SYNTHESIS AND REACTIVITY OF *UMPOLUNG* REAGENTS THROUGH TRANSITION METAL CATALYSIS

ANDREI NIKOLAEV

A DISSERTATION SUBMITTED TO THE FACULTY OF GRADUATE STUDIES IN PARTIAL FULFILLMENT OF THE REQUIREMENTS FOR THE DEGREE OF DOCTOR OF PHILOSOPHY

GRADUATE PROGRAM IN CHEMISTRY
YORK UNIVERSITY
TORONTO, CANADA

DECEMBER, 2018

Abstract

The cyclopropanol-derived palladium-homoenolates have previously been exploited as a unique class of cross-coupling partners in our group. The major advantage of using cyclopropanols as the cross-coupling partners is the fact that the functional group content is preserved. Specifically, cyclopropanol forms the corresponding β-functionalized carbonyl product which can be used for further transformations. We developed an efficient method towards the synthesis of quinoline derivatives with broad functional group tolerance using series of cyclopropanols and *ortho*-bromoanilines as the cross-coupling partners in the presence of a palladium-catalyst. A deuterium labeling study revealed that a second equivalent of *ortho*-bromoaniline is the terminal oxidant in this reaction.

Considering the importance of aza-aromatic heterocycles in biologically active drug molecules, there is a continuous demand for rapid and benign methods towards their functionalization. Hence, we wanted to exploit a transition-metal catalyzed free-radical ring opening reaction of cyclopropanols towards rapid and efficient functionalization of pyridine derivatives. We development a silver-catalyzed direct functionalization of heteroaromatic compounds with a well-defined silver catalyst. Through this study, we gained strong evidence which suggests that silver-pyridine complexes are the catalytically active species for free-radical ring-opening of the cyclopropanol.

Acylsilanes are classic *umpolung* reagents with broad synthetic applications. Specifically, acylsilanes undergo polarity inversion at the carbonyl-carbon via the 1,2-Brook rearrangement with a concomitant reaction with an electrophile. Unfortunately, synthetic methods for acylsilanes often involve many steps and harsh conditions. We explored a mild synthetic method for the preparation of α,β-unsaturated acylsilanes via perrhenate-catalyzed Meyer-Schuster rearrangement of 3-silyl propargylic alcohols.

Dedications

It is my delight to dedicate this thesis to my family. Their unconditional love, support, inspiration, warmth and kindness allowed me to focus on my goals and to reach my dreams. I also dedicate my work to my best friend Max, I am truly thankful for your friendship and for your advices that you gave me.

Acknowledgements

First, I would like to give my special thanks to my supervisor Prof. Arturo Orellana for providing me with the opportunity to conduct research as a graduate student in his group. Your guidance, help and support throughout the years allowed me to develop into a confident and motivated chemist that I am today. Your constructive criticism and feedback throughout the years allowed me to develop my problem-solving skills and critical thinking. I would also like to extend my thanks to Prof. Michael G. Organ and Prof. Gino Lavoie for your constructive criticism and feedback during my research evaluations.

To my examining comminittee members, I thank you for taking your time with preparing for my defense.

Next, I would like to thank Dr. Howard Hunter for his expert help, support and knowledge in NMR spectroscopy. Thank you for your help with various NMR experiments and giving me the opportunity to look after the spectrometers.

I would like to show my thanks to all my colleagues that I had the privilege to work with and collaborate in sharing ideas and insightful discussion about chemistry. To Abir Khadra for her passion and useful discussions about reaction mechanisms, to David Rosa, Faizan Rasheed, Minhao Zhang, Nour Wasfy, Zi Wang, Bojan Dragisic, Sadaf Samadi and Nisha Nithiy, for their interest in organic chemistry and willingness to engage in question-answer discussions. To Dr. Mahmoud Sayah for his knowledge in organometallics and friendship inside and outside of the lab. I would like to also express my gratitude to my friends outside of York University. To my best friend Max for his advices and support and to Leila for her support, care and love.

Finally, this work would not be possible without the help and support from my family. Thank you, dad, for financial and moral support. To my mom for her care, love and best-tasting cooking. To my sister for her support and help.

Table of Contents

List of Tables

List of Figures

List of Schemes

List of Abbreviations

acac	Acetylacetonate
ACS	American chemical society
CFL	Compact fluorescent light
DBU	1,8-Diazabicyclo[5.4.0]undec-7-ene
DCE	1,2-Dichloroethane
DCM	Dichloromethane
DIAD	Diisopropyl azodicarboxylate
DMA	*N,N*-Dimethylacetamide
DMF	*N,N*-Dimethylformamide
DMSO	Dimethyl sulfoxide
dppb	1,4-Bis(diphenylphosphino)butane
dppm	Bis(diphenylphosphino)methan
EA	Electron affinity
EI	Electron ionization
ESI	Electrospray ionization
EtOAc	Ethyl Acetate
eV	Electron Volt
FG	Functional group
HMPA	Hexamethylphosphoramide
HRMS	High resolution mass spectrometry
Hz	Hertz
IR	Infrared
LED	Light-emitting diode
LUMO	Lowest unoccupied molecular orbital
m.p.	Melting point
MeCN	Acetonitrile
MW	Microwave
NHC	*N*-Heterocyclic Carbene
NMR	Nuclear Magnetic Resonance

$PhCH_3$	Toluene
PhH	Benzene
pic	Picolinate
ppm	Parts per million
PTSA	*p*-Toluenesulfonic acid
QPhos	1,2,3,4,5-Pentaphenyl-1’-(di-*tert*-butylphosphino)ferrocene
S_EAr	Electrophilic Aromatic Substitution
S_N2	Substitution Nucleophilic Bimolecular
S_NAr	Nucleophilic Aromatic Substitution
TBAF	Tetra-*n*-butylammonium fluoride
TBHP	*tert*-Butyl hydroperoxide
TBS	*tert*-Butyldimethylsilyl
TEA	Triethylamine
TEMPO	(2,2,6,6-Tetramethylpiperidin-1-yl)oxyl
TES	Triethylsilyl
TFA	Trifluoroacetic acid
THF	Tetrahydrofuran
TIPS	Triisopropylsilyl
TMS	Trimethylsilyl
TOF	Time of flight
UV	Ultraviolet
UVA	Ultraviolet A
XPhos	2-Dicyclohexylphosphino-2’,4’,6’-triisopropylbiphenyl

Chapter 1: Introduction

1.1 Umpolung Logic in Organic Synthesis

The realm of organic synthesis stems from the ability to construct new carbon-carbon and carbon-heteroatom bonds with the aid of reagents, auxiliaries and catalysts.[1] In general, the carbon framework and functional group content determines the overall reactivity and properties of a molecule. Therefore, much focus has been placed on the development of efficient and environmentally benign synthetic strategies for the formation of carbon-heteroatom, carbon-carbon single, double, and triple bonds. Specifically, strategies that utilize organotransition metal catalysis,[2] elimination, substitution, and free radical reactions have been developed.[3] Despite the advances in synthetic strategies, there is still a continuous demand for more efficient and benign carbon-carbon and carbon-heteroatom bond formation methodologies for expedient synthesis of small and complex molecules.

The most common logic for new bond formation is based on a polar bond disconnection between a nucleophile and an electrophile. Conceptually and in practise, the action of electron density transfer from a nucleophile to an electrophilic center forges a new chemical bond (Fig. 1).

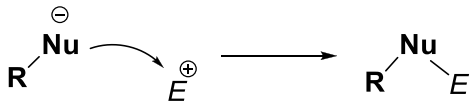

Figure 1. Traditional bond formation between a nucleophile (- or δ^-) and an electrophile (+ or δ^+).

A plethora of reactions in organic synthesis utilize this strategy for construction of carbon-carbon and carbon-heteroatom bonds. Some of the prototypical examples of such reactions include the Arbuzov phosphonate ester preparation, the Kolbe nitrile synthesis, the Mitsunobu inversion/esterification and the Finkelstein S_N2 alkyl iodide synthesis (Scheme 1).[4,5,6,7]

Examination of these reactions reveal a general trend. Particularly, the carbon-heteroatom bond formation is between a nucleophilic heteroatom (- or δ^-) and an electrophilic carbon (+ or δ^+). Hence, traditional bond formation stems from the combination of opposite polarity reactive partners.

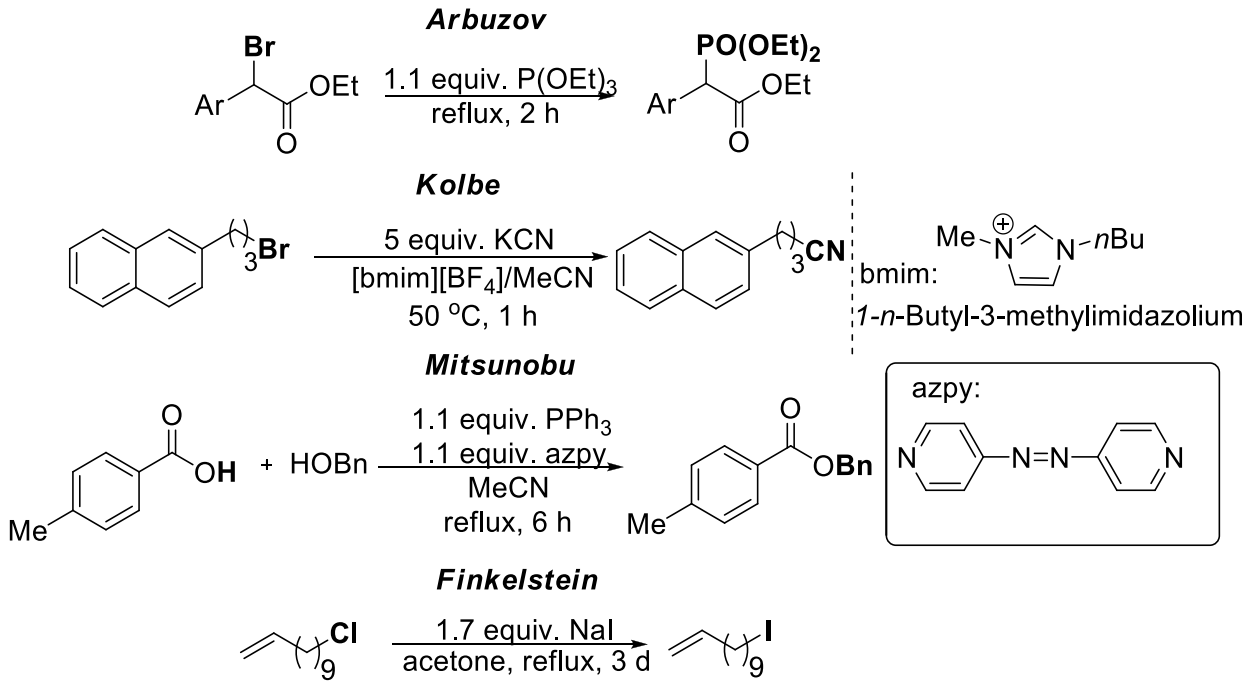

Scheme 1. Prototypical reactions in organic synthesis that exploit complimentary polarity between reactive partners.

The mechanism of the Arbuzov reaction is a great example where multiple such complimentary nucleophile-electrophile bond formations events occur in a sequence (Scheme 2). In the first step, the carbon-phosphorus bond is formed via an S_N2 reaction between triethyl phosphite and the α-bromo ester derivative. The second step produces the phosphonate ester after S_N2 reaction between the bromide and one of the ethyl groups.

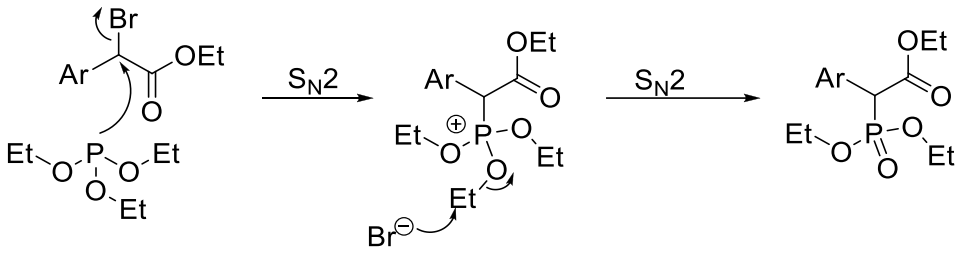

Scheme 2. The mechanism of the Arbuzov reaction displays two sequential S_N2 steps.

Generally, electronegative heteroatoms such as nitrogen, oxygen and the halogens impose an alternating donor and acceptor reactivity pattern on the carbon skeleton (Fig. 2).[8] This alternating pattern of donor (**d**) and acceptor (**a**) atoms implies that in principle 1,(2n+1) substituted products can be formed through nucleophilic attack at the acceptor carbons. The same bond-making approach would fail for odd substitution products because the two atoms making a bond have a non-complementary relationship. Hence, formation of synthetic targets with 1,(2n) substitution patterns is difficult to achieve using traditional reactivity owing to the charge affinity mismatch. This mismatched bonding relationship is commonly referred to as dissonant.

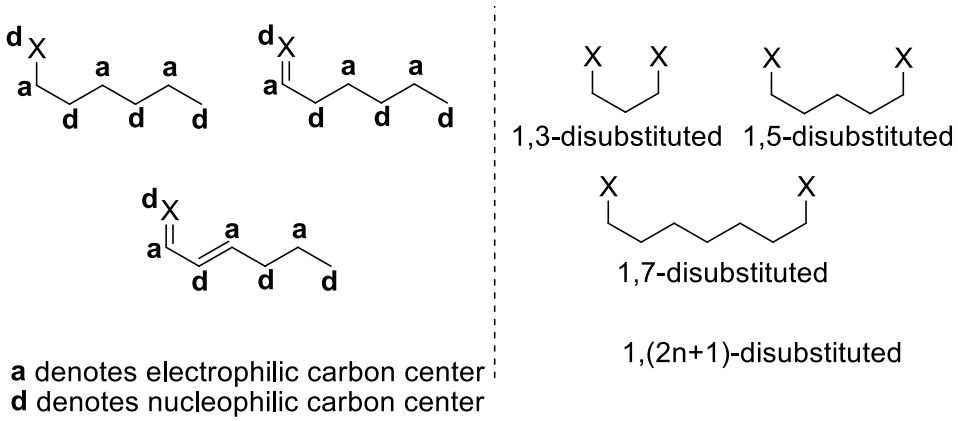

Figure 2. An alternating donor and acceptor reactivity pattern on the carbon skeleton framework for 1,(2n+1) disubstituted patterns.

Access to 1,(2n)-disubstituted patterns necessitates a change in polarity from acceptor to donor at the 2n carbon atom positions. This process of polarity inversion is termed *umpolung* and

was introduced by D. Seebach together with E. J. Corey and has proven to be a useful conceptual tool in organic synthesis for the construction of simple and complex molecular targets.[8,9]

The aldehyde group has proved to be a particulary useful *umpolung* reagent in organic synthesis. Its innate electrophilic character makes the carbonyl group highly susceptible to nucleophilic attack at the carbonyl carbon. This reactivity pattern, however, can be reversed in the presence of nucleophilic organic catalysts such as cyanide or N-heterocyclic carbene (NHC), which render the carbonyl carbon nucleophilic.[10] This unique reactivity inversion is widely exploited for the synthesis of α-hydroxy ketones. This reactions proceeds through carbon-carbon bond formation between two electrophilic carbons via an aldehyde-derived acyl anion equivalent formed by the nucleophilic addition of NHC catalyst to the aldehyde function (Eq. 1).[11]

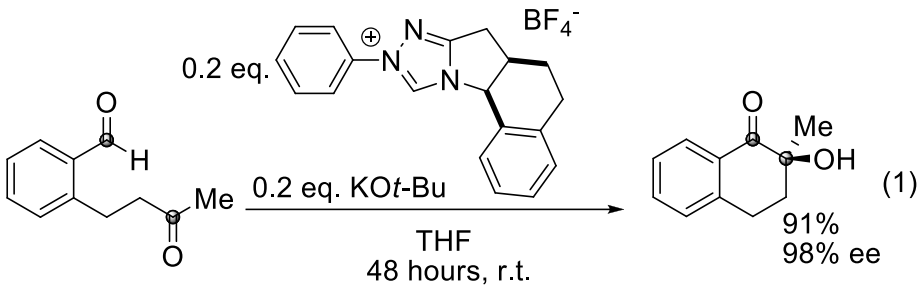

(1)

The general mechanism of nucleophile-catalyzed carbonyl polarity inversion commences with the attack at the carbonyl carbon by the nucleophilic catalyst, forming the tetrahedral intermediate reversibly. For example, in the case of cyanide as the nucleophilic catalyst during the benzoin condensation reaction, deprotonation of the acidic α-proton generates a nitrile stabilized anion which undergoes a subsequent 1,2 addition to a carbonyl function. Finally, the nucleophilic catalyst is regenerated through collapse of the tetrahedral intermediate, revealing the ketone product (Scheme 3).

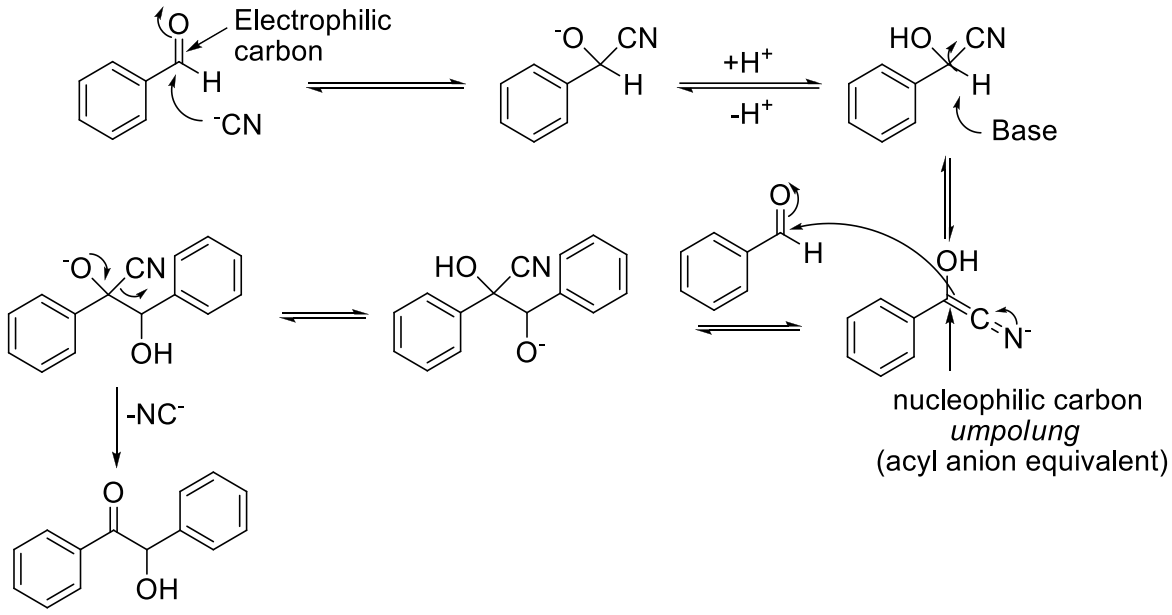

Scheme 3. The mechanism of the benzoin condensation displays *umpolung* reactivity.

A somewhat different variant of *umpolung* reactivity involves stoichiometric pre-modification of the carbonyl function prior to the polarity inversion step. Specifically, an aldehyde function is converted to a 1,3-dithiane via a Lewis-acid catalyzed condensation with 1,3-propanedithiol. The polarization and the inductive effects of the two sulfur atoms render the adjacent proton acidic and can readily undergo deprotonation with a strong base and generate a nucleophilic carbon atom (Scheme 4).[12] The carbonyl function is then regenerated after hydrolysis of the dithiane.[13,14,15] However, the need for stoichiometric modification of the aldehyde function and the dithiane formation and hydrolysis steps are major drawbacks of this approach.

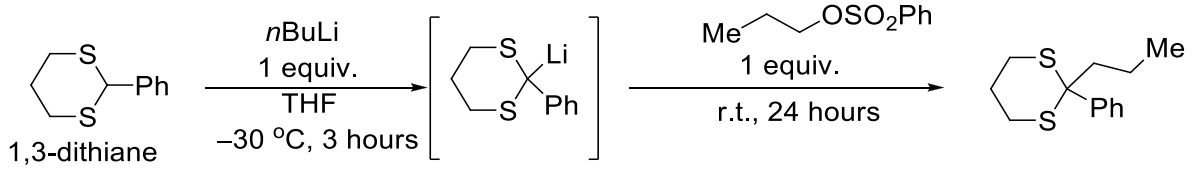

Scheme 4. Dithiane induces carbonyl *umpolung* reactivity for new carbon-carbon bond formation.

Examples of *umpolung* methods presented so far have relied on the removal of an acidic proton to generate a nucleophilic carbon. These methods, therefore, are limited to the aldehyde functional group. Alternatively, switching to the acylsilane functionality allows for an *umpolung* strategy that does not depend on a deprotonation step. In this case, polarity inversion is achieved via a 1,2-Brook rearrangement initiated by the addition of a nuclephile to the acyl silane (Scheme 5).[16] Generally, the 1,2-Brook rearrangement is a reversible process and is therefore controlled by the relative thermodynamic stability of the equilibrating species. The fundamental driving force for the forward 1,2-Brook rearrangement is the formation of the stronger oxygen-silicon bond (110 kcal/mol) at the expense of the weaker carbon-silicon bond (85 kcal/mol).[17] The resulting silyl ether carbanion intermediate reacts with an electrophilic species and forges a new carbon-carbon bond irreversibly.

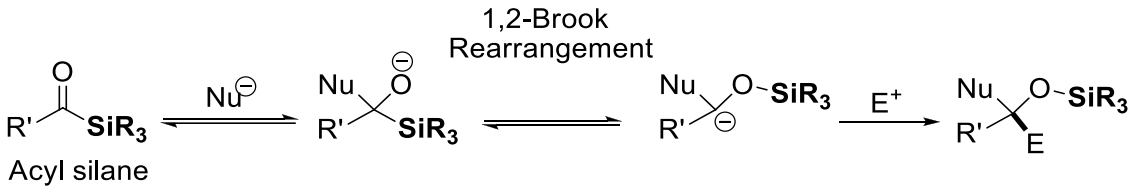

Scheme 5. General mechanism for nucleophile promoted *umpolung* of acyl silanes via 1,2-Brook rearrangement.

Acylsilanes are highly versatile *umpolung* reagents and have found applications in the synthesis of natural products and small molecules.[18,19] Okamoto *et. al.* utilized acyl silane derived polarity inversion for the synthesis of decorated eight-membered rings with broad functional group content (Scheme 6).[20]

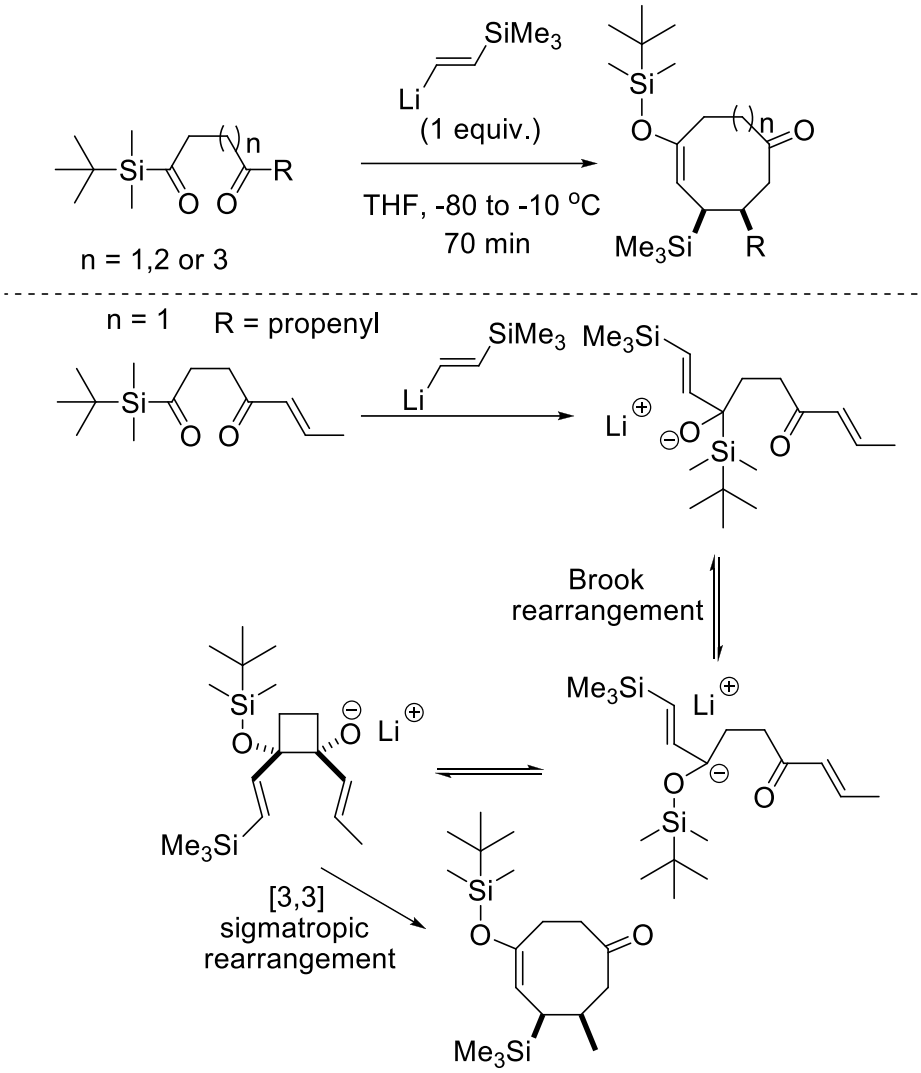

Scheme 6. Formation of functionalized eight-membered rings using the *umpolung* reactivity of acyl silanes.[20]

The mechanism of this transformation begins with a nucleophilic attack by the 1,2-lithiovinyl silane on the acylsilane carbonyl carbon, followed by dynamic 1,2-Brook rearrangement. In the second step, the silyl ether carbanion intermediate adds to the pendant ketone function to generate a four-membered ring reversibly. The forward direction of this equilibrium is driven by the subsequent irreversible [3,3]-sigmatropic rearrangement when the two vicinal vinyl groups have a *cis*-relationship. The driving force for this step is the release of the strain-energy associated with the cyclobutane.

Umpolung logic is not limited to carbonyl function as demonstrated by its extension to substitution reactions of aromatic rings. Benzene reacts through Friedel-Crafts electrophilic aromatic substitution (S_EAr) with an alkyl or acyl chloride substrates in the presence of a Lewis acid.[21] Interestingly, this reactivity pattern can be reversed using Semmelhack's method which renders the benzene ring electron deficient upon complexation with chromium tricarbonyl that facilitates a nucleophilic aromatic substitution reaction with an overall inversion in reactivity (Scheme 7).[22]

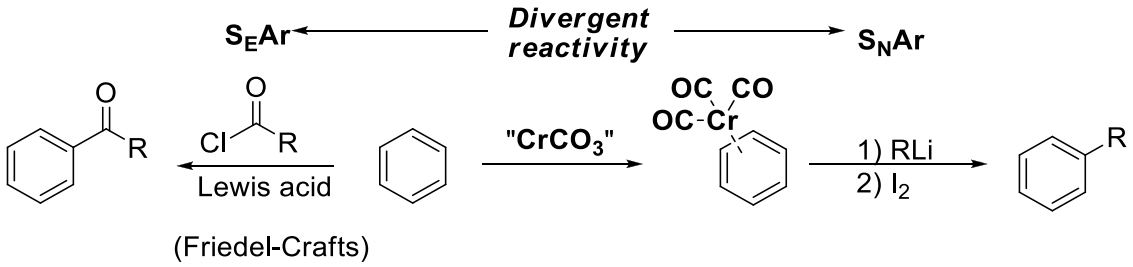

Scheme 7. Extension of *umpolung* principle towards divergent reactivity of an aromatic ring.

The series of *umpolung* examples with aldehydes presented so far have all been limited to the polarity inversion at the carbonyl carbon. Extension of *umpolung* logic to distal sites away from the carbonyl group is far more challenging. For example, consider the reaction between a ketone-derived enolate and an aldehyde. Bond formation in this reaction occurs between complimentary reactivity sites, which provides the β-hydroxy ketone and preserves the alternating distribution of charge along the carbon chain in a 1,3-relationship between the carbonyl and alcohol functions (Path A, Fig. 3).

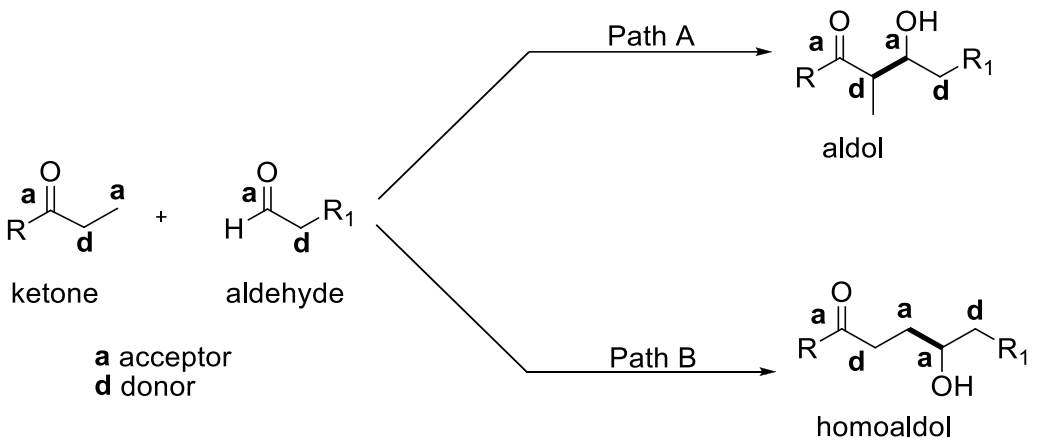

Figure 3. Formation of aldol and homoaldol products using alternating charge affinity patters.

However, the formation of a homoaldol product displaying a 1,4-relationship between the carbonyl and alcohol function is challenging owing to the dissonant relationship between the carbon atoms (Path B, Fig. 3). Construction of carbonyl function with 1,4-relationship therefore, requires a reversal of polarity at the β-carbon, from an electrophile to a nucleophile via homoenolate formation. Nickon and co-workers have shown that homoenolates can be generated from conformationally constrained ketones.[23,24] Specifically, they have shown that (+)-camphenoline racemizes in the presence of base at elevated temperatures via homoenolate formation followed by the formation of *meso*-cyclopropoxide (Scheme 8). However, this method requires special substrates and harsh reaction-conditions that limit its synthetic utility.

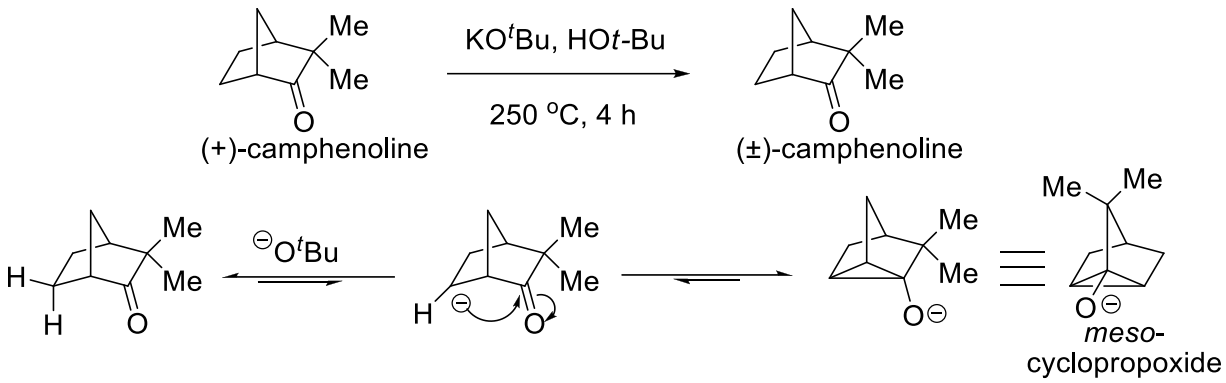

Scheme 8. Racemization of (+)-camphenoline via homoenolate formation.

1.2 TMS-Protected Cyclopropanols & Acyl Silanes in Umpolung Logic

While the formation of an enolate derived from a ketone can be achieved readily by treatment with strong base, there are no general methods for the formation of homoenolate analogs. The few examples of direct homoenolate formation are limited to substrates derived from conformationally constrained ketones and use forcing conditions, which limits their application.[23] [24] The major challenge of direct generation of homoenolates by deprotonation at the β-position is the lack of resonance stabilization, which significantly increases the pKa and hinders their formation. In an effort to circumvent this limitation a number of strategies have been developed. For example, the use of acetal containing Grignard substrates were shown to be suitable homoenolate equivalents by Büchi and Wüest (Scheme 9).[25] Unfortunately, this method suffers from the need for protection and deprotection steps, which significantly limits the synthetic utility.

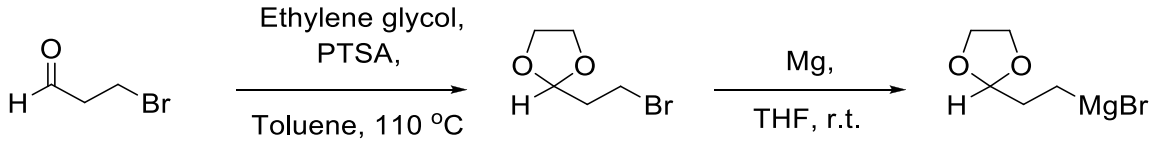

Scheme 9. Synthesis of acetal-protected Grignard reagent as homoenolate equivalent.

A protecting-group-free homoenolate equivalent was synthesized using 3-bromopropionic acid *via* a deprotonation and reduction sequence (Eq. 2).[26] However, this method is limited to carboxylic acids.

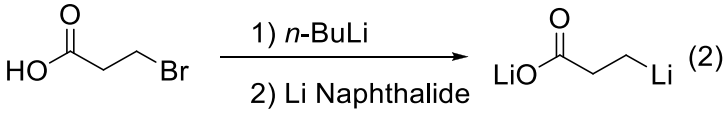

In 1977, Kuwajima introduced a method for the synthesis of 4-hydroxy esters via the titanium(IV)-mediated reaction of 1-alkoxy-1-siloxy-cyclopropanes with aldehydes (Scheme 10).[27]

He suggested that this transformation proceeds through the formation of a titanium homoenolate intermediate prior to an aldol-type condensation. This result shows that homoenolates can be readily accessed via treatment of siloxycyclopropanes with an appropriate metal halide source. Overall, this method utilizes the alleviation of ring strain in cyclopropanes towards the formation of various homoenolate equivalents.

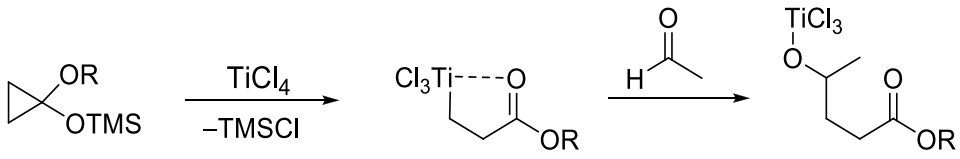

Scheme 10. Cyclopropanol-derived titanium(IV) homoenolates in homoaldol-condensation as suggested by Kuwajima.

Following the seminal discovery by Kuwajima, a number of cyclopropanol-derived metal homoenolate equivalents were prepared with stoichiometric metal salts (Fig. 4). Particularly, a mixture of zinc chloride and siloxycyclopropane forms zinc homoenolates,[28] which can be transmetallated to metals such as palladium, nickel and copper.[29,30,31] Homoenolates based on mercury and tin metals have also been prepared in a similar manner.[32,33,34]

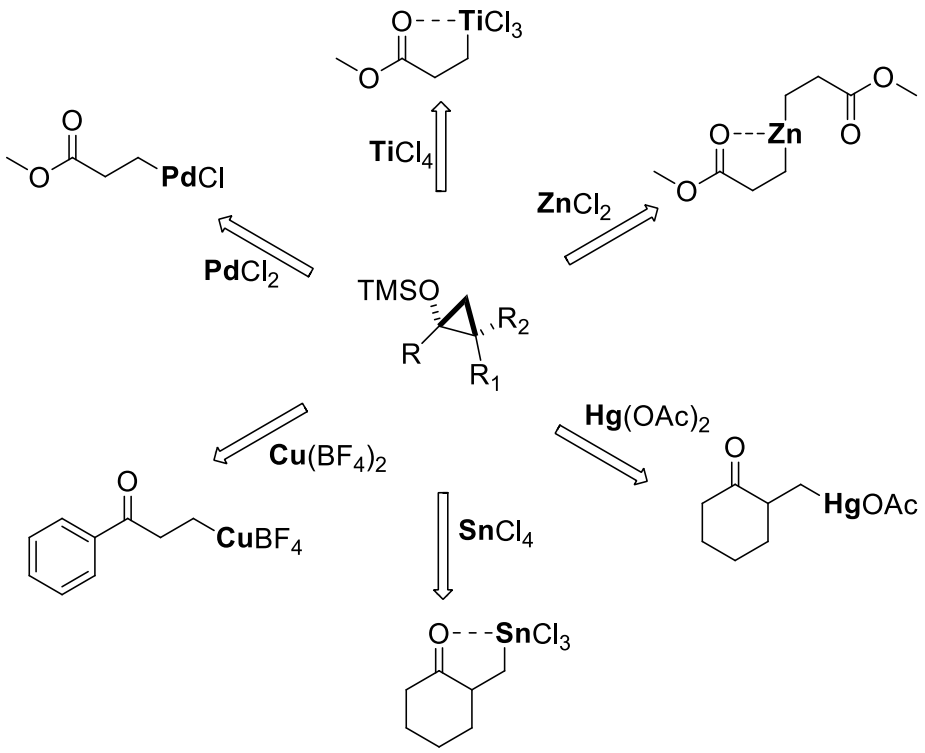

Figure 4. Siloxycyclopropane-derived metal-coordinated homenolates.

An alternative method for homoenolate formation introduced by Kuwajima utilizes the acyl silane functionality and its ability to undergo a 1,2-Brook rearrangement (Scheme 5) as an *umpolung* precursor.[35] The two-step protocol begins with the treatment of an acyl silane with a vinyl Grignard reagent, which generates 1-trimethylsilyl allylic alcohol upon workup. In the second step, lithium alkoxide of 1-trimethylsilyl allylic alcohol is formed via deprotonation with *sec*-butyllithium and undergoes a 1,2-Brook rearrangement with concomitant formation of the silyl homoenolate equivalent (Scheme 11). Treatment of this homoenolate with a wide array of 1˚ and 2˚ alkyl iodides affords the corresponding β-functionalized silyl enol ether equivalent.

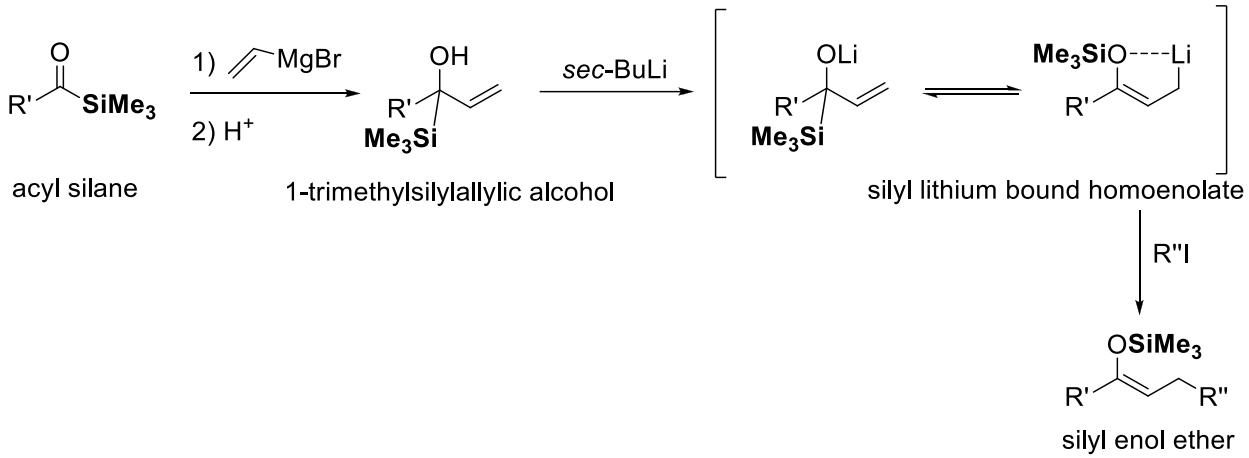

Scheme 11. Acylsilane-derived, lithium-coordinated silyl homoenolate formation and its reaction with alkyl iodides.

Seminal work by Kuwajima with siloxycyclopropanes and acylsilanes demonstrated a practical solution to the limitations associated with previously reported methods for homoenolate formation. Since their discovery, metal bound homoenolates have proven to be highly useful for construction of new carbon-carbon bonds via direct substitution (S_N2), addition and transition metal catalyzed cross-coupling reactions. Advances in transition metal catalyzed homoenolate formation protocols using cyclopropanols, facilitated their use in broad range of carbon-carbon and carbon-heteroatom bond formation strategies.

1.3 Transition-Metal-Catalyzed Reactions of Cyclopropanols

Initial reports by Kuwajima *et al.* demonstrated that silyl-protected cyclopropanols are compatible substrates for palladium-catalyzed cross-coupling with aryl triflates but fail with aryl halides (Scheme 12).[36,37,38,39,40,41] Following the seminal work by Kuwajima, an immense number of transition metal-catalyzed C-C and C-X bond forming reactions were developed using homoenolate umpolung strategies. Unlike the previous examples, many of the new methods are compatible with aryl halides and unprotected cyclopropanols in the presence of a transition metal-catalyst.

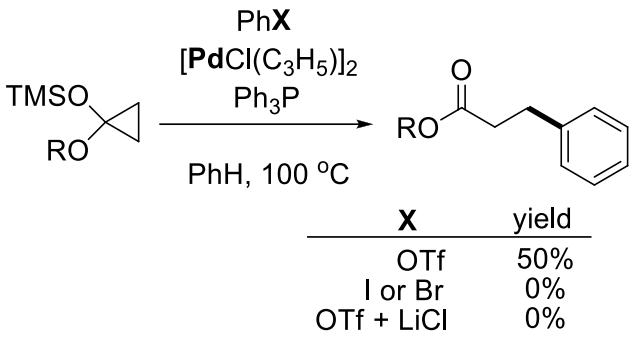

Scheme 12. Cross-coupling of cyclopropane acetals with aryl triflates, catalyzed by palladium reported by Kuwajima.

Methodologies developed by the Orellana group represent the first examples of palladium-catalysis using cyclopropanols as unique cross-coupling partners with aryl halides. In their initial report, the palladium-catalyzed cross-coupling reaction between aryl halides (X = Br or I) and cyclopropanol was shown to be a competent method for C-C bond formation at the β-position of the resulting ketone function (Eq. 3).[42] In this methodology, the substrates were designed to prevent the potential β-hydride elimination reaction. As an extension to this method, the same group developed the cross-coupling of cyclopropanol-derived homoenolates bearing β-hydrogens relative to the palladium (Eq. 4).[43] Interestingly, the choice of bidentate phosphine ligand 1,4-bis(diphenylphosphino)butane (dppb) was critical for suppressing the formation of undesired β-hydride elimination product. In a separate report by the Orellana group, the scope of palladium-catalyzed cross-coupling reactions with cyclopropanols was extended to include benzyl chlorides as cross-coupling partners (Eq. 5).[44] The Cha group exploited palladium-catalyzed cross-coupling reactions of cyclopropanols using aryl triflates and bromides as cross-coupling partners for the synthesis of cycloheptanones (Eq. 6).[45] An advantage of these methods is that they reveal a ketone group at the same time that a new C-C bond between two electrophilic carbon atoms is formed.

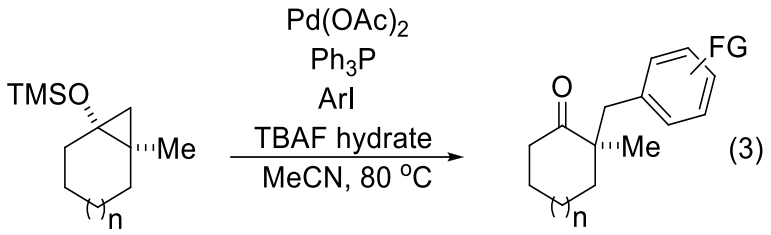

(3)

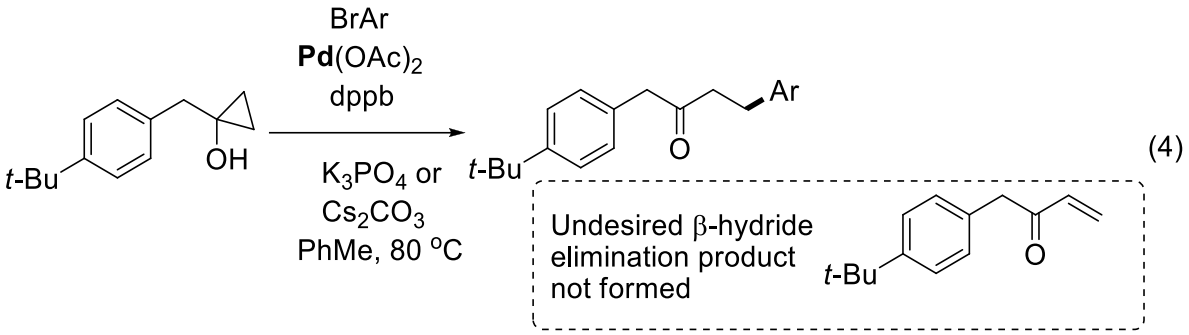

(4)

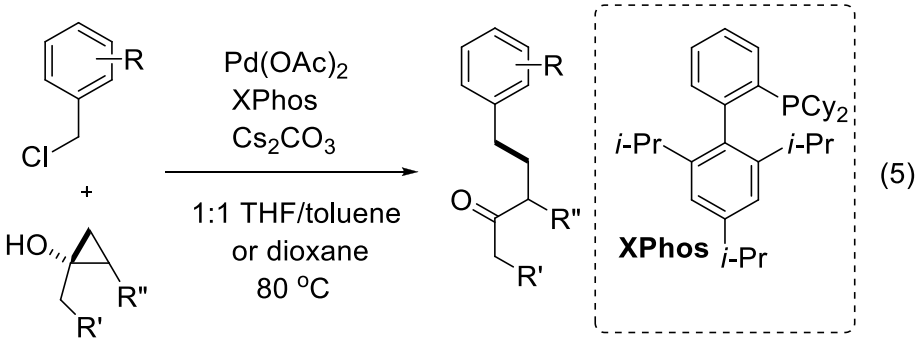

(5)

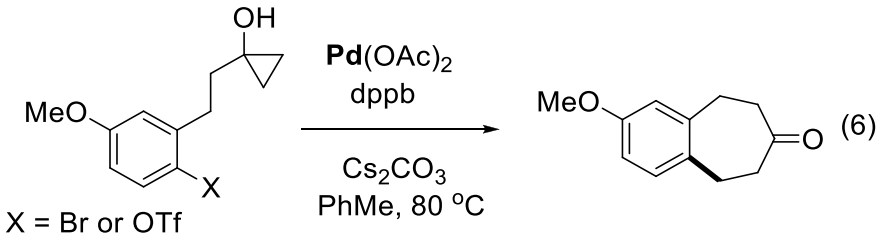

(6)

The exact mechanism of the ring-opening step in the above reactions remains unclear. In a report based on palladium-catalyzed oxidative transformation of unprotected cyclopropanols to α,β-unsaturated ketones, Cha proposed a mechanism involving coordination of the cyclopropanol oxygen to the palladium(II) centre prior to the C-C bond cleavage.[46] Therefore, a putative general catalytic cycle of palladium catalyzed cross-coupling reactions with cyclopropanols begins with

direct insertion of palladium(0) catalyst into C-X (X = Cl, Br, I or pseudohalide) bond which formally oxidizes the metal center to palladium(II) (Scheme 13). Coordination of cyclopropanol followed by deprotonation would yield a palladium(II)-alkoxide intermediate which then undergoes β-carbon elimination and yields the palladium homoenolate. Formation of a new carbon-carbon bond through reductive elimination from the palladium(II) centre would generate the cross-coupled product and regenerate the palladium(0) catalyst.

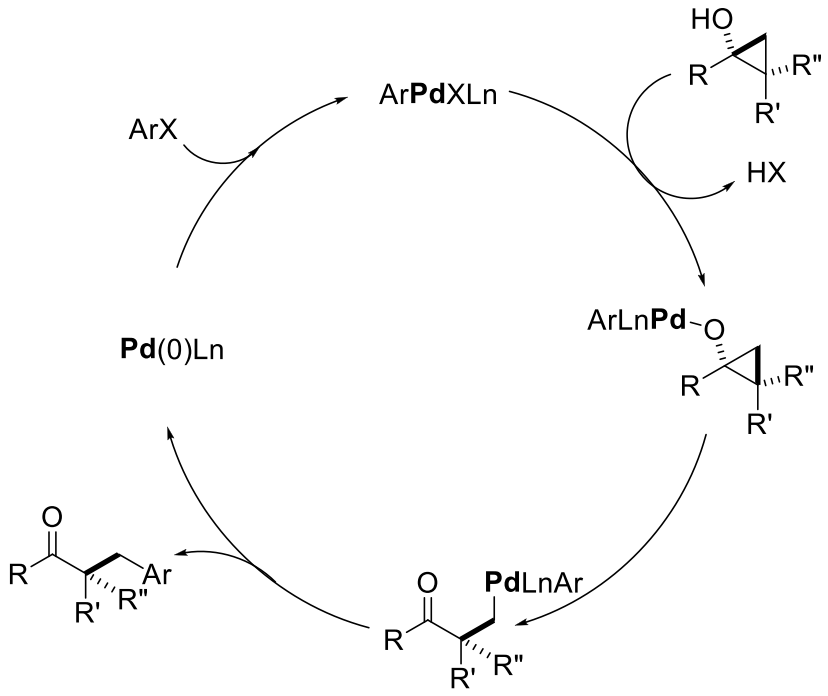

Scheme 13. Proposed general catalytic cycle for palladium-catalyzed cross-coupling between cyclopropanols and aryl halides.

The transition metal catalyzed cross-coupling reactions with symmetric cyclopropanol substrates occur with no choice in regioselectivity during the ring opening step and can therefore only form a single cross-coupled product. In the case of asymmetric cyclopropanols however, two different cross-coupled products can potentially form depending on the regioselectivity during the ring-opening step. Nevertheless, palladium-catalysts show remarkable regioselectivity for the formation of the cross-coupled product at the less substituted carbon. Although details about the

mechanism of this ring opening event are currently lacking, it is believed that the palladium-catalyzed ring opening step is under the steric control. This regioselectivity pattern was first exemplified by series of methodologies developed by the Orellana group with asymmetric cyclopropanols (Eq. 3 & Eq. 5). Following these contributions, similar regioselectivity was observed in the palladium-catalyzed cross-coupling of cyclopropanol-derived aldehyde homoenolates reported by Walsh (Eq. 7).[47] The palladium-catalyzed ring opening and cross-coupling occur exclusively at the primary carbon. Overall, these methods provide the coupled products in good yields and tolerate wide range of functional groups.

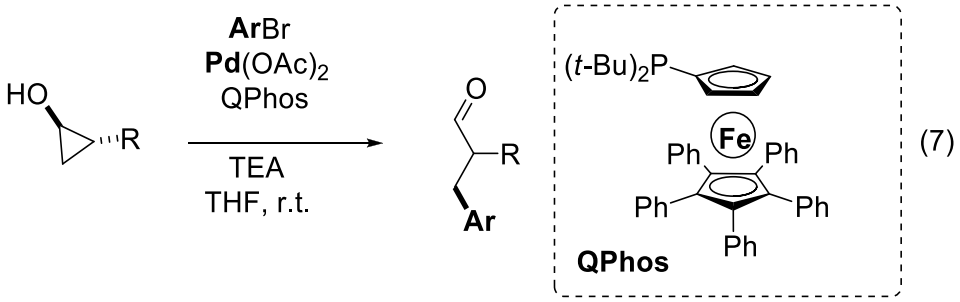

(7)

In general, reactions involving transition metals can be classified based on radical and nonradical processes. Palladium-catalyzed cyclopropanol ring opening is believed to occur through a concerted mechanism without radical intermediates. Transition metals capable of single electron redox processes should in principle facilitate the free-radical ring-opening of cyclopropanols. Examples of single electron oxidative homolytic cleavage of cyclopropanols mediated by transition metals were reported decades ago.[48] These reactions are believed to proceed through single-electron oxidation of cyclopropanol with concomitant fragmentation to the carbon-based radical (Scheme 14).

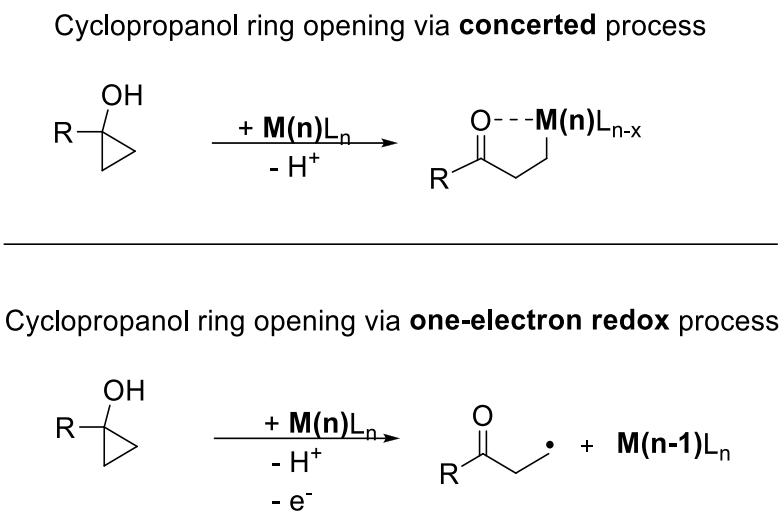

Scheme 14. Cyclopropanol ring opening via concerted and radical processes.

The synthetic utility of the free radical ring opening reactivity of cyclopropanols remained dormant until recently. The Narasaka group showed that β-keto radicals generated from single-electron oxidation of cyclopropanols with manganese(III) tris(pyridine-2-carboxylate) are capable of adding to electron-deficient and electron-rich olefins.[49,50,51,52] The utility of this method was demonstrated in the synthesis of bicyclic molecules by intramolecular radical cyclization (Scheme 15).[53] Although useful, this method requires superstoichiometric loading of the manganese reagent. An improved method developed by the same group, uses substoichiometric silver nitrate as single-electron oxidant and ammonium persulfate as the terminal oxidant.[54]

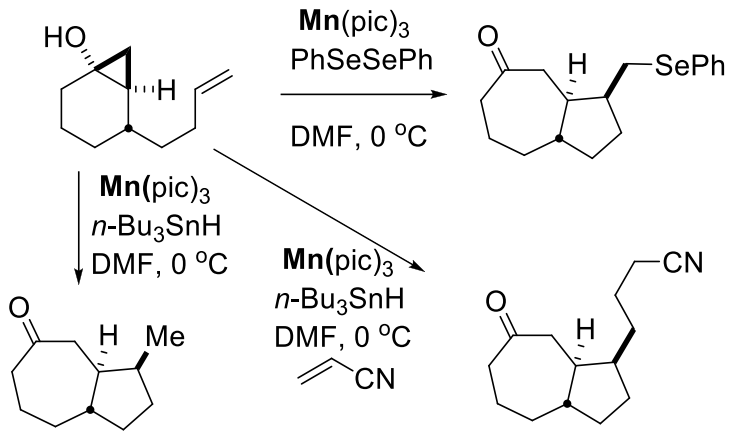

Scheme 15. The use of Mn(III)-mediated oxidative ring opening of cyclopropanols for the synthesis of bicyclic systems via free-radical addition to alkenes.

The Zhu and Murakami groups used silver(I) fluoride catalyst with mono-and disubstituted cyclopropanols for the synthesis of β-fluroketones.[55,56] The C-F bond formation occurred predominantly at the more substituted carbon with 1,2-disubstituted cyclopropanols (Eq. 8).

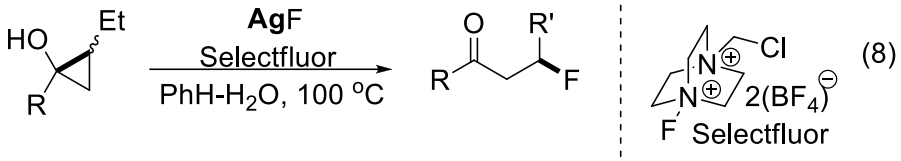

(8)

The proposed mechanism of the formation of β-fluorinated ketone products commences with two-electron oxidation of Ag(I) catalyst to high-valent Ag(III) species with selectfluor as the terminal oxidant. The next step is coordination of the cyclopropanol and the loss of a proton followed by oxidation via homolytic silver-oxygen bond cleavage to generate oxyradical species, which ring opens to a β-keto radical intermediate. Coupling with Ag(II)FX, followed by reductive-elimination, forms the product and regenerates the Ag(I)X catalyst (Scheme 16). A body of experimental evidence provides support for this proposed radical mechanism. For example, control experiments with stoichiometric amounts of silver(I) fluoride or silver(II) fluoride did not promote this reaction, implying that the high-valent silver(III) species is involved. Addition of

(2,2,6,6-tetramethylpiperidin-1-yl)oxyl (TEMPO) completely shut down the reaction. Using 1,2-disubstituted cyclopropanol furnished C-F coupled product at the more substituted carbon. Taken together, these results are strongly suggestive of a free-radical mechanism during the ring opening step.

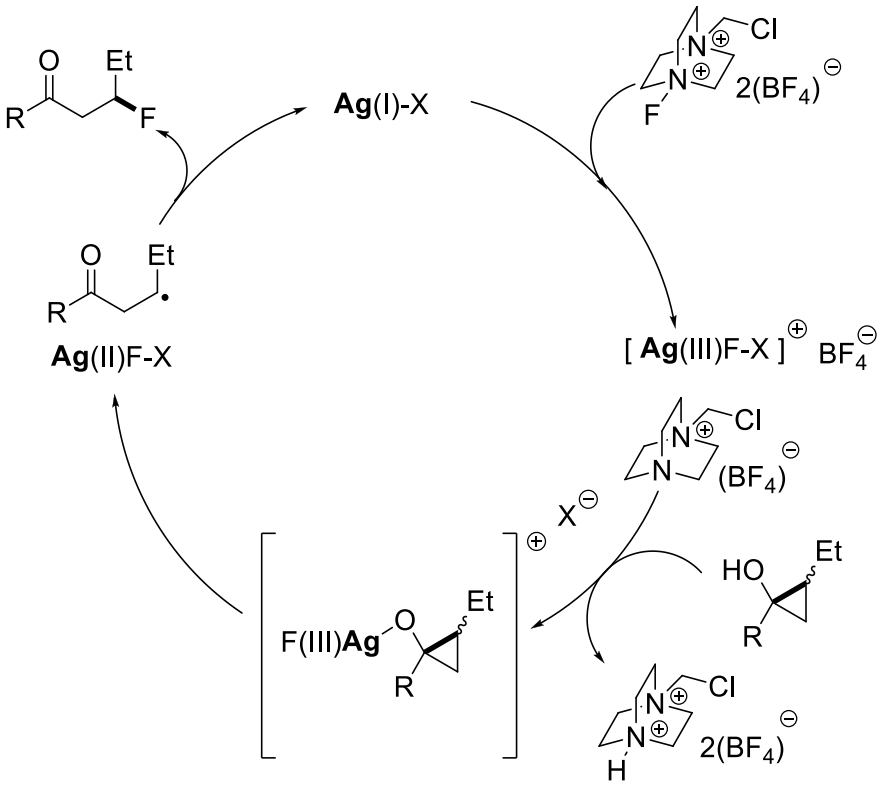

Scheme 16. Proposed catalytic cycle for silver-catalyzed synthesis of β-fluoro ketones from cyclopropanols reported by Murakami.

Using silver triflate as catalyst, the Zhang group developed synthesis of β-chloro ketones from cyclopropanols using *tert*-butyl hypochlorite as the terminal oxidant and phenanthroline as the ligand (Eq. 9).[57] Consistent with a radical mechanism, in the case of disubstituted cyclopropanol substrates, a more substituted C-Cl bond was formed selectively.

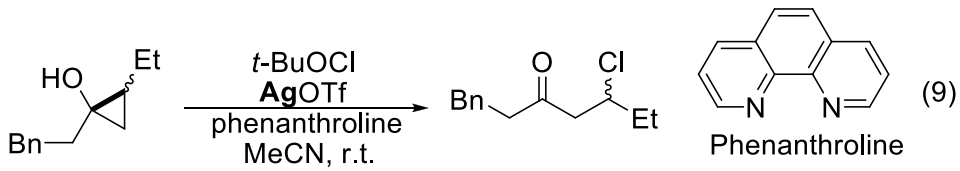

(9)

Catalysts for cyclopropanol ring-opening reactions span the early, middle and late transition metals. For example, Mn(III)-picolinate and Fe(III)-chloride mediated free-radical cyclopropanol reactions proved to be a competent method for tandem synthesis of bicyclic molecules,[53 58] $Cu(MeCN)_4BF_4$ efficiently catalyzes the formation of β-trifluormethyl ketones from cyclopropanols in the presence of Togni's reagent,[59] and a $VO(acac)_2$ catalyst transforms cyclopropanols to β-oxygenated ketones under atmosphere of dioxygen as the terminal oxidant.[60]

Transition-metal catalyzed ring opening reactions of cyclopropanols have rapidly developed into a versatile synthetic tool for C-C and C-X bond formation that exploits nonintuitive retrosynthetic *umpolung* disconnections. The regioselectivity of the ring opening step is primarily controlled by judicious choice of metal catalyst. In the case of C-C bond formation reactions, cyclopropanols offer unique reactivity patterns that allow for facile bond formation between carbons of non-complimentary polarity, and that would otherwise be difficult to make. Despite the considerable number of examples exploiting this reactivity, there are many reactions that remain to be explored.

1.4 Research Plan

Given the synthetic utility of cyclopropanol-derived palladium-homoenolates in cross-coupling reactions, we became interested in extending this strategy towards the synthesis of aromatic heterocycles. The major advantage of using cyclopropanols as the cross-coupling partner is the fact that the functional group content is preserved. Specifically, cyclopropanol forms the corresponding β-functionalized carbonyl product which can be used for further transformations. We envisioned that using a cyclopropanol and an *ortho*-bromoaniline as cross-coupling partners in the presence of a palladium-catalyst, should provide an expedient method for synthesis of quinoline derivatives in the presence of terminal oxidant. Gratifyingly, after a thorough optimization study, this reaction proved to be an efficient method towards the synthesis

of quinoline derivatives with broad functional group tolerance. The details of this method including the optimization and the scope studies are described in Chapter 2 of this dissertation.

Considering the importance of aza-aromatic heterocycles in pharmaceutical drug molecules, there is a continuous demand for rapid and benign methods towards their functionalization. Hence, we wanted to exploit a transition metal-catalyzed free-radical ring opening reaction of cyclopropanols towards the functionalization of pyridine derivatives. We were pleased to find that approach based on free radical addition to heterocyles, lead to the development of silver-catalyzed direct functionalization of heteroaromatic compounds with a well-defined silver catalyst. Throughout this study, we gained strong evidence that suggests that silver-pyridine complexes are the catalytically active species for free-radical ring-opening of the cyclopropanol. The details of the development of this method, including the optimization and the scope studies, are described in Chapter 3 of this dissertation.

Acylsilanes are classic *umpolung* reagents with broad synthetic applications. Specifically, acylsilanes undergo polarity inversion at the carbonyl-carbon via the 1,2-Brook rearrangement with a concomitant reaction with an electrophile. Unfortunately, synthetic methods for acylsilanes often involve many steps, harsh conditions and toxic reagents. We were interested in developing a mild synthetic method for the preparation of α,β-unsaturated acylsilanes via perrhenate-catalyzed Meyer-Schuster rearrangement of 3-silyl propargylic alcohols. The details of the development of this method, including the optimization and the scope studies, are described in Chapter 4 of this dissertation.

Chapter 2: Synthesis of Quinolines via Palladium-Catalyzed Cross-Coupling of Cyclopropanols with *ortho*-Bromoanilines.

2.1 Introduction

Heterocycles and heterocycle-containing molecules are ubiquitous in nature and find application in chemistry, biology, medicine, agriculture and materials science. Considering their broad applications, there is continued demand for new synthetic methods based on mild and environmentally benign reaction conditions. Classical approaches to synthesis of heterocycles often require elevated temperatures under strongly basic or acidic conditions, which significantly limit their scope (Eq. 10).[61,62,63]

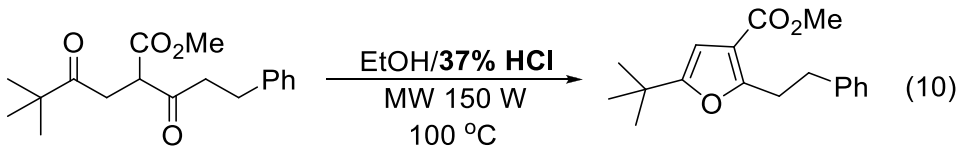

(10)

Compared to classical methods, the transition metal catalyzed synthesis of heterocycles generally benefits from milder reaction conditions and broader scope.[64,65] Importantly, most of the transition metals are relatively non-toxic, a feature which is particularly advantageous for reactions conducted on large scale. For example, using relatively non-toxic copper(I) iodide as a catalyst, the synthesis of substituted indolizine derivatives was carried out at room temperature and with mild base (Eq. 11).[66] In light of all these benefits, novel methods for the synthesis of heterocycles using transition metal catalysis are therefore worth pursuing.

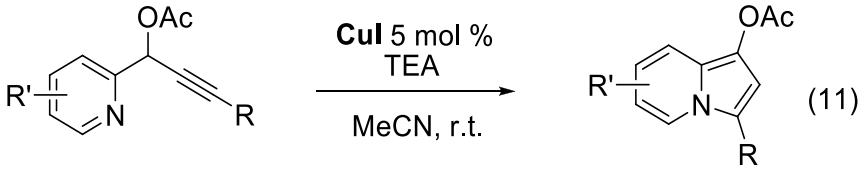

(11)

As discussed previously, palladium-catalyzed cross-coupling reactions of cyclopropanol-derived homoenolates with a wide array of electrophiles are well documented. One of the key advantages of these reactions is that the functional group content is preserved. Specifically, the cyclopropanol is transformed into a carbonyl function in the cross-coupled product that can be used for further synthetic transformations (Eq. 12).

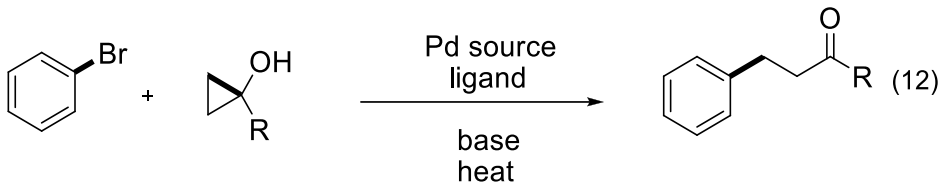

(12)

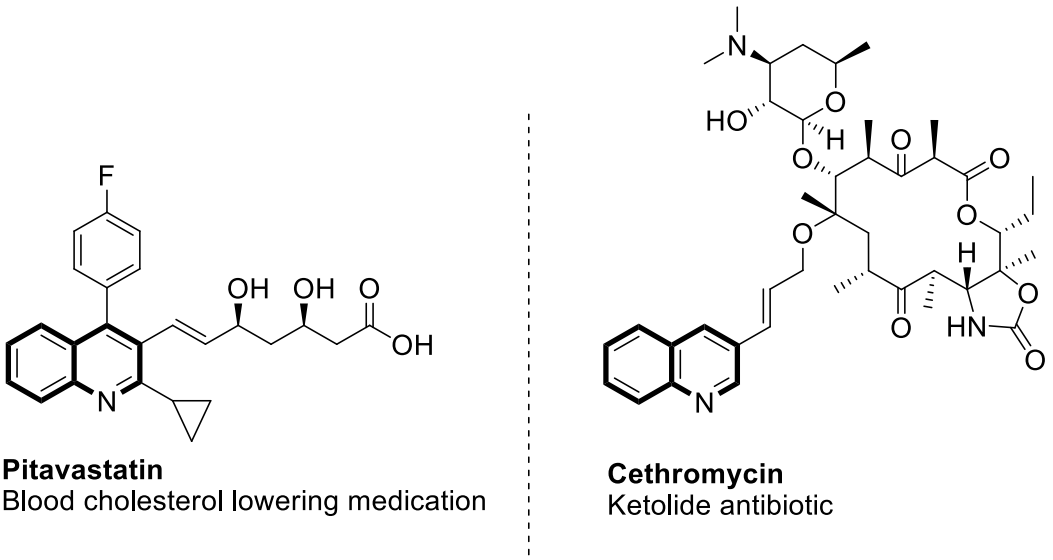

Pitavastatin
Blood cholesterol lowering medication

Cethromycin
Ketolide antibiotic

Figure 5: Examples of quinoline containing molecules with biological function.

Substituted quinoline derivatives are common structural motifs in many pharmaceutical drugs (Fig. 5) and for that reason there has been great interest in new methodologies for their synthesis. Exploiting palladium-catalysis, Larock developed the synthesis of substituted quinoline derivatives from *ortho*-iodoanilines and an allylic alcohol (Eq.13).[67] It is proposed that quinoline formation in this transformation begins with Heck reaction followed by imine formation and subsequent oxidation to yield the final quinoline product. In the presence of polar solvent such as

DMF, DMSO, MeOH and MeCN, mixtures of quinolines and tetrahydroquinoline products were observed, which implies a likely disproportionation step. Interestingly, when HMPA was used as solvent for the reaction, only quinoline product was observed.

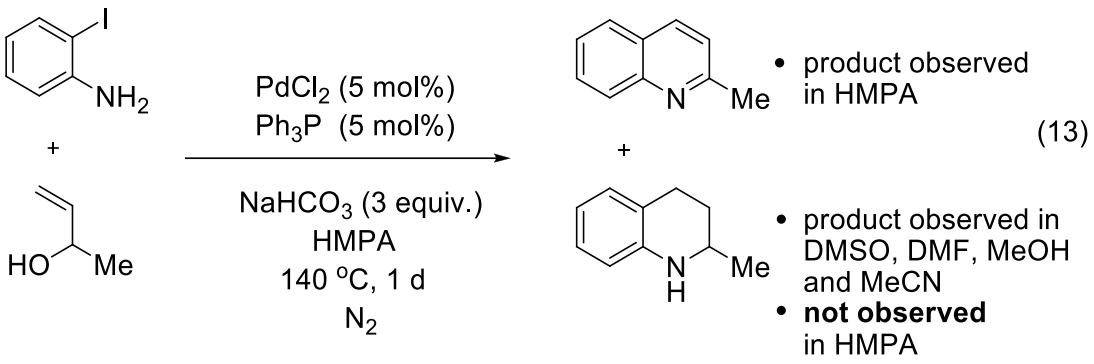

(13)

Following the seminal contributions by the Larock group, similar methodologies have been developed.[68,69,70,71,72,73] In a two-step methodology developed by Stone,[74] palladium-catalyzed quinoline synthesis was carried out via initial cross-coupling between allylic alcohols and *ortho*-bromoanilines, followed by oxidation with diisopropyl azodicarboxylate (DIAD) in a second step (Eq. 14). Although this method is an improvement to the initial report by Larock, it is far from ideal. The need for DIAD as an oxidant and acetic acid as solvent in the second step limits the functional group tolerance and scope.

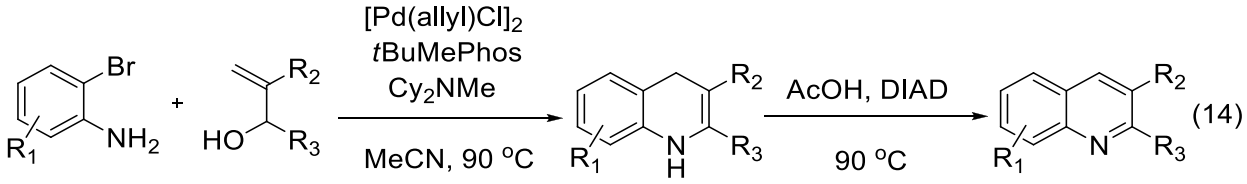

(14)

We envisioned that palladium-catalyzed cross-coupling of cyclopropanols could be extended towards the synthesis of substituted quinolines under mild reaction conditions. Our proposed catalytic cycle involves: (1) oxidative addition of a Pd(0) catalyst to the ortho-bromoaniline, (2) formation of palladium(II) alkoxide species (**II**, in Scheme 17) via coordination-deprotonation of the cyclopropanol **I**, (3) cyclopropanol to palladium homoenolate rearrangement

III, (4) reductive elimination to form β-(2-aniline)-ketone **IV** and concomitant condensation-oxidation to prepare quinoline **VI**. We believe that this transformation will provide an expedient route to substituted quinoline derivatives.

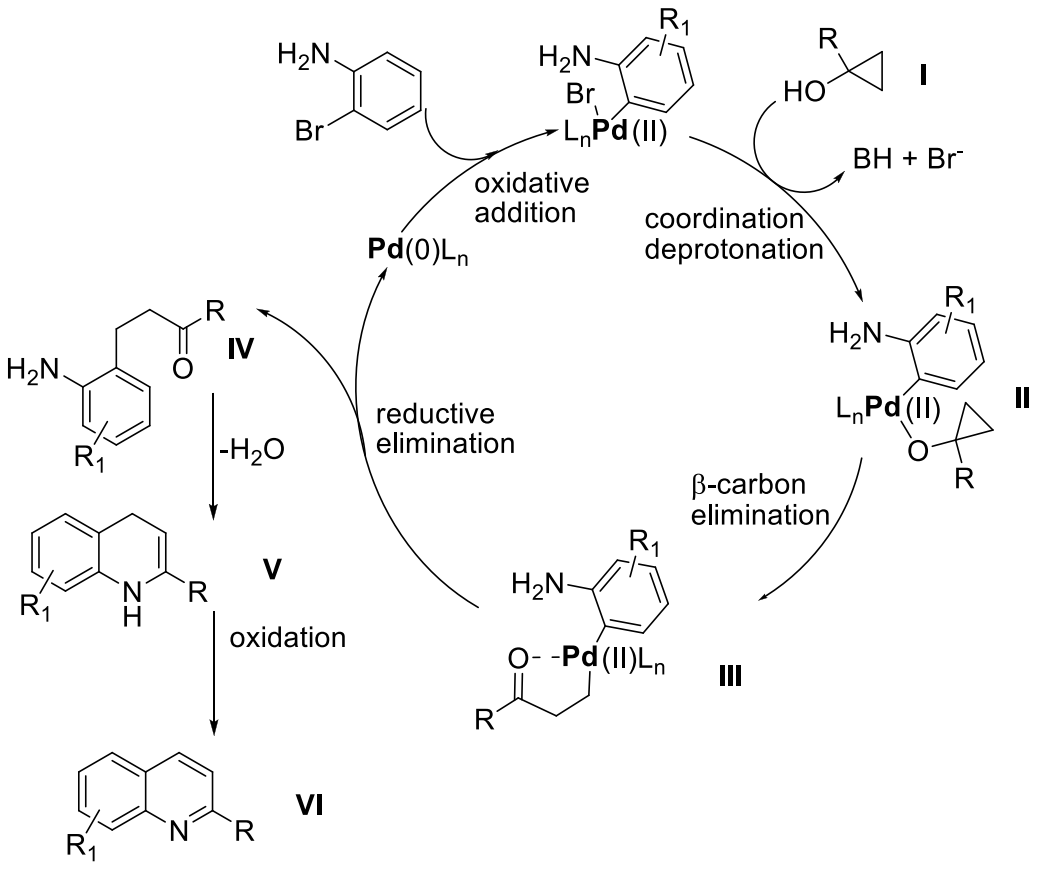

Scheme 17. Catalytic cycle for the proposed synthesis of substituted quinoline derivatives.

Results and Discussion:

*2.2 Preparation of Model Substrate **1***

To test the feasibility of the proposed quinoline synthesis we decided to prepare cyclopropanol **1**. The same model substrate was previously prepared in our group for the cross-coupling of cyclopropanol-derived homoenolates bearing β-hydrogens.[43] The ^{1}H-NMR resonance signals for cyclopropanol **1** were consistent with the expected structure bearing the diagnostic cyclopropanol proton resonance signals at 0.85 and 0.68 ppm. This and related substrates can be readily synthesized using the Kulinkovich method using an ester, a titanium(IV) catalyst and a Grignard reagent (Eq. 15).[75] Also, the proton NMR spectroscopic analysis of the quinoline product would be simplified due to the symmetry of **1**. Hence, methyl-2-(4-*tert*-butylphenyl)acetate was used as the precursor for our model substrate.

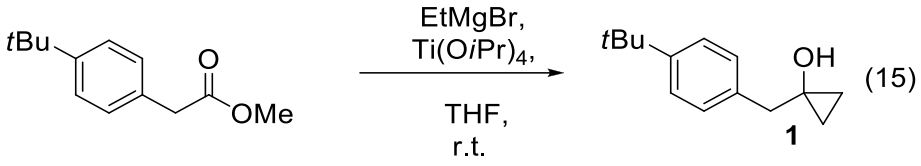

(15)

2.3 Proof of Concept

With cyclopropanol **1** synthesized, we were excited to test the feasibility of the quinoline synthesis proposed in Scheme 17. Our group had previously demonstrated that the bidentate phosphine ligands such as 1,4-bis(diphenylphosphino)butane (dppb) are competent in palladium-catalyzed cross-coupling reaction of cyclopropanols. Hence, we decided to test our proposed quinoline synthesis using previously optimized reaction conditions by cross-coupling *ortho*-bromoaniline with cyclopropanol **1**.[42] We were pleased to isolate the desired quinoline **2** in 43% yield along with the aniline product **3** in almost 1:1 ratio (Eq. 16). Analysis of the ^{1}H-NMR spectrum of quinoline **2** revealed the diagnostic resonance signals at 8.13, 8.04 and 4.36 ppm for protons labelled (II), (III) and (I) respectively as compared to a similar compound previously reported.[76]

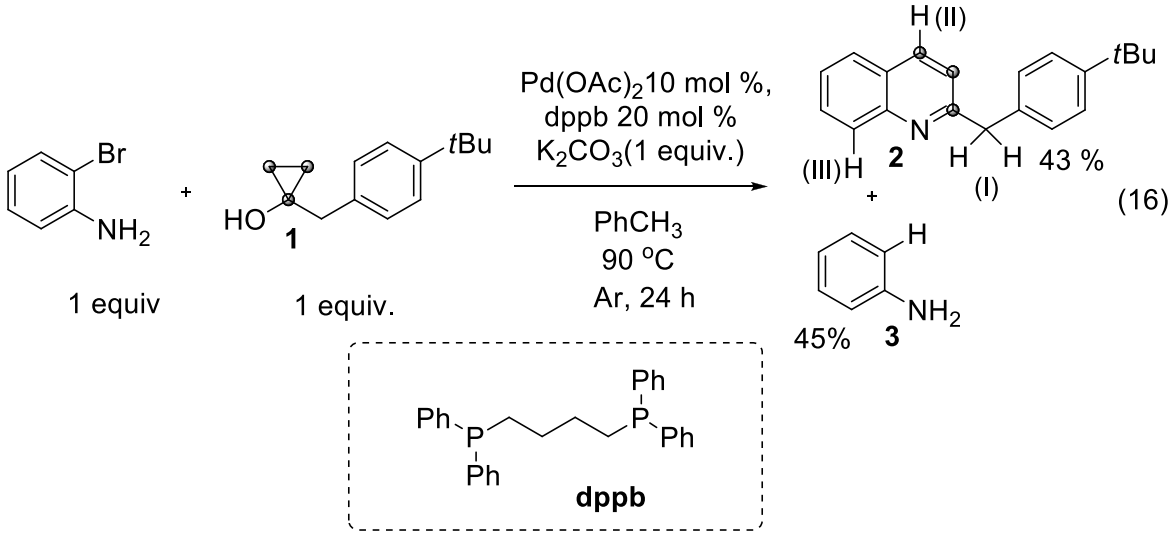

(16)

2.4 Optimization Study

Motivated by this initial result, we decided to optimize the reaction conditions for this methodology. Isolation of products **2** and **3** in nearly 1:1 ratio implied that *ortho*-bromoaniline plays a dual role as the substrate and as the terminal oxidant. Doubling the number of equivalents of *ortho*-bromoaniline relative to cyclopropanol **1** improved the yield of **2** from 43% to 64%. Employing dppb as ligand, $Pd(OAc)_2$ as the precatalyst and toluene as the solvent, a screen of

common organic and inorganic bases was undertaken (Table 1). Interestingly, carbonate bases were required for quinoline synthesis while biphosphate, acetate and organic bases furnished trace or no quinoline product along with recovered starting material. Using four equivalents of K_2CO_3 proved to be optimal and furnishing quinoline product in 76% isolated yield.

Table 1. Optimization Study – Base Screen[a]

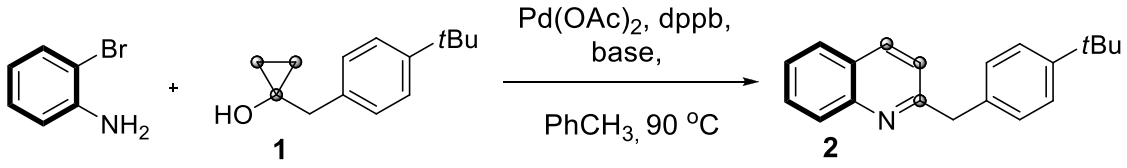

Entry	Base	2[b]	Entry	Base	2[b]
1	K_2HPO_4	trace	6	Cs_2CO_3	trace
2	proton sponge	0%	7	K_2CO_3	64% (76%)[c]
3	DBU	0%	8	NaOAc	0%
4	TEA	0%	9	KOAc	0%
5	Na_2CO_3	38%			

[a] All reactions were carried out with 0.49 mmol of substrate at 0.12 M concentration in toluene, 10 mol % of $Pd(OAc)_2$, 20 mol % of dppb, 2.0 equiv. of *ortho*-bromoaniline and 1.0 equiv. of base. [b] Isolated yields of pure product after column chromatography on silica. [c] Using 4.0 equiv. of base.

2.5 Substrate Scope Study

With optimized reaction conditions for the synthesis of substituted quinolines in hand, we investigated the scope of this transformation. First, we explored a range of cyclopropanol substrates with *ortho*-bromoaniline (Table 2). The cyclopropanol substrates used in this study were synthesized using known methods.[43,77,50,78] In general, monocyclic monosubstituted cyclopropanols provided the corresponding quinoline in 75-89% yield (Table 2, entries 1,2, and 4-6). The reaction conditions developed also tolerated a cyclopropanol bearing a cyclohexenyl substituent (Table 2, entry 3). However, the quinoline product **13** was isolated in only 41% yield. Employing a cyclopropanol substituted at position two (Table 2, entry 5) furnished quinoline **15**

bearing a substituent at the 3-position in 80% isolated yield. This makes the method particularly useful considering that generally, functionalization of quinolines at the “meta” position of the aza ring is challenging due to lack of activation at that site. Ring-fused cyclopropanols **9** and **10** allow access to tricyclic quinolines **17** and **18** in fair yields respectively.

Table 2. Scope of Cyclopropanol Substrates for the Synthesis of Quinoline Derivatives[a,b]

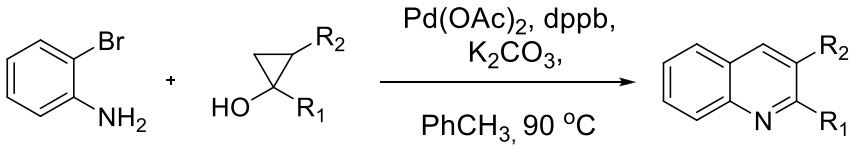

Entry	Cyclopropanol	Quinoline
1	**1** 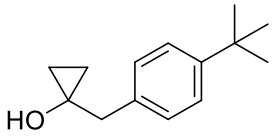	**11** 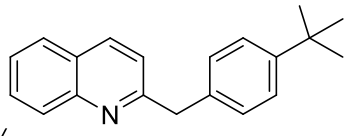 76%
2	**4** 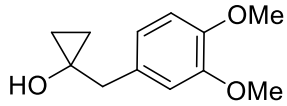	**12** 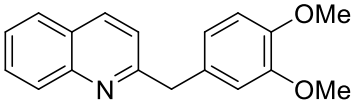 75%
3	**5** 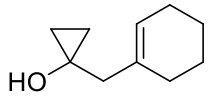	**13** 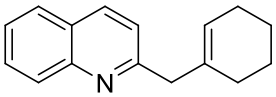 41%
4	**6** 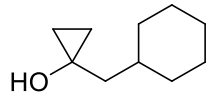	**14** 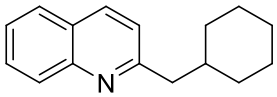 77%
5	**7** 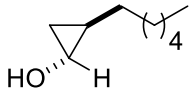	**15** 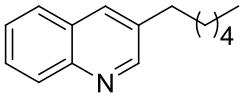 80%
6	**8** 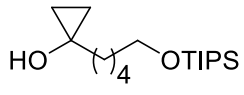	**16** 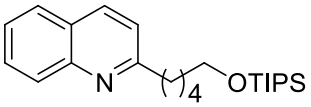 89%
7	**9** 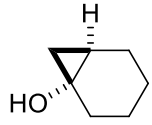	**17** 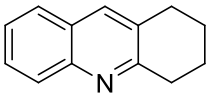 51%
8	**10** 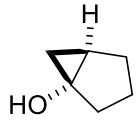	**18** 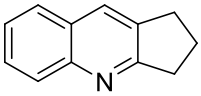 48%

[a] All reactions were carried out with 0.25 mmol of substrate at 0.12 M concentration in toluene, 10 mol % of $Pd(OAc)_2$, 20 mol % of dppb, 2.0 equiv. of *ortho*-bromoaniline and 4.0 equiv. of base. [b] Isolated yields of pure product after column chromatography on silica.

Next, the scope of this methodology was investigated with substituted bromoanilines (Table 3, entries 1-8) and 1-(4-*tert*-butylbenzyl)cyclopropanol **1**. Overall this reaction shows wide functional group compatibility under the optimized conditions. Specifically, this methodology tolerates alkyl, halogen, ester, sulfonamide and nitro substituents in 65-89% isolated yields. It is worth noting that in the case of quinoline **28**, the chloro substituent allows for further functionalization and derivatization via standard cross-coupling methods.[66] Overall this method allows for an expedient construction of functionalized quinoline derivatives with simple palladium-catalyst system.

Table 3. Scope of Bromoaniline Substrates for the Synthesis of Quinoline Derivatives[a,b]

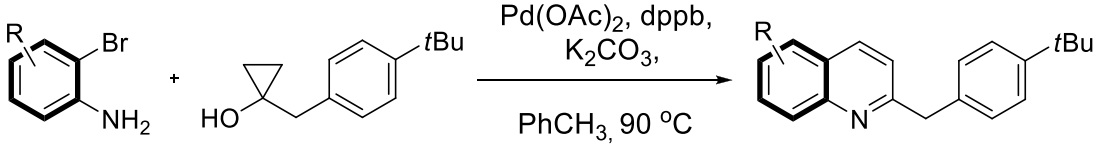

Entry	Bromoaniline	Quinoline
1	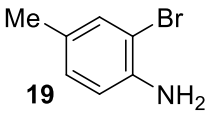 **19**	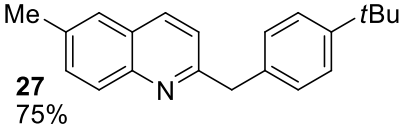 **27** 75%
2	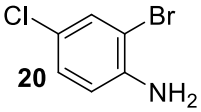 **20**	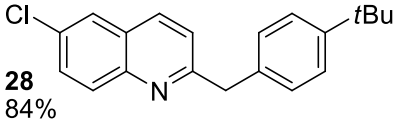 **28** 84%
3	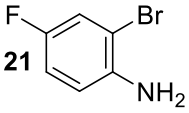 **21**	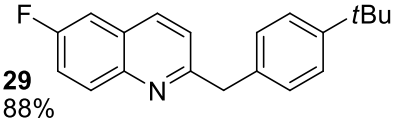 **29** 88%
4	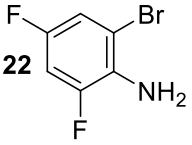 **22**	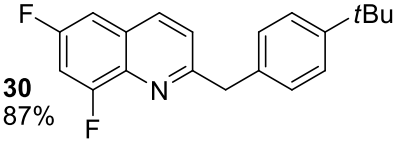 **30** 87%
5	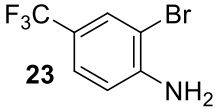 **23**	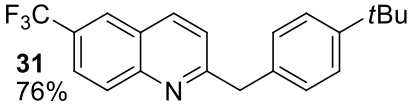 **31** 76%
6	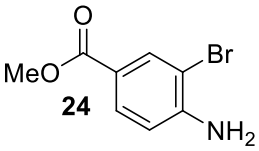 **24**	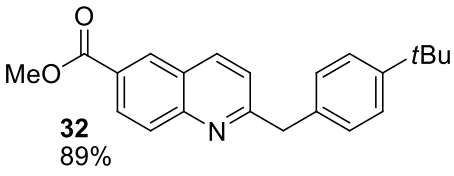 **32** 89%
7	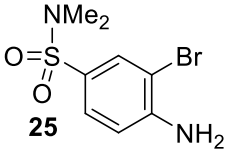 **25**	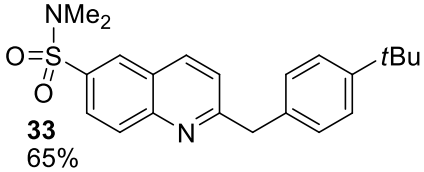 **33** 65%
8	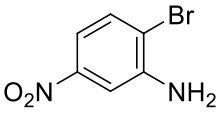 **26**	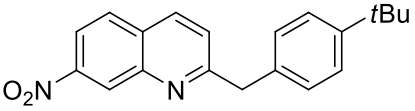 **34** 87%

[a] All reactions were carried out with 0.25 mmol of substrate at 0.12 M concentration in toluene, 10 mol % of $Pd(OAc)_2$, 20 mol % of dppb, 2.0 equiv. of *ortho*-bromoaniline and 4.0 equiv. of base. [b] Isolated yields of pure product after column chromatography on silica.

Intrigued by the need for two equivalents of *ortho*-bromoaniline for good yields, we hypothesised that the second *ortho*-bromoaniline equivalent functions as the terminal oxidant during the oxidation of a dihydroquinoline to a quinoline. To test this hypothesis, we decided to carry out a deuterium-labeling experiment. A strategically deuterated cyclopropanol **1**-d_4 was synthesized using the Kulinkovich reaction conditions using methyl-2-(4-*tert*-butylphenyl)acetate and the Grignard reagent derived from bromoethane-d_5 (Eq. 17).[75] Next, cyclopropanol **1**-d_4 was subjected to the optimized reaction conditions with bromoaniline **24**. If our hypothesis is correct, the deuterium labels will be located at the 3- and 4-positions of the quinoline product and 2-position in the reduced aniline. Indeed, this reaction furnished quinoline **32**-d_2 in 85% yield and the 2-deutero-aniline **35** in 83% yield (Eq. 18).

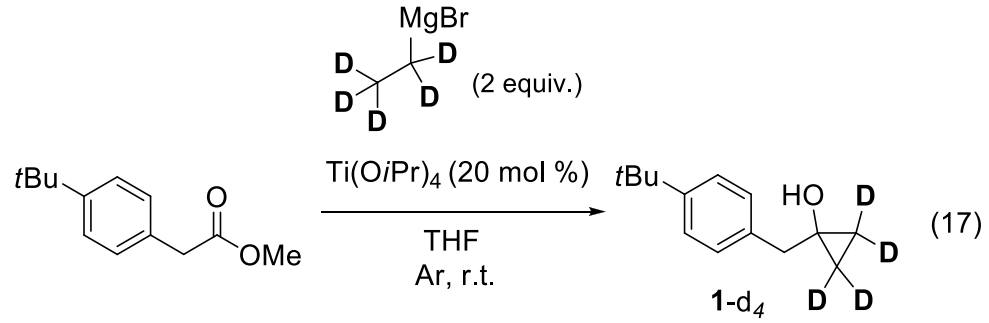

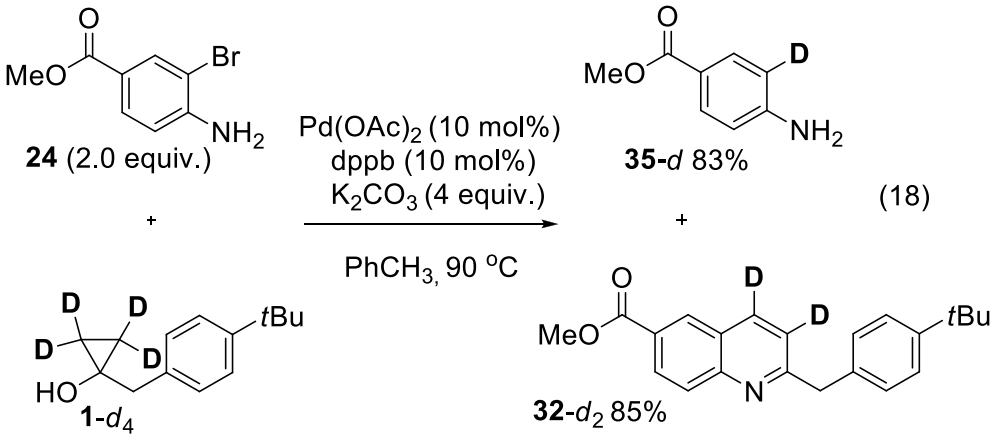

Based on this mechanistic evidence, a proposed mechanism of the oxidation would commence with the oxidative insertion of the Pd(0) catalyst to the *ortho*-bromoaniline generating

a Pd(II) intermediate, followed by its coordination to the enamine tautomer of the 1,4-dihydroquinoline forming complex (**IV** in Scheme 18). This complex would then undergo β-deuteride elimination and generate the quinoline product (**V**) and the palladium aryl deuteride intermediate (**VI**), which upon reductive elimination would generate the aniline (**VII**) and regenerate Pd(0) catalyst.

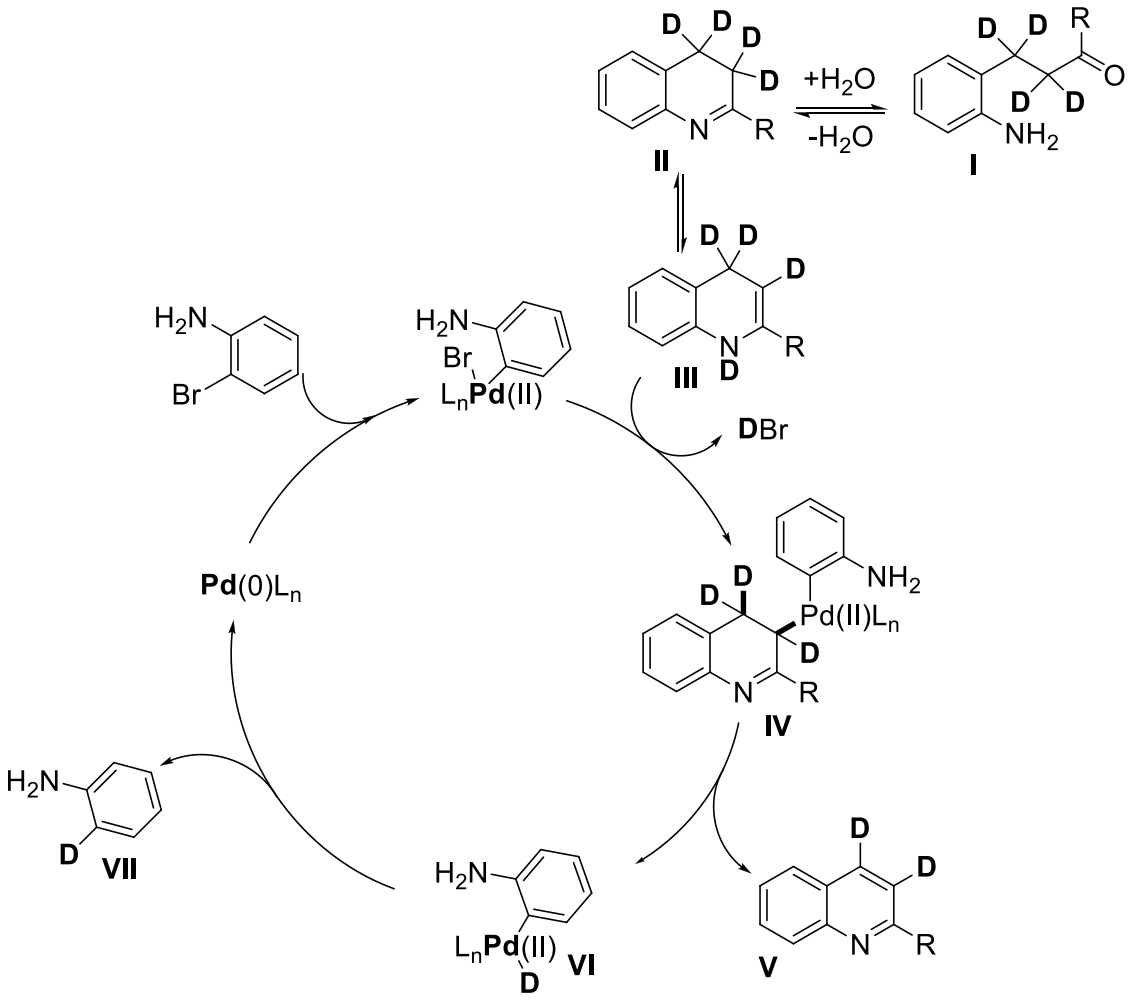

Scheme 18. Proposed catalytic cycle for the oxidation of 1,4-dihydroquinoline by stoichiometric *ortho*-bromoaniline and catalytic palladium.

2.6 Conclusion

In conclusion, we have developed a methodology for the synthesis of substituted quinoline derivatives using palladium-catalyzed cross-coupling between cyclopropanol-derived palladium-homoenolates and *ortho*-bromoanilines as the key step. The reaction conditions use a simple catalyst system and provides quinoline derivative products in good yields. Also, the optimized reaction conditions are compatible with a range of functionality and tolerate various substituted cyclopropanols. The second equivalent of bromoaniline serves as the terminal oxidant for the oxidation of 1,4-dihydroquinoline intermediate to the quinoline product.

Chapter 3: The Acid-Free Cyclopropanol-Minisci Reaction and the Catalytic Role of Silver-Pyridine Complexes

3.1 Introduction

Nitrogen-containing aromatic heterocycles are common in many biologically-active molecules and play a significant role in drug development.[79] Therefore, methods that allow for their expedient functionalization are continuously sought-after. The electrophilic aromatic substitution (S_EAr) is one of the common methods for functionalization of aromatic compounds. Generally, this reaction proceeds via an electrophilic addition of the cationic species to an aromatic ring followed by the loss of a proton to restore the aromaticity (Scheme 19). However, this approach fails with pyridines, owing to their intrinsic electron-deficient ring and the Lewis basicity of the nitrogen, which interferes with the Lewis acidic reagents and/or catalysts and makes the pyridine ring even more electron deficient.

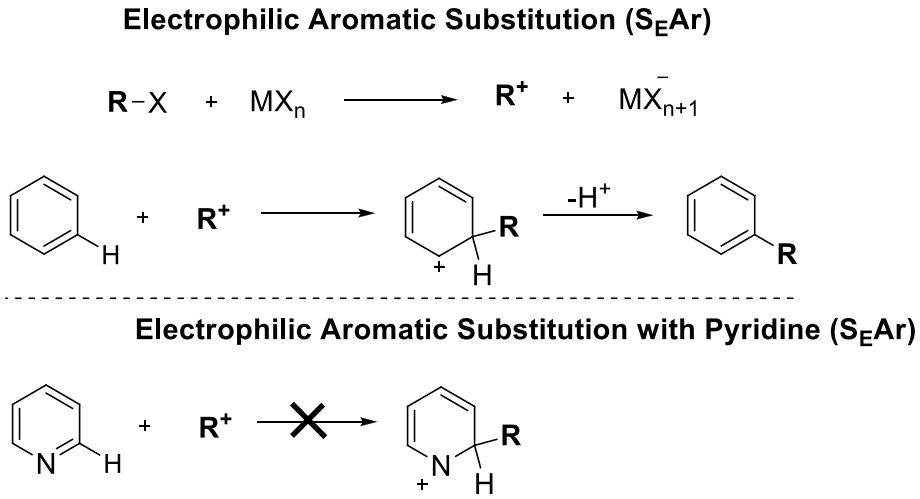

Scheme 19. Electrophilic aromatic substitution comparison between benzene and pyridine rings.

A common approach for pyridine functionalization involves its conversion to pyridine-*N*-oxide which renders the aza-aromatic ring electron-rich and facilitates the electrophilic substitution (Fig. 6). The disadvantage of this approach is the need for an oxidation and a reduction steps.

Other common methods for pyridine functionalization include nucleophilic aromatic substitution (S_NAr) and transition metal-catalyzed cross-coupling reactions (Fig. 7).[80] However, these methods require a pre-existing leaving group on the heterocyclic ring.

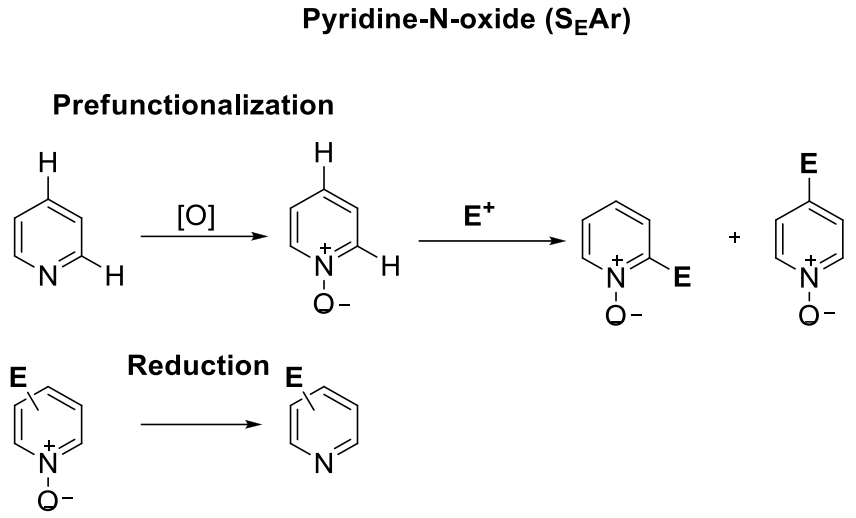

Figure 6. Conversion of pyridine to pyridine-N-oxide and functionalization via S_EAr.

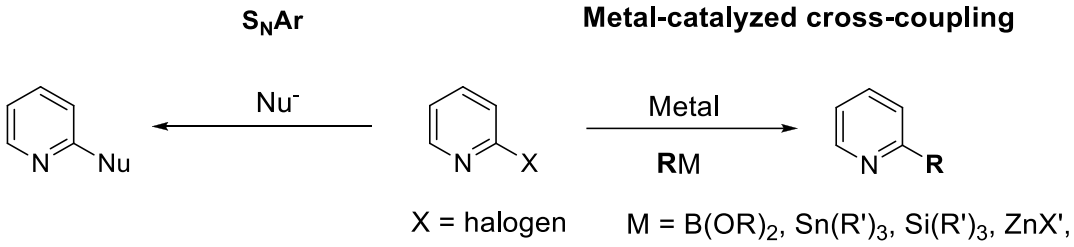

Figure 7. Cross-coupling and S_NAr as methods for functionalization of pyridines.

An alternative method of pyridine functionalization involves radical addition and subsequent oxidation of the resulting radical intermediate as the means for converting a C-H to a C-C bond. The major advantage of this method is that it avoids the need for prefunctionalization of the pyridine ring. The Minisci reaction is a classic method of a direct functionalization of pyridines. Specifically, the carboxylic acid function serves as the radical precursor in the presence of a silver catalyst, persulfate terminal oxidant and sulfuric acid (Scheme 20).[81,82] Oxidation of the carboxylate function by the silver catalyst generates a carboxyl radical that subsequently

fragments to CO_2 and a nucleophilic radical. Addition of the nucleophilic radical to the protonated pyridine ring and oxidation of the resulting dearomatized radical-cation intermediate yields the substituted pyridine product(s). However, the requirement of superstoichiometric amount of strong acid and high catalyst loading are the major disadvantages of this method.

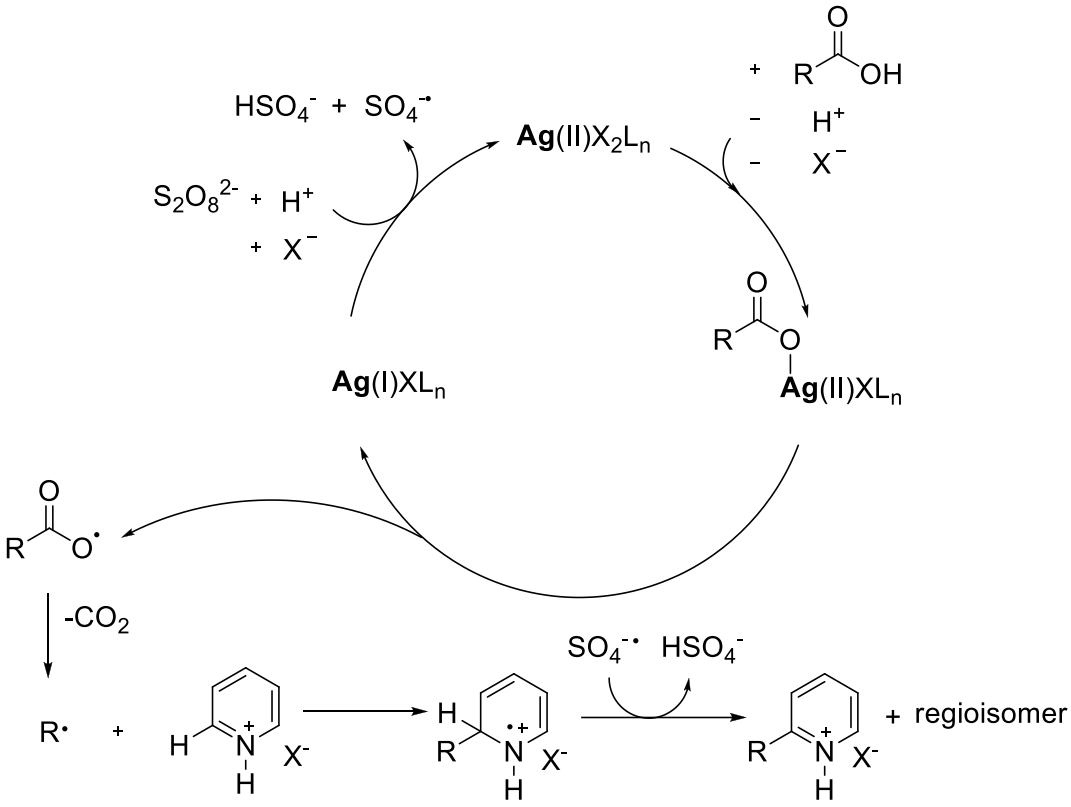

Scheme 20. Functionalization of pyridine using silver-catalyzed Minisci reaction.

In 2010, Baran *et al.* exploited this fundamental reactivity using boronic acid as the aryl radical precursor (Eq. 19).[83] This method benefits from mild reaction conditions and compatibility with a range of electron-deficient heterocycles. However, this approach requires a second catalyst loading for reactions over 3 hours due to catalyst decomposition. The Minisci-type reactivity however, is not limited to boronic acids. The functionalization of aromatic heterocycles via addition of the nucleophilic carbon radicals derived from alkylsulfinates,[84,85,86] alkenes,[87] amino acids,[88] alcohols,[89] trifluoroborate salts[90] and alkyl bromides[91] were also reported (Fig. 8).[83,92,93,94,95,96,97,98]

The major limitation in many of these methods however, is the loss of the functional group content during the free radical generation.

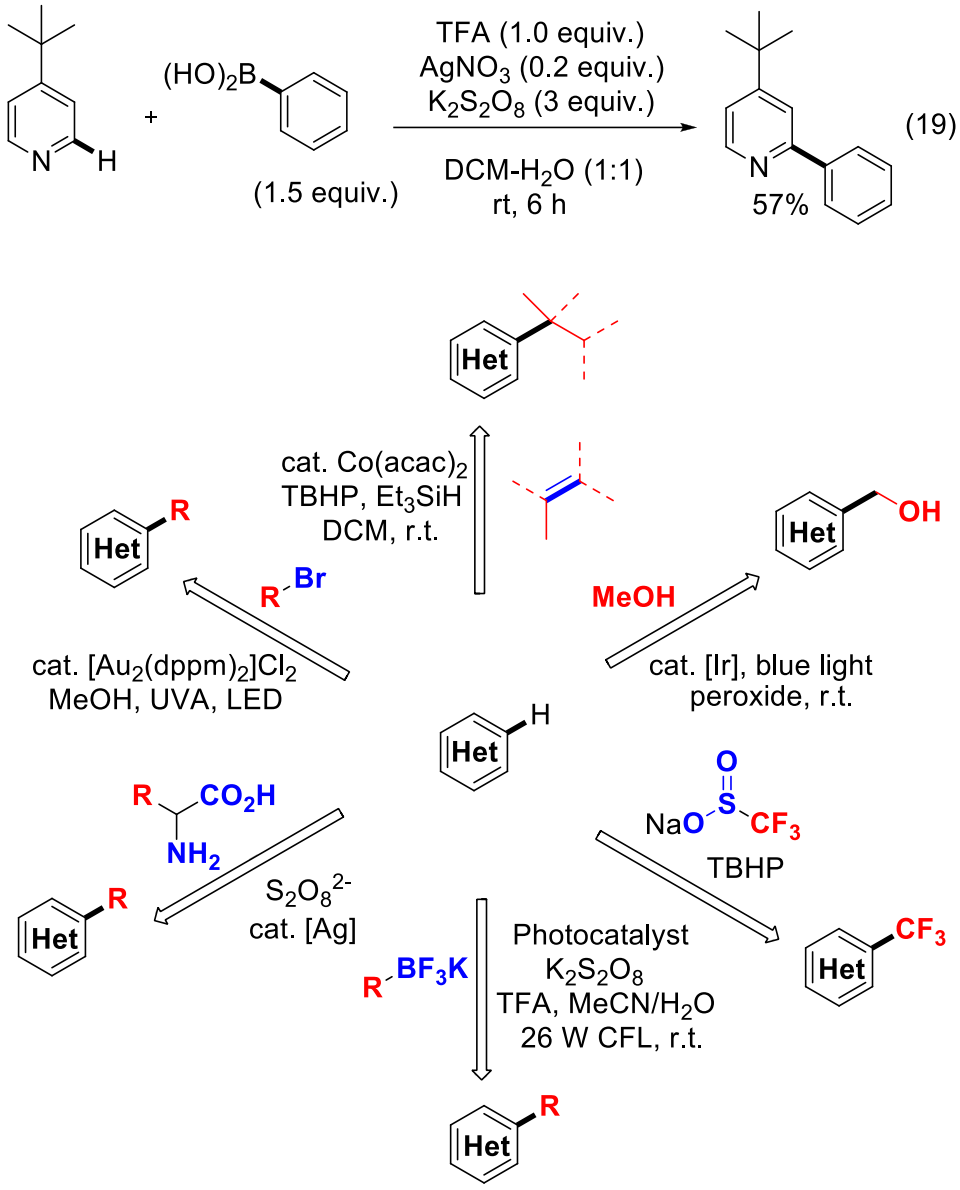

Figure 8. Examples of Minisci-type reactivity for direct functionalization of aromatic heterocycles.

We became interested in extending the free radical approach to heterocycle functionalization by merging the transition metal-catalyzed ring-opening of cyclopropanols to β-keto radicals[55,56,57,54] with the Minisci-type radical addition to electrophilic heterocycles. A unique feature of this approach is that it installs a ketone function that may be used for further reactions.

Exploiting this reactivity platform, Lectka developed a method using MnO_2 reagent towards functionalization of heteroaromatics (Eq. 20).[99] In this transformation, it is proposed that the cyclopropanol undergoes single-electron oxidation by MnO_2, followed by the formation of the nucleophilic β-keto radical, which adds to the protonated azaheterocycle. The substitution product is formed after the oxidation/aromatization step. However, this method requires superstoichiometric loadings of MnO_2, five equivalents of both trifluoroacetic acid (TFA) and the azaheterocycle which makes it non-ideal. A similar method based on silver-catalyzed reaction was reported by Li (Eq. 21).[100] However, this method requires high catalyst loading and is limited to benzo-fused heterocycles.

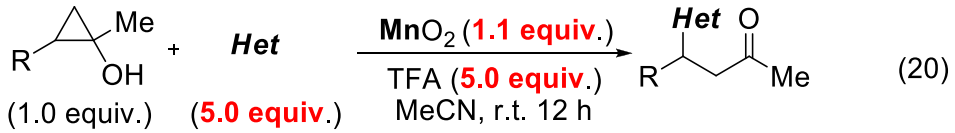

(20)

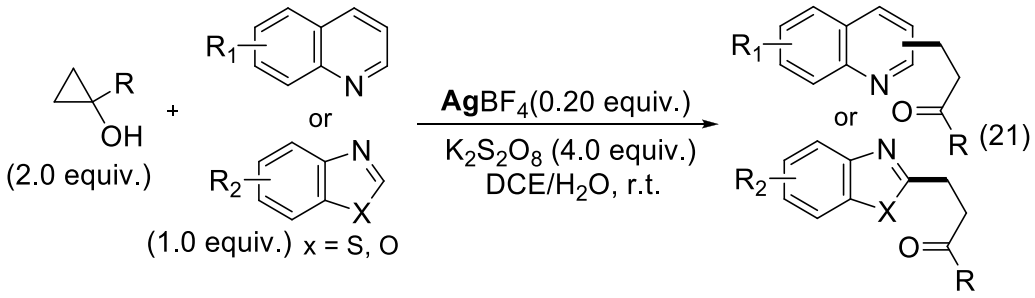

(21)

The mechanistic studies conducted by Bonchev and Aleksiev with persulfate terminal oxidant and catalytic amounts of silver(I) precatalyst have shown that Ag(I)/Ag(II) redox-couple operates during the single-electron oxidation of sulphanilic acid.[101,102] Anderson and Kochi observed the same redox-couple during the oxidative-decarboxylation of carboxylic acids in the presence of catalytic Ag(I) and stoichiometric persulfate.[103] Hence, we envisioned catalytic cycle involving a Ag(I)/Ag(II) redox couple during the cyclopropanol-Minisci reaction (Scheme 21). The cycle begins with the persulfate-oxidation of silver(I) (**VII** in Scheme 21) to the high-valent silver(II) complex (**I** in Scheme 21) followed by the coordination-deprotonation of the cyclopropanol to form

cyclopropoxide-silver(II) complex (**II** in Scheme 21). Subsequent fragmentation of **II** via the homolytic silver-oxygen bond cleavage generates the cyclopropoxy radical (**III** in Scheme 21) and regenerates the active silver(I) catalyst **VII**. In the off-cycle, **III** opens to the nucleophilic β-keto radical **IV**, which adds to the pyridine ring forming the dearomatized radical intermediate **V**. A concomitant oxidation-aromatization furnishes the final substituted pyridine product **VI**. We believe that this transformation will provide a direct approach to functionalization of electron-deficient aromatic heterocycles.

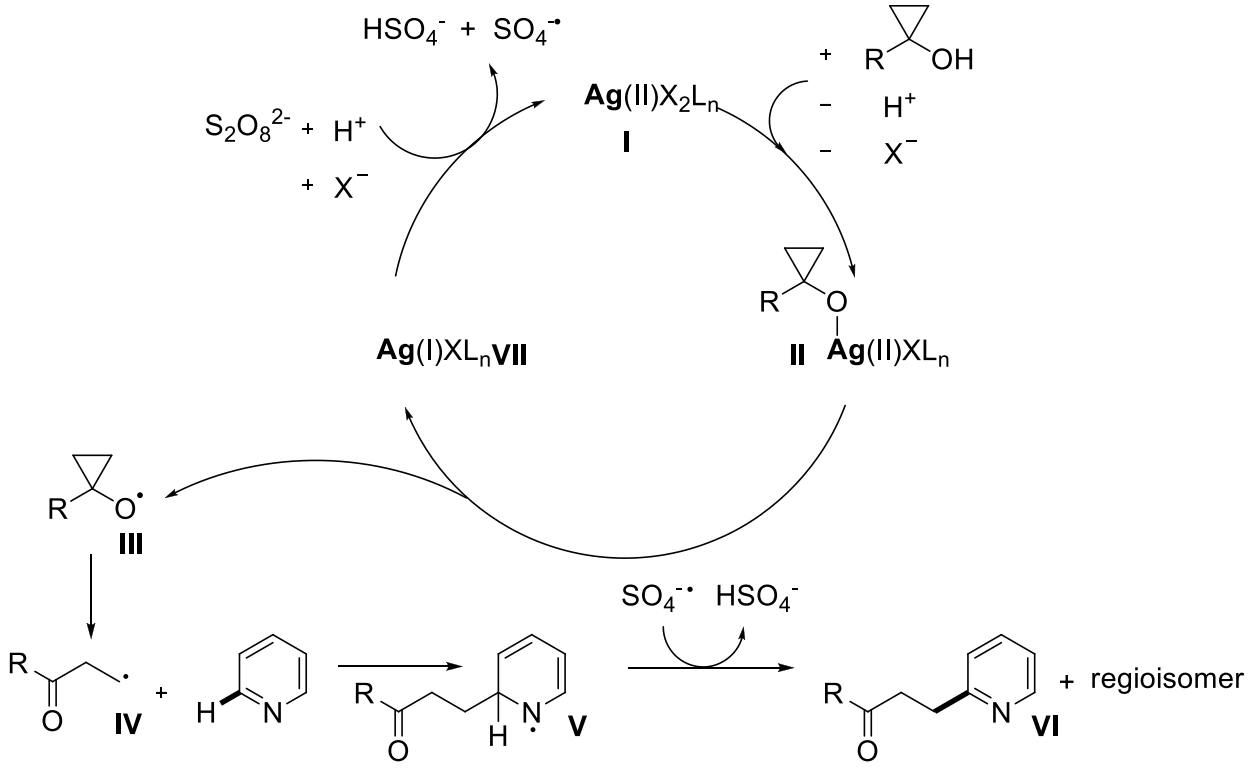

Scheme 21. Proposed catalytic cycle for the functionalization of pyridine using silver-catalyzed cyclopropanol-Minisci reaction.

Results and Discussion:

3.2 Preparation of Model Substrate **36**

To test the feasibility of the proposed pyridine functionalization reaction we decided to synthesize cyclopropanol **36**. The proton NMR resonance signals for cyclopropanol **36** were consistent with the previously reported structure bearing the diagnostic cyclopropanol proton resonance signals at 0.72 and 0.43 ppm.[104] This and related substrates can be readily synthesized using Kulinkovich method using esters in the presence of a titanium(IV) catalyst and a Grignard reagent (Eq. 22).[75] Also, the ^{1}H-NMR spectroscopic analysis of the desired product would be simplified due to lack of aromatic protons and symmetry of **36**. Hence, methyl hexanoate was used as the precursor for our model substrate.

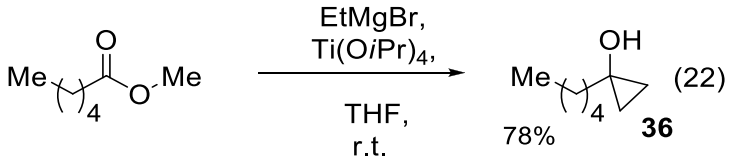

3.3 Proof of Concept

With cyclopropanol **36** in hand, we set out to test the feasibility of the cyclopropanol-Minisci reaction. Considering that Minisci reactions generally proceed well with pyridines bearing an electron-withdrawing group, we decided to test this transformation using methyl isonicotinate. Also, the symmetry of this substrate can only give one product and will simplify the interpretation of ^{1}H-NMR spectroscopy data. Gratifyingly, reaction conditions employing silver nitrate as the catalyst, ammonium persulfate as the oxidant and acetonitrile as the solvent provided the desired functionalized pyridine **37** in 28% isolated yield along with the ring-opened product (**38** in Eq. 23). Analysis of the ^{1}H-NMR spectrum of pyridine **37** revealed a set of diagnostic proton resonance signals that are consistent with the expected structure. Specifically, a doublet at 8.65 ppm with 4.8 Hz coupling constant, a singlet at 7.76 ppm and a doublet at 7.66 ppm with 4.8 Hz coupling constant corresponding to protons labelled (III), (I) and (II) respectively.

(23)

3.4 Optimization Study

Encouraged by this initial result, we proceeded towards the optimization of the reaction conditions for this transformation. We hypothesized that by increasing the equivalents of methyl isonicotinate, the yield of **37** may be improved. Indeed, conducting this reaction with 3 equivalents of methyl isonicotinate afforded pyridine **37** in 40% isolated yield (Table 4, entry 3). Further

increase in the number of equivalents did not improve the yield significantly (Table 4, entries 4 and 5).

Table 4. Optimization Study – Equivalents of Methyl Isonicotinate Screen[a]

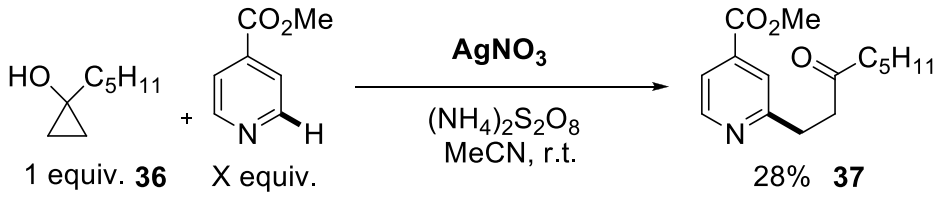

1 equiv. **36** X equiv. 28% **37**

Entry	X equiv.	37[b]
1	1.0	28%
2	2.0	34%
3	3.0	40%
4	4.0	41%
5	5.0	42%

[a] All reactions were carried out with 0.49 mmol of substrate at 0.30 M concentration in acetonitrile, 10 mol % of $AgNO_3$ and 1.1 equiv. of $(NH_4)_2S_2O_8$. [b] Isolated yields of pure product after column chromatography on silica.

Next, a screen of $(NH_4)_2S_2O_8$ equivalents was undertaken. It was found that using 3 equivalents of the stoichiometric oxidant was optimal for this transformation (Table 5, entry 3).

Table 5. Optimization Study - Equivalents of $(NH_4)_2S_2O_8$ Screen[a]

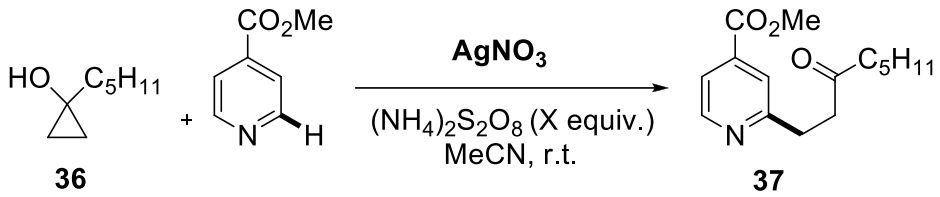

36 **37**

Entry	X equiv.	37[b]	Entry	X equiv.	37[b]
1	1.0	40%	3	3.0	47%
2	2.0	44%	4	4.0	48%

[a] All reactions were carried out with 0.49 mmol of substrate at 0.30 M concentration in acetonitrile, 10 mol % of $AgNO_3$ and 3.0 equiv. of methyl isonicotinate. [b] Isolated yields of pure product after column chromatography on silica

With these semi-optimized reaction conditions in hand, we wanted to establish the generality of this method. Specifically, we were interested to see if this transformation was compatible with other aza-heteroaromatic substrates such as benzo fused pyridines and pyridines bearing alkyl groups. During the course of this study, we were surprised to find that the steric environment around the heterocyclic nitrogen played a critical role in the reactivity towards the substitution (Fig. 9). Specifically, reaction with 3,5-dimethylpyridine furnished the expected mixture of substituted products, while the electronically similar but sterically different 2,6-dimethylpyridine did not. Reaction with the isoquinoline substrate yielded the alkylated product, whereas the quinoline isomer did not. In view of these observations we hypothesized that the aza-heteroaromatic substrates may function as ligands in a silver complex and generate the active catalyst. Hence, if the nitrogen of the heteroaromatic substrate is sterically shielded, the catalytically active complex cannot form, and the reaction does not occur. It is also likely that silver functions as the Lewis acid for the heterocycle and activated it towards the radical addition, hence if the nitrogen of the heteroaromatic substrate is sterically shielded such activation is not possible and reaction does not occur.

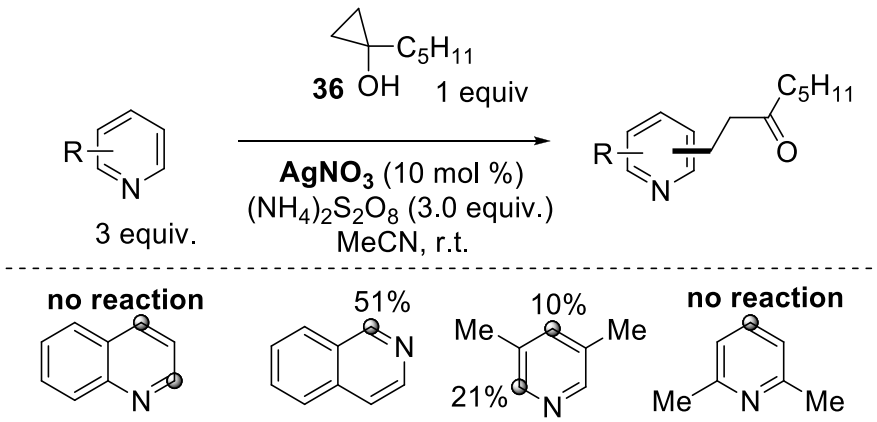

Figure 9. Electronically similar azaheterocycles reveal an apparent steric-effect during cyclopropanol-Minisci reaction with $AgNO_3$ precatalyst.

Intrigued by these results, we set out to conduct series of control experiments to test our hypothesis regarding silver-pyridine complexes as active catalysts in the cyclopropanol-Minisci

reaction (Scheme 22). If our hypothesis is correct, then subjecting a reluctant aza-heteroaromatic substrate to the pre-optimized reaction conditions (Eq. 2 in Scheme 22) should not yield any substituted product.[105] Indeed, when benzimidazole was used as the heterocyclic substrate the reaction failed. We thought that if methyl isonicotinate and $AgNO_3$ combination forms the active catalyst (Eq. 1 in Scheme 22), then the same complex might catalyze alkylation of benzimidazole. We were pleased to find that, mixing methyl isonicotinate, $AgNO_3$ and the oxidant in acetonitrile before the addition of benzimidazole furnished the expected benzimidazole-alkylated product in 37% isolated yield (Eq. 3 in Scheme 22).

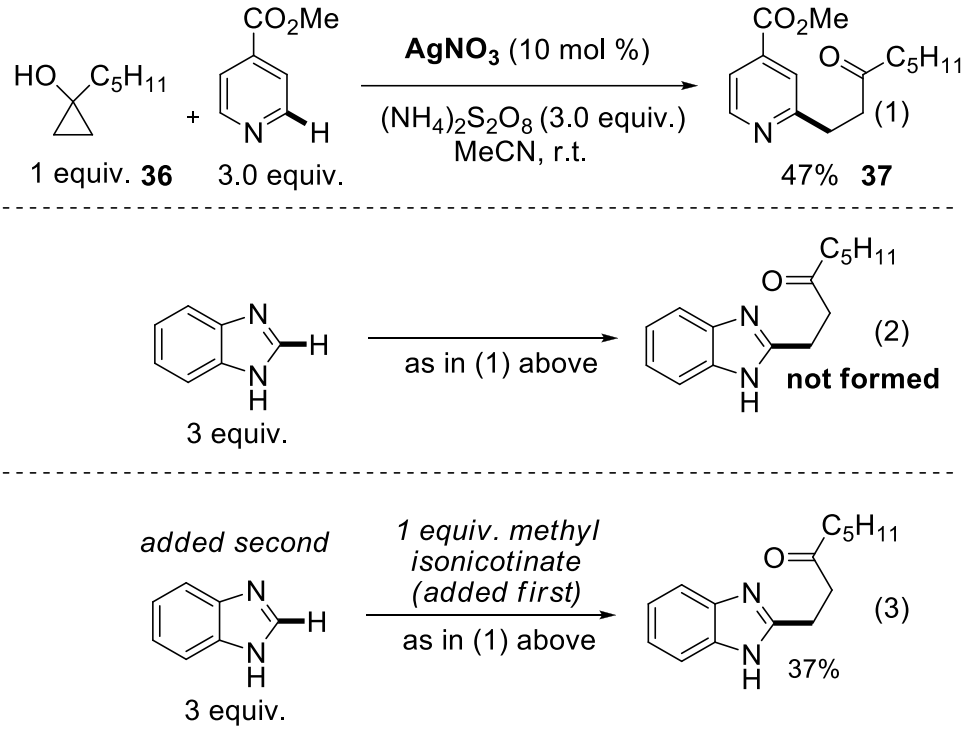

Scheme 22. Control Experiments Reveal Silver-Pyridine Complexes as Catalysts in the Cyclopropanol-Minisci Reaction.

Based on these results, we thought that using preformed silver-pyridine complex may serve as a precatalyst and promote reactions that would otherwise fail with catalytic $AgNO_3$. In 1981, Pehl and coworkers demonstrated that isolable bis(2,2'-bipyridine)silver(I) and bis(2,2'-bipyridine)silver(II) complexes readily underwent a reversible Ag(I)/Ag(II) redox-couple without

decomposition.[106] More recently, bis(2,2'-bipyridine)silver(II) persulfate complex was shown to be redox active in oxidation.[107,108] This bench-stable silver(II) complex is readily prepared from silver nitrate, 2,2'-bipyridine and potassium persulfate in water as the solvent. We were pleased to find that using $[Ag(II)(bipy)_2]S_2O_8$ as the catalyst, the benzimidazole-coupled product was formed in 42% isolated yield (Eq. 24). Therefore, we chose this catalyst for further optimization study due to its bidentate homoleptic ligands that enhance the catalyst stability by disfavoring catalyst decomposition via ligand substitution and its ability to support a reversible redox-couple.

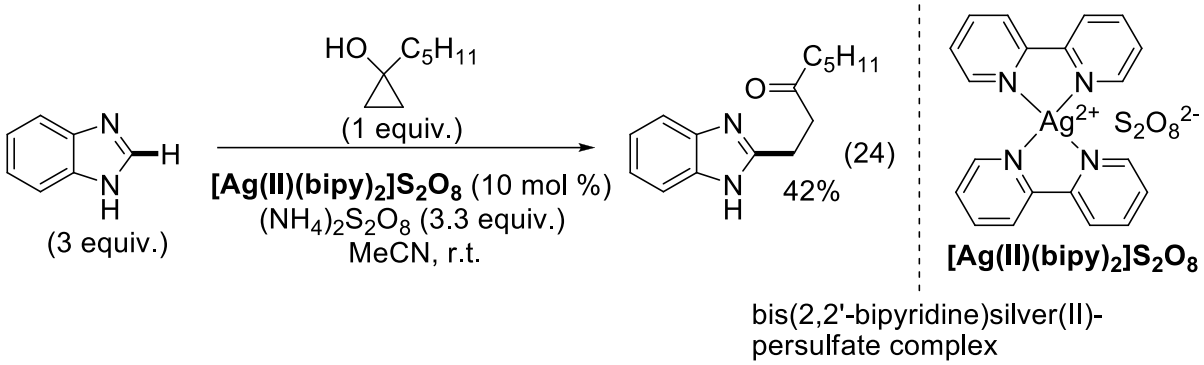

A screen of solvents revealed that THF, ether and CH_2Cl_2 were not effective for this methodology (Table 6, entries 3, 4 and 5). A similar result was observed when MeOH and nonpolar solvents were surveyed (entries 1, 2, 6 and 10). When DMSO was employed, a significant amount of dimethyl sulfone was isolated along with 43% of **37**. Gratifyingly, reactions utilizing DMA or DMF furnished the pyridine **37** product in 66% and 65% isolated yields respectively (entries 11 and 12). We decided to use DMF to continue the optimization due to its greater solubility in water which simplified the workup.

Table 6. Optimization Study – Solvent Screen.[a]

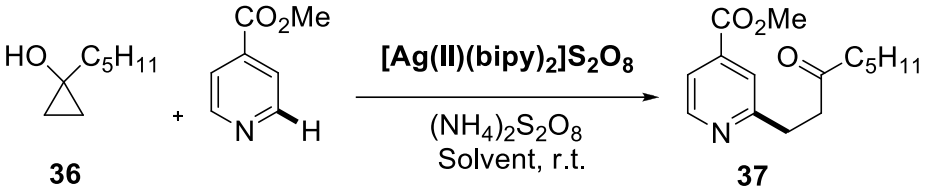

36 **37**

Entry	Solvent	37[b]	Entry	Solvent	37[b]
1	PhH	0%	7	$MeCN/H_2O$	0%
2	PhMe	0%	8	MeCN	55%
3	THF	0%	9	MeCN/DMSO	37%
4	Et_2O	0%	10	DMSO	43%
5	CH_2Cl_2	0%	11	DMA	66%
6	MeOH	0%	12	DMF	65%

[a] All reactions were carried out with 0.49 mmol of substrate at 0.30 M concentration, 10 mol % of $[Ag(II)(bipy)_2]S_2O_8$ and 3.0 equiv. of methyl isonicotinate and 3.0 equiv. $(NH_4)_2S_2O_8$. [b] Isolated yields of pure product after column chromatography on silica.

During the course of our optimization, we noticed that a significant amount of heat was evolved upon the addition of $(NH_4)_2S_2O_8$ to the solution of the cyclopropanol and the catalyst when DMF was used as solvent. In effort to control the temperature of this reaction, the stoichiometric oxidant was added portionwise to a solution at 0 ^oC and allowed to warm up to ambient temperature. Gratifyingly, the isolated yield of **37** increased to 69% (Table 7, entry 1). The highest yield was achieved with 0.9 M methyl isonicotinate solution in argon-purged DMF (entry 4). Decreasing the catalyst loading from 10 mol % to 5 mol % did not have a significant effect on the yield (entry 5). A reaction conducted with 1 mol % catalyst loading furnished **37** in 53% isolated yield (entry 6). It is important to note that such low catalyst loading is uncommon for Minisci-type reactions with silver.

Table 7. Optimization Study – Fine-Tuning the Reaction Conditions

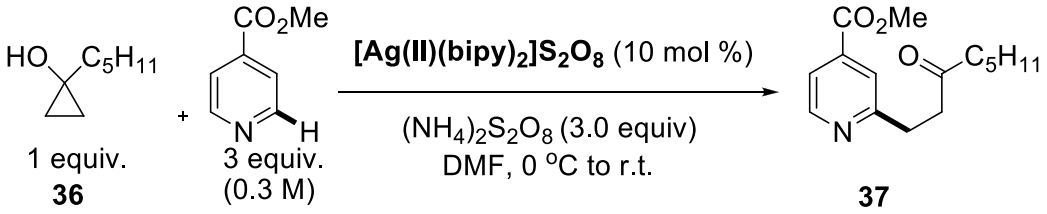

Entry	change from above	37
1	oxidant added portionwise	69%
2	oxidant added portionwise, 0.6 M in Py	73%
3	oxidant added portionwise, 0.9 M in Py	75%
4	**oxidant added portionwise, 0.9 M in Py, Ar purge**	78%
5	5% catalyst, oxidant added portionwise, 0.9 M in Py, Ar purge	77%
6	1% catalyst, oxidant added portionwise, 0.9 M in Py, Ar purge	53%
7	0.9 M in Py, Ar purge, alcohol added dropwise	67%
8	1 equiv. oxidant added portionwise, 0.9 M in Py, Ar purge	60%
9	oxidant solution added dropwise, 0.9 M in Py, Ar purge	63%
10	oxidant + alcohol solution added dropwise, 0.9 M in Py, Ar purge	61%
11	Entry 5 but 1:1 ratio of pyridine and alcohol	30%
12	3 equiv. of pyridinium trifluoroacetate salt	57%

3.5 Electron Affinity (EA)

The electron affinity of an atom or a molecule can be formally defined as the amount of energy required to remove an electron from the negative ion, or the amount of energy gained due to the addition of an extra electron to a neutral atom or molecule in the gas phase.[109] Calculated molecular electron affinity represents the difference between the total energies of the neutral and the negatively charged molecules at their corresponding equilibrium nuclear positions and

generally correlates well with the experimentally-determined values.[93] The theoretically-determined molecular electron affinity typically correlate linearly with the energy of the LUMO of the molecule. This is logical, considering that the extra electron populates the lowest empty orbital of the molecule. Therefore, during free radical addition, molecules with higher electron affinity (low LUMO energy) should react with a relatively higher rate. It is therefore reasonable to use the calculated EA of the heterocylic molecules as a measure of their susceptibility to the free radical addition. Also, the calculated EA of the heterocycles should have a positive correlation with the yields of the coupled products, since the free radical addition to the heterocycle is generally the rate-determining step. Claude Legault therefore calculated the EA of the heterocyles studied with the hope of gaining insight into the reaction.[110]

3.6 Substrate Scope Study

With reliable reaction conditions for the cyclopropanol-Minisci reaction in hand, we explored the scope of this transformation with cyclopropanol (**36**) and various pyridine-heterocycles using $[Ag(II)(bipy)_2]S_2O_8$ and $AgNO_3$ catalysts (Table 8). As expected, pyridines bearing an electron-withdrawing group (**37**-**40**) furnished the alkylated products in overall good yields (57-78%) although, yields were generally lower (45-65%) with $AgNO_3$. Pyridine (**43**) and monoalkylated pyridine substrates (**44**-**46**) yielded the expected mixture of products in good combined yields (48-66%). It is worth noting that the isolated yields generally increased with an increase in EA values unless the nitrogen was sterically hindered. For example, 2-phenylpyridine (**47**) (EA = -0.01 eV) yielded the expected mixture of substituted products in lower combined yields (15-29%) as compared to the pyridine (**43**) (15-44%) (EA = -0.91). As expected, owing to steric shielding around the pyridine nitrogen, 2,6-dimethylpyridine (**49**) did not provide the desired product with $AgNO_3$. Surprisingly, this heterocycle also failed to yield the desired product with $[Ag(II)(bipy)_2]S_2O_8$ as catalyst. These results suggest that Lewis-acid activation via silver-heterocycle coordination is also important and such activation of the pyridine (**49**) is hindered due

to sterics. In comparison, 3,5-dimethylpyridine (**48**) gave the desired substituted products at the 2- and 4-positions with either catalyst. 4-Bromopyridine (**50**) and 4-dimethylaminopyridine (**51**) did not provide the coupled product with either catalyst. We hypothesized that in the case of 4-bromopyridine, release of free-bromide causes catalyst decomposition via silver-bromide adduct formation. 4-Dimethylaminopyridine, due to its strongly coordinating property, likely forms catalytically inactive electron-rich silver-pyridine complex. To our delight, we did manage to functionalize 3- and 4-methoxypyridines (**52** and **53**) albeit in low yields. It is worth noting that pyridines bearing an electron donating group in the four position are generally unreactive under Minisci-type conditions.[111,112] Impressively, pyridine substrates with acid-sensitive functional groups such as a TIPS-protected alcohol (**61**), a Boc-protected amine (**62**), and a dimethyl acetal (**63**) were well tolerated and gave the desired functionalized products in 35-38% yield range. Such protecting groups would not be compatible with standard Minisci reaction conditions due to strong acid.[113]

Next, we explored the scope of this transformation with cyclopropanol (**36**) and various non-pyridine heterocycles bearing imine-type nitrogens using $[Ag(II)(bipy)_2]S_2O_8$ and $AgNO_3$ catalysts (Table 8). Isoquinoline (**41**) gave the expected substituted product at the position one in good yield with either catalyst; but, quinoline (**42**) furnished the alkylated products only with $[Ag(II)(bipy)_2]S_2O_8$. These results are surprising since both benzopyridine substrates have similar electron affinities and therefore, are expected to have similar reactivity towards a nucleophilic radical addition. The fact that quinoline does not form the alkylated products with $AgNO_3$ suggests that the steric environment about the nitrogen hinders the formation of the catalytically active silver-quinoline complex. Benzimidazole (**54**) and thiazole (**55**) gave the expected functionalized products only when $[Ag(II)(bipy)_2]S_2O_8$ was used as the catalyst, which suggests that silver-pyridine complexes are the catalytically-active species for cyclopropanol-Minisci reaction under these conditions. Pyrazine (**56**) furnished the alkylated product in good yields with $AgNO_3$ and

[Ag(II)(bipy)$_2$]S_2O_8, pyrimidine (**57**) yielded inseparable mixture of products. However, substituted pyrimidine (**58**) gave the expected product in 67% isolated yields with [Ag(II)(bipy)$_2$]S_2O_8 and 33% with $AgNO_3$. Pyridazine (**59**) was unreactive under the optimized conditions with either catalyst. To our surprise, acridine (**60**) also failed to yield the expected alkylated product despite having the highest calculated electron affinity of all the heterocycles examined. This observation further supports the notion of Lewis-acid activation of the heterocycle by silver catalyst. Hence, due to sterically shielded acridine nitrogen, no such activation can take place and reaction fails.

Table 8. Scope of Aromatic Heterocycles.[a, b]

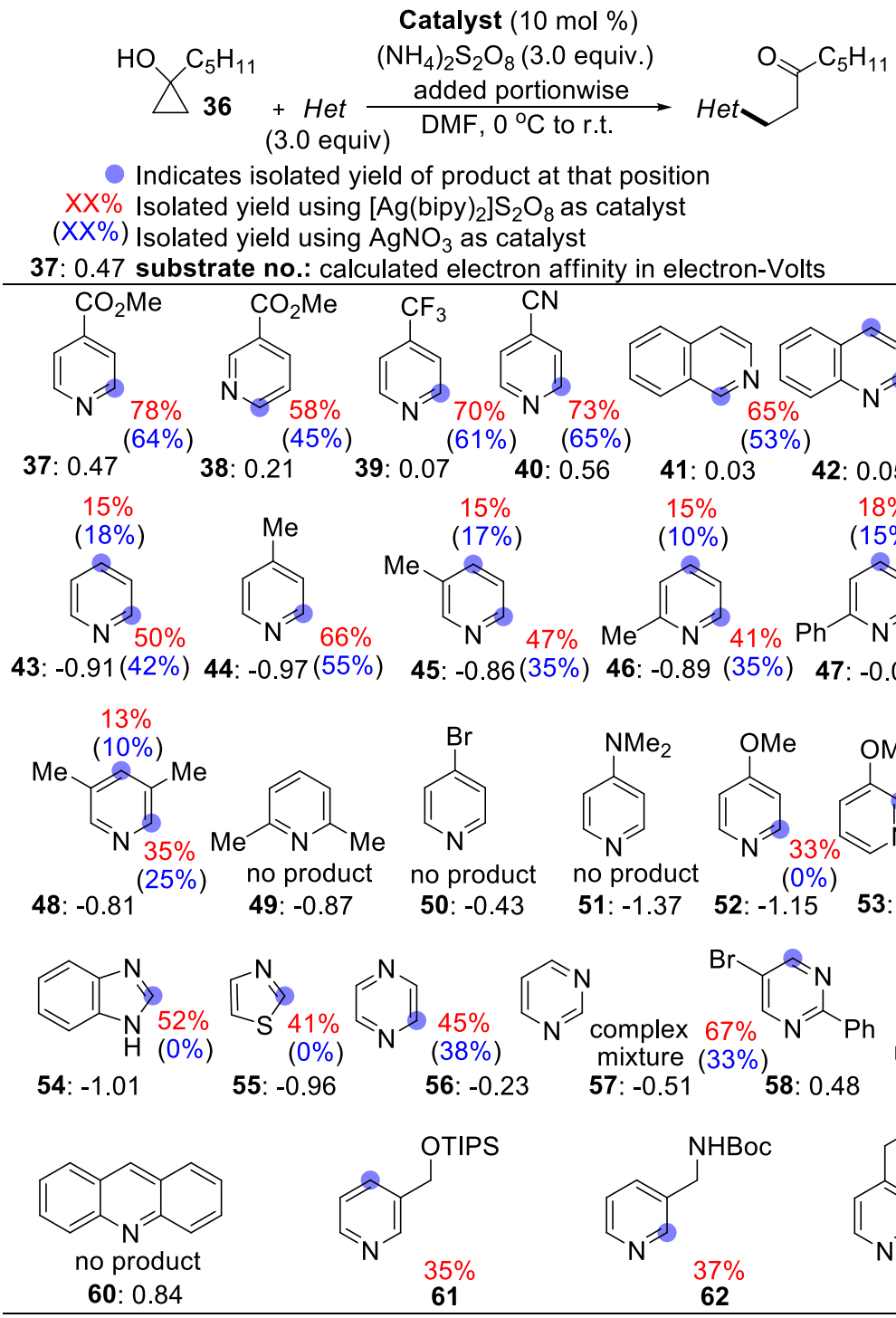

[a] All reactions were carried out with 0.49 mmol of substrate at 0.90 M concentration in pyridine using argon purged DMF. [b] Isolated yields of pure product after column chromatography on silica.

Considering that the functionalization of 4-methoxypyridine (**52**) is the first such example with Minisci-like reaction, we were interested to gain some insight into its reactivity under our optimized conditions. The fact that 4-methoxypyridine is not sterically hindered suggests that it can readily form a silver complex in solution. However, the fact that it is unreactive when $AgNO_3$ is used as the catalyst suggests that 4-methoxypyridine-silver complex is not redox active. It is reasonable to assume that 4-methoxypyridine ligands render silver catalyst relatively electron-rich and hinder its oxidative properties. In addition, it is also likely that such a complex is not Lewis-acidic enough to activate 4-methoxypyridine towards radical addition, owing to the relatively electron-rich silver-pyridine complex. Hence, we concluded that the nature of the pyridine ligand has a direct effect on the catalytic activity during the cyclopropanol-Minisci reaction. To corroborate this hypothesis, a series of reactions were carried out (Scheme 23).

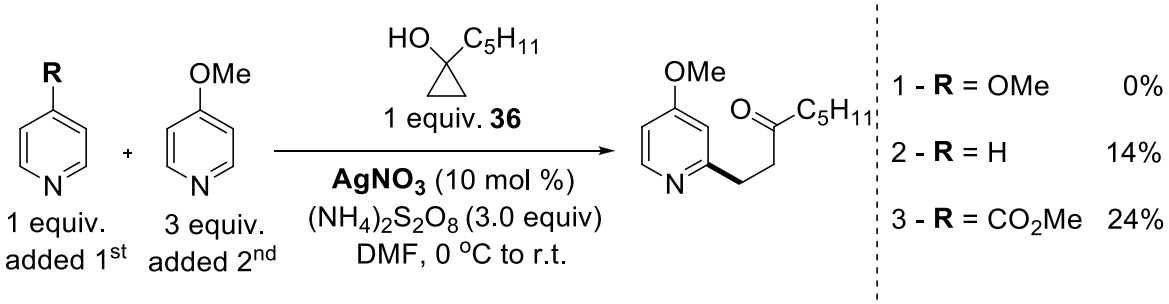

Scheme 23. Evidence for silver-pyridine complexes as Lewis-acid for activation of pyridines.

Functionalization of 4-methoxy pyridine does not occur with $AgNO_3$ as catalyst (entry 1). Adding one equivalent of pyridine and **36** to the optimized conditions followed by the addition of 4-methoxypyridine gave the functionalized 4-methoxypyridine product in 14% yield (entry 2). Strikingly, adding one equivalent of the more electron-deficient methyl isonicotinate and **36** to the optimized conditions followed by the addition of 4-methoxypyridine gave the functionalized 4-methoxypyridine product in an improved yield of 24% (entry 3). These experiments strongly suggest that the nature of the pyridine ligands is critical for the formation of the catalytic active

silver-pyridine complexes in cyclopropanol-Minisci reactions. These results also suggest that pyridine ligands may play a role in tuning the Lewis-acidity of the silver-pyridine complexes.

Next, the scope of this methodology was investigated with an array of cyclopropanol substrates (Table 8, entries **a-f**) and pyridine **37**.

Table 9. Scope of Cyclopropanol Substrates for the Cyclopropanol-Minisci Reaction.[a, b]

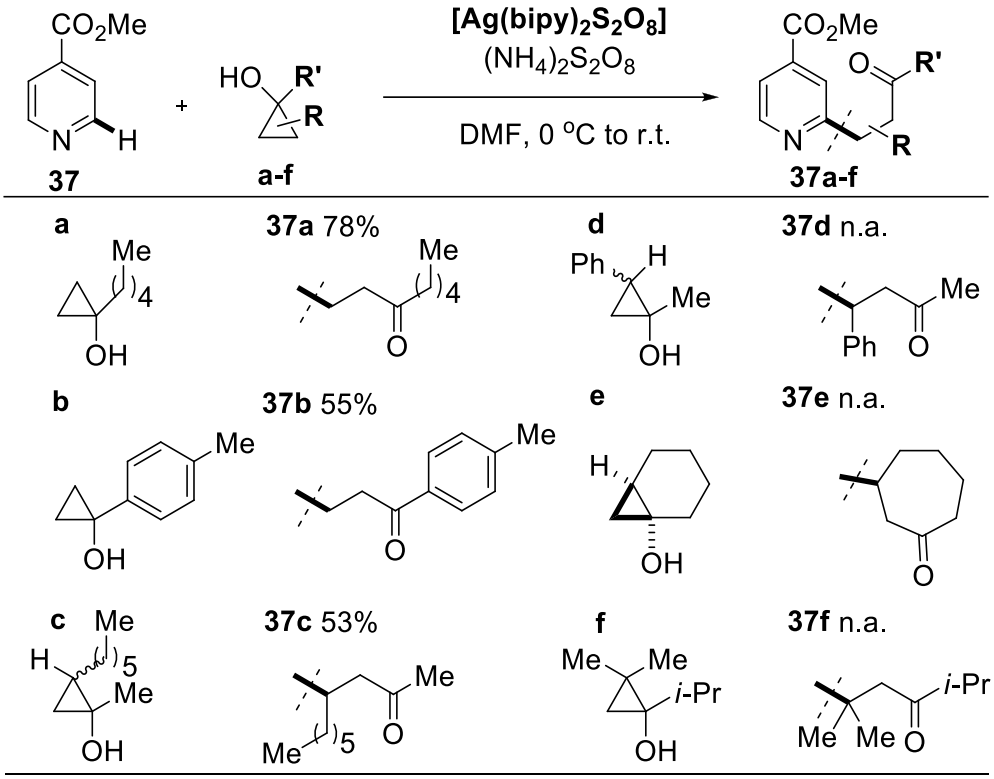

[a] All reactions were carried out with 0.49 mmol of substrate at 0.90 M concentration in argon purged DMF, 10 mol % of $[Ag(II)(bipy)_2]S_2O_8$ and 3.0 equiv. of methyl isonicotinate and 3.0 equiv. $(NH_4)_2S_2O_8$. [b] Isolated yields of pure product after column chromatography on silica.

This methodology is compatible with monosubstituted cyclopropanols bearing 1-alkyl (**a**) and 1-aryl (**b**) substituents, yielding the corresponding functionalized pyridine **37** product derived from primary alkyl radical addition in good isolated yields. Employing cyclopropanol bearing 1,2-dialkyl-substituents provided the expected product (**37c**) derived from addition of a secondary radical in 53% isolated yield. Cyclopropanols (**d-f**) did not furnish the expected products. Specifically,

substrate **d** was unstable under the optimized reaction conditions and substrates **e** and **f** yielded mostly ring-opened product.

3.7 Conclusion

In conclusion, we have developed an efficient cyclopropanol-Minisci reaction under acid-free conditions with a well-defined silver catalyst. The conditions developed accommodate functionalization of a broad range of nitrogen-containing aromatic-heterocycles. Furthermore, this methodology is compatible with aza-heterocycles containing acid-sensitive functional group. We also showed that our optimized conditions allow for reaction with silver catalyst loading as low as 1 mol %. More importantly, we gained significant evidence that silver-pyridine complexes are critical for homolytic cleavage of cyclopropanols and the Lewis-acid activation of pyridine towards alkyl-radical addition.

.

Chapter 4: Synthesis of α,β-Unsaturated Acylsilanes via Perrhenate-Catalyzed Meyer-Schuster Rearrangement of 3-Silylalkyn-1-ols

4.1 Introduction

Since the initial report of their synthesis in 1957,[114] acylsilanes have drawn great interest and significant effort has focused on exploring both their synthesis and synthetic utility in organic chemistry.[115] Specifically, acylsilanes are valuable organosilicon reagents that display *umpolung* reactivity via the Brook rearrangement, which involves a 1,2-shift of the silyl group from carbon to oxygen (Scheme 24).[16,114] This unique reactivity has been exploited in a number of synthetic transformations.[116,117,118,119,120,121] However, although acylsilanes are synthetically useful, their preparation is difficult and has limited their utility.[115]

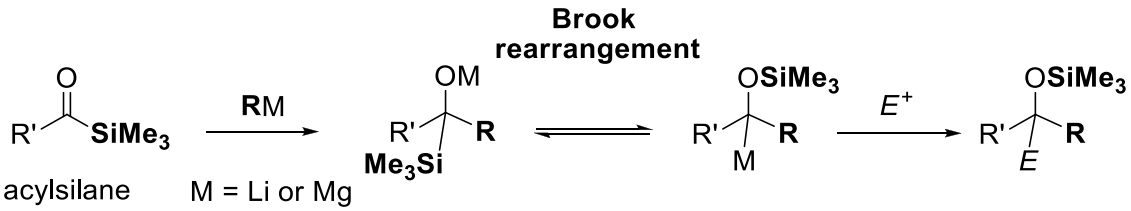

Scheme 24. Acylsilane *umpolung* reactivity via the Brook rearrangement.

α,β-Unsaturated acylsilanes stand out as particularly attractive synthetic targets. The combination of an acylsilane motif and a conjugated double bond offers a diverse range of potential reactivity patterns such as Diels-Alder reaction, Michael addition, Brook rearrangement, palladium-catalyzed cross-coupling and cascade processes (Fig. 10). Unfortunately, methods for preparation of α,β-unsaturated acylsilanes often involve many steps and elaborate procedures which render them non-ideal.[122,123,124,125]

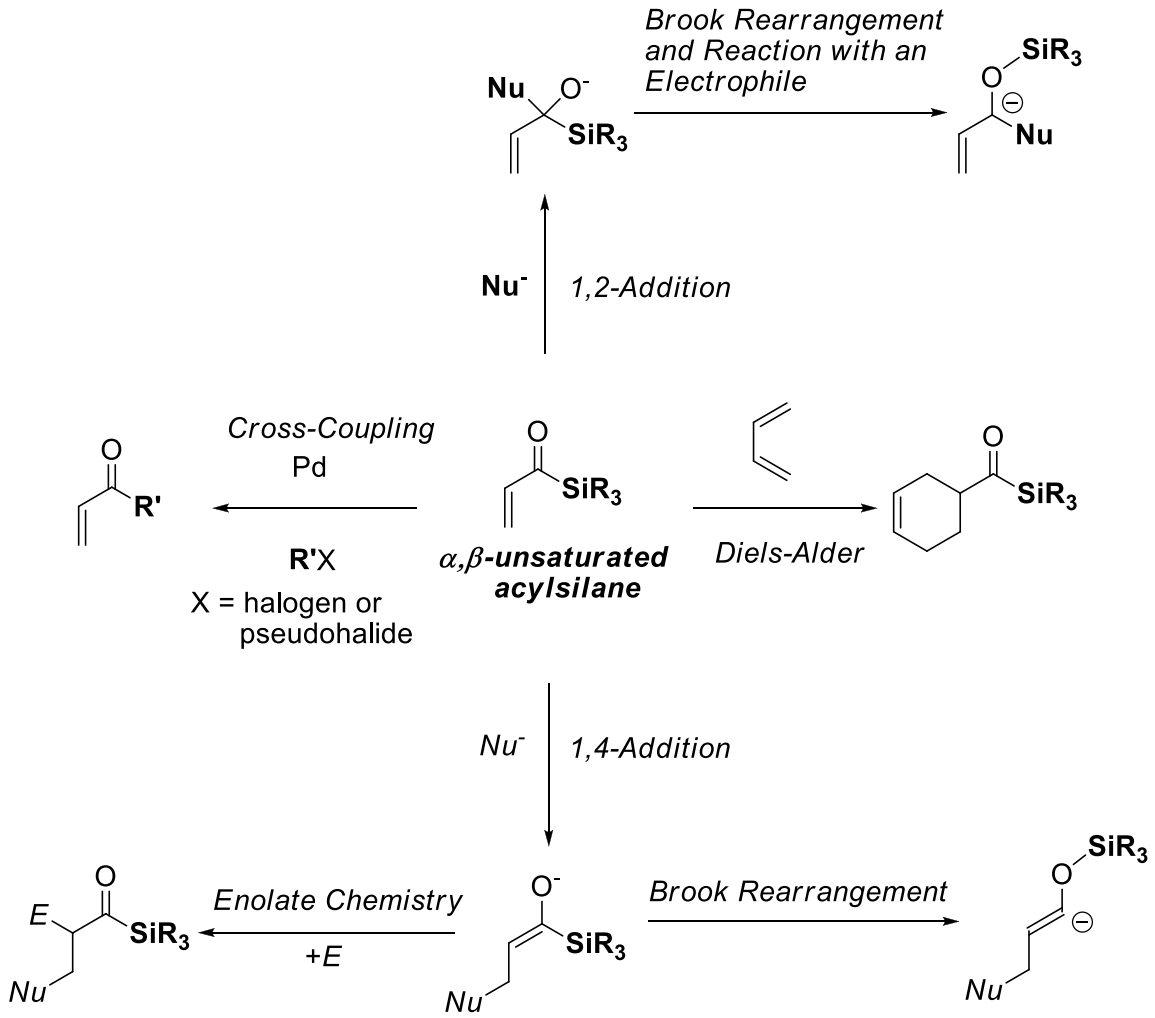

Figure 10. Potential reactivity patterns of α,β-Unsaturated acylsilanes in organic synthesis.

Since its discovery in 1922, the Meyer-Schuster rearrangement has proven to be a useful method for the preparation of α,β-unsaturated aldehydes and ketones from propargylic alcohols.[126,127,128,129] We envisioned that the α,β-unsaturated acylsilanes may be accessed via Meyer-Schuster rearrangement of readily prepared 3-silylalkyn-1-ols. In 1991, Hayashi introduced a mild and practical approach to Meyer-Schuster rearrangement that utilizes a simple catalyst system consisting of catalytic tetra-*n*-butylammonium perrhenate (nBu$_4$NReO$_4$) and toluenesulfonic acid in dichloromethane at room temperature (Scheme 25).[130,131] The proposed catalytic-cycle begins with the formation of a propargyl perrhenate ester (**III** in Scheme 25) from the condensation reaction between (**I**) and (**II**), followed by [1,3]-transposition of the oxygen via a

[3,3]-sigmatropic rearrangement forming the allenoate ester (**IV**). The rhenium(VII) catalyst (**I**) is regenerated and the α,β-unsaturated ketone (**V**) is formed after hydrolysis of (**IV**).

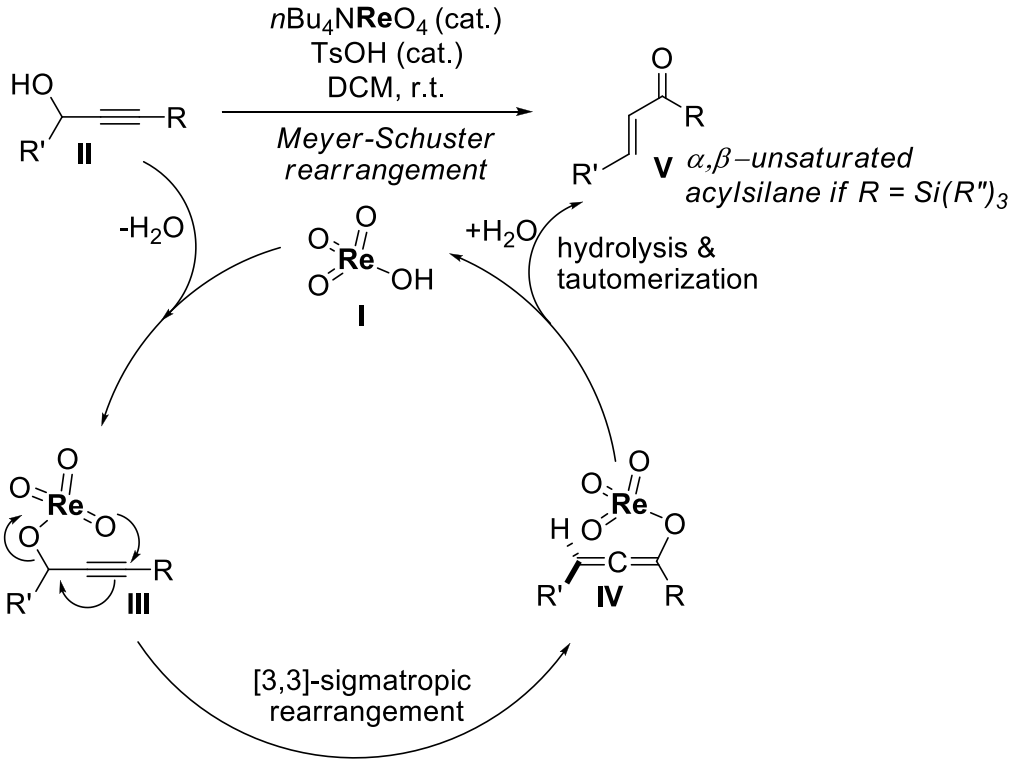

Scheme 25. Proposed catalytic cycle for the synthesis of α,β-unsaturated ketones via perrhenate catalyzed Meyer-Shuster rearrangement of propargyl alcohols.

We envisioned that the perrhenate-catalyzed Meyer-Schuster rearrangement of 3-silylalkyn-1-ols (R = Si(R")$_3$ in Scheme 25) should yield the corresponding α,β-unsaturated acylsilanes and provide a practical approach towards the synthesis of α,β-unsaturated acylsilanes under mild conditions. Therefore, given the immense potential of α,β-unsaturated acylsilanes in synthesis, we set out to explore their preparation via the perrhenate catalyzed Meyer-Schuster rearrangement with a range of 3-silylalkyn-1-ol substrates.

Results and Discussion:

4.2 Preparation of 3-Silylalkyn-1-ol Substrates

To explore the synthetic scope of the transformation described in Scheme 25, a convenient route towards the synthesis of 3-silylalkyn-1-ol substrates was required. We envisioned that synthesis of propargyl alcohols can be readily achieved by deprotonation of commercially available silyl acetylenes with *n*-butyllithium and addition of the corresponding lithium silylacetylide to a series of ketones and aldehydes. This method provided the desired propargyl alcohol **64a** in 77% isolated yield (Eq.25). The ^{1}H- and ^{13}C-NMR spectra were consistent with the previously reported structure.[132] The diagnostic proton attached to the carbinol carbon was observed as a singlet at 5.44 ppm. The related substrates for this study, were readily synthesized using this method.

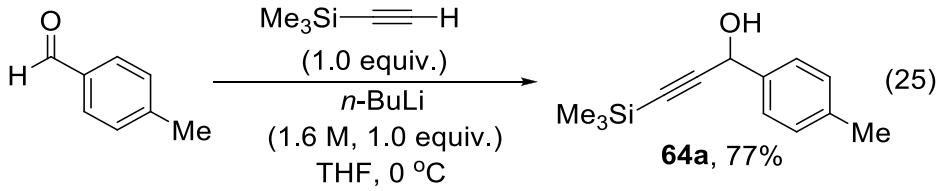

(25)

4.3 Proof of Concept

In the first and the only example, Hayashi showed that Meyer-Schuster rearrangement of 3-silylalkyn-1-ol yields the corresponding α,β-unsaturated acylsilane. Specifically, 1-phenyl-2-(trimethylsilyl)prop-2-yn-1-ol was converted to the corresponding acylsilane in 75% yield (Eq.26).[130,131] We were pleased to confirm the Hayashi conditions and to use them for the substrate scope study.

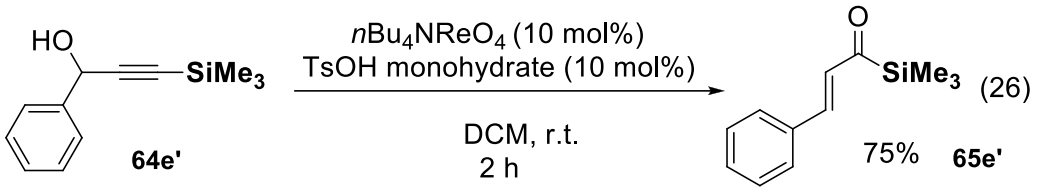

(26)

4.4 Substrate Scope Study

We began the substrate study by exploring the effect of the silyl group on the Meyer-Schuster rearrangement catalyzed by the tetra-*n*-butylammonium perrhenate and the toluenesulfonic acid. Gratifyingly, 3-silylalkyn-1-ol substrates **64a-c** containing trimethylsilyl (TMS), triethylsilyl (TES) and *tert*-butyldimethylsilyl (TBS) groups furnished the expected α,β-unsaturated acylsilane products **65a-c** in uniformly good yields (Scheme 26). However, subjecting substrate **64d** bearing a triisopropylsilyl group (TIPS) to the same reaction conditions did not transform to the corresponding acylsilane product **65d** and instead yielded the diastereomeric mixture of ether products **66d** and **67d** (Scheme 26). We rationalized that these products maybe formed via acid-catalyzed self-condensation of the propargylic alcohol through the formation of a carbocation and subsequent reaction with another alcohol equivalent. This divergent reactivity of **64d** is likely due to the steric demand of the TIPS group, which hinders the [3,3]-sigmatropic rearrangement and prevents the acylsilane formation.

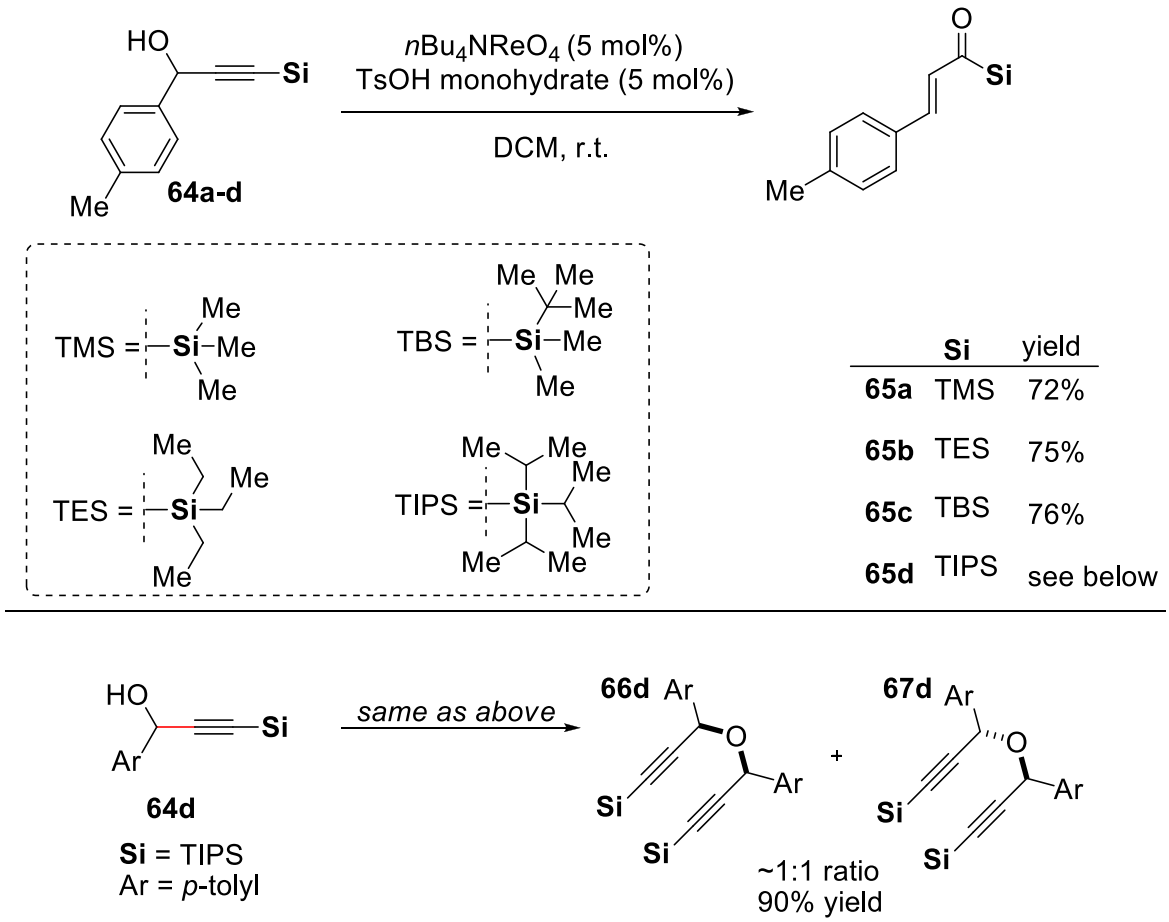

Scheme 26. Exploration of the Effect of the Silyl Group on the Formation of α,β-Unsaturated Acylsilane through Meyer-Schuster Rearrangement.

Considering that 3-silylalkyn-1-ol bearing TES and TBS groups provided the α,β-unsaturated acylsilane in similar yields, we decided to proceed with 3-silylalkyn-1-ol bearing TES group due to its low cost. Hence, we next explored a range of 3-silylalkyn-1-ol substrates derived from substituted benzaldehydes and TES-acetylene (Table 10). We were pleased to find that the propargylic alcohols bearing electron-deficient and electron-neutral aryl motifs were well tolerated and smoothly transformed to the corresponding acylsilane products in 58-80% isolated yields (**65e-h**, **k-m**, Table 10). Interestingly, this transformation is insensitive to the steric environment at the *ortho* positions of the aryl ring as demonstrated by the formation of the acysilane product **65f**. However, subjecting propargylic alcohols bearing a methoxy group either in the meta or para positions (**65i** and **65j**) led to an inseparable complex mixture of products. We hypothesized that

electron-donating groups on the aryl ring facilitate benzylic carbocation formation catalyzed by strong acid (TsOH pKa = -2.8 (water))[133] which leads to the substrate decomposition. Hence, we thought that the strong-acid free reaction conditions would circumvent the decomposition pathways and favor the formation of the corresponding acylsilane with acid sensitive propargylic alcohol substrates. Specifically, we decided to employ triphenylsilyl perrhenate (Osborn's reagent) as the Re(VII) catalyst for the Meyer-Schuster rearrangement (**conditions B**). Utilizing these conditions allowed for the formation of the corresponding acylsilane products **65i** and **65j** in 30% and 52% isolated yields respectively.

Table 10. Evaluation of Aryl-Substituted Secondary Propargylic Alcohols for the Synthesis of α,β-Unsaturated Acylsilanes.[a,b]

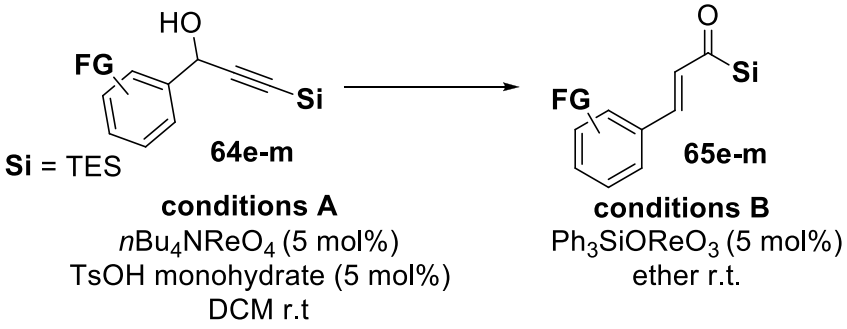

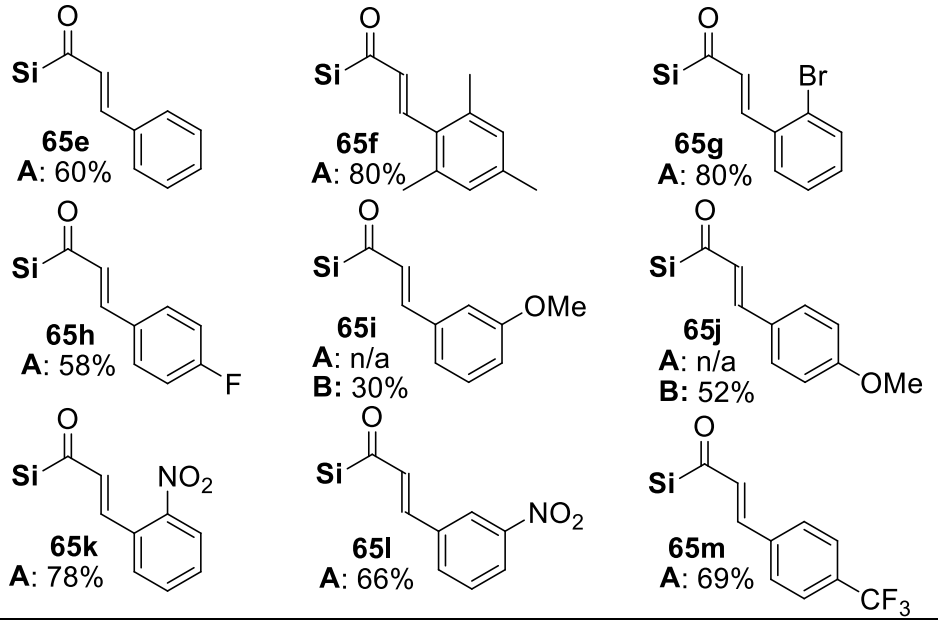

[a] All reactions were carried out at 0.20 M substrate concentration. [b] Isolated yields of pure product after column chromatography on silica.

Next, we wanted to evaluate the scope of tertiary propargylic alcohols derived from TES-acetylene and a series of ketones. We were surprised to find that alcohol prepared form benzophenone and TES-acetylene **64n** did not furnish the expected acylsilane **65n** under conditions **A** or **B** (Eq. 27). Instead, *β*-silyl-1-indanone **66n** was isolated in 55% yield, bearing the AB set of doublets at 3.00 ppm with 19.6 Hz as the coupling constant, a ketone ^{13}C resonance at 205.6 ppm and an IR stretch at 1705 cm^{-1} as the diagnostic signals.

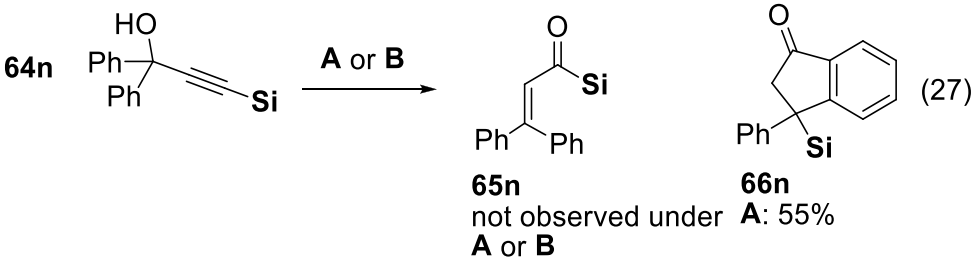

Interestingly, when alcohol **64o** prepared form 4,4'-dichlorobenzophenone and TES-acetylene was subjected to conditions **B**, the expected acylsilane **65o** was isolated in 78% yield bearing the diagnostic ^{13}C signal at 239.3 ppm and a strong IR stretching signal at 1622 cm^{-1} consistent with the acylsilane carbonyl group (Eq. 28). Considering that alcohol **64o** did not yield the corresponding indanone **66o** suggests that *β*-silyl-1-indanone **66n** formation likely involves an electrophilic aromatic substitution as one of its steps. In the presence of chlorine substituents however, the aromatic ring is deactivated towards such a reaction and **66o** does not form.

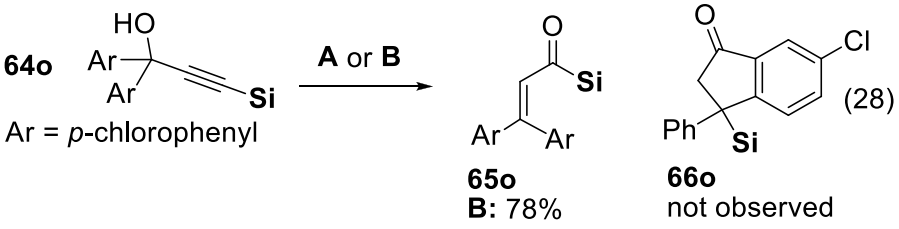

Overall, the formation of *β*-silyl-1-indanone **66n** maybe rationalized by the initial formation of an acylsilane **65n** which undergoes the intramolecular electrophilic aromatic addition of the

acylsilane followed by the aromatization and sequential 1,5-shifts of the TES group (Scheme 27). Enol-tautomerization furnishes the final *β*-silyl-1-indanone **66n** product.

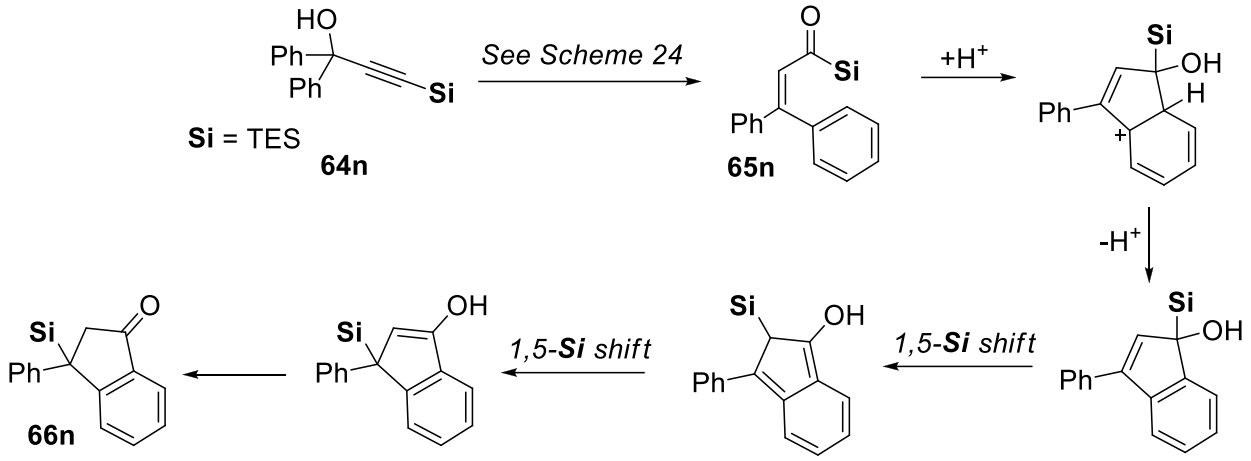

Scheme 27. Proposed mechanism for the formation of *β*-silyl-1-indanone **66n** from the propargylic alcohol **64n**

In the case of alcohol prepared from acetophenone and TES-acetylene **64p**, the desired acylsilane **65p** was isolated in 75% yield under conditions **B** (Eq. 29). However, when conditions **A** were employed, alcohol **65p** yielded the dehydration product **66p** in excellent yield. The spectroscopic data of **66p** consists of the aromatic protons, a set of two singlets for the alkene (5.96 ppm & 5.74 ppm), the aliphatic proton signals for the TES group (1.08 ppm triplet & 0.70 ppm quartet), alkyne ^{13}C signals (105.2 & 93.3), alkene ^{13}C signals (121.2 & 126.0), four aromatic ^{13}C signals and two ^{13}C signals in the aliphatic region.

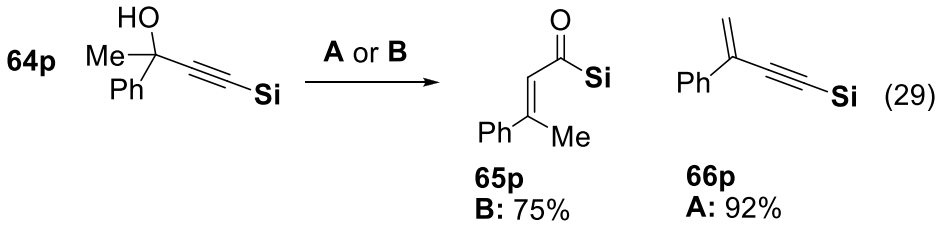

Alcohol prepared form cyclohexanone and TES-acetylene **64q** yielded α-silyl ketone **66q** under either conditions (Eq. 30). The ^{1}H-NMR spectroscopy data of **66q** consists of a singlet for the alkene at 6.93 ppm, a singlet for the ketone α-protons at 2.30 ppm, the aliphatic protons of the cyclohexenyl ring between 2.27-1.64 ppm, signals for the TES group (0.95 ppm triplet & 0.54 ppm quartet). The ^{13}C-NMR spectroscopy data of **66q** consists of ketone signal at 199.2 ppm, alkene signals (140.8 & 139.6 ppm) and seven aliphatic signals in the 26.0-6.3 ppm range.

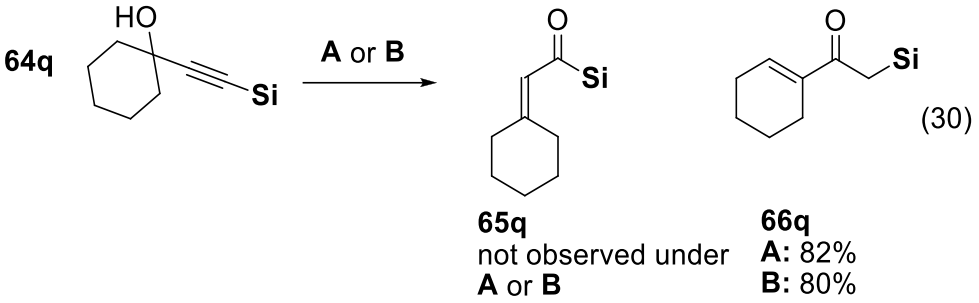

The formation of α-silyl-ketone **66q** from alcohol **64q** maybe rationalized by invoking a Rupe rearrangement (Scheme 28).[134] The generally accepted mechanism involves the dehydration of the tertiary propargylic alcohol to an enyne intermediate followed by hydration of the alkyne.

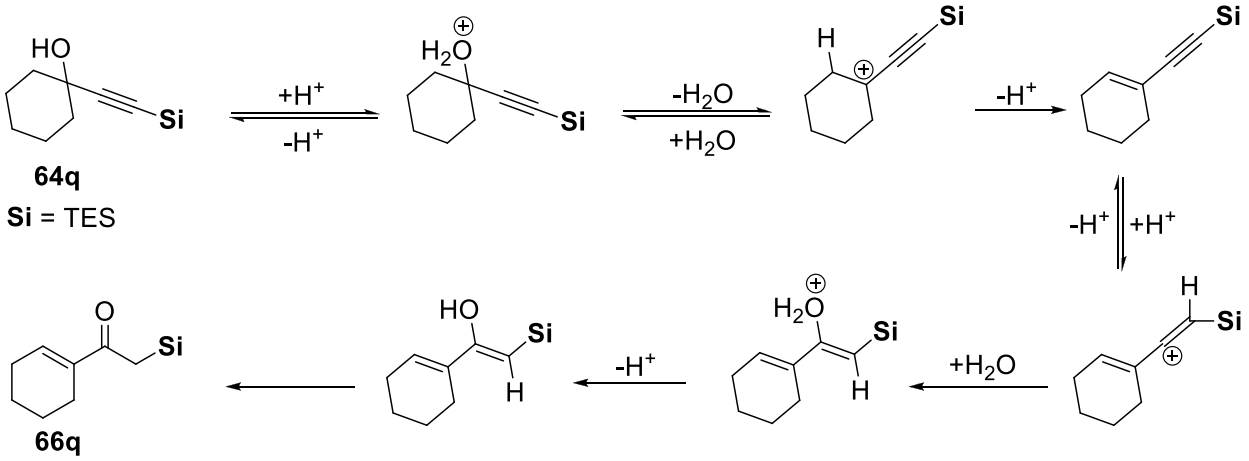

Scheme 28. The formation of α-silyl-ketone **66q** from the propargylic alcohol **64q** via Rupe rearrangement.

Next, we explored the scope of secondary propargylic alcohols derived from TES-acetylene and series of aliphatic aldehydes (**64r-v**, Table 11). For reasons that are unclear, alcohols bearing a secondary (**64r**) or tertiary (**64s**) center adjacent to the carbinol carbon, proved to be unreactive at room temperature in DCM or in refluxing dioxane as solvent. In contrast, alcohol **64t** bearing a quaternary center adjacent to the carbinol carbon, transformed to the corresponding α,β-unsaturated acylsilane **65t** in 80% isolated yield when heated at refluxing dioxane. Such difference in reactivity maybe attributed to the hyperconjugation effect of the *tert*-butyl group which likely stabilizes the transition state during the [3,3]-sigmatropic rearrangement of perrhenate-bound alcohol **64t** (Fig. 11).

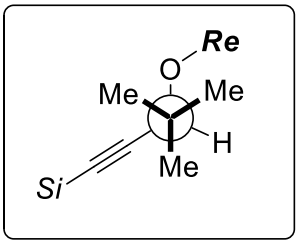

Figure 11. The hyperconjugation effect of the adjacent *tert*-butyl group.

Lastly, we investigated the compatibility of propargylic alcohols derived from TES-acetylene and *α,β*-unsaturated ketones (**64u** and **64v**) for the synthesis of α,β,γ,δ-unsaturated acylsilane products (**65u** and **65v**) through Meyer-Schuster rearrangement. Subjecting alcohol **64u** to conditions **A** resulted in substrate decomposition. When the same alcohol was subjected to refluxing ether with catalytic amount of Osborn's reagent, a mixture of starting alcohol **64u** and its 1,3-allylic transposition product **66u** were isolated as an inseparable mixture in 4:1 ratio. We hypothesized that formation of this mixture was due to minor difference in the thermodynamic stability between **64u** and **66u**. This observation also implies that the activation energy for [3,3]-sigmatropic rearrangement between the perrhenate ester and the alkyne group is greater than the [3,3]-sigmatropic rearrangement between the perrhenate ester and the alkene functional group due to geometric constraints of the former (Fig. 12). We thought that conducting this

reaction at an elevated temperature would provide sufficient energy to overcome the activation barrier for [3,3]-sigmatropic rearrangement between the perrhenate ester and the alkyne group and yield the desired acylsilane **65u**. Indeed, subjecting alcohol **64u** to refluxing THF with catalytic amount of Osborn's reagent provided the α,β,γ,δ-unsaturated acylsilane **65u** in 51% isolated yield as an orange oil. Subjecting propargylic alcohol **64v** to conditions **B** furnished an inseparable mixture of conjugated alcohols **66v** and **66v'** in ~ 1:0.7 ratio with combined yield of 90%. Alcohol **64v** did not transform to the corresponding acylsilane **65v** even at elevated temperatures and instead provided α,β,γ,δ-unsaturated ketone **67v** in 74% isolated yield. Spectroscopic data for **67v** was consistent with the previously reported structure.[89] Formation of **67v** maybe rationalized by invoking dehydration followed by the hydration of the alkyne and the loss of the silyl group (Scheme 29).

Table 11. Evaluation of Secondary Aliphatic Propargylic Alcohols for the Synthesis of α,β-Unsaturated Acylsilanes through Meyer-Schuster Rearrangement.[a,b]

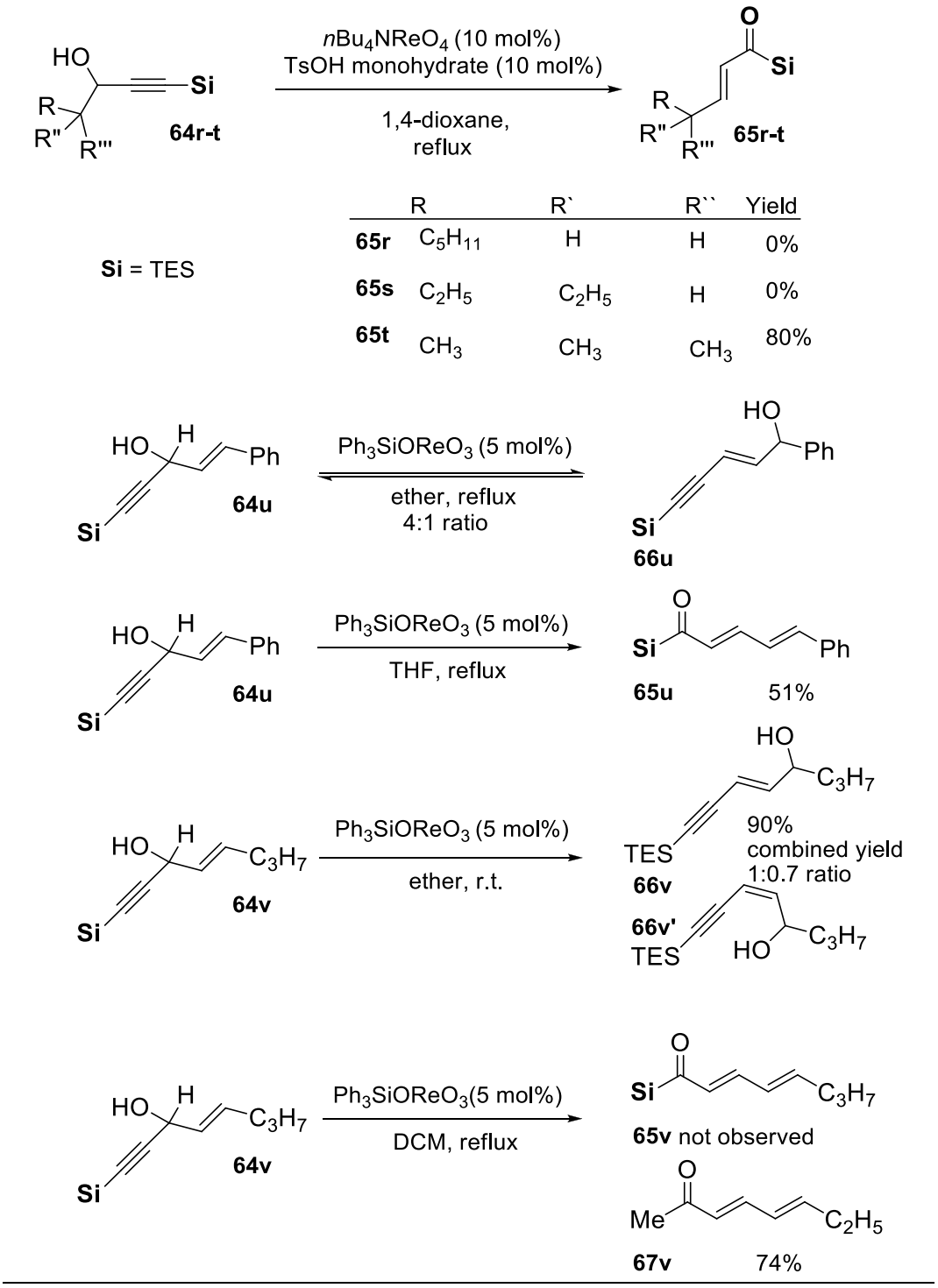

[a] All reactions were carried out at 0.20 M substrate concentration. [b] Isolated yields of pure product after column chromatography on silica.

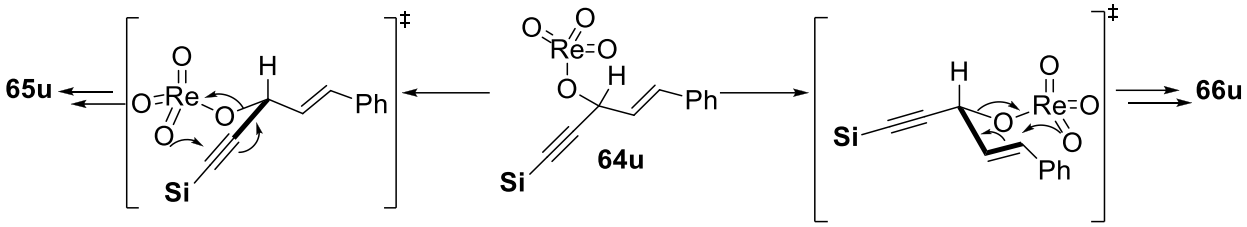

Figure 12. [3,3]-Sigmatropic rearrangement transition states comparison of alkyne versus alkene functions and the perrhenate ester.

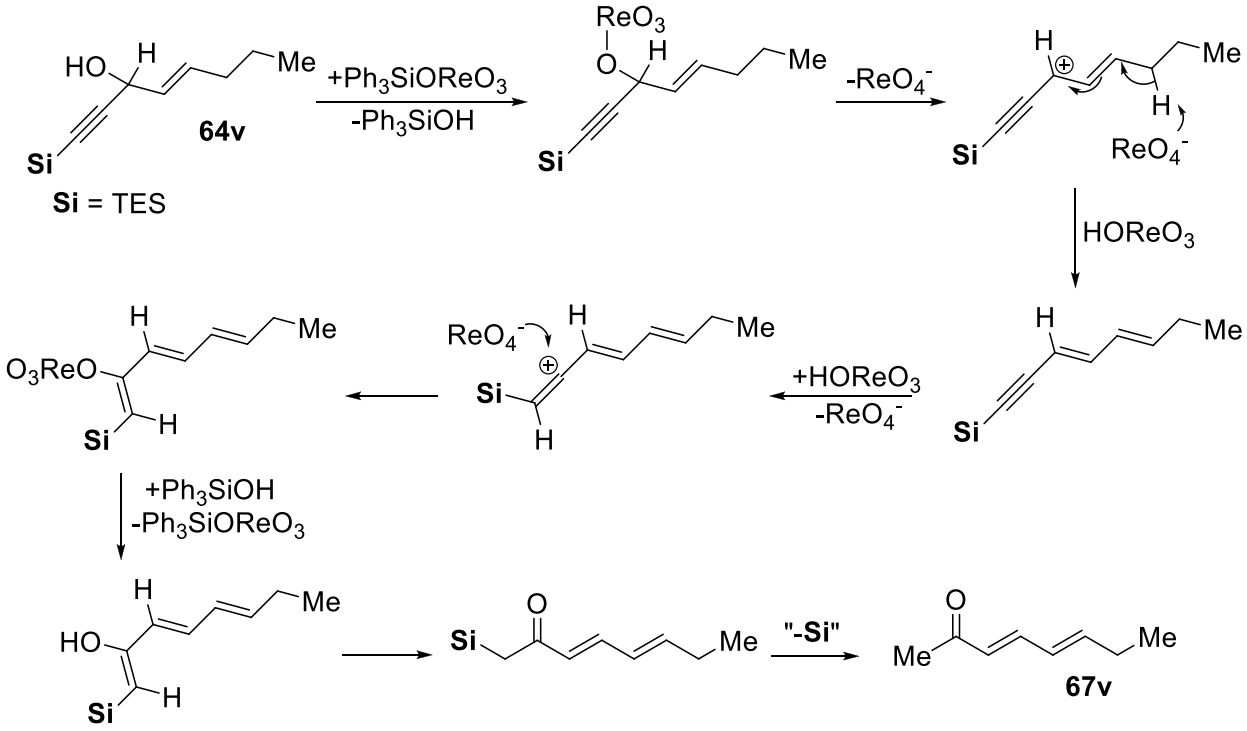

Scheme 29. Proposed mechanism for the formation of ketone **67v** catalyzed by Osborn's reagent.

4.5 Conclusion

In conclusion, we have explored the synthesis of acylsilanes from series of 3-silylalkyn-1-ol substrates through perrhenate-catalyzed Meyer-Schuster rearrangement reaction. Generally, propargylic alcohol substrates prepared from benzaldehyde derivatives smoothly transformed to the corresponding acylsilanes in the presence of catalytic amount of TsOH monohydrate and *n*-Bu_4NReO_4. With substrate that were prone to Brönsted acid catalyzed ionization, the use of

catalytic amount of Osborn's reagent ($Ph_3SiOReO_3$) allowed for acylsilane formation with most substrates. Interestingly, the secondary aliphatic propargylic alcohols that were evaluated proved to be generally unreactive. Lastly, propargylic alcohol derived from cinnamaldehyde and TES-acetylene transformed to the corresponding α,β,γ,δ-unsaturated acylsilane with Osborn's reagent in refluxing THF.

Chapter 5. Experimental Protocols and Compound Data

5.1 General Experimental

Reactions were conducted in flame- or oven-dried glassware under an atmosphere of argon using freshly distilled solvents unless specified otherwise. Commercial reagents were used as received. Thin-layer chromatography was performed on Merck silica gel 60 F254 plates. Visualisation was carried out using UV light (254 nm) and/or $KMnO_4$, anisaldehyde or $(NH_4)_2Ce(NO_3)_6$ solutions. Hexanes (ACS grade) and ethyl acetate (ACS grade) were used as received. Flash column chromatography was carried out using Aldrich silica gel (230-400 mesh, 40-63 µ, 60 Å pore size). ^{1}H-, ^{2}H-, ^{13}C-, ^{19}F- and ^{29}Si-NMR spectra were recorded on a Bruker 400 AV or Bruker 300 AV spectrometer in chloroform-d (99.8% deuterated) or methanol-d*4* (99.8% deuterated), and using chloroform (7.24 ppm ^{1}H and 77.2 ppm ^{13}C) or methanol (3.35 ppm ^{1}H and 49.3 ppm ^{13}C) as a reference. Chemical shifts (δ) are reported in ppm and multiplicities are indicated by s (singlet), d (doublet), t (triplet), q (quartet), p (pentet), m (multiplet), br (broad). Coupling constants *J* are reported in Hertz (Hz). Infrared (IR) spectra were recorded using Alpha-Platinum ATR Bruker instrument.

5.2 Experimental Procedures – Synthesis of Quinolines via Palladium-Catalyzed Cross-Coupling of Cyclopropanols with ortho-Bromoanilines

General Procedure 1. *Synthesis of Quinolines via Palladium-Catalyzed Cross-Coupling of Cyclopropanols with ortho-Bromoanilines*.

Quinoline **11**

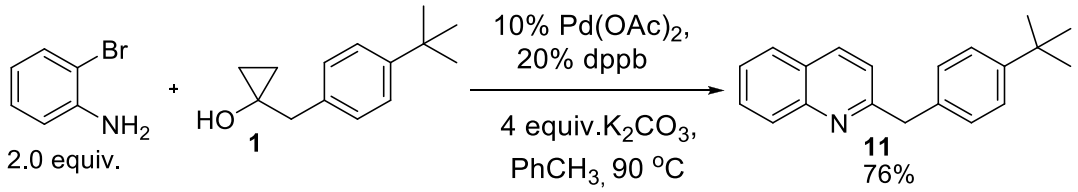

An over dried vial equipped with a stir bar was charged with $Pd(OAc)_2$ (0.0055 g, 0.025 mmol, 0.10 equiv.), dppb (0.020 g, 0.049 mmol, 0.2 equiv.) and K_2CO_3 (0.15 g, 0.98 mmol, 4.0 equiv.). 1 ml of distilled $PhCH_3$ was introduced into the vial *via* syringe and contents allowed to stir. A second oven dried vial equipped with a stir bar was charged with cyclopropanol **1** (0.05 g, 0.25 mmol, 1 equiv.) and 2-bromoaniline (0.084 g, 0.49 mmol, 2 equiv.). 1 ml of distilled $PhCH_3$ was introduced into the vial *via* syringe and contents allowed to stir. The contents of the second vial were mixed with the pre-stirred palladium catalyst in the first vial. The reaction vessel was purged with a stream of Ar. The reaction mixture was heated to 110 °C under an argon atmosphere for 24 hours. Upon completion, the reaction mixture was filtered through a pad of Celite using EtOAc and concentrated *in vacuo*. The crude product was purified by flash column chromatography, eluting with 20% EtOAc in hexanes as solvent mixture to afford the desired quinoline product **11** as a yellow oil (0.051 g, 0.19 mmol) in 76% yield.

Data for **11**
^{1}H NMR (400 MHz, $CDCl_3$)
δ 8.13 (d, *J* = 8.4 Hz, 1 H), 8.04 (d, *J* = 8.4 Hz, 1 H), 7.78 (d, *J* = 8.1 Hz, 1 H), 7.73 (dd, *J* = 8.4, 7.8 Hz, 1 H), 7.52 (dd, *J* = 8.4, 7.8 Hz,1 H), 7.36 (d, *J* = 8.1 Hz, 1 H), 7.30-7.26 (m, 3 H), 4.36 (s, 2H), 1.33 (s, 9 H).
^{13}C NMR (100 MHz, $CDCl_3$)
δ 161.4, 149.2, 147.8, 136.3, 136.1, 129.3, 128.9, 128.8, 127.4, 126.7, 125.8, 125.4, 121.5, 45.0, 34.3, 31.3
IR Alpha-Platinum ATR, Bruker, diamond crystal
υ = 3057, 2960, 1655, 1618, 1599, 1504, 742 cm^{-1}
HRMS TOF EI
Calculated for $[C_{20}H_{21}N]^+$ = 275.1674, found = 275.1669

Quinoline **12**

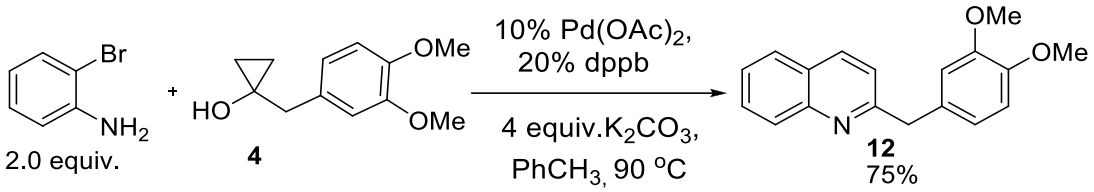

Following *General Procedure 1* cyclopropanol **4** (0.050 g, 0.24 mmol, 1 equiv.) and 2-bromoaniline (0.083 g, 0.48 mmol, 2 equiv.) were converted to quinoline. Purification by flash column chromatography using 35 % solution of EtOAc in hexanes afforded the quinoline **12** (0.050 g, 0.18 mmol) as a brown oil in 75 % yield.[135]

Data for **12**
^{1}H NMR (400 MHz, $CDCl_3$)
δ 8.12 (d, *J* = 8.4 Hz, 1 H), 8.05 (d, *J* = 8.4 Hz, 1 H), 7.78 (d, *J* = 8.0 Hz, 1 H), 7.74 (dd, *J* = 8.4, 7.6 Hz, 1 H), 7.52 (dd, *J* = 8.0, 7.6 Hz, 1 H), 7.25 (d, *J* = 8.4 Hz,1 H), 6.89-6.82 (m, 3 H), 4.31 (s, 2 H), 3.87 (s, 3 H), 3.84 (s, 3 H)
^{13}C NMR (100 MHz, $CDCl_3$)
δ 161.4, 149.0, 147.63, 147.60, 136.5, 131.6, 129.4, 128.8, 127.4, 126.7, 125.9, 121.3, 121.1, 112.3, 111.2, 55.8, 55.7, 45.0.
IR.Alpha-Platinum ATR, Bruker, diamond crystal
υ = 3056, 2955, 1610, 1597, 1512, 754 cm^{-1}

Quinoline **13**

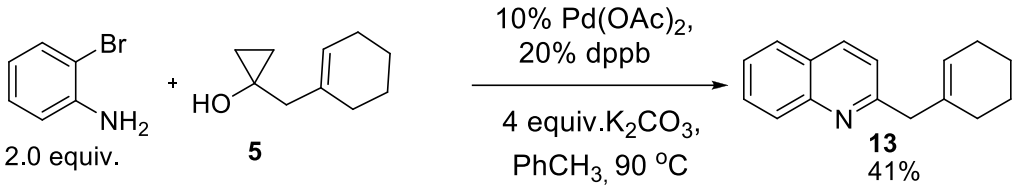

Following *General Procedure 1* cyclopropanol **5** (0.050 g, 0.33 mmol, 1 equiv.) and 2-bromoaniline (0.11 g, 0.66 mmol, 2 equiv.) were converted to quinoline. Purification by flash column chromatography using triple solvent system 2 % EtOAc, 20 % $PhCH_3$ in DCM afforded the quinoline **13** (0.030 g, 0.13 mmol) as a yellow oil in 41 % yield.

Data for **13**
^{1}H NMR (400 MHz, $CDCl_3$)
δ 8.09 (d, *J* = 8.0 Hz, 1 H), 8.08 (d, *J* = 8.4 Hz, 1 H), 7.81 (d, *J* = 8.0 Hz, 1 H), 7.72 (dd, *J* = 8.4, 7.6 Hz, 1 H), 7.51 (dd, *J* = 8.0, 7.6 Hz, 1 H), 7.36 (d, *J* = 8.4 Hz, 1 H), 5.55 (br s, 1 H), 3.65 (s, 2 H), 2.06 (br s, 2 H), 1.97 (br s, 2 H), 1.63-1.56 (m, 4 H)
^{13}C NMR (100 MHz, $CDCl_3$)
δ 161.0, 147.7, 135.9, 135.8, 129.2, 128.9, 127.4, 126.7, 125.7, 124.1, 121.3, 47.9, 28.3, 25.3, 22.8, 22.2
IR Alpha-Platinum ATR, Bruker, diamond crystal
υ = 3056, 2922, 1618, 1601, 1503, 1425, 1310, 752, 475 cm^{-1}
HRMS TOF EI
Calculated for $[C_{16}H_{17}N]^+$ = 223.1361, found = 223.1368

Quinoline **14**

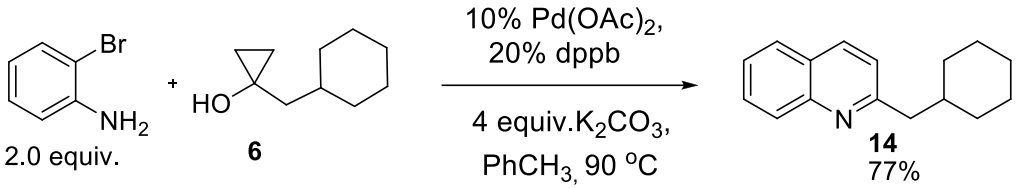

Following *General Procedure 1* cyclopropanol **6** (0.050 g, 0.32 mmol, 1 equiv.) and 2-bromoaniline (0.11 g, 0.65 mmol, 2 equiv.) were converted to quinoline. Purification by flash column chromatography using 10% EtOAc solution in hexanes afforded the quinoline **14** (0.056 g, 0.25 mmol) as a slight yellow oil in 77% yield.

Data for **14**
^{1}H NMR (400 MHz, $CDCl_3$)
δ 8.08 (d, *J* = 9.2 Hz, 1 H), 8.06 (d, *J* = 9.2 Hz, 1 H), 7.79 (d, *J* = 8.0 Hz, 1 H), 7.69 (dd, *J* = 8.4, 7.6 Hz 1 H), 7.49 (dd, *J* = 8.0, 7.6 Hz, 1 H), 7.27 (d, *J* = 8.4 Hz,1 H), 2.88 (d, *J* = 7.2 Hz, 2 H), 1.92-1.86 (m, 1 H), 1.71 (m, 6 H), 1.26-1.10 (m, 4 H)
^{13}C NMR (100 MHz, $CDCl_3$)
δ 161.9, 147.9, 135.7, 129.1, 128.8, 127.4, 126.6, 125.5, 122.1, 47.0, 38.8, 33.2, 26.4, 26.1
IR Alpha-Platinum ATR, Bruker, diamond crystal
υ = 3056, 2919, 1618, 1599, 1503, 1446, 847, 739 cm^{-1}
HRMS TOF EI
Calculated for $[C_{16}H_{19}N]^+$ = 225.1361, found = 225.1368

Quinoline **15**

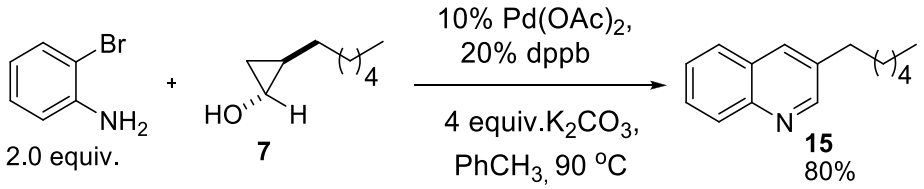

Following *General Procedure 1* cyclopropanol **7** (0.050 g, 0.35 mmol, 1 equiv.) and 2-bromoaniline (0.12 g, 0.70 mmol, 2 equiv.) were converted to quinoline. Purification by flash column chromatography using 20% EtOAc solution in hexanes afforded the quinoline **15** (0.060g, 0.28 mmol) as a slight yellow oil in 80% yield.[136]

Data for **15**
^{1}H NMR (400 MHz, $CDCl_3$)
δ 8.80 (s, 1 H), 8.09 (d, *J* = 8.4 Hz, 1 H), 7.92 (s, 1 H), 7.78 (d, *J* = 8.0 Hz, 1 H), 7.67 (dd, *J* = 8.4, 7.2 Hz,1 H), 7.53 (dd, *J* = 8.0, 7.2 Hz,1 H), 2.81 (t, *J* = 7.6 Hz, 2 H), 1.73 (m, 2H), 1.42-1.32 (m, 6 H), 0.91 (t, *J* = 6.4 Hz, 3 H)
^{13}C NMR (100 MHz, $CDCl_3$)
δ 152.1, 146.7, 135.3, 133.9, 129.1, 128.3, 128.1, 127.2, 126.4, 33.1, 31.5, 31.0, 28.7, 22.5, 14.0.
IR Alpha-Platinum ATR, Bruker, diamond crystal
υ = 3064, 2955, 1604, 1570, 1494, 748 cm^{-1}

Quinoline **16**

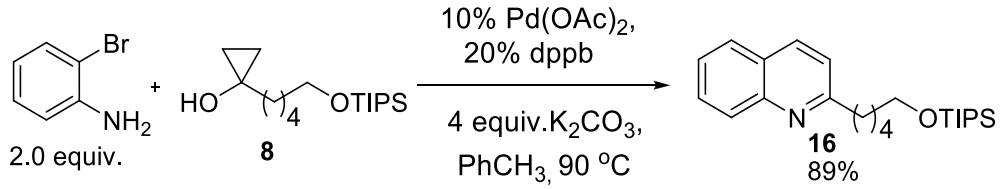

Following *General Procedure 1* cyclopropanol **8** (0.050 g, 0.17 mmol, 1 equiv.) and 2-bromoaniline (0.057 g, 0.33 mmol, 2 equiv.) were converted to quinoline. Purification by flash column chromatography using 5% EtOAc solution in hexanes afforded the quinoline **16** (0.055 g, 0.148 mmol) as a slight yellow oil in 89% yield.

Data for **16**
^{1}H NMR (400 MHz, $CDCl_3$)
δ 8.08 (d, *J* = 8.4 Hz, 1 H), 8.06 (d, *J* = 9.2 Hz, 1 H), 7.80 (d, *J* = 8.4 Hz, 1 H), 7.70 (dd, *J* = 8.0, 7.2 Hz 1 H), 7.50 (dd, *J* = 8.4, 7.2 Hz, 1 H), 7.32 (d, *J* = 8.0 Hz,1 H), 3.70 (t, *J* = 6.0 Hz, 2 H), 3.00 (t, *J* = 8.0 Hz, 2 H), 1.87 (dt, *J* = 7.6, 6.0 Hz, 2 H), 1.63 (dt, *J* = 8.0, 6.8 Hz, 2 H), 1.51 (dt, *J* = 7.6, 6.8 Hz, 2 H), 1.08 (m, 21 H)
^{13}C NMR (100 MHz, $CDCl_3$)
δ 162.9, 147.8, 136.1, 129.2, 128.7, 127.4, 126.6, 125.5, 121.3, 63.2, 39.3, 32.8, 29.9, 25.7, 17.9, 11.9.
IR Alpha-Platinum ATR, Bruker, diamond crystal
υ = 3057, 2892, 1619, 1601, 1561, 1089, 881, 678 cm^{-1}
HRMS TOF EI
Calculated for $[C_{23}H_{37}NOSi]^{+}$ = 371.2644 found = 371.2638

Quinoline **17**

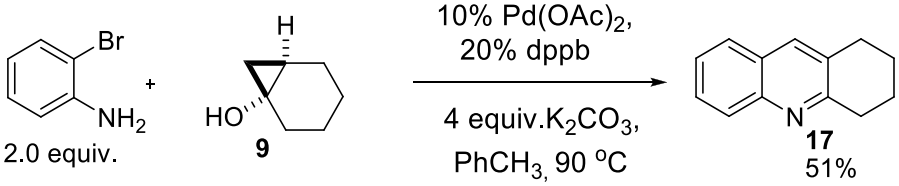

Following *General Procedure 1* cyclopropanol **9** (0.050 g, 0.45 mmol, 1 equiv.) and 2-bromoaniline (0.15 g, 0.90 mmol, 2 equiv.) were converted to quinoline. Purification by flash column chromatography using 25% EtOAc solution in hexanes afforded the quinoline **17** (0.042 g, 0.23 mmol) as a brown solid in 51% yield.[137]

Data for **17**
^{1}H NMR (400 MHz, $CDCl_3$)
δ 7.99 (d, *J* = 8.8 Hz, 1 H), 7.82 (s,1 H), 7.72 (d, *J* = 8.00 Hz, 1 H), 7.63 (dd, *J* = 8.0, 7.2 Hz, 1 H), 7.45 (dd, *J* = 8.0, 7.2 Hz,1 H), 3.15 (t, *J* = 6.4 Hz, 2 H), 2.99 (t, *J* = 6.0 Hz, 2 H), 2.00 (m, 2 H), 1.92 (m, 2H)
^{13}C NMR (100 MHz, $CDCl_3$)
δ 159.2, 146.5, 134.9, 130.9, 128.4, 128.1, 127.1, 126.8, 125.4, 33.5, 29.2, 23.1, 22.8
IR Alpha-Platinum ATR, Bruker, diamond crystal
υ = 3052, 2926, 1618, 1598, 1488, 746 cm^{-1}
m.p. 54-55 °C

Quinoline **18**

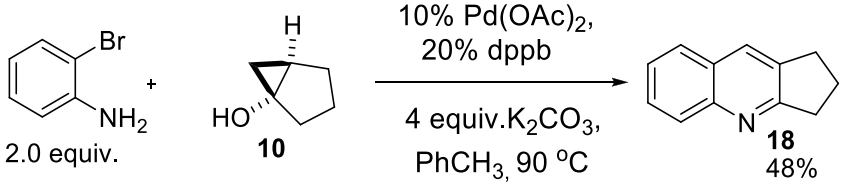

Following *General Procedure 1* cyclopropanol **10** (0.050 g, 0.51 mmol, 1 equiv.) and 2-bromoaniline (0.18 g, 1.0 mmol, 2 equiv.) were converted to quinoline. Purification by flash column chromatography using 40% EtOAc solution in hexanes afforded the quinoline **18** (0.041 g, 0.24 mmol) as a brown oil in 48% yield.[138]

Data for **18**
^{1}H NMR (400 MHz, $CDCl_3$)
δ 8.03 (d, *J* = 8.4 Hz 1 H), 7.89 (s, 1 H), 7.74 (d, *J* = 8.1 Hz 1 H), 7.63 (dd, *J* = 8.4, 8.0 Hz 1 H), 7.47 (d, *J* = 8.1, 8.0 Hz 1 H), 3.18 (t, *J* = 7.5 Hz, 2 H), 3.10 (t, *J* = 7.2 Hz 2 H), 2.27 (dt, 7.5, 7.2 Hz, 2 H)
^{13}C NMR (100 MHz, $CDCl_3$)
δ 167.8, 147.4, 135.5, 130.2, 128.7, 128.5, 128.2, 127.3, 125.4, 34.5, 30.4, 23.5
IR Alpha-Platinum ATR, Bruker, diamond crystal
υ = 3055, 2953, 1617, 1569, 1496, 1404, 900, 859, 748 cm^{-1}

Quinoline **27**

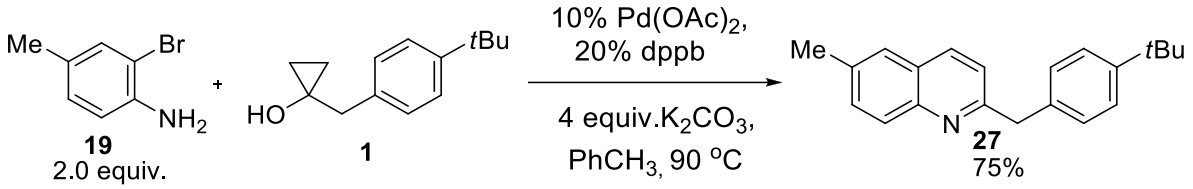

Following *General Procedure 1* cyclopropanol **1** (0.050 g, 0.25 mmol, 1 equiv.) and 2-bromoaniline **19** (0.091 g, 0.49 mmol, 2 equiv.) were converted to quinoline. Purification by flash column chromatography using 10% solution of EtOAc in hexanes afforded the quinoline **27** (0.053 g, 0.18 mmol) as a yellow solid in 75% yield.

Data for **27**
^{1}H NMR (400 MHz, $CDCl_3$)
δ 8.02 (d, *J* = 8.4 Hz, 1 H), 7.95 (d, *J* = 8.4 Hz, 1 H), 7.55 (d, J = 8.0 Hz, 1 H), 7.54 (s, 1H), 7.36 (d, *J* = 8.0 Hz, 2 H), 7.28 (d, *J* = 8.0 Hz,2 H), 7.23 (d, *J* = 8.4 Hz 3 H), 4.33 (s, 2 H), 2.54 (s, 3 H), 1.33 (s, 9 H)
^{13}C NMR (100 MHz, $CDCl_3$)
δ 160.4, 149.1, 146.3, 136.2, 135.7, 135.6, 131.6, 128.8, 128.6, 126.7, 126.3, 125.4, 121.5, 44.9, 34.3, 31.3, 21.4.
IR Alpha-Platinum ATR, Bruker, diamond crystal
υ = 3064, 2961, 1599, 1496, 1114, 1227, 824, 692 cm^{-1}
HRMS TOF EI
Calculated for $[C_{21}H_{23}N]^+$ = 289.1830, found = 289.1825
m.p. 64-65 °C

Quinoline **28**

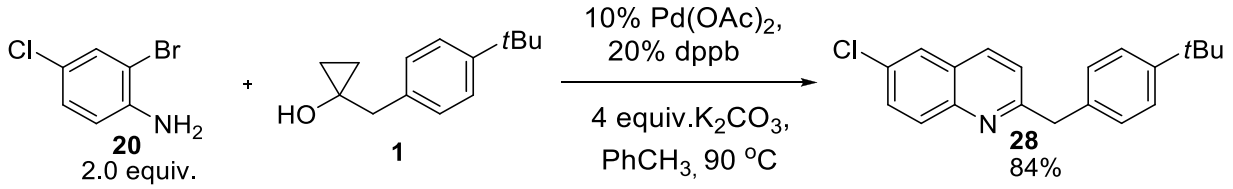

Following *General Procedure 1* cyclopropanol **1** (0.050 g, 0.25 mmol, 1 equiv.) and 2-bromoaniline **20** (0.10 g, 0.49 mmol, 2 equiv.) were converted to quinoline. Purification by flash column chromatography using 8% solution of EtOAc in hexanes afforded the quinoline **28** (0.064 g, 0.20 mmol) as a slight yellow solid in 84% yield.

Data for **28**
^{1}H NMR (400 MHz, $CDCl_3$)
δ 8.04 (d, *J* = 9.2 Hz, 1 H), 7.94 (d, *J* = 8.4 Hz, 1 H), 7.75 (d, *J* = 2.0 Hz, 1 H), 7.65 (dd, *J* = 9.2, 2.0 Hz, 1 H), 7.36 (d, *J* = 8.0 Hz, 2 H), 7.28 (d, *J* = 8.4 Hz,1 H), 7.26 (d, *J* = 8.0 Hz, 2 H), 4.32 (s, 2 H), 1.33 (s, 9 H)
^{13}C NMR (100 MHz, $CDCl_3$)
δ 161.7, 149.3, 146.1, 135.7, 135.4, 131.4, 130.5, 130.2, 128.7, 127.3, 126.1, 125.5, 122.4, 44.9, 34.3, 31.3.
IR Alpha-Platinum ATR, Bruker, diamond crystal
υ = 3089, 2956, 1600, 1594, 1512, 1110, 828, 798, 546 cm^{-1}
HRMS TOF EI
Calculated for $[C_{20}H_{20}NCl]^+$ = 309.1284, found = 309.1279
m.p. 77-78 °C

Quinoline **29**

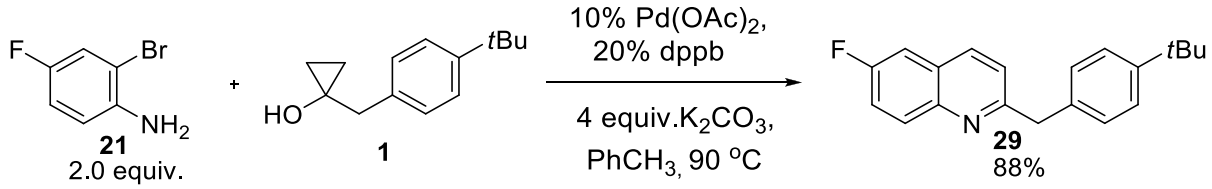

Following *General Procedure 1* cyclopropanol **1** (0.050 g, 0.25 mmol, 1 equiv.) and 2-bromoaniline **21** (0.093 g, 0.49 mmol, 2 equiv.) were converted to quinoline. Purification by flash column chromatography using 10% solution of EtOAc in hexanes afforded the quinoline **29** (0.063 g, 0.22 mmol) as a slight yellow oil in 88% yield.

Data for **29**
^{1}H NMR (400 MHz, $CDCl_3$)
δ 8.10 (dd, *J* = 9.2, 5.2 Hz, 1 H), 7.99 (d, *J* = 8.8 Hz, 1H), 7.49 (ddd, *J* = 8.9, 8.8, 2.4 Hz,1 H), 7.39 (dd, *J* = 9.0, 2.4 Hz, 1 H), 7.36 (d, *J* = 8.4 Hz, 2 H), 7.29 (d, *J* = 8.8 Hz, 1 H), 7.27 (d, *J* = 8.4 Hz, 2 H), 4.32 (s, 2 H), 1.33 (s, 9 H)
^{13}C NMR (100 MHz, $CDCl_3$)
δ 160.7 (d, $^{4}J_{C\text{-}F}$= 2.6 Hz),160.0 (d, $^{1}J_{C\text{-}F}$= 246 Hz),149.3, 144.8, 135.9, 135.6 (d, $^{4}J_{C\text{-}F}$ = 5.1 Hz), 131.3 (d, $^{3}J_{C\text{-}F}$ = 9.1 Hz), 128.7, 127.2 (d, $^{3}J_{C\text{-}F}$ = 9.9 Hz), 125.5, 122.3, 119.4 (d, $^{2}J_{C\text{-}F}$ = 25.4 Hz), 110.4 (d, $^{2}J_{C\text{-}F}$ = 21.4 Hz), 44.8, 34.3, 31.2
^{19}F-NMR (376 MHz, $CDCl_3$)
δ −114.5
IR Alpha-Platinum ATR, Bruker, diamond crystal
υ = 3056, 2960, 1628, 1605, 1504, 1227, 820, 552 cm^{-1}
HRMS TOF EI
Calculated for $[C_{20}H_{20}NF]^{+}$ = 293.1580, found = 293.1578

Quinoline **30**

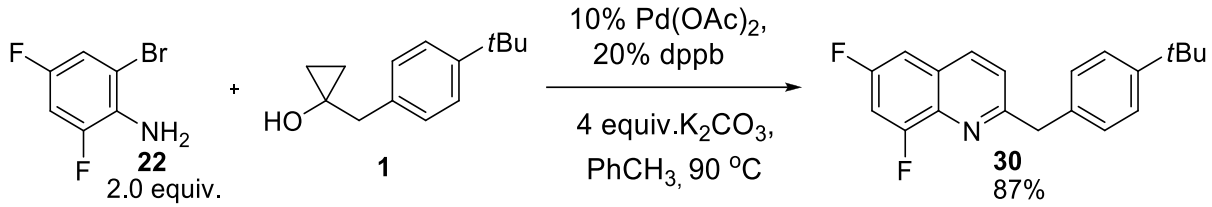

Following *General Procedure 1* cyclopropanol **1** (0.050 g, 0.25 mmol, 1 equiv.) and 2-bromoaniline **22** (0.10 g, 0.49 mmol, 2 equiv.) were converted to quinoline. Purification by flash column chromatography using 5% solution of EtOAc in hexanes afforded the quinoline **30** (0.066 g, 0.21 mmol) as a yellow oil in 87% yield.

Data for **30**
^{1}H NMR (400 MHz, $CDCl_3$)
δ 7.99 (d, *J* = 8.4 Hz,1 H), 7.37-7.21 (m, 7 H), 4.37 (s, 2 H), 1.32 (s, 9 H)
^{13}C NMR (100 MHz, $CDCl_3$)
δ 161.2, 159.0 (dd, $^{1}J_{C\text{-}F}$ = 247Hz, $^{3}J_{C\text{-}F}$ = 11 Hz), 158.2 (dd,$^{1}J_{C\text{-}F}$ = 258 Hz, $^{3}J_{C\text{-}F}$ = 13 Hz), 149.4, 135.6, 135.5, 135.1 (d, $^{3}J_{C\text{-}F}$ = 10 Hz), 128.8, 127.9 (dd, $^{2}J_{C\text{-}F}$ = 11 Hz, $^{4}J_{C\text{-}F}$ = 3.3 Hz), 125.5, 123.5, 106.4 (dd, $^{2}J_{C\text{-}F}$ = 21Hz, $^{4}J_{C\text{-}F}$ = 4.8 Hz), 105.0 (dd, $^{2}J_{C\text{-}F}$ = 29 Hz, $^{2}J_{C\text{-}F'}$ = 23 Hz), 44.3, 34.3, 31.23
^{19}F-NMR (376 MHz, $CDCl_3$)
δ −111.5, −120.3
IR Alpha-Platinum ATR, Bruker, diamond crystal
υ = 3089, 2961, 1648, 1606, 1501, 1122, 986, 544 cm^{-1}
HRMS TOF EI
Calculated for $[C_{20}H_{19}NF_2]^+$ = 311.1486, found = 311.1479

Quinoline **31**

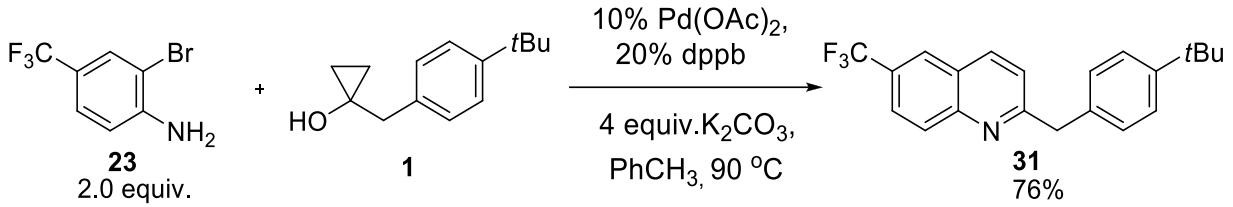

Following *General Procedure 1* cyclopropanol **1** (0.050 g, 0.25 mmol, 1 equiv.) and 2-bromoaniline **23** (0.12 g, 0.49 mmol, 2 equiv.) were converted to quinoline. Purification by flash column chromatography using 10% solution of EtOAc in hexanes afforded the quinoline **31** (0.064 g, 0.19 mmol) as a slight yellow solid in 76% yield.

Data for **31**
^{1}H NMR (400 MHz, $CDCl_3$)
δ 8.22 (d, *J* = 8.8 Hz 1 H), 8.12 (d, *J* = 9.2 Hz, 1 H), 8.10 (s, 1 H), 7.89 (d, *J* = 8.8 Hz 1 H), 7.38 (d, *J* = 9.2 Hz, 1 H), 7.37 (d,*J* = 8.0 Hz, 2 H), 7.28 (d, *J* = 8.0 Hz 2 H), 4.37 (s, 2 H), 1.33 (s, 9 H)
^{13}C NMR (100 MHz, $CDCl_3$)
δ 163.8, 149.5, 148.7, 136.9, 135.4, 130.1, 128.8, 127.7 (q, $^{2}J_{C\text{-}F}$ = 32 Hz), 125.6, 125.5, 125.3 (q, $^{3}J_{C\text{-}F}$ = 5.0 Hz), 125.0 (q, $^{3}J_{C\text{-}F}$ = 3.0 Hz), 124.0 (q, $^{1}J_{C\text{-}F}$ = 270 Hz) 122.7, 45.0, 34.3, 31.2
^{19}F-NMR (376 MHz, $CDCl_3$)
δ −62.15
IR Alpha-Platinum ATR, Bruker, diamond crystal
υ = 3087, 2959, 1631, 1599, 1305, 1135, 1062, 840 cm^{-1}
HRMS TOF EI
Calculated for $[C_{21}H_{20}NF_3]^+$ = 343.1548, found = 343.1542
m.p. 97-98 °C

Quinoline **32**

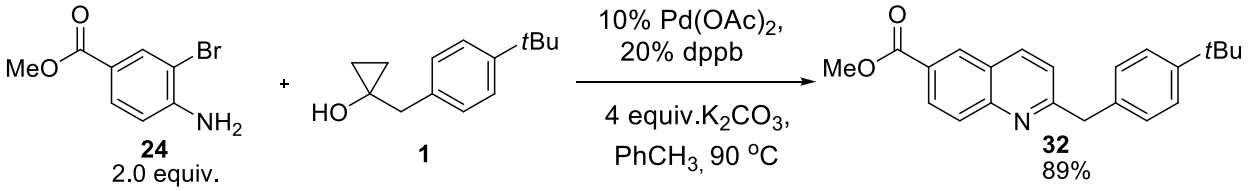

Following *General Procedure 1* cyclopropanol **1** (0.050 g, 0.25 mmol, 1 equiv.) and 2-bromoaniline **24** (0.11 g, 0.49 mmol, 2 equiv.) were converted to quinoline. Purification by flash column chromatography using 25% solution of EtOAc in hexanes afforded the quinoline **32** (0.073 g, 0.22 mmol) as a slight yellow solid in 89% yield.

Data for **32**
^{1}H NMR (400 MHz, $CDCl_3$)
δ 8.54 (s, 1 H), 8.31 (d, *J* = 8.8 Hz, 1 H), 8.13 (dd, *J* = 8.6, 3.6Hz, 2 H), 7.36 (d, *J* = 8 Hz, 2 H), 7.33 (d, *J* = 8.6 Hz, 1 H), 7.27 (d, *J* = 8 Hz, 2 H), 4.35 (s, 2 H), 4.00 (s, 3 H), 1.32 (s, 9 H)
^{13}C NMR (100 MHz, $CDCl_3$)
δ 166.7, 163.9, 149.7, 149.5, 137.5, 135.6, 130.7, 129.3, 129.0, 128.9, 127.4, 125.9, 125.6, 122.4, 52.3, 45.2, 34.4, 31.3
IR Alpha-Platinum ATR, Bruker, diamond crystal
υ = 3057, 2966, 1706, 1620, 1600, 1475, 1271, 1250, 1071, 764 cm^{-1}
HRMS TOF EI
Calculated for $[C_{22}H_{23}NO_2]^+$ = 333.1729, found = 333.1729
m.p. 92-93 °C

Quinoline **33**

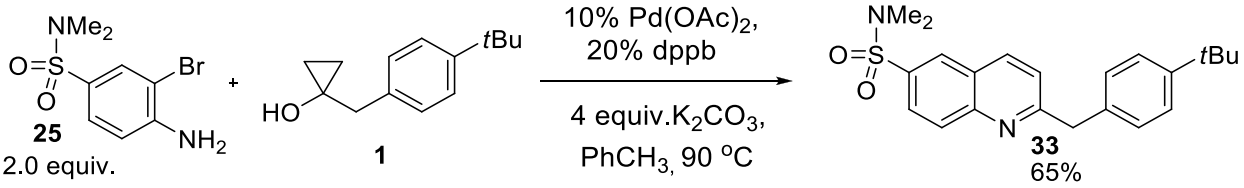

Following *General Procedure 1* cyclopropanol **1** (0.050 g, 0.25 mmol, 1 equiv.) and 2-bromoaniline **25** (0.14 g, 0.49 mmol, 2 equiv.) were converted to quinoline. Purification by flash column chromatography using 45% solution of EtOAc in hexanes afforded the quinoline **33** (0.061 g, 0.16 mmol) as a slight yellow solid in 65% yield.

Data for **33**
^{1}H NMR (400 MHz, $CDCl_3$)
δ 8.30 (s, 1 H), 8.23 (d, *J* = 8.8 Hz, 1 H), 8.17 (d, *J* = 8.4 Hz, 1 H), 8.01 (d, *J* = 9.2 Hz, 1 H), 7.41 (d, *J* = 8.4 Hz, 1 H), 7.36 (d, *J* = 8.0 Hz, 2 H), 7.27 (d, *J* = 8.0 Hz, 2 H), 4.36 (s, 2 H), 2.78 (s, 6 H), 1.32 (s, 9 H)
^{13}C NMR (100 MHz, $CDCl_3$)
δ 164.5, 149.5, 149.0, 137.3, 135.3, 132.8, 130.3, 128.8, 128.6, 126.6, 125.8, 125.6, 123.1, 45.1, 37.9, 34.3, 31.2
IR Alpha-Platinum ATR, Bruker, diamond crystal
υ = 3090, 2959, 1614, 1592, 1331, 1135, 1142, 956, 712, 607, 481 cm^{-1}
HRMS TOF EI
Calculated for $[C_{22}H_{26}N_2O_2S]^+$ = 382.1715, found = 382.1709
m.p. 156-157 °C

Quinoline **34**

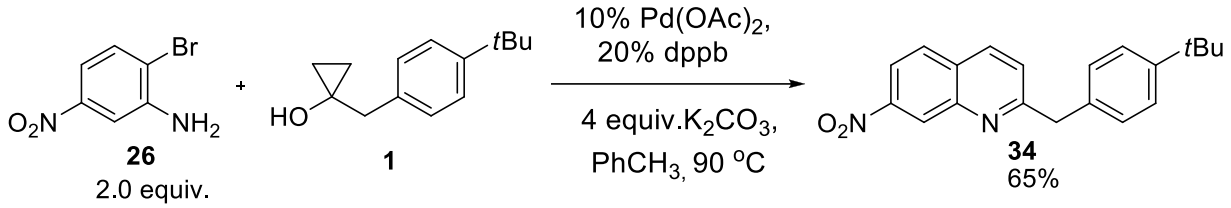

Following *General Procedure 2* cyclopropanol **1** (0.050 g, 0.25 mmol, 1 equiv.) and 2-bromoaniline **26** (0.11 g, 0.49 mmol, 2 equiv.) were converted to quinoline. Purification by flash column chromatography using 15% solution of EtOAc in hexanes afforded the quinoline **34** (0.068 g, 0.21 mmol) as a bright yellow solid in 87% yield.

Data for **34**
^{1}H NMR (400 MHz, $CDCl_3$)
δ 9.01 (d, *J* = 1.6 Hz 1 H), 8.28 (dd, *J* = 8.6,1.6 Hz, 1 H), 8.14 (d, *J* = 8.8 Hz, 1 H), 7.92 (d, *J* = 8.8 Hz,1 H), 7.46 (d, *J* = 8.6 Hz, 1 H), 7.37 (d, *J* = 8.0 Hz, 2 H), 7.28 (d, *J* = 8.0 Hz, 2 H), 4.37 (s, 2 H), 1.32 (s, 9 H)
^{13}C NMR (100 MHz, $CDCl_3$)
δ 164.0, 149.6, 148.0, 146.7, 136.0, 135.2, 129.9, 128.9, 128.8, 125.6, 125.3, 124.5, 119.4, 44.9, 34.3, 31.2.
IR Alpha-Platinum ATR, Bruker, diamond crystal
υ = 3090, 2960, 1627, 1599, 1528, 1343, 1071, 827, 739 cm^{-1}
HRMS TOF EI
Calculated for $[C_{20}H_{20}N_2O_2]^+$ = 320.1525, found = 320.1525
m.p. 97-98 °C

Cyclopropanol **1-*d*$_4$**

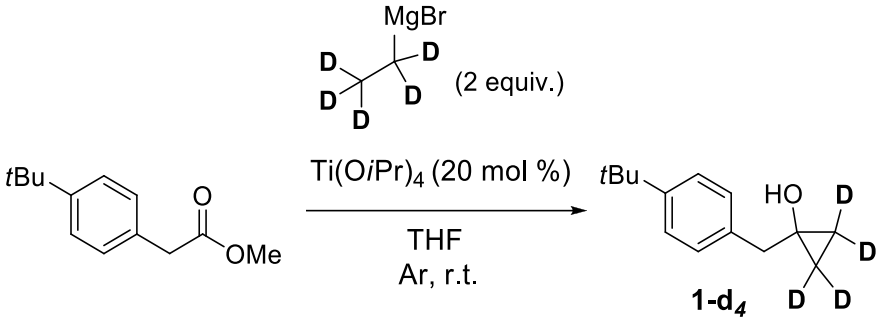

To a round-bottom flask equipped with a magnetic stir bar were added methyl 3-phenylpropanoate (0.50 g, 2.4 mmol), freshly distilled THF (7.00 mL) and titanium (IV) isopropoxide (0.22 mL, 0.73 mmol, 0.3 equiv.). The reaction vessel was purged with argon and a freshly made solution of d_5-EtMgBr (3.00 mL, 4.9 mmol, 2.0 equiv.) in THF (3 mL) was transferred dropwise via a cannula under an argon atmosphere. After stirring overnight, the resultant mixture was quenched with 1 M HCl and extracted with ethyl acetate three times. The combined organic layers were washed with brine and dried with $MgSO_4$. Filtration, concentration in vacuo, and purification of the crude product by flash coloumn chromatography (20% EtOAc:hexanes) provided cyclopropanol **1-d$_4$** as a colourless oil in 76% yield (0.38 g).

Data for **1-d$_4$**
^{1}H NMR (400 MHz, $CDCl_3$)
δ 7.38 (d, *J* = 8.4 Hz, 2 H), 7.27 (d, *J* = 8.4 Hz, 2 H), 2.88 (s, *J* = 8.8 Hz, 2 H), 2.05 (s, 1 H), 1.36 (s, 9 H)
^{13}C NMR (100 MHz, $CDCl_3$)
δ 149.2, 135.7, 129.2, 125.3, 55.6, 43.5, 34.4, 31.5, 12.16 (pentet, $^1J_{CD}$ = 24 Hz)
IR Alpha-Platinum ATR, Bruker, diamond crystal
υ = 3253, 3056, 2961, 2196, 1616, 1509, 1362, 1229, 1167, 816, 559 cm^{-1}
HRMS TOF EI
Calculated for $[C_{14}H_{16}D_4O]^+$ = 208.1765, found = 208.1765
m.p. 44-45 °C

Quinoline **32-d2**

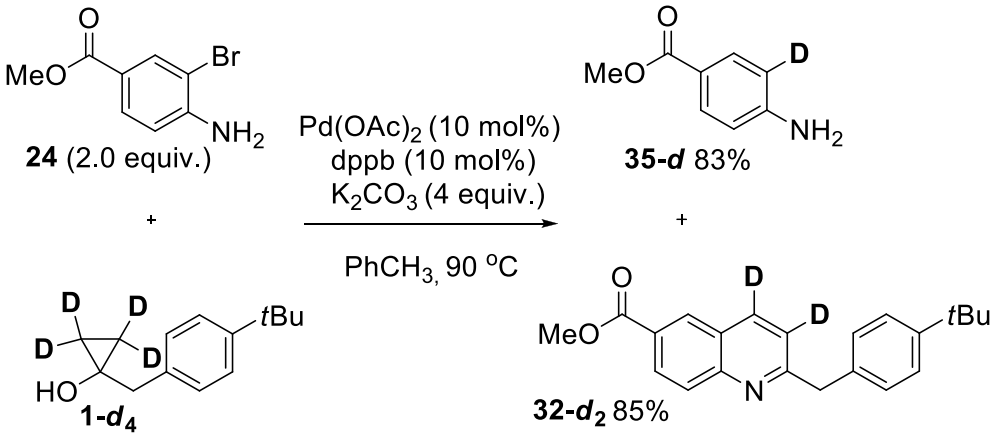

Following *General Procedure 1* cyclopropanol **1-d₄** (0.050 g, 0.24 mmol, 1 equiv.) and 2-bromoaniline **24** (0.11 g, 0.48 mmol, 2 equiv.) were converted to quinoline and aniline. Purification by flash column chromatography using 25% EtOAc solution in hexanes afforded the quinoline **32-d₂** (0.068 g, 0.20 mmol) as a yellow solid in 85% yield and aniline **35-d** (0.030 g, 0.39 mmol) as a yellow oil in 83% yield.

Data for **32-d2**
^{1}H NMR (400 MHz, $CDCl_3$)
δ 8.54 (s, 1 H), 8.30 (d, *J* = 8.8 Hz 1 H), 8.14 (d, *J* = 8.8 Hz 1 H), 7.36 (d, *J* = 8.4 Hz 2 H), 7.27 (d, *J* = 8.4 Hz 2 H), 4.35 (s, 2 H), 4.00 (s, 3 H), 1.32 (s, 9 H)
^{13}C NMR (100 MHz, $CDCl_3$)
δ 166.6, 163.8, 149.6, 149.4, 137.0 (t,$^{1}J_{CD}$ = 24.5 Hz), 135.5, 130.5, 129.2, 128.9, 128.8, 127.4, 125.7, 125.5, 121.9 (t,$^{1}J_{CD}$ = 24.8 Hz), 52.2, 45.0, 34.3, 31.2
^{2}H NMR (61 MHz, $CDCl_3$)
δ 8.14 (s, 1 D), 7.35 (s, 1 D)
IR Alpha-Platinum ATR, Bruker, diamond crystal
υ = 3057, 2952, 1707, 1618, 1445, 1251, 1107, 768, 540, 463 cm^{-1}
HRMS TOF EI
Calculated for $[C_{22}H_{21}D_2NO_2]^+$ = 335.1854, found = 335.1849
m.p. 94-95 °C

Data for **35-d**
^{1}H NMR (400 MHz, $CDCl_3$)
δ 7.87 (d, *J* = 6.8 Hz, 2 H), 6.65 (d, *J* = 8.4 Hz, 1 H), 4.09 (br s, 2 H), 3.87 (s, 3 H)
^{13}C NMR (100 MHz, $CDCl_3$)
δ 167.1, 150.8, 131.5, 131.4, 119.5, 113.7, 113.4 (t,$^{1}J_{CD}$ = 24 Hz), 51.5
^{2}H NMR (61 MHz, $CDCl_3$)
δ 6.69 (s, 1 D)
IR Alpha-Platinum ATR, Bruker, diamond crystal
υ = 3336, 3226, 3032, 2944, 1682, 1601, 1434, 1284, 768, 492 cm^{-1}
HRMS TOF EI
Calculated for $[C_8H_8DNO_2]^+$ = 152.0696, found =152.0691

5.3 Experimental Procedures – The Acid-Free Cyclopropanol-Minisci Reaction and the Catalytic Role of Silver-Pyridine Complexes

General Procedure 2. *The Acid-Free Cyclopropanol-Minisci Reaction and the Catalytic Role of Silver-Pyridine Complexes*.

Cyclopropanol Minisci reaction using **$AgNO_3$**

To a flame-dried round-bottomed flask equipped with a stir bar and charged with $AgNO_3$ (0.016 g, 0.094 mmol, 0.1 equiv.) was added aza-heterocycle (3.00 equiv.) and a 0.95 M solution of cyclopropanol a (0.12 g, 0.94 mmol, 1.0 equiv.) in anhydrous DMF (1 mL). This solution was allowed to stir at room temperature for 10 minutes before cooling to 0 °C. $(NH_4)_2S_2O_8$ (0.64 g, 2.81 mmol, 3.0 equiv.) was added portion-wise to avoid overheating. The progress of the reaction was monitored by TLC. Upon completion, the reaction was quenched with 1 N NaOH, diluted with ethyl acetate, and the phases were separated. The organic phase was washed with brine, dried with Na_2SO_4, and concentrated in vacuo. The crude product was purified by flash column chromatography, eluting with the indicated solvent mixture to afford the desired product.

General Procedure 3. *The Acid-Free Cyclopropanol-Minisci Reaction and the Catalytic Role of Silver-Pyridine Complexes*.

Cyclopropanol Minisci reaction using **$(Ag[bipy]_2)•S_2O_8$**

To a flame-dried round-bottomed flask equipped with a stir bar and charged with $(Ag[bipy]_2)S_2O_8$ (0.057 g, 0.094 mmol, 0.1 equiv.) was added aza-heterocycle (3.00 equiv.) and a 0.95 M solution of cyclopropanol a (0.12 g, 0.94 mmol, 1.0 equiv.) in anhydrous DMF (1 mL). This solution was allowed to stir at room temperature for 10 minutes before cooling to 0 °C. $(NH_4)_2S_2O_8$ (0.64 g, 2.8 mmol, 3.0 equiv.) was added portion-wise to avoid overheating. The progress of the reaction was monitored by TLC. Upon completion, the reaction was quenched with 1 N NaOH, diluted with ethyl acetate, and the phases were separated. The organic phase was washed with brine, dried with Na_2SO_4, and concentrated in vacuo. The crude product was purified by flash column chromatography, eluting with the indicated solvent mixture to afford the desired product.

Procedure 4: <u>One gram scale Cyclopropanol Minisci reaction using $[Ag(bipy)_2]•S_2O_8$</u>

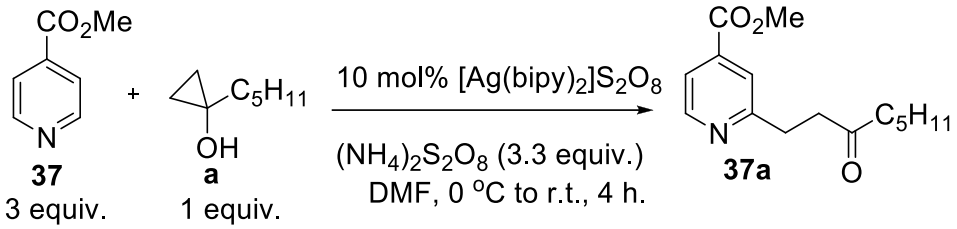

To a flame-dried round-bottomed flask equipped with a stir bar and charged with $(Ag[bipy]_2)S_2O_8$ (0.48 g, 0.78 mmol, 0.1 equiv.) was added aza-heterocycle **37** (3.2 g, 23 mmol, 3.0 equiv.) and a 0.90 M solution of cyclopropanol **a** (1.0 g, 7.8 mmol, 1.0 equiv.) in anhydrous DMF (8.70 mL). This solution was allowed to stir at room temperature for 10 minutes before cooling to 0 °C. $(NH_4)_2S_2O_8$ (5.9 g, 26 mmol, 3.3 equiv.) was added portion-wise to avoid overheating. The progress of the reaction was monitored by TLC. Upon completion, the reaction was quenched with 1 N NaOH, diluted with ethyl acetate, and the phases were separated. The organic phase was washed with brine, dried with Na_2SO_4, and concentrated *in vacuo*. The crude product was purified by flash column chromatography, eluting with 7:13 EtOAc:Hexanes and provided product **37a** (1.5 g, 5.6 mmol) in 72% yield.

Pyridine coupled products 43a (CAS 1597445-03-8) **and 43a'** (1596778-44-7)

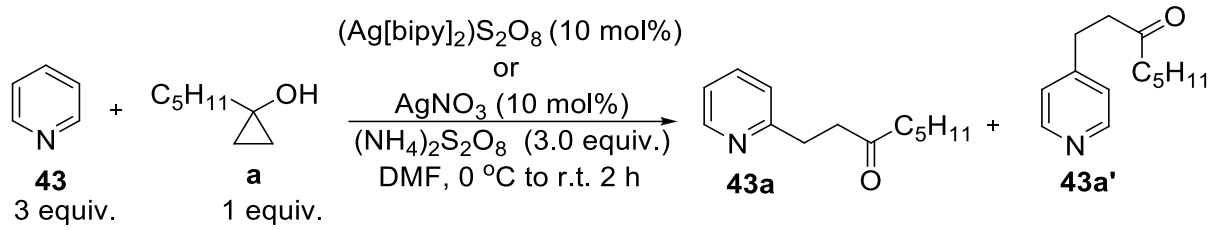

Following *General Procedure 2*, pyridine **43** (0.19 g, 2.4 mmol, 3 equiv.) was converted to coupled products **43a** (0.060 g, 0.30 mmol) in 38% and **43a'** (0.025 g, 0.12 mmol) in 15%. Following *General Procedure 3* produced **43a** (0.070 g, 0.35 mmol) in 44% and **43a'** (0.028 g, 0.13 mmol) in 17%. Chromatography: 1:3 Acetone:hexanes.

Data for **43a**
^{1}H-NMR (400 MHz, $CDCl_3$)
δ 8.50 (d, *J* = 5.2 Hz, 2 H), 7.13 (d, *J* = 5.2 Hz, 2 H), 2.91 (t, *J* = 7.2 Hz, 2 H), 2.77 (t, *J* = 7.2 Hz, 2 H), 2.41 (t, *J* = 7.2 Hz, 2 H), 1.58 (p, *J* = 7.2 Hz, 2 H), 1.27 (m, 4 H), 0.89 (t, *J* = 7.2 Hz, 3 H).
^{13}C-NMR (100 MHz, $CDCl_3$)
δ 209.2, 150.4, 149.4, 123.7, 42.8, 42.5, 31.2, 28.7, 23.3, 22.3, 13.8.
IR Alpha-Platinum ATR, Bruker, diamond crystal
υ = 3109, 2956, 1712, 1603, 1501, 694 cm^{-1}
HRMS ESI
Calculated for M+H$^+$ $[C_{13}H_{20}NO]^+$ = 206.1593, found 206.1534

Data for **43a'**
^{1}H-NMR (400 MHz, $CDCl_3$)
δ 8.52 (d, *J* = 4.4 Hz, 1 H), 7.59 (dd, *J* = 7.9, 7.6 Hz, 1 H), 7.20 (d, *J* = 7.6 Hz, 1 H), 7.12 (dd, *J* = 7.9, 4.8 Hz, 1 H), 3.08 (t, *J* = 7.2 Hz, 2 H), 2.93 (t, *J* = 7.2 Hz, 2 H), 2.44 (t, *J* = 7.2 Hz, 2 H), 1.59 (p, *J* = 7.2 Hz, 2 H), 1.29 (m, 4 H), 0.89 (t, *J* = 7.2 Hz, 3 H).
^{13}C-NMR (100 MHz, $CDCl_3$)
δ 210.3, 160.5, 149.0, 136.2, 123.1, 122.1, 42.8, 41.4, 31.6, 31.3, 23.4, 22.3, 13.8.
IR Alpha-Platinum ATR, Bruker, diamond crystal
υ = 3045, 2956, 1710, 1603, 1501, 655 cm^{-1}
HRMS ESI
Calculated for M+H$^+$ $[C_{13}H_{20}NO]^+$ = 206.1593, found 206.1532

4-Methylpyridine coupled product 44a

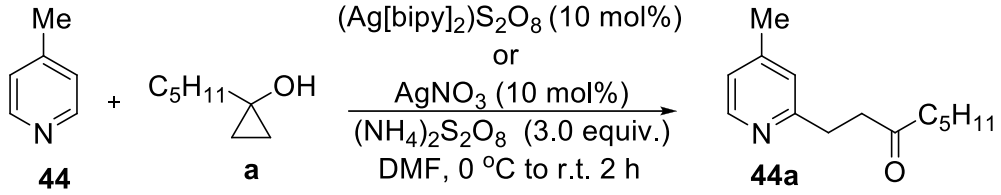

Following *General Procedure 2,* 4-methylpyridine **44** (0.26 g, 2.8 mmol, 3 equiv.) was converted to coupled product **44a** (0.11 g, 0.51 mmol) in 55% yield. Following *General Procedure 3* produced **44a** (0.13 g, 0.62 mmol) in 66% isolated yield. Chromatography: 7:3 EtOAc:hexanes.

Data for **44a**
^{1}H-NMR (400 MHz, $CDCl_3$)
δ 8.36 (d, *J* = 4.8 Hz, 1 H), 7.03 (s, 1 H), 6.93 (d, *J* = 4.8 Hz, 1 H), 3.03 (t, *J* = 7.2 Hz, 2 H), 2.92 (t, *J* = 7.2 Hz, 2 H), 2.43 (t, *J* = 7.2 Hz, 2 H), 2.33 (s, 3 H), 1.58 (p, *J* = 7.2 Hz, 2 H), 1.28 (m, 4 H), 0.89 (t, *J* = 7.2 Hz, 3 H).
^{13}C-NMR (100 MHz, $CDCl_3$)
δ 210.4, 160.2, 148.7, 147.3, 123.9, 122.1, 42.7, 41.5, 31.4, 31.2, 23.4, 22.3, 20.8, 13.8.
IR Alpha-Platinum ATR, Bruker, diamond crystal
υ = 3056, 2929, 1710, 1605, 1561, 1374, 821 cm^{-1}
HRMS TOF EI
Calculated for $[C_{14}H_{21}NO]^+$ = 219.1623, found 219.1620

3-Methylpyridine coupled products 45a and 45a'

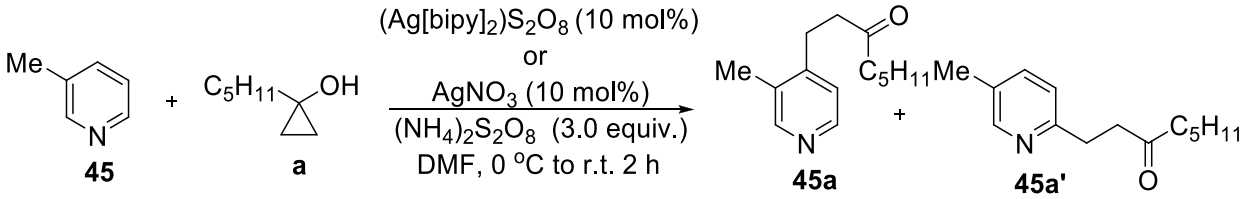

Following *General Procedure 2*, 3-methylpyridine **45** (0.22 g, 2.3 mmol, 3 equiv.) was converted to coupled products **45a** (0.03 g, 0.14 mmol) in 18% yield and **45a'** (0.050 g, 0.23 mmol) in 30%. Following *General Procedure 3* produced **45a** (0.031 g, 0.14 mmol) in 19% yield and **45a'** (0.071 g, 0.32 mmol) in 44%. Chromatography: 35% Acetone in hexanes.

Data for **45a**
^{1}H-NMR (300 MHz, $CDCl_3$)
δ 8.33 (m, 2 H), 7.02 (d, *J* = 6.8 Hz, 1 H), 2.88 (t, *J* = 7.5 Hz, 2 H), 2.71 (t, *J* = 7.5 Hz, 2 H), 2.42 (t, *J* = 7.5 Hz, 2 H), 2.30 (s, 3 H), 1.59 (p, *J* = 7.5 Hz, 2 H), 1.26 (m, 4 H), 0.89 (t, *J* = 7.0 Hz, 3 H).
^{13}C-NMR (100 MHz, $CDCl_3$)
δ 209.3, 150.6, 148.2, 147.5, 131.5, 123.0, 42.9, 41.3, 31.2, 25.9, 23.4, 22.3, 16.0, 13.8.
IR Alpha-Platinum ATR, Bruker, diamond crystal
υ = 3056, 2929, 1712, 1595, 1406, 831 cm^{-1}
HRMS TOF EI
Calculated for $[C_{14}H_{21}NO]^+$ = 219.1623, found 219.1620

Data for **45a'**
^{1}H-NMR (300 MHz, $CDCl_3$)
δ 8.33 (d, *J* = 3.3 Hz, 1 H), 7.40 (d, *J* = 7.5 Hz, 1 H), 7.03 (dd, *J* = 7.5, 3.3 Hz, 1 H), 3.05 (t, *J* = 6.3 Hz, 2 H), 2.96 (t, *J* = 6.3 Hz, 2 H), 2.51 (t, *J* = 7.5 Hz, 2 H),
2.34 (s, 3 H), 1.61 (p, *J* = 7.5 Hz, 2 H), 1.28 (m, 4 H), 0.90 (t, *J* = 7.2 Hz, 3 H).
^{13}C-NMR (100 MHz, $CDCl_3$)
δ 210.9, 158.3, 146.2, 137.2, 131.1, 121.0, 42.9, 39.9, 31.3, 28.3, 23.5, 22.3, 18.6, 13.8.
IR Alpha-Platinum ATR, Bruker, diamond crystal
υ = 3055, 2929, 1712, 1573, 1464, 787 cm^{-1}
HRMS TOF EI
Calculated for $[C_{14}H_{21}NO]^+$ = 219.1623, found 219.1618

2-Methylpyridine coupled products 46a and 46a'

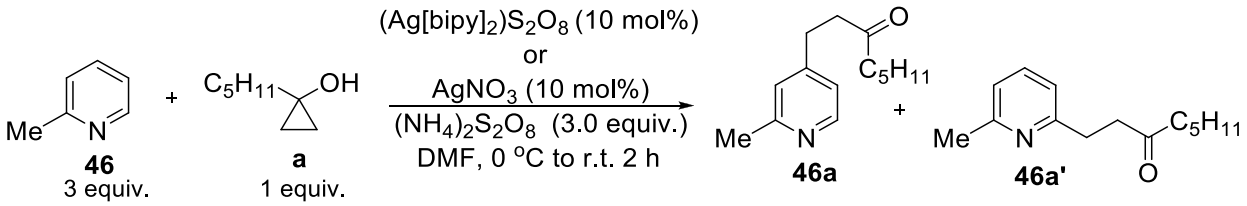

Following *General Procedure 2*, 2-methylpyridine **46** (0.22 g, 2.3 mmol, 3 equiv.) was converted to coupled products **46a** (0.020 g, 0.093 mmol) in 12% and **46a'** (0.059 g, 0.26 mmol) in 34%. Following *General Procedure 3* produced **46a** (0.025 g, 0.12 mmol) in 15% and **46a'** (0.065 g, 0.31 mmol) in 38%. Chromatography: 30% Acetone in hexanes.

Data for **46a**
^{1}H-NMR (400 MHz, $CDCl_3$)
δ 8.37 (d, *J* = 5.2 Hz, 1 H), 7.00 (s, 1 H), 6.92 (d, *J* = 5.2 Hz, 1 H), 2.87 (t, *J* = 7.6 Hz, 2 H), 2.74 (t, *J* = 7.5 Hz, 2 H), 2.52 (s, 3 H), 2.40 (t, *J* = 7.6 Hz, 2 H), 1.57 (p, *J* = 7.5 Hz, 2 H), 1.26 (m, 4 H), 0.89 (t, *J* = 7.0 Hz, 3 H).
^{13}C-NMR (100 MHz, $CDCl_3$)
δ 209.3, 158.2, 150.5, 148.9, 123.3, 120.7, 42.9, 42.7, 31.2, 28.7, 24.1, 23.4, 22.3, 13.8.
IR Alpha-Platinum ATR, Bruker, diamond crystal
υ = 3056, 2929, 1711, 1605, 1373, 834 cm^{-1}
HRMS TOF EI
Calculated for $[C_{14}H_{21}NO]^+$ = 219.1623, found 219.1629

Data for **46a'**
^{1}H-NMR (400 MHz, $CDCl_3$)
δ 7.48 (t, *J* = 7.6 Hz, 1 H), 6.98 (t, *J* = 7.6 Hz, 2 H), 3.04 (t, *J* = 7.6 Hz, 2 H), 2.89 (t, *J* = 7.6 Hz, 2 H), 2.53 (s, 3 H), 2.44 (t, *J* = 7.6 Hz, 2 H), 1.59 (p, *J* = 7.5 Hz, 2 H), 1.28 (m, 4 H), 0.90 (t, *J* = 7.6 Hz, 3 H).
^{13}C-NMR (100 MHz, $CDCl_3$)
δ 210.4, 159.8, 157.6, 136.5, 120.5, 119.8, 42.8, 41.8, 31.8, 31.3, 24.3, 23.4, 22.3,13.8.
IR Alpha-Platinum ATR, Bruker, diamond crystal
υ = 3064, 2955, 1712, 1591, 1456, 780 cm^{-1}
HRMS TOF EI
Calculated for $[C_{14}H_{21}NO]^+$ = 219.1623, found 219.1628

2-Phenylpyridine coupled products 47a and 47a'

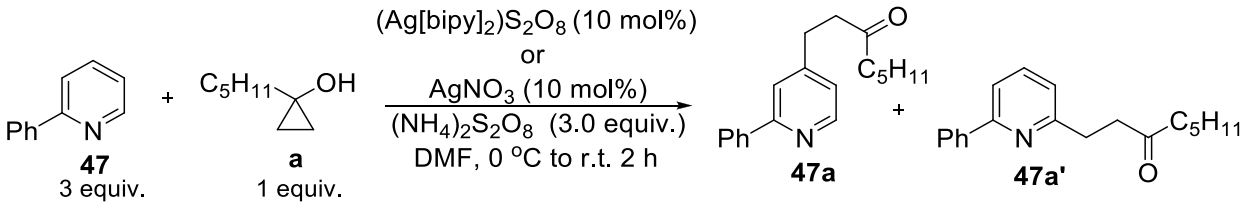

Following *General Procedure 2*, 2-phenylpyridine **47** (0.44 g, 2.2 mmol, 3 equiv.) was converted to coupled products **47a** (0.037 g, 0.13 mmol) in 15% yield and **47a'** (0.050 g, 0.19) in 25%. Following *General Procedure 3* produced **47a** (0.052 g, 0.18 mmol) in 18% yield and **47a'** (0.052 g, 0.19 mmol) in 29%. Chromatography: 2:3 EtOAc:hexanes.

Data for **47a**
^{1}H-NMR (400 MHz, $CDCl_3$)
δ 8.60 (d, *J* = 5.2 Hz, 1 H), 7.96 (d, *J* = 7.6 Hz, 2 H), 7.57 (s, 1 H), 7.49 (dd, *J* = 7.6, 7.2 Hz, 2 H), 7.44 (t, *J* = 7.6 Hz, 1 H), 2.97 (t, *J* = 7.6 Hz, 2 H), 2.81 (t, *J* = 7.6 Hz, 2 H), 2.42 (t, *J* = 7.2 Hz, 2 H), 1.59 (p, *J* = 7.2 Hz, 2 H), 1.27 (m, 4 H), 0.89 (t, *J* = 7.2 Hz, 3 H).
^{13}C-NMR (100 MHz, $CDCl_3$)
δ 209.3, 157.5, 151.0, 149.5, 139.2, 128.8, 128.6, 126.9, 122.2, 120.8, 42.9, 42.7, 31.2, 28.9, 23.4, 22.3, 13.8.
IR Alpha-Platinum ATR, Bruker, diamond crystal
υ = 3057, 2929, 1711, 1600, 1556, 1405, 776, 695 cm^{-1}
HRMS TOF EI
Calculated for $[C_{19}H_{23}NO]^+$ = 281.1780, found 281.1785

Data for **47a'**
^{1}H-NMR (300 MHz, $CDCl_3$)
δ 7.98 (d, *J* = 7.2 Hz, 2 H), 7.65 (t, *J* = 7.8 Hz, 1 H), 7.50 (m, 4 H), 7.13 (d, *J* = 7.5 Hz, 1 H), 3.16 (t, *J* = 7.2 Hz, 2 H), 3.02 (t, *J* = 7.2 Hz, 2 H), 2.50 (t, *J* = 7.5 Hz, 2 H), 1.58 (p, *J* = 7.6 Hz, 2 H), 1.29 (m, 4 H), 0.89 (t, *J* = 7.2 Hz, 3 H).
^{13}C-NMR (100 MHz, $CDCl_3$)
δ 210.6, 160.2, 156.5, 139.5, 136.8, 128.6, 128.5, 126.8, 121.4, 117.8, 42.9, 41.2, 31.7, 31.3, 23.4, 22.4, 13.8.
IR Alpha-Platinum ATR, Bruker, diamond crystal
υ = 3062, 2929, 1710, 1572, 1409, 758, 693 cm^{-1}
HRMS TOF EI
Calculated for $[C_{19}H_{23}NO]^+$ = 281.1780, found 281.1788

3,5-Dimethylpyridine coupled products 48a and 48a'

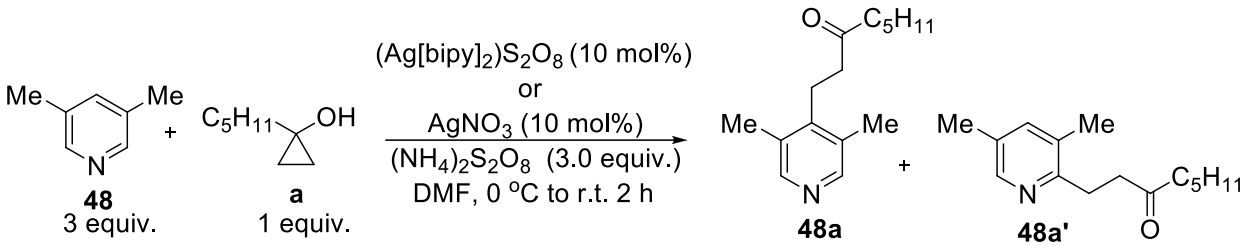

Following *General Procedure 2*, 3,5-dimethylpyridine **48** (0.30 g, 2.8 mmol, 3 equiv.) was converted to coupled products **48a** (0.022 g, 0.092 mmol) in 10% yield and **48a'** (0.054 g, 0.23 mmol) in 25% yield. Following *General Procedure 3* produced **48a** (0.028 g, 0.12 mmol) in 13% yield and **48a'** (0.075 g, 0.33 mmol) in 35% yield. Chromatography: 1:1 EtOAc:hexanes.

Data for **48a**
^{1}H-NMR (400 MHz, $CDCl_3$)
δ 8.22 (s, 2 H), 2.90 (t, *J* = 7.6 Hz, 2 H), 2.55 (t, *J* = 7.6 Hz, 2 H), 2.45 (t, *J* = 7.2 Hz, 2 H), 2.28 (s, 6 H), 1.62 (p, *J* = 7.6 Hz, 2 H), 1.31 (m, 4 H), 0.91 (t, *J* = 7.0 Hz, 3 H).
^{13}C-NMR (100 MHz, $CDCl_3$)
δ 209.5, 148.7, 146.8, 130.9, 42.7, 40.4, 31.3, 23.5, 23.0, 22.3, 16.1, 13.8.
IR Alpha-Platinum ATR, Bruker, diamond crystal
υ = 3113, 2926, 1715, 1600, 1457, 881 cm^{-1}
HRMS TOF EI
Calculated for $[C_{15}H_{23}NO]^+$ = 233.1780, found 233.1782

Data for **48a'**
^{1}H-NMR (400 MHz, $CDCl_3$)
δ 8.16 (s, 1 H), 7.23 (s, 1 H), 3.00 (t, *J* = 7.2 Hz, 2 H), 2.92 (t, *J* = 7.2 Hz, 2 H), 2.49 (t, *J* = 7.6 Hz, 2 H), 2.29 (s, 3 H), 2.26 (s, 3 H), 1.60 (p, *J* = 7.6 Hz, 2 H),1.27 (m, 4 H), 0.89 (t, *J* = 7.2 Hz, 3 H).
^{13}C-NMR (100 MHz, $CDCl_3$)
δ 211.0, 155.4, 146.5, 138.1, 130.5, 130.3, 42.9, 40.2, 31.3, 27.9, 23.5, 22.4, 18.5, 17.7, 13.8.
IR Alpha-Platinum ATR, Bruker, diamond crystal
υ = 3115, 2926, 1712, 1569, 879 cm^{-1}
HRMS TOF EI
Calculated for $[C_{15}H_{23}NO]^+$ = 233.1780, found 233.1788

4-Methoxypypyridine coupled product 52a

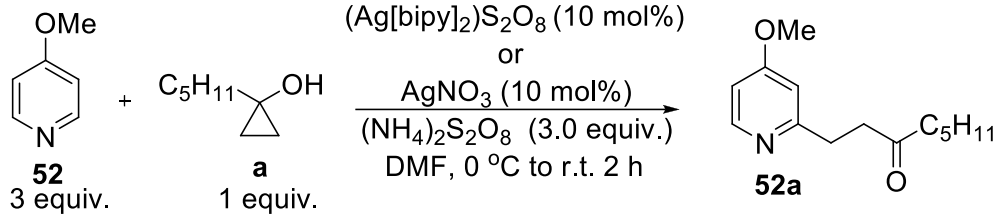

Following *General Procedure 2,* 4-methoxypyridine **52** (0.31 g, 2.8 mmol, 3 equiv.) was converted to coupled product **52a** (0.064 g, 0.27 mmol) in 33% yield. Chromatography: 7:3 EtOAc:hexanes.

Data for **52a**
^{1}H-NMR (400 MHz, $CDCl_3$)
δ 8.33 (d, *J* = 5.6 Hz, 1 H), 6.72 (d, *J* = 2.4 Hz, 1 H), 6.66 (dd, *J* = 5.6, 2.4 Hz, 1 H), 3.85 (s, 1 H), 3.03 (t, *J* = 7.2 Hz, 2 H), 2.92 (t, *J* = 7.2 Hz, 2 H), 2.43 (t, *J* = 7.2 Hz, 2 H), 2.43 (p, *J* = 7.2 Hz, 2 H), 1.30 (m, 4 H), 0.89 (t, *J* = 7.2 Hz, 3 H)
^{13}C-NMR (75 MHz, $CDCl_3$)
δ 210.3, 165.9, 162.1, 150.1, 108.8, 107.6, 54.9, 42.8, 41.5, 31.7, 31.2, 23.4, 22.3, 13.8.
IR Alpha-Platinum ATR, Bruker, diamond crystal
υ = 3066, 2933, 1715, 1602, 1432, 1250, 1152, 992, 740 cm^{-1}
HRMS TOF EI (M+)
Calculated for $[C_{14}H_{21}NO_2]^+$ = 235.1572, found 235.1577

3-Methoxypyridine coupled product 53a

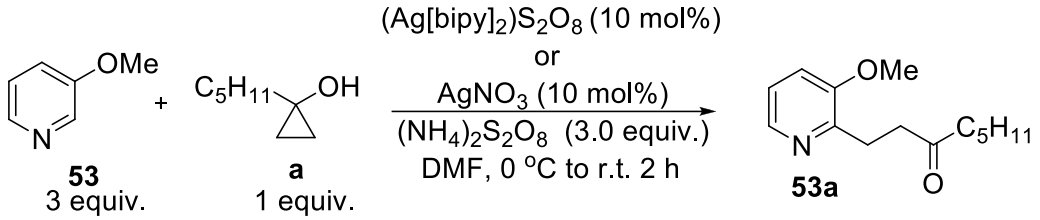

53 3 equiv. + **a** 1 equiv. → **53a**

Following *General Procedure 2,* 3-methoxypyridine **53** (0.51 g, 4.7 mmol, 3 equiv.) was converted to coupled product **53a** (0.055 g, 0.24 mmol) in 15% yield. Following *General Procedure 3* produced **53a** (0.14 g, 0.58 mmol) in 37% yield. Chromatography: 6:4 EtOAc:hexanes.

Data for **53a**
^{1}H-NMR (400 MHz, $CDCl_3$)
δ 8.02 (t, *J* = 5.6 Hz, 1 H), 7.04 (s, 2 H), 3.78 (s, 3 H), 3.05 (t, *J* = 7.2 Hz, 2 H), 2.83 (t, *J* = 7.2 Hz, 2 H), 2.43 (t, *J* = 7.2 Hz, 2 H), 1.56 (p, *J* = 7.2 Hz, 2 H), 1.25 (m, 4 H), 0.84 (t, *J* = 7.2 Hz, 3 H)
^{13}C-NMR (75 MHz, $CDCl_3$)
δ 210.7, 153.4, 150.2, 140.0, 121.7, 116.2, 54.9, 42.7, 39.7, 31.3, 26.0, 23.4, 22.3, 13.8.
IR Alpha-Platinum ATR, Bruker, diamond crystal
υ = 3032, 2950, 1717, 1600, 1432, 1250, 1152 cm^{-1}
HRMS TOF EI (M+)
Calculated for $[C_{14}H_{21}NO_2]^+$ = 235.1572, found 235.1576

4-(Trifluoromethyl)pyridine coupled product 39a

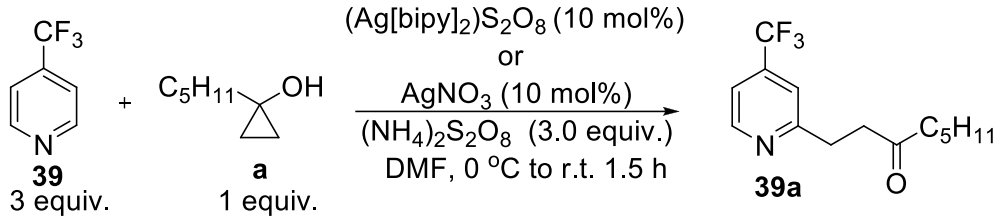

Following *General Procedure 2*, 4-(trifluromethyl)pyridine **39** (0.41 g, 2.8 mmol, 3 equiv.) was converted to coupled product **39a** (0.16 g, 0.57 mmol) in 61% yield. Following *General Procedure 3* produced **39a** (0.18 g, 0.66 mmol) in 70% yield. Chromatography: 1:3 EtOAc:hexanes.

Data for **39a**
^{1}H-NMR (400 MHz, $CDCl_3$)
δ 8.68 (d, *J* = 5.2 Hz, 1 H), 7.44 (s, 1 H), 7.33 (d, *J* = 5.2 Hz, 1 H), 3.17 (t, *J* = 7.0 Hz, 2 H), 2.97 (t, *J* = 7.0 Hz, 2 H), 2.46 (t, *J* = 7.2 Hz, 2 H), 1.58 (p, *J* = 7.6 Hz, 2 H), 1.28 (m, 4 H), 0.90 (t, *J* = 7.0 Hz, 3 H).
^{13}C-NMR (100 MHz, $CDCl_3$)
δ 209.6, 162.1, 149.9, 138.2 (q, $^{2}J_{C\text{-}F}$ = 33.0 Hz), 122.9 (q, $^{1}J_{C\text{-}F}$ = 271.4 Hz), 118.7, 116.5, 42.7, 40.7, 31.4, 31.2, 23.3, 22.2, 13.6.
^{19}F-NMR (376 MHz, $CDCl_3$)
δ –64.4
IR Alpha-Platinum ATR, Bruker, diamond crystal
υ = 3064, 2932, 1714, 1609, 1327, 1133, 841, 668 cm^{-1}
HRMS TOF EI
Calculated for $[C_{14}H_{18}F_3NO]^+$ = 273.1340, found 273.1348

Methyl isonicotinate coupled product 37a

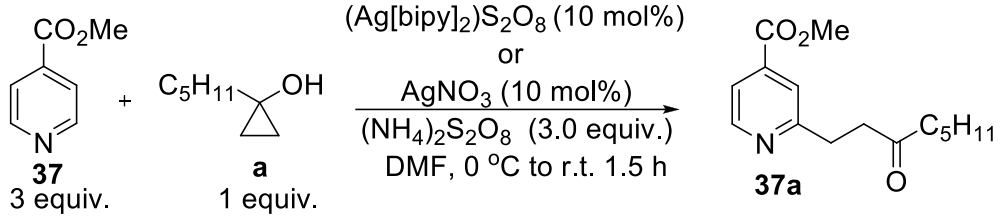

Following *General Procedure 2*, methyl isonicotinate **37** (0.39 g, 2.8 mmol, 3 equiv.) was converted to coupled product **37a** (0.15 g, 0.60 mmol) in 64% yield. Following *General Procedure 3* produced **37a** (0.19 g, 0.73 mmol) in 78% yield. Chromatography: 7:13 EtOAc:hexanes.

Data for **37a**
^{1}H-NMR (400 MHz, $CDCl_3$)
δ 8.65 (d, *J* = 4.8 Hz, 1 H), 7.76 (s, 1 H), 7.66 (d, *J* = 4.8 Hz, 1 H), 3.97 (s, 3 H), 3.16 (t, *J* = 7.2 Hz, 2 H), 2.96 (t, *J* = 7.2 Hz, 2 H), 2.45 (t, *J* = 7.6 Hz, 2 H), 1.59 (p, *J* = 7.6 Hz, 2 H), 1.29 (m, 4 H), 0.89 (t, *J* = 7.2 Hz, 3 H).
^{13}C-NMR (100 MHz, $CDCl_3$)
δ 209.2, 164.8, 162.0, 151.6, 138.7, 123.1, 121.3, 52.8, 42.6, 41.4, 33.5, 31.1, 23.2, 22.2, 13.7.
IR Alpha-Platinum ATR, Bruker, diamond crystal
υ = 3057, 2931, 1731, 1713, 1602, 1561, 1436, 1289, 1209,1111, 762 cm^{-1}
HRMS TOF EI
Calculated for $[C_{15}H_{21}NO_3]^+$ = 263.1521, found 263.1525

Methyl isonicotinate coupled product 37b

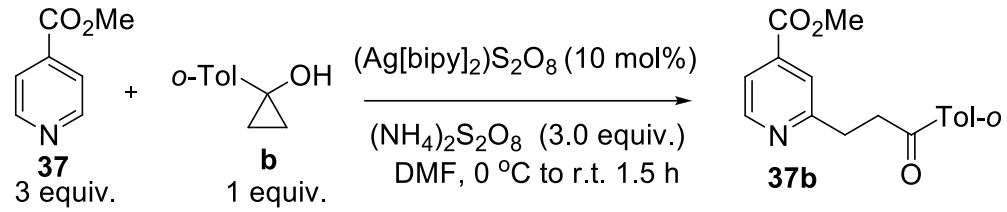

Following *General Procedure 2*, methyl isonicotinate **37** (0.28 g, 2.0 mmol, 3 equiv.) was converted to coupled product **37b** (0.11 g, 0.37 mmol) in 55% yield. Chromatography: 9:11 EtOAc:hexanes.

Data for **37**
^{1}H-NMR (400 MHz, $CDCl_3$)
δ 8.67 (d, *J* = 5.2 Hz, 1 H), 7.91 (d, *J* = 8.0 Hz, 1 H), 7.85 (s, 1 H), 7.67 (d, *J* = 5.2 Hz, 1 H), 7.27 (d, *J* = 8.0 Hz, 1 H), 3.97 (s, 3 H), 3.53 (t, *J* = 6.9 Hz, 2 H), 3.33 (t, *J* = 6.9 Hz, 2 H), 2.43 (s, 3 H).
^{13}C-NMR (75 MHz, $CDCl_3$)
δ 198.5, 165.7, 162.0, 150.0, 143.7, 137.5, 134.2, 129.1, 128.1, 122.4, 120.3, 52.5, 37.3, 32.0, 21.5.
IR Alpha-Platinum ATR, Bruker, diamond crystal
υ = 3050, 2930, 1729, 1698, 1600, 1500, 1289, 805 cm^{-1}
HRMS TOF EI (M+)
Calculated for $[C_{17}H_{17}NO_3]^+$ = 283.1208, found 283.1202

Methyl isonicotinate coupled product 37c (CAS 1830288-80-6)

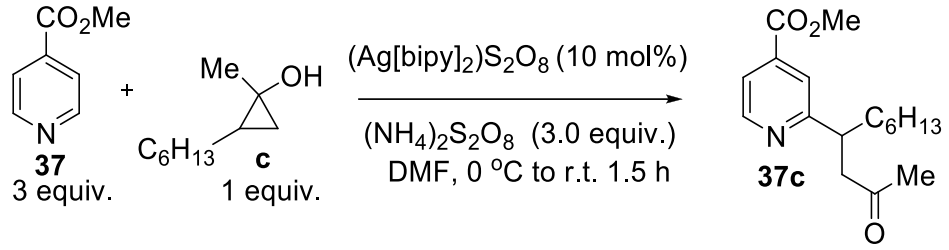

Following *General Procedure 2*, methyl isonicotinate **37** (0.28 g, 2.0 mmol, 3 equiv.) was converted to coupled product **37c** (0.12 g, 0.41 mmol) in 58% yield. Chromatography: 9:11 EtOAc:hexanes.[99]

Data for **37c**
^{1}H-NMR (400 MHz, $CDCl_3$)
δ 8.66 (d, *J* = 5.2 Hz, 1 H), 7.74 (s, 1 H), 7.65 (d, *J* = 5.2 Hz, 1 H), 3.96 (s, 3 H), 3.39 (m,1 H), 3.13 (dd, *J* = 17.2, 8.4 Hz, 1 H), 2.75 (dd, *J* = 17.2, 5.2 Hz, 1 H), 2.09 (s, 3 H), 1.66 (m, 2 H), 1.21 (m, 8 H), 0.85 (t, *J* = 6.8 Hz, 1 H).
^{13}C-NMR (100 MHz, $CDCl_3$)
δ 207.7, 165.8, 165.1,149.9, 137.3, 122.6, 120.4, 52.5, 48.3, 42.4, 35.5, 31.5, 30.4, 29.1, 27.1, 22.4, 13.9.
IR Alpha-Platinum ATR, Bruker, diamond crystal
υ = 3060, 2938, 1733, 1708, 1605, 1561, 1436, 1290 cm^{-1}

Ethyl nicotinate coupled product 38a

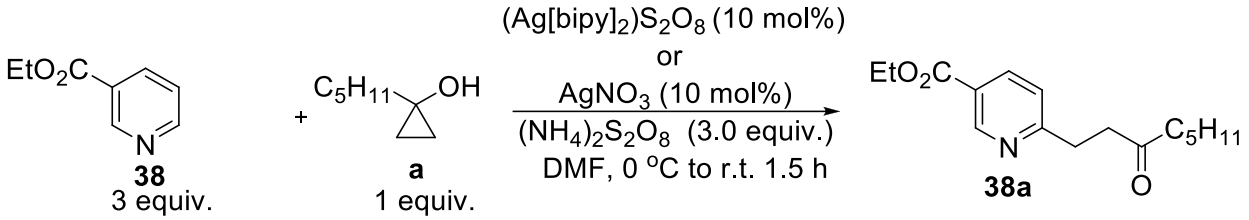

Following *General Procedure 2*, ethyl nicotinate **38** (0.28 g, 2.0 mmol, 3 equiv.) was converted to coupled product **38a** (0.10 g, 0.30 mmol) in 45% yield. Following *General Procedure 3* produced **38a** (0.13 g, 0.39 mmol) in 58% yield. Chromatography: 7:13 EtOAc:hexanes.

Data for **38a**
^{1}H-NMR (400 MHz, $CDCl_3$)
δ 9.11 (d, *J* = 1.6 Hz, 1 H), 8.20 (dd, *J* = 8.0, 1.6 Hz, 1 H), 7.29 (d, *J* = 8.0 Hz, 1 H), 4.40 (q, *J* = 7.2 Hz, 3 H), 3.14 (t, *J* = 7.2 Hz, 2 H), 2.96 (t, *J* = 7.2 Hz, 2 H), 2.45 (t, *J* = 7.6 Hz, 2 H),1.59 (p, *J* = 7.6 Hz, 2 H), 1.40 (t, *J* = 7.2 Hz, 2 H), 1.29 (m, 4 H), 0.89 (t, *J* = 7.2 Hz, 3 H).
^{13}C-NMR (100 MHz, $CDCl_3$)
δ 209.2, 165.3, 165.0, 150.3, 137.1, 123.9, 122.7, 61.1, 42.8, 40.9, 33.7, 31.2, 23.4, 22.3, 14.2, 13.8.
IR Alpha-Platinum ATR, Bruker, diamond crystal
υ = 3064, 2933, 1729, 1710, 1605, 1561, 1436, 1290 cm^{-1}
HRMS TOF EI
Calculated for $[C_{16}H_{23}NO_3]^+$ = 277.1678, found 277.1670

4-Cyanopyridine coupled product 13a

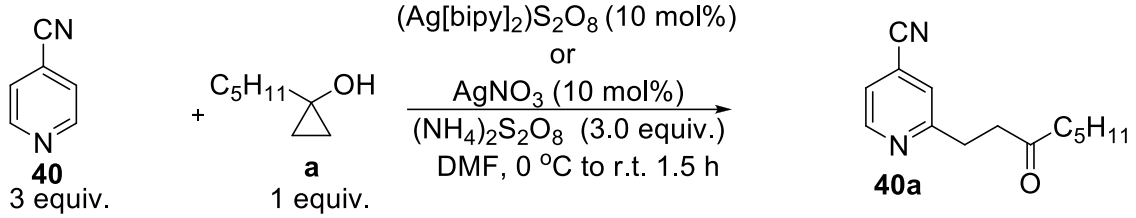

Following *General Procedure 2*, 4-cyanopyridine **40** (0.29 g, 2.8 mmol, 3 equiv.) was converted to coupled product **40a** (0.14 g, 0.61 mmol) in 65% yield. Following *General procedure 3* produced **40a** (0.16 g, 0.69 mmol) in 73% yield. Chromatography: 9:11 EtOAc:hexanes.

Data for **40a**
^{1}H-NMR (400 MHz, $CDCl_3$)
δ 8.69 (d, *J* = 5.2 Hz, 1 H), 7.49 (s, 1 H), 7.36 (d, *J* = 5.2 Hz, 1 H), 3.16 (t, *J* = 7.0 Hz, 2 H), 2.98 (t, *J* = 7.0 Hz, 2 H), 2.45 (t, *J* = 7.6 Hz, 2 H),1.59 (p, *J* = 7.6 Hz, 2 H), 1.28 (m, 4 H), 0.90 (t, *J* = 7.2 Hz, 3 H).
^{13}C-NMR (100 MHz, $CDCl_3$)
δ 209.4, 162.4, 150.5, 125.2, 122.8, 120.8, 116.31, 42.7, 40.6, 31.9, 31.2, 23.3, 22.3, 13.8.
IR Alpha-Platinum ATR, Bruker, diamond crystal
υ = 3058, 2928, 2238, 1709, 1594, 1548, 1374, 1077, 841 cm^{-1}
HRMS TOF EI
Calculated for $[C_{14}H_{18}N_2O]^+$ = 230.1419, found 230.1413

Isoquinoline coupled product 41a

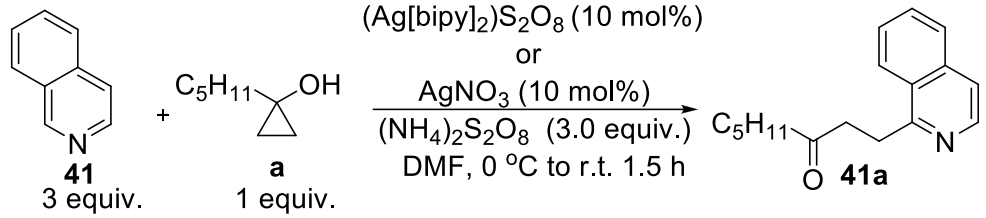

Following *General Procedure 2*, isoquinoline **41** (0.36 g, 2.8 mmol, 3 equiv.) was converted to coupled product **41a** (0.13 g, 0.50 mmol) in 53% yield. Following *General Procedure 3* produced **41a** (0.16 g, 0.61 mmol) in 65% yield. Chromatography: 9:11 EtOAc:hexanes.

Data for **41a**
^{1}H-NMR (400 MHz, $CDCl_3$)
δ 8.40 (d, *J* = 5.7 Hz, 1 H), 8.21 (d, *J* = 8.1 Hz, 1 H), 7.82 (d, *J* = 8.1 Hz, 1 H), 7.67 (m, 2 H), 7.52 (d, *J* = 5.7 Hz, 1 H), 3.62 (t, *J* = 7.2 Hz, 2 H), 3.11 (t, *J* = 7.2 Hz, 2 H), 2.56 (t, *J* = 7.5 Hz, 2 H),1.65 (p, *J* = 7.5 Hz, 2 H), 1.32 (m, 4 H), 0.91 (t, *J* = 7.0 Hz, 3 H).
^{13}C-NMR (100 MHz, $CDCl_3$)
δ 210.7, 159.7, 141.4, 135.8, 129.7, 127.18, 127.0, 126.9, 124.8, 119.2, 42.9, 40.0, 31.3, 28.1, 23.5, 22.4, 13.9.
IR Alpha-Platinum ATR, Bruker, diamond crystal
υ = 3052, 2928, 1710, 1623, 1562, 1503, 1457, 1362, 821, 744 cm^{-1}
HRMS TOF EI
Calculated for $[C_{17}H_{21}NO]^+$ = 255.1623, found 255.1630

Quinoline coupled products 42a and 42a'

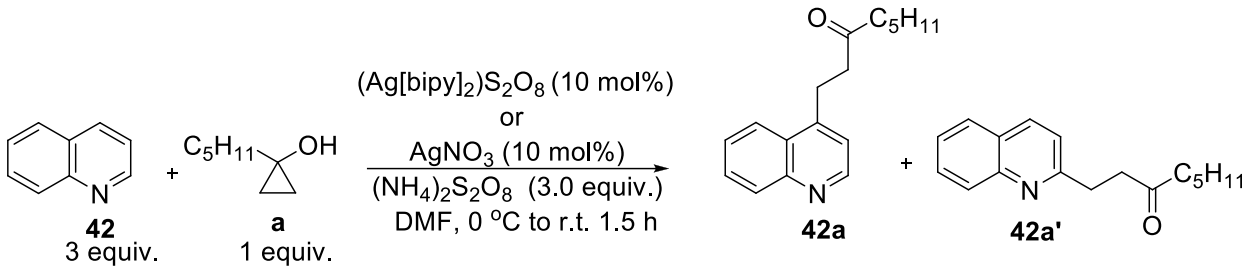

Following *General Procedure 2* did not furnish the desired products. Following *General Procedure 3,* quinoline **42** (0.34 g, 2.2 mmol, 3 equiv.) was converted to coupled product **42a** (0.10 g, 0.38 mmol) in 42% yield and product **42a'** (0.095 g, 0.40 mmol) in 36% yield. Chromatography: 40% Acetone in hexanes.

Data for **42a**
^{1}H-NMR (400 MHz, MeOH *d4*)
δ 8.75 (d, *J* = 4.4 Hz, 1 H), 8.19 (d, *J* = 8.4 Hz, 1 H), 8.04 (d, *J* = 8.4 Hz, 1 H), 7.71 (dd, *J* = 8.4, 6.4 Hz, 1 H), 7.57 (dd, *J* = 8.4, 6.4 Hz, 1 H), 7.41 (d, *J* = 4.4 Hz, 1 H), 3.42 (t, *J* = 7.6 Hz, 2 H), 2.98 (t, *J* = 7.6 Hz, 2 H), 2.50 (t, *J* = 7.2 Hz, 2 H), 1.56 (p, *J* = 7.6 Hz, 2 H), 1.30 (m, 4 H), 0.89 (t, *J* = 7.0 Hz, 3 H).
^{13}C-NMR (100 MHz, $CDCl_3$)
δ 209.2, 150.1, 148.1, 147.0, 130.2, 129.1, 127.1, 126.5, 123.1, 120.7, 42.9, 42.2, 31.2, 25.6, 23.4, 22.3, 13.8.
IR Alpha-Platinum ATR, Bruker, diamond crystal
υ = 3063, 2929, 1711, 1593, 1501, 1372, 807, 795 cm^{-1}
HRMS TOF EI
Calculated for $[C_{17}H_{21}NO]^+$ = 255.1623, found 255.1628

Data for **42a'**
^{1}H-NMR (400 MHz, $CDCl_3$)
δ 8.06 (d, *J* = 8.4 Hz, 1 H), 8.00 (d, *J* = 8.4 Hz, 1 H), 7.78 (d, *J* = 8.0 Hz, 1 H), 7.69 (dd, *J* = 8.0, 7.6 Hz, 1 H), 7.50 (dd, *J* = 8.4, 7.6 Hz, 1 H), 7.33 (d, *J* = 8.4 Hz, 1 H), 3.28 (t, *J* = 7.2 Hz, 2 H), 3.05 (t, *J* = 7.2 Hz, 2 H), 2.51 (t, *J* = 7.2 Hz, 2 H), 1.61 (p, *J* = 7.6 Hz, 2 H), 1.27 (m, 4 H), 0.89 (t, *J* = 7.2 Hz, 3 H).
^{13}C-NMR (100 MHz, $CDCl_3$)
δ 210.4, 160.9, 147.7, 136.1, 129.2, 128.6, 127.4, 126.7, 125.7, 121.7, 42.9, 41.1, 32.3, 31.3, 23.5, 22.4, 13.8.
IR Alpha-Platinum ATR, Bruker, diamond crystal
υ = 3058, 2929, 1711, 1601, 1505, 826, 754 cm^{-1}
HRMS TOF EI
Calculated for $[C_{17}H_{21}NO]^+$ = 255.1623, found 255.1629

Benzimidazole coupled product 54a

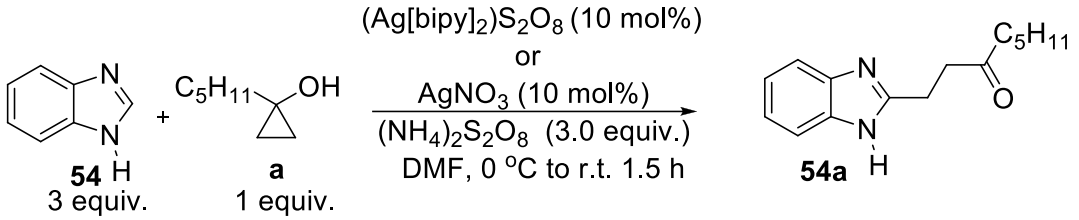

Following *General Procedure 2*, did not provide the expected coupled product. Following *General Procedure 3,* benzimidazole **54** (0.33 g, 2.8 mmol, 3 equiv.) was converted to coupled product **54a** (0.11 g, 0.47 mmol) in 48% yield. Chromatography: 30% Acetone in hexanes.

Data for **54a**
^{1}H-NMR (300 MHz, MeOH *d4*)
δ 7.49 (m, 2 H), 7.20 (m, 2 H), 3.08 (m, 4 H), 2.51 (t, *J* = 7.0 Hz, 2 H), 1.58 (p, *J* = 7.5 Hz, 2 H), 1.30 (m, 4 H), 0.91 (t, *J* = 7.2 Hz, 3 H).
^{13}C-NMR (75 MHz, $CDCl_3$)
δ 211.1, 154.3, 137.9, 122.3, 114.6, 42.7, 40.3, 31.2, 23.4, 22.7, 22.4, 13.8.
IR Alpha-Platinum ATR, Bruker, diamond crystal
υ = 3381, 3057, 2929, 1697, 1624, 1534, 1407, 1271 cm^{-1}
m.p. 50-51 °C
HRMS TOF EI
Calculated for $[C_{15}H_{20}N_2O]^+$ = 244.1576, found 244.1571

Thiazole coupled product 55a

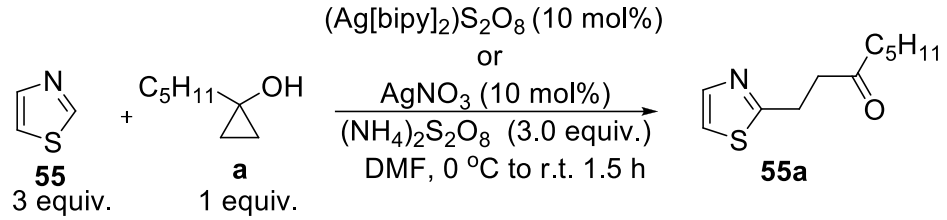

Following *General Procedure 2* did not provide the expected coupled product. Following *General Procedure 3*, thiazole **55** (0.23 g, 2.2 mmol, 3 equiv.) was converted to coupled product **55a** (0.075 g, 0.38 mmol) in 39%. Chromatography: 25% Acetone in hexanes

Data for **55a**
^{1}H-NMR (400 MHz, $CDCl_3$)
δ 7.65 (d, *J* = 3.2 Hz, 1 H), 7.19 (d, *J* = 4.2 Hz, 1 H), 3.30 (t, *J* = 7.2 Hz, 2 H), 2.98 (t, *J* = 7.2 Hz, 2 H), 2.45 (t, *J* = 7.2 Hz, 2 H),1.60 (p, *J* = 7.2 Hz, 2 H), 1.28 (m, 4 H), 0.90 (t, *J* = 7.2 Hz, 3 H).
^{13}C-NMR (100 MHz, $CDCl_3$)
δ 209.1, 169.4, 142.03, 118.3, 42.8, 41.4, 31.2, 26.8, 23.4, 22.3, 13.8.
IR Alpha-Platinum ATR, Bruker, diamond crystal
υ = 3116, 2955, 1712, 1653, 1504, 1374, 1118, 720 cm^{-1}
HRMS TOF EI
Calculated for $[C_{11}H_{17}NOS]^+$ = 211.1031, found 211.1025

Pyrazine coupled product 56a

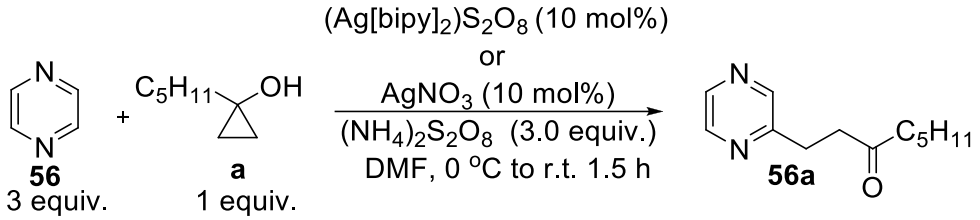

Following *General Procedure 2*, pyrazine **56** (0.23 g, 2.8 mmol, 3 equiv.) was converted to coupled product **56a** (0.073 g, 0.35 mmol) in 38% yield. Following *General Procedure 3* produced **56a** (0.087 g, 0.42 mmol) in 45% yield. Chromatography: 13:7 EtOAc:hexanes.

Data for **56a**
^{1}H-NMR (400 MHz, $CDCl_3$)
δ 8.53 (s, 1 H), 8.47 (s, 1 H), 8.41 (s, 1 H), 3.11 (t, *J* = 7.2 Hz, 2 H), 2.96 (t, *J* = 7.2 Hz, 2 H), 2.46 (t, *J* = 7.2 Hz, 2 H),1.60 (p, *J* = 7.2 Hz, 2 H), 1.28 (m, 4 H), 0.90 (t, *J* = 7.2 Hz, 3 H).
^{13}C-NMR (100 MHz, $CDCl_3$)
δ 209.6, 156.2, 144.9, 143.7, 142.1, 42.7, 40.4, 31.2, 28.6, 23.4, 22.3, 13.8.
IR Alpha-Platinum ATR, Bruker, diamond crystal
υ = 3055, 2929, 1712, 1582, 1456, 1404, 1374, 1018, 778 cm^{-1}
HRMS TOF EI
Calculated for $[C_{12}H_{18}N_2O]^+$ = 206.1419, found 206.1411

5-Bromo-2-phenylpyrimidine coupled product 58a

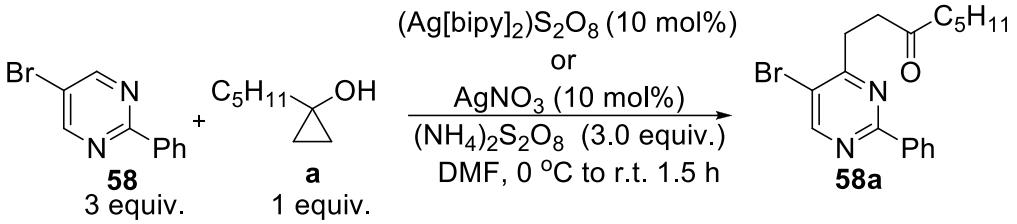

Following *General Procedure 2*, 5-bromo-2-phenylpyrimidine **58** (0.28 g, 1.2 mmol, 3 equiv.) was converted to coupled product **58a** (0.047 g, 0.13 mmol) in 33% yield. Following *General Procedure 3*, produced **58a** (0.095 g, 0.26 mmol) in 67% yield. Chromatography: 1:19 EtOAc:hexanes.

Data for **58a**
^{1}H-NMR (400 MHz, $CDCl_3$)
δ 8.75 (s, 1 H), 8.36 (dd, *J* = 7.0, 1.6 Hz, 2 H), 7.50 (m, 3 H), 3.26 (t, *J* = 7.0 Hz, 2 H), 3.07 (t, *J* = 7.0 Hz, 2 H), 2.59 (t, *J* = 7.2 Hz, 2 H), 1.65 (p, *J* = 7.2 Hz, 2 H), 1.32 (m, 4 H), 0.89 (t, *J* = 7.0 Hz, 3 H).
^{13}C-NMR (100 MHz, $CDCl_3$)
δ 209.3, 166.6, 162.4, 158.0, 136.7, 130.7, 128.4, 128.0, 119.2, 42.9, 38.3, 31.3, 30.3, 23.4, 22.4, 13.8.
IR Alpha-Platinum ATR, Bruker, diamond crystal
υ = 3067, 3037, 2951, 1707, 1552, 1525, 1427, 1403, 1368, 1027, 738, 688 cm^{-1}
m.p. 49-50 °C
HRMS TOF EI
Calculated for $[C_{18}H_{21}BrN_2O]^+$ = 360.0837, found 360.0831

3-((triisopropylsilyloxy)methyl)pyridine coupled product 61a

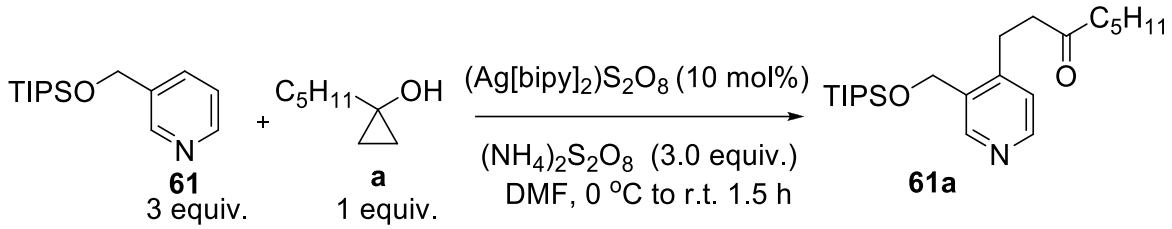

Following *General Procedure 3,* 3-((triisopropylsilyloxy)methyl)pyridine **61** (0.73 g, 2.2 mmol, 3 equiv.) was converted to coupled product **61a** (0.13 g, 0.38 mmol) in 35% yield. Chromatography: 20% Acetone in hexanes

Data for **61a**
^{1}H-NMR (400 MHz, $CDCl_3$)
δ 8.61 (s,1 H), 8.44 (d, *J* = 5.1 Hz, 1 H), 7.08 (d, *J* = 5.1 Hz, 1 H), 4.86 (s, 2 H), 2.93 (t, *J* = 6.6 Hz, 2 H), 2.78 (t, *J* = 6.6 Hz, 2 H), 2.40 (t, *J* = 7.5 Hz, 2 H), 1.59 (p, *J* = 7.5 Hz, 2 H), 1.27 (m, 4 H), 1.18 (m, 3 H), 1.11 (d, *J* = 6.3 Hz, 18 H), 0.90 (t, *J* = 7.0 Hz, 3 H)
^{13}C-NMR (100 MHz, $CDCl_3$)
δ 209.3, 148.8, 148.7, 148.1,134.2, 123.3, 61.4, 42.8, 42.3, 31.3, 25.1, 23.4, 22.3, 17.9, 13.8, 11.9.
IR Alpha-Platinum ATR, Bruker, diamond crystal
υ = 3066, 2925, 1710, 1608, 1566, 1260, 1210, 851 cm^{-1}
HRMS TOF ESI (M+H+)
Calculated for $[C_{23}H_{42}NO_2Si]^+$ = 392.2979, found 392.2991

***tert*-Butyl pyridine-3-ylmethylcarbamate coupled product 62a**

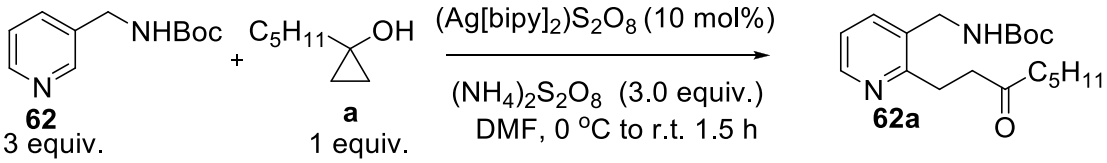

Following *General Procedure 3, tert*-butyl pyridine-3-ylmethylcarbamate **62** (0.59 g, 2.8 mmol, 3 equiv.) was converted to coupled product **62a** (0.12 g, 0.35 mmol) in 37% yield. Chromatography: 3:2 EtOAc:hexanes.

Data for **62a**
^{1}H-NMR (400 MHz, $CDCl_3$)
δ 8.40 (d, *J* = 4.8 Hz, 1 H), 7.58 (d, *J* = 7.6 Hz, 1 H), 7.10 (dd, *J* = 7.6, 4.8 Hz, 1 H), 5.23 (br s,1 H), 4.40 (d, *J* = 5.6 Hz, 2 H), 3.04 (m, 4 H), 2.47 (t, *J* = 7.6 Hz, 2 H), 1.59 (p, *J* = 7.2 Hz, 2 H), 1.59 (p, *J* = 7.2 Hz, 2 H), 1.48 (s, 9 H), 1.31 (m, 4 H), 0.89 (t, *J* = 7.0 Hz, 3 H)
^{13}C-NMR (100 MHz, $CDCl_3$)
δ 210.9, 158.0, 155.8, 147.7, 135.9, 131.9, 121.3, 42.8, 41.6, 40.2, 31.3, 29.6, 28.3, 27.5, 23.4, 22.3, 13.8.
IR Alpha-Platinum ATR, Bruker, diamond crystal
υ = 3452, 3049, 2980, 1733, 1709, 1601, 1436, 1289, 1209,1115, 742 cm^{-1}
HRMS TOF EI (M+)
Calculated for $[C_{19}H_{30}N_2O_3]^+$ = 334.2251, found 334.2251

4-(3,3-Diethoxypropyl)pyridine coupled product 63a

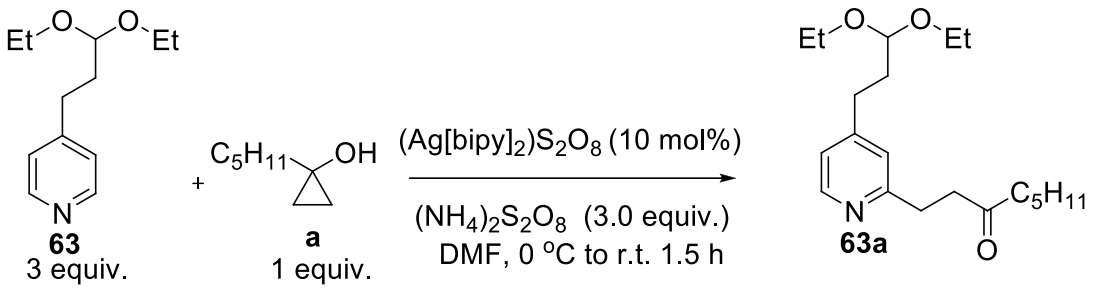

Following *General Procedure 3*, 4-(3,3-diethoxypropyl)pyridine **63** (0.57 g, 2.2 mmol, 3 equiv.) was converted to coupled product **63a** (0.12 g, 0.39 mmol) in 38% yield. Chromatography: 40% Ethyl acetate in hexanes.

Data for **63a**
^{1}H-NMR (400 MHz, $CDCl_3$)
δ 8.38 (d, *J* = 4.8 Hz, 1 H), 7.04 (s, 1 H), 6.96 (d, *J* = 4.8 Hz, 1 H), 4.49 (t, *J* = 5.6 Hz, 1 H), 3.67 (p, *J* = 7.2 Hz, 2 H), 3.52 (p, *J* = 7.2 Hz, 2 H), 3.04 (t, *J* = 7.2 Hz, 2 H), 2.91 (t, *J* = 7.2 Hz, 2 H), 2.67 (t, *J* = 8.0 Hz, 2 H), 2.43 (t, *J* = 7.6 Hz, 2 H), 1.95 (p, *J* = 6.0 Hz, 2 H), 1.60 (m, 2 H), 1.55 (m, 10 H), 0.89 (t, *J* = 7.2 Hz, 3 H).
^{13}C-NMR (100 MHz, $CDCl_3$)
δ 210.4, 160.4,151.1, 148.9,123.2, 121.3, 101.8, 61.2, 42.8, 41.53, 33.9, 31.6, 31.3, 30.1, 23.4, 22.3, 15.2, 13.8.
IR Alpha-Platinum ATR, Bruker, diamond crystal
υ = 3051, 2988, 1710, 1602, 1555, 1150, 908, 650 cm^{-1}
HRMS TOF ESI (M+H+)
Calculated for $[C_{20}H_{34}NO_3]^+$ = 336.2533, found 336.2543

5.4 Experimental Procedures – Synthesis of α,β-Unsaturated Acylsilanes via Perrhenate-Catalyzed Meyer-Schuster Rearrangement of 3-Silylalkyn-1-ols

General Procedure 5. *Synthesis of α,β-Unsaturated Acylsilanes via Perrhenate-Catalyzed Meyer-Schuster Rearrangement of 3-Silylalkyn-1-ols*.

A flame-dried round-bottomed flask equipped with a stir bar was charged with the appropriate silyl acetylene (1.0 equiv.) and placed under an argon atmosphere. Freshly distilled THF was introduced into the flask *via* syringe to prepare a 0.2 M solution of the acetylene and the resulting solution was cooled to 0 °C. While stirring at 0 °C, a 1.6 M solution of *n*-butyllithium in hexanes (1.0 equiv.) was added. After 30 minutes of stirring at 0 °C the reaction was charged with a 0.2 M solution of appropriate aldehyde or ketone (1.0 equiv.) in THF. The progress of the reaction was monitored by TLC analysis. Upon completion, the reaction was quenched with a saturated aqueous solution of ammonium chloride and diluted with EtOAc. The layers were separated and the organic layer was washed with brine, dried using Na_2SO_4, and concentrated *in vacuo*. The crude product was purified by flash column chromatography, eluting with the indicated solvent mixture to afford the desired alcohol.

Alcohol 64a

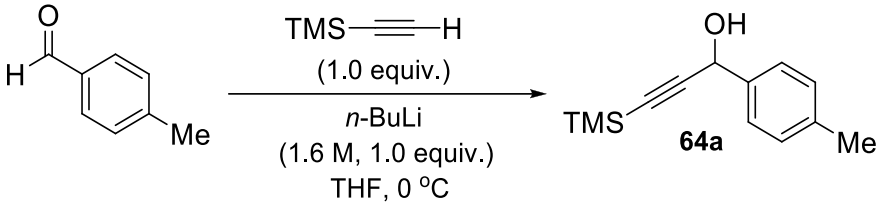

Propargyl alcohol **64a** was prepared following *General Procedure 5*, using 4-methylbenzaldehyde (0.30 g, 2.5 mmol, 1.0 equiv.) and TMS-acetylene (0.25 g, 2.5 mmol, 1.0 equiv.). Purification by flash column chromatography using a 10% solution of EtOAc in hexanes yielded alcohol **64a** (0.42 g, 1.9 mmol, 77%) as a white solid. Data acquired on this material matched that previously reported.[132]

Data for **64a**
^{1}H-NMR (400 MHz, $CDCl_3$)
δ 7.46 (d, *J* = 8.0 Hz, 2 H), 7.22 (d, *J* = 8.0 Hz, 2 H), 5.44 (s, 1 H), 2.38 (s, 3 H), 2.11 (s, 1 H), 0.22 (s, 9 H).
^{13}C-NMR (100 MHz, $CDCl_3$)
δ 137.9, 137.5, 129.2, 126.7, 105.5, 91.0, 64.6, 21.1, –0.2.
^{29}Si-NMR (80 MHz, $CDCl_3$)
δ –17.5
IR Alpha-Platinum ATR, Bruker, diamond crystal
υ = 3327, 3052, 2957, 2174, 1612, 1510, 1283, 1058 cm^{-1}
m.p. = 34-35 °C

Alcohol 64b

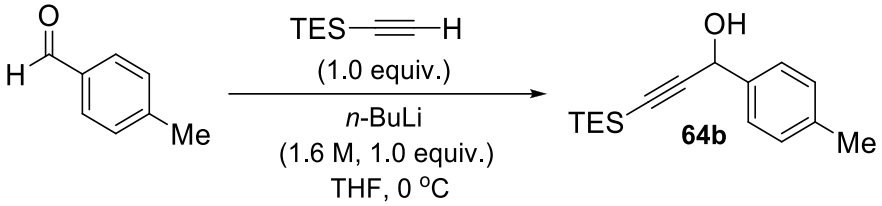

Propargyl alcohol **64b** was prepared following *General Procedure 5*, using 4-methylbenzaldehyde (0.30 g, 2.5 mmol, 1.0 equiv.) and TES-acetylene (0.35 g, 2.5 mmol, 1.0 equiv.). Purification by flash column chromatography using a 10% solution of EtOAc in hexanes yielded alcohol **64b** (0.44 g, 1.7 mmol, 68%) as a clear oil. Data acquired on this material matched that previously reported.[139]

Data for **64b**
^{1}H-NMR (400 MHz, $CDCl_3$)
δ 7.48 (d, *J* = 8.0 Hz, 2 H), 7.21 (d, *J* = 8.0 Hz, 2 H), 5.46 (d, *J* = 6.0 Hz, 1 H), 2.38 (s, 3 H), 2.11 (d, *J* = 6.0 Hz, 1 H), 1.03 (t, *J* = 7.6 Hz, 9 H), 0.65 (q, *J* = 7.6 Hz, 6 H).
^{13}C-NMR (100 MHz, $CDCl_3$)
δ 137.9, 137.6, 129.1, 126.7, 106.6, 88.5, 64.7, 21.1, 7.4, 4.2.
^{29}Si-NMR (80 MHz, $CDCl_3$)
δ −7.1
IR Alpha-Platinum ATR, Bruker, diamond crystal
υ = 3353, 3062, 2954, 2170, 1613, 1512, 1236, 1110 cm^{-1}

Alcohol 64c

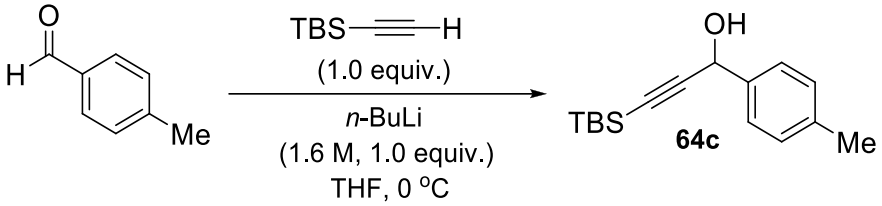

Propargyl alcohol **64c** was prepared following *General Procedure 5*, using 4-methylbenzaldehyde (0.30 g, 2.5 mmol, 1.0 equiv.) and TBS-acetylene (0.35 g, 2.5 mmol, 1.0 equiv.). Purification by flash column chromatography using a 10% solution of EtOAc in hexanes yielded alcohol **64c** (0.49 g, 1.9 mmol, 76%) as a white solid. Data acquired on this material matched that previously reported.[140]

Data for **64c**
^{1}H-NMR (400 MHz, $CDCl_3$)
δ 7.47 (d, *J* = 8.0 Hz, 2 H), 7.21 (d, *J* = 8.0 Hz, 2 H), 5.45 (d, *J* = 2.8 Hz, 1 H), 2.38 (s, 3 H), 2.09 (d, *J* = 2.8 Hz, 1 H), 0.98 (s, 9 H), 0.16 (s, 6 H).
^{13}C-NMR (100 MHz, $CDCl_3$)
δ 137.9, 137.6, 129.1, 126.7, 106.1, 89.3, 64.6, 26.1, 21.1, 16.5, –4.7.
^{29}Si-NMR (80 MHz, $CDCl_3$)
δ –7.7
IR Alpha-Platinum ATR, Bruker, diamond crystal
υ = 3356, 3054, 2927, 2176, 1514, 1281, 1032 cm^{-1}
m.p. = 39-40 °C

Alcohol 64d

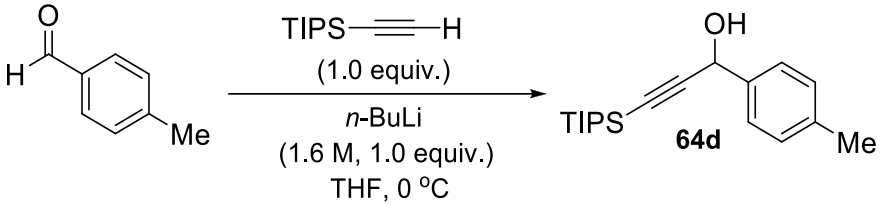

Propargyl alcohol **64d** was prepared following *General Procedure 5*, using 4-methylbenzaldehyde (0.30 g, 2.5 mmol, 1.0 equiv.) and TIPS-acetylene (0.46 g, 2.5 mmol, 1.0 equiv.). Purification by flash column chromatography using a 10% solution of EtOAc in hexanes yielded alcohol **64d** (0.49 g, 1.5 mmol, 65%) as a clear oil.

Data for **64d**
^{1}H-NMR (400 MHz, $CDCl_3$)
δ 7.49 (d, *J* = 7.6 Hz, 1 H), 7.21 (d, *J* = 7.6 Hz, 1 H), 5.47 (d, *J* = 6.4 Hz, 1 H), 2.38 (s, 3 H), 2.08 (d, *J* = 6.4 Hz, 1 H), 1.11 (s, 21 H).
^{13}C-NMR (100 MHz, $CDCl_3$)
δ 137.9, 137.7, 129.1, 126.7, 107.2, 87.4, 64.8, 21.1, 18.5, 11.5
^{29}Si-NMR (80 MHz, $CDCl_3$)
δ −1.9
IR Alpha-Platinum ATR, Bruker, diamond crystal
υ = 3378, 3040, 2941, 2170, 1606, 1512, 1241, 1178 cm^{-1}
HRMS ESI
Calculated for $C_{20}H_{31}OSi$ ($[M+H]^+$) = 303.2139, found = 303.2136

Alcohol 64e

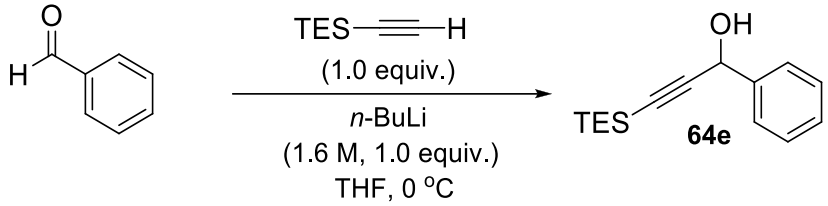

Propargyl alcohol **64e** was prepared following *General Procedure 5*, using benzaldehyde (0.30 g, 2.8 mmol, 1.0 equiv.) and TES-acetylene (0.40 g, 2.8 mmol, 1.0 equiv.). Purification by flash column chromatography using a 8% solution of EtOAc in hexanes yielded alcohol **64e** (0.53 g, 2.2 mmol, 77%) as a clear oil.

Data for **64e**
^{1}H-NMR (400 MHz, $CDCl_3$)
δ 7.6 (d, *J* = 7.6 Hz, 2 H), 7.37 (m, 3 H), 5.50 (s, 1 H), 2.15 (s, 1 H), 1.03 (t, *J* = 8.0 Hz, 9 H), 0.66 (q, *J* = 8.0 Hz, 6 H).
^{13}C-NMR (100 MHz, $CDCl_3$)
δ 140.4, 128.4, 128.2, 126.7, 106.2, 88.9, 64.9, 7.4, 4.2.
^{29}Si-NMR (80 MHz, $CDCl_3$)
δ −7.0
IR Alpha-Platinum ATR, Bruker, diamond crystal
υ = 3350, 3055, 2954, 2171, 1601, 1493, 1237, 1083 cm^{-1}
HRMS ESI
Calculated for $C_{15}H_{23}OSi$ ($[M+H]^+$) = 247.1513, found = 247.1504

Alcohol 64f

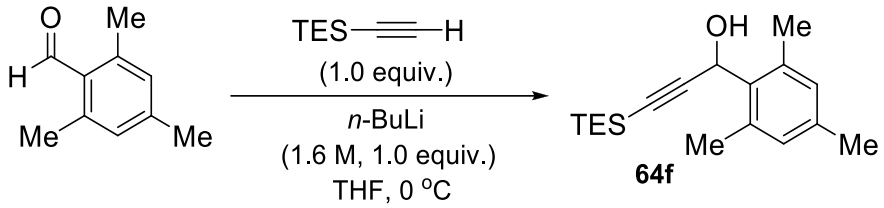

Propargyl alcohol **64f** was prepared following *General Procedure 5*, using 2,4,6-trimethylbenzaldehyde (0.30 g, 2.0 mmol, 1.0 equiv.) and TES-acetylene (0.28 g, 2.0 mmol, 1.0 equiv.). Purification by flash column chromatography using a 9% solution of EtOAc in hexanes yielded alcohol **64f** (0.53 g, 2.2 mmol, 40%) as a clear oil.

Data for **64f**
^{1}H-NMR (400 MHz, $CDCl_3$)
δ 6.88 (s, 2 H), 5.92 (s, 1 H), 2.53 (s, 6 H), 2.29 (s, 3 H), 2.09 (s, 1 H), 1.00 (t, *J* = 7.6 Hz, 9 H), 0.64 (q, *J* = 7.6 Hz, 6 H).
^{13}C-NMR (100 MHz, $CDCl_3$)
δ 137.6, 136.5, 133.4, 129.8, 106.1, 88.0, 60.6, 20.8, 20.2, 7.3, 4.2.
^{29}Si-NMR – (80 MHz, $CDCl_3$)
δ −7.5
IR Alpha-Platinum ATR, Bruker, diamond crystal
υ = 3395, 3072, 2166, 1609, 1236, 1038 cm^{-1}
HRMS ESI
Calculated for $C_{18}H_{29}OSi$ ($[M+H]^+$) = 289.1982, found = 289.1971

Alcohol 64g

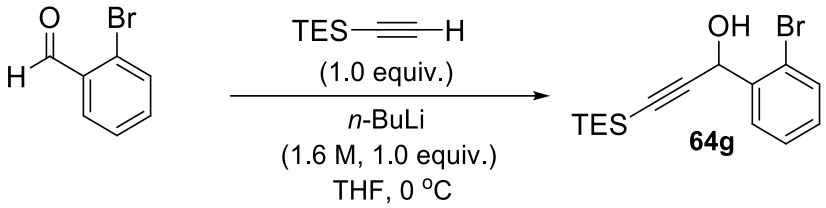

Propargyl alcohol **64g** was prepared following *General Procedure 5*, using 2-bromobenzaldehyde (0.30 g, 1.6 mmol, 1.0 equiv.) and TES-acetylene (0.22 g, 1.6 mmol, 1.0 equiv.). Purification by flash column chromatography using a 7% solution of EtOAc in hexanes yielded alcohol **64g** (0.34 g, 1.0 mmol, 65%) as a clear oil.

Data for **64g**
^{1}H-NMR (400 MHz, $CDCl_3$)
δ 7.83 (d, *J* = 6.4 Hz, 1 H), 7.59 (d, *J* = 8.0 Hz, 1 H), 7.40 (dd, *J* = 8.0 Hz, 7.6 Hz, 1 H), 7.22 (dd, *J* = 7.6 Hz, 6.4 Hz, 1 H), 5.80 (d, *J* = 3.6 Hz, 1 H), 2.42 (d, *J* = 3.6 Hz, 1 H), 1.02 (t, *J* = 8.0 Hz, 9 H), 0.65 (q, *J* = 8.0 Hz, 6 H).
^{13}C-NMR (100 MHz, $CDCl_3$)
δ 139.3, 132.9, 129.8, 128.5, 127.7, 122.9, 104.9, 89.4, 64.5, 7.3, 4.1.
^{29}Si-NMR (80 MHz, $CDCl_3$)
δ –6.8
IR Alpha-Platinum ATR, Bruker, diamond crystal
υ = 3380, 3064, 2954, 2172, 1591, 1235, 1037 cm^{-1}
HRMS ESI
Calculated for $C_{15}H_{21}BrNaOSi$ ($[M+Na]^+$) = 347.0437, found = 347.0435

Alcohol 64h

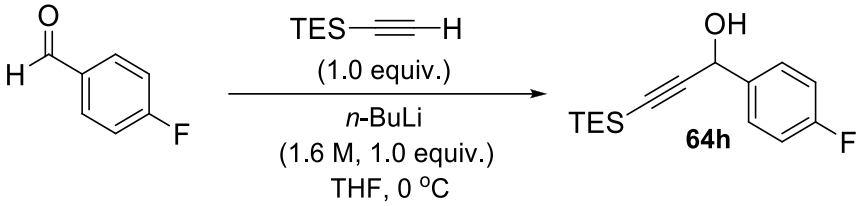

Propargyl alcohol **64h** was prepared following *General Procedure 5*, using 4-fluorobenzaldehyde (0.30 g, 2.4 mmol, 1.0 equiv.) and TES-acetylene (0.34 g, 2.4 mmol, 1.0 equiv.). Purification by flash column chromatography using a 10% solution of EtOAc in hexanes yielded alcohol **64h** (0.44 g, 1.7 mmol, 70%) as a clear oil.

Data for **64h**
^{1}H-NMR (400 MHz, $CDCl_3$)
δ 7.56 (dd, $^{3}J_{H-H}$ = 8.6 Hz, $^{4}J_{H-F}$ = 5.2 Hz, 2 H), 7.08 (dd, $^{3}J_{H-F}$ = 8.8 Hz, $^{3}J_{H-H}$ = 8.6 Hz, 2 H), 5.48 (d, J = 4.8 Hz, 1 H), 2.16 (d, J = 4.8 Hz, 1 H), 1.03 (t, J = 8.0 Hz, 9 H), 0.66 (q, J = 8.0 Hz, 6 H).
^{13}C-NMR (100 MHz, $CDCl_3$)
δ 162.5 (d, $^{1}J_{C-F}$ = 245.0 Hz), 136.3 (d, $^{4}J_{C-F}$ = 3.0 Hz), 128.5 (d, $^{3}J_{C-F}$ = 8.0 Hz), 115.1 (d, $^{2}J_{C-F}$ = 21.0 Hz), 106.1, 89.0, 64.0, 7.3, 4.1.
^{29}Si-NMR (80 MHz, $CDCl_3$)
δ −6.9
^{19}F-NMR (376 MHz, $CDCl_3$)
δ −113.9
IR Alpha-Platinum ATR, Bruker, diamond crystal
υ = 3335, 3040, 2955, 2172, 1604, 1508, 1225, 1037 cm^{-1}
HRMS ESI
Calculated for $C_{15}H_{21}FNaOSi$ ($[M+Na]^+$) = 287.1238, found = 287.1228

Alcohol 64i

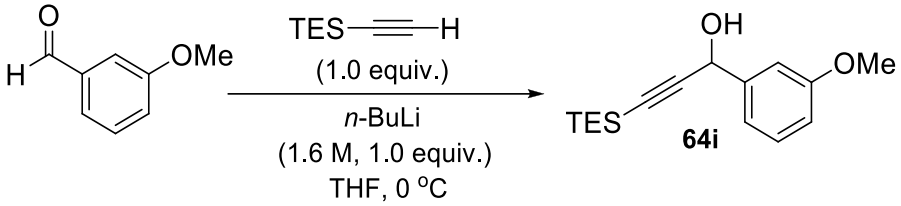

Propargyl alcohol **64i** was prepared following *General Procedure 5*, using 3-methoxylbenzaldehyde (0.30 g, 2.2 mmol, 1.0 equiv.) and TES-acetylene (0.31 g, 2.2 mmol, 1.0 equiv.). Purification by flash column chromatography using a 20% solution of EtOAc in hexanes yielded alcohol **64i** (0.49 g, 1.8 mmol, 81%) as a clear oil.

Data for **64i**
^{1}H-NMR (400 MHz, $CDCl_3$)
δ 7.32 (dd, *J* = 8.4 Hz, 8.0 Hz, 1 H), 7.17 (m, 2 H), 6.90 (dd, *J* = 8.4 Hz, 2.0 Hz, 1 H), 5.47 (d, *J* = 6.0 Hz, 1 H), 3.85 (s, 3 H), 2.14 (d, *J* = 6.0 Hz, 1 H), 1.03 (t, *J* = 8.0 Hz, 9 H), 0.66 (q, *J* = 8.0 Hz, 6 H),
^{13}C-NMR (100 MHz, $CDCl_3$)
δ 159.5, 142.0, 129.4, 119.0, 114.2, 111.7, 106.3, 88.6, 64.7, 55.0, 7.3, 4.2
^{29}Si-NMR (80 MHz, $CDCl_3$)
δ –7.0
IR Alpha-Platinum ATR, Bruker, diamond crystal
υ = 3410, 3058, 2954, 2170, 1600, 1258, 1038, 722 cm^{-1}
HRMS ESI
Calculated for $C_{16}H_{24}NaO_2Si$ ($[M+Na]^+$) = 299.1438, found = 299.1441

Alcohol 64j

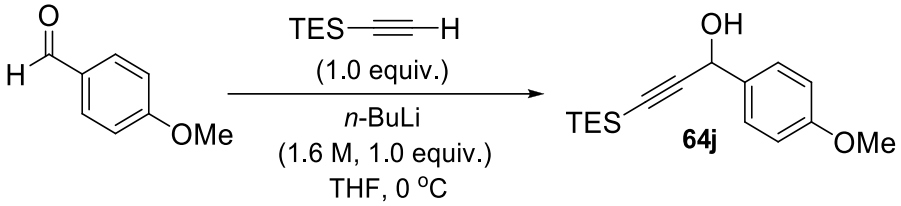

Propargyl alcohol **64j** was prepared following *General Procedure 1*, using 4-methoxylbenzaldehyde (0.30 g, 2.2 mmol, 1.0 equiv.) and TES-acetylene (0.31 g, 2.2 mmol, 1.0 equiv.). Purification by flash column chromatography using a 20% solution of EtOAc in hexanes yielded alcohol **64j** (0.46 g, 1.5 mmol, 75%) as a clear oil. Data acquired on this material matched that previously reported.[139]

Data for **64j**
^{1}H-NMR (400 MHz, $CDCl_3$)
δ 7.51 (d, *J* = 8.4 Hz, 2 H), 6.93 (d, *J* = 8.4 Hz, 2 H), 5.45 (d, *J* = 6.4 Hz, 1 H), 3.84 (s, 3H), 2.09 (d, *J* = 6.4 Hz, 1 H), 1.03 (t, *J* = 7.6 Hz, 9 H), 0.66 (q, *J* = 7.6 Hz, 6 H).
^{13}C-NMR (100 MHz, $CDCl_3$)
δ 159.4, 132.9, 128.1, 113.7, 106.7, 88.3, 64.3, 55.1, 7.4, 4.2.
^{29}Si-NMR (80 MHz, $CDCl_3$)
δ −7.2
IR Alpha-Platinum ATR, Bruker, diamond crystal
υ = 3395, 3068, 2954, 2171, 1610, 1510, 1246, 1172, 978 cm^{-1}

Alcohol 64k

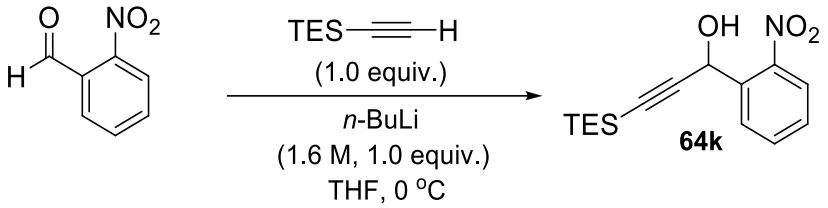

Propargyl alcohol **64k** was prepared following *General Procedure 5*, using 2-nitrobenzaldehyde (0.30 g, 2.0 mmol, 1.0 equiv.) and TES-acetylene (0.28 g, 2.0 mmol, 1.0 equiv.). Purification by flash column chromatography using a 17% solution of EtOAc in hexanes yielded alcohol **64k** (0.42 g, 1.5 mmol, 73%) as a clear oil.

Data for **64k**
^{1}H-NMR (400 MHz, $CDCl_3$)
δ 7.98 (d, *J* = 8.0 Hz, 1 H), 7.97 (d, *J* = 8.0 Hz, 1 H), 7.69 (dd, *J* = 8.0 Hz, 7.4 Hz, 1 H), 7.53 (dd, *J* = 8.0 Hz, 7.4 Hz, 1 H), 6.01 (d, *J* = 5.2 Hz, 1 H), 3.16 (d, *J* = 5.2 Hz, 1 H), 1.00 (t, *J* = 7.6 Hz, 9 H), 0.64 (q, *J* = 7.6 Hz, 6 H).
^{13}C-NMR (100 MHz, $CDCl_3$)
δ 148.0, 135.2, 133.5, 129.2, 129.1, 124.8, 103.8, 89.4, 61.5, 7.2, 4.0.
^{29}Si-NMR (80 MHz, $CDCl_3$)
δ –6.7
IR Alpha-Platinum ATR, Bruker, diamond crystal
υ = 3430, 3042, 2955, 2174, 1609, 1527, 1349, 1236, 1086 cm^{-1}
HRMS ESI
Calculated for $C_{15}H_{22}NO_3Si$ ($[M+H]^+$) = 292.1369, found = 292.1365

Alcohol 64l

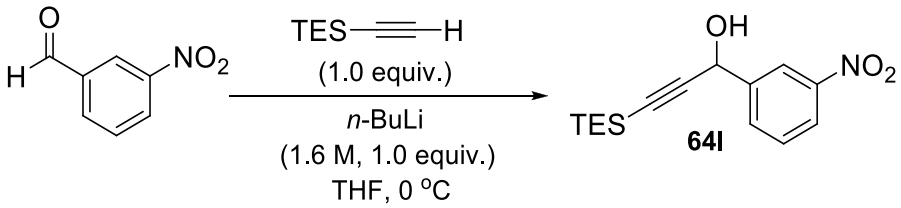

Propargyl alcohol **64l** was prepared following *General Procedure 5*, using 3-nitrobenzaldehyde (0.30 g, 2.0 mmol, 1.0 equiv.) and TES-acetylene (0.28 g, 2.0 mmol, 1.0 equiv.). Purification by flash column chromatography using a 13% solution of EtOAc in hexanes yielded alcohol **64l** (0.42 g, 1.5 mmol, 71%) as a clear oil.

Data for **64l**
^{1}H-NMR (400 MHz, $CDCl_3$)
δ 8.50 (s, 1 H), 8.22 (d, *J* = 8.4 Hz, 1 H), 7.92 (d, *J* = 7.6 Hz, 1 H), 7.59 (dd, *J* = 8.4 Hz, 7.6 Hz, 1 H), 5.60 (d, *J* = 4.8 Hz, 1 H), 2.36 (d, *J* = 4.8 Hz, 1 H), 1.04 (t, *J* = 8.0 Hz, 9 H), 0.67 (q, *J* = 8.0 Hz, 6 H).
^{13}C-NMR (100 MHz, $CDCl_3$)
δ 148.1, 142.5, 132.7, 129.3, 123.0, 121.6, 104.9, 90.3, 63.7, 7.2, 4.0.
^{29}Si-NMR (80 MHz, $CDCl_3$)
δ –6.5
IR Alpha-Platinum ATR, Bruker, diamond crystal
υ = 3420, 3080, 2955, 2174, 1609, 1529, 1347, 1236, 1093 cm^{-1}
HRMS ESI
Calculated for $C_{15}H_{21}NaO_3NSi$ ($[M+Na]^+$) = 314.1183, found = 314.1170

Alcohol 64m

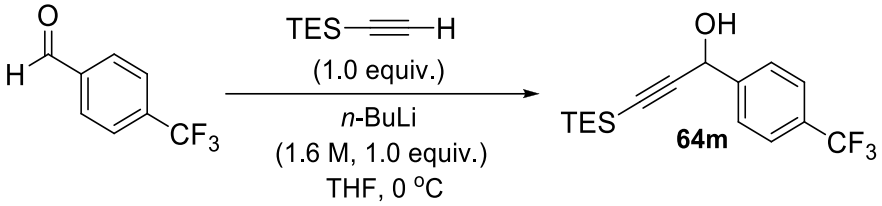

Propargyl alcohol **64m** was prepared following *General Procedure 5*, using 4-(trifluoromethyl)benzaldehyde (0.30 g, 1.7 mmol, 1.0 equiv.) and TES-acetylene (0.24 g, 1.7 mmol, 1.0 equiv.). Purification by flash column chromatography using a 6% solution of EtOAc in hexanes yielded alcohol **64m** (0.37 g, 1.2 mmol, 68%) as clear oil.

Data for **64m**
^{1}H-NMR (400 MHz, $CDCl_3$)
δ 7.71 (d, *J* = 8.4 Hz, 2 H), 7.67 (d, *J* = 8.4 Hz, 2 H), 5.55 (d, *J* = 5.6 Hz, 1 H), 2.24 (d, *J* = 5.6 Hz, 1 H), 1.03(t, *J* = 8.4 Hz, 9 H), 0.66 (q, *J* = 8.4 Hz, 6 H).
^{13}C-NMR (100 MHz, $CDCl_3$)
δ 144.1, 130.3 (q, $^{2}J_{C\text{-}F}$ = 32.3 Hz), 126.8, 125.3, 123.9 (q, $^{1}J_{C\text{-}F}$ = 270.4 Hz), 105.4, 89.7, 64.1, 7.1, 4.1.
^{29}Si-NMR (80 MHz, $CDCl_3$)
δ –6.7
^{19}F-NMR (376 MHz, $CDCl_3$)
δ –62.6
IR Alpha-Platinum ATR, Bruker, diamond crystal
υ = 3329, 3042, 2957, 2174, 1619, 1237, 1125 cm^{-1}
HRMS ESI
Calculated for $C_{16}H_{22}F_3OSi$ ($[M+H]^+$) = 315.3138, found = 315.1373

Alcohol 64n

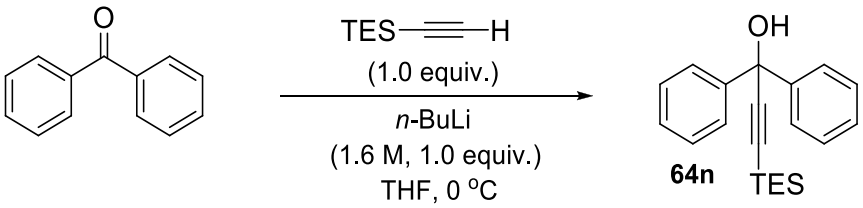

Propargyl alcohol **64n** was prepared following *General Procedure 5*, using benzophenone (0.30 g, 1.6 mmol, 1.0 equiv.) and TES-acetylene (0.22 g, 1.6 mmol, 1.0 equiv.). Purification by flash column chromatography using a 6% solution of EtOAc in hexanes yielded alcohol **64n** (0.40 g, 1.2 mmol, 75%) as a clear oil.

Data for **64n**
^{1}H-NMR (400 MHz, $CDCl_3$)
δ 7.65 (d, *J* = 8.8 Hz, 4 H), 7.34 (dd, *J* = 8.8 Hz, 7.2 Hz, 4 H), 7.27 (t, *J* = 7.2 Hz, 2 H), 2.77 (s, 1 H), 1.05 (t, *J* = 8.0 Hz, 9 H), 0.69 (q, *J* = 8.0 Hz, 6 H).
^{13}C-NMR (100 MHz, $CDCl_3$)
δ 145.0, 128.1, 127.5, 126.0, 109.3, 89.4, 74.7, 7.5, 4.4.
^{29}Si-NMR (80 MHz, $CDCl_3$)
δ −6.6
IR Alpha-Platinum ATR, Bruker, diamond crystal
υ = 3447, 3086, 2955, 2169, 1598, 1236, 1163, 978 cm^{-1}
HRMS ESI
Calculated for $C_{21}H_{26}NaOSi$ ($[M+Na]^+$) = 345.1645, found = 345.1631

Alcohol 64o

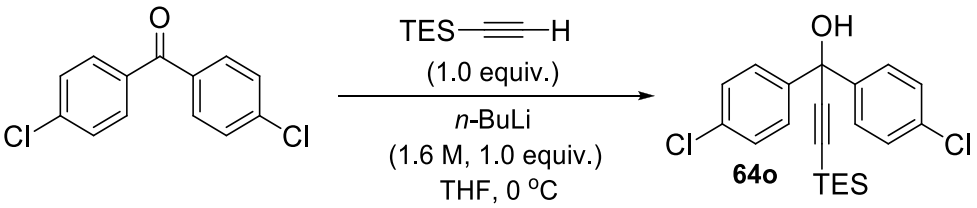

Propargyl alcohol **64o** was prepared following *General Procedure 5*, using 4,4'-dichlorobenzophenone (0.30 g, 1.2 mmol, 1.0 equiv.) and TES-acetylene (0.17 g, 1.2 mmol, 1.0 equiv.). Purification by flash column chromatography using a 4% solution of EtOAc in hexanes yielded alcohol **64o** (0.25 g, 0.90 mmol, 75%) as a clear oil.

Data for **64o**

^{1}H-NMR (400 MHz, $CDCl_3$)
δ 7.54 (d, *J* = 8.8 Hz, 4 H), 7.31 (d, *J* = 8.8 Hz, 4 H), 2.81 (br s, 1 H), 1.03 (t, *J* = 7.6 Hz, 9 H), 0.68 (q, *J* = 7.6 Hz, 6 H).
^{13}C-NMR (100 MHz, $CDCl_3$)
δ 143.0, 133.7, 128.3, 127.3, 107.9, 90.5, 73.8, 7.4, 4.2.
^{29}Si-NMR (80 MHz, $CDCl_3$)
δ –6.3
IR Alpha-Platinum ATR, Bruker, diamond crystal
υ = 3437, 3080, 2950, 2171, 1599, 1233, 1160, 980 cm^{-1}
HRMS ESI
Calculated for $C_{21}H_{24}NaOCl_2Si$ ($[M+Na]^+$) = 413.0866, found = 413.0853

Alcohol 64p

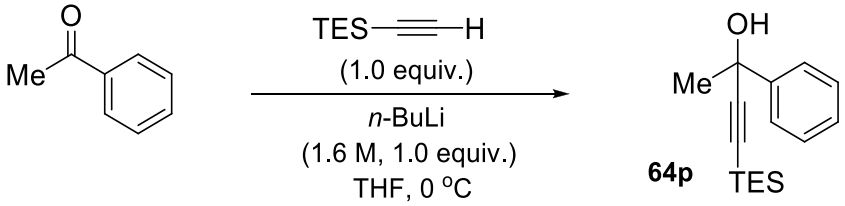

Propargyl alcohol **64p** was prepared following *General Procedure 5*, using acetophenone (0.30 g, 2.5 mmol, 1.0 equiv.) and TES-acetylene (0.35 g, 2.5 mmol, 1.0 equiv.). Purification by flash column chromatography using a 10% solution of EtOAc in hexanes yielded alcohol **64p** (0.52 g, 2.0 mmol, 80%) as clear oil. Data acquired on this material matched that previously reported.[141]

Data for **64p**
^{1}H-NMR (400 MHz, $CDCl_3$)
δ 7.70 (d, *J* = 7.2 Hz, 2 H), 7.39 (dd, *J* = 7.6 Hz, 7.2 Hz, 2 H), 7.31 (t, *J* = 7.6 Hz, 1 H), 2.34 (s, 1 H), 1.79 (s, 3 H), 1.04 (t, *J* = 8.0 Hz, 9 H), 0.66 (q, *J* = 8.0 Hz, 6 H)
^{13}C-NMR (100 MHz, $CDCl_3$)
δ 145.6, 128.1, 127.5, 125.0, 110.4, 86.5, 70.2, 33.5, 7.4, 4.3.
^{29}Si-NMR (80 MHz, $CDCl_3$)
δ −7.1
IR Alpha-Platinum ATR, Bruker, diamond crystal
υ = 3307, 3063, 2980, 2164, 1224, 1073, 946, 695 cm^{-1}
m.p. 44-46 °C

Alcohol 64q

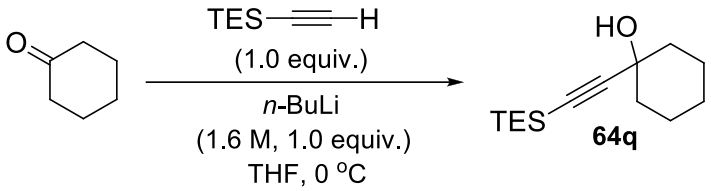

Propargyl alcohol **64q** was prepared following *General Procedure 5*, using cyclohexanone (0.30 g, 3.1 mmol, 1.0 equiv.) and TES-acetylene (0.43 g, 3.1 mmol, 1.0 equiv.). Purification by flash column chromatography using a 10% solution of EtOAc in hexanes yielded alcohol **64q** (0.58 g, 2.4 mmol, 79%) as a clear oil. Data collected on this material matched that previously reported.[142]

Data for **64q**
^{1}H-NMR (400 MHz, $CDCl_3$)
δ 1.97 (m, 2 H), 1.68-1.46 (m, 8 H), 1.19 (t, *J* = 8.0 Hz, 9 H), 0.73 (q, *J* = 8.0 Hz, 6 H)
^{13}C-NMR (100 MHz, $CDCl_3$)
δ 110.8, 85.6, 69.0, 39.9, 25.1, 23.4, 7.3, 4.3
^{29}Si-NMR (80 MHz, $CDCl_3$)
δ −7.5
IR Alpha-Platinum ATR, Bruker, diamond crystal
υ = 3339, 2933, 2164, 1068, 1016, 1006, 965, 765, 724 cm^{-1}

Alcohol 64r

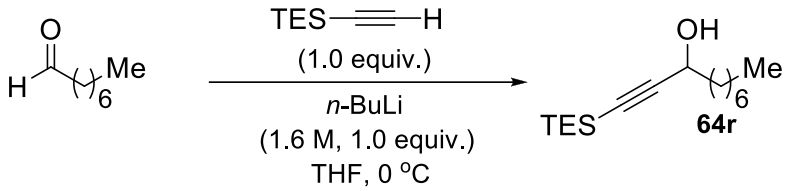

Propargyl alcohol **64r** was prepared following *General Procedure 5*, using octanal (0.30 g, 2.3 mmol, 1.0 equiv.) and TES-acetylene (0.32 g, 2.3 mmol, 1.0 equiv.). Purification by flash column chromatography using a 5% solution of EtOAc in hexanes yielded alcohol **64r** (0.50 g, 1.9 mmol, 81%) as a clear oil.

Data for **64r**
^{1}H-NMR (400 MHz, $CDCl_3$)
δ 4.39 (ddd, *J* = 7.0, 6.8, 6.4 Hz, 1 H), 1.73 (d, *J* = 6.4 Hz, 1H), 1.5 (m, 2 H) 1.31 (m, 10 H), 1.01 (t, *J* = 8.0 Hz, 9 H), 0.90 (t, *J* = 7.0 Hz, 3 H), 0.62 (q, *J* = 8.0 Hz, 6 H).
^{13}C-NMR (100 MHz, $CDCl_3$)
δ 108.3, 86.2, 62.7, 37.7, 31.6, 29.2, 29.1, 25.0, 22.5, 13.9, 7.2, 4.1.
^{29}Si-NMR (80 MHz, $CDCl_3$)
δ −7.5
IR Alpha-Platinum ATR, Bruker, diamond crystal
υ = 3339, 2954, 2169, 1236, 1127 cm^{-1}
HRMS ESI
Calculated for $C_{16}H_{32}NaOSi$ ($[M+Na]^+$) = 291.2115, found = 291.2105

Alcohol 64s

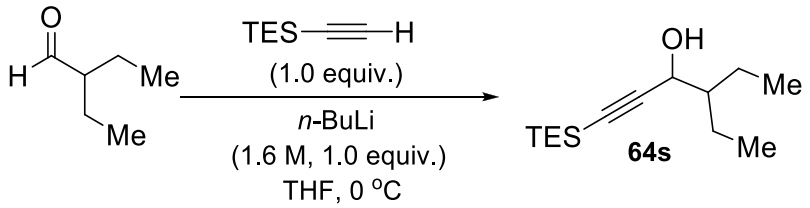

Propargyl alcohol **64s** was prepared following *General Procedure 5*, using 2-ethylbutanal (0.30 g, 3.0 mmol, 1.0 equiv.) and TES-acetylene (0.42 g, 3.0 mmol, 1.0 equiv.). Purification by flash column chromatography using a 6% solution of EtOAc in hexanes yielded alcohol **64s** (0.58 g, 2.4 mmol, 80%) as a clear oil.

Data for **64s**
^{1}H-NMR (400 MHz, $CDCl_3$)
δ 4.43 (dd, *J* = 6.0, 5.2 Hz, 1 H), 1.68 (d, *J* = 6.0 Hz, 1 H), 1.42-1.66 (m, 5 H), 1.01 (t, *J* = 8 Hz, 9 H), 0.96 (t, *J* = 8.8 Hz, 6 H), 0.61 (q, *J* = 8.0 Hz, 6 H)
^{13}C-NMR (100 MHz, $CDCl_3$)
δ 107.3, 86.8, 64.8, 47.2, 22.0, 21.6, 11.4, 11.3, 7.1, 4.2.
^{29}Si-NMR (80 MHz, $CDCl_3$)
δ −7.6
IR Alpha-Platinum ATR, Bruker, diamond crystal
υ = 3307, 2980, 2161, 1254, 1053, 936, 695 cm^{-1}
HRMS ESI
Calculated for $C_{14}H_{28}NaOSi$ ($[M+Na]^+$) = 263.1810, found = 263.1793

Alcohol 64t

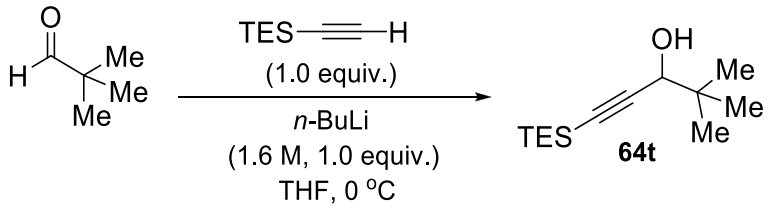

Propargyl alcohol **64t** was prepared following *General Procedure 5*, using pivaldehyde (0.30 g, 3.5 mmol, 1.0 equiv.) and TES-acetylene (0.49 g, 3.5 mmol, 1.0 equiv.). Purification by flash column chromatography using a 5% solution of EtOAc in hexanes yielded alcohol **64t** (0.59 g, 2.6 mmol, 75%) as a clear oil.

Data for **64t**
^{1}H-NMR (400 MHz, $CDCl_3$)
δ 4.03 (d, *J* = 5.2 Hz, 1 H), 1.7 (d, *J* = 5.2 Hz, 1 H), 1.02 (m, 18 H), 0.62 (q, *J* = 8.0 Hz, 6 H).
^{13}C-NMR (100 MHz, $CDCl_3$)
δ 106.8, 87.1, 71.5, 35.5, 25.1, 7.3, 4.2.
^{29}Si-NMR (80 MHz, $CDCl_3$)
δ −7.5
IR Alpha-Platinum ATR, Bruker, diamond crystal
υ = 3301, 3050, 2935, 2167, 1588, 1289, 1070, 993 cm^{-1}
HRMS ESI
Calculated for $C_{13}H_{26}NaOSi$ ($[M+Na]^+$) = 249.1635, found = 249.1635

Alcohol 64u

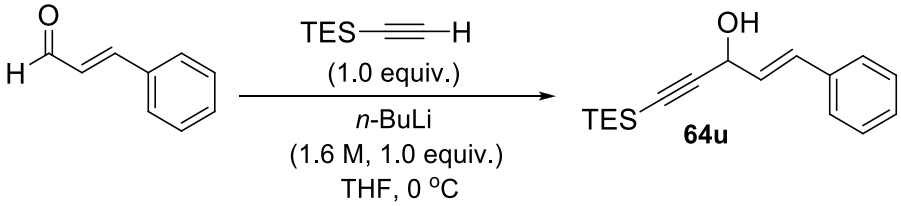

Propargyl alcohol **64u** was prepared following *General Procedure 5*, using cinnamaldehyde (0.30 g, 2.3 mmol, 1.0 equiv.) and TES-acetylene (0.32 g, 2.3 mmol, 1.0 equiv.). Purification by flash column chromatography using a 10% solution of EtOAc in hexanes yielded alcohol **64u** (0.49 g, 1.8 mmol, 79%) as clear oil.

Data for **64u**
^{1}H-NMR (400 MHz, $CDCl_3$)
δ 7.43 (d, *J* = 8.0 Hz, 2 H), 7.36 (dd, *J* = 8.2, 8.0 Hz, 2 H), 7.29 (t, *J* = 8.2 Hz, 1 H), 6.85 (d, *J* = 15.6 Hz 1 H), 6.33 (dd, *J* = 15.6, 5.6 Hz, 1 H), 5.09 (dd, *J* = 6.4 Hz, 5.6 Hz, 1 H), 1.96 (d, *J* = 6.4 Hz, 1 H), 1.05 (t, *J* = 8.2 Hz, 9 H), 0.66 (q, *J* = 8.2 Hz, 6 H)
^{13}C-NMR (100 MHz, $CDCl_3$)
δ 136.0, 132.0, 128.5, 128.0, 127.9, 126.7, 105.3, 88.8, 63.3, 7.4, 4.2.
^{29}Si-NMR (80 MHz, $CDCl_3$)
δ –7.0
IR Alpha-Platinum ATR, Bruker, diamond crystal
υ = 3318, 3001, 2955, 2170, 1235, 1016, 963, 722 cm^{-1}
HRMS ESI
Calculated for $C_{17}H_{24}NaOSi$ ($[M+Na]^+$) = 295.1489, found = 295.1478

Alcohol 64v

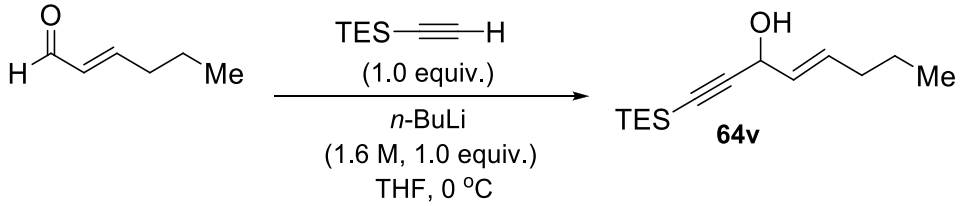

Propargyl alcohol **64v** was prepared following *General Procedure 5*, using trans-2-Hexenal (0.30 g, 3.0 mmol, 1.0 equiv.) and TES-acetylene (0.42 g, 3.0 mmol, 1.0 equiv.). Purification by flash column chromatography using an 8% solution of EtOAc in hexanes yielded alcohol **64v** (0.49 g, 1.8 mmol, 78%) as a clear oil.

Data for **64v**
^{1}H-NMR (400 MHz, $CDCl_3$)
δ 5.94 (m, 1 H), 5.62 (dd, *J* = 15.0 Hz, 6.0 Hz, 1 H), 4.86 (d, *J* = 5.6 Hz, 1 H), 2.07 (m, 2 H), 1.44 (sex, *J* = 7.6 Hz, 2 H), 1.02 (t, *J* = 7.6 Hz, 9 H), 0.94 (t, *J* = 7.6 Hz, 3 H), 0.63 (q, *J* = 7.6 Hz, 6 H)
^{13}C-NMR (100 MHz, $CDCl_3$)
δ 133.4, 129.0, 106.3, 87.5, 63.0, 33.8, 22.0, 13.4, 7.2, 4.1.
^{29}Si-NMR (80 MHz, $CDCl_3$)
δ −7.4
IR Alpha-Platinum ATR, Bruker, diamond crystal
υ = 3010, 2955, 2171, 1233, 1010, 960, 715 cm^{-1}
HRMS ESI
Calculated for $C_{15}H_{24}OSi$ ($[M+H]^+$) = 237.1667, found = 237.1660

Part 2 – Synthesis of Acyl Silanes from Propargylic Alcohols 64a-v.

Two reaction protocols were developed for the Meyer-Schuster rearrangement of propargylic alcohols to acyl silanes. **Conditions A** involved the use of *p*-TSA•H_2O and *n*Bu_4N•ReO_4 in DCM at r.t. When this method failed or the substrates were deemed to be sensitive to acid-catalyzed ionization **Conditions B**, which involved the use of $Ph_3SiOReO_3$ in anhydrous solvents (Et_2O or THF), were utilized.

General Procedure 6 (Conditions A).

To a round-bottomed flask equipped with a stir bar and charged with *n*Bu_4N•ReO_4 (0.05 equiv.), *p*-TsOH•H_2O (0.05 equiv.) was added a 0.2 M solution of propargyl alcohol (1.00 equiv.) in DCM. After overnight stirring at ambient temperature the reaction was diluted with water and the aqueous phase separated. The organic phase was washed with brine, dried with $MgSO_4$, and concentrated *in vacuo*. The crude product was purified by flash column chromatography, eluting with the indicated solvent mixture to afford the desired product.

General Procedure 7 (Conditions B)

A flame-dried round-bottomed flask equipped with a stir bar was charged with $Ph_3SiOReO_3$ (0.05 equiv.) followed by 0.2 M solution of propargyl alcohol (1.0 equiv.) in freshly distilled Et_2O or THF. After overnight stirring at r.t. the reaction was diluted with water and the aqueous phase separated. The organic phase was washed with brine, dried using sodium sulphate and concentrated *in vacuo*. The crude product was purified by flash column chromatography, eluting with the indicated solvent mixture to afford the desired product.

α,β-Unsaturated Acyl Silane 65a

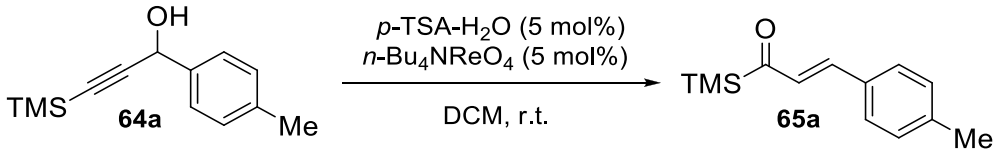

Following *General Procedure 6*, propargyl alcohol **64a** (0.15 g, 0.69 mmol, 1.0 equiv.) was converted to α,β-unsaturated acyl silane **65a**. Purification by flash column chromatography using 6% solution of EtOAc in hexanes yielded the product (0.11 g, 0.50 mmol, 72%) as an orange oil.

Data for **65a**
^{1}H-NMR (400 MHz, $CDCl_3$)
δ 7.47 (d, *J* = 8.0 Hz, 2 H), 7.44 (d, *J* = 16.4 Hz, 1 H), 7.23 (d, *J* = 8.0 Hz, 2 H), 6.89 (d, *J* = 16.4 Hz, 1 H), 2.40 (s, 3 H), 0.34 (s, 9 H).
^{13}C-NMR (100 MHz, $CDCl_3$)
δ 236.0, 143.0, 140.9, 132.0, 130.5, 129.6, 128.1, 21.4, −2.1.
^{29}Si-NMR (80 MHz, $CDCl_3$)
δ −8.5
IR Alpha-Platinum ATR, Bruker, diamond crystal
υ = 3109, 2956, 1637, 1609, 1511, 1248, 1210, 975 cm^{-1}
HRMS ESI
Calculated for $C_{13}H_{20}OSi$ ($[M+H]^+$) = 219.1200, found = 219.1192

α,β-Unsaturated acyl silane 65b

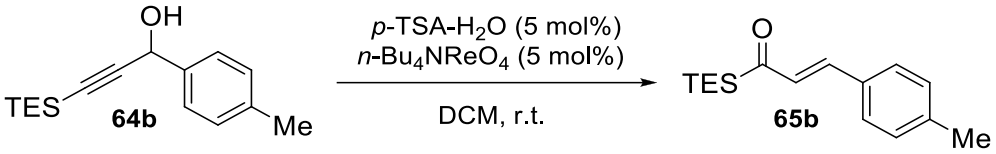

Following *General Procedure 6*, propargyl alcohol **64b** (0.15 g, 0.58 mmol, 1.0 equiv.) was converted to α,β-unsaturated acyl silane **65b**. Purification by flash column chromatography using 5% solution of EtOAc in hexanes yielded acyl silane **65b** (0.11 g, 0.44 mmol, 75%) as an orange solid.

Data for **65b**
^{1}H-NMR (400 MHz, $CDCl_3$)
δ 7.48 (d, *J* = 8.0 Hz, 2 H), 7.40 (d, *J* = 16.4 Hz, 1 H), 7.23 (d, *J* = 8.0 Hz, 2 H), 6.92 (d, *J* = 16.4 Hz, 1 H), 2.40 (s, 3 H), 1.04 (t, *J* = 7.6 Hz, 9 H), 0.87 (q, *J* = 7.6 Hz, 6 H)
^{13}C-NMR (100 MHz, $CDCl_3$)
δ 235.9, 141.8, 140.8, 132.0, 131.1, 129.6, 128.2, 21.4, 7.3, 2.9.
^{29}Si-NMR (80 MHz, $CDCl_3$)
δ −1.2
IR Alpha-Platinum ATR, Bruker, diamond crystal
υ = 3085, 2953, 1636, 1609, 1510, 1238, 975 cm^{-1}
HRMS ESI
Calculated for $C_{16}H_{26}OSi$ ($[M+H]^+$) = 261.1670, found = 261.1658
m.p. = 28 - 30 °C

α,β-Unsaturated acyl silane 65c

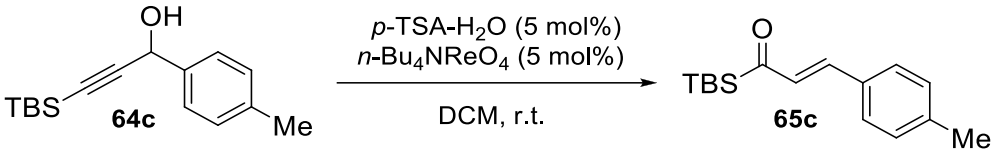

Following *General Procedure 6*, propargyl alcohol **64c** (0.15 g, 0.58 mmol, 1.0 equiv.) was converted to α,β-unsaturated acyl silane **65c**. Purification by flash column chromatography using 4% solution of EtOAc in hexanes yielded the product (0.11 g, 0.44 mmol, 76%) as an orange solid.

Data for **65c**
^{1}H-NMR (400 MHz, $CDCl_3$)
δ 7.48 (d, *J* = 8.0 Hz, 2 H), 7.38 (d, *J* = 16.4 Hz, 1 H), 7.22 (d, *J* = 8.0 Hz, 2 H), 7.00 (d, *J* = 16.4 Hz, 1 H), 2.40 (s, 3 H), 0.99 (s, 9 H), 0.32 (s, 6 H).
^{13}C-NMR (100 MHz, $CDCl_3$)
δ 235.0, 140.8, 132.0, 130.2, 129.6, 128.9, 128.2, 26.5, 21.4, 16.7, −6.2.
^{29}Si-NMR (80 MHz, $CDCl_3$)
δ −2.0
IR Alpha-Platinum ATR, Bruker, diamond crystal
υ = 3028, 2952, 1636, 1609, 1509, 1260, 1166, 983 cm^{-1}
HRMS ESI
Calculated for $C_{16}H_{25}OSi$ ($[M+H]^+$) = 261.1669, found = 261.1671
m.p. = 68 - 69 °C

Ethers 66d and 67d.

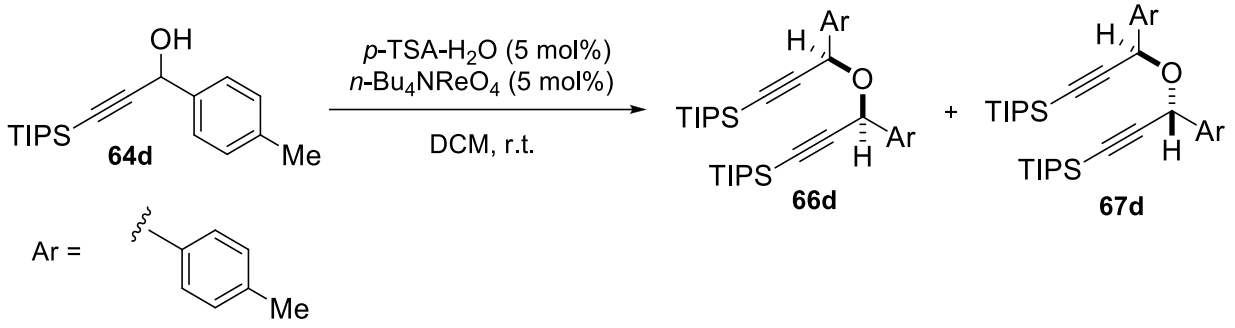

Using *General Procedure 6* alcohol **64d** (0.15 g, 0.49 mmol, 1.0 equiv.) did not provide the expected acyl silane **65d**, but rather gave an inseparable mixture of *meso* ether **66d** and its diastereomer **67d** in a nearly 1:1 ratio. Purification by flash column chromatography using 6% solution of EtOAc in hexanes yielded the mixture of products (0.26 g, 0.44 mmol, 90%) as a clear oil.

Data for **66d** and **67d**
^{1}H-NMR (400 MHz, $CDCl_3$)
δ 7.50 (d, *J* = 7.6 Hz, 4 H), 7.44 (d, *J* = 7.6 Hz, 4 H), 7.17 (m, 8 H), 5.76 (s, 2 H), 5.33 (s, 2 H), 2.37 (s, 6 H), 2.35 (s, 6 H), 1.15 (s, 42 H), 1.13 (s, 6 H), 1.09 (s, 36 H).
^{13}C-NMR (100 MHz, $CDCl_3$)
δ 137.9, 137.8, 135.5, 135.4, 129.0, 128.9, 127.9, 127.8, 127.5, 105.5, 105.6, 89.3, 88.4, 70.0, 68.9, 21.14, 21.10, 18.6, 18.5, 11.2
^{29}Si-NMR (80 MHz, $CDCl_3$)
δ −1.6, −1.9
IR Alpha-Platinum ATR, Bruker, diamond crystal
υ = 3053, 2942, 2168, 1513, 1007 cm^{-1}
HRMS ESI
Calculated for $C_{38}H_{58}NaOSi_2$ ($[M+Na]^+$) = 609.3918, found = 609.3893

α,β-Unsaturated acyl silane 65e

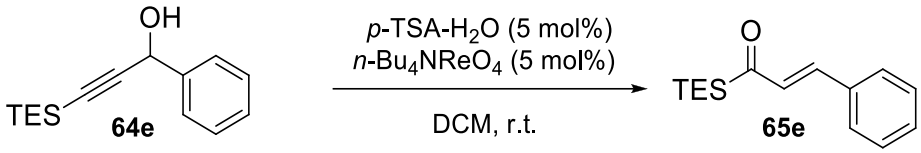

Following *General Procedure 6*, propargyl **64e** (0.15 g, 0.61 mmol, 1.0 equiv.) was converted to α,β-unsaturated acyl silane **65e**. Purification by flash column chromatography using 4% solution of EtOAc in hexanes yielded the product (0.090 g, 0.37 mmol, 60%) as an orange oil.

Data for **65e**
^{1}H-NMR (400 MHz, $CDCl_3$)
δ 7.59 (m, 2 H), 7.42 (m, 4 H), 6.96 (d, *J* = 16.0 Hz, 1 H), 1.04 (t, *J* = 8.0 Hz, 9 H), 0.88 (q, *J* = 8.0 Hz, 6 H)
^{13}C-NMR (100 MHz, $CDCl_3$)
δ 236.1, 141.6, 134.8, 131.8, 130.3, 128.8, 128.2, 7.3, 2.9.
^{29}Si-NMR (80 MHz, $CDCl_3$)
δ −1.0
IR Alpha-Platinum ATR, Bruker, diamond crystal
υ = 3083, 2954, 1638, 1577, 2171, 1495, 1238, 1153, 973 cm^{-1}
HRMS ESI
Calculated for $C_{15}H_{24}OSi$ ($[M+H]^+$) = 247.1513, found = 247.1502

α,β-Unsaturated acyl silane 65f

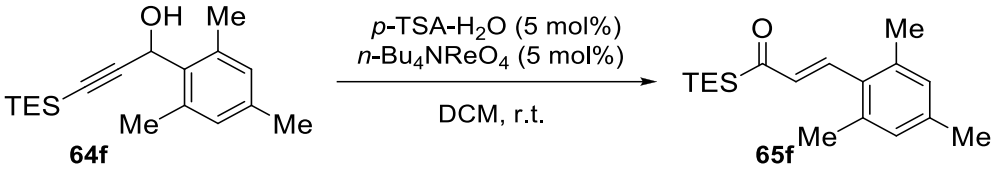

Following *General Procedure 6*, propargyl alcohol **64f** (0.15 g, 0.52 mmol, 1.0 equiv.) was converted to α,β-unsaturated acyl silane **65f**. Purification by flash column chromatography using 4% solution of EtOAc in hexanes yielded the product (0.12 g, 0.42 mmol, 80%) as an orange oil.

Data for **65f**
^{1}H-NMR (400 MHz, $CDCl_3$)
δ 7.59 (d, *J* = 16.8 Hz, 1 H), 6.93 (s, 2 H), 6.56 (d, *J* = 16.8 Hz, 1 H), 2.36 (s, 6 H), 2.31 (s, 3 H), 1.05 (t, *J* = 8.0 Hz, 9 H), 0.87 (q, *J* = 8.0 Hz, 6 H).
^{13}C-NMR (100 MHz, $CDCl_3$)
δ 236.3, 140.8, 138.4, 137.9, 136.7, 131.3, 129.2, 21.1, 20.9, 7.3, 3.0.
^{29}Si-NMR (80 MHz, $CDCl_3$)
δ −1.3
IR Alpha-Platinum ATR, Bruker, diamond crystal
υ = 3121, 2953, 1636, 1610, 1237, 1162, 982 cm^{-1}
HRMS ESI
Calculated for $C_{18}H_{29}OSi$ ($[M+H]^+$) = 289.1982, found = 289.1973

α,β-Unsaturated acyl silane 65g

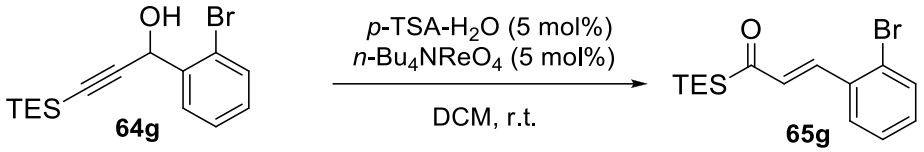

Following *General Procedure 6*, propargyl alcohol **64g** (0.15 g, 0.46 mmol, 1.0 equiv.) was converted to α,β-unsaturated acyl silane **65g**. Purification by flash column chromatography using 5% solution of EtOAc in hexanes yielded the product (0.12 g, 0.37 mmol, 80%) as an orange oil.

Data for **65g**
^{1}H-NMR (400 MHz, $CDCl_3$)
δ 7.89 (d, *J* = 16.8 Hz, 1 H), 7.67 (m, 2 H), 7.37 (dd, *J* = 7.4, 7.2 Hz, 1 H), 7.25 (dd, *J* = 7.2, 7.0 Hz, 1 H), 6.74 (d, *J* = 16.8 Hz, 1 H), 1.05 (t, *J* = 8.0 Hz, 9 H), 0.92 (q, *J* = 8.0 Hz, 6 H).
^{13}C-NMR (100 MHz, $CDCl_3$)
δ 237.0, 142.1, 135.2, 134.8, 133.3, 131.2, 127.7, 127.3, 125.8, 7.3, 3.1.
^{29}Si-NMR (80 MHz, $CDCl_3$)
δ –0.3
IR Alpha-Platinum ATR, Bruker, diamond crystal
υ = 3064, 2953, 1617, 1582, 1591, 1239, 1155, 971 cm^{-1}
HRMS ESI
Calculated for $C_{15}H_{23}BrOSi$ ($[M+H]^+$) = 325.0610, found = 325.0610

α,β-Unsaturated acyl silane 65h

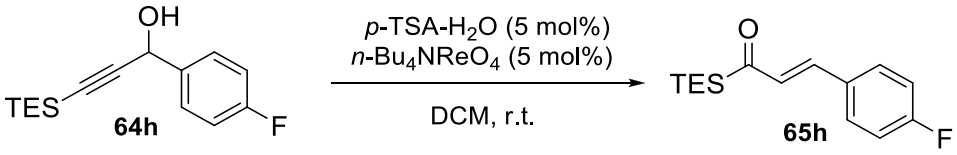

Following *General Procedure 6*, propargyl alcohol **64h** (0.15 g, 0.57 mmol, 1.0 equiv.) was converted to α,β-unsaturated acyl silane **65h**. Purification by flash column chromatography using 4% solution of EtOAc in hexanes yielded the product (0.090 g, 0.33 mmol, 58%) as an orange oil.

Data for **65h**
^{1}H-NMR (400 MHz, $CDCl_3$)
δ 7.57 (dd, $^{4}J_{H\text{-}F}$ = 5.6 Hz, J = 8.6 Hz, 2 H), 7.37 (d, J = 16.0 Hz, 1 H), 7.11 (dd, $^{3}J_{H\text{-}F}$ = 8.8 Hz, J = 8.6 Hz, 2 H), 6.89 (d, J = 16.0 Hz, 1 H), 1.04 (t, J = 8.0 Hz, 9 H), 0.87 (q, J = 8.0 Hz, 6 H).
^{13}C-NMR (100 MHz, $CDCl_3$)
δ 235.8, 163.8 (d, $^{1}J_{C\text{-}F}$ = 251.0 Hz), 139.9, 131.3 (d, $^{5}J_{C\text{-}F}$ = 1.0 Hz), 131.0 (d, $^{4}J_{C\text{-}F}$ = 3.0 Hz), 130.0 (d, $^{3}J_{C\text{-}F}$ = 9.0 Hz), 116.0 (d, $^{2}J_{C\text{-}F}$ = 22.0 Hz), 7.2, 2.8.
^{29}Si-NMR (80 MHz, $CDCl_3$)
δ −1.0
^{19}F-NMR (376 MHz, $CDCl_3$)
δ −109.3
IR Alpha-Platinum ATR, Bruker, diamond crystal
υ = 3072, 2956, 1638, 1600, 1506, 1232, 1156, 974 cm^{-1}
HRMS ESI
Calculated for $C_{15}H_{23}FOSi$ ($[M+H]^+$) = 265.1418, found = 265.1406

α,β-Unsaturated acyl silane 65i

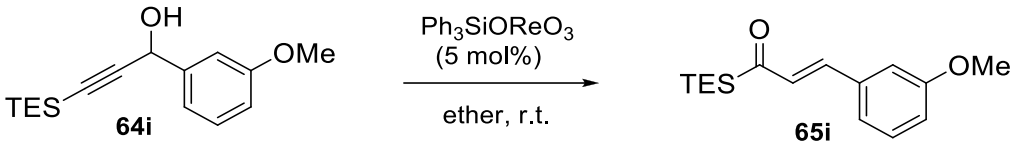

Following *General Procedure 7*, propargyl alcohol **64i** (0.15 g, 0.54 mmol, 1.0 equiv.) was converted to α,β-unsaturated acyl silane **65i**. Purification by flash column chromatography using 7% solution of EtOAc in hexanes yielded the product (0.045 g, 0.16 mmol, 30%) as an orange oil.

Data for **65i**
^{1}H-NMR (400 MHz, $CDCl_3$)
δ 7.38 (d, *J* = 16.8 Hz, 1 H), 7.32 (d, *J* = 8.0 Hz, 1 H), 7.17 (d, *J* = 7.5 Hz, 1 H), 7.10 (s, 1 H), 6.97 (dd, *J* = 8.0, 7.5 Hz, 1 H), 6.92 (d, *J* = 16.8 Hz, 1 H), 3.87 (s, 3 H), 1.04 (t, *J* = 8.0 Hz, 9 H), 0.87 (q, *J* = 8.0 Hz, 6 H).
^{13}C-NMR (100 MHz, $CDCl_3$)
δ 236.2, 159.8, 141.6, 136.2, 132.1, 129.8, 120.9, 116.1, 113.0, 55.2, 7.3, 2.9.
^{29}Si-NMR (80 MHz, $CDCl_3$)
δ −1.30
IR Alpha-Platinum ATR, Bruker, diamond crystal
υ = 3120, 2953, 1637, 1600, 1501, 1245, 1160, 966 cm^{-1}
HRMS ESI
Calculated for $C_{21}H_{26}O_2Si$ ($[M+H]^+$) = 277.1618, found = 277.1607

α,β-Unsaturated acyl silane 65j

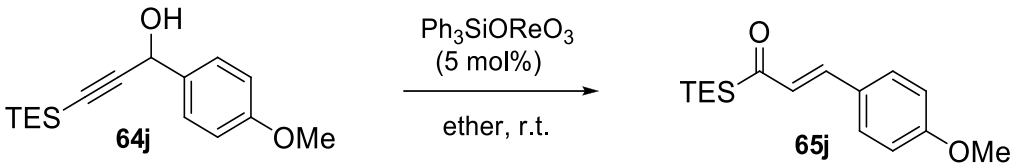

Following *General Procedure 7*, propargyl alcohol **64j** (0.15 g, 0.54 mmol, 1.0 equiv.) was converted to α,β-unsaturated acyl silane **65j**. Purification by flash column chromatography using 7% solution of EtOAc in hexanes yielded the product (0.078 g, 0.28 mmol, 52%) as an orange oil.

Data for **65j**
^{1}H-NMR (400 MHz, $CDCl_3$)
δ 7.53 (d, *J* = 8.4 Hz, 2 H), 7.39 (d, *J* = 16.4 Hz, 1 H), 6.94 (d, *J* = 8.4 Hz, 2 H), 6.86 (d, *J* = 16.4 Hz, 1 H), 3.87 (s, 3 H), 1.04 (t, *J* = 8.0 Hz, 9 H), 0.86 (q, *J* = 8.0 Hz, 6 H).
^{13}C-NMR (100 MHz, $CDCl_3$)
δ 235.5, 161.5, 141.6, 130.1, 129.9, 127.4, 114.3, 55.3, 7.3, 2.9.
^{29}Si-NMR (80 MHz, $CDCl_3$)
δ −1.32
IR Alpha-Platinum ATR, Bruker, diamond crystal
υ = 3119, 2954, 1635, 1603, 1508, 1248, 1159, 974 cm^{-1}
HRMS ESI
Calculated for $C_{16}H_{25}O_2Si$ ($[M+H]^+$) = 277.1618, found = 277.1607

α,β-Unsaturated acyl silane 65k

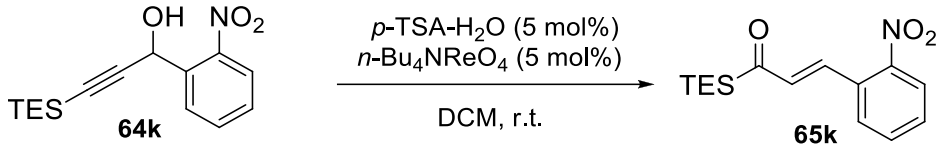

Following *General Procedure 6*, propargyl alcohol **64k** (0.15 g, 0.52 mmol, 1.0 equiv.) was converted to α,β-unsaturated acyl silane **65k**. Purification by flash column chromatography using 15% solution of EtOAc in hexanes yielded the product (0.12 g, 0.40 mmol, 78%) as an orange oil.

Data for **65k**
^{1}H-NMR (400 MHz, $CDCl_3$)
δ 8.10 (d, *J* = 8.0 Hz, 1 H), 8.00 (d, *J* = 16.0 Hz, 1 H), 7.69 (m, 2 H), 7.58 (dd, *J* = 5.0, 4.4 Hz, 1 H), 6.69 (d, *J* = 16.0 Hz, 1 H), 1.04 (t, *J* = 7.6 Hz, 9 H), 0.90 (q, *J* = 7.6 Hz, 6 H).
^{13}C-NMR (100 MHz, $CDCl_3$)
δ 237.1, 148.2, 138.3, 137.0, 133.5, 131.2, 129.3, 128.7, 125.0, 7.2, 2.9.
^{29}Si-NMR (80 MHz, $CDCl_3$)
δ −0.4
IR Alpha-Platinum ATR, Bruker, diamond crystal
υ = 3105, 2955, 1638, 1523, 1343, 1237, 1138, 970 cm^{-1}
HRMS ESI
Calculated for $C_{15}H_{22}NO_3Si$ ($[M+H]^+$) = 292.1364, found = 292.1365

α,β-Unsaturated acyl silane 65l

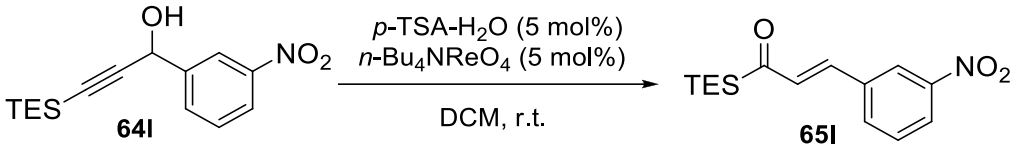

Following *General Procedure 6*, propargyl alcohol **64l** (0.15 g, 0.52 mmol, 1.0 equiv.) was converted to α,β-unsaturated acyl silane **65l**. Purification by flash column chromatography using 15% solution of EtOAc in hexanes yielded the product (0.10 g, 0.34 mmol, 66%) as as an orange oil.

Data for **65l**
^{1}H-NMR (400 MHz, $CDCl_3$)
δ 8.42 (s, 1 H), 8.26 (d, *J* = 8.0 Hz, 1 H), 7.88 (d, *J* = 7.6 Hz, 1 H), 7.61 (dd, *J* = 8.0, 7.6 Hz, 1 H), 7.40 (d, *J* = 16.0 Hz, 1 H), 7.05 (d, *J* = 16.0 Hz, 1 H), 1.05 (t, *J* = 7.6 Hz, 9 H), 0.89 (q, *J* = 7.6 Hz, 6 H).
^{13}C-NMR (100 MHz, $CDCl_3$)
δ 236, 148.6, 137.4, 136.8, 133.7, 133.0, 129.8, 124.4, 122.5, 7.2, 2.7.
^{29}Si-NMR (80 MHz, $CDCl_3$)
δ –0.3
IR Alpha-Platinum ATR, Bruker, diamond crystal
υ = 3088, 2954, 1642, 1582, 1527, 1350, 1153, 973 cm^{-1}
HRMS ESI
Calculated for $C_{15}H_{23}NO_3Si$ ($[M+H]^+$) = 292.1364, found = 292.1352

α,β-Unsaturated acyl silane 65m

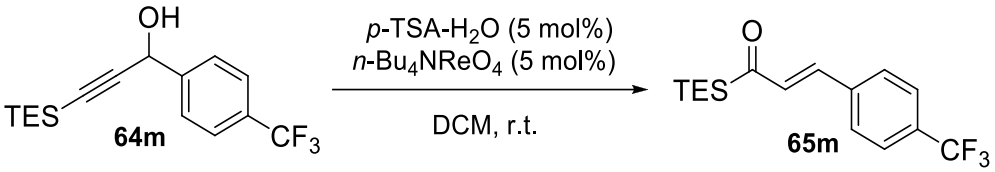

Following *General Procedure 6*, propargyl alcohol **64m** (0.15 g, 0.48 mmol, 1.0 equiv.) was converted to α,β-unsaturated acyl silane **65m**. Purification by flash column chromatography using 10% solution of EtOAc in hexanes yielded the product (0.10 g, 0.33 mmol, 69%) as an orange oil in.

Data for **65m**
^{1}H-NMR (400 MHz, $CDCl_3$)
δ 7.67 (s, 4 H), 7.39 (d, *J* = 16.4 Hz, 1 H), 6.99 (d, *J* = 16.4 Hz, 1 H), 1.05 (t, *J* = 8.0 Hz, 9 H), 0.88 (q, *J* = 8.0 Hz, 6 H).
^{13}C-NMR (100 MHz, $CDCl_3$)
δ 236.2, 138.8, 138.3, 132.9, 131.7 (q, $^{2}J_{C\text{-}F}$ = 33.0 Hz), 128.2, 125.7, 123.7 (q, $^{1}J_{C\text{-}F}$ = 270.8 Hz), 7.2, 2.7.
^{29}Si-NMR (80 MHz, $CDCl_3$)
δ −0.6
^{19}F-NMR (376 MHz, $CDCl_3$)
δ −62.8
IR Alpha-Platinum ATR, Bruker, diamond crystal
υ = 3040, 2956, 1641, 1617, 1321, 1237, 1125, 976 cm^{-1}
HRMS ESI
Calculated for $C_{16}H_{22}F_3OSi$ ($[M+H]^+$) = 315.1392, found 315.1387

1-Indanone 66n

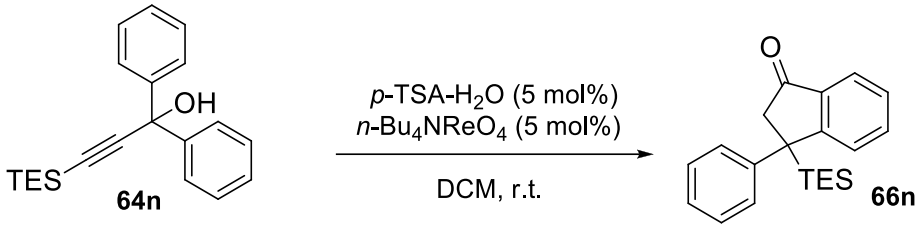

Following *General Procedure 6*, propargyl alcohol **64n** (0.15 g, 0.45 mmol, 1.0 equiv.) was converted to 1-indanone **66n**. Purification by flash column chromatography using 7% solution of EtOAc in hexanes yielded the product (0.083 g, 0.25 mmol, 55%) as a yellow oil.

Data for **66n**
^{1}H-NMR (400 MHz, $CDCl_3$)
δ 7.84 (d, *J* = 7.6 Hz, 1 H), 7.80 (d, *J* = 8.0 Hz, 1 H), 7.70 (dd, *J* = 8.0, 7.4 Hz, 1 H), 7.43 (dd, *J* = 7.6, 7.4 Hz, 1 H), 7.36 (d, *J* = 7.6 Hz, 2 H), 7.31 (dd, *J* = 8.0, 7.6 Hz, 2 H), 7.18 (t, *J* = 8.0 Hz, 1 H), 3.40 (d, *J* = 19.6 Hz, 1 H), 2.99 (d, *J* = 19.6 Hz, 1 H), 0.77 (t, *J* = 7.6 Hz, 9 H), 0.64 (m, 6 H)
^{13}C-NMR (100 MHz, $CDCl_3$)
δ 205.6, 158.9, 144.8, 136.6, 133.9, 128.3, 128.2, 127.2, 126.7, 125.4, 124.2, 50.3, 43.4, 7.6, 3.0.
^{29}Si-NMR (80 MHz, $CDCl_3$)
δ 9.0
IR Alpha-Platinum ATR, Bruker, diamond crystal
υ = 3085, 2953, 1705, 1609, 1510, 1238 cm^{-1}
HRMS ESI
Calculated for $C_{21}H_{28}OSi$ ($[M+H]^+$) = 323.1826, found 323.1812

α,β-Unsaturated acyl silane 65o

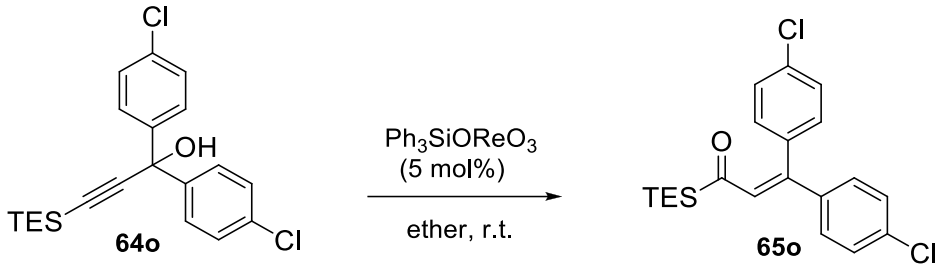

Following *General Procedure 7*, propargyl alcohol **64o** (0.15 g, 0.38 mmol, 1.0 equiv.) was converted to α,β-unsaturated acyl silane **65o**. Purification by flash column chromatography using 7% solution of EtOAc in hexanes yielded the product (0.12 g, 0.30 mmol, 78%) as red oil.

Data for **65o**
^{1}H-NMR (400 MHz, $CDCl_3$)
δ 7.33 (m, 4 H), 7.22 (d, *J* = 8.0 Hz, 2 H), 7.10 (d, *J* = 8.0 Hz, 2 H), 6.82 (s, 1 H), 0.97 (t, *J* = 8.0 Hz, 9 H), 0.67 (q, *J* = 8.0 Hz, 6 H).
^{13}C-NMR (100 MHz, $CDCl_3$)
δ 239.3, 145.5, 139.5, 136.7, 135.3, 134.6, 131.5, 130.3, 129.7, 128.6, 128.2, 7.2, 2.2.
^{29}Si-NMR (80 MHz, $CDCl_3$)
δ −1.49
IR Alpha-Platinum ATR, Bruker, diamond crystal
υ = 3080, 2954, 1622, 1589, 1488, 1237, 1089, 825 cm^{-1}
HRMS ESI
Calculated for $C_{21}H_{26}Cl_2OSi$ ($[M+H]^+$) = 391.1046, found 391.1038

Enyne 66p

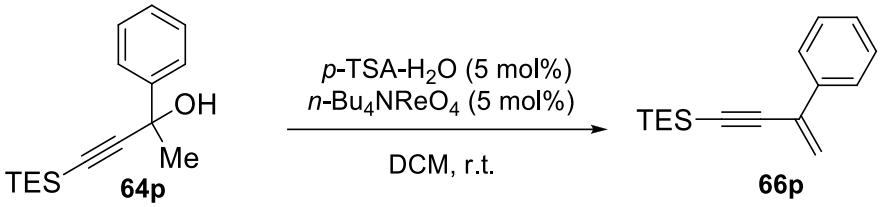

Following *General Procedure 6*, propargyl alcohol **64p** (0.15 g, 0.58 mmol, 1.0 equiv.) was converted to dehydration product **66p**. Filtration through celite® yielded the product (0.13 g, 0.53 mmol, 92%) as yellow oil.

Data for **66p**
^{1}H-NMR (400 MHz, $CDCl_3$)
δ 7.69 (d, *J* = 7.6 Hz, 2 H), 7.36 (m, 3 H), 5.96 (s, 1 H), 5.74 (s, 1 H), 1.08 (t, *J* = 8.0 Hz, 9 H), 0.70 (q, *J* = 8.0 Hz, 6 H).
^{13}C-NMR (100 MHz, $CDCl_3$)
δ 136.9, 130.7, 128.2, 128.1, 126.0, 121.2, 105.2, 93.3, 7.4, 4.4.
^{29}Si-NMR (80 MHz, $CDCl_3$)
δ –7.0
IR Alpha-Platinum ATR, Bruker, diamond crystal
υ = 3104, 2954, 2148, 1236, 950, 895, 700 cm^{-1}
HRMS ESI
Calculated for $C_{16}H_{23}Si$ ($[M+H]^+$) = 243.1564, found 243.1564

α,β-Unsaturated acyl silane 65p

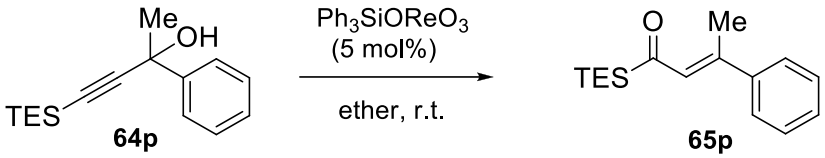

Following *General Procedure 7*, propargyl alcohol **64p** (0.15 g, 0.58 mmol, 1.0 equiv.) was converted to α,β-unsaturated acyl silane **65p**. Purification by flash column chromatography using 2.5% solution of EtOAc in hexanes yielded the product (0.11 g, 0.43 mmol, 75%) as an orange oil.

Data for **65p**
^{1}H-NMR (400 MHz, $CDCl_3$)
δ 7.52 (m, 2 H), 7.41 (m, 3 H), 6.96 (s, 1 H), 2.48 (s, 3 H), 1.04 (t, *J* = 7.6 Hz, 9 H), 0.81 (q, *J* = 7.6 Hz, 6 H).
^{13}C-NMR (100 MHz, $CDCl_3$)
δ 239.2, 147.2, 142.6, 128.9, 128.4, 128.0, 126.6, 18.4, 7.3, 2.2.
^{29}Si-NMR (80 MHz, $CDCl_3$)
δ −2.54
IR Alpha-Platinum ATR, Bruker, diamond crystal
υ = 3083, 2953, 1624, 1553, 1237, 1005, 864 cm^{-1}
HRMS ESI
Calculated for $C_{16}H_{26}OSi$ ($[M+H]^+$) = 261.1670, found 261.1660

α,β-Unsaturated ketone 66q

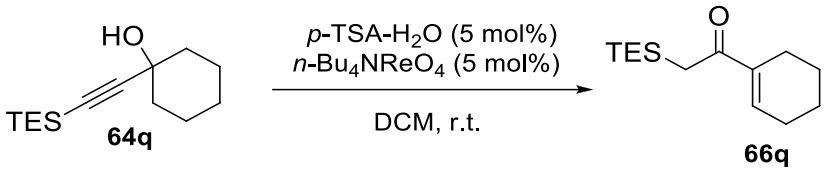

Following *General Procedure 6*, propargyl alcohol **64q** (0.15 g, 0.63 mmol, 1.0 equiv.) was converted to α,β-unsaturated ketone **66q**. Purification by flash column chromatography using 5% solution of EtOAc in hexanes yielded the product (0.12 g, 0.52 mmol, 82%) as yellow oil.

Data for **66q**
^{1}H-NMR (400 MHz, $CDCl_3$)
δ 6.93 (s, 1 H), 2.30 (s, 2 H), 2.27 (m, 4 H), 1.64 (m, 4 H), 0.95 (t, *J* = 8.0 Hz, 9 H), 0.54 (q, *J* = 8.0 Hz, 6 H).
^{13}C-NMR (100 MHz, $CDCl_3$)
δ 199.2, 140.8, 139.6, 26.0, 25.0, 22.8, 21.8, 21.4, 6.6, 6.3.
^{29}Si-NMR (80 MHz, $CDCl_3$)
δ 8.9
IR Alpha-Platinum ATR, Bruker, diamond crystal
υ = 3002, 2953, 1669, 1234, 1065, 1003, 727 cm^{-1}
HRMS ESI
Calculated for $C_{14}H_{26}NaOSi$ ($[M+Na]^+$) = 261.1670, found 261.1657

α,β-Unsaturated acyl silane 65t

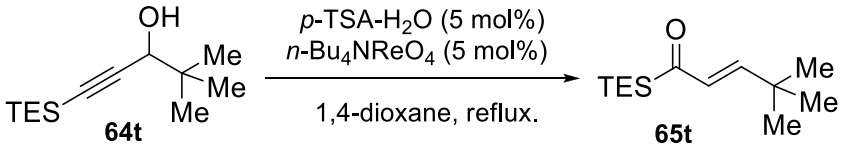

A flame-dried round-bottomed flask equipped with a stir bar was charged with nBu$_4$N•ReO$_4$ (0.016 g, 0.033 mmol, 0.05 equiv.), TsOH•H$_2$O (0.0063 g, 0.033 mmol, 0.05 equiv.) followed by propargyl alcohol **1t** (0.15 g, 0.66 mmol, 1.0 equiv.) in 1,4-dioxane. After refluxing for 24 hours the reaction was diluted with water and the aqueous phase separated. The organic phase was washed with brine, dried using sodium sulphate and concentrated *in vacuo*. Purification by flash column chromatography using 4% solution of EtOAc in hexanes yielded α,β-unsaturated acyl silane **65t** (0.12 g, 0.53 mmol, 80%) as a yellow oil.

Data for **65t**
^{1}H-NMR (400 MHz, CDCl$_3$)
δ 6.72 (d, *J* = 16.8 Hz, 1 H), 6.19 (d, *J* = 16.8 Hz, 1 H), 1.12 (s, 9 H), 0.99 (t, *J* = 8.1 Hz, 9 H), 0.79 (q, *J* = 8.1 Hz, 6 H),
^{13}C-NMR (100 MHz, CDCl$_3$)
δ 236.8, 157.8, 132.3, 28.5, 25.7, 7.2, 3.1.
^{29}Si-NMR (80 MHz, CDCl$_3$)
δ −1.51
IR Alpha-Platinum ATR, Bruker, diamond crystal
υ = 3001, 2955, 1634, 1591, 1268, 1004, 981, 724 cm^{-1}
HRMS ESI
Calculated for $C_{13}H_{28}OSi$ ([M+H]$^+$) = 227.1826, found 227.1817

Isomeric alcohols 64u and 66u

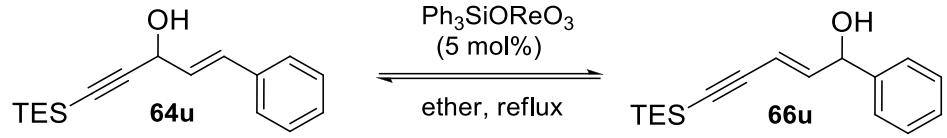

A flame-dried round-bottomed flask equipped with a stir bar was charged with $Ph_3SiOReO_3$ (0.0094 g, 0.018 mmol, 0.05 equiv.) followed by propargyl alcohol **64u** (0.15 g, 0.55 mmol, 1.0 equiv.) in freshly distilled Et_2O. After refluxing for 24 hours the reaction was diluted with water and the aqueous phase separated. The organic phase was washed with brine, dried using Na_2SO_4 and concentrated *in vacuo*. Purification by flash column chromatography using 10% solution of EtOAc in hexanes yielded an inseparable mixture of **64u** and **66u** in a 4:1 ratio (0.13 g, 0.48 mmol, 88% recovered) as a yellow oil.

Data for **64u** and **66u**
^{1}H-NMR (400 MHz, $CDCl_3$)
δ 7.47 (d, *J* = 7.6 Hz, 0.40 H), 7.43 (d, *J* = 7.6 Hz, 2 H), 7.36 (d, *J* = 7.6 Hz, 3 H), 7.31 (m, 2 H), 6.84 (d, *J* = 15.6, 1 H), 6.38 (d, *J* = 5.6 Hz, 0.1 H), 6.32 (dd, *J* = 15.6, 5.6 Hz, 1 H), 5.86 (m, 0.4 H), 5.65 (d, *J* = 11.0, 0.1 H), 5.1 (dd, *J* = 5.6, 3 Hz, 1 H), 1.03 (m, 14 H), 0.66 (m, 10 H).
^{13}C-NMR (100 MHz, $CDCl_3$)
δ 145.3, 145.2, 142.4, 141.7, 136.1, 135.1, 131.9, 128.5, 128.5, 127.9, 127.6, 126.7, 126.4, 125.7, 110.3, 109.8, 105.4, 104.0, 102.0, 98.5, 93.2, 88.7, 74.3, 72.0, 63.2, 7.3, 4.3, 4.2.
^{29}Si-NMR (80 MHz, $CDCl_3$)
δ -7.00, -7.50.
IR Alpha-Platinum ATR, Bruker, diamond crystal
υ = 3081, 2954, 1627, 1601, 1543, 1234, 997, 688 cm^{-1}
HRMS ESI
Calculated for $C_{17}H_{24}NaOSi$ ($[M+Na]^+$) = 295.1494, found 295.1694

α,β,γ,δ-Unsaturated acyl silane 65u

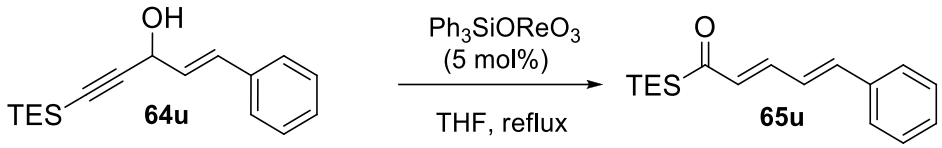

A flame-dried round-bottomed flask equipped with a stir bar was charged with $Ph_3SiOReO_3$ (0.0094 g, 0.018 mmol, 0.05 equiv.) followed by propargyl alcohol **64u** (0.15 g, 0.55 mmol, 1.0 equiv.) in frishely distilled THF. After refluxing for 24 hours the reaction was diluted with water and the aqueous phase separated. The organic phase was washed with brine, dried using Na_2SO_4 and concentrated *in vacuo*. Purification by flash column chromatography using 2.5% solution of EtOAc in hexanes yielded α,β,γ,δ-unsaturated acyl silane **65u** (0.078 g, 0.28 mmol, 51%) as an orange oil.

Data for **65u**
^{1}H-NMR (400 MHz, $CDCl_3$)
δ 7.50 (d, *J* = 7.2 Hz, 2 H), 7.38 (m, 3 H), 7.20 (dd, *J* = 15.6, 13.0 Hz, 1 H), 6.99 (d, *J* = 15.6, 1 H), 6.92 (dd, *J* = 15.6, 10.4 Hz, 1 H), 6.52 (d, *J* = 15.6 Hz, 1 H), 1.03 (t, *J* = 8.0 Hz, 9 H), 0.84 (q, *J* = 8.0 Hz, 6 H).
^{13}C-NMR (100 MHz, $CDCl_3$)
δ 236.1,141.4, 140.9, 136.0, 134.8,129.0, 128.7, 127.3, 127.1, 7.2, 2.8.
^{29}Si-NMR (80 MHz, $CDCl_3$)
δ −1.38
IR Alpha-Platinum ATR, Bruker, diamond crystal
υ = 3081, 2954, 1627, 1601, 1543, 1234, 997, 688 cm^{-1}
HRMS ESI
Calculated for $C_{17}H_{26}OSi$ ($[M+H]^+$) = 273.1670, found 273.1656

Isomeric alcohols 66v and 66v'

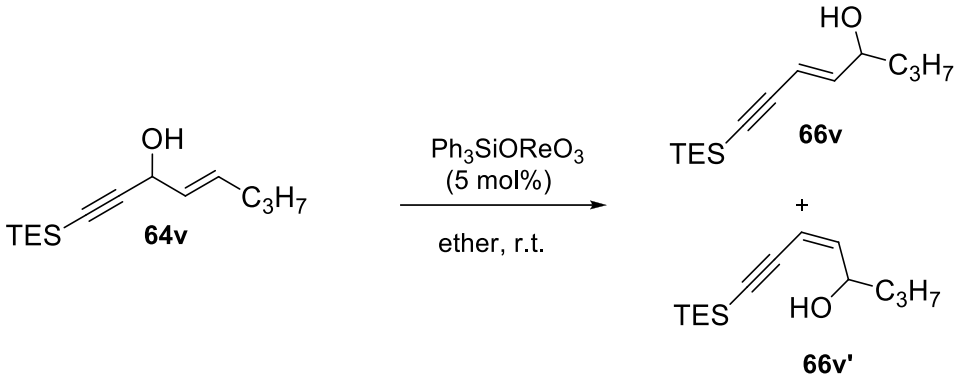

A flame-dried round-bottomed flask equipped with a stir bar was charged with $Ph_3SiOReO_3$ (0.0094 g, 0.018 mmol, 0.05 equiv.) followed by propargyl alcohol **64v** (0.15 g, 0.63 mmol, 1.0 equiv.) in freshly distilled Et_2O. After stirring at room temperature for 24 hours the reaction was diluted with water and the aqueous phase separated. The organic phase was washed with brine, dried using Na_2SO_4 and concentrated *in vacuo*. Purification by flash column chromatography using 8% solution of EtOAc in hexanes yielded an inseparable mixture cis/trans mixture of **66v** and **66v'** in a 1:0.7 ratio (0.14 g, 0.57 mmol, 90% yield) as a clear oil.

Data for **66v** and **66v'**
^{1}H-NMR (400 MHz, $CDCl_3$)
δ 6.22 (dd, *J* = 16.0, 6.0 Hz, 1 H), 5.95 (dd, *J* = 12.0, 8.4 Hz, 0.8 H), 5.77 (d, *J* = 16.0 Hz, 1 H), 5.59 (d,12.0 Hz, 0.8 H), 4.73 (m, 0.7 H), 4.18 (m, 1.0 H), 1.46 (m, 10 H), 1.00 (m, 29 H), 0.66 (m, 12 H).
^{13}C-NMR (100 MHz, $CDCl_3$)
δ 146.7, 146.6, 109.8, 109.6, 104.2, 101.9, 97.8, 92.3, 71.8, 69.9, 38.9, 38.5, 31.3, 18.4, 18.3, 13.8, 7.3, 6.6, 6.3, 4.2.
^{29}Si-NMR (80 MHz, $CDCl_3$)
δ -7.26, -7.62.
IR Alpha-Platinum ATR, Bruker, diamond crystal
υ = 3081, 2954, 1644, 1543, 1234, 968, 702 cm^{-1}
HRMS ESI
Calculated for $C_{14}H_{25}OSi$ ($[M-2H+H]^+$) = 237.1674, found 237.1669

α,β,γ,δ-Unsaturated ketone 67v

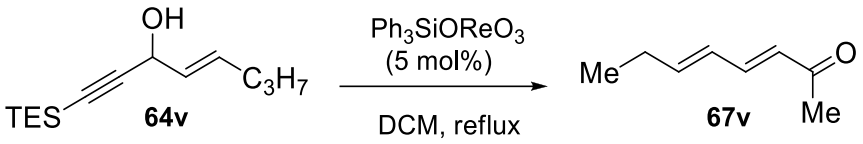

A flame-dried round-bottomed flask equipped with a stir bar was charged with $Ph_3SiOReO_3$ (0.0094 g, 0.031 mmol, 0.05 equiv.) followed by propargyl alcohol **64v** (0.15 g, 0.63 mmol, 1.0 equiv.) in frishely distilled DCM. After refluxing for 24 hours the reaction was diluted with water and the aqueous phase separated. The organic phase was washed with brine, dried using Na_2SO_4 and concentrated *in vacuo*. Purification by flash column chromatography using 10% solution of EtOAc in hexanes yielded α,β,γ,δ-unsaturated ketone **67v** (0.058 g, 0.47 mmol, 74%) as yellow oil.[143]

Data for **67v**
^{1}H-NMR (400 MHz, $CDCl_3$)
δ 7.10 (dd, *J* = 16.0, 9.2 Hz, 1 H), 6.20 (m, 2 H), 6.05 (d, *J* = 15.6 Hz, 1 H), 2.26 (s, 3 H), 2.21 (m, 2 H), 1.05 (t, *J* = 7.2 Hz, 3 H).
^{13}C-NMR (100 MHz, $CDCl_3$)
δ 198.6, 146.9, 144.0, 128.7, 127.7, 27.0, 26.0, 12.7.
IR Alpha-Platinum ATR, Bruker, diamond crystal
υ = 3080, 2954, 1670, 1543, 998, 688 cm^{-1}

5.5 ^{1}H-, ^{2}H-, ^{13}C, ^{19}F-, ^{29}Si-NMR Spectra

^{1}H (400 MHz, $CDCl_3$) and ^{13}C (100 MHz, $CDCl_3$)-NMR spectra of quinoline **11**

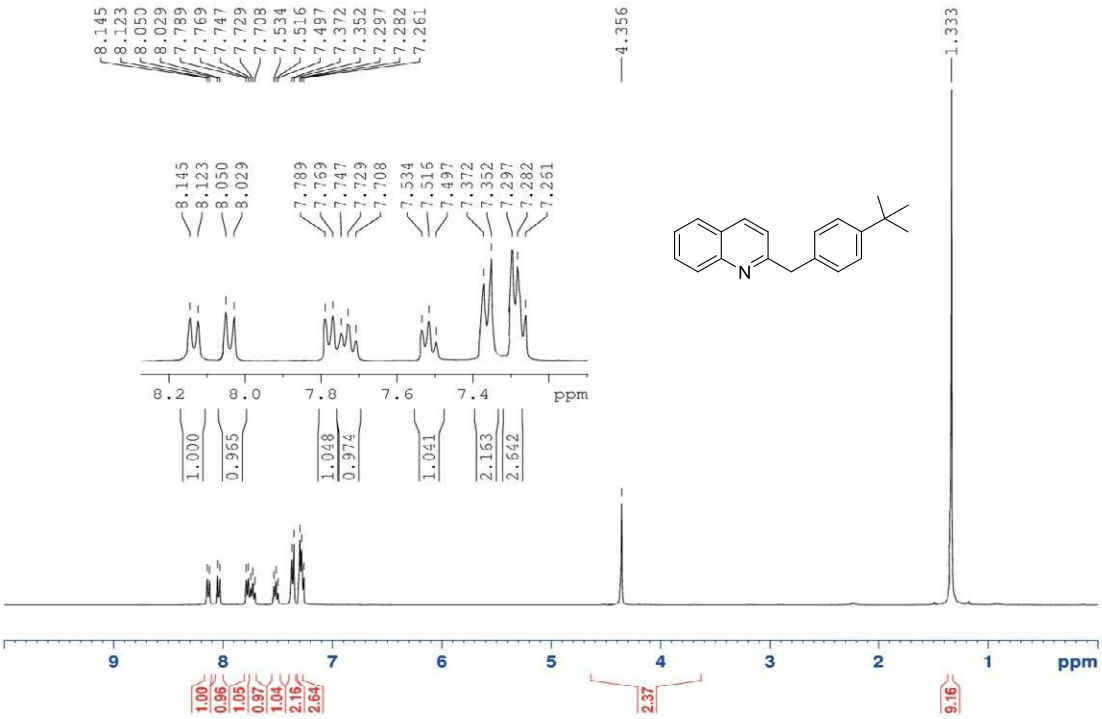

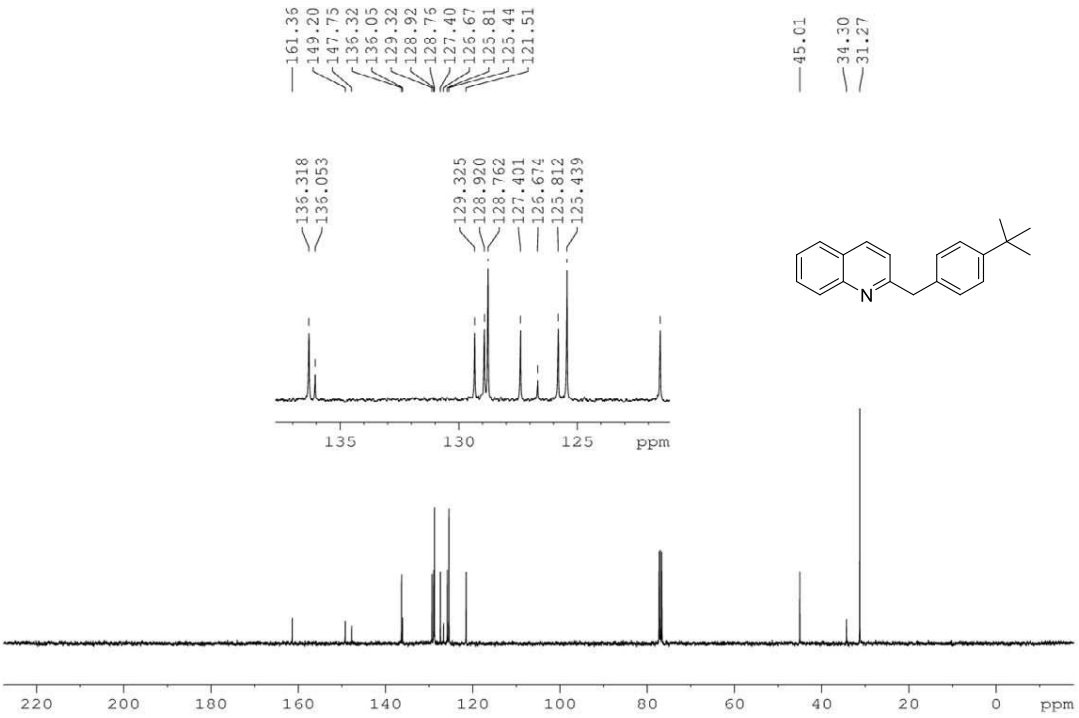

^{1}H (400 MHz, $CDCl_3$) and ^{13}C (100 MHz, $CDCl_3$)-NMR spectra of quinoline **12**

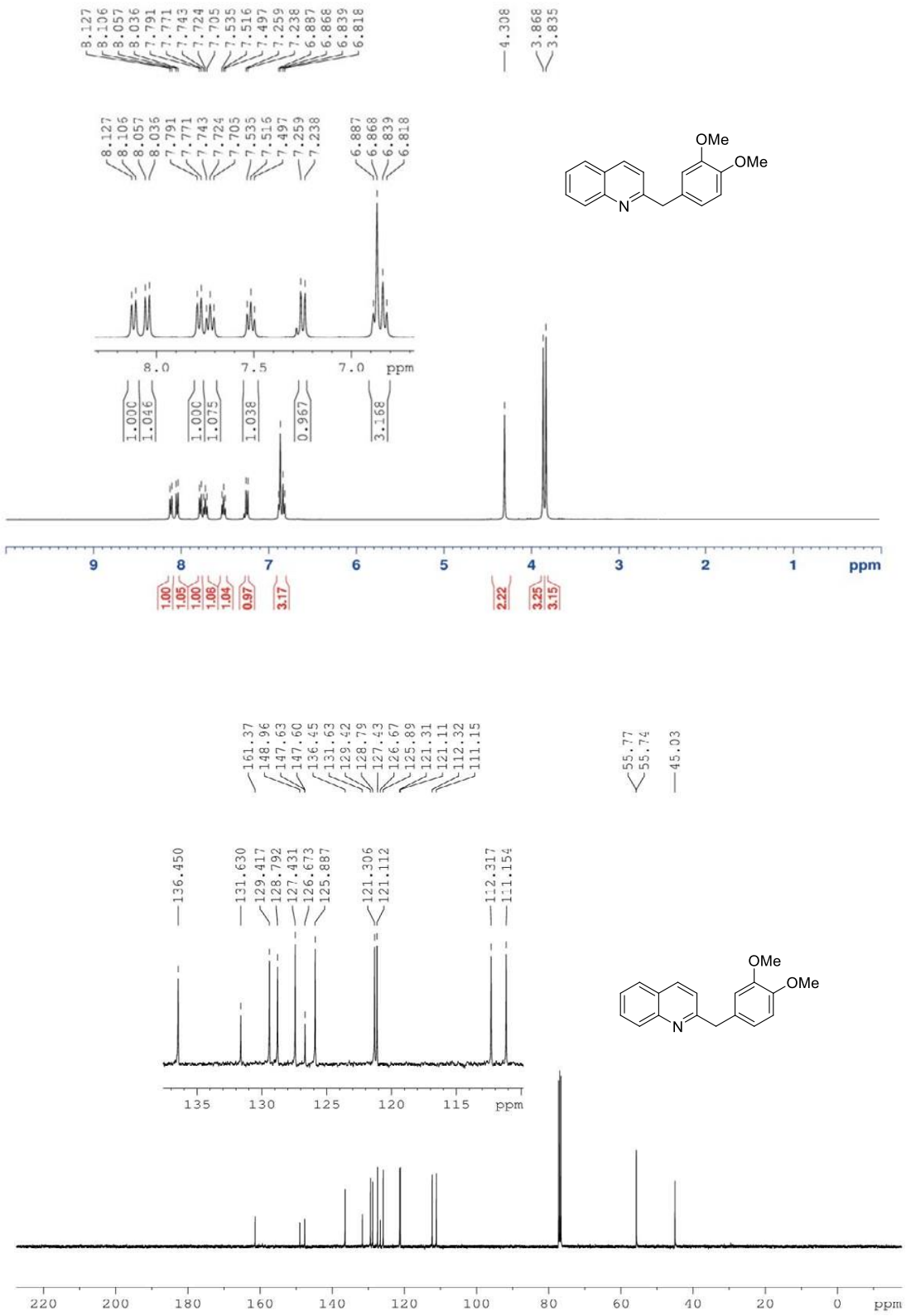

^{1}H (400 MHz, $CDCl_3$) and ^{13}C (100 MHz, $CDCl_3$)-NMR spectra of quinoline **13**

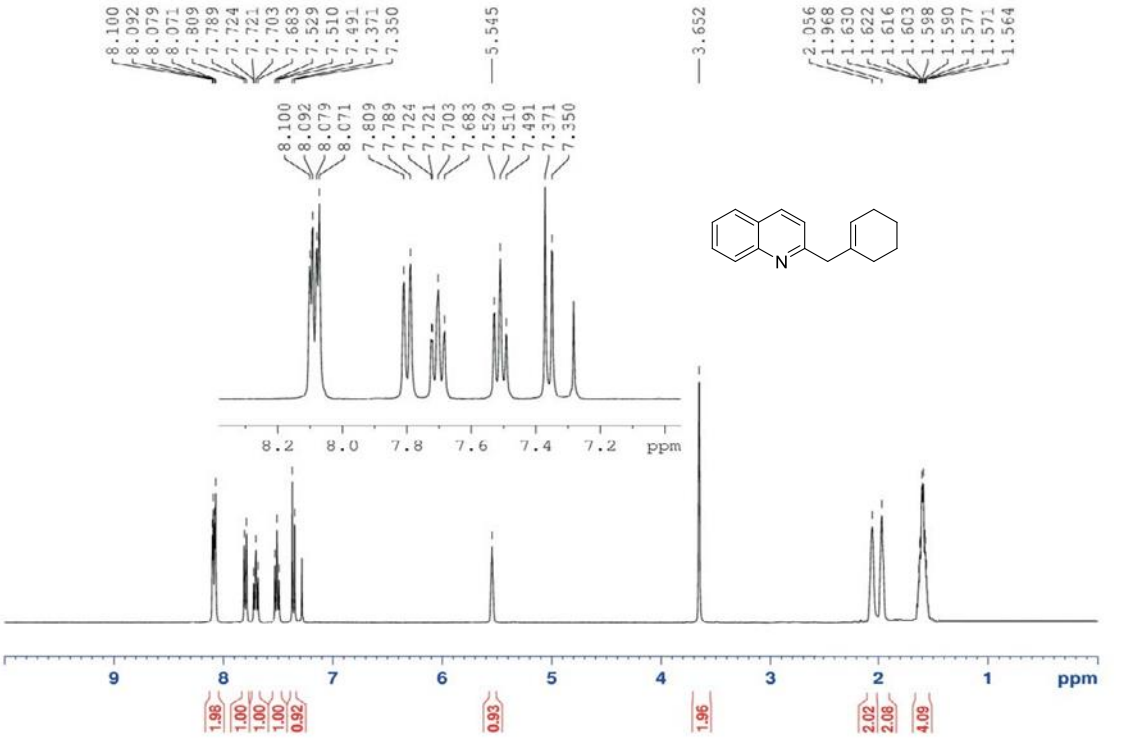

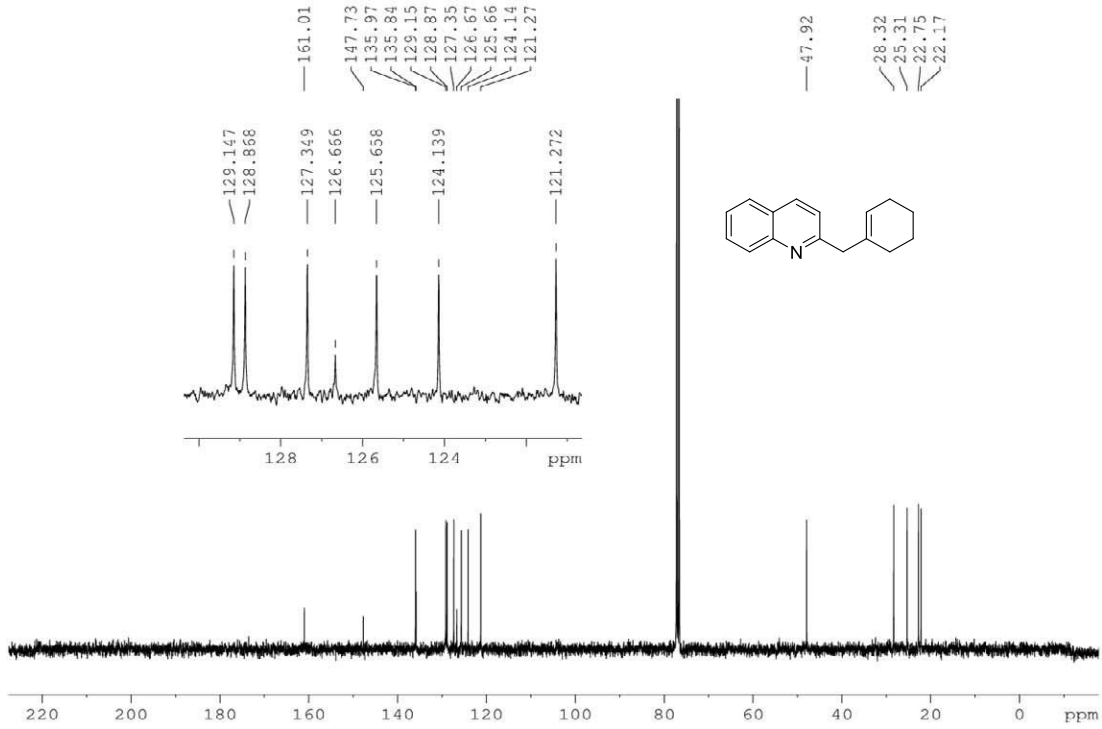

^{1}H (400 MHz, $CDCl_3$) and ^{13}C (100 MHz, $CDCl_3$)-NMR spectra of quinoline **14**

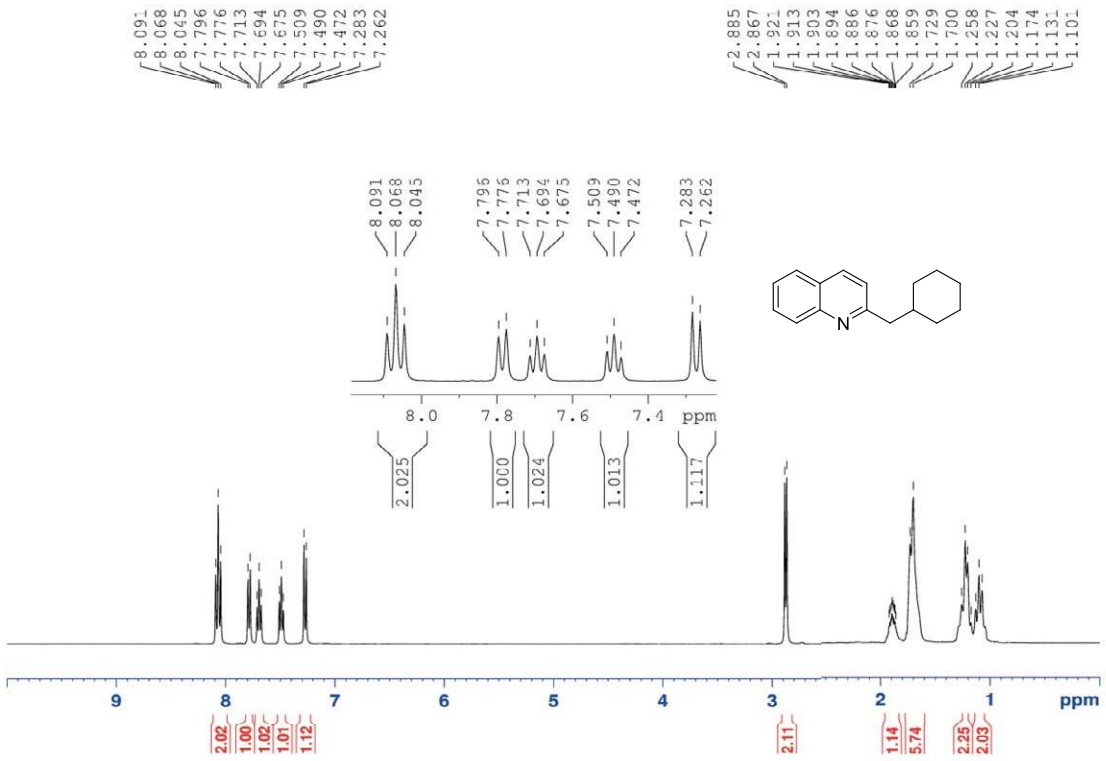

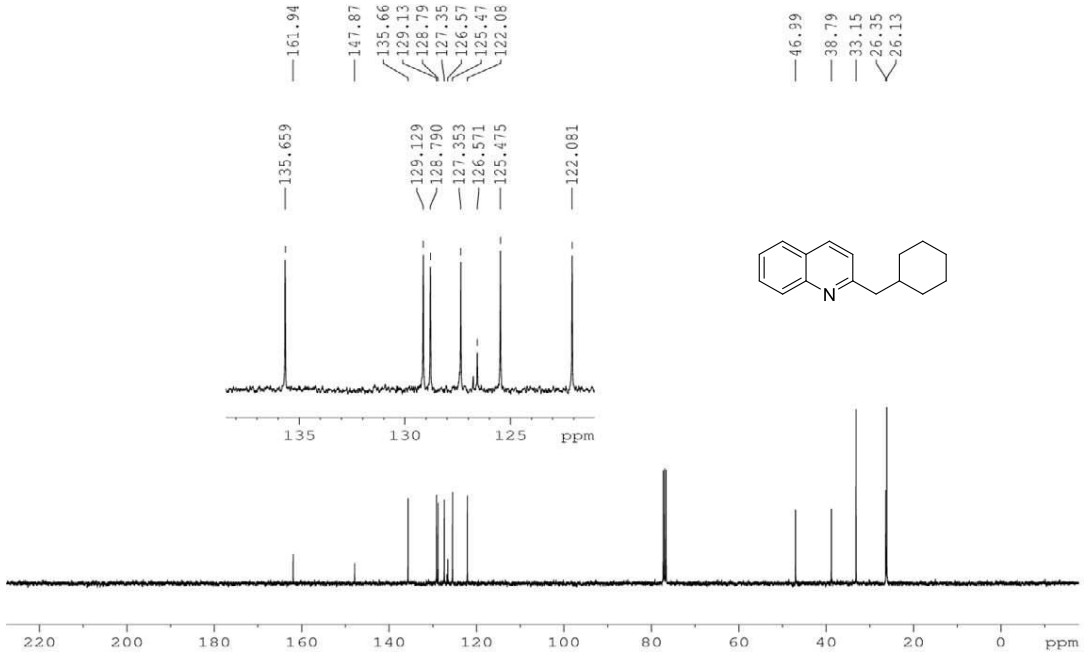

^{1}H (400 MHz, $CDCl_3$) and ^{13}C (100 MHz, $CDCl_3$)-NMR spectra of quinoline **15**

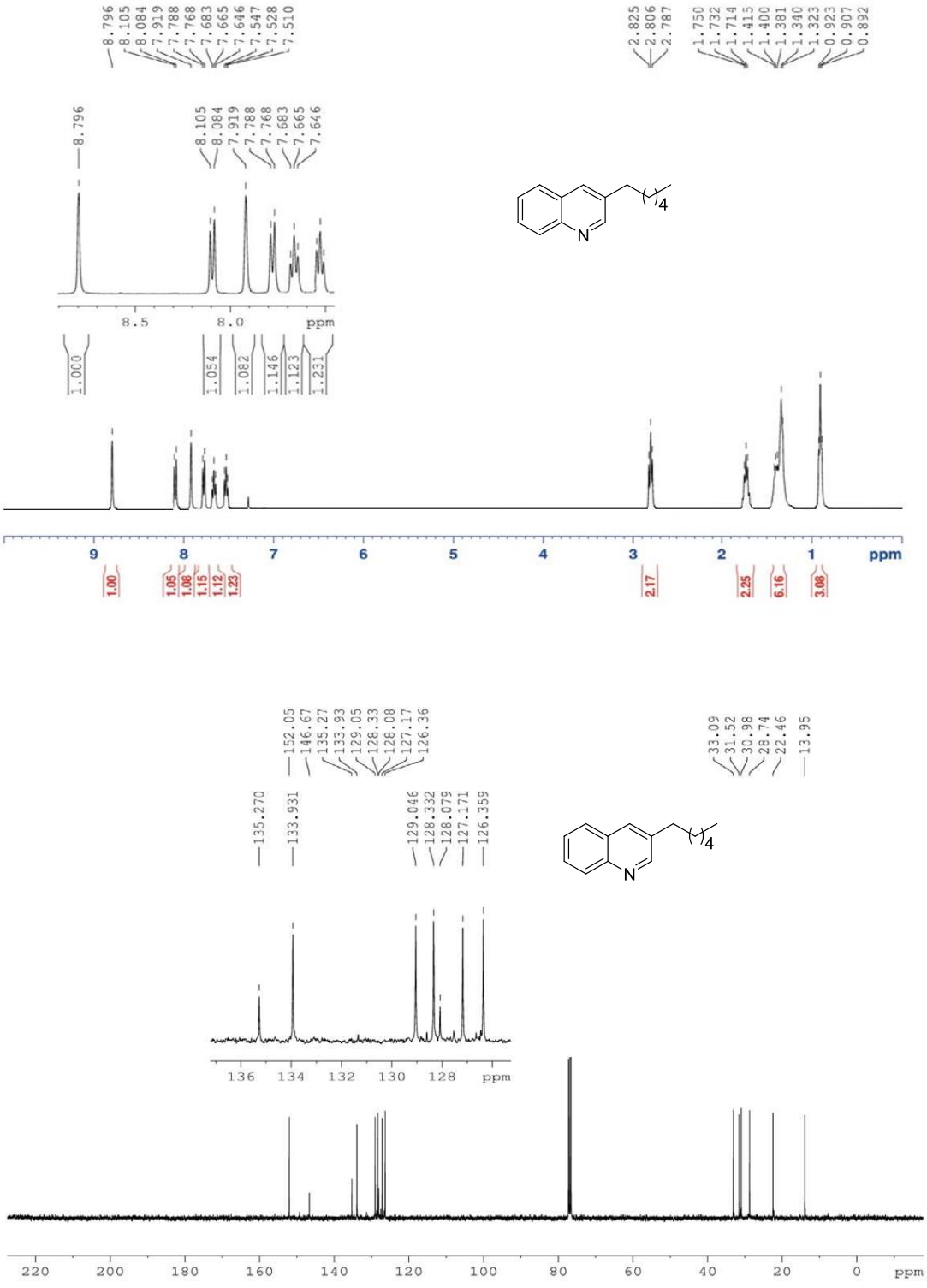

^{1}H (400 MHz, $CDCl_3$) and ^{13}C (100 MHz, $CDCl_3$) -NMR spectra of quinoline **16**

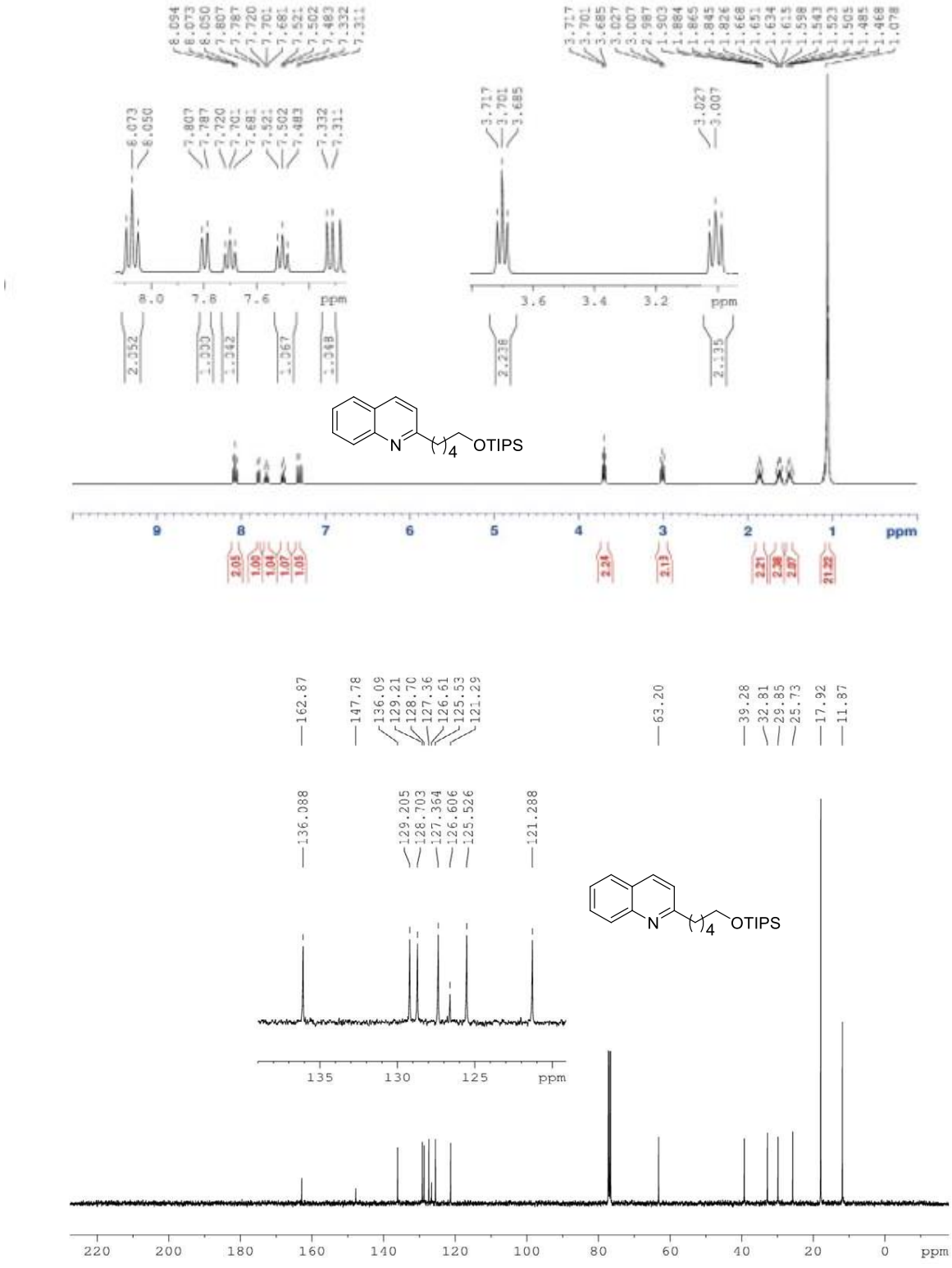

^{1}H (400 MHz, $CDCl_3$) and ^{13}C (100 MHz, $CDCl_3$)-NMR spectra of quinoline **17**

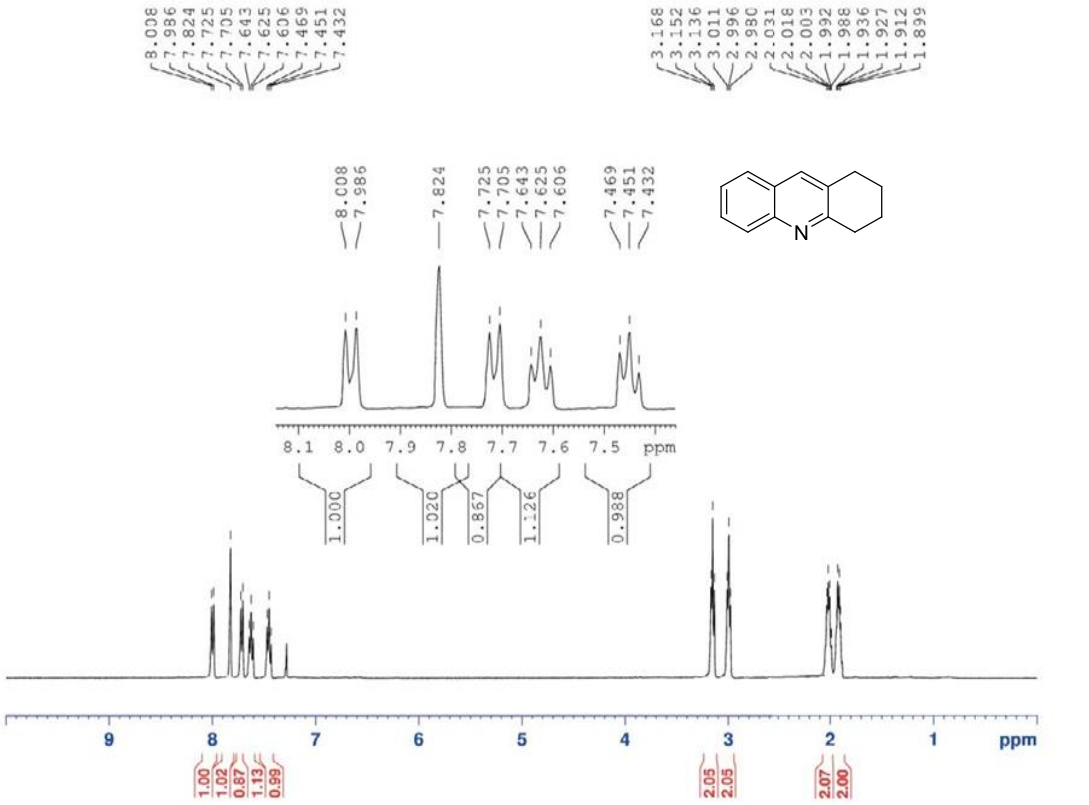

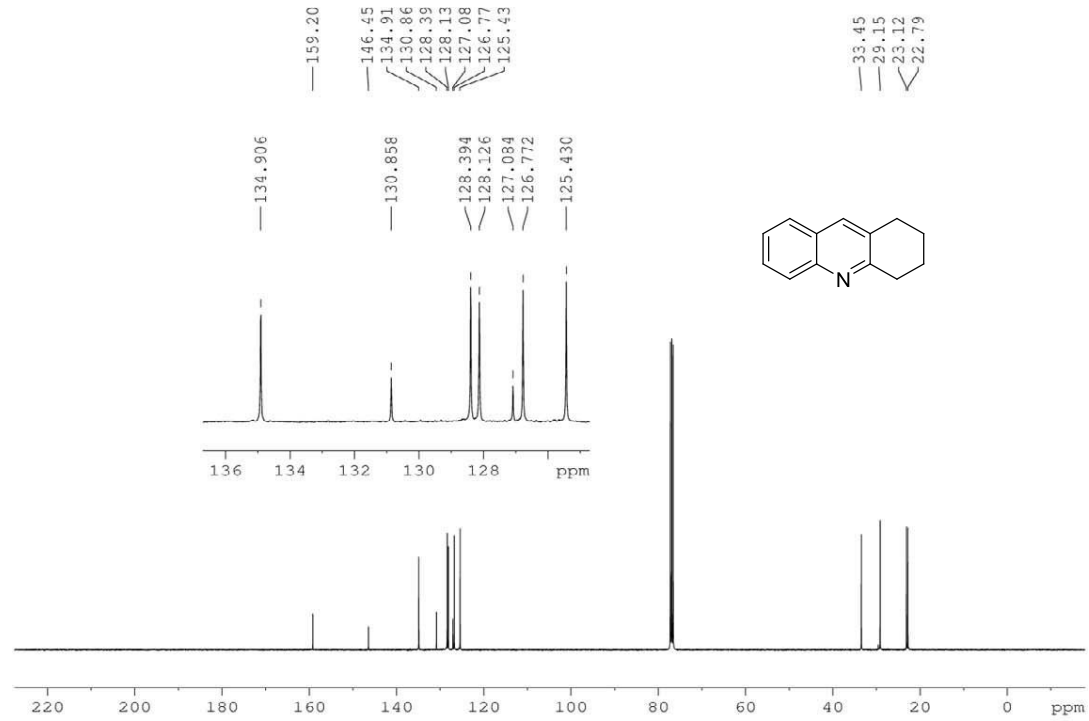

^{1}H (400 MHz, $CDCl_3$) and ^{13}C (100 MHz, $CDCl_3$)-NMR spectra of quinoline **18**

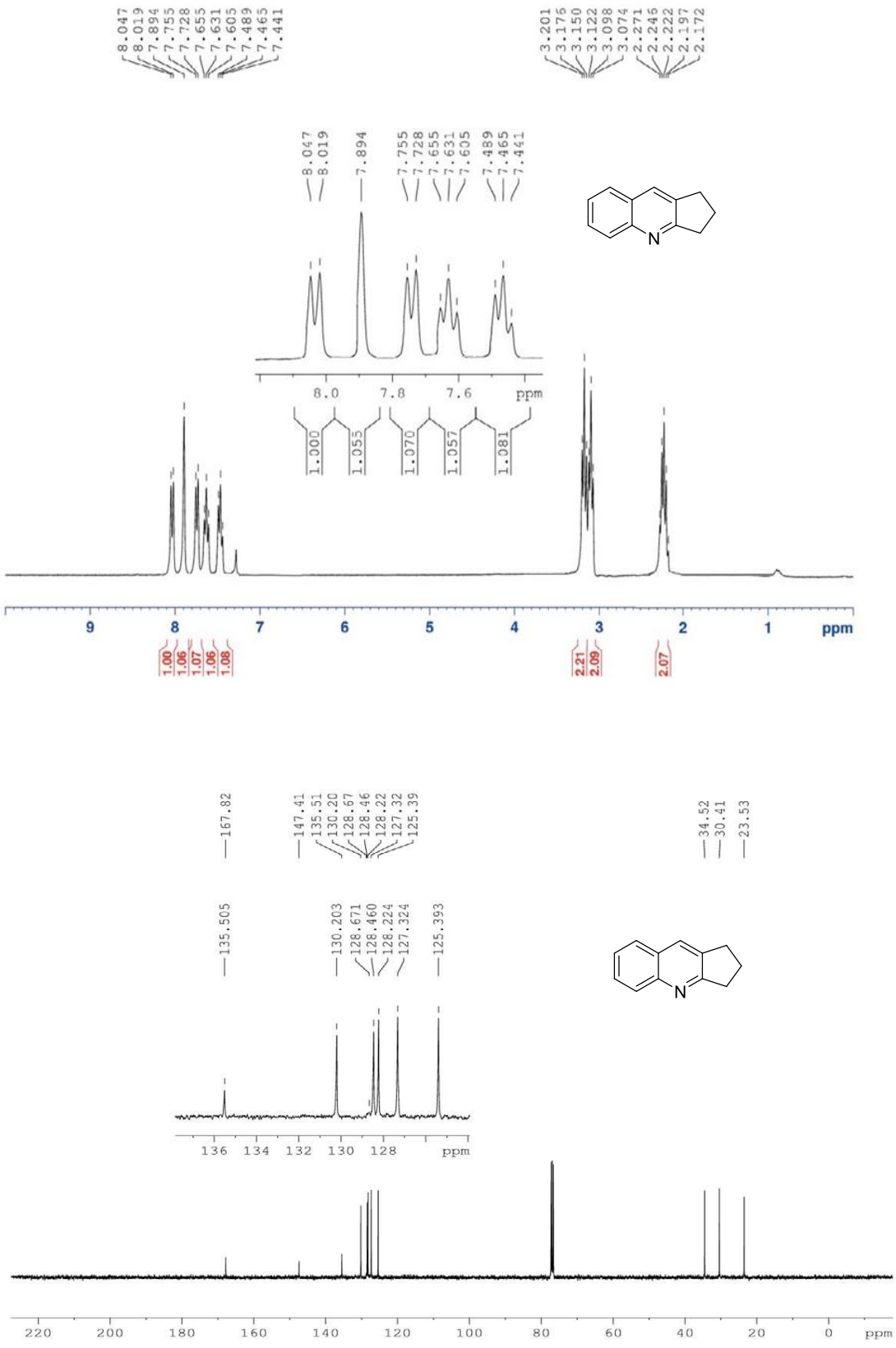

^{1}H (400 MHz, $CDCl_3$) and ^{13}C (100 MHz, $CDCl_3$)-NMR spectra of quinoline **27**

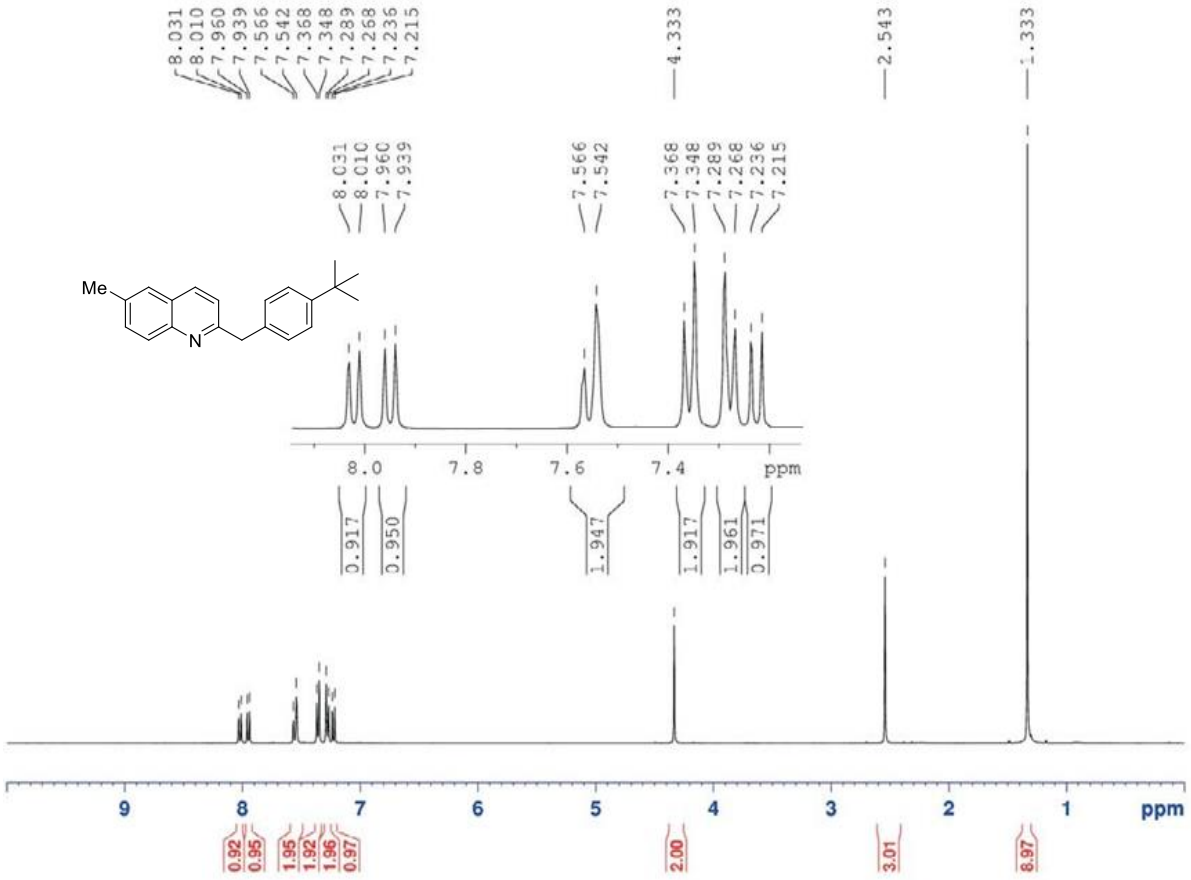

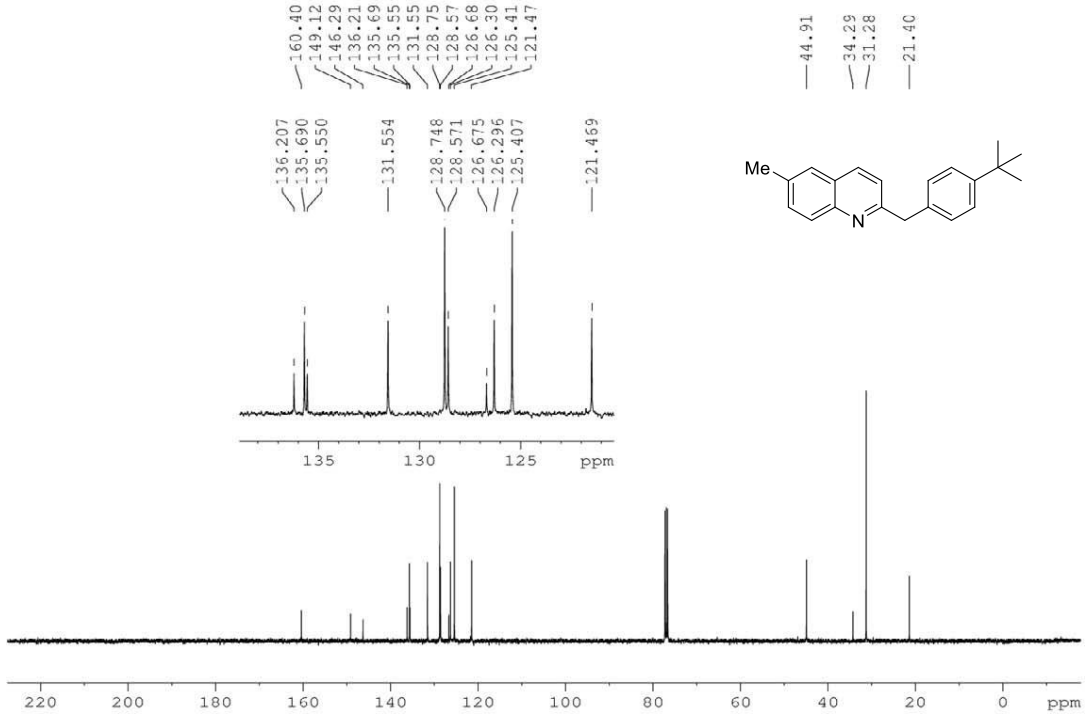

^{1}H (400 MHz, $CDCl_3$) and ^{13}C (100 MHz, $CDCl_3$)-NMR spectra of quinoline **28**

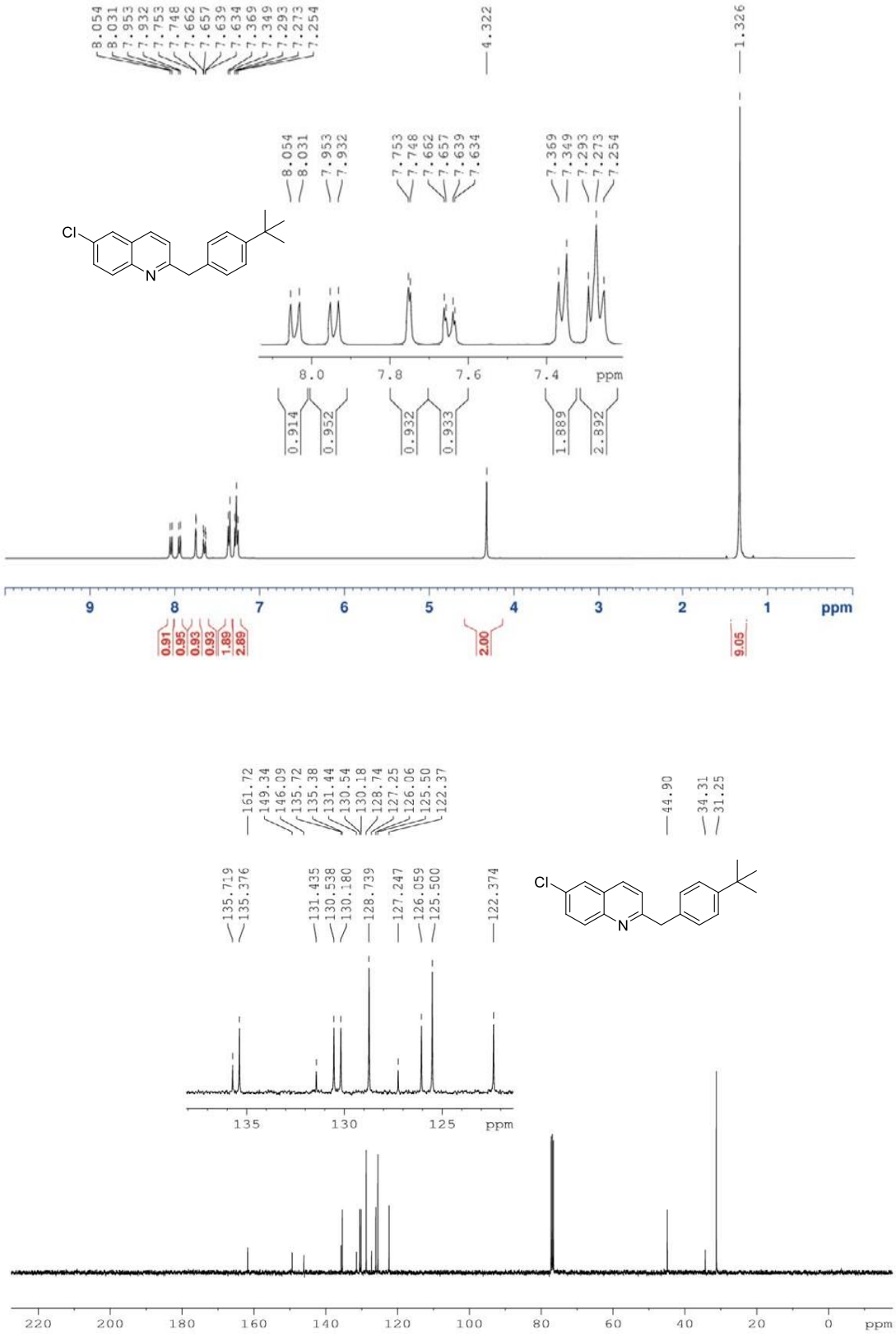

^{1}H (400 MHz, $CDCl_3$) and ^{13}C (100 MHz, $CDCl_3$)-NMR spectra of quinoline **29**

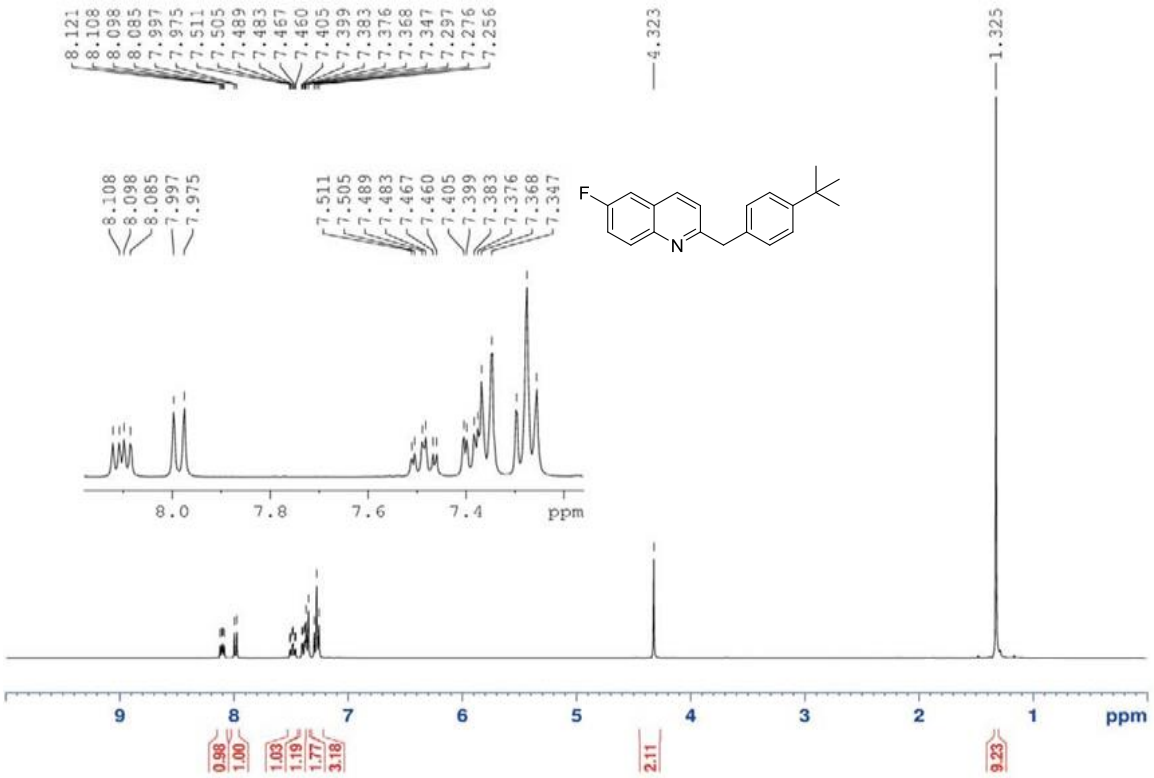

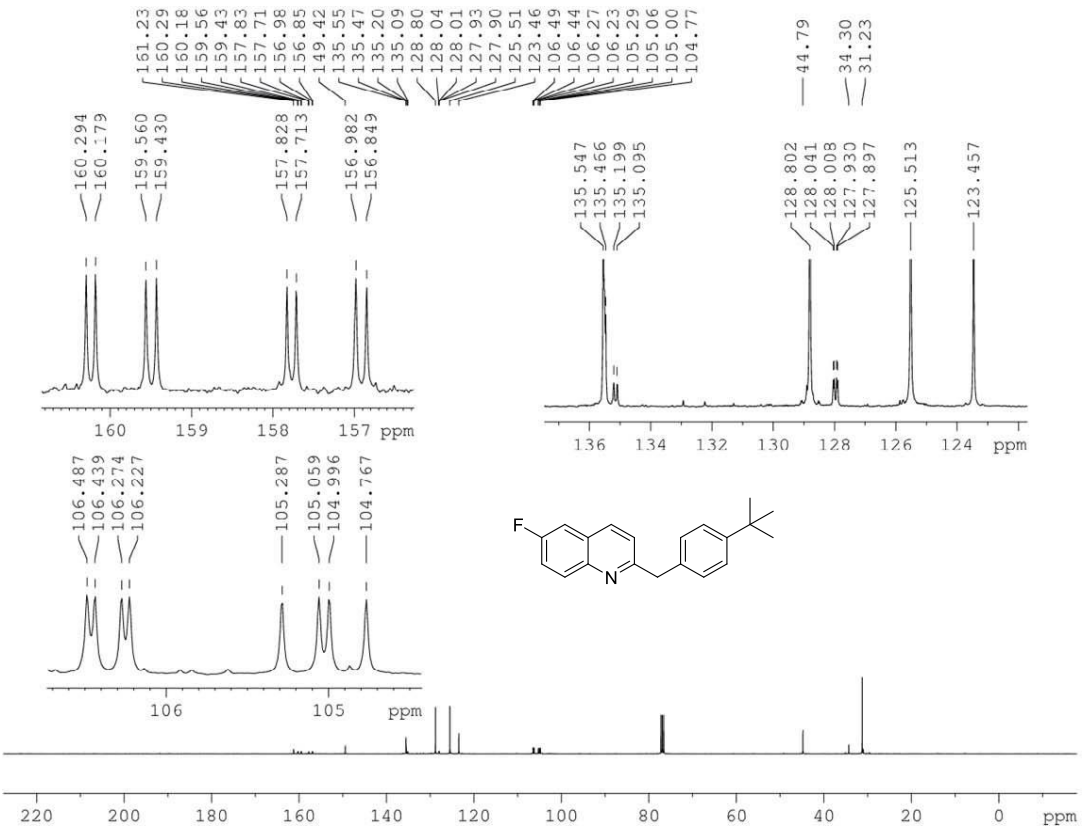

^{19}F (376 MHz, $CDCl_3$)-NMR spectrum of quinoline **29**

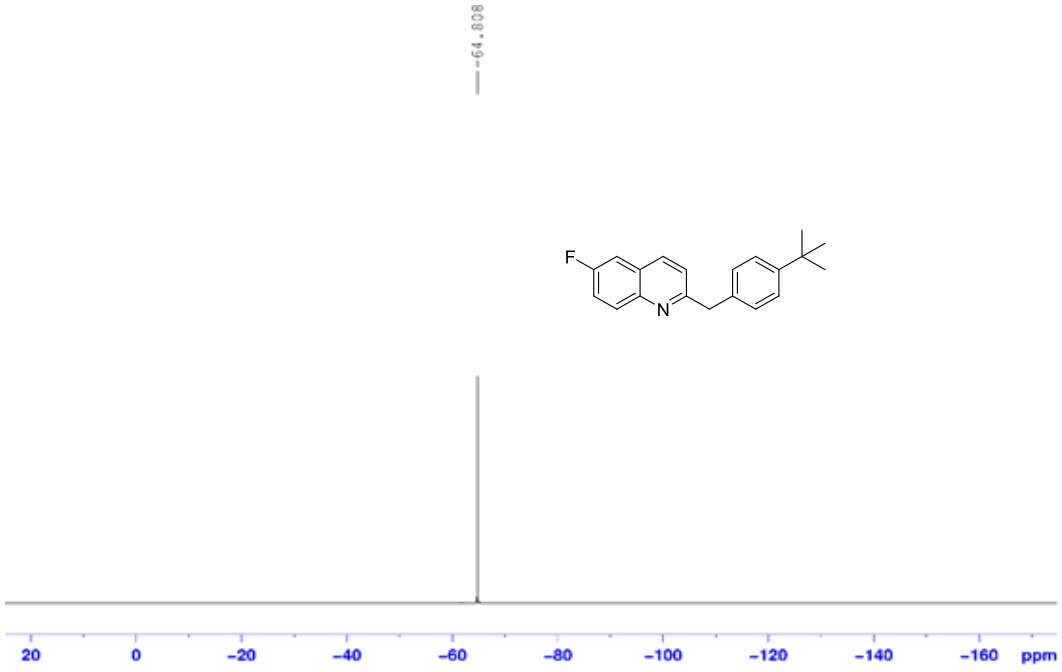

^{1}H (400 MHz, $CDCl_3$) and ^{13}C (100 MHz, $CDCl_3$)-NMR spectra of quinoline **30**

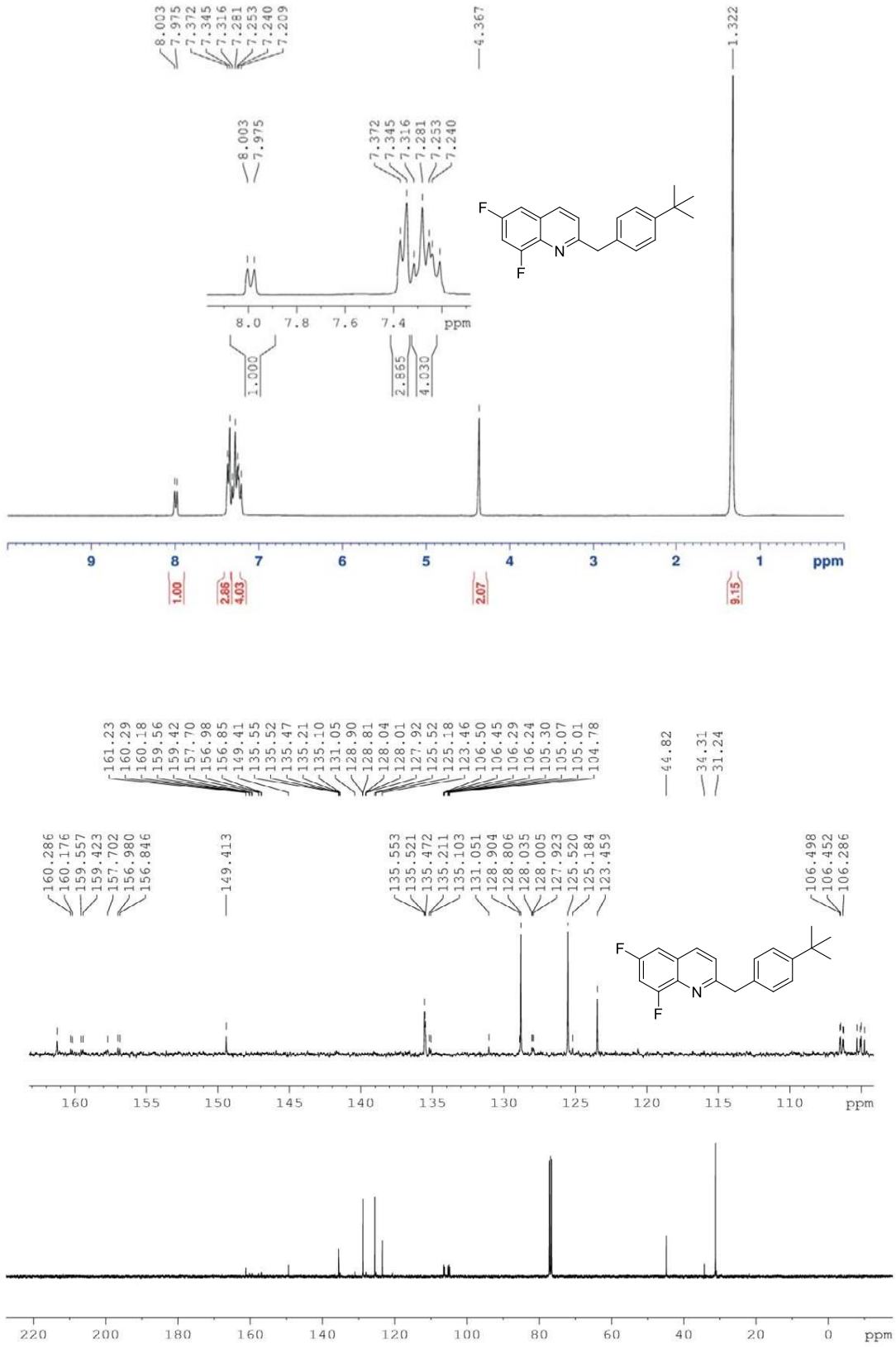

^{19}F (376 MHz, $CDCl_3$)-NMR spectrum of quinoline **30**

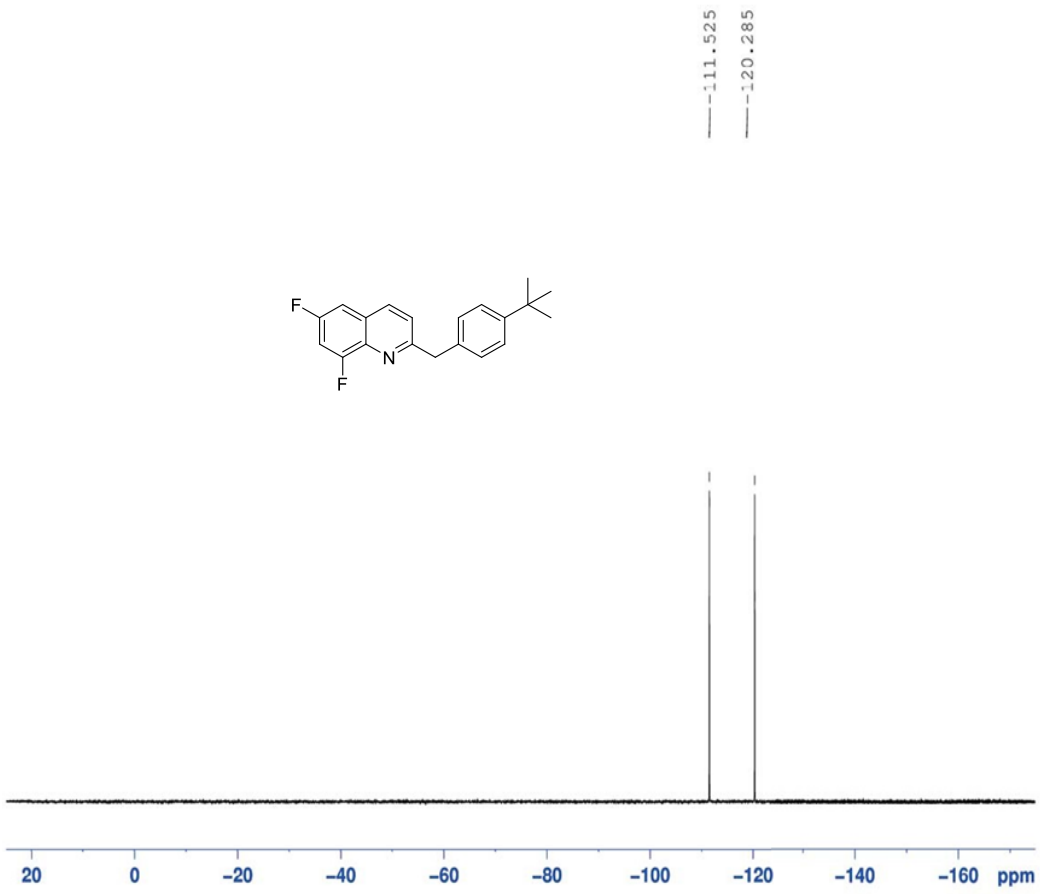

^{1}H (400 MHz, $CDCl_3$) and ^{13}C (100 MHz, $CDCl_3$)-NMR spectra of quinoline **31**

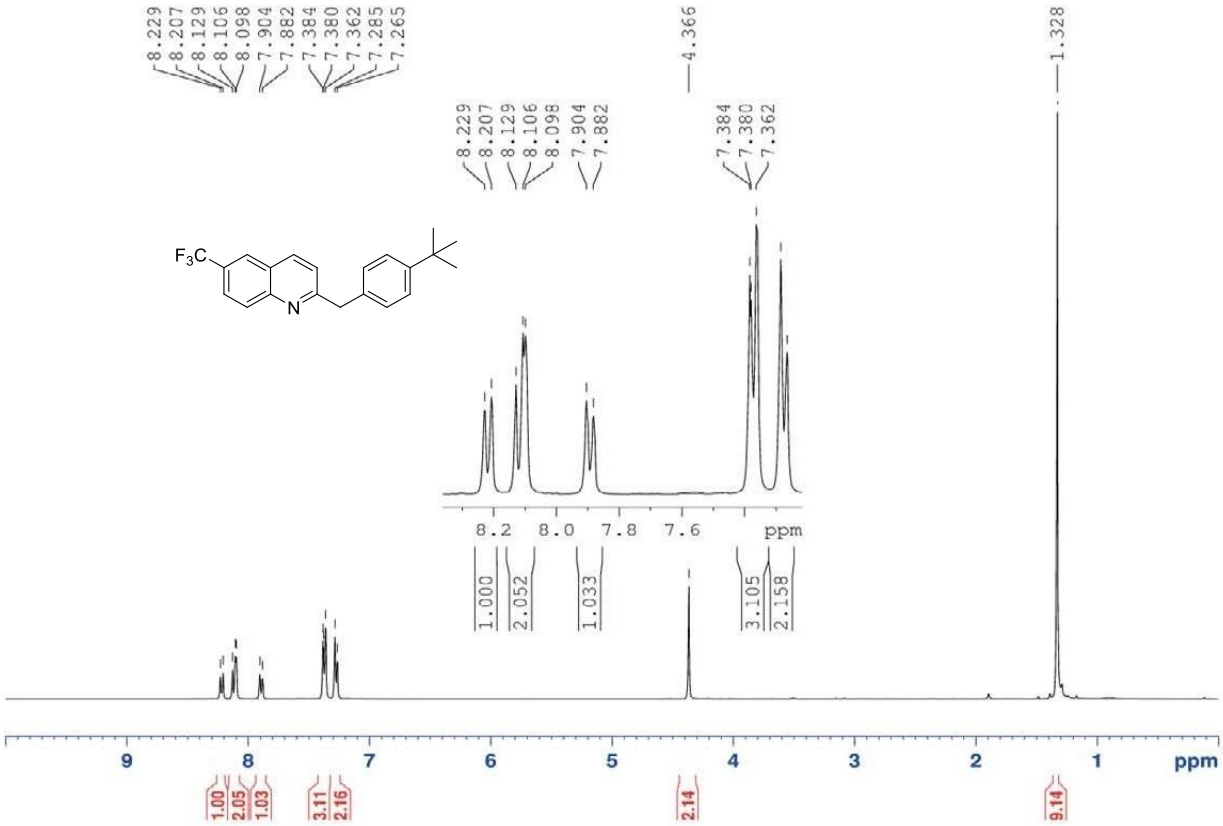

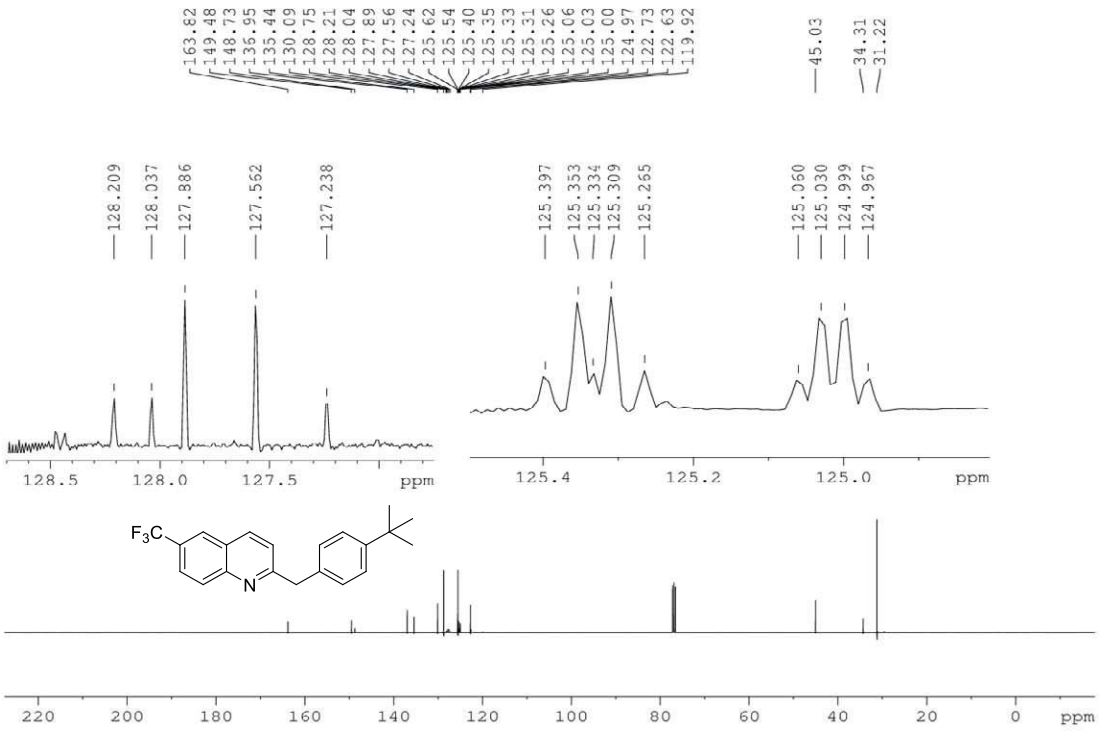

^{19}F (376 MHz, $CDCl_3$)-NMR spectrum of quinoline **31**

^{1}H (400 MHz, $CDCl_3$) and ^{13}C (100 MHz, $CDCl_3$)-NMR spectra of quinoline **32**

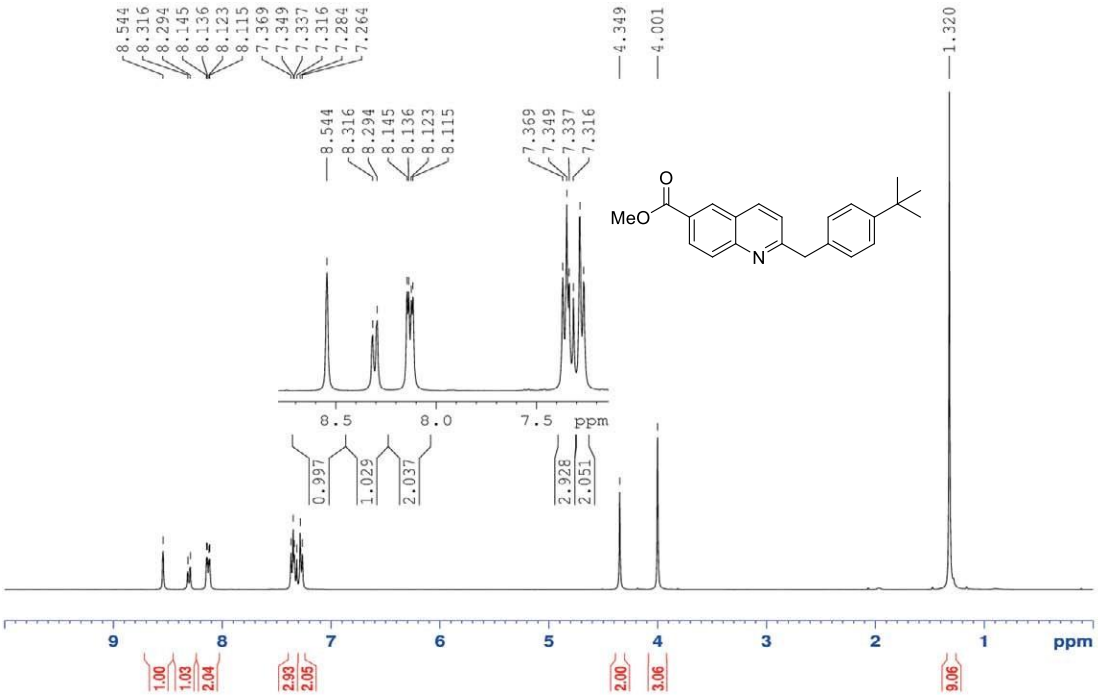

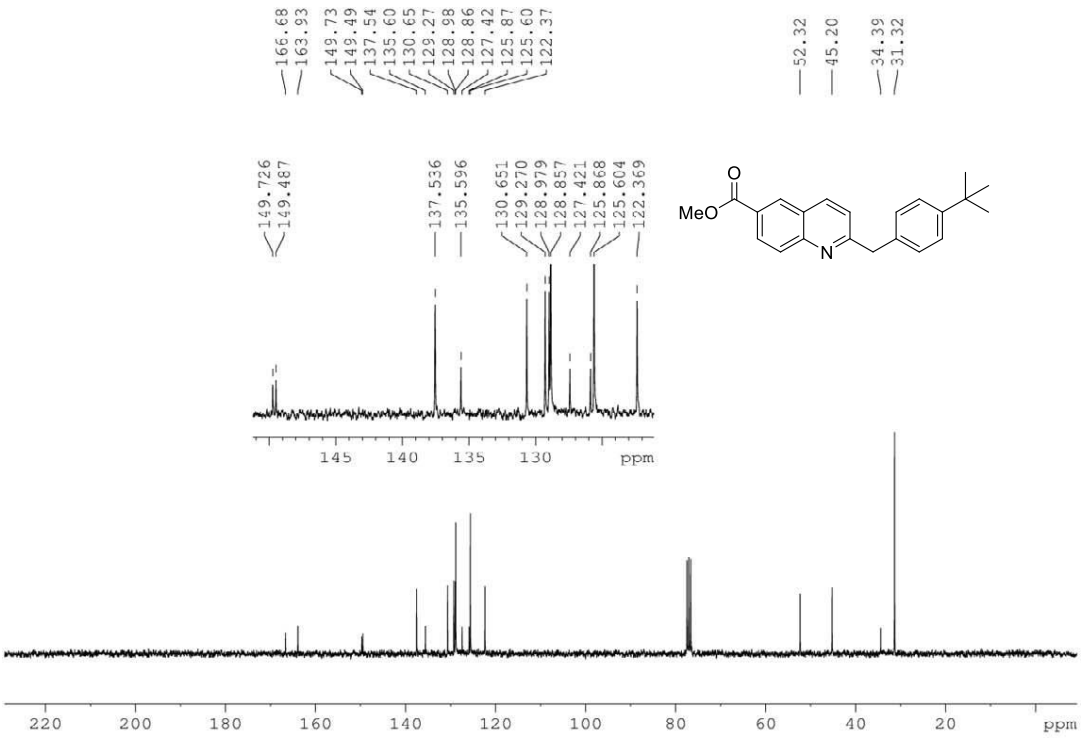

^{1}H (400 MHz, $CDCl_3$) and ^{13}C (100 MHz, $CDCl_3$)-NMR spectra of quinoline **33**

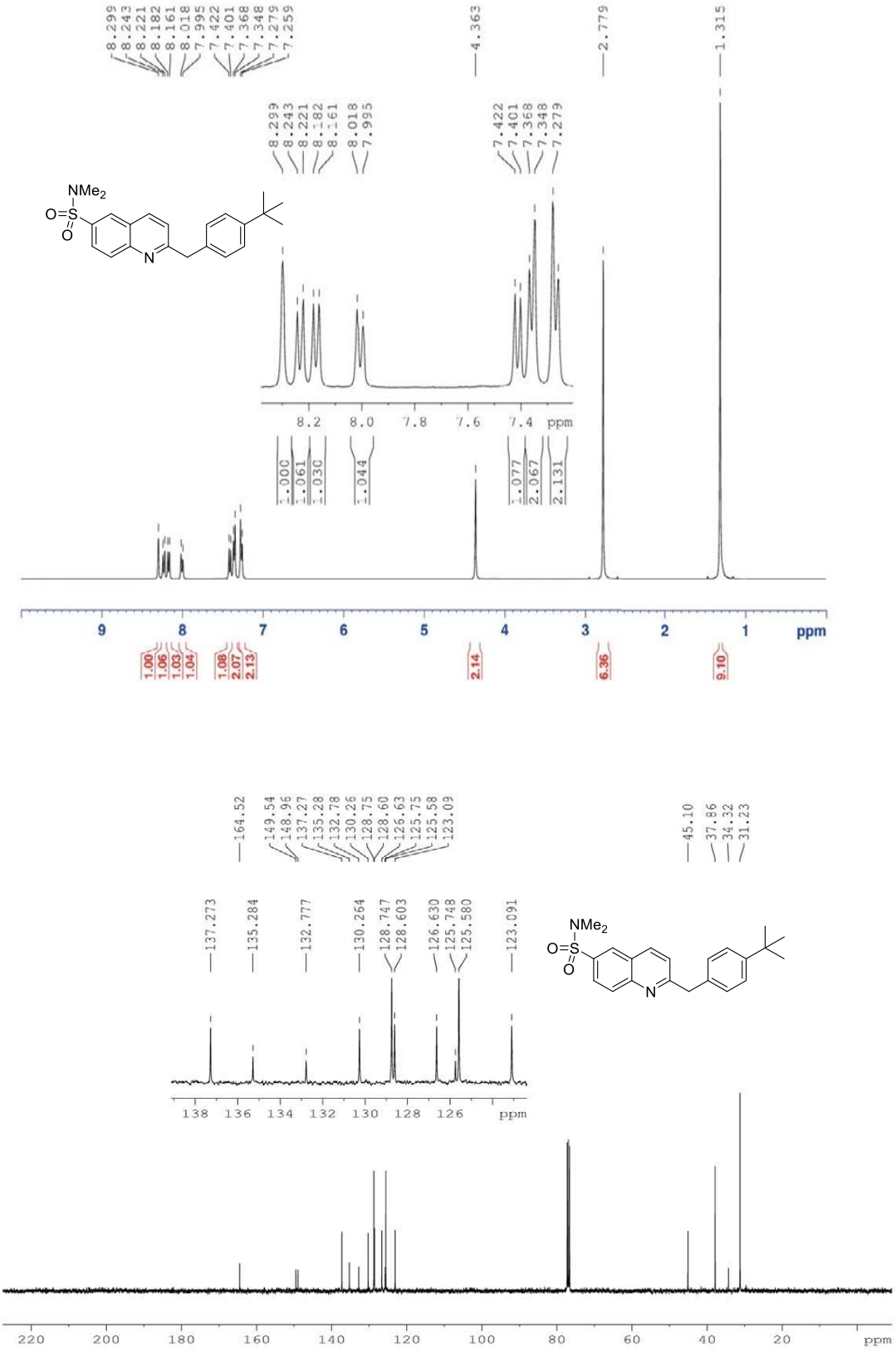

^{1}H (400 MHz, $CDCl_3$) and ^{13}C (100 MHz, $CDCl_3$)-NMR spectra of quinoline **34**

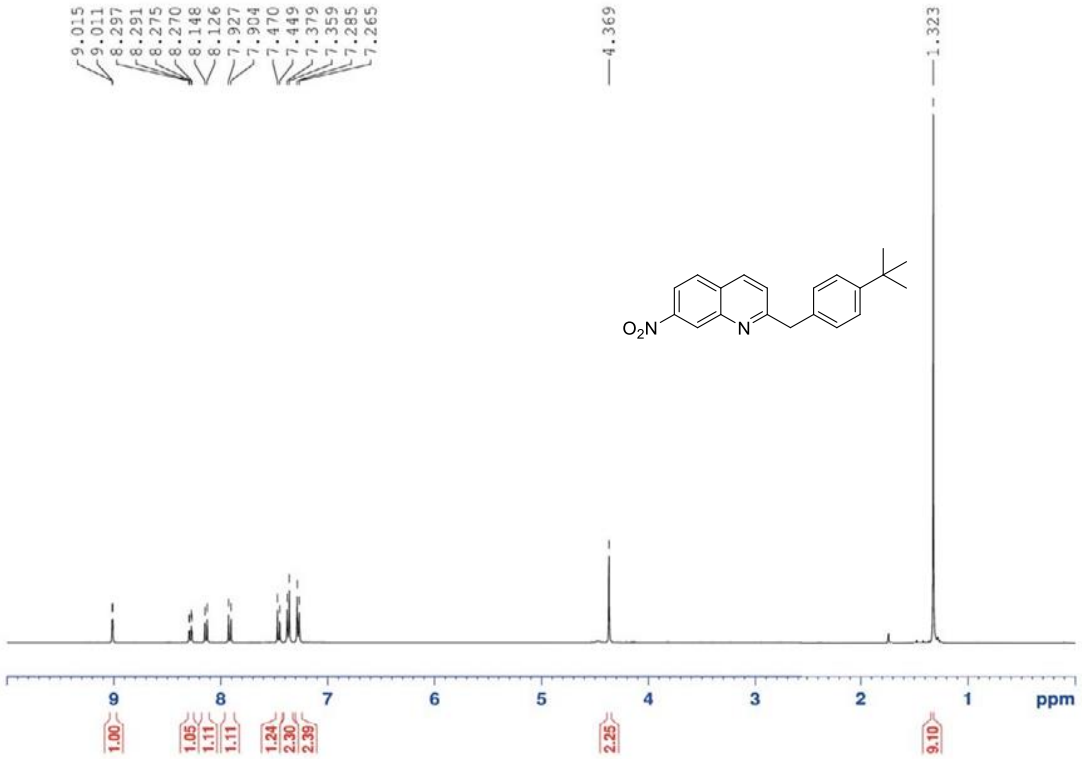

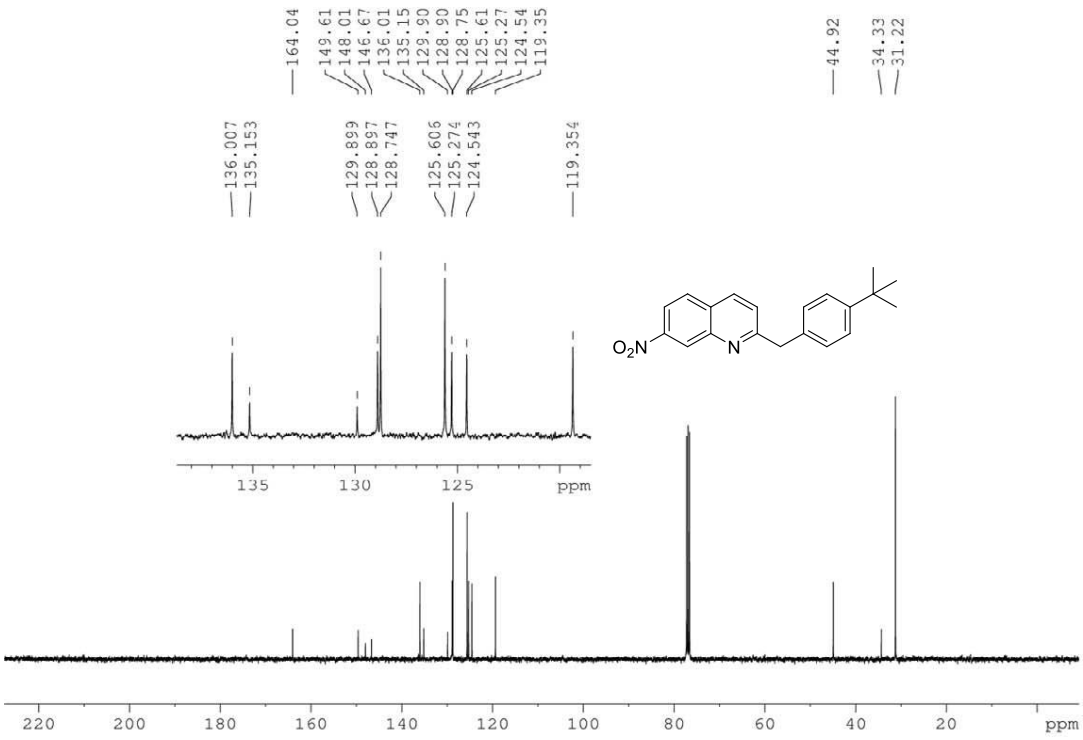

^{1}H (400 MHz, $CDCl_3$) and ^{13}C (100 MHz, $CDCl_3$)-NMR spectra of cyclopropanol **1-d$_4$**

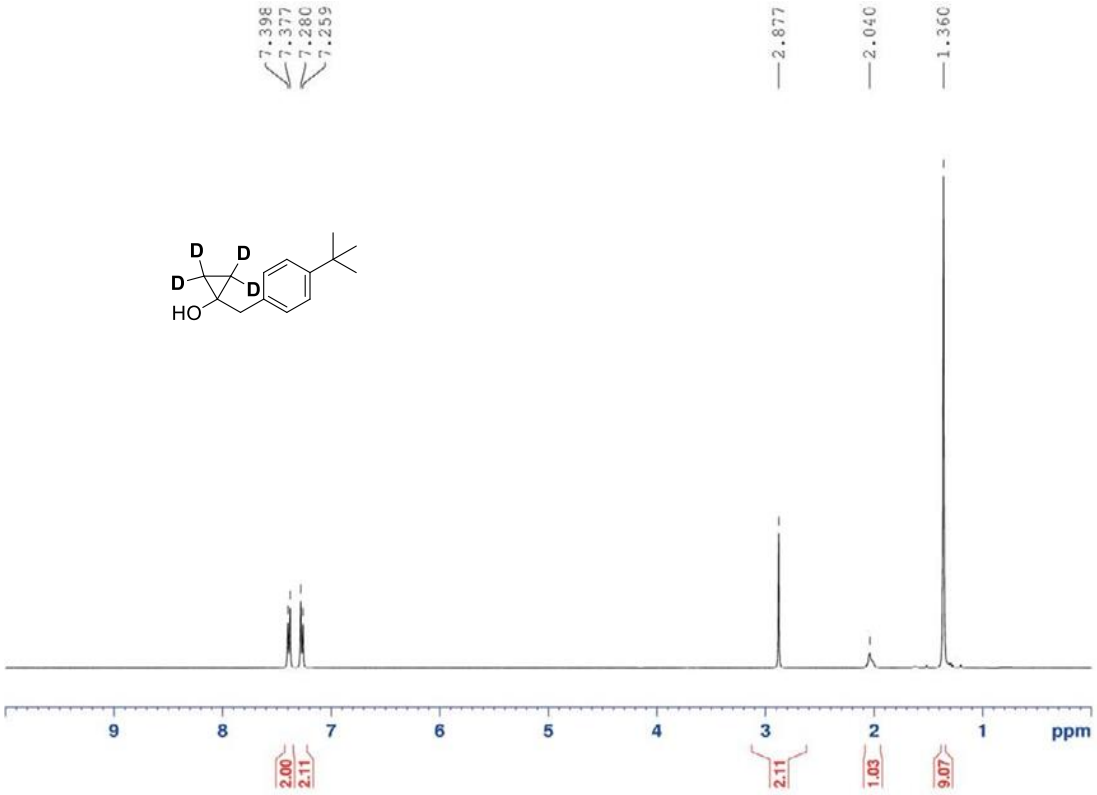

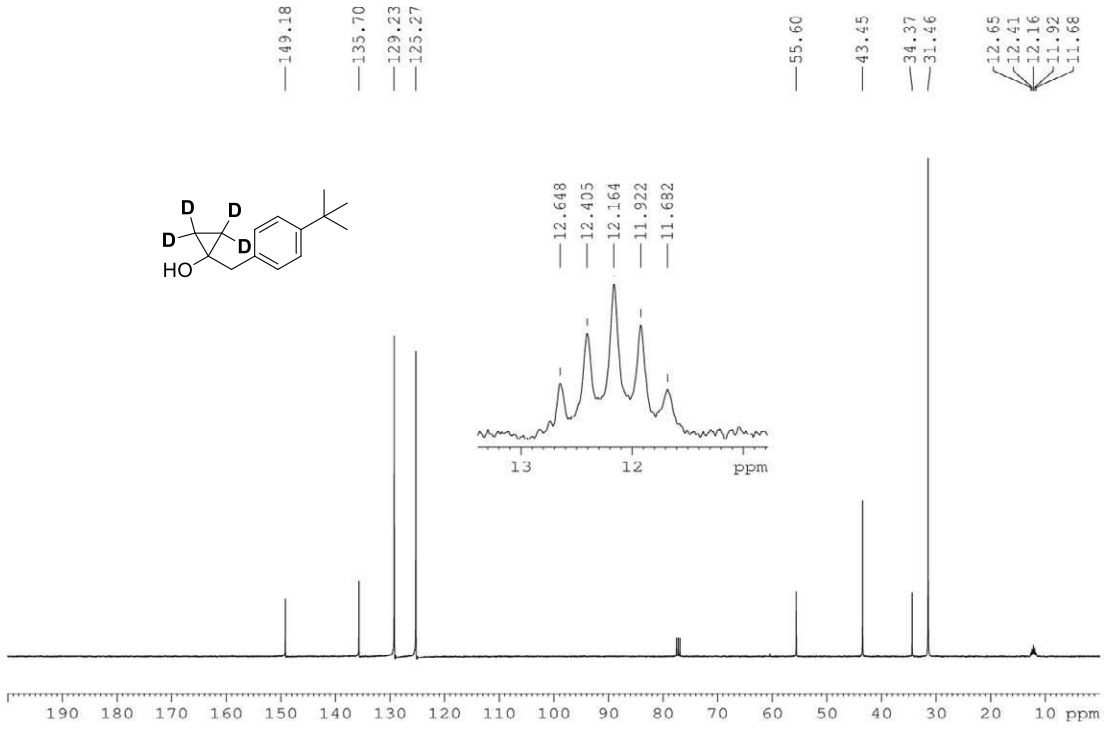

^{1}H (400 MHz, $CDCl_3$) and ^{13}C (100 MHz, $CDCl_3$)-NMR spectra of quinoline **32-d_2**

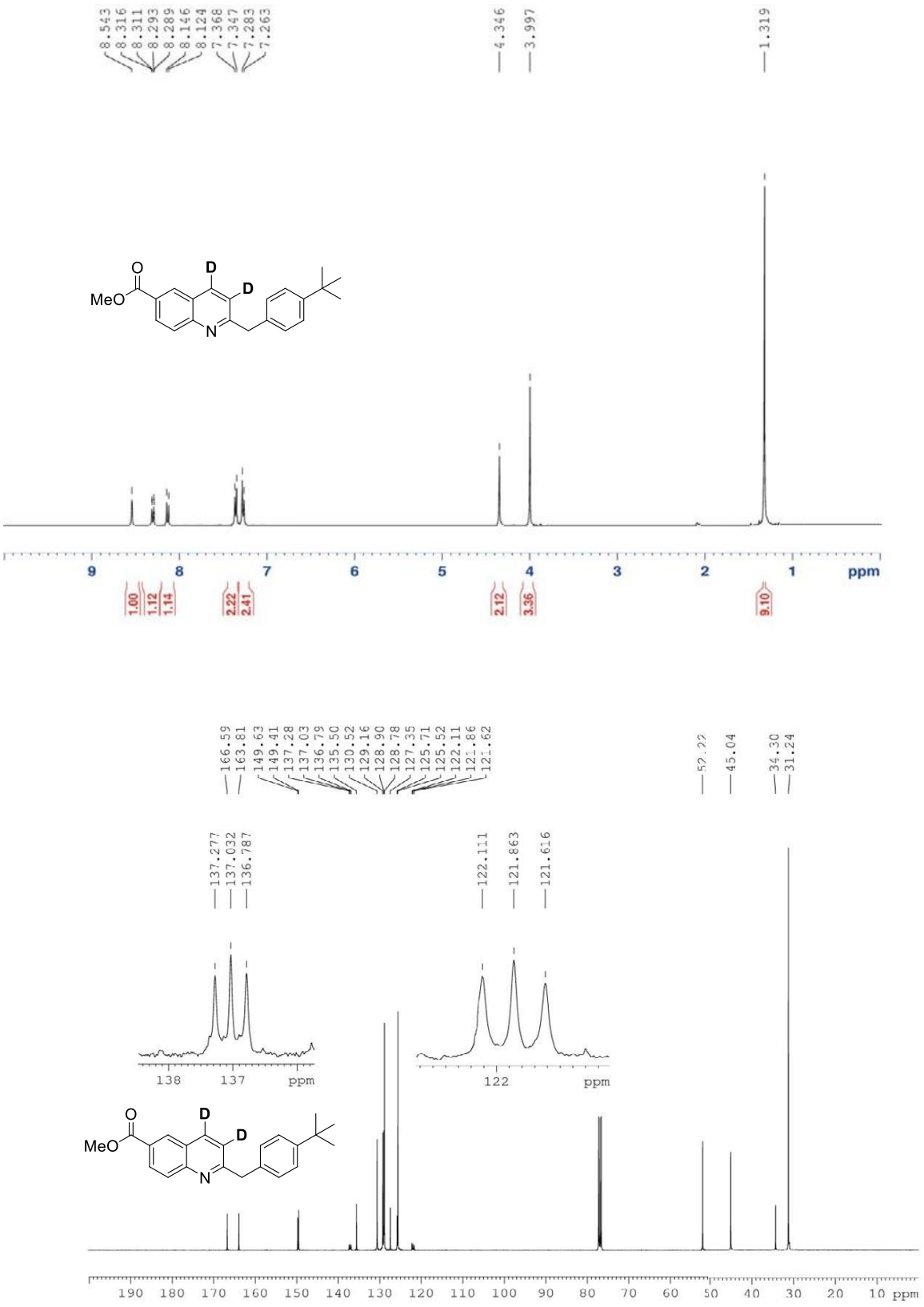

^{2}H (61 MHz, $CDCl_3$)-NMR spectrum of quinoline **32-d_2**

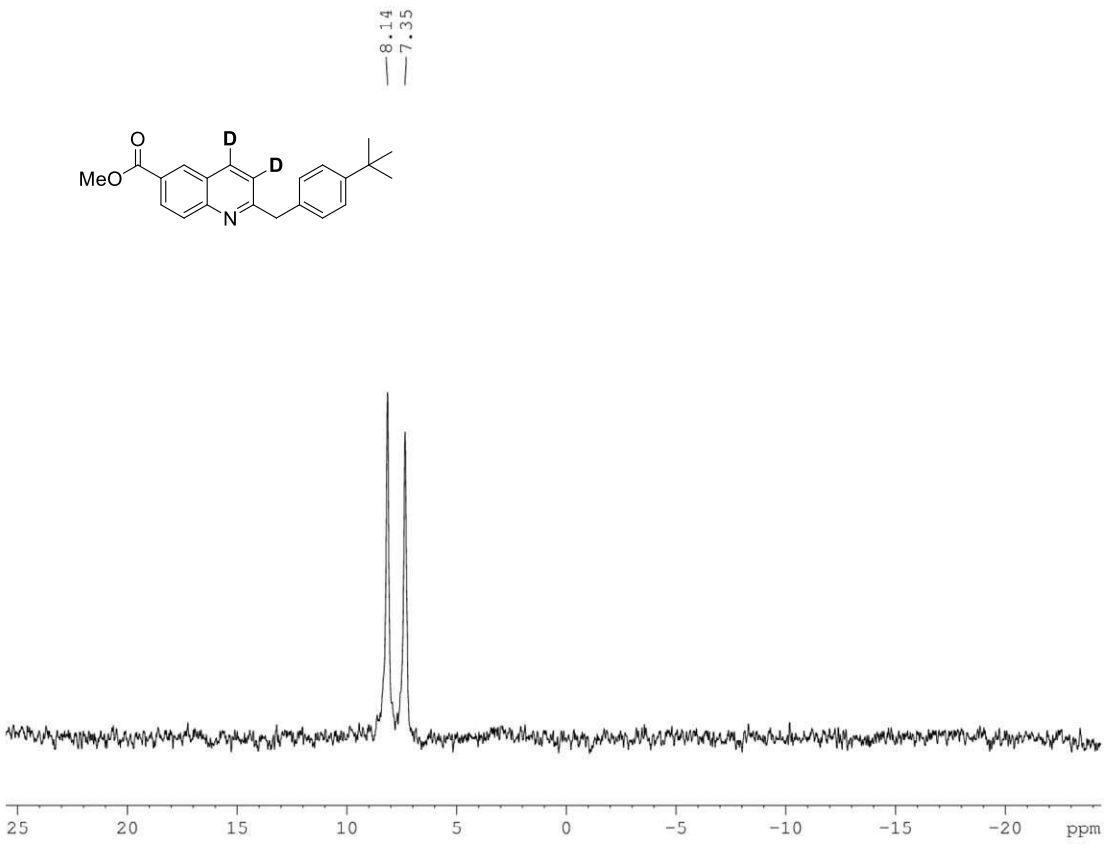

^{1}H (400 MHz, $CDCl_3$) and ^{13}C (100 MHz, $CDCl_3$)-NMR spectra of aniline **35-d**

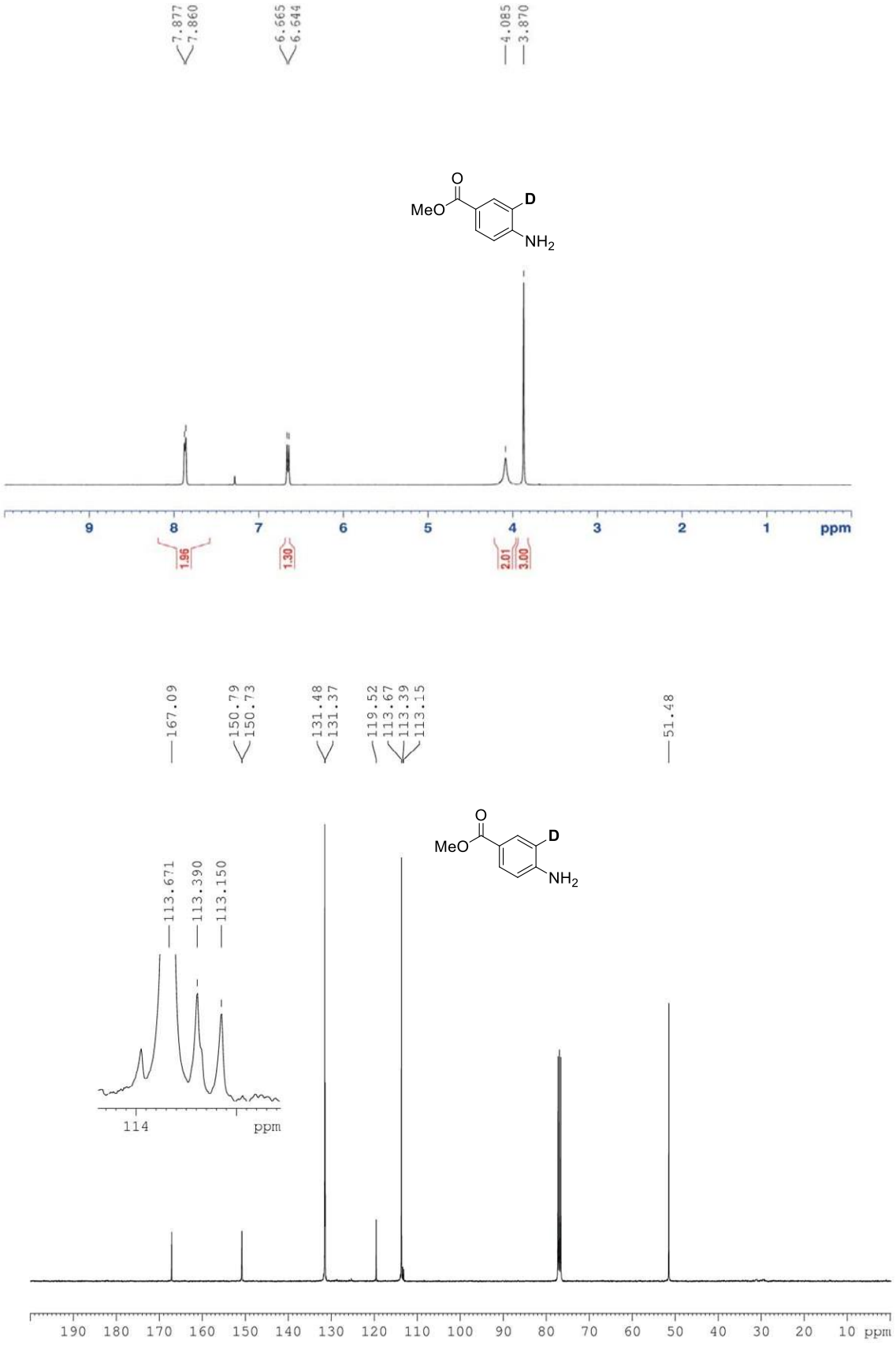

^{2}H (61 MHz, $CDCl_3$)-NMR spectrum of aniline **35-d**

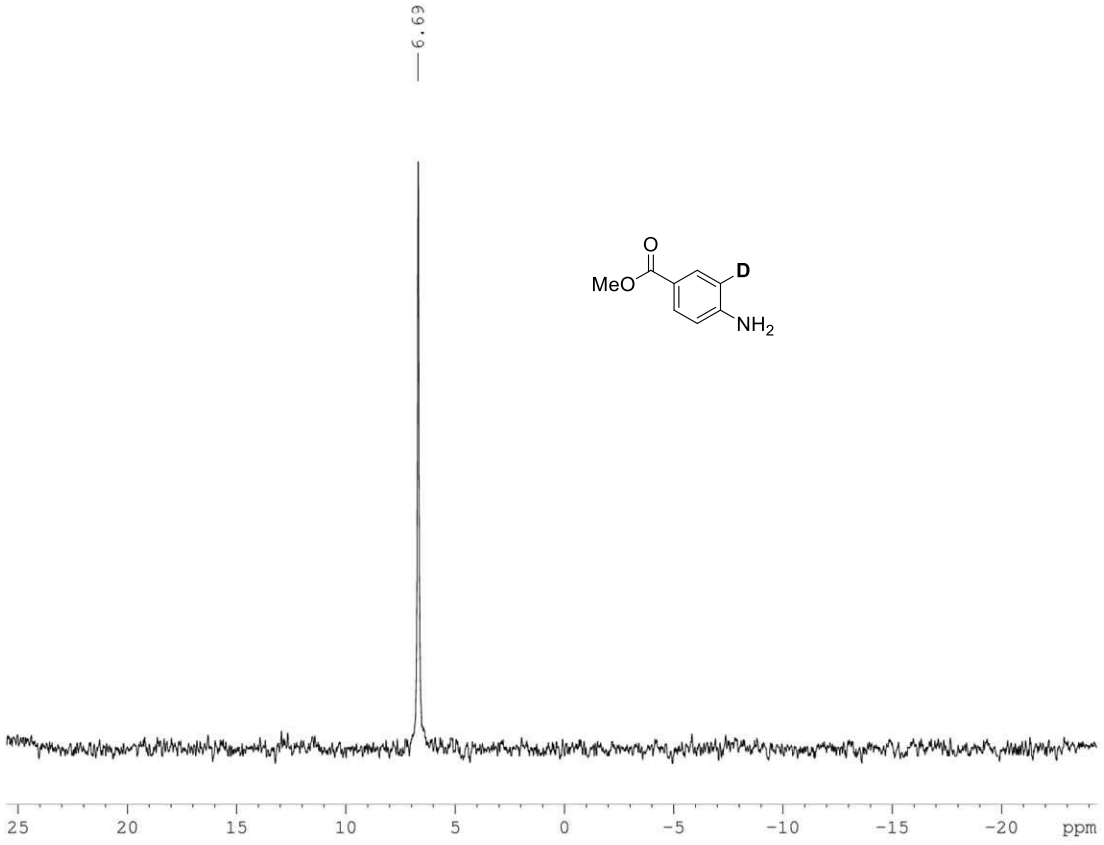

^{1}H (400 MHz, $CDCl_3$) and ^{13}C (100 MHz, $CDCl_3$)-NMR spectra of heterocycle **37a**

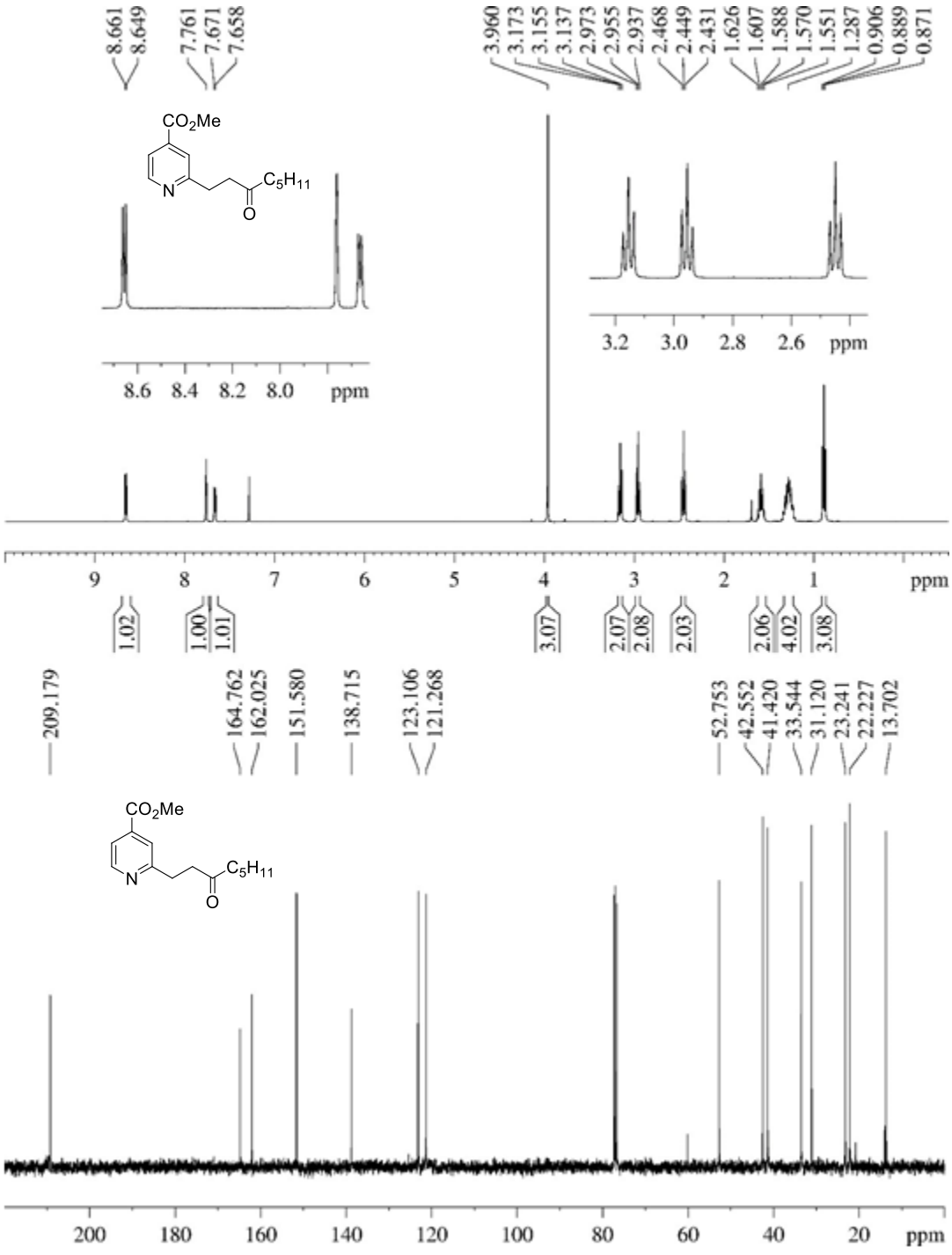

^{1}H (400 MHz, $CDCl_3$) and ^{13}C (100 MHz, $CDCl_3$)-NMR spectra of heterocycle **38a**

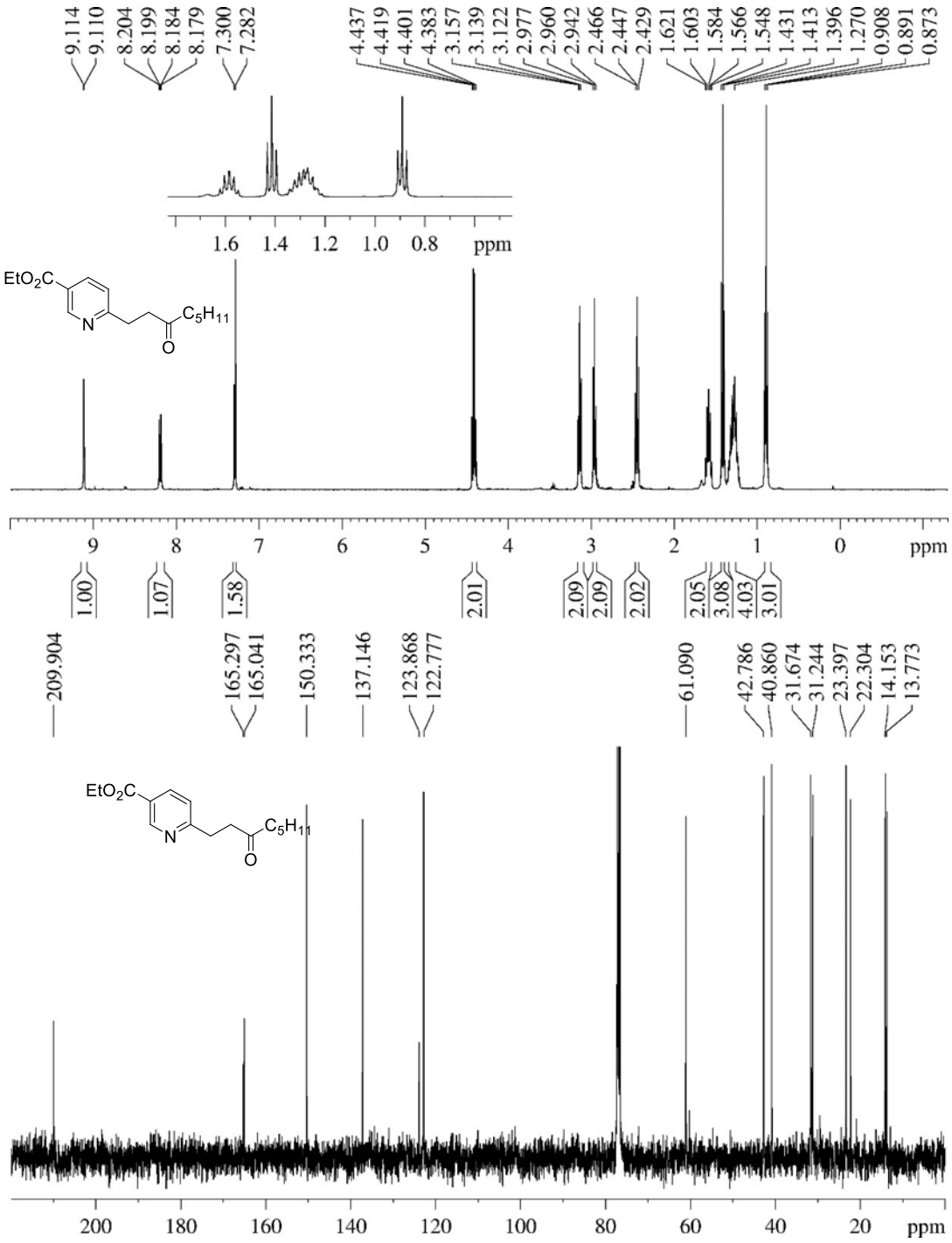

^{1}H (400 MHz, $CDCl_3$) and ^{13}C (100 MHz, $CDCl_3$)-NMR spectra of heterocycle **39a**

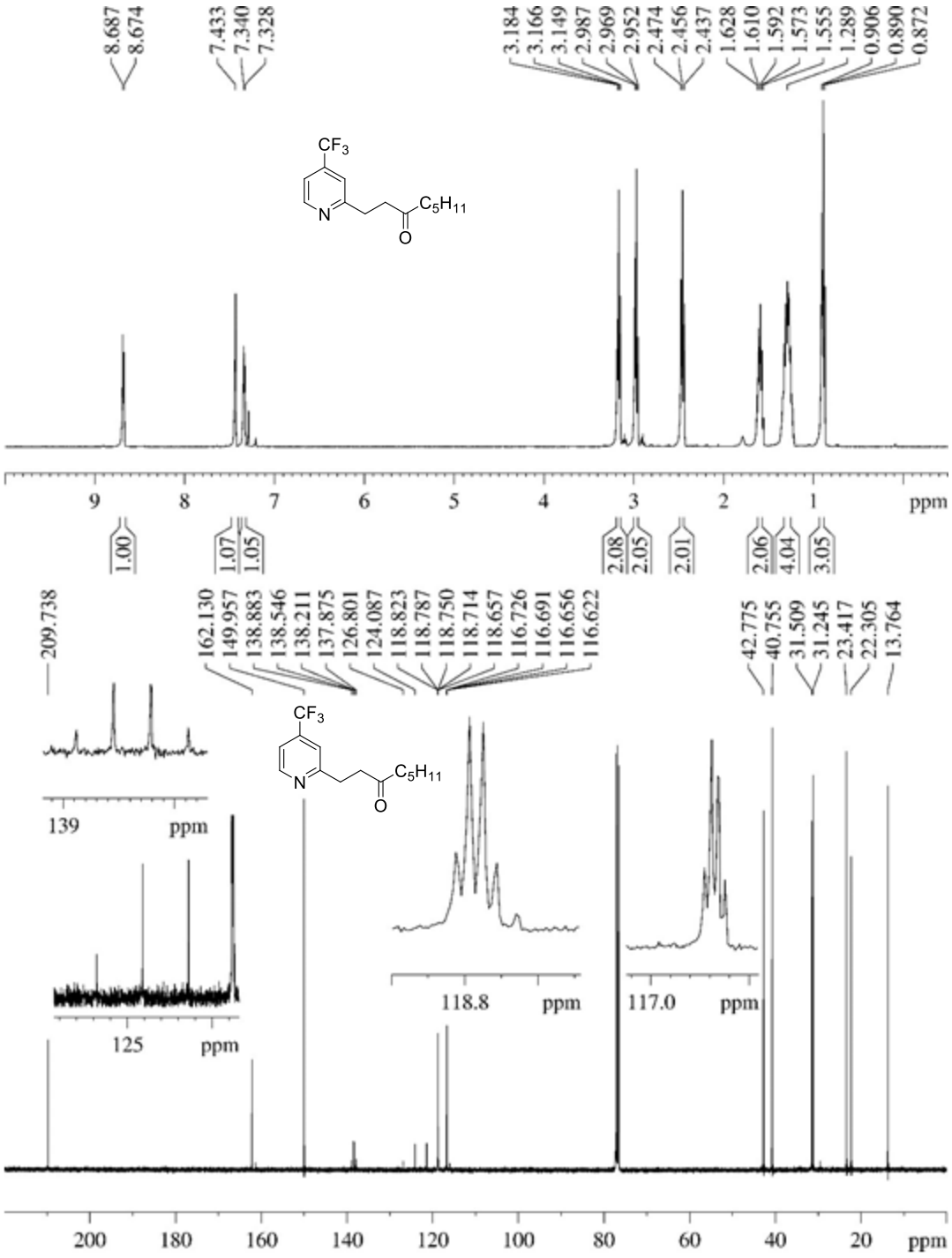

^{19}F (376 MHz, $CDCl_3$)-NMR spectra of heterocycle **39a**

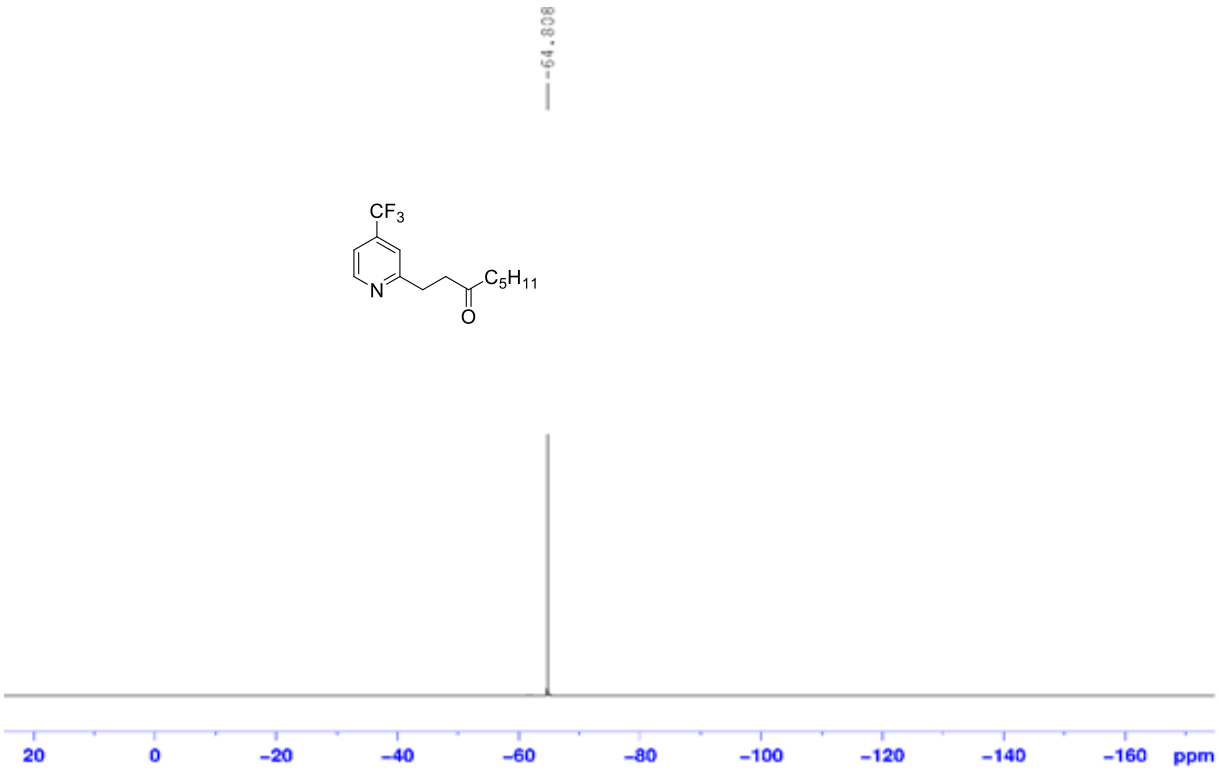

^{1}H (400 MHz, $CDCl_3$) and ^{13}C (100 MHz, $CDCl_3$)-NMR spectra of heterocycle **40a**

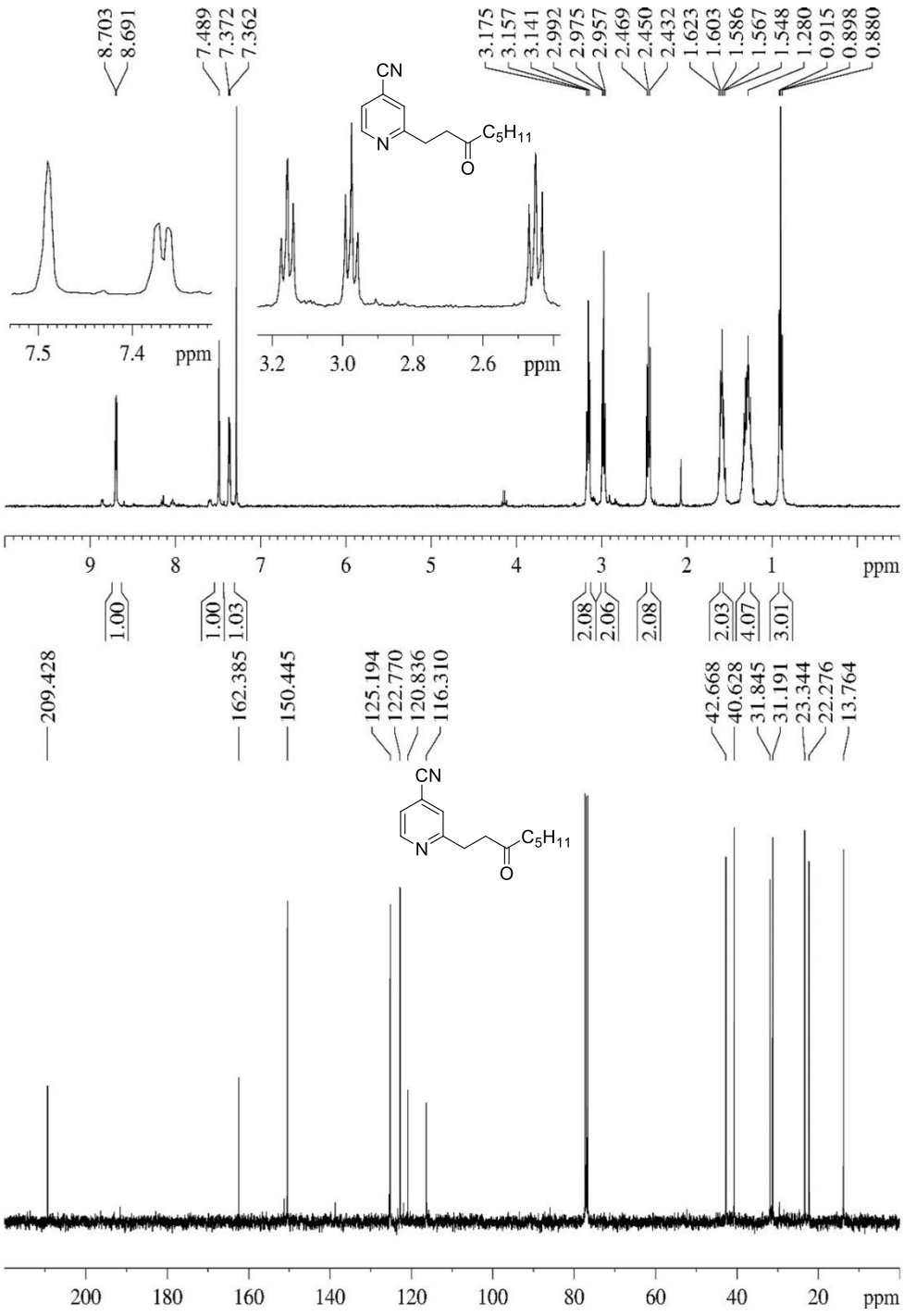

^{1}H (400 MHz, $CDCl_3$) and ^{13}C (100 MHz, $CDCl_3$)-NMR spectra of heterocycle **41a**

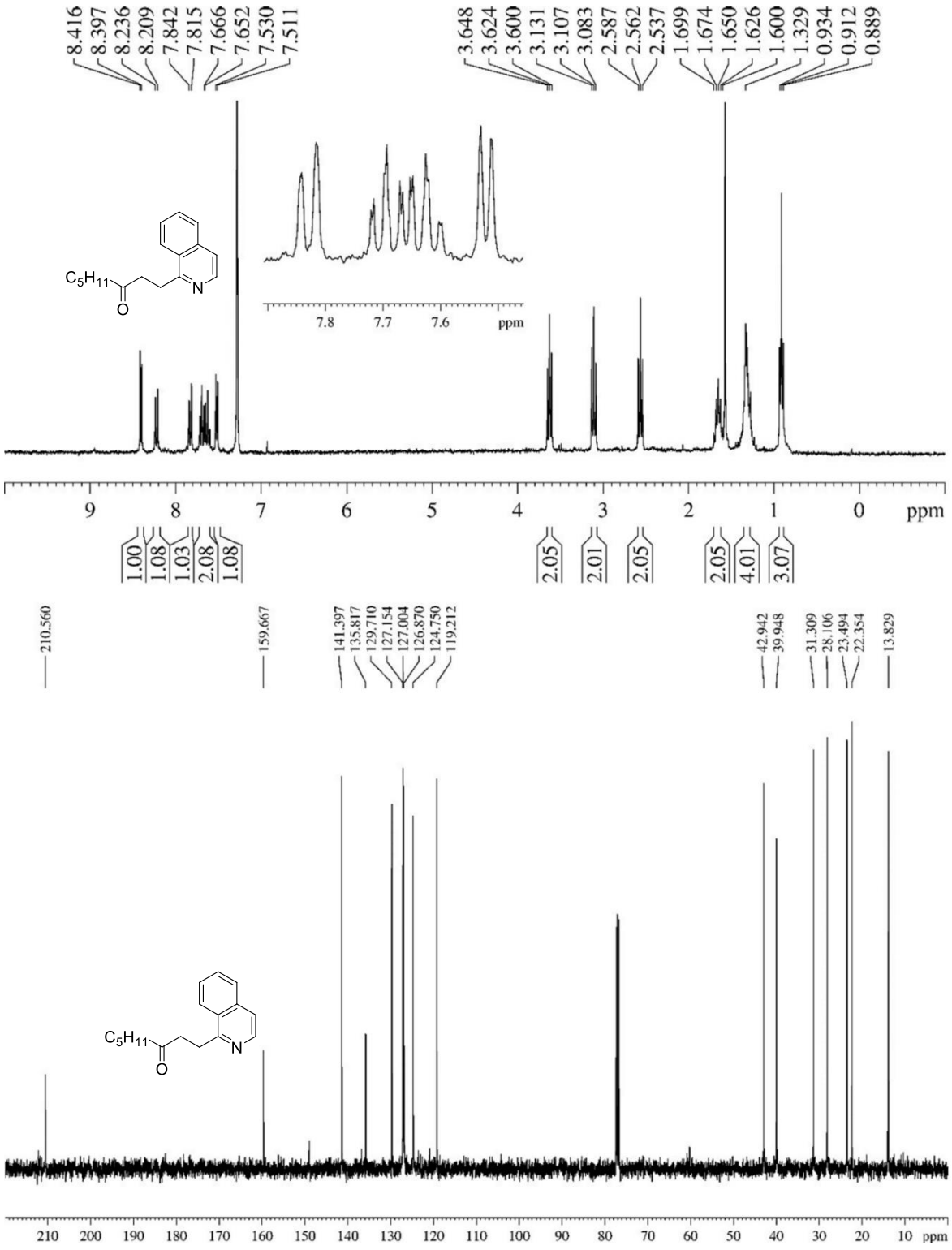

^{1}H (400 MHz, MeOH *d4*) and ^{13}C (100 MHz, $CDCl_3$)-NMR spectra of heterocycle **42a**

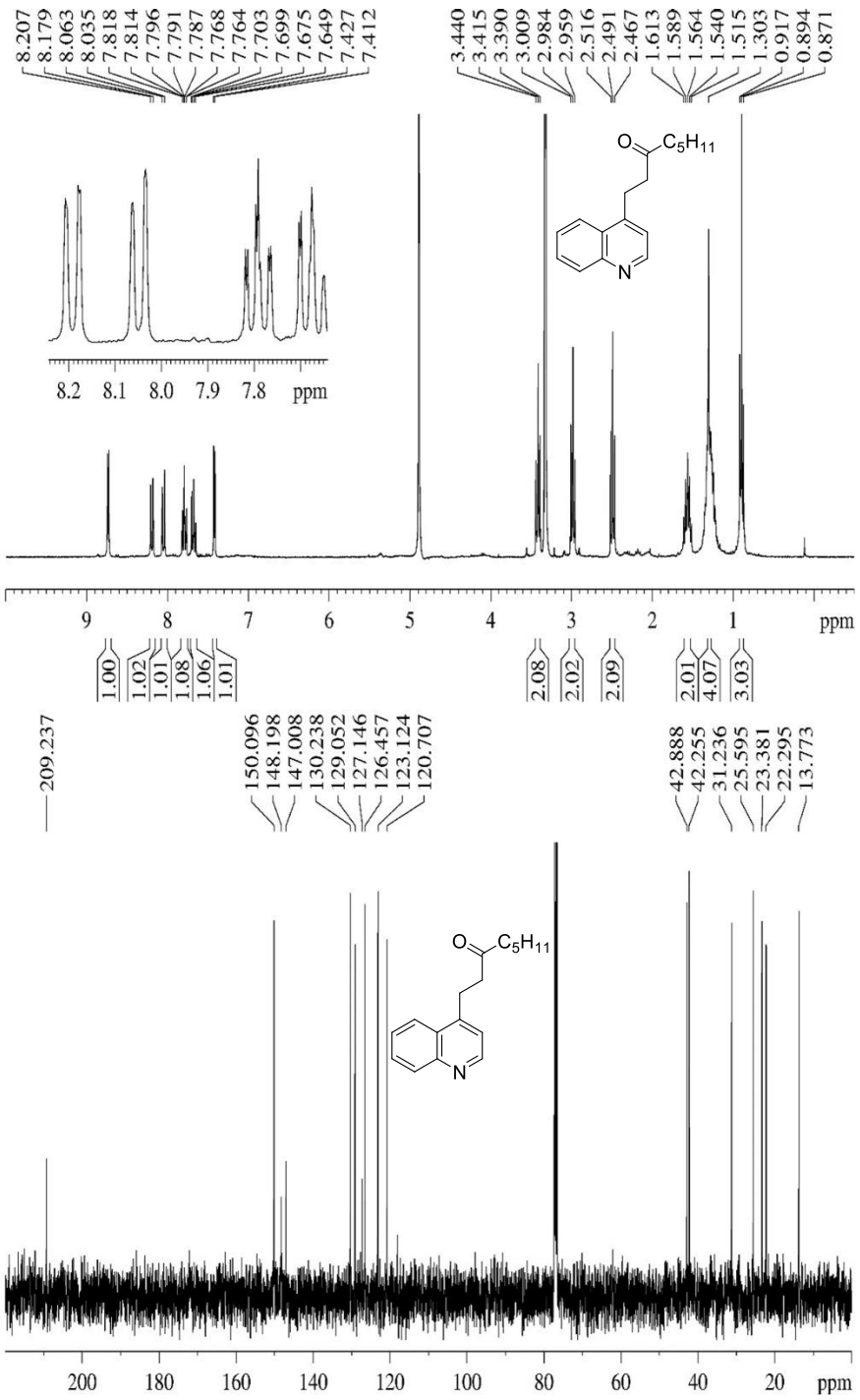

^{1}H (400 MHz, MeOH *d4*) and ^{13}C (100 MHz, $CDCl_3$)-NMR spectra of heterocycle **42a'**

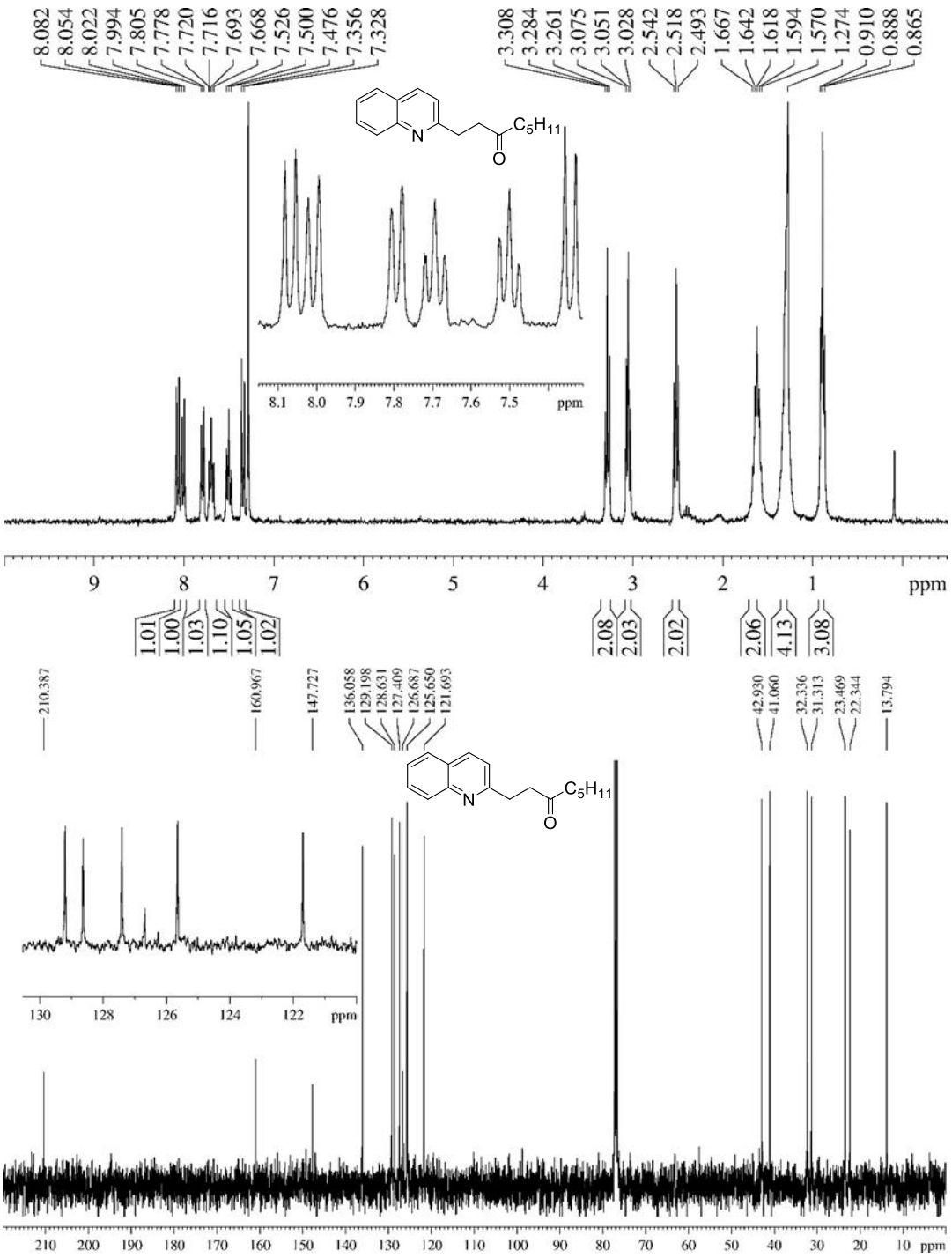

^{1}H (400 MHz, $CDCl_3$) and ^{13}C (100 MHz, $CDCl_3$)-NMR spectra of heterocycle **43a**

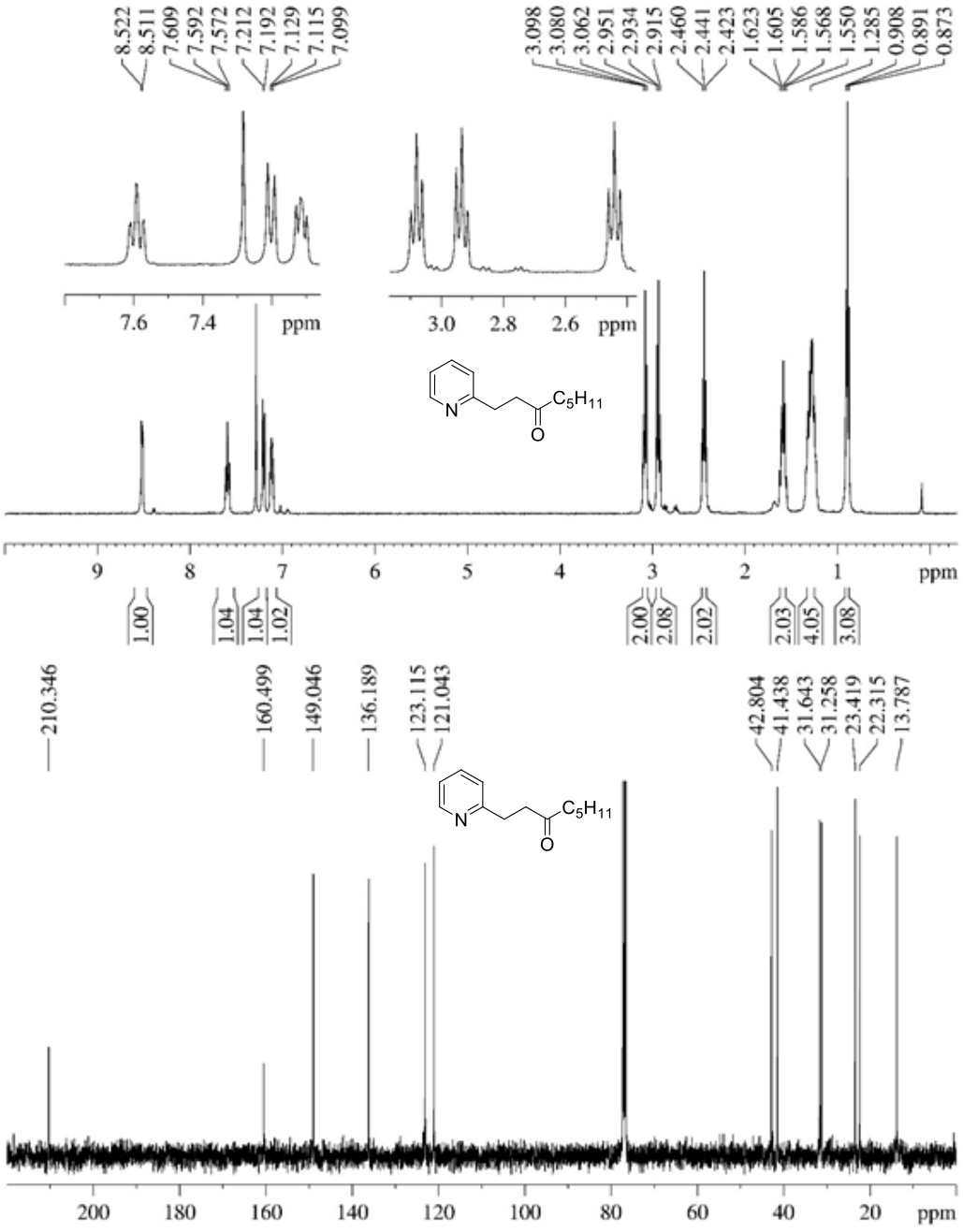

^{1}H (400 MHz, $CDCl_3$) and ^{13}C (100 MHz, $CDCl_3$)-NMR spectra of heterocycle **43a'**

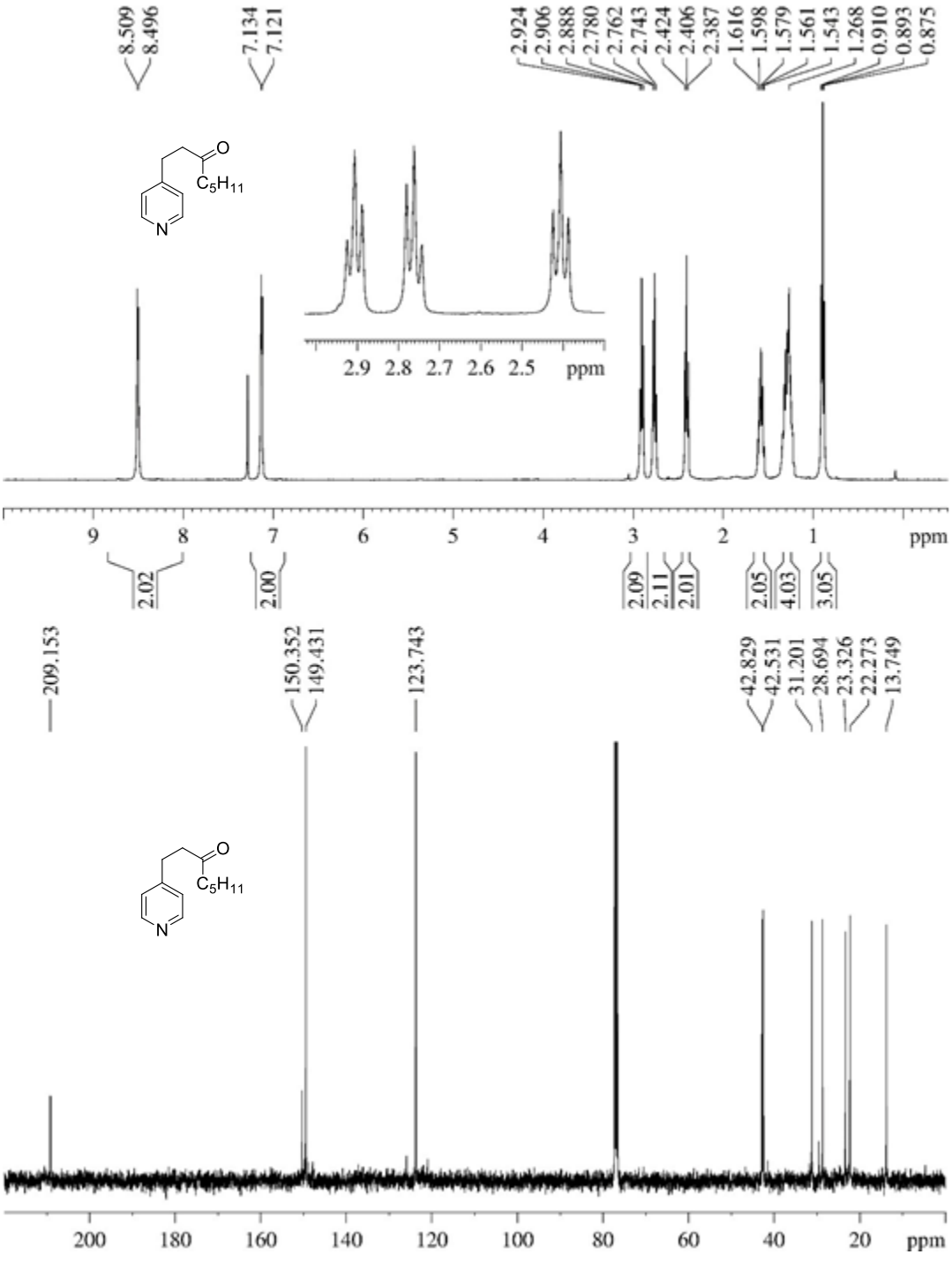

^{1}H (400 MHz, $CDCl_3$) and ^{13}C (100 MHz, $CDCl_3$)-NMR spectra of heterocycle **44a**

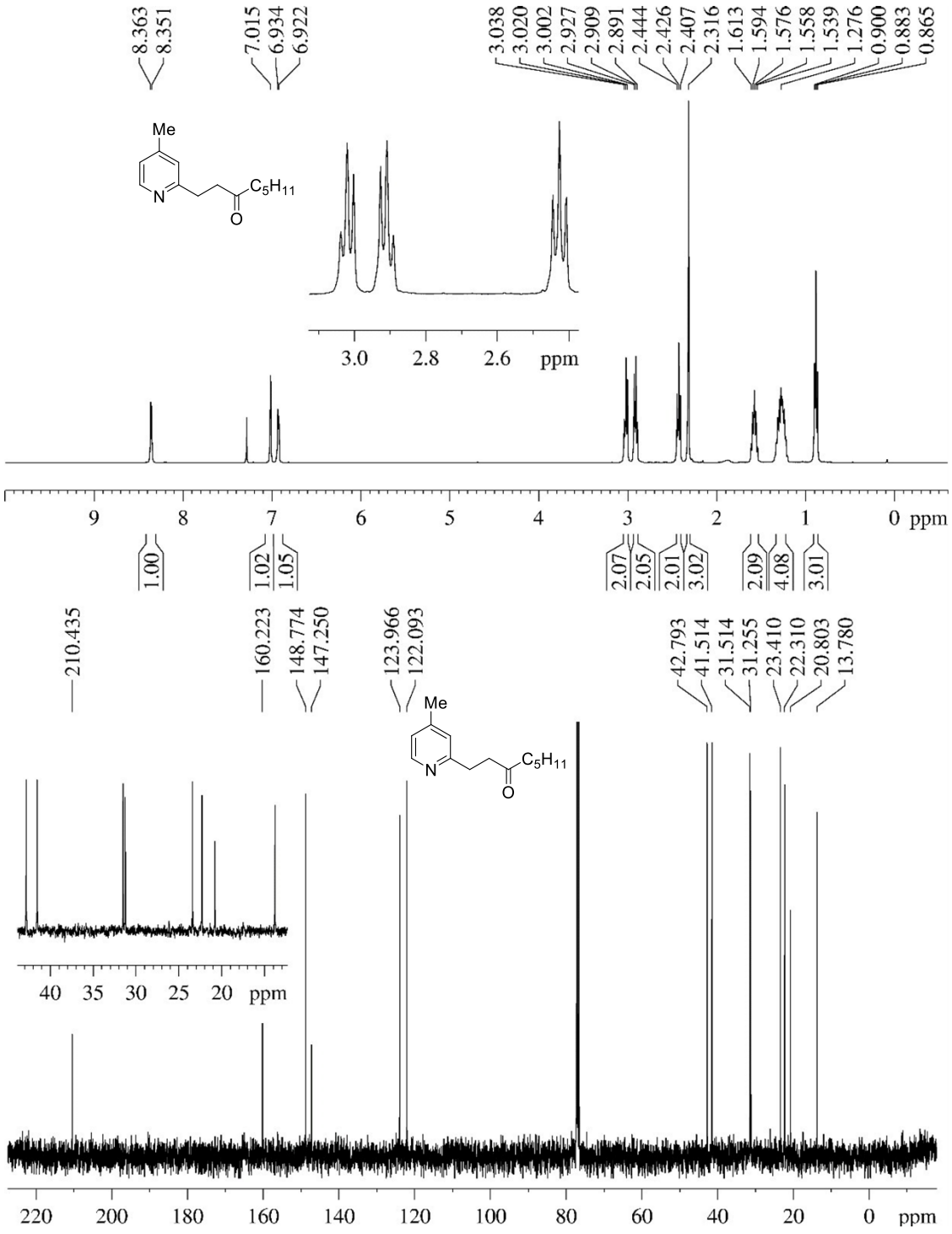

^{1}H (300 MHz, $CDCl_3$) and ^{13}C (100 MHz, $CDCl_3$)-NMR spectra of heterocycle **45a**

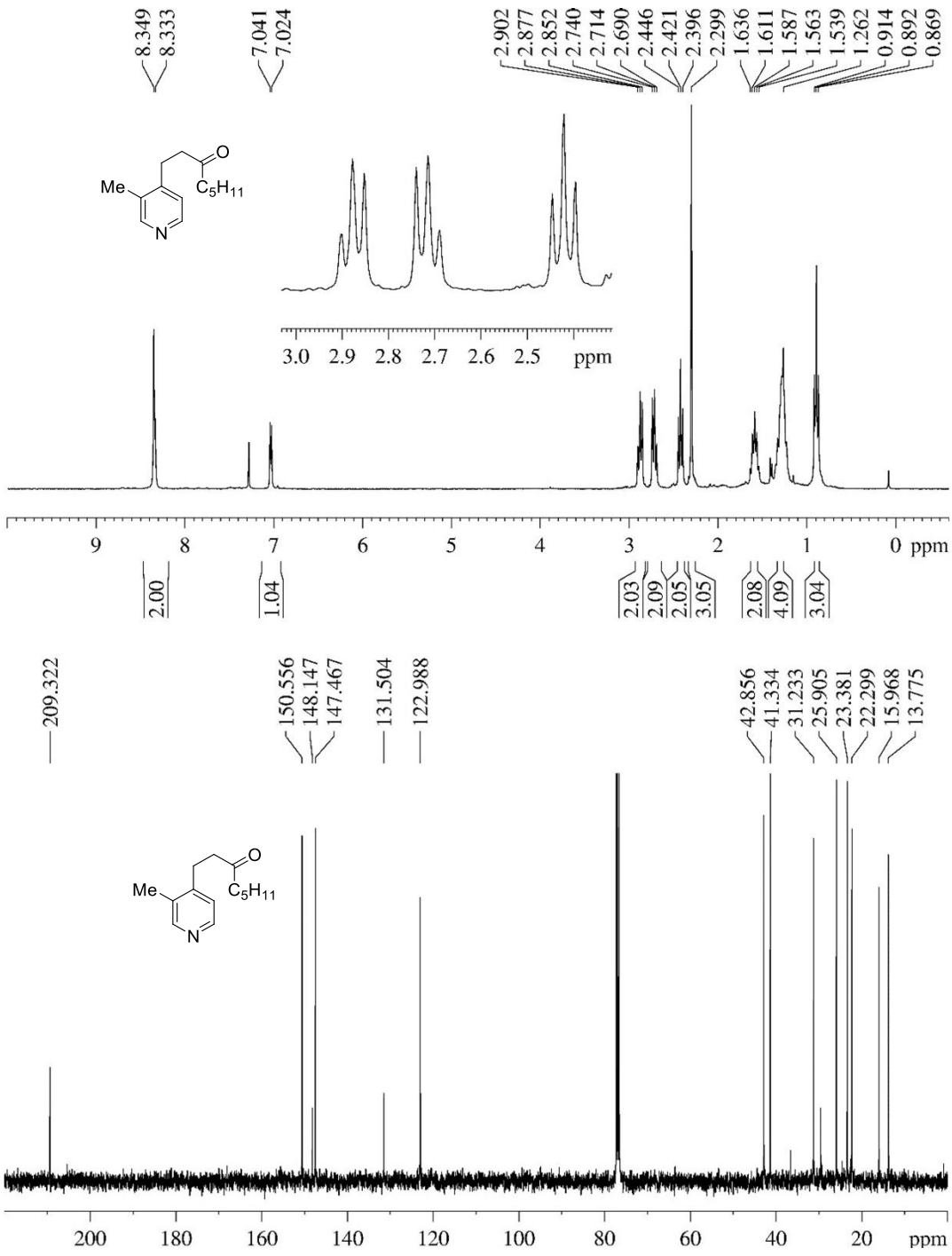

^{1}H (300 MHz, $CDCl_3$) and ^{13}C (100 MHz, $CDCl_3$)-NMR spectra of heterocycle **45a'**

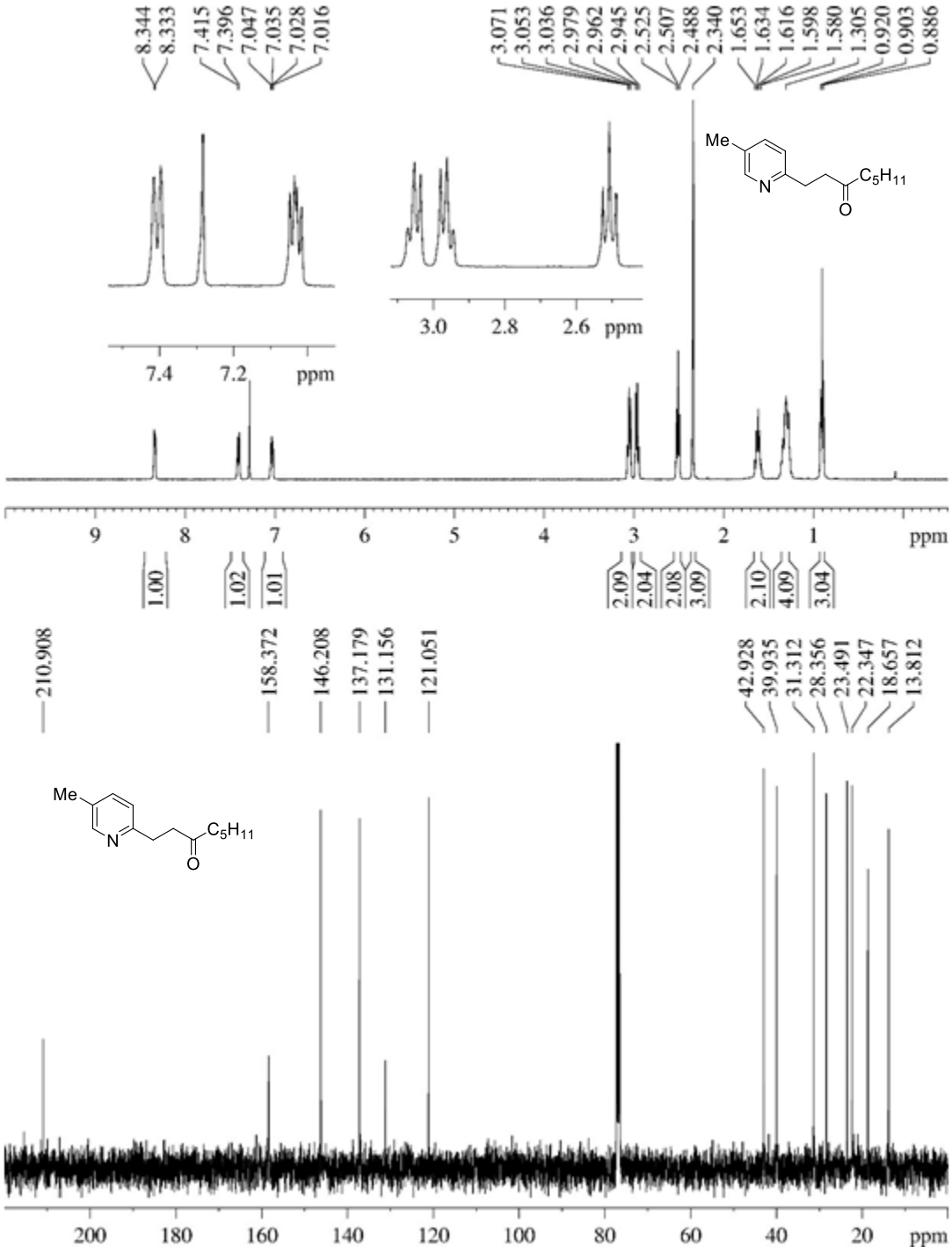

^{1}H (400 MHz, $CDCl_3$) and ^{13}C (100 MHz, $CDCl_3$)-NMR spectra of heterocycle **46a**

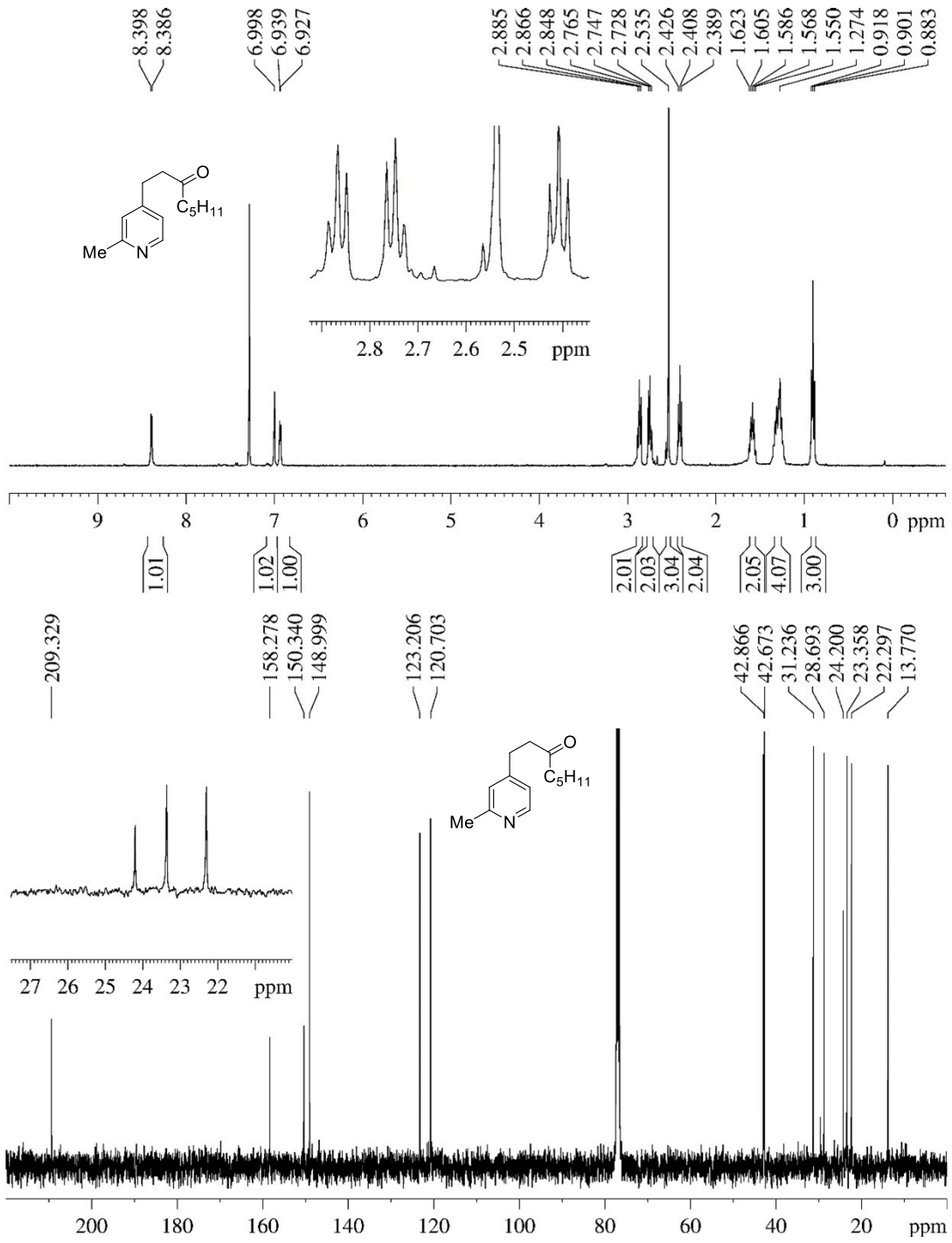

^{1}H (400 MHz, $CDCl_3$) and ^{13}C (100 MHz, $CDCl_3$)-NMR spectra of heterocycle **46a'**

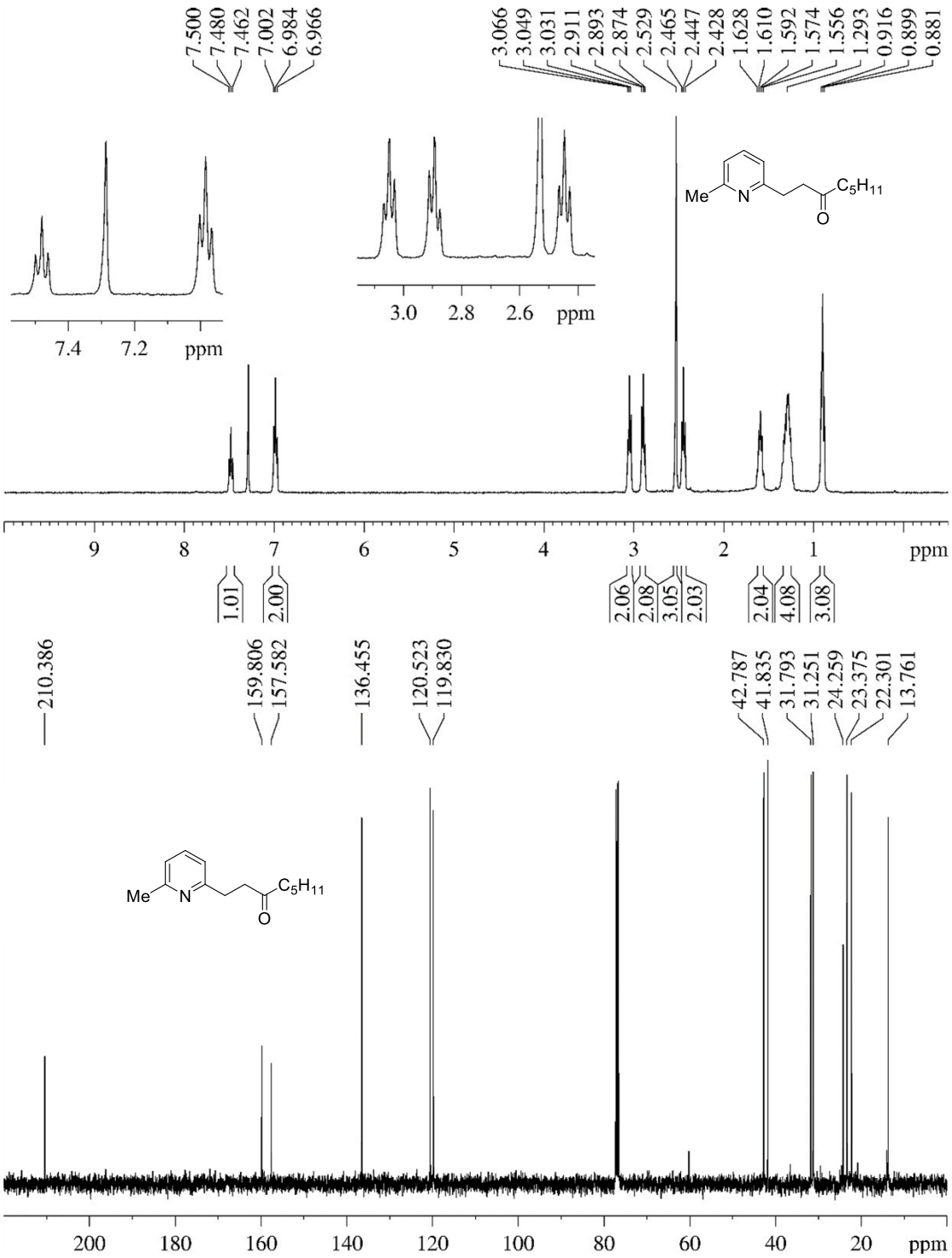

^{1}H (400 MHz, $CDCl_3$) and ^{13}C (100 MHz, $CDCl_3$)-NMR spectra of heterocycle **47a**

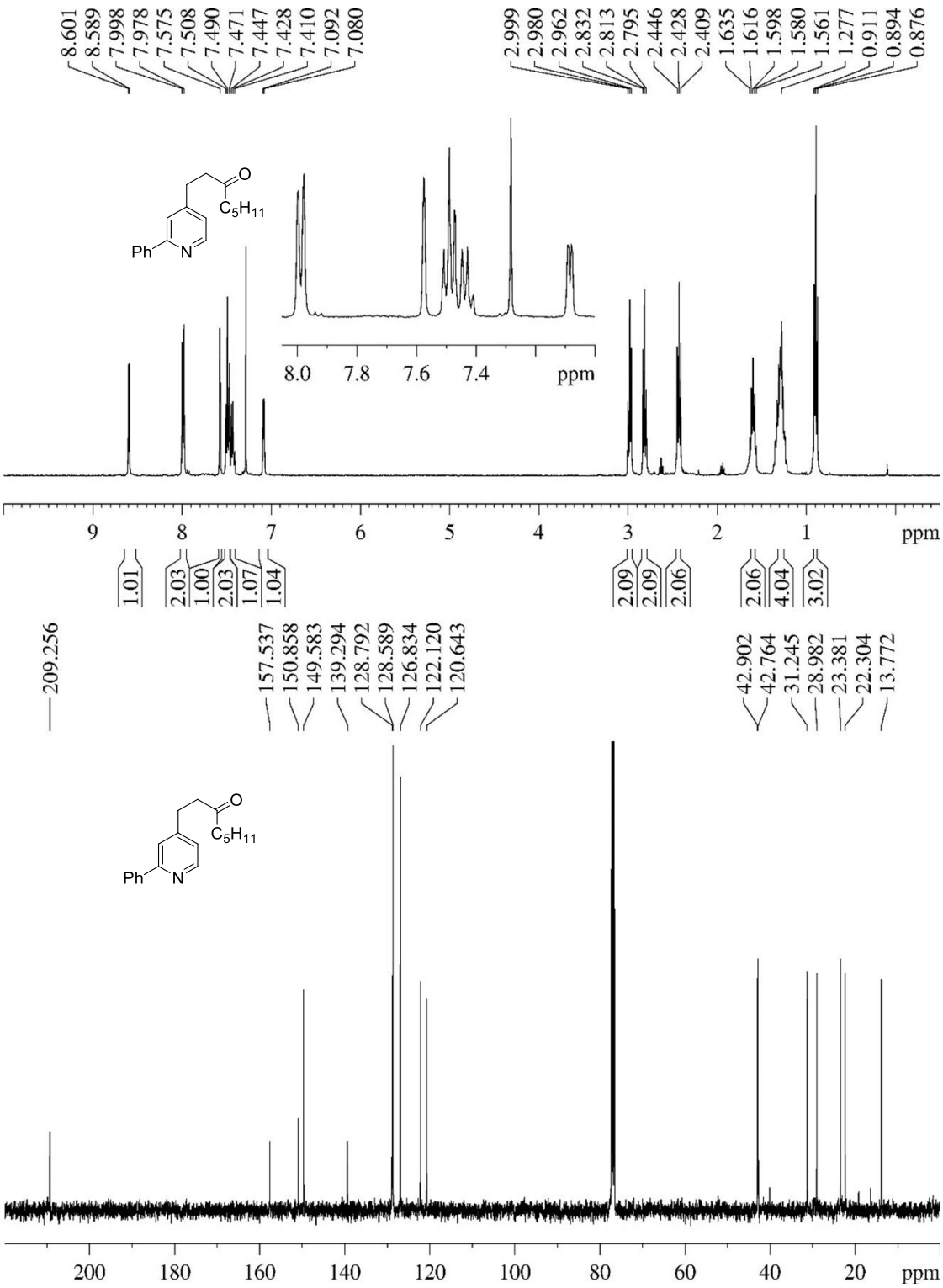

^{1}H (400 MHz, $CDCl_3$) and ^{13}C (100 MHz, $CDCl_3$)-NMR spectra of heterocycle **47a'**

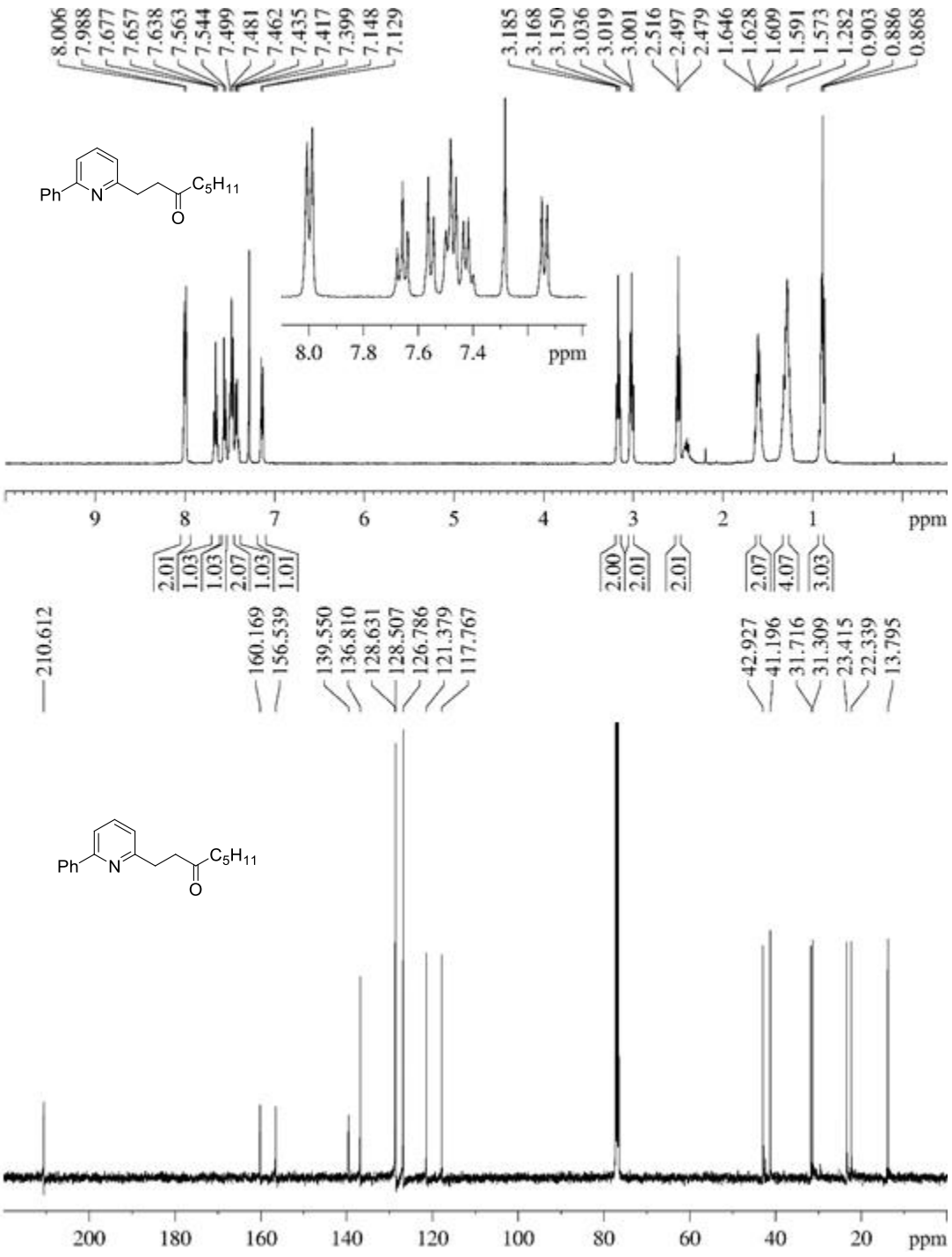

^{1}H (400 MHz, $CDCl_3$) and ^{13}C (100 MHz, $CDCl_3$)-NMR spectra of heterocycle **48a**

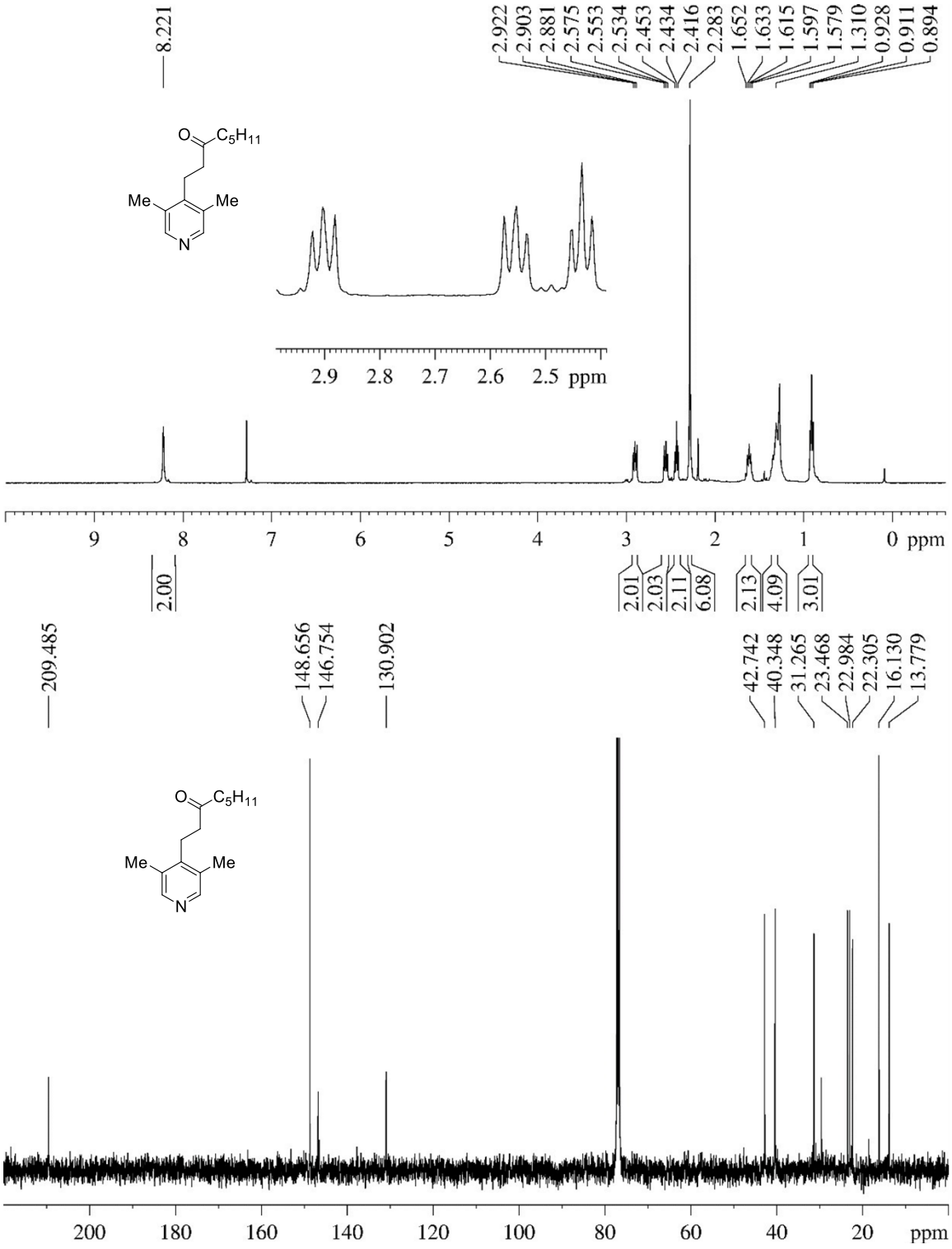

^{1}H (400 MHz, $CDCl_3$) and ^{13}C (100 MHz, $CDCl_3$)-NMR spectra of heterocycle **48a'**

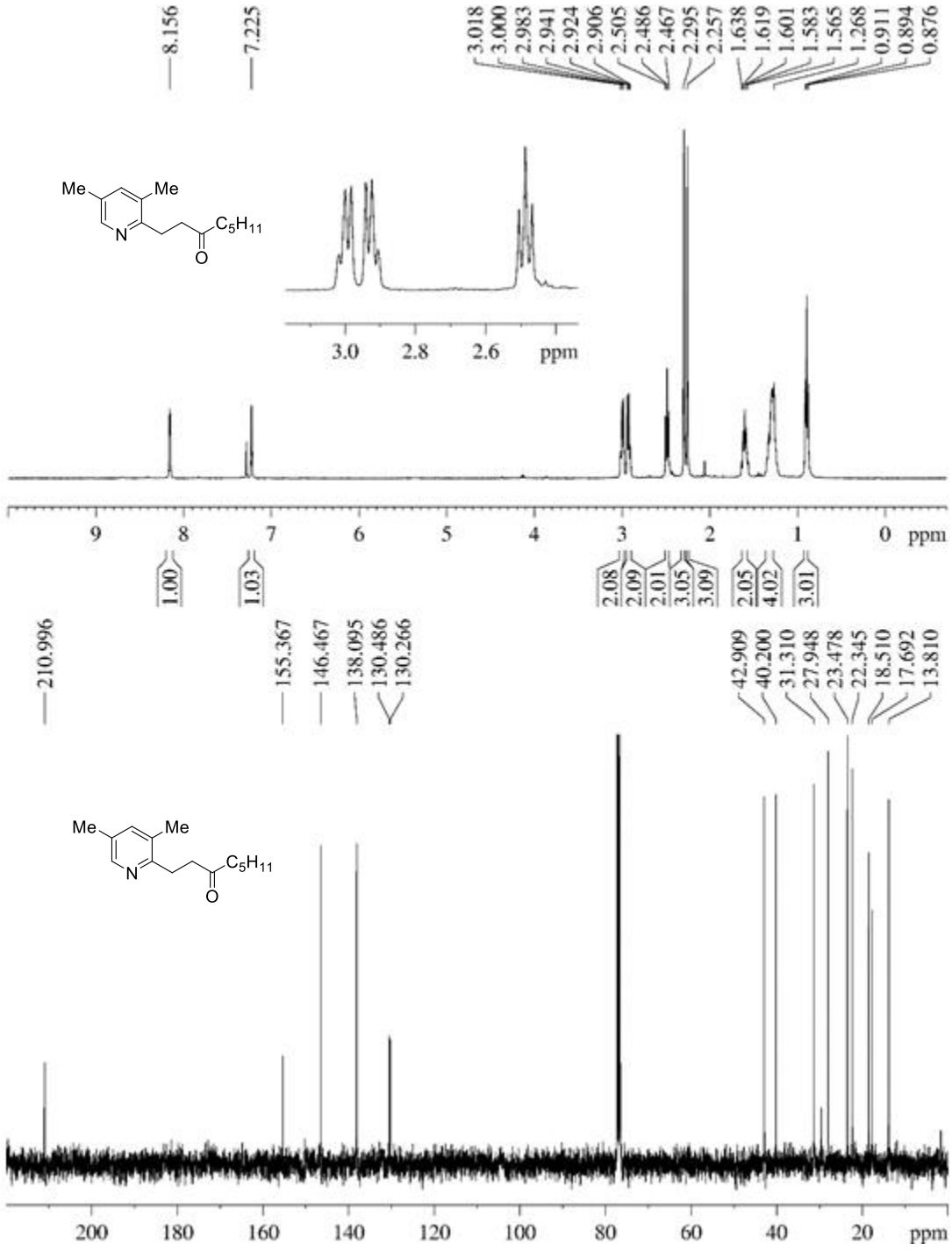

^{1}H (400 MHz, $CDCl_3$) and ^{13}C (75 MHz, $CDCl_3$)-NMR spectra of heterocycle **52a**

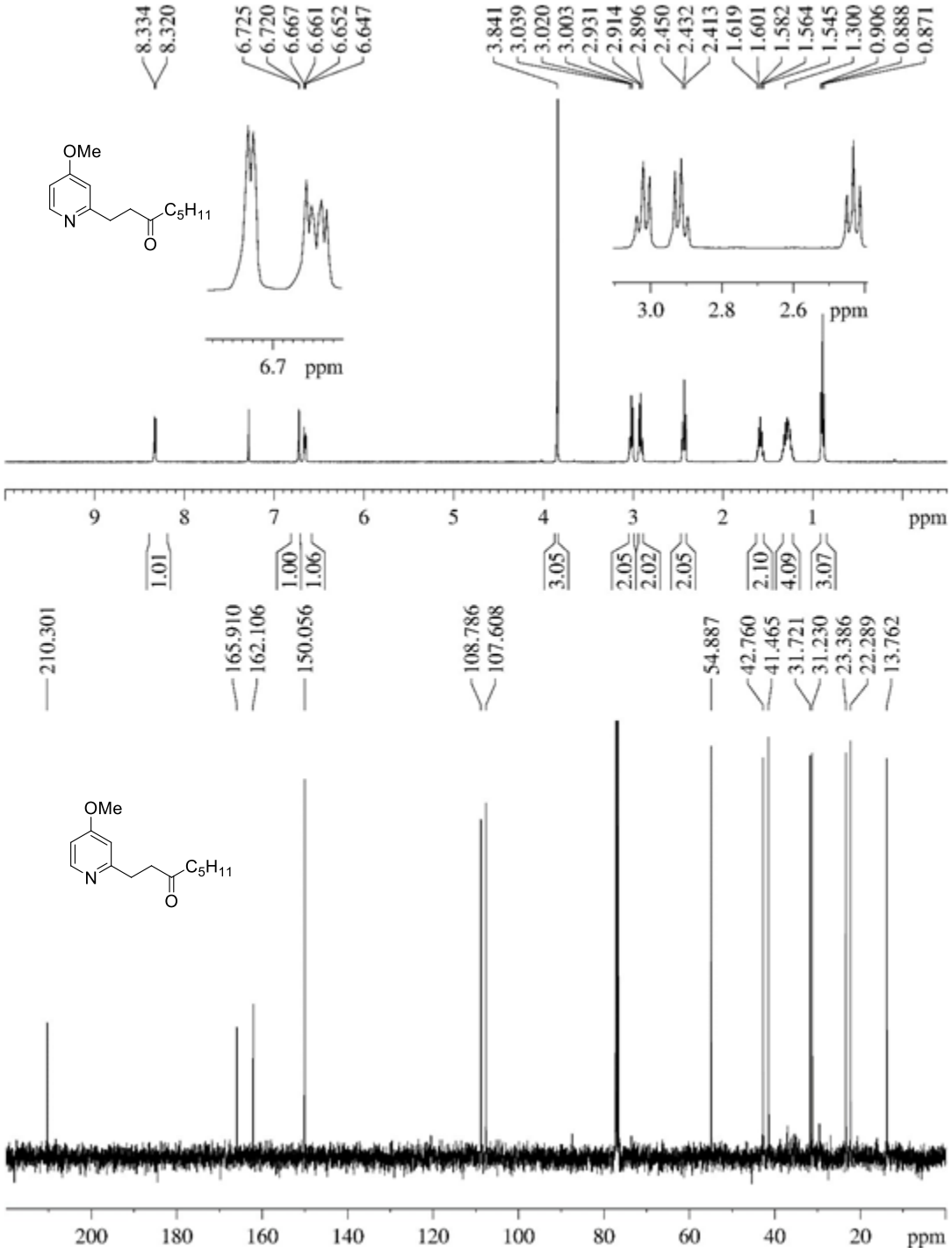

^{1}H (400 MHz, $CDCl_3$) and ^{13}C (75 MHz, $CDCl_3$)-NMR spectra of heterocycle **53a**

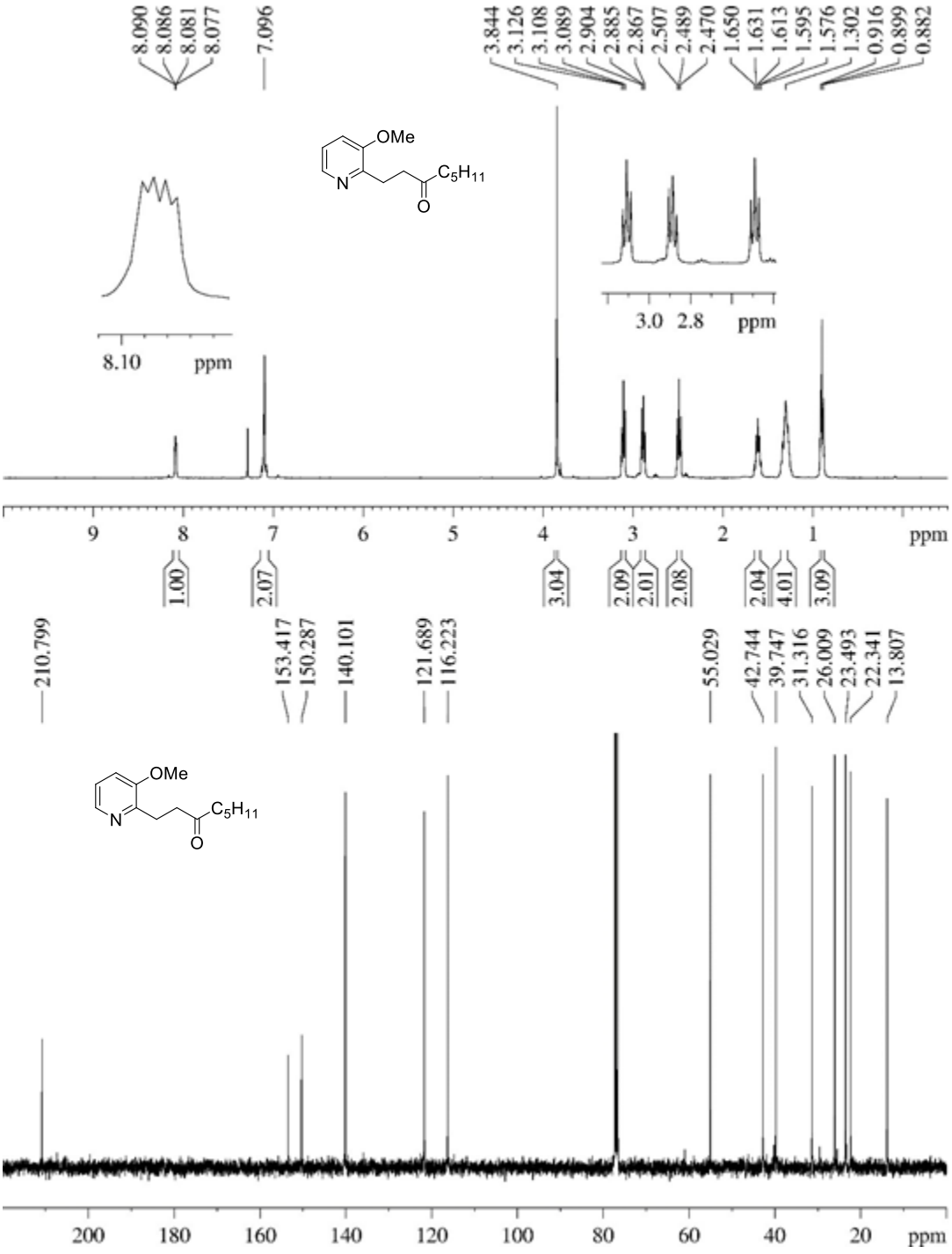

^{1}H (300 MHz, MeOH d_4) and ^{13}C (75 MHz, $CDCl_3$)-NMR spectra of heterocycle **54a**

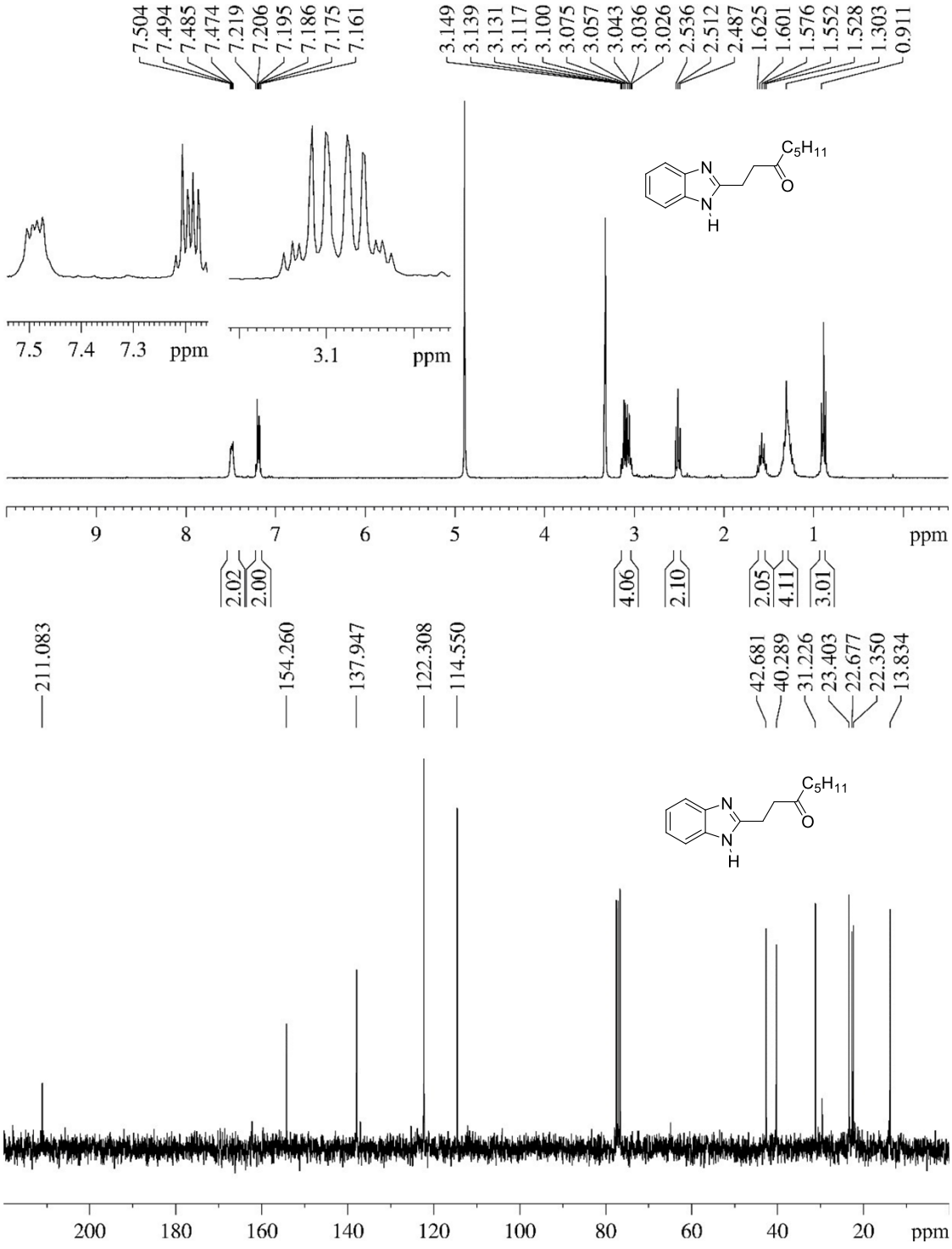

^{1}H (400 MHz, $CDCl_3$) and ^{13}C (100 MHz, $CDCl_3$)-NMR spectra of heterocycle **55a**

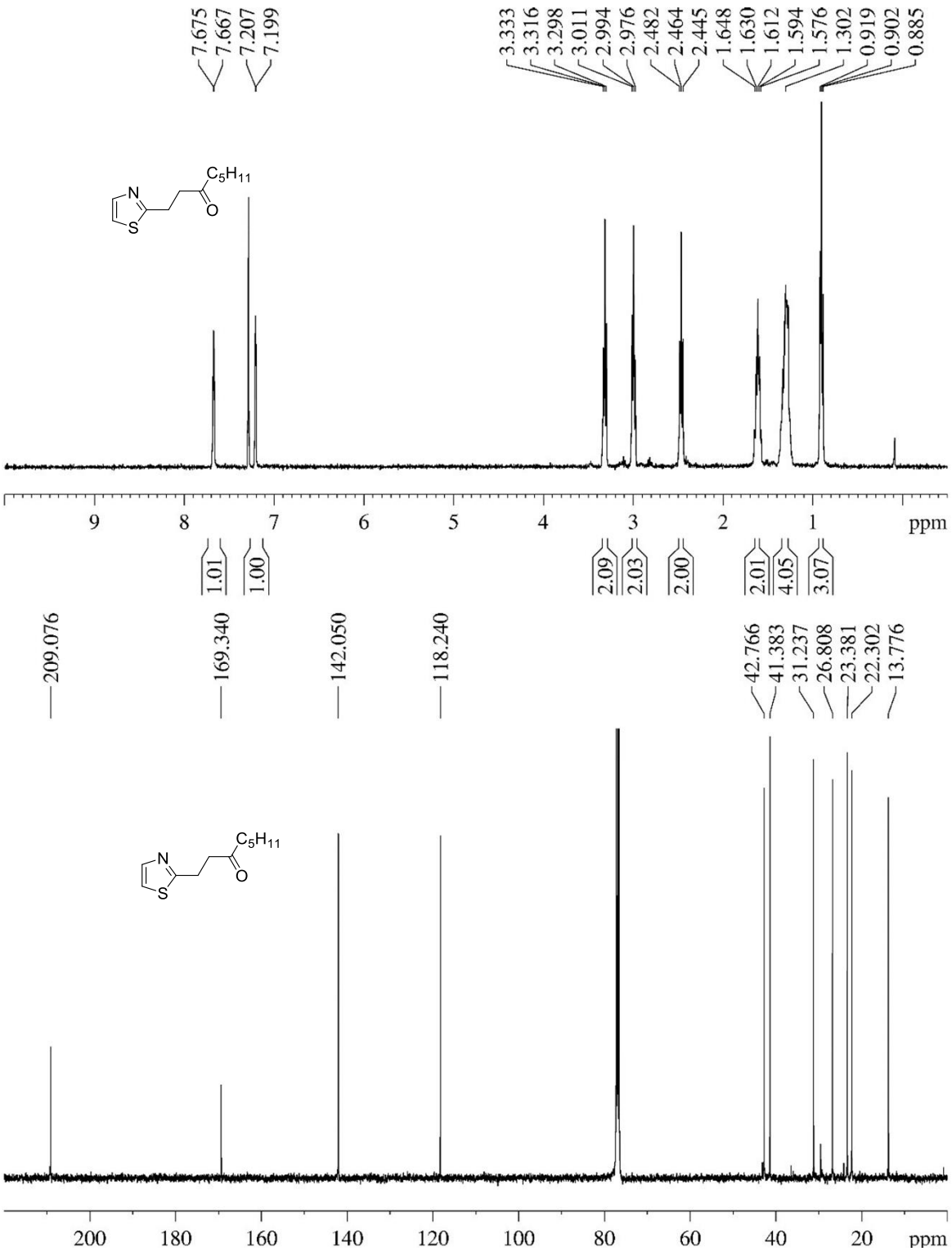

^{1}H (400 MHz, $CDCl_3$) and ^{13}C (100 MHz, $CDCl_3$)-NMR spectra of heterocycle **56a**

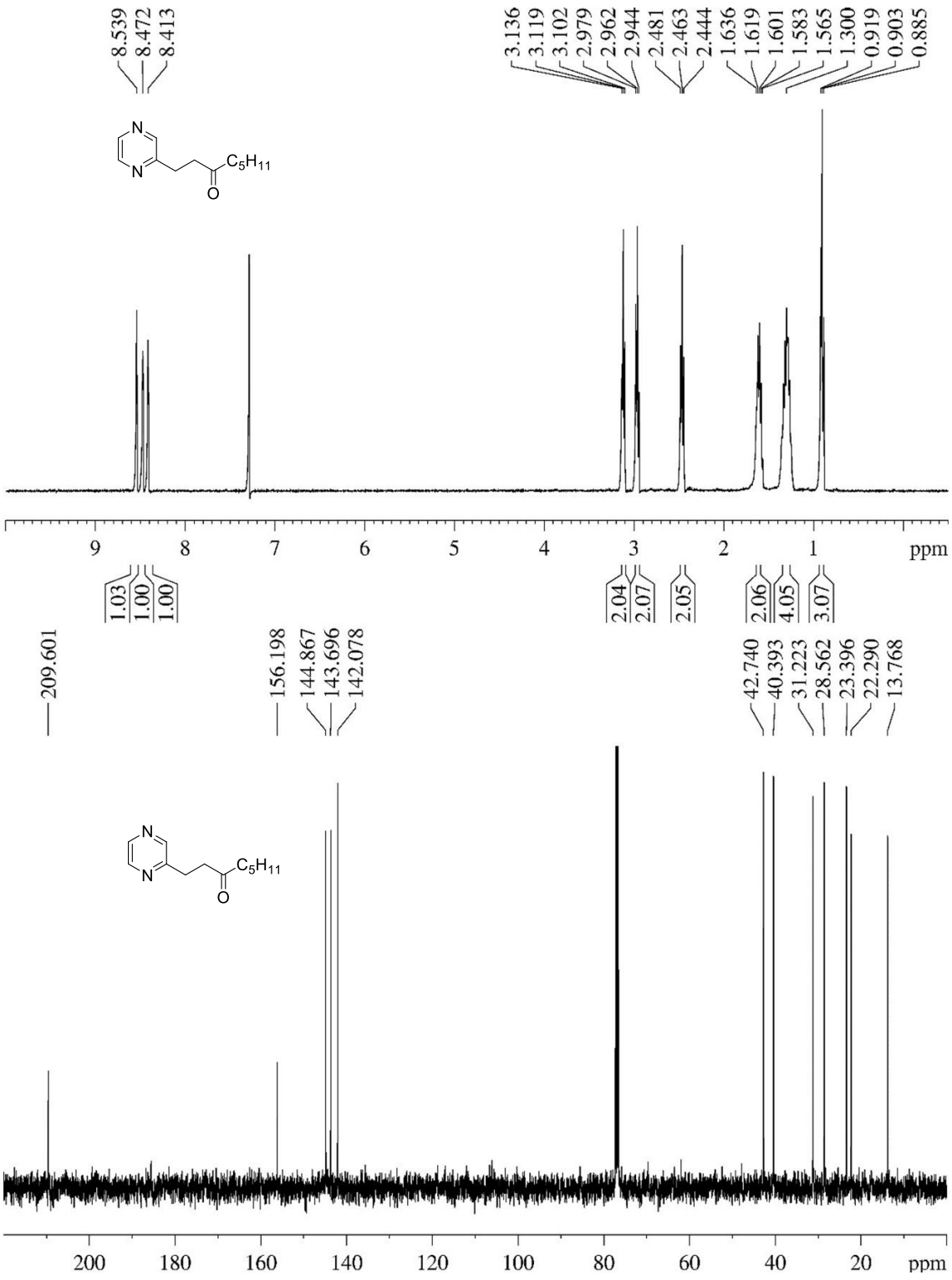

^{1}H (400 MHz, $CDCl_3$) and ^{13}C (100 MHz, $CDCl_3$)-NMR spectra of heterocycle **58a**

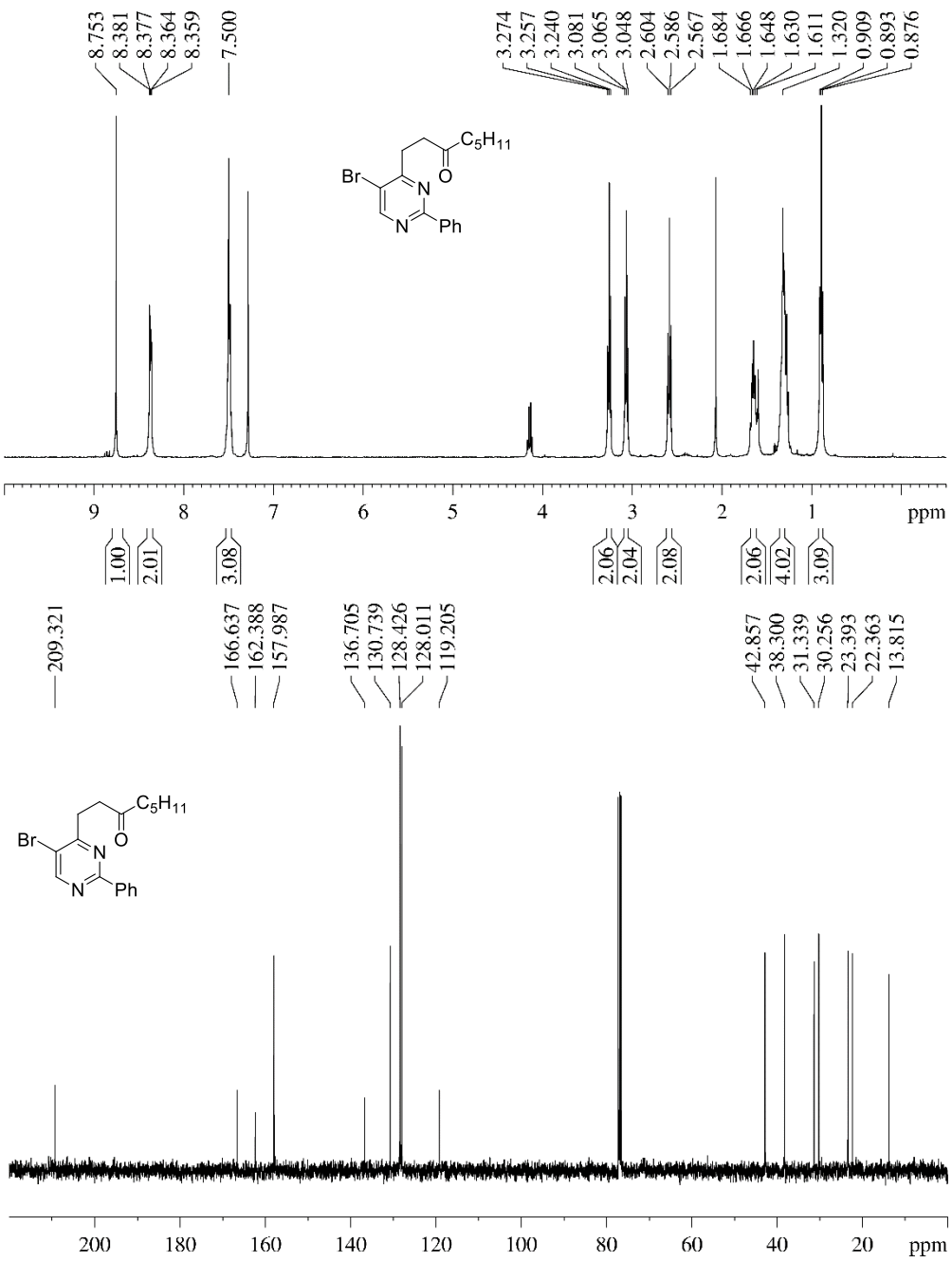

^{1}H (400 MHz, $CDCl_3$) and ^{13}C (100 MHz, $CDCl_3$)-NMR spectra of heterocycle **61a**

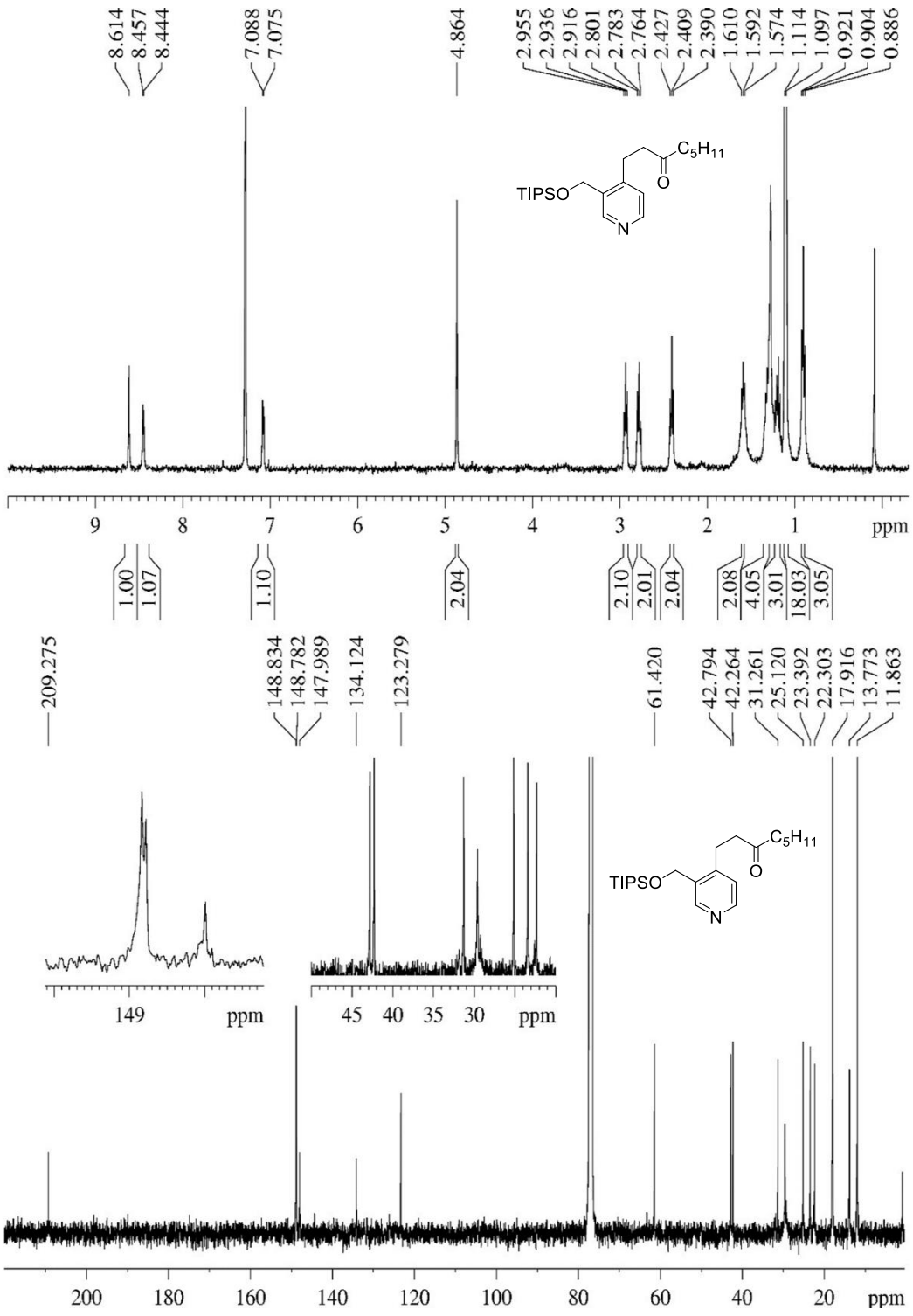

^{1}H (400 MHz, $CDCl_3$) and ^{13}C (100 MHz, $CDCl_3$)-NMR spectra of heterocycle **62a**

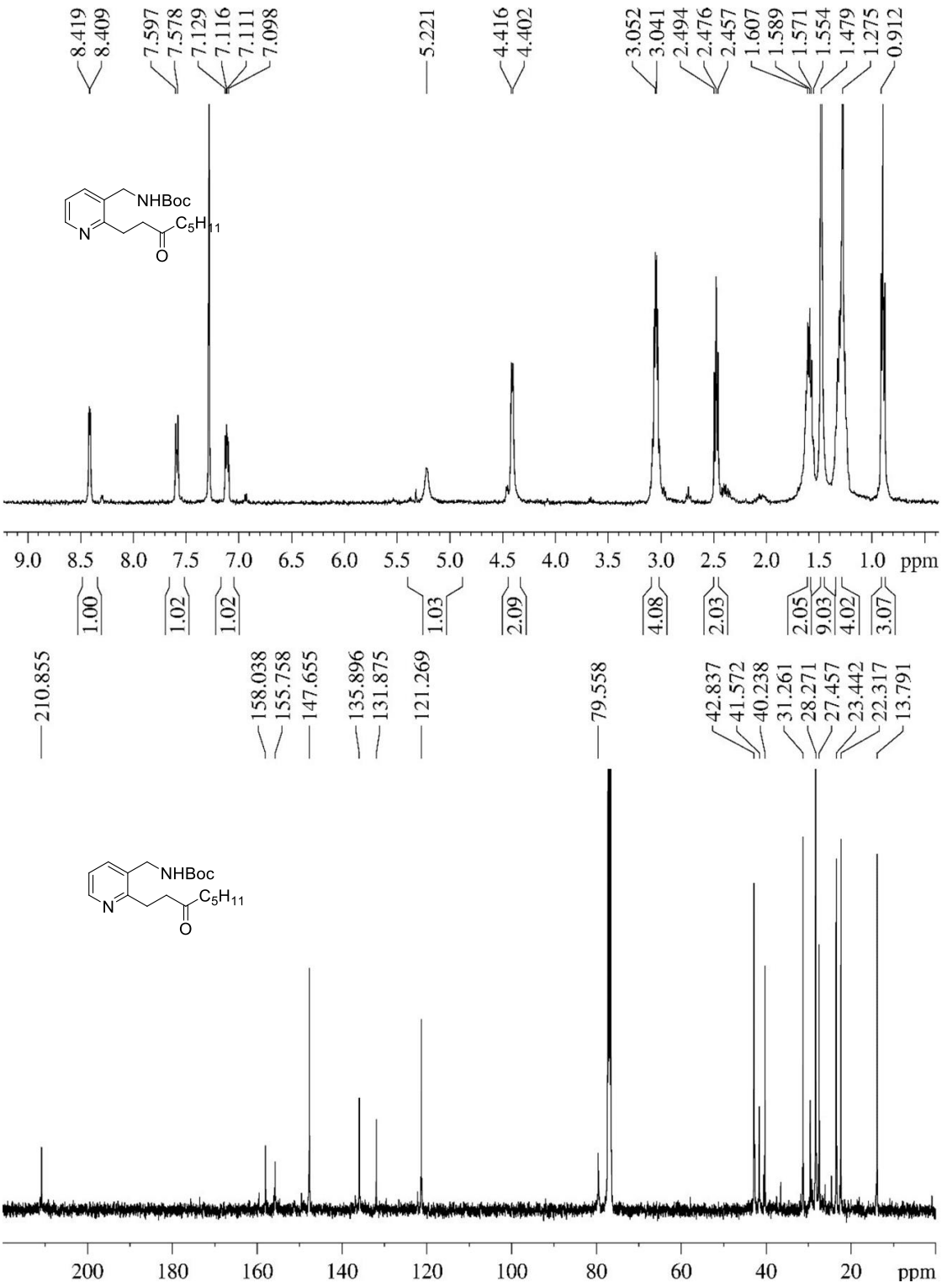

^{1}H (400 MHz, $CDCl_3$) and ^{13}C (100 MHz, $CDCl_3$)-NMR spectra of heterocycle **63a**

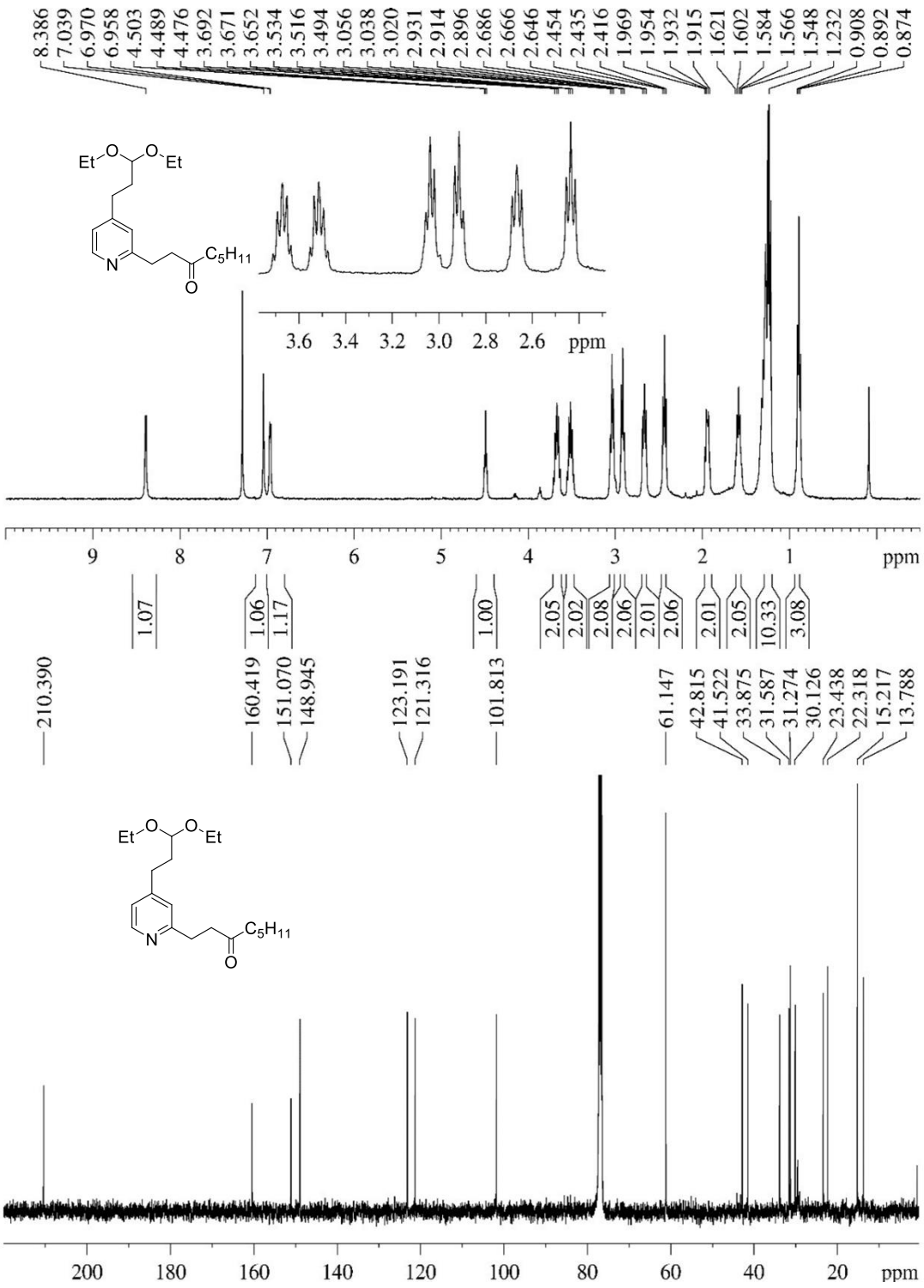

^{1}H (400 MHz, $CDCl_3$) and ^{13}C (100 MHz, $CDCl_3$)-NMR spectra of heterocycle **37b**

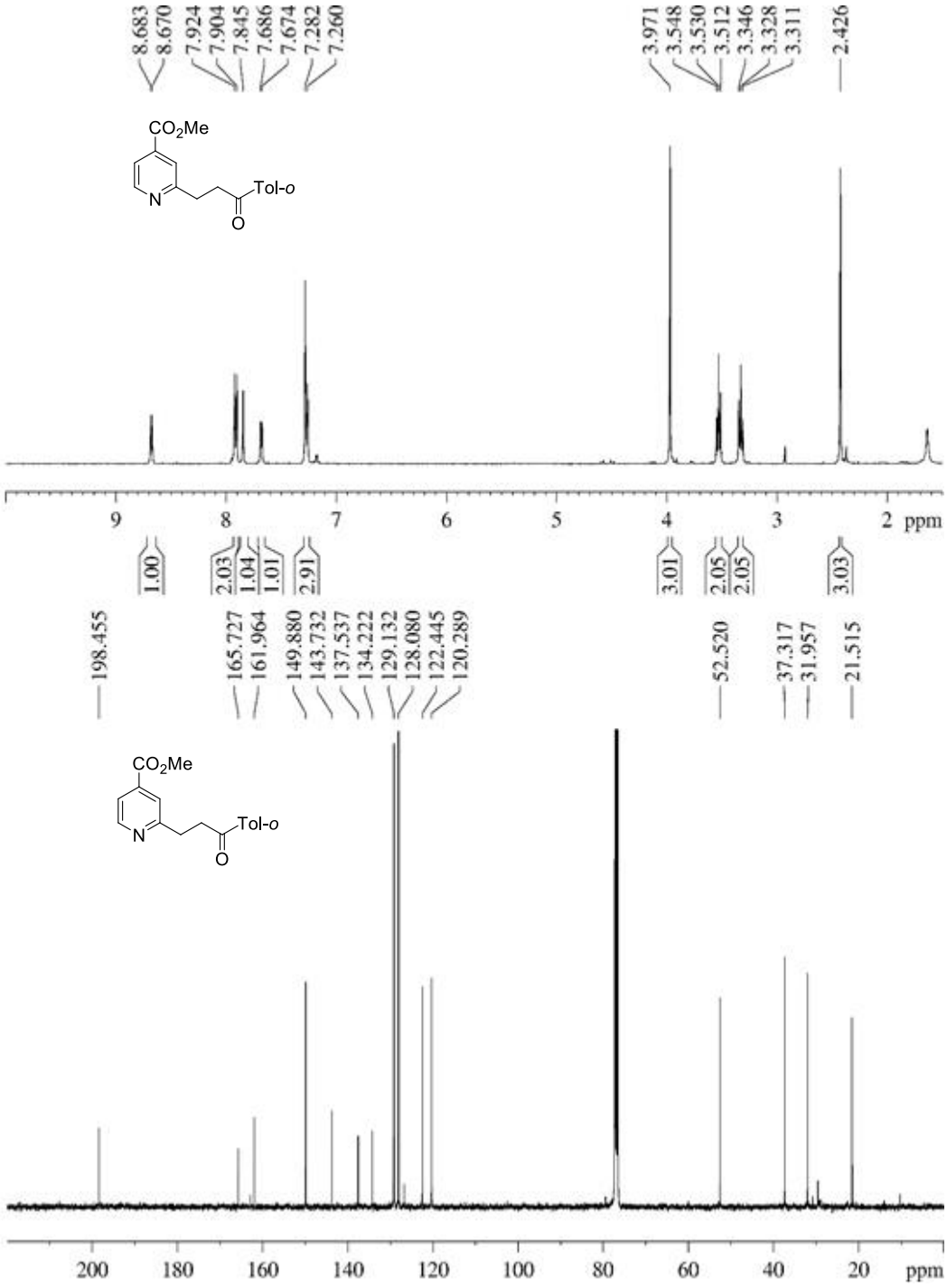

^{1}H (400 MHz, $CDCl_3$) and ^{13}C (100 MHz, $CDCl_3$)-NMR spectra of heterocycle **37c**

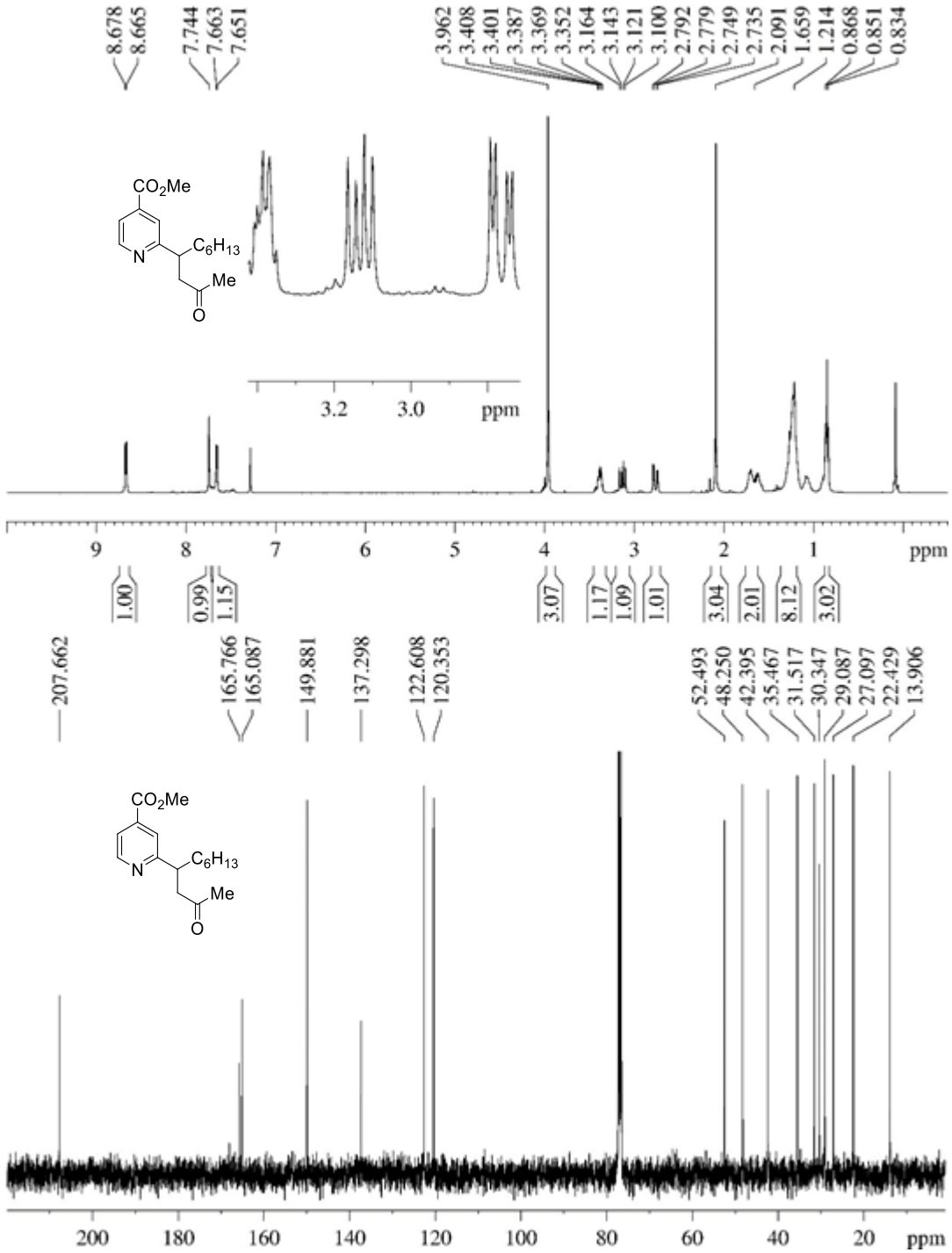

^{1}H (400 MHz, $CDCl_3$) and ^{13}C (100 MHz, $CDCl_3$)-NMR spectra of alcohol **64a**

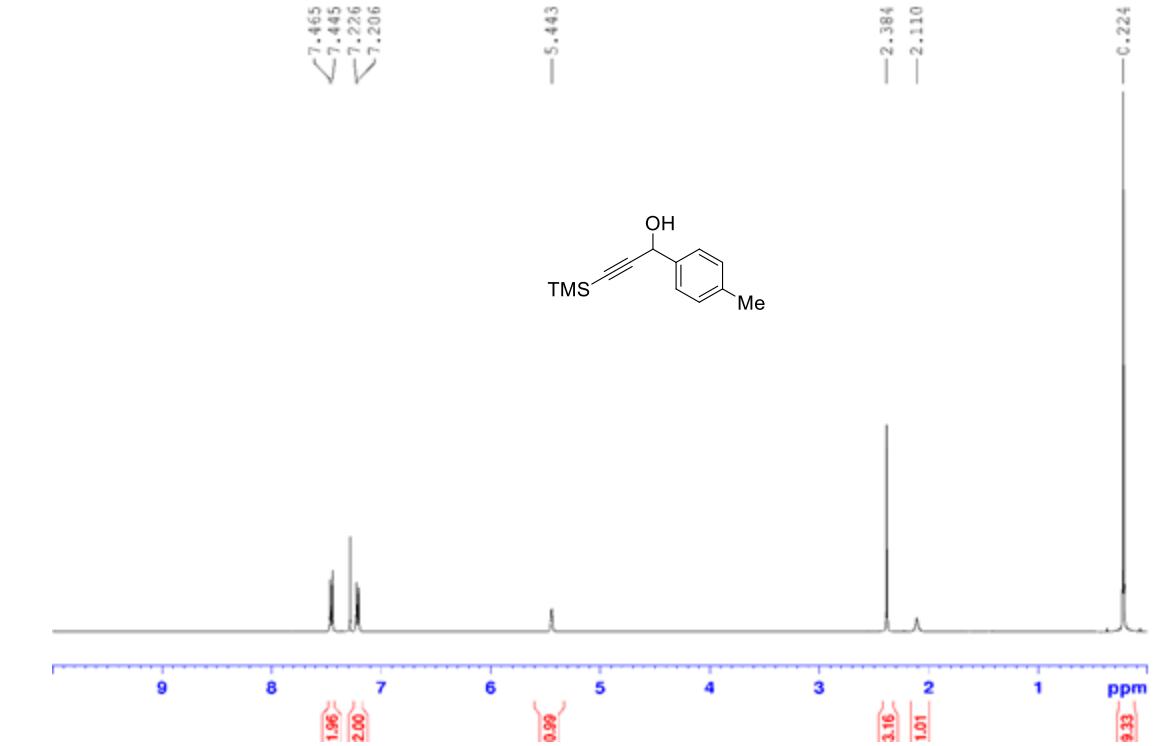

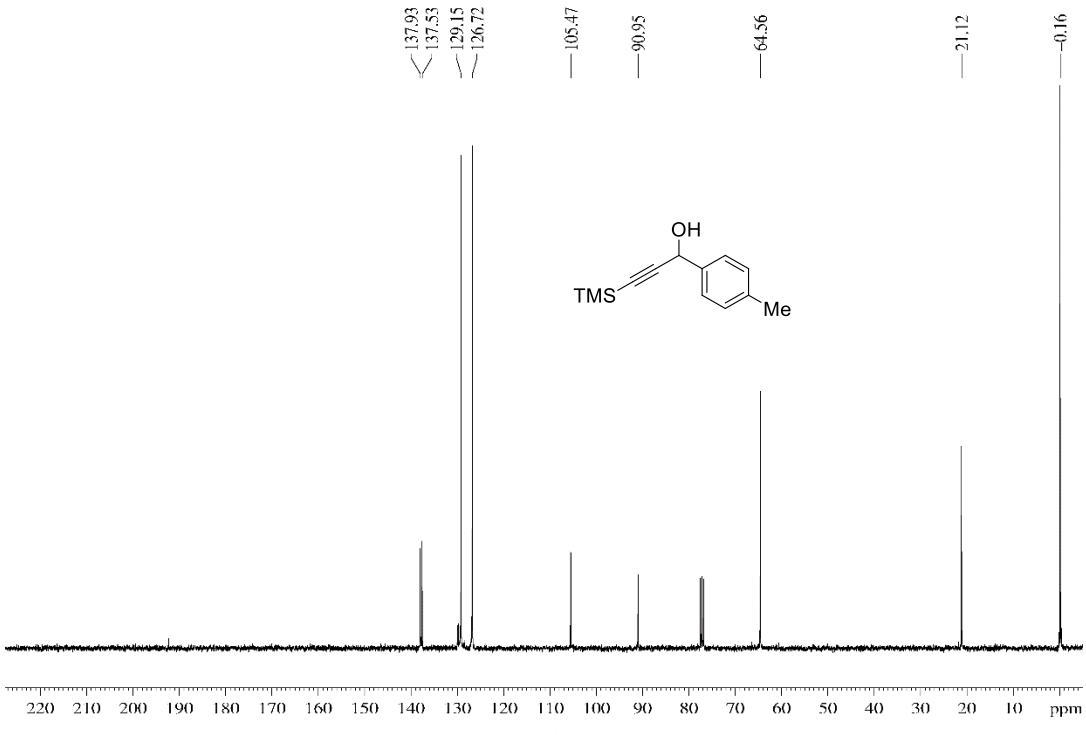

^{29}Si (80 MHz, $CDCl_3$)-NMR spectra of alcohol **64a**

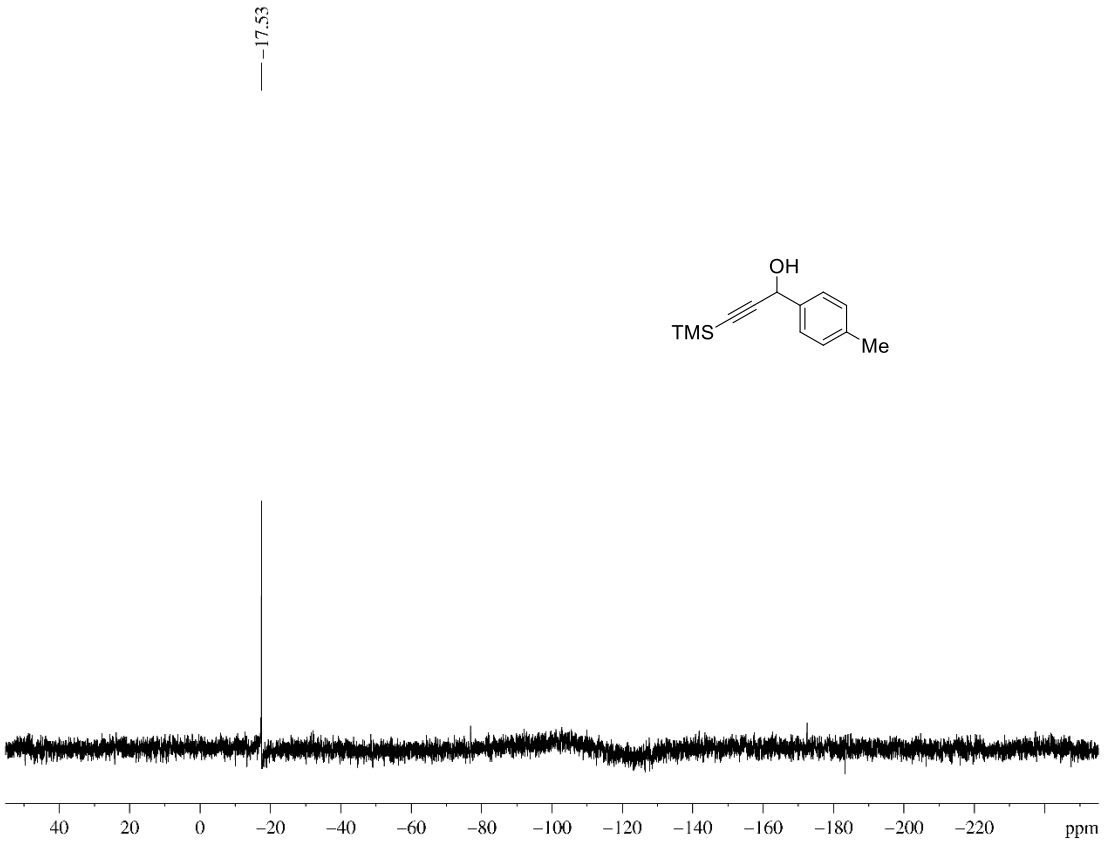

^{1}H (400 MHz, $CDCl_3$) and ^{13}C (100 MHz, $CDCl_3$)-NMR spectra of alcohol **64b**

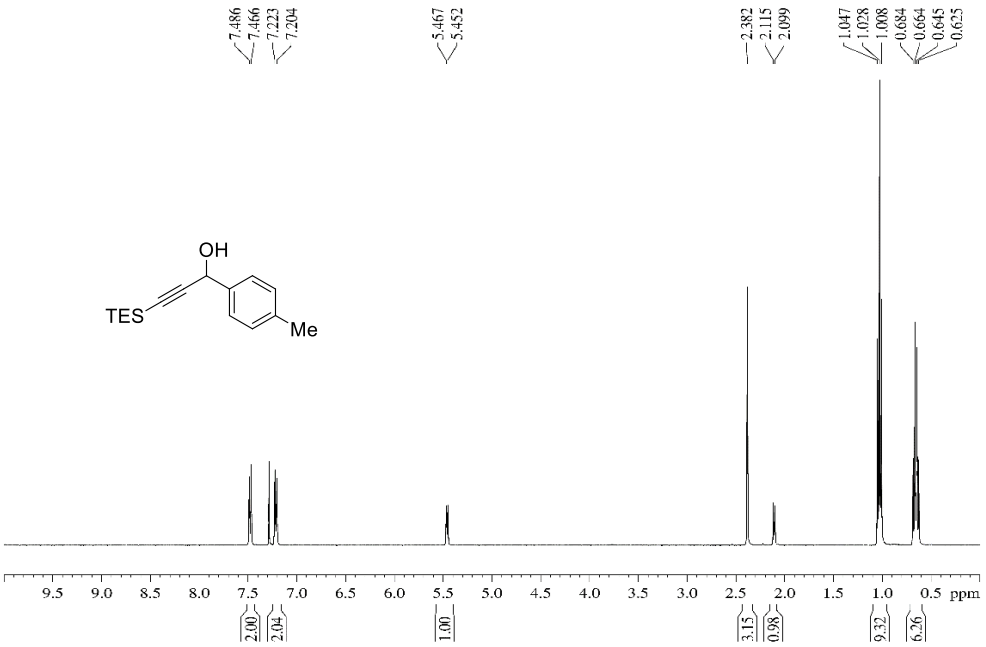

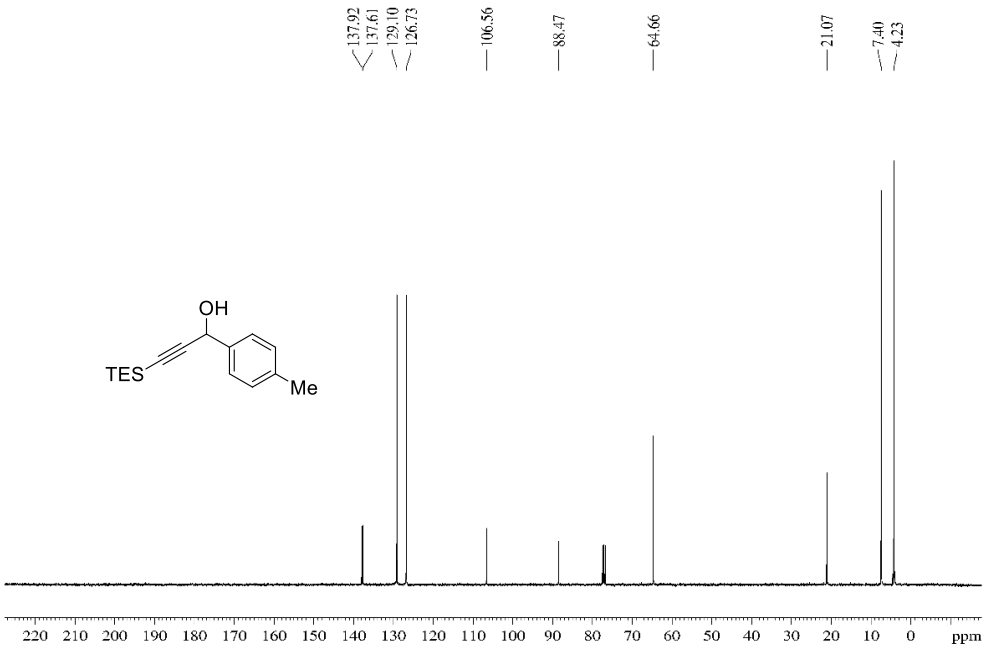

^{29}Si (80 MHz, $CDCl_3$)-NMR spectra of alcohol **64b**

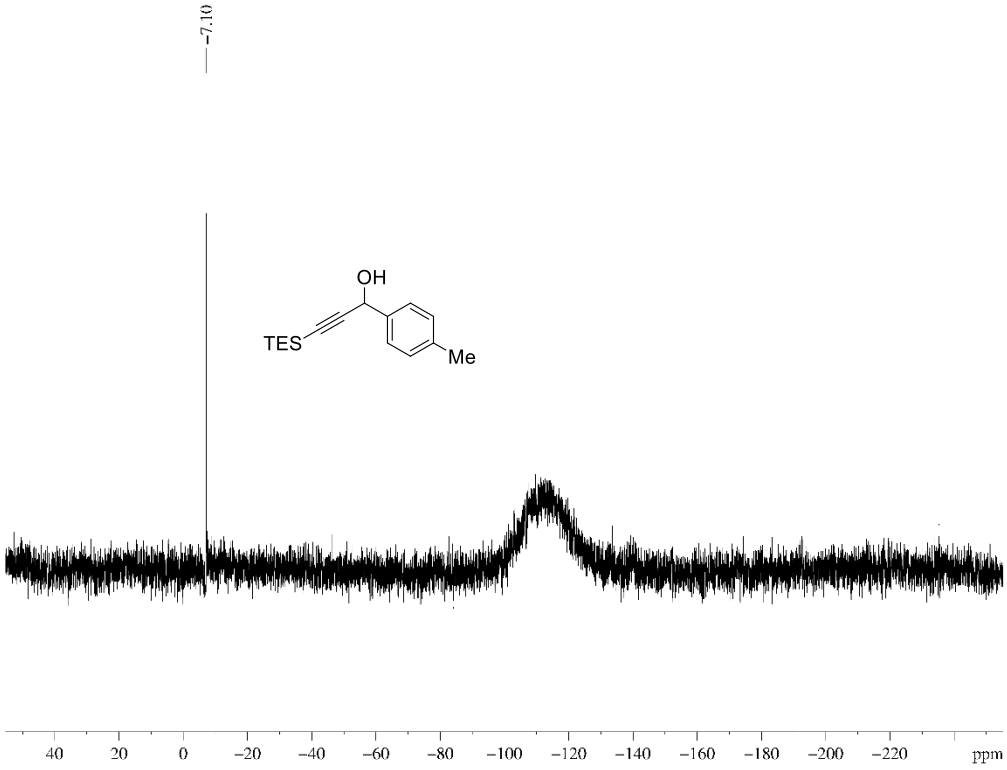

^{1}H (400 MHz, $CDCl_3$) and ^{13}C (100 MHz, $CDCl_3$)-NMR spectra of alcohol **64c**

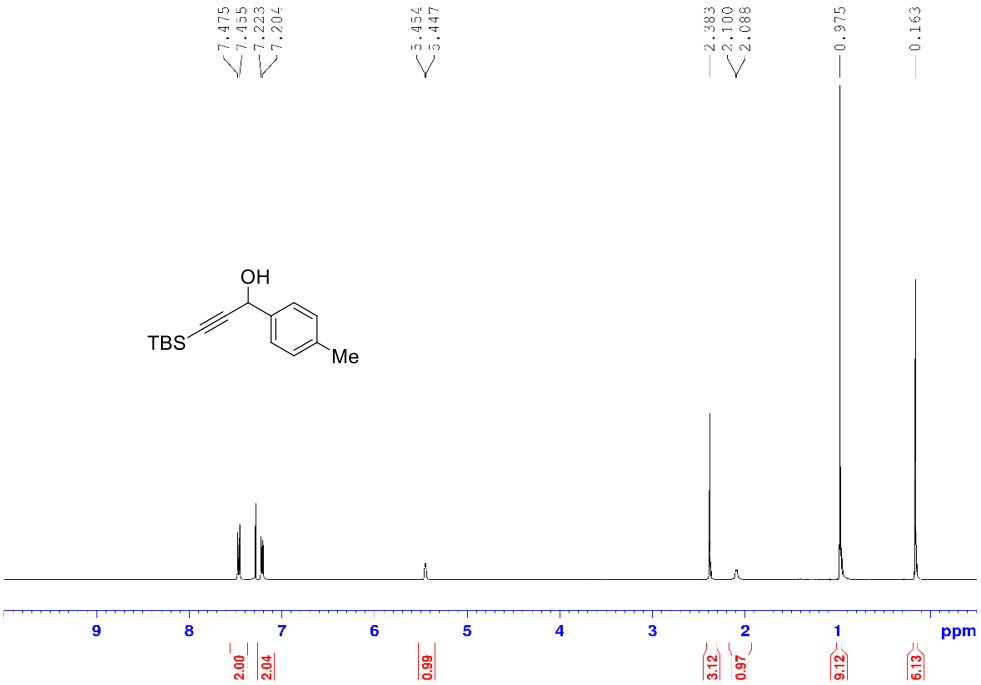

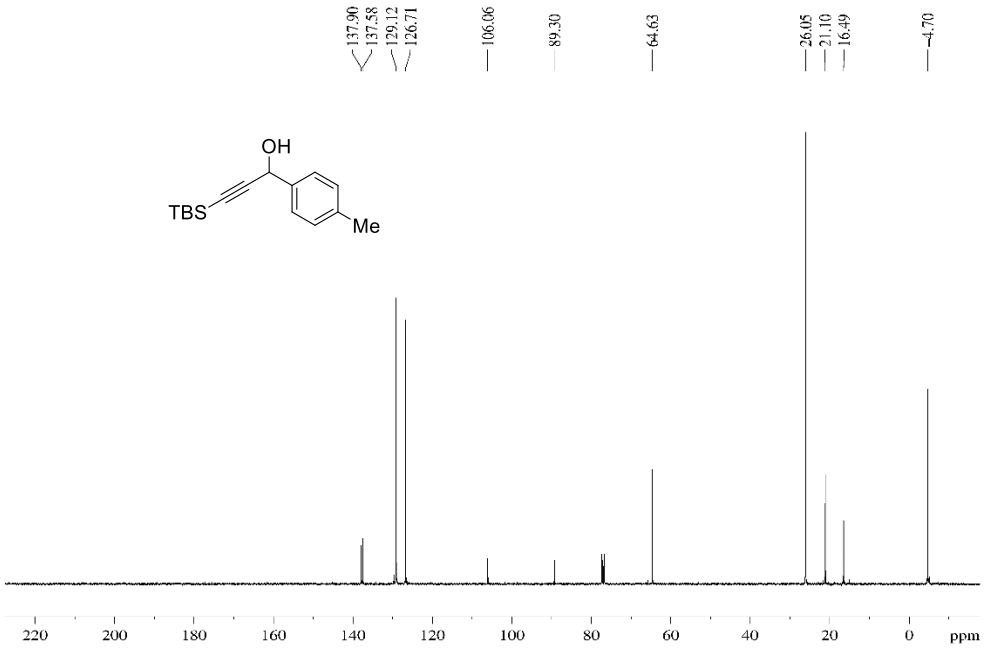

^{29}Si (80 MHz, $CDCl_3$)-NMR spectra of alcohol **64c**

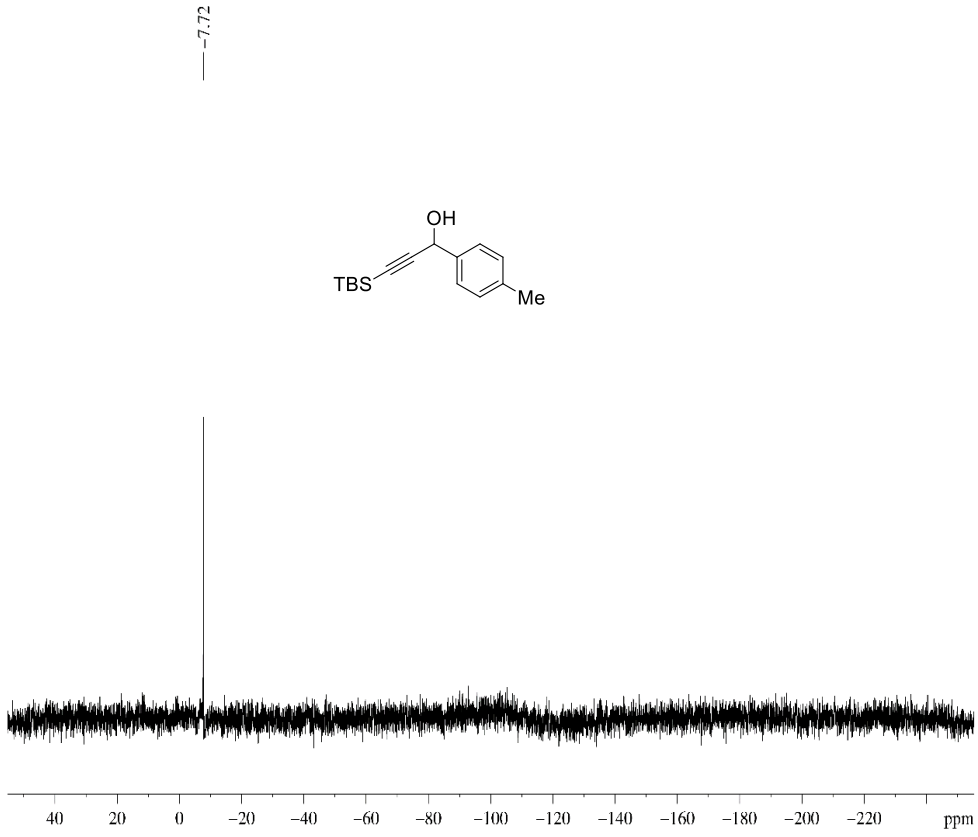

^{1}H (400 MHz, $CDCl_3$) and ^{13}C (100 MHz, $CDCl_3$)-NMR spectra of alcohol **64d**

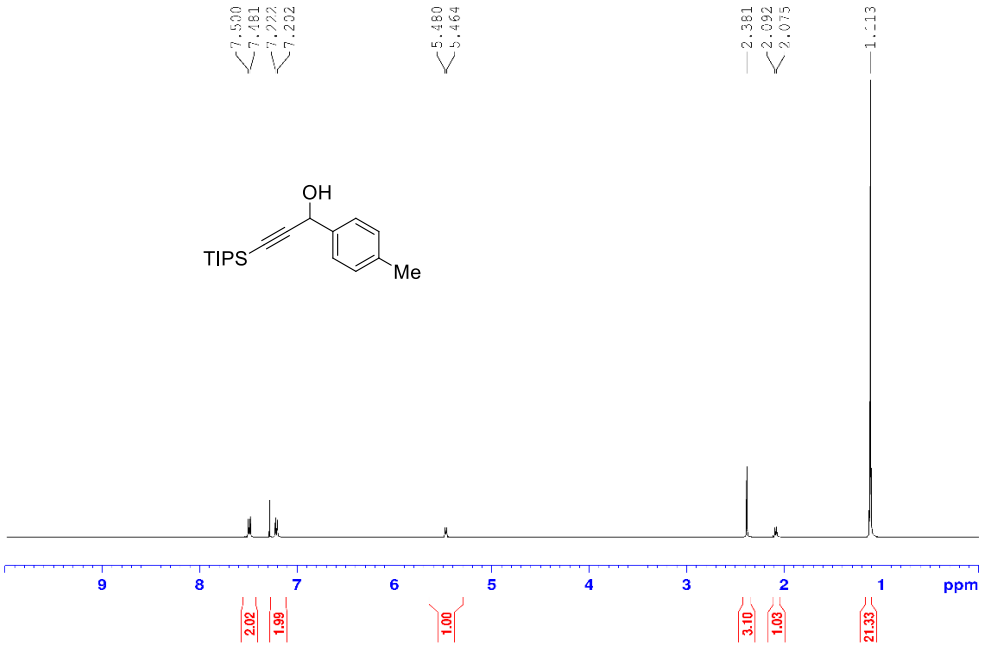

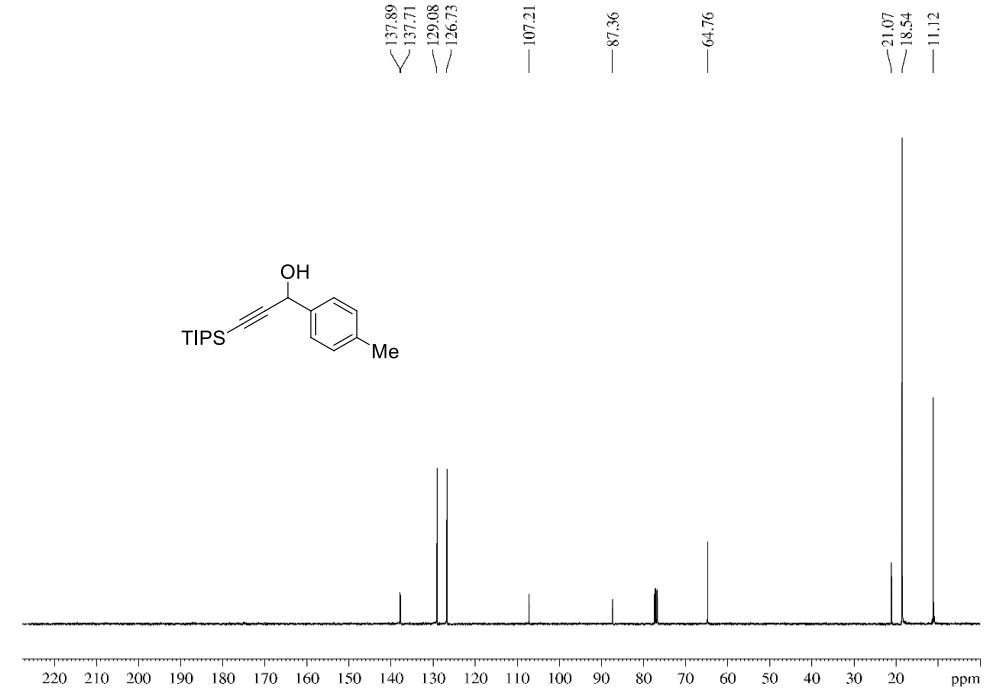

^{29}Si (80 MHz, $CDCl_3$)-NMR spectra of alcohol **64d**

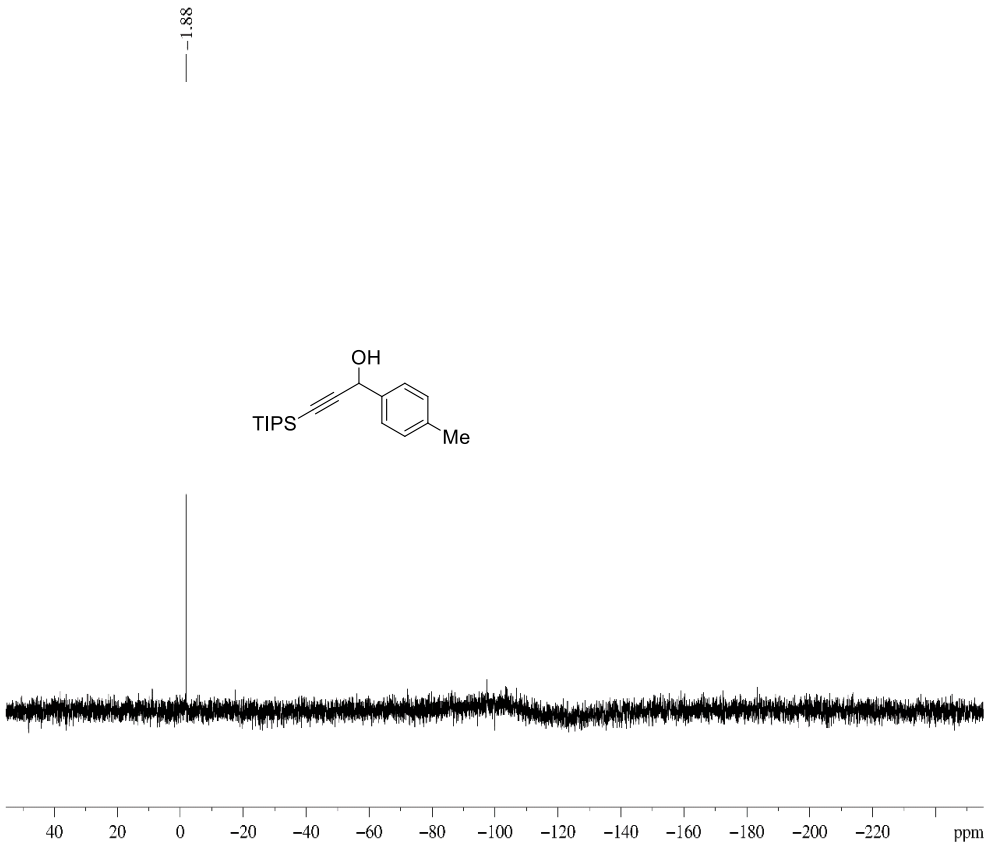

^{1}H (400 MHz, $CDCl_3$) and ^{13}C (100 MHz, $CDCl_3$)-NMR spectra of alcohol **64e**

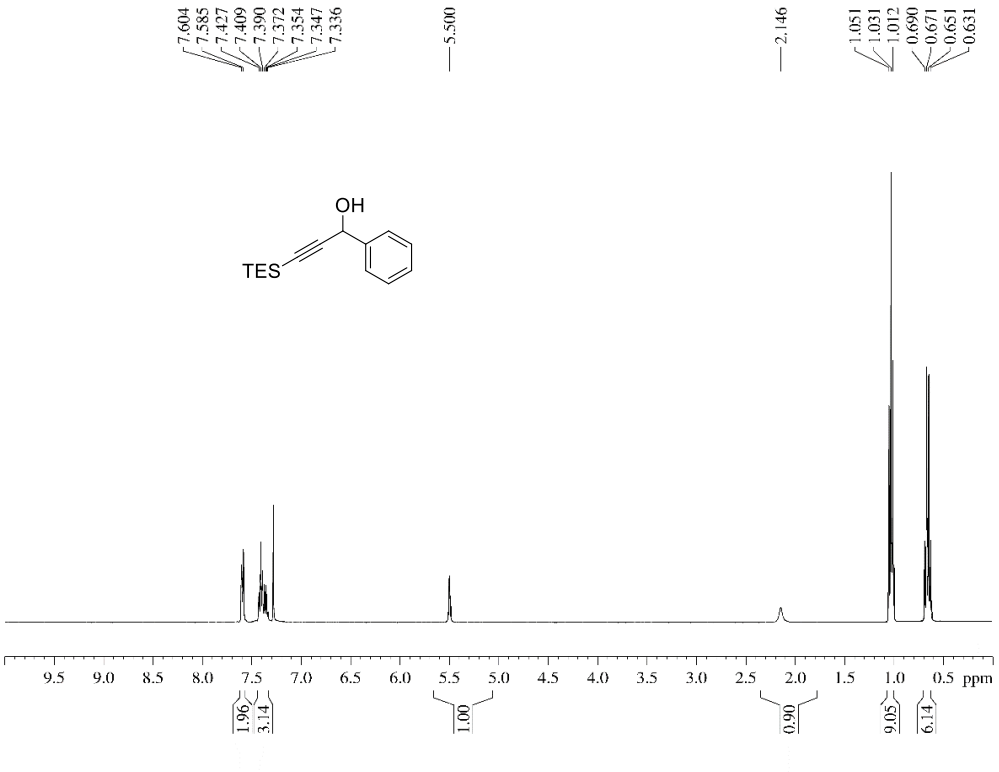

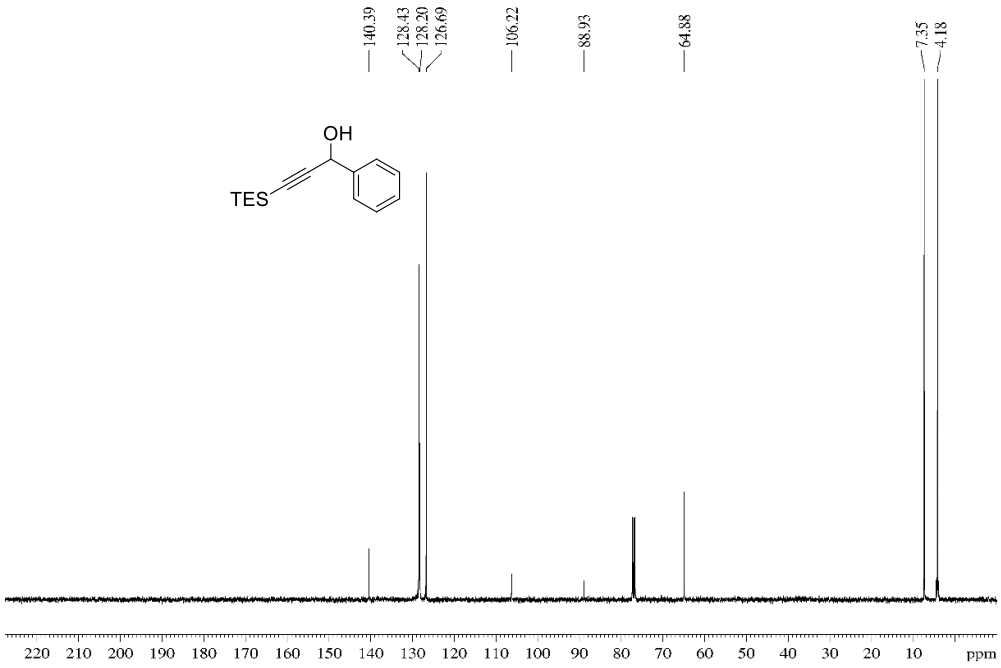

^{29}Si (80 MHz, $CDCl_3$)-NMR spectra of alcohol **64e**

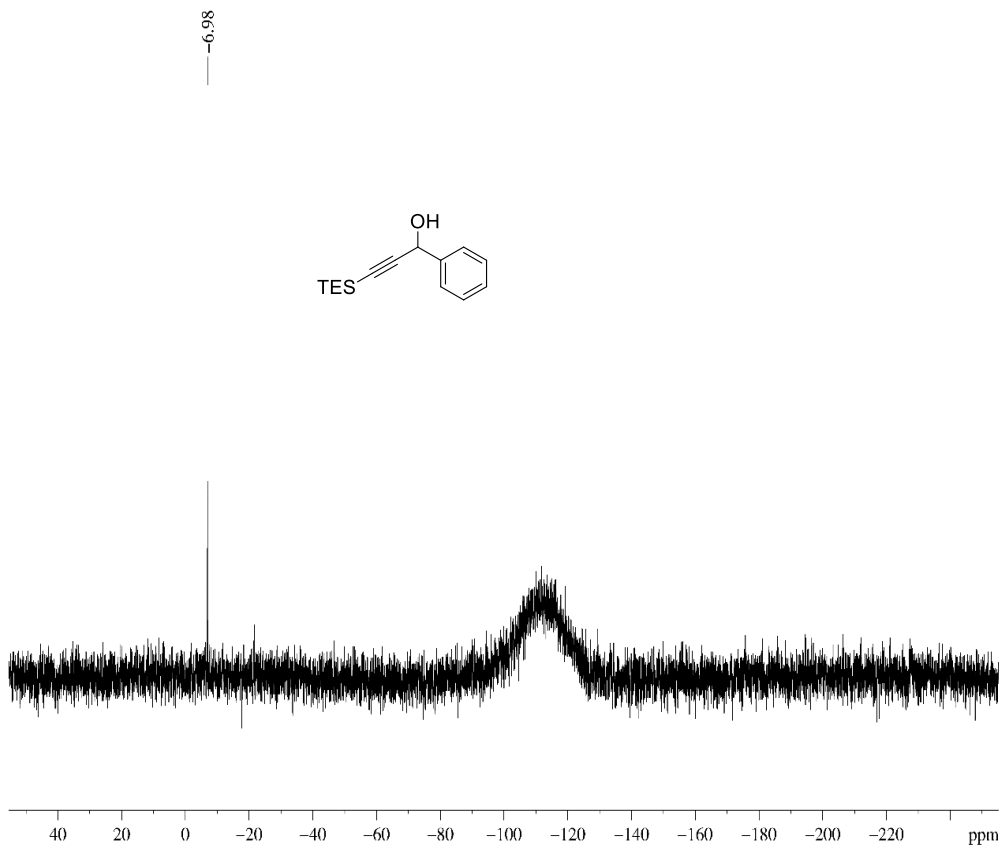

^{1}H (400 MHz, $CDCl_3$) and ^{13}C (100 MHz, $CDCl_3$)-NMR spectra of alcohol **64f**

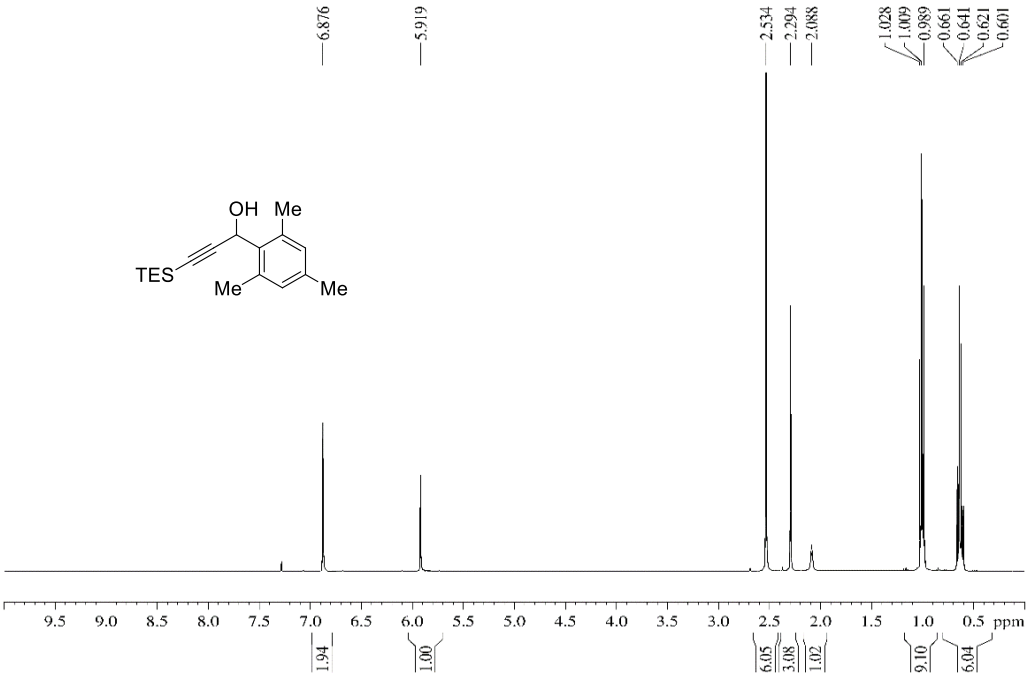

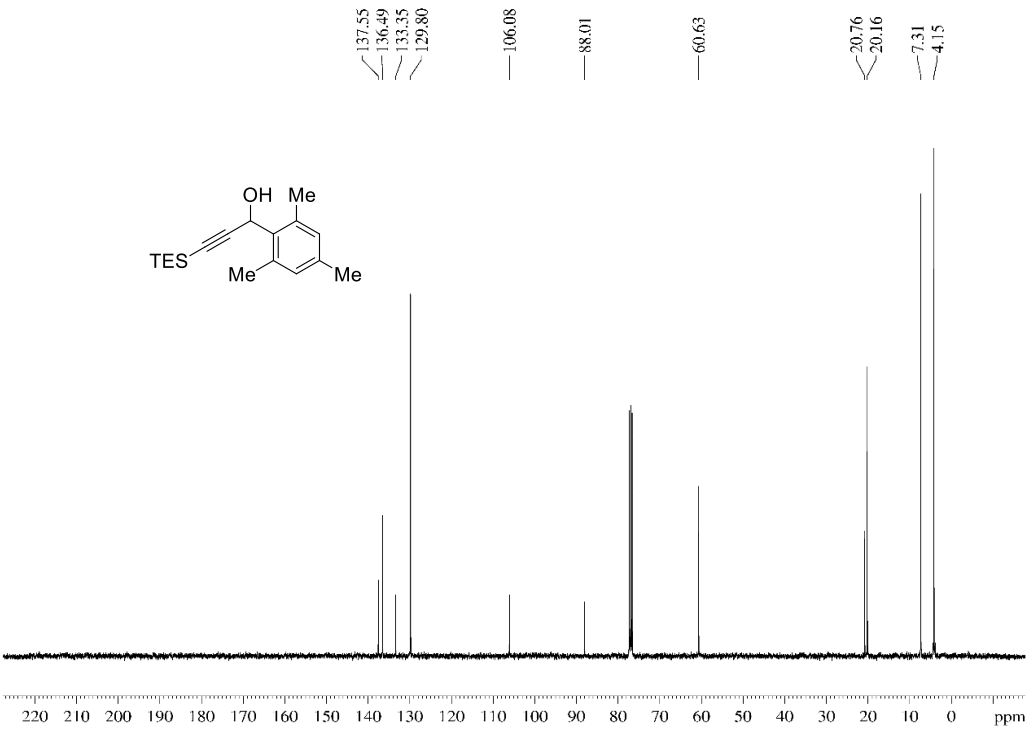

^{29}Si (80 MHz, $CDCl_3$)-NMR spectra of alcohol **64f**

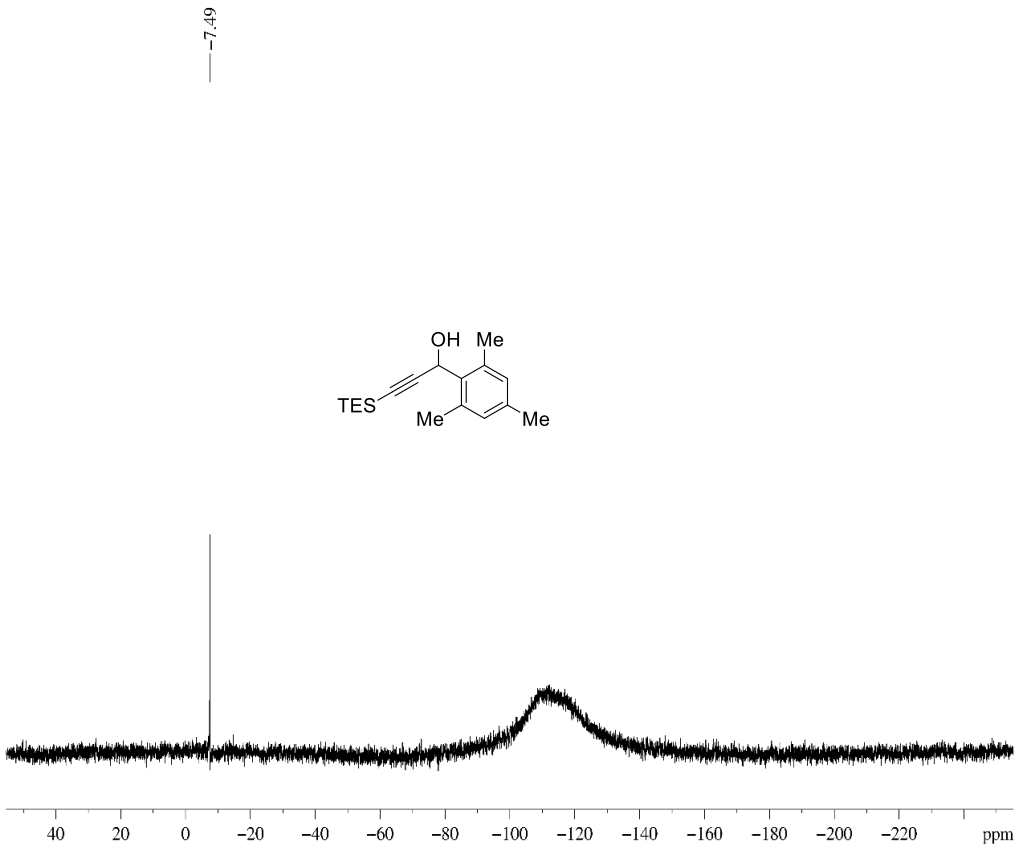

^{1}H (400 MHz, $CDCl_3$) and ^{13}C (100 MHz, $CDCl_3$)-NMR spectra of alcohol **64g**

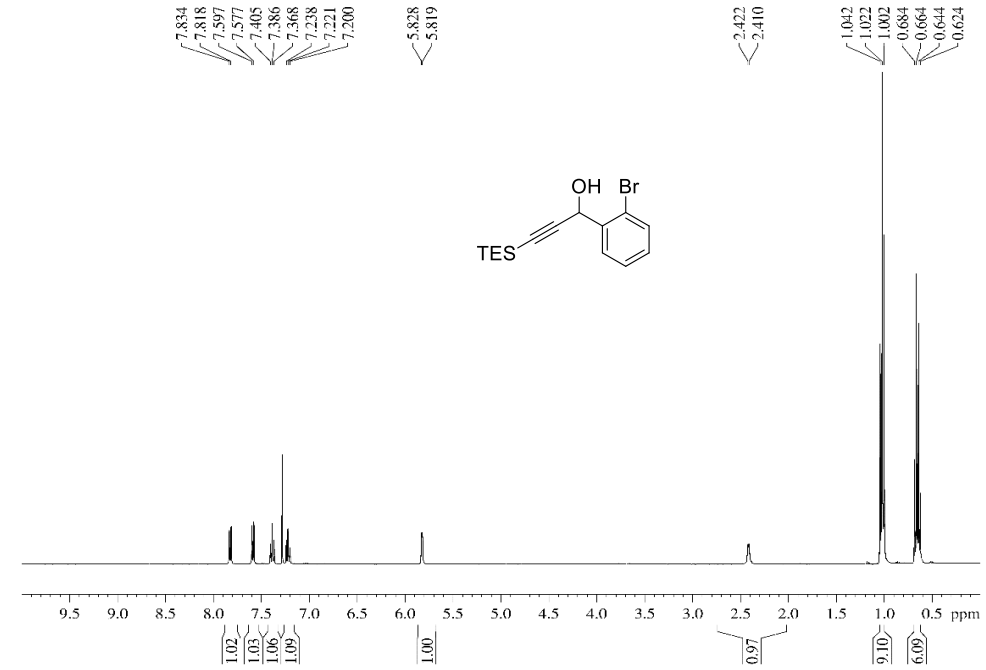

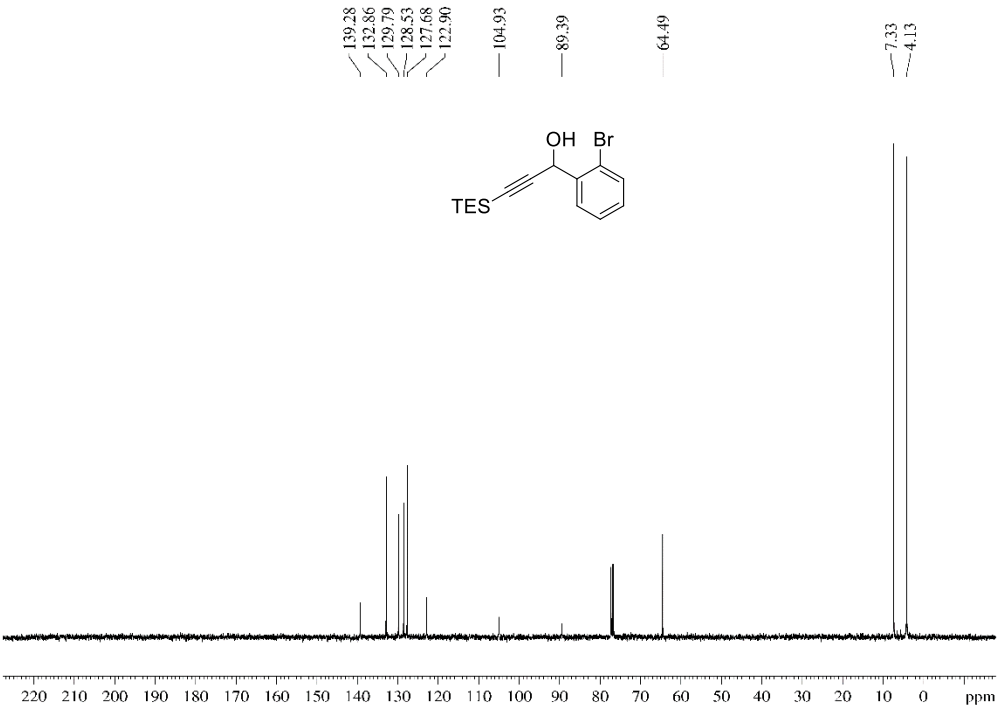

^{29}Si (80 MHz, $CDCl_3$)-NMR spectra of alcohol **64g**

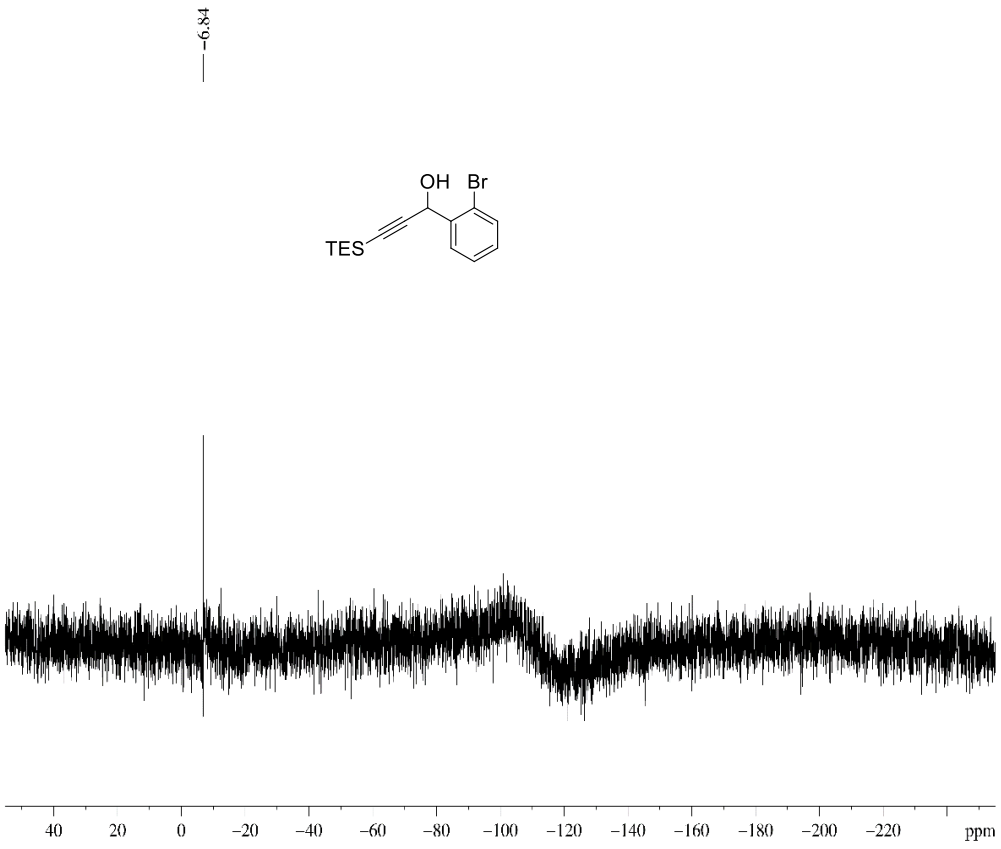

^{1}H (400 MHz, $CDCl_3$) and ^{13}C (100 MHz, $CDCl_3$)-NMR spectra of alcohol **64h**

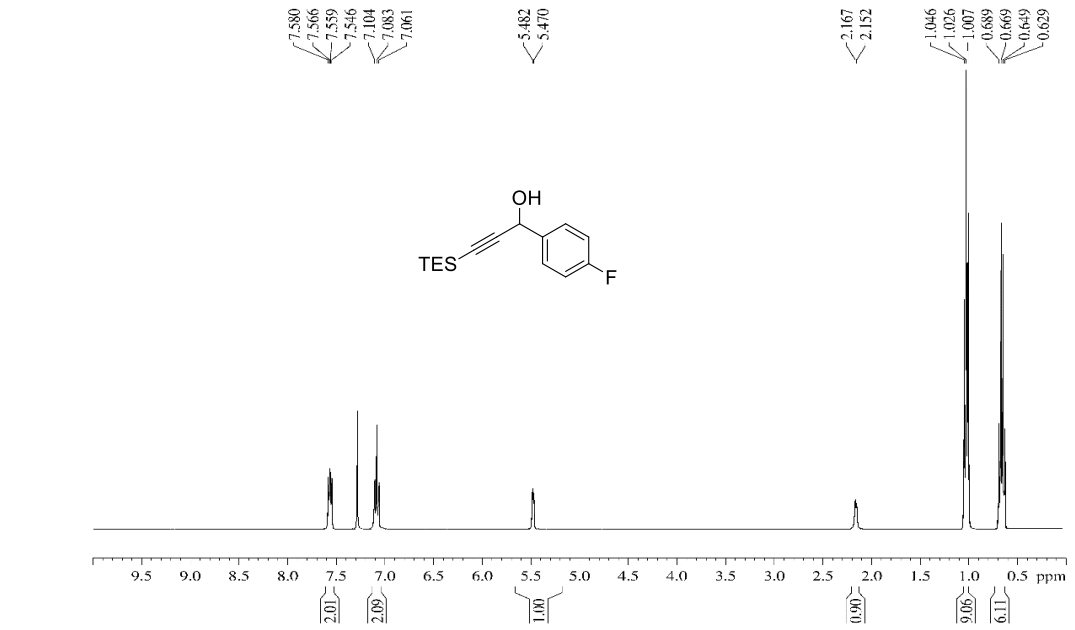

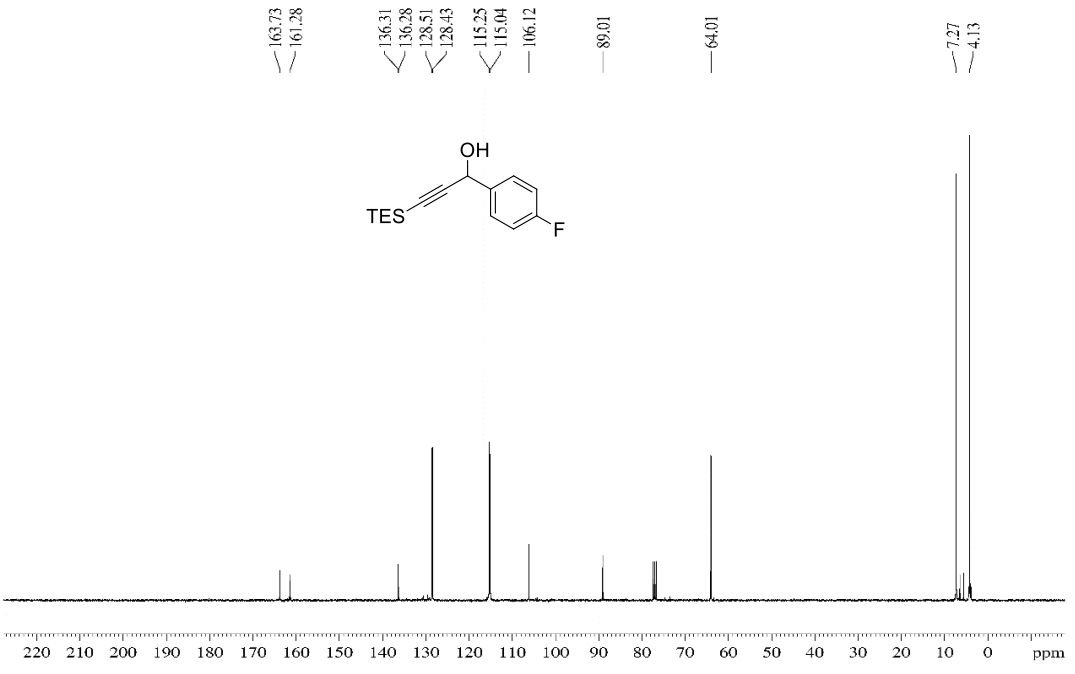

^{29}Si (80 MHz, $CDCl_3$)-NMR spectra of alcohol **64h**

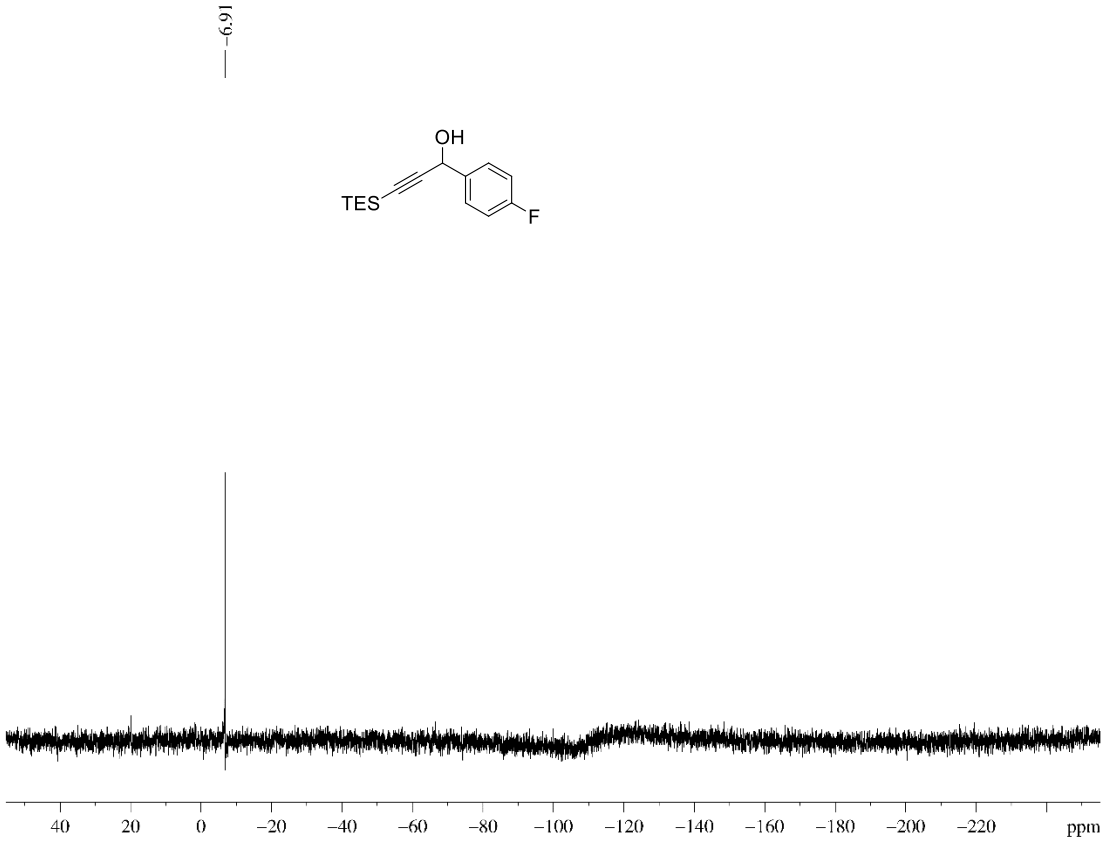

^{19}F (376 MHz, $CDCl_3$)-NMR spectra of alcohol **64h**

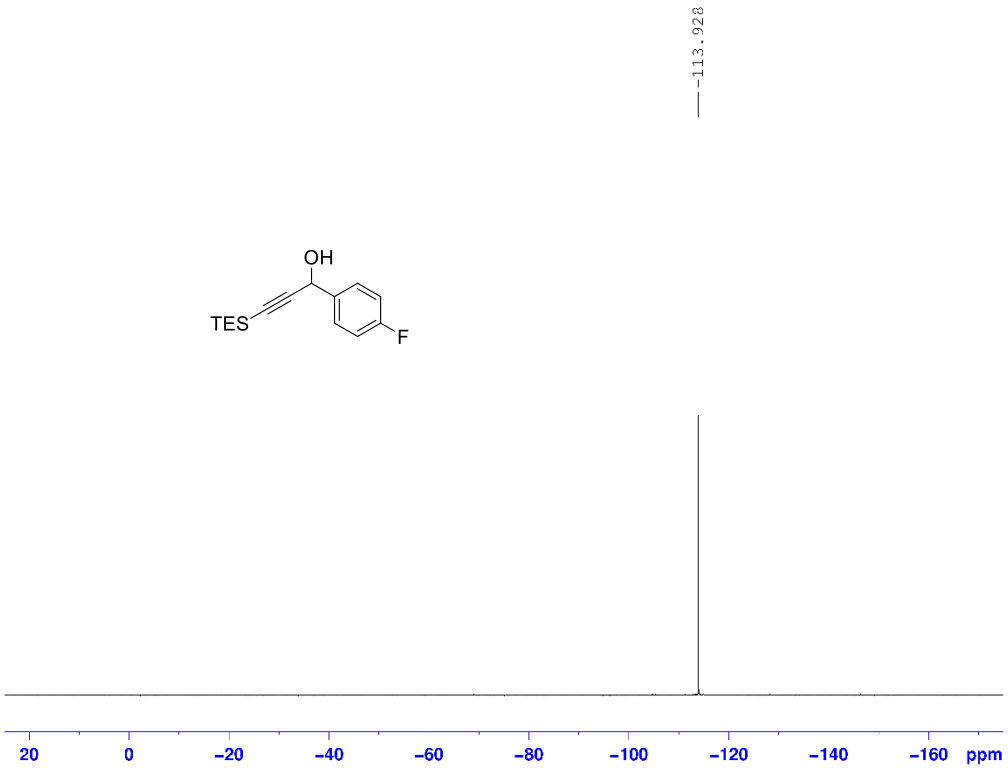

^{1}H (400 MHz, $CDCl_3$) and ^{13}C (100 MHz, $CDCl_3$)-NMR spectra of alcohol **64i**

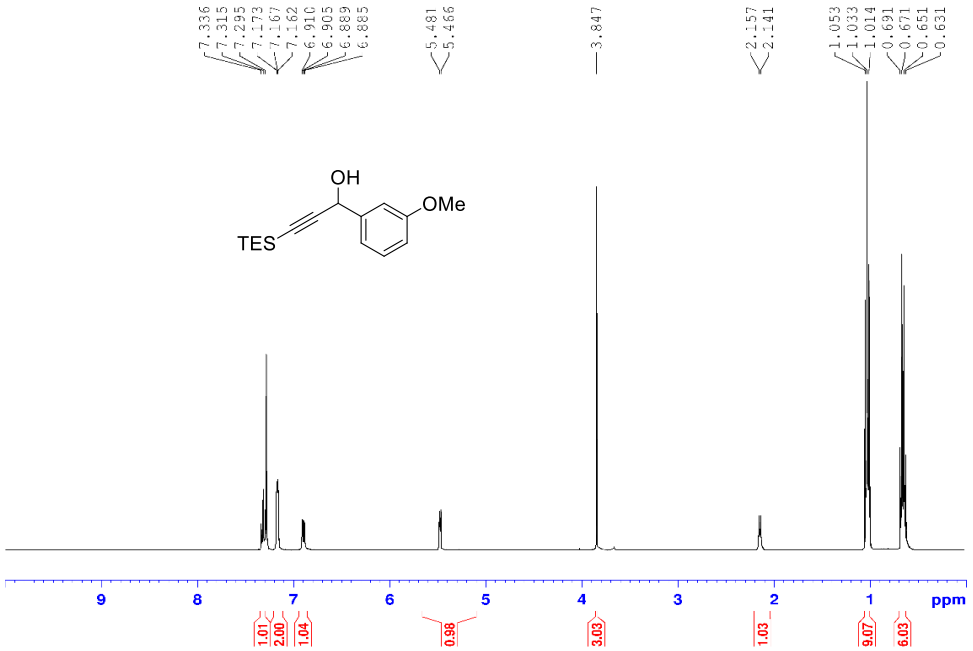

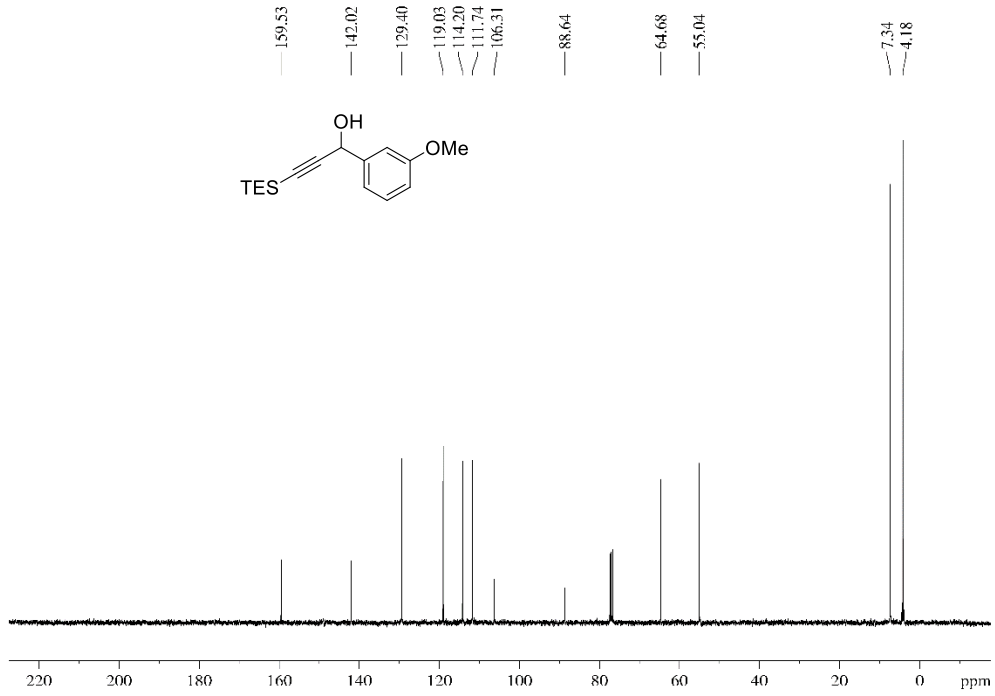

^{29}Si (80 MHz, $CDCl_3$)-NMR spectra of alcohol **64i**

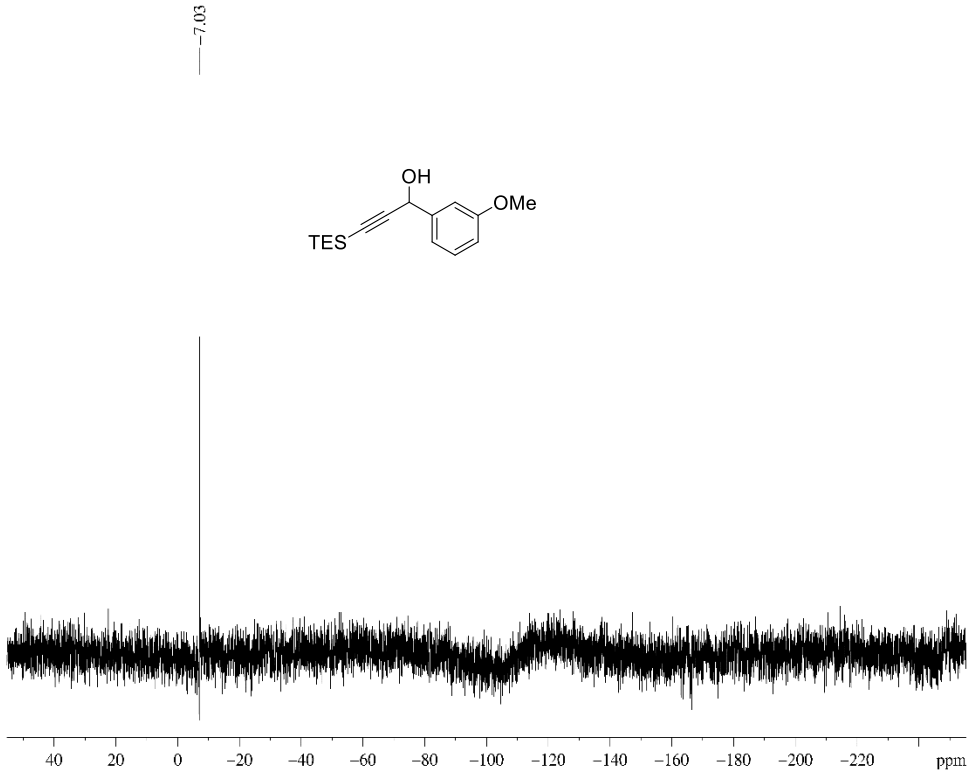

^{1}H (400 MHz, $CDCl_3$) and ^{13}C (100 MHz, $CDCl_3$)-NMR spectra of alcohol **64j**

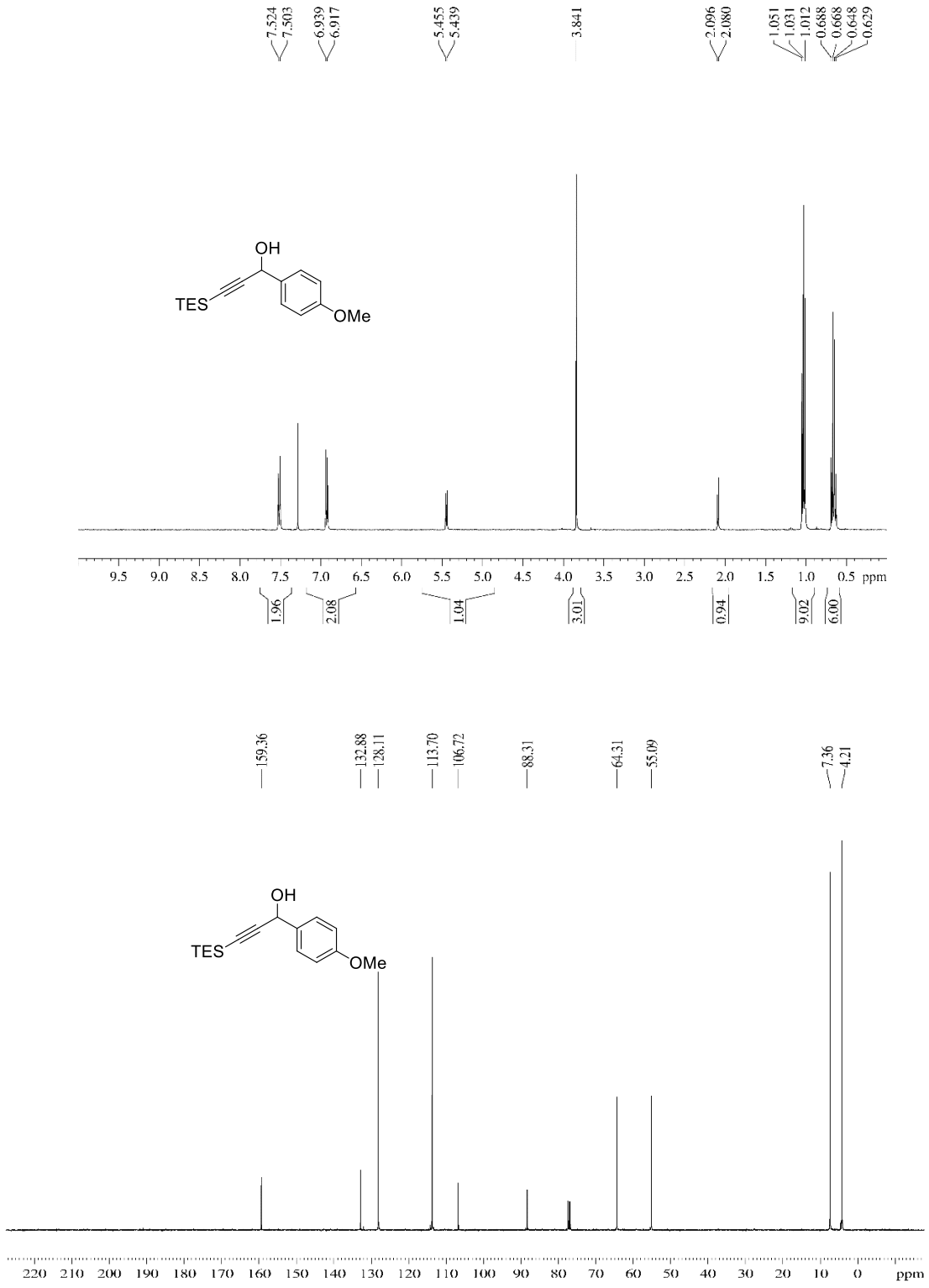

^{29}Si (80 MHz, $CDCl_3$)-NMR spectra of alcohol **64j**

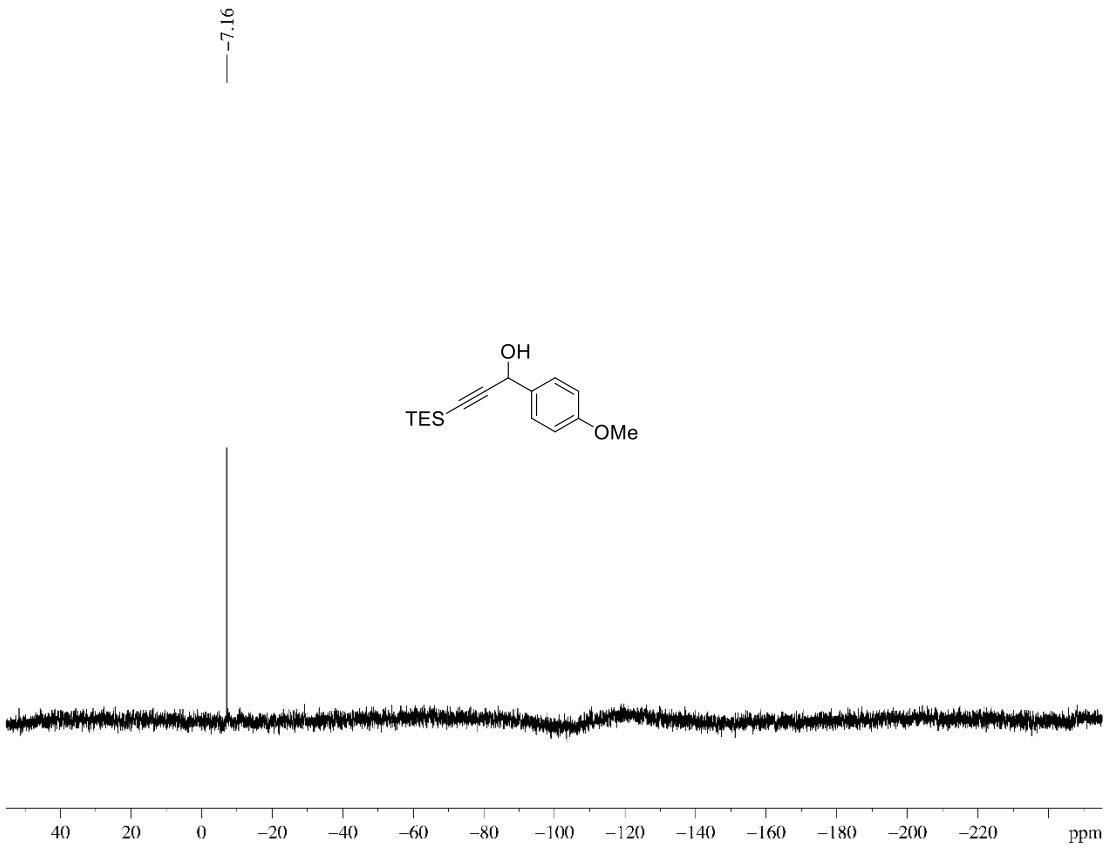

^{1}H (400 MHz, $CDCl_3$) and ^{13}C (100 MHz, $CDCl_3$)-NMR spectra of alcohol **64k**

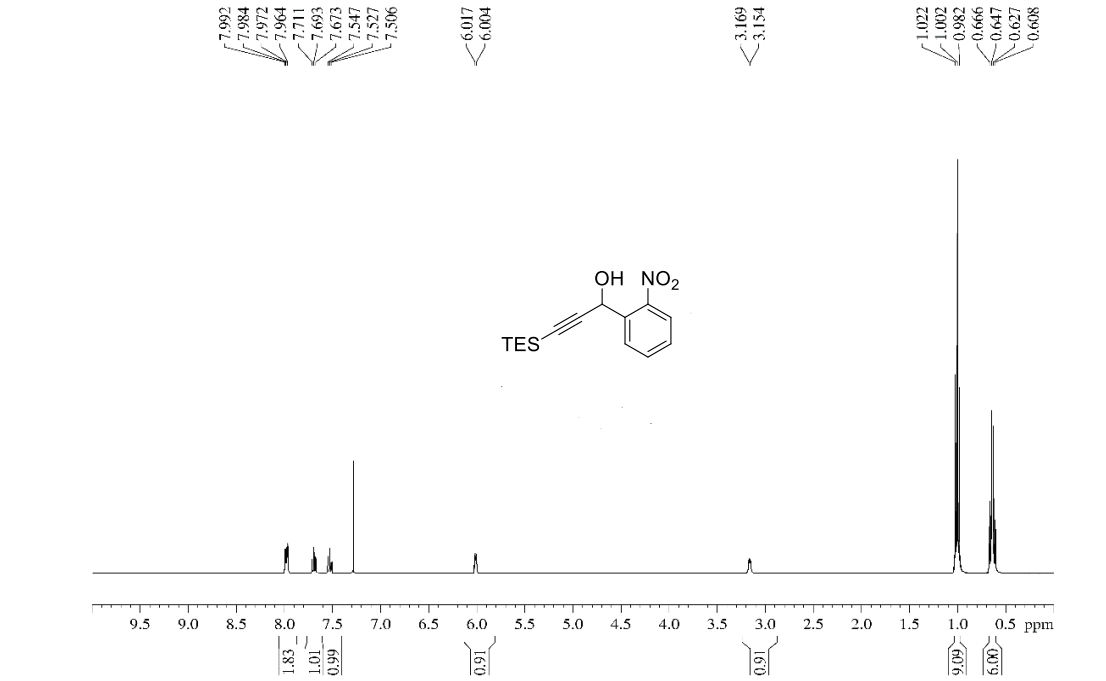

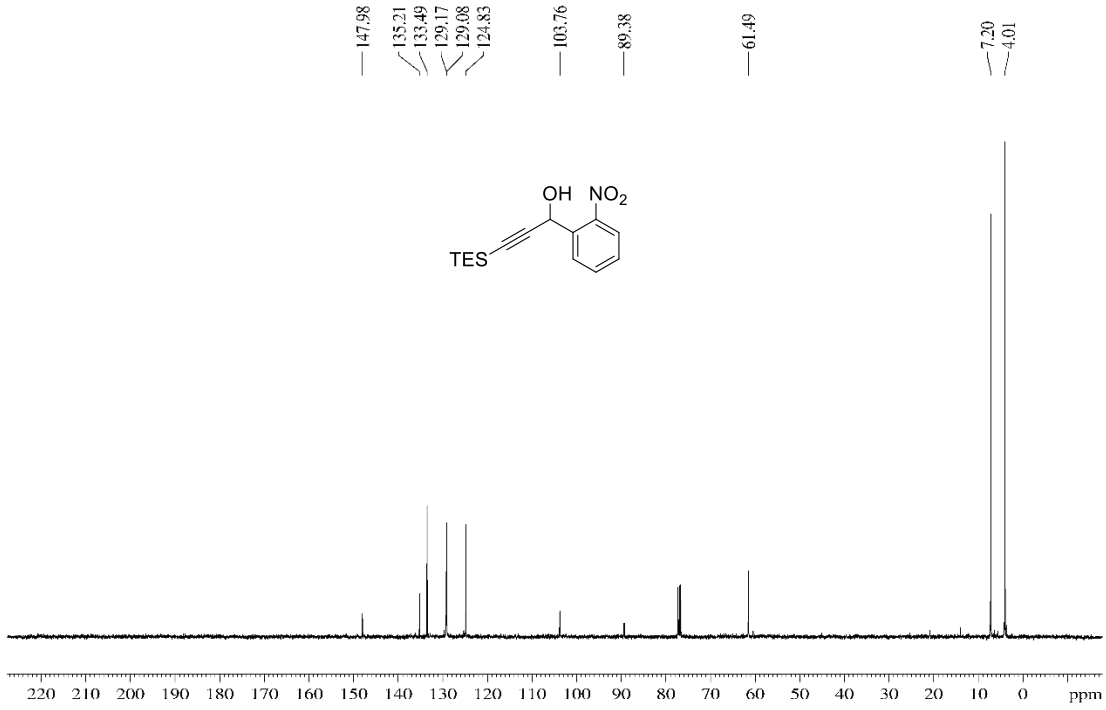

^{29}Si (80 MHz, $CDCl_3$)-NMR spectra of alcohol **64k**

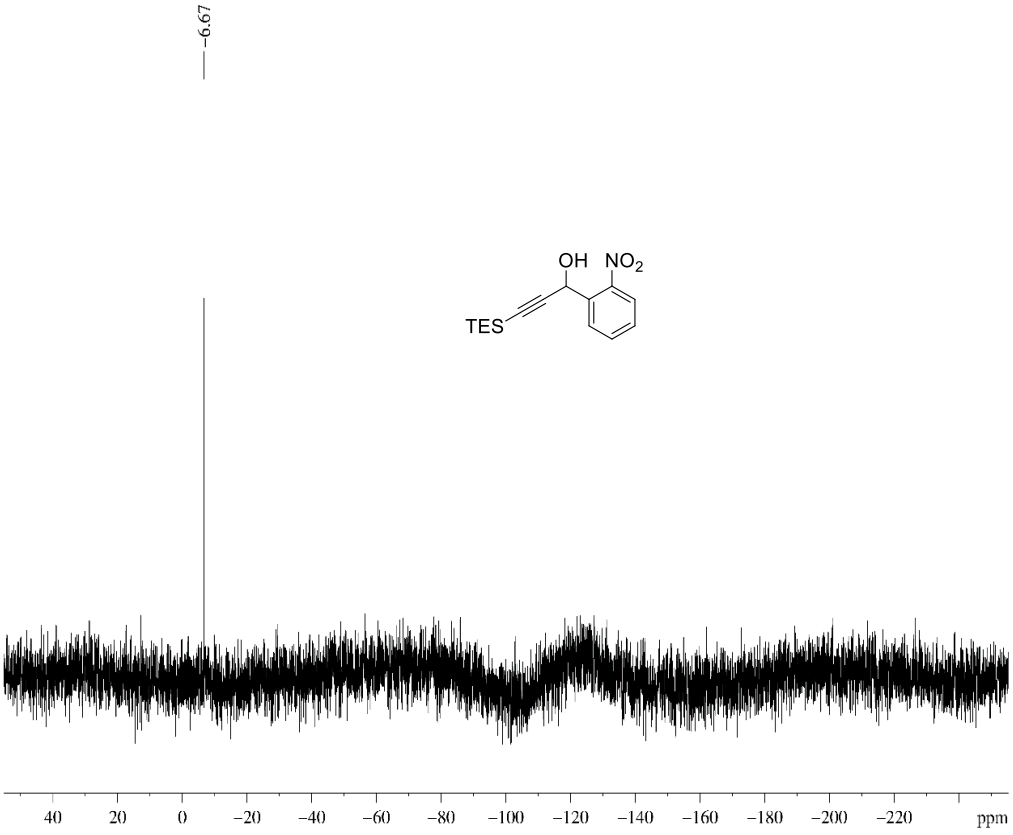

^{1}H (400 MHz, $CDCl_3$) and ^{13}C (100 MHz, $CDCl_3$)-NMR spectra of alcohol **64l**

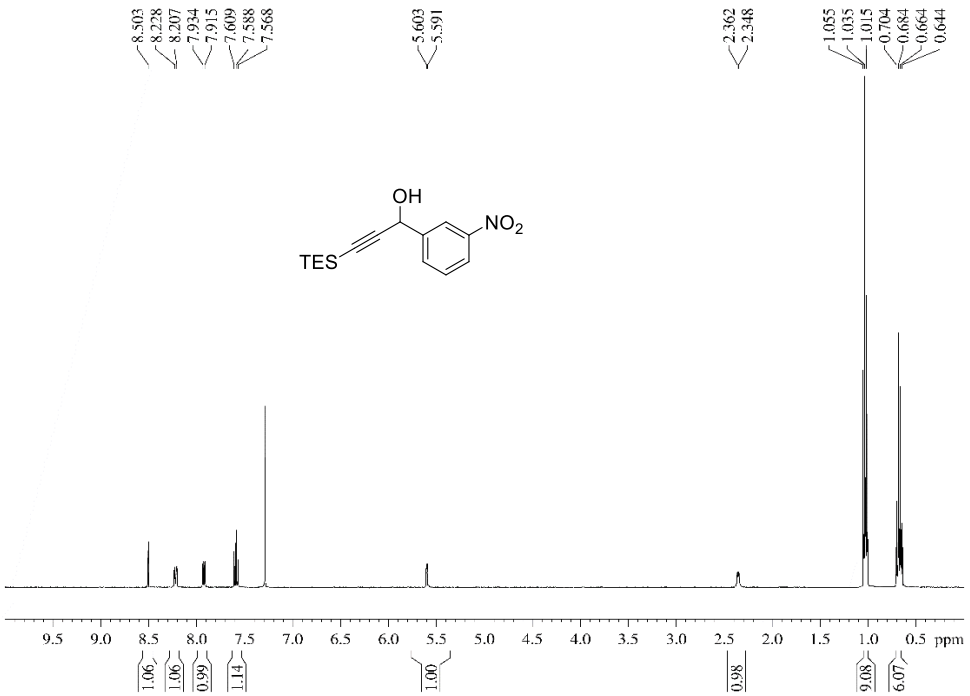

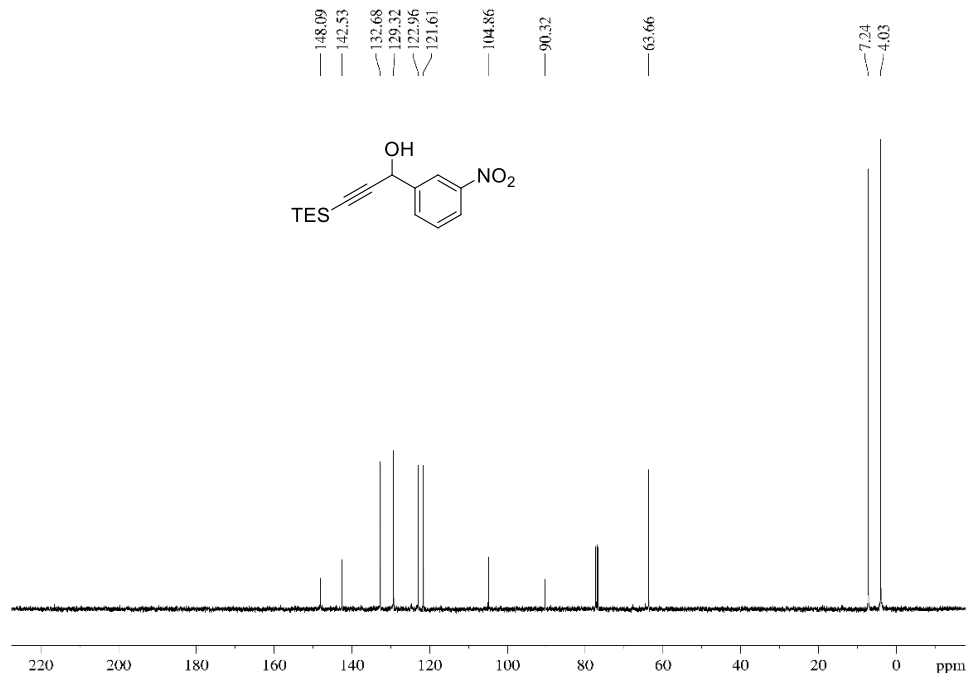

^{29}Si (80 MHz, $CDCl_3$)-NMR spectra of alcohol **64l**

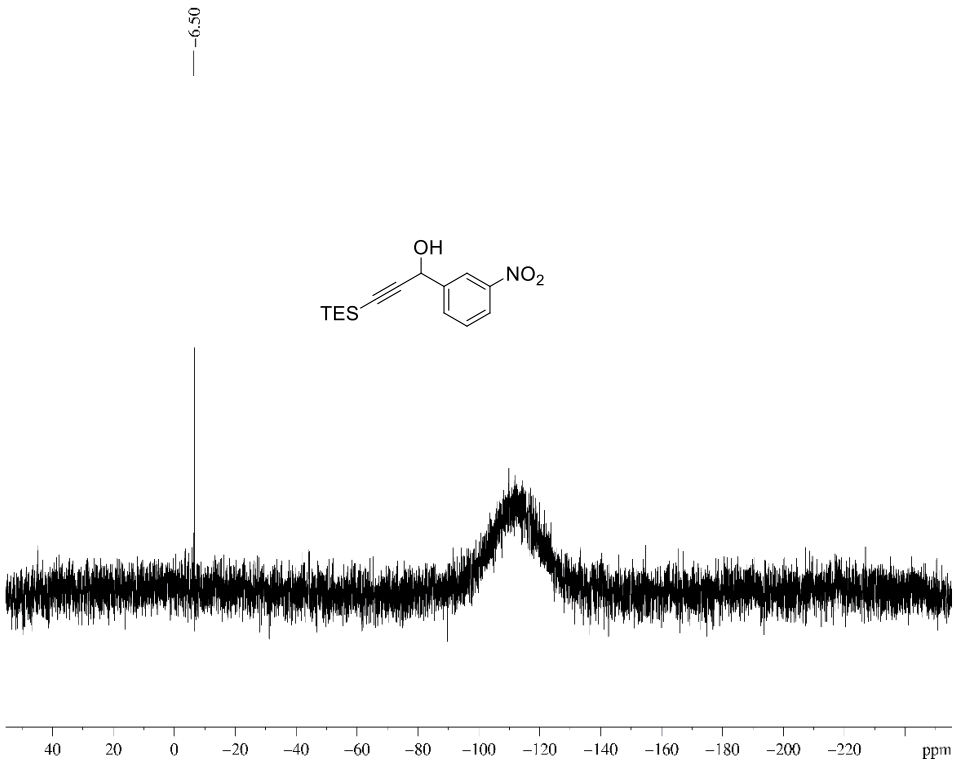

^{1}H (400 MHz, $CDCl_3$) and ^{13}C (100 MHz, $CDCl_3$)-NMR spectra of alcohol **64m**

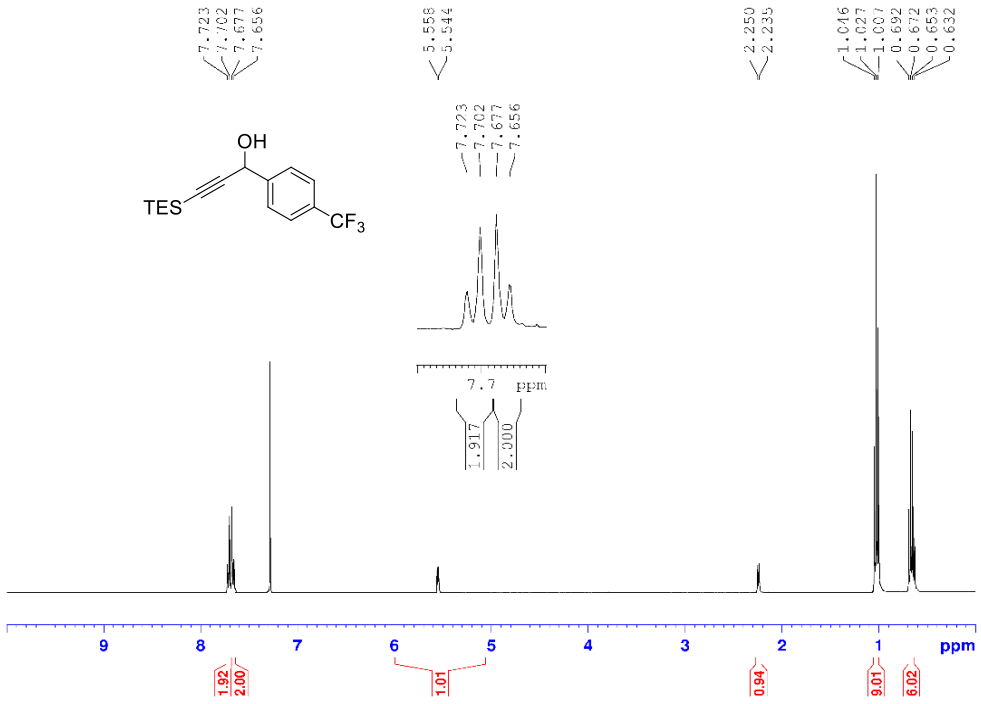

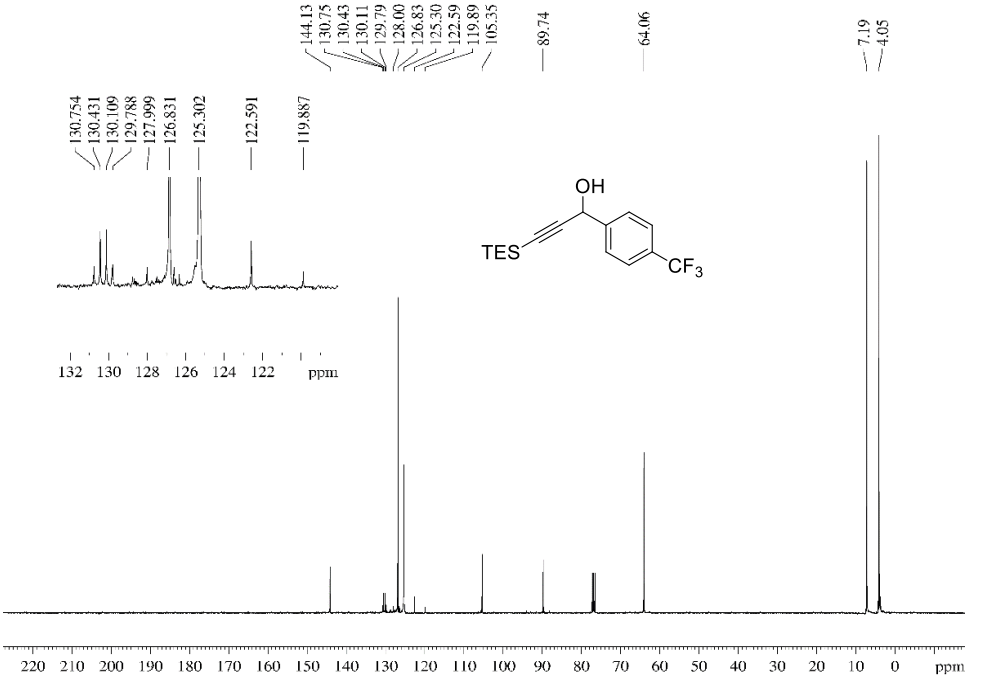

^{29}Si (80 MHz, $CDCl_3$)-NMR spectra of alcohol **64m**

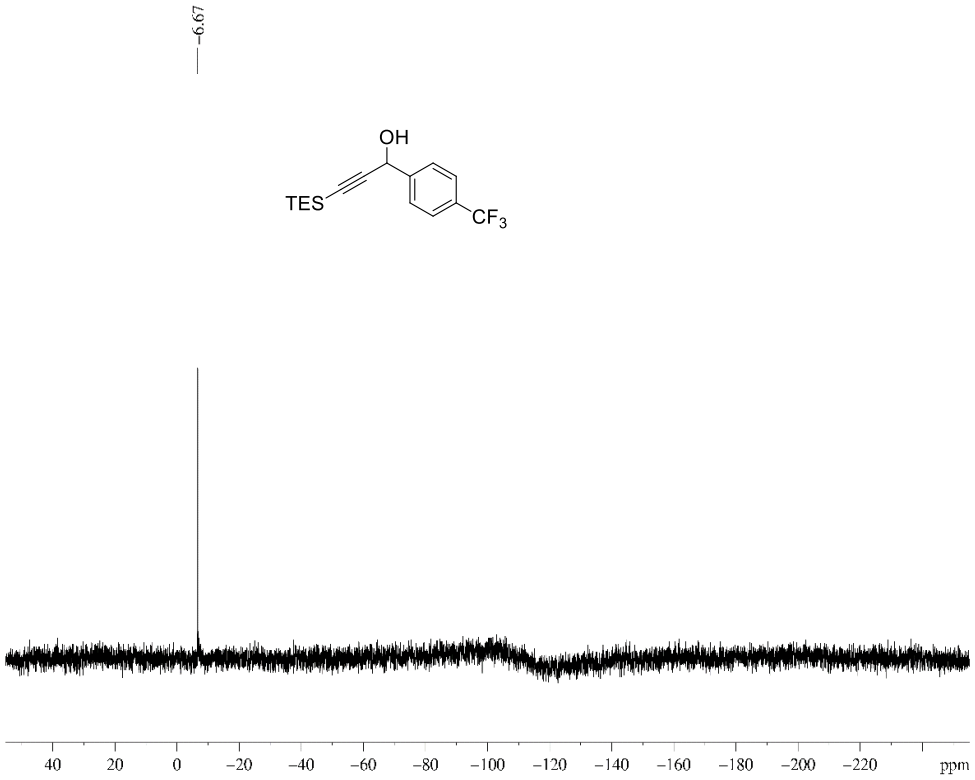

^{19}F (376 MHz, $CDCl_3$)-NMR spectra of alcohol **64m**

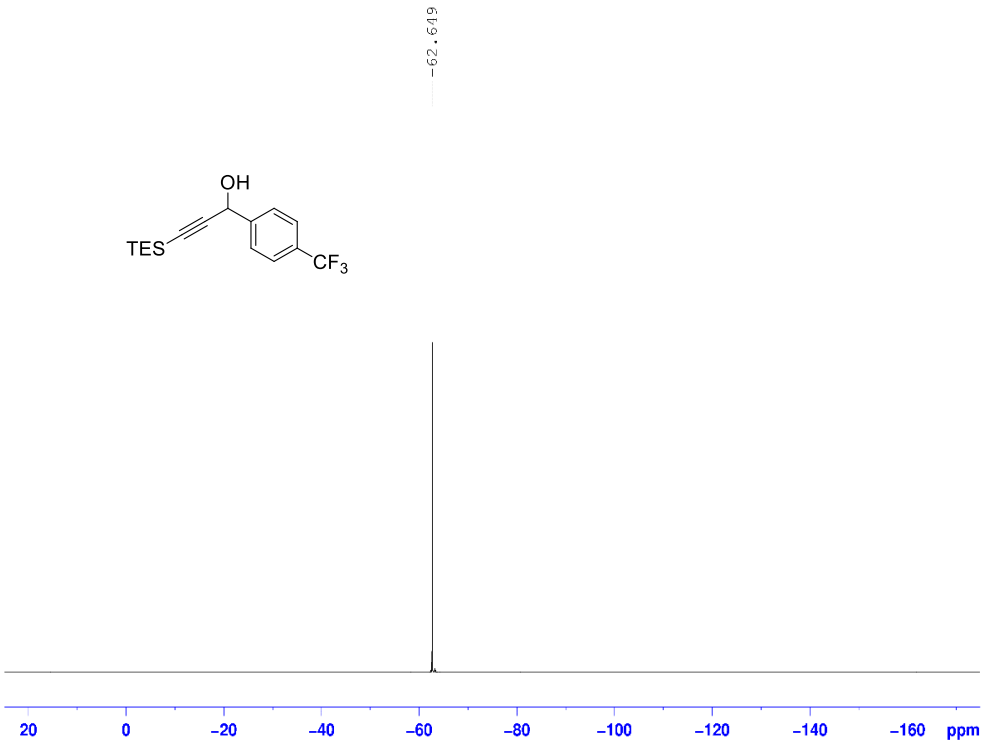

^{1}H (400 MHz, $CDCl_3$) and ^{13}C (100 MHz, $CDCl_3$)-NMR spectra of alcohol **64n**

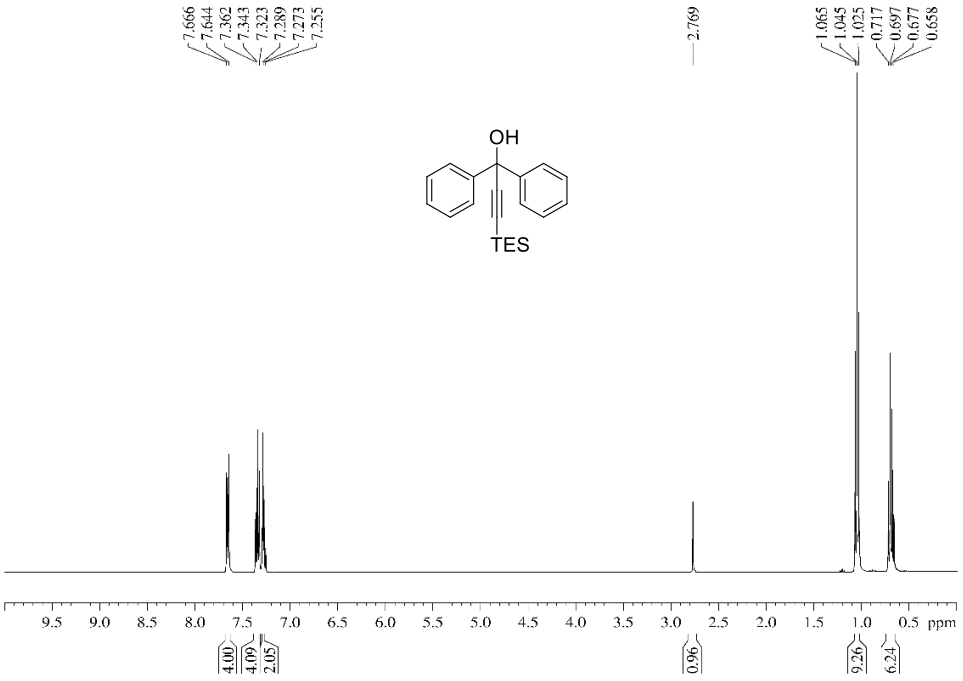

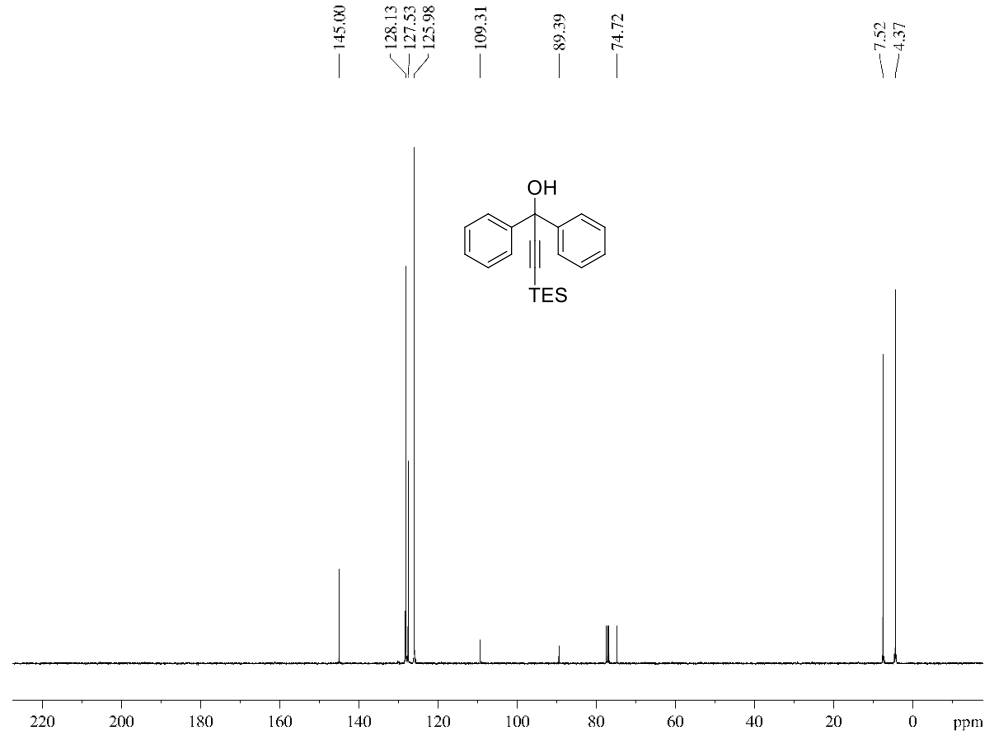

^{29}Si (80 MHz, $CDCl_3$)-NMR spectra of alcohol **64n**

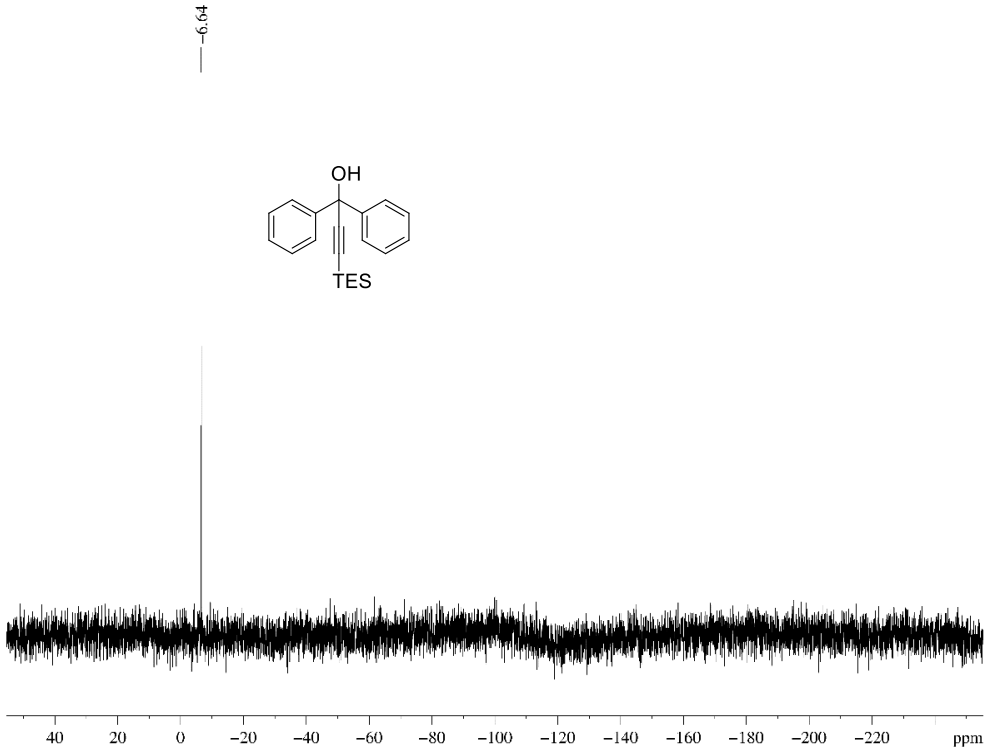

^{1}H (400 MHz, $CDCl_3$) and ^{13}C (100 MHz, $CDCl_3$)-NMR spectra of alcohol **64o**

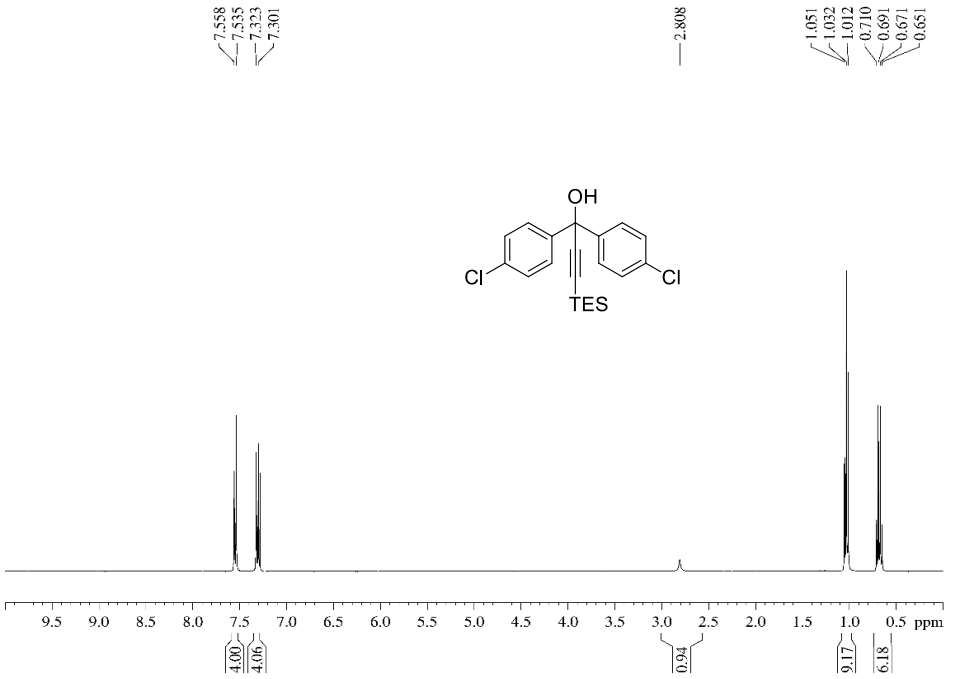

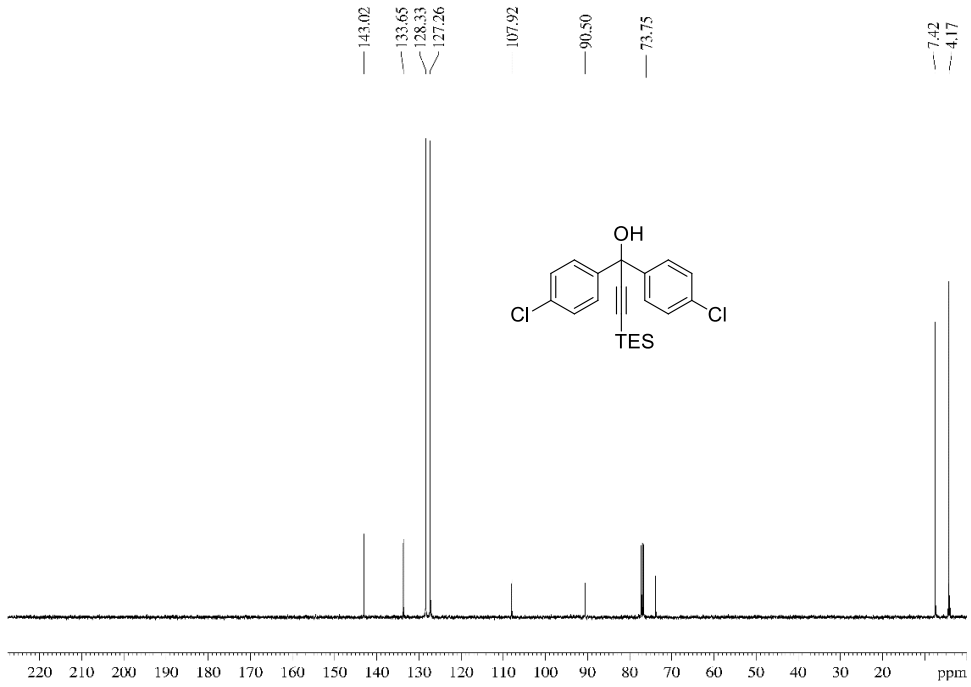

^{29}Si (80 MHz, $CDCl_3$)-NMR spectra of alcohol **64o**

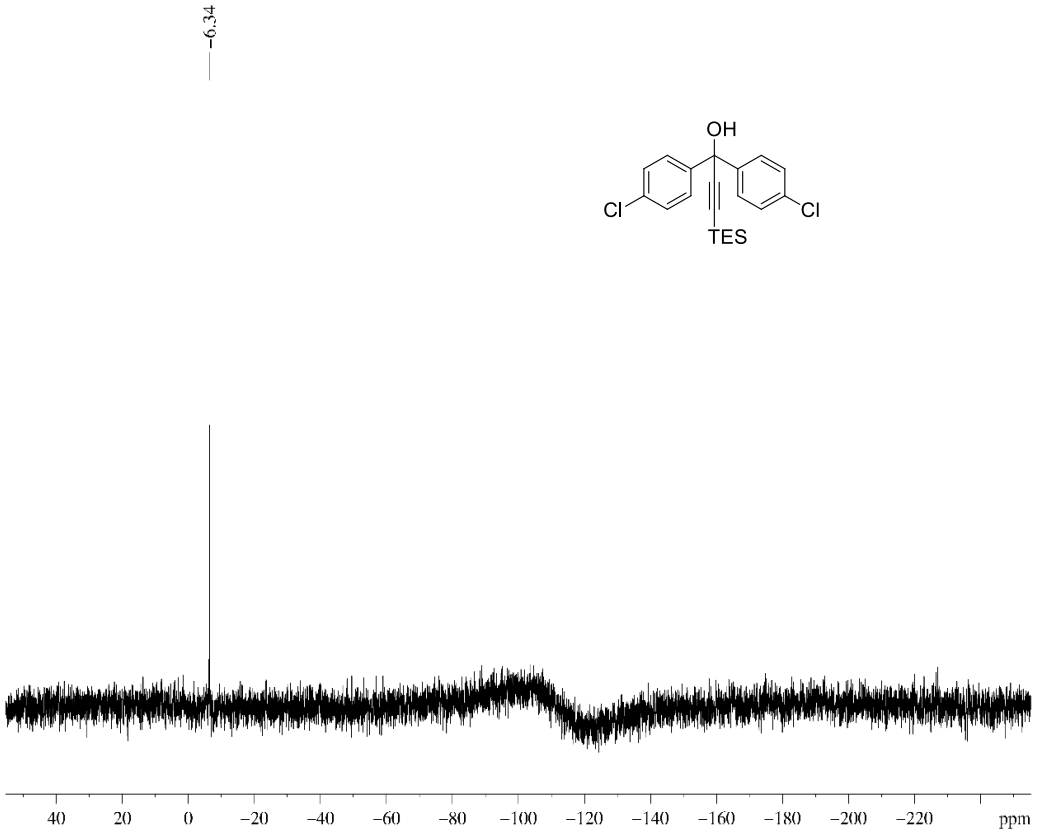

^{1}H (400 MHz, $CDCl_3$) and ^{13}C (100 MHz, $CDCl_3$)-NMR spectra of alcohol **64p**

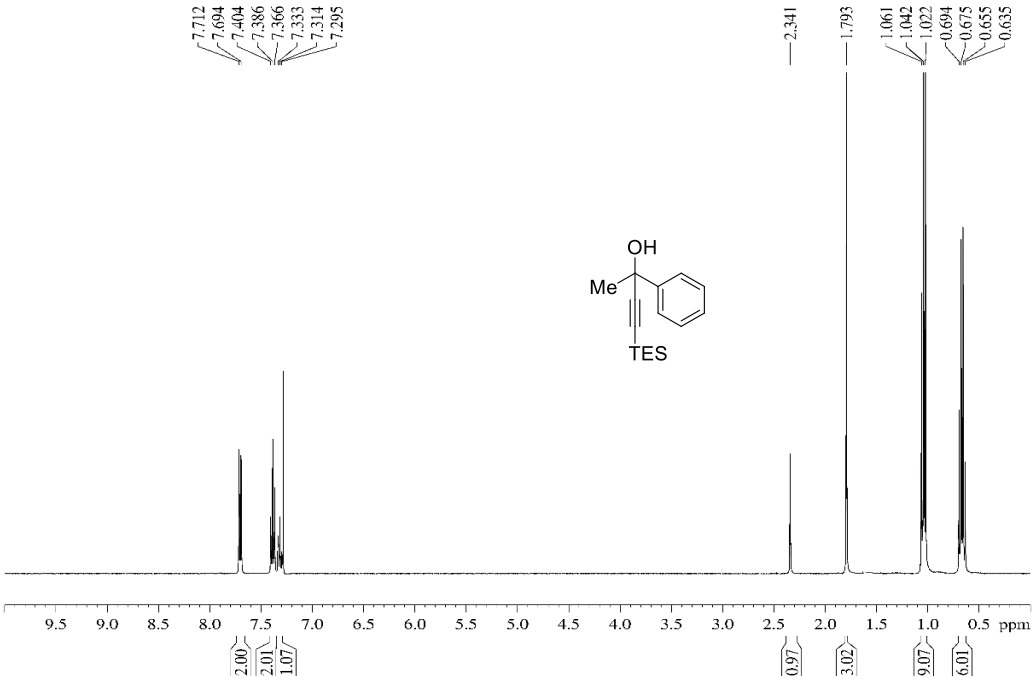

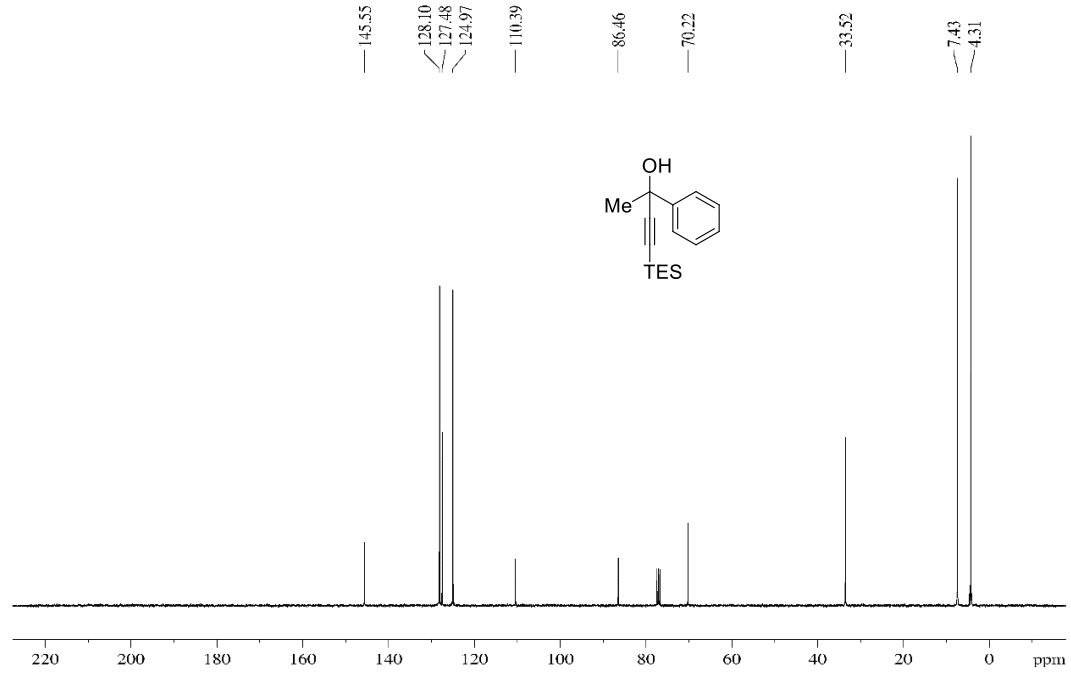

^{29}Si (80 MHz, $CDCl_3$)-NMR spectra of alcohol **64p**

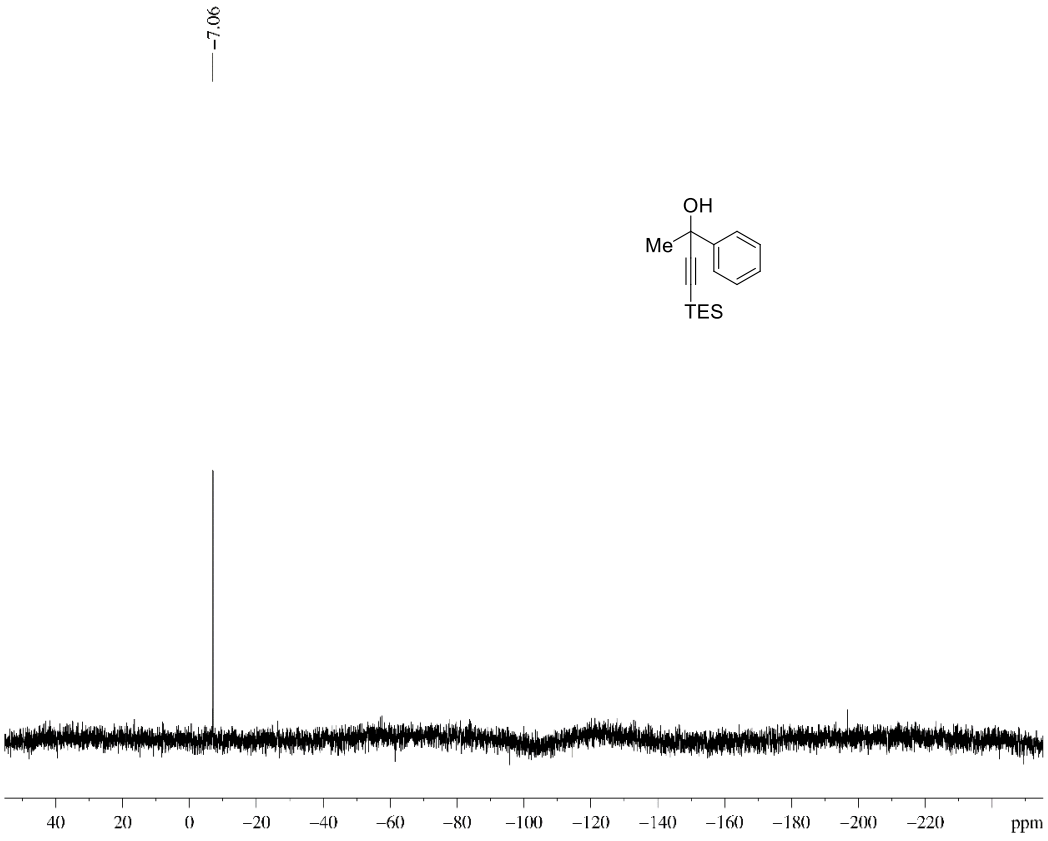

^{1}H (400 MHz, $CDCl_3$) and ^{13}C (100 MHz, $CDCl_3$)-NMR spectra of alcohol **64q**

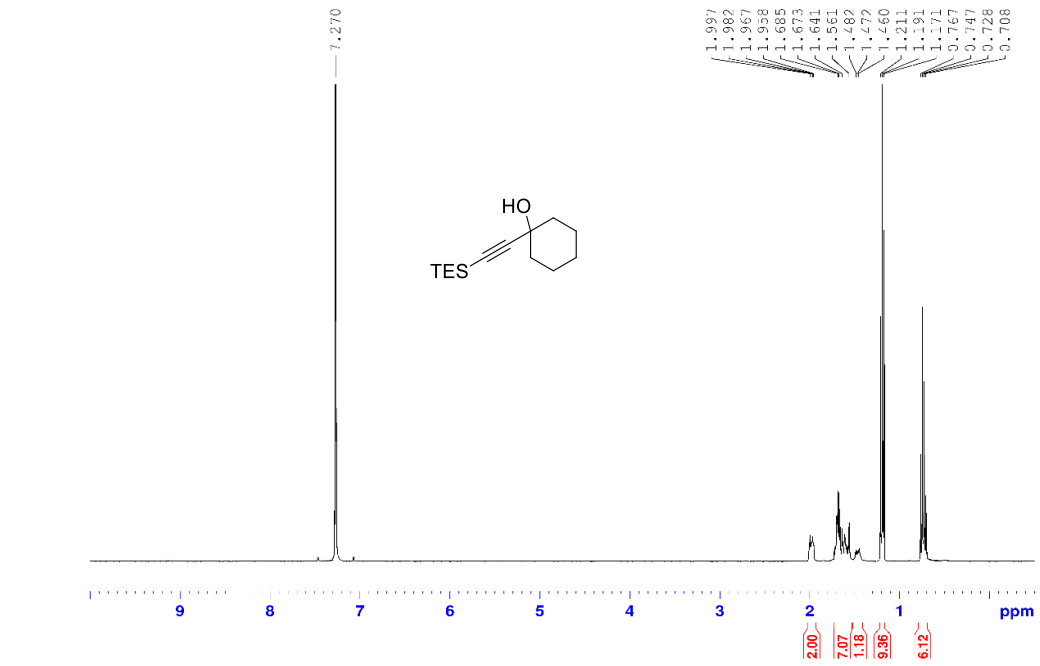

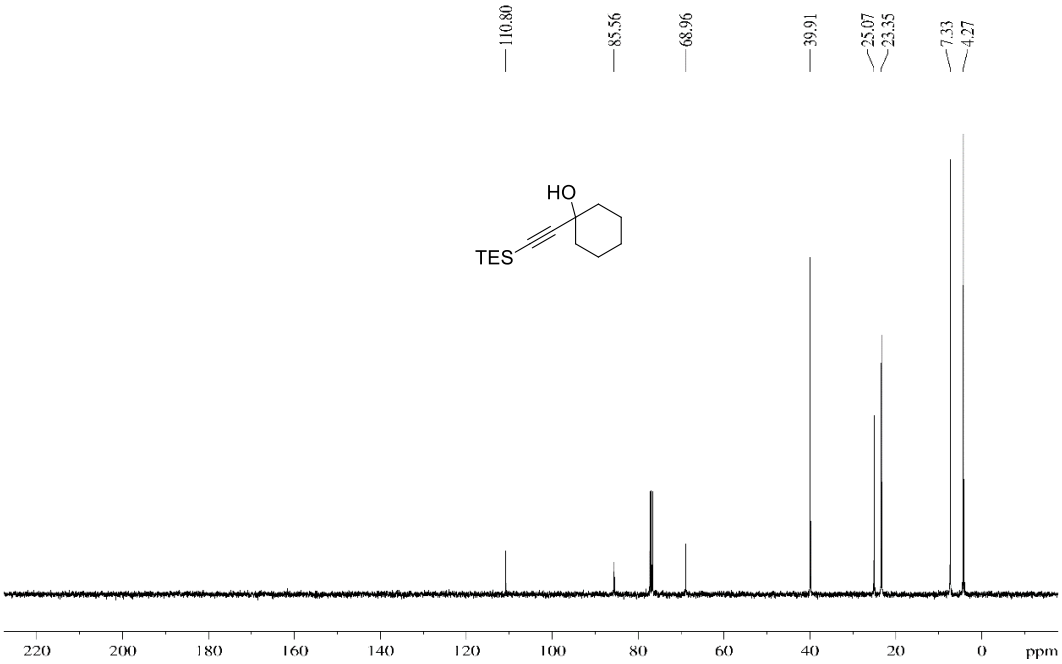

^{29}Si (80 MHz, $CDCl_3$)-NMR spectra of alcohol **64q**

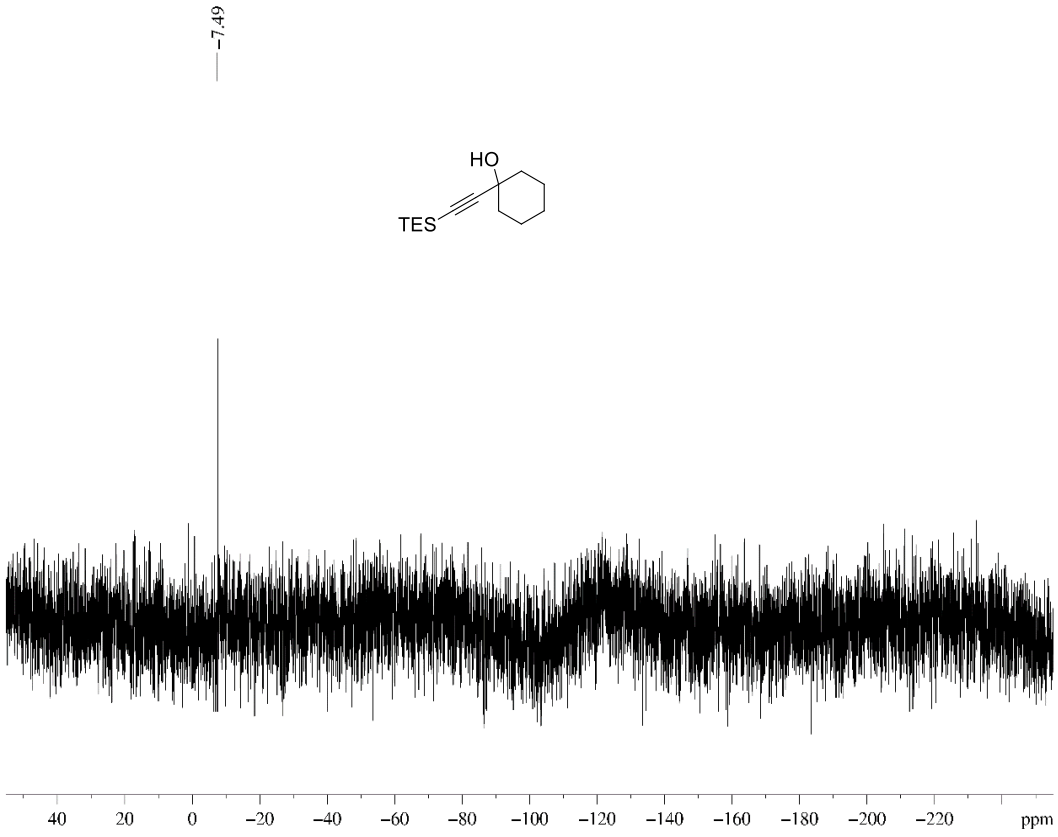

^{1}H (400 MHz, $CDCl_3$) and ^{13}C (100 MHz, $CDCl_3$)-NMR spectra of alcohol **64r**

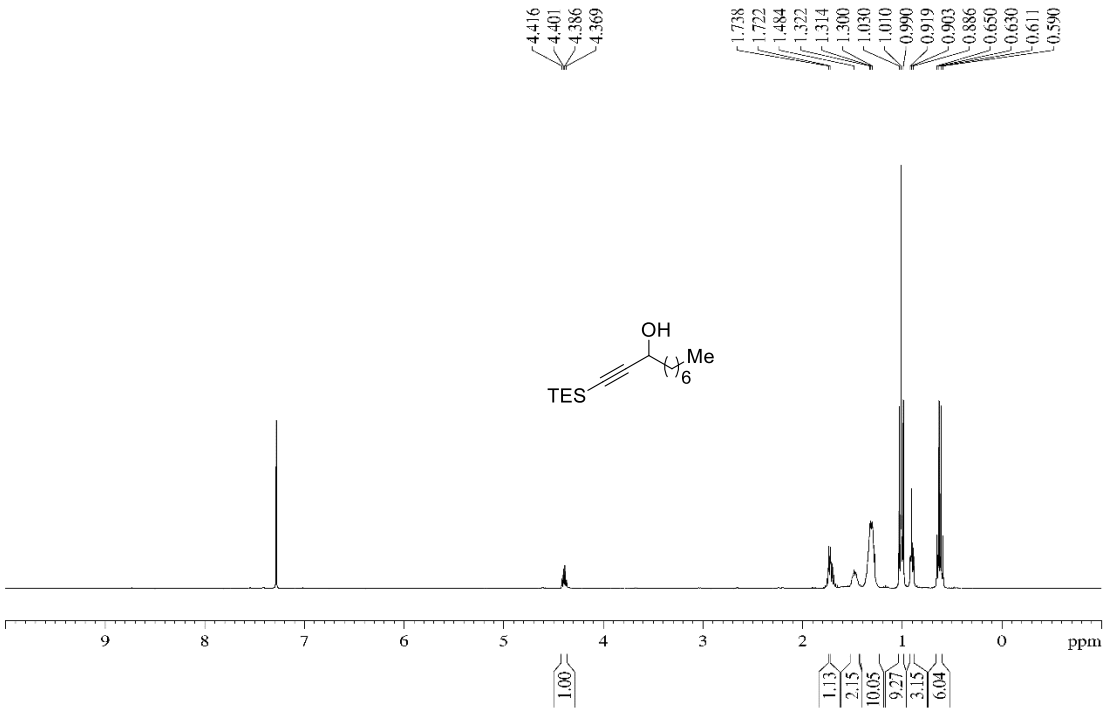

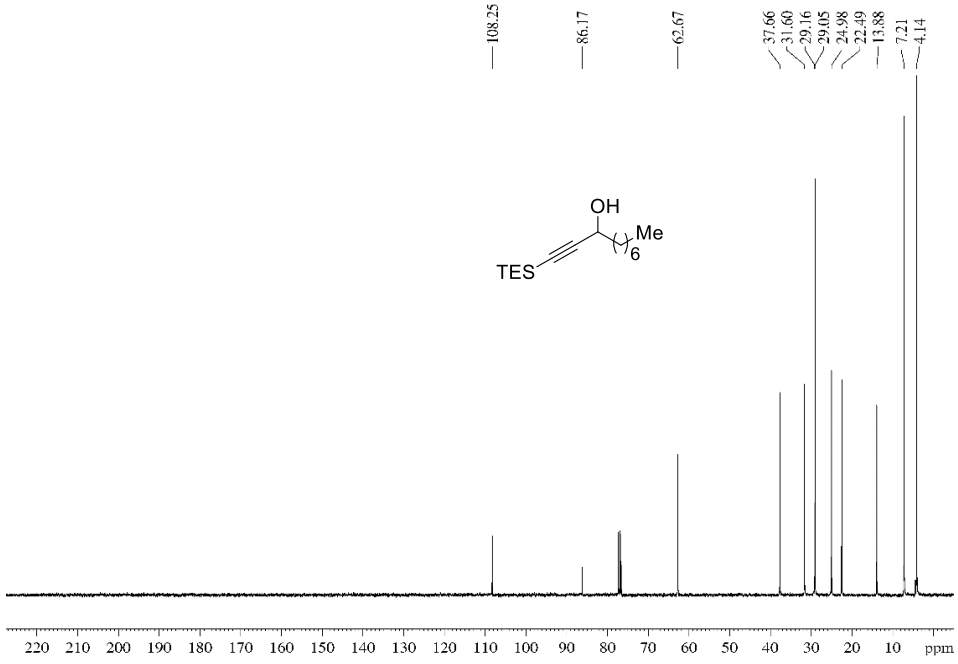

^{29}Si (80 MHz, $CDCl_3$)-NMR spectra of alcohol **64r**

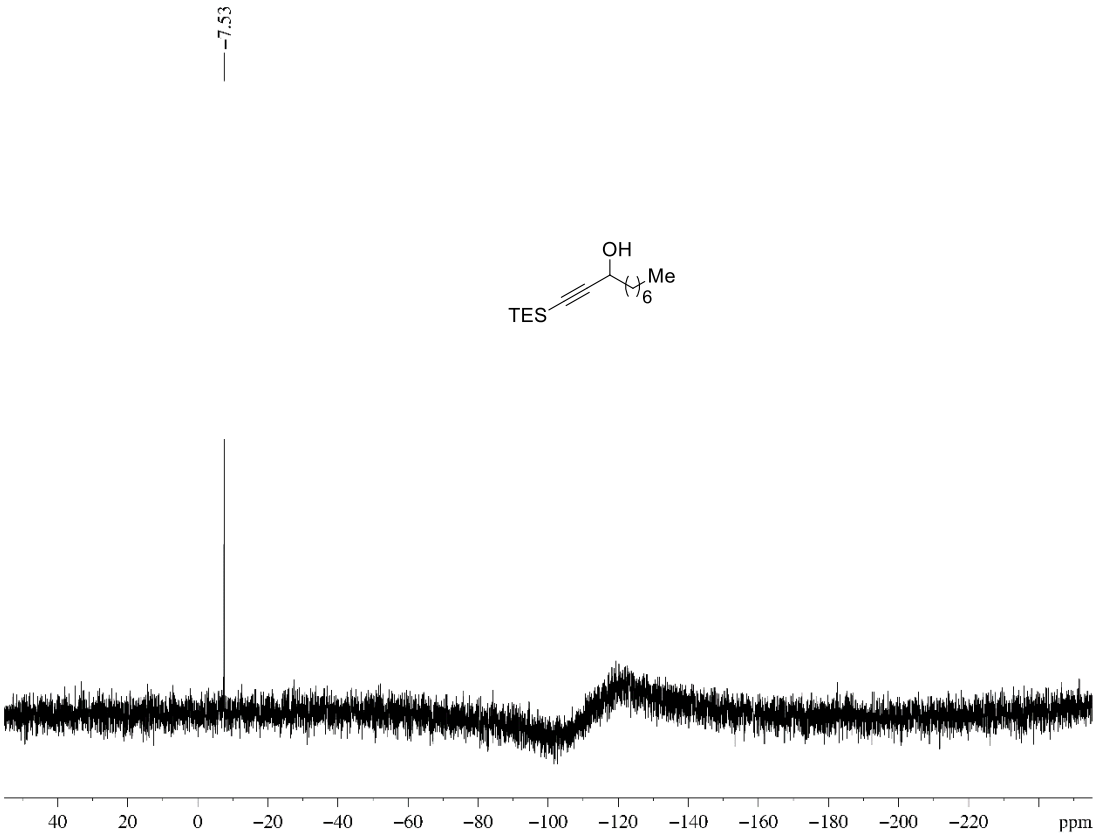

^{1}H (400 MHz, $CDCl_3$) and ^{13}C (100 MHz, $CDCl_3$)-NMR spectra of alcohol **64s**

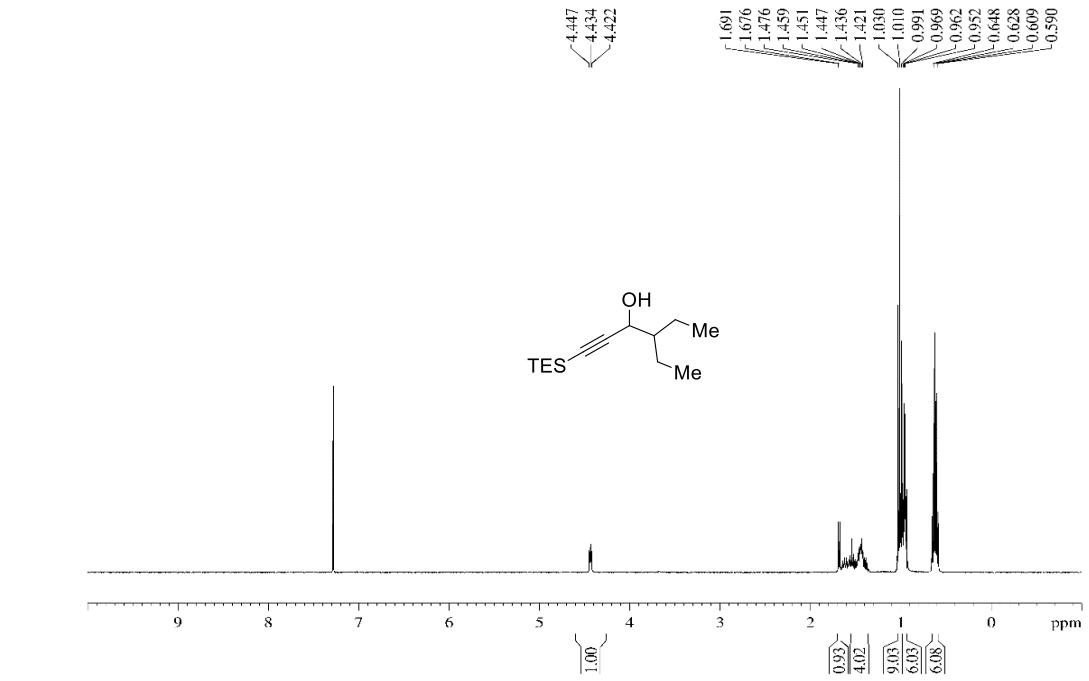

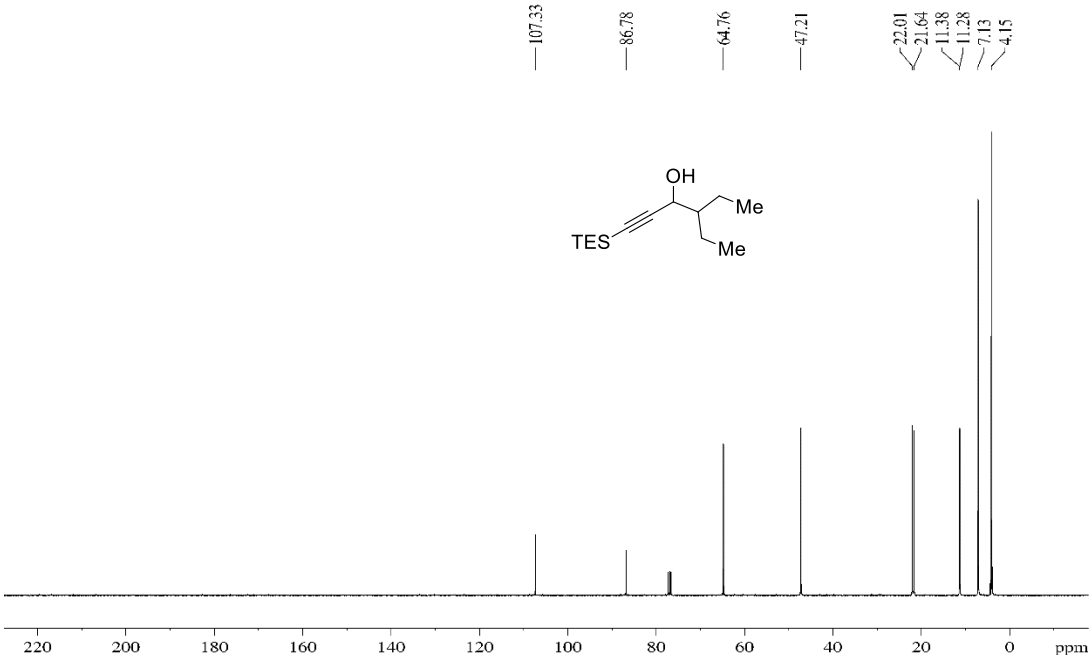

^{29}Si (80 MHz, $CDCl_3$)-NMR spectra of alcohol **64s**

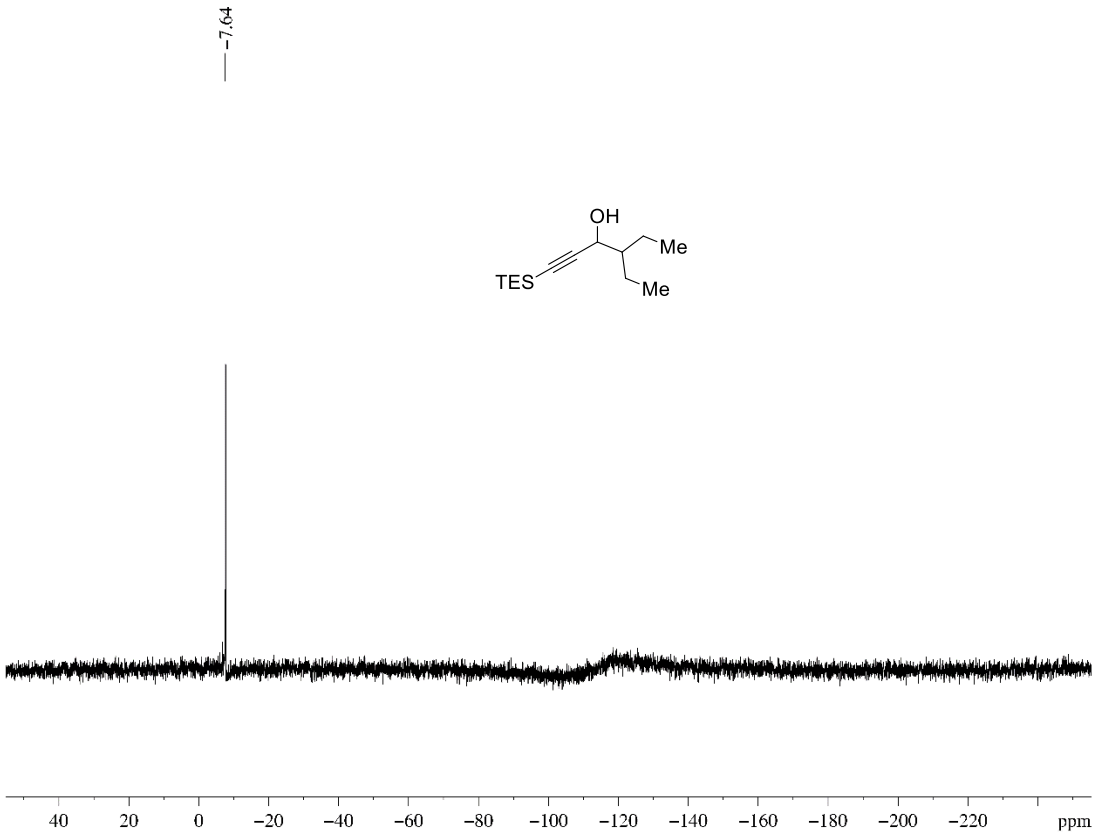

^{1}H (400 MHz, $CDCl_3$) and ^{13}C (100 MHz, $CDCl_3$)-NMR spectra of alcohol **64t**

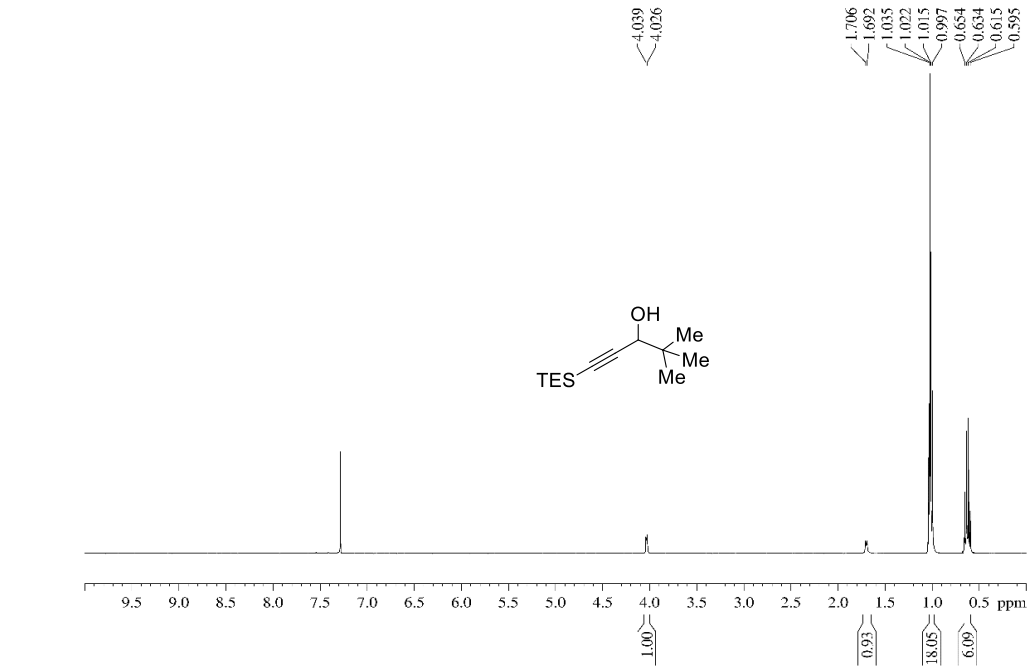

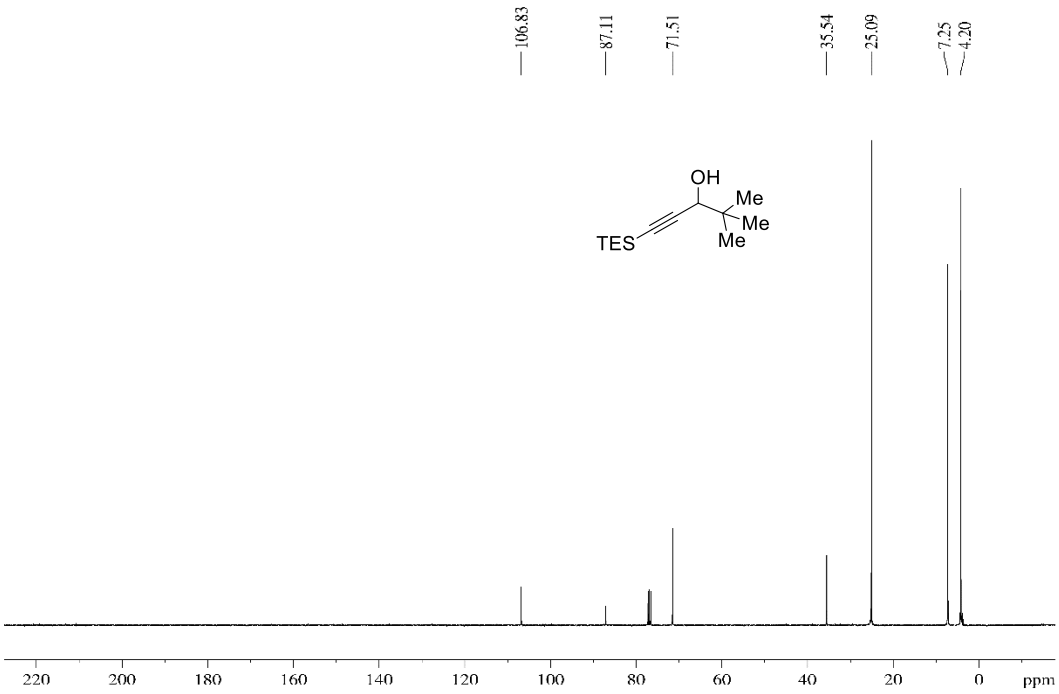

^{29}Si (80 MHz, $CDCl_3$)-NMR spectra of alcohol **64t**

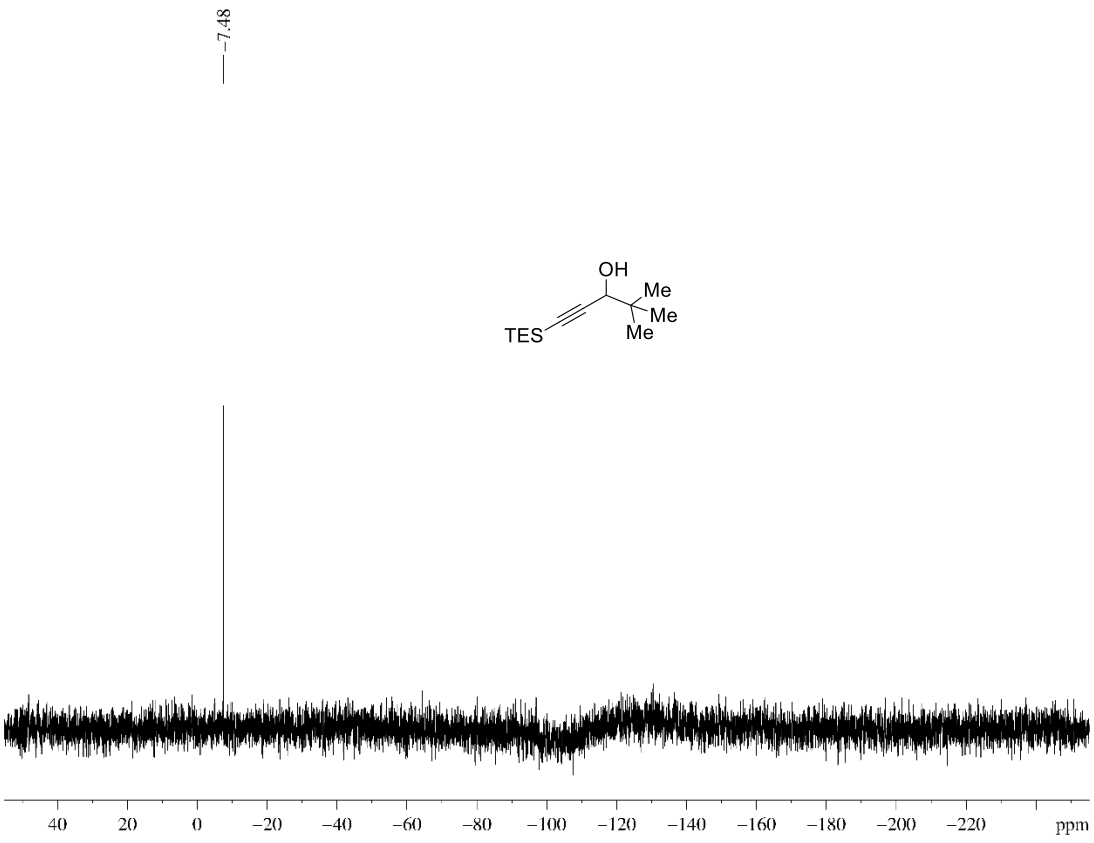

^{1}H (400 MHz, $CDCl_3$) and ^{13}C (100 MHz, $CDCl_3$)-NMR spectra of alcohol **64u**

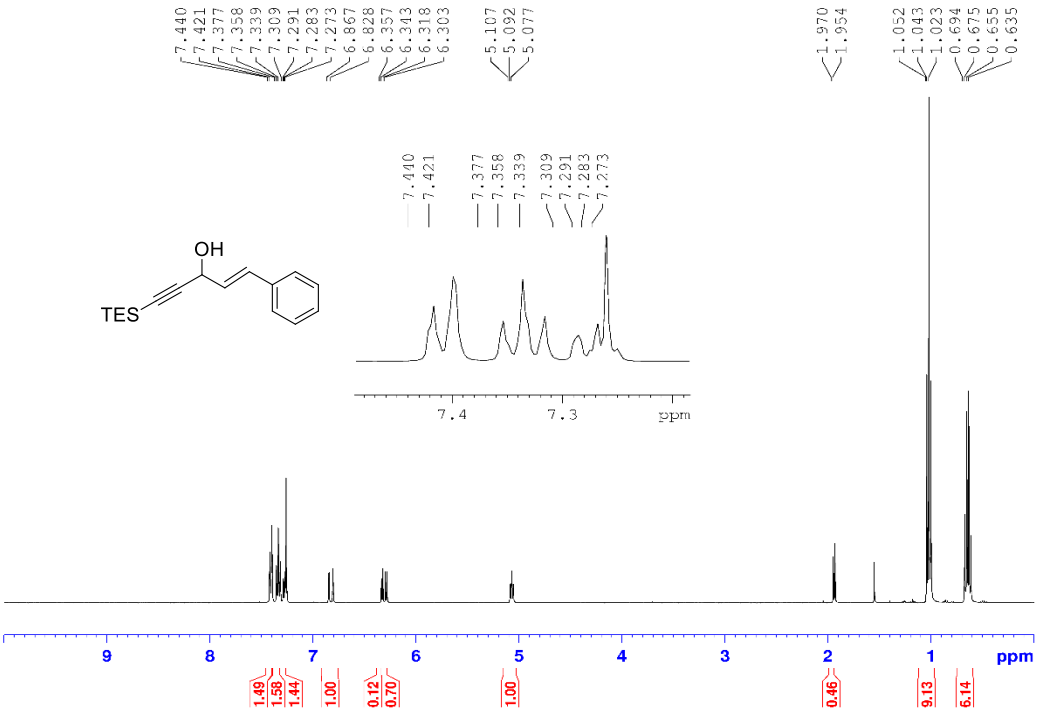

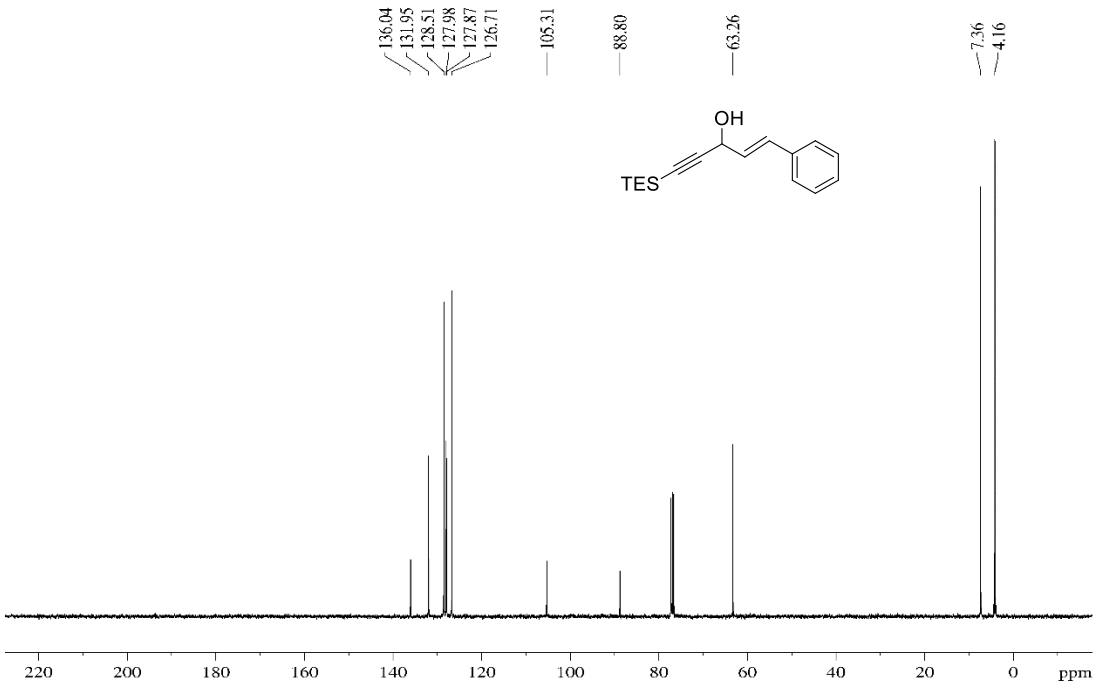

^{29}Si (80 MHz, $CDCl_3$)-NMR spectra of alcohol **64u**

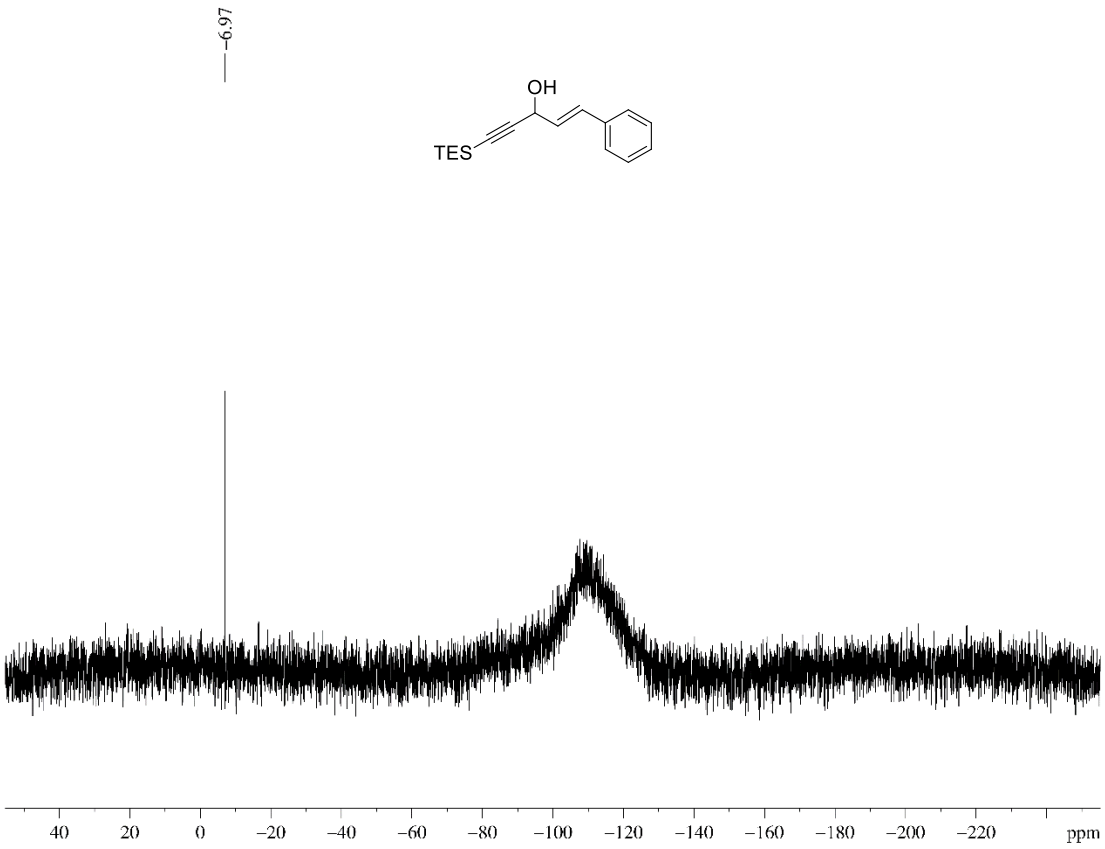

^{1}H (400 MHz, $CDCl_3$) and ^{13}C (100 MHz, $CDCl_3$)-NMR spectra of alcohol **64v**

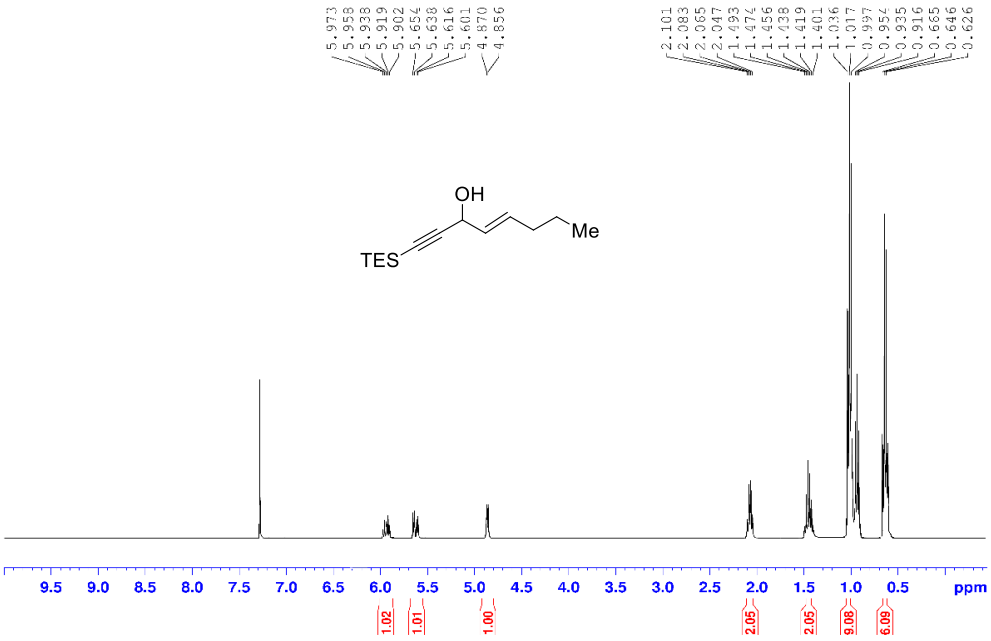

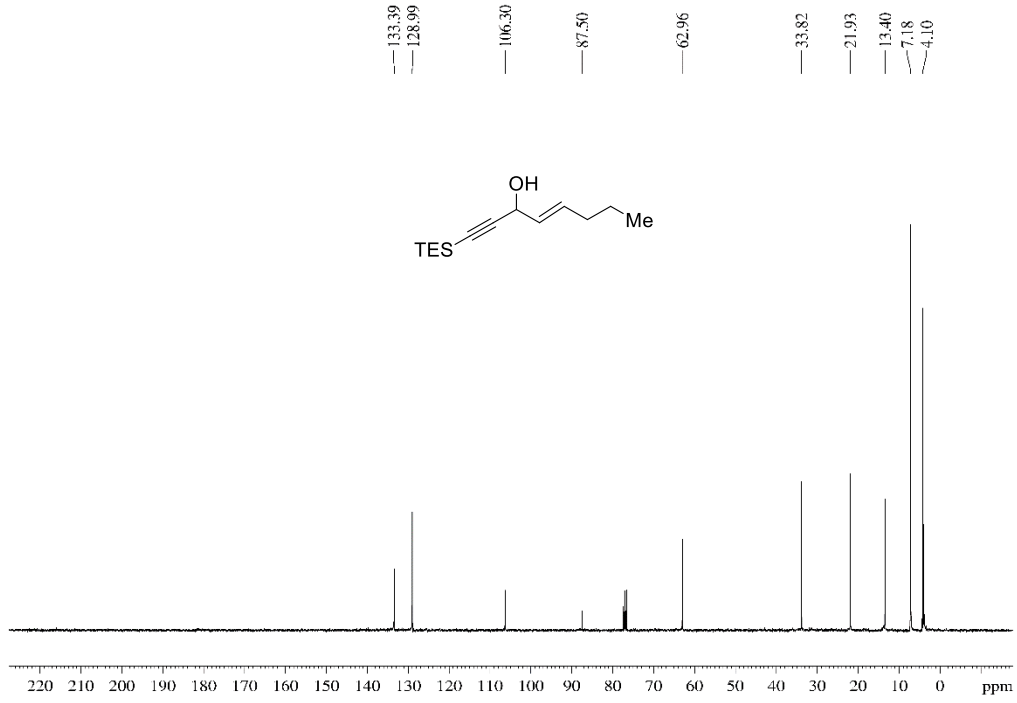

^{29}Si (80 MHz, $CDCl_3$)-NMR spectra of alcohol **64v**

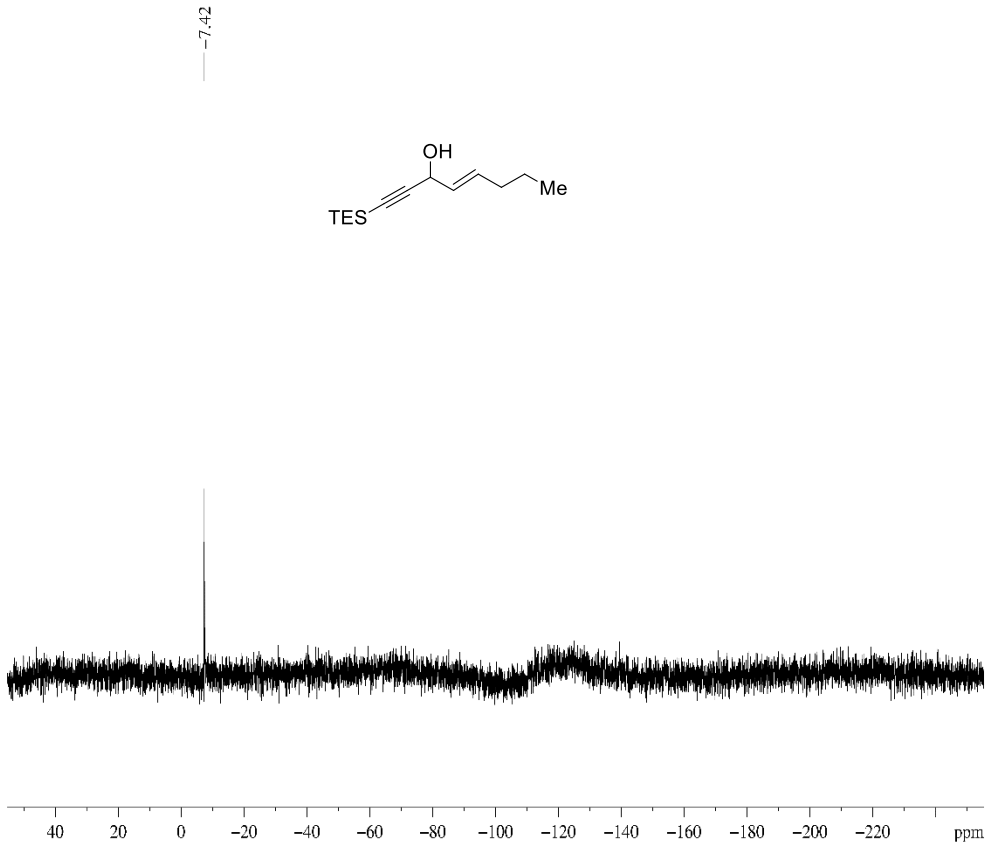

^{1}H (400 MHz, $CDCl_3$) and ^{13}C (100 MHz, $CDCl_3$)-NMR spectra of acylsilane **65a**

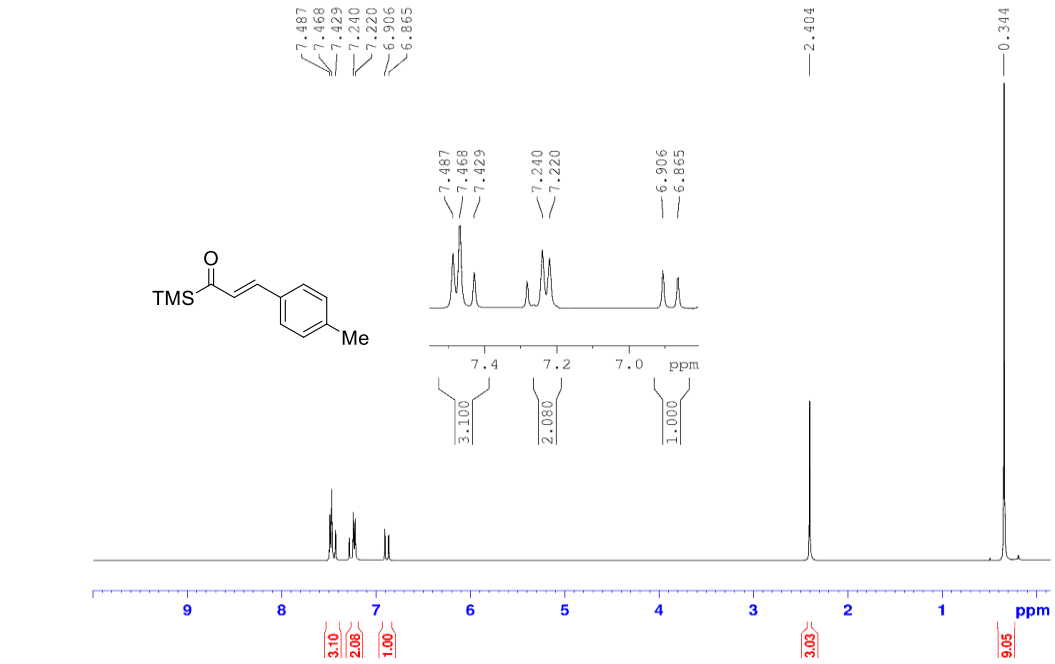

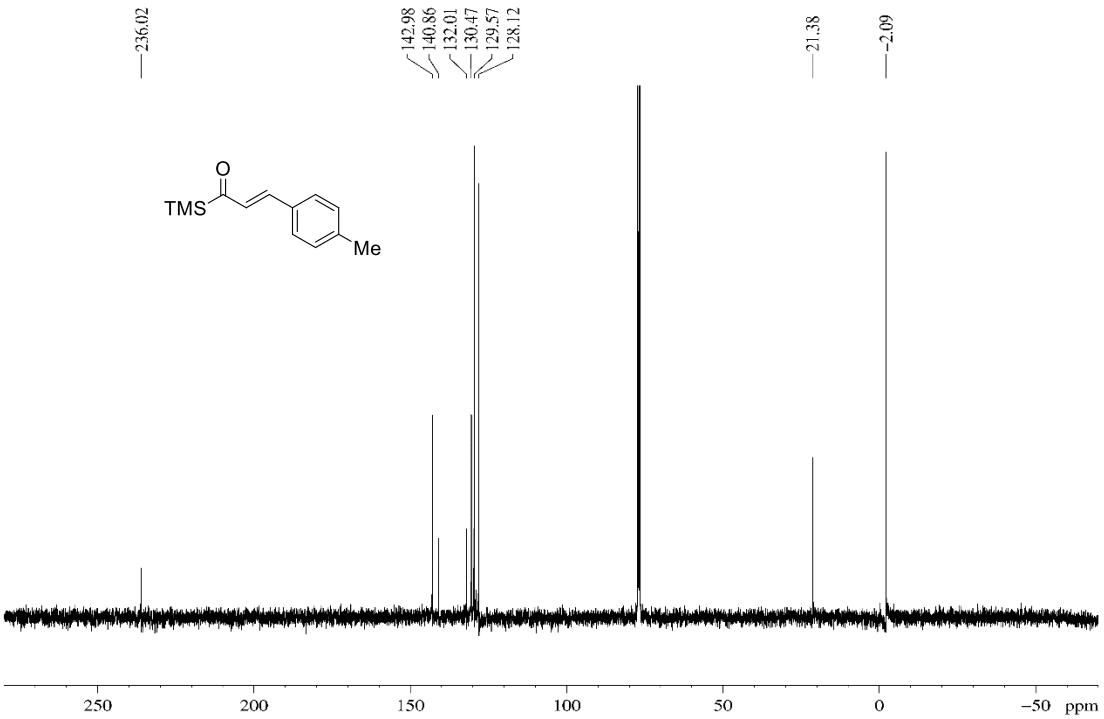

^{29}Si (80 MHz, $CDCl_3$)-NMR spectra of acylsilane **65a**

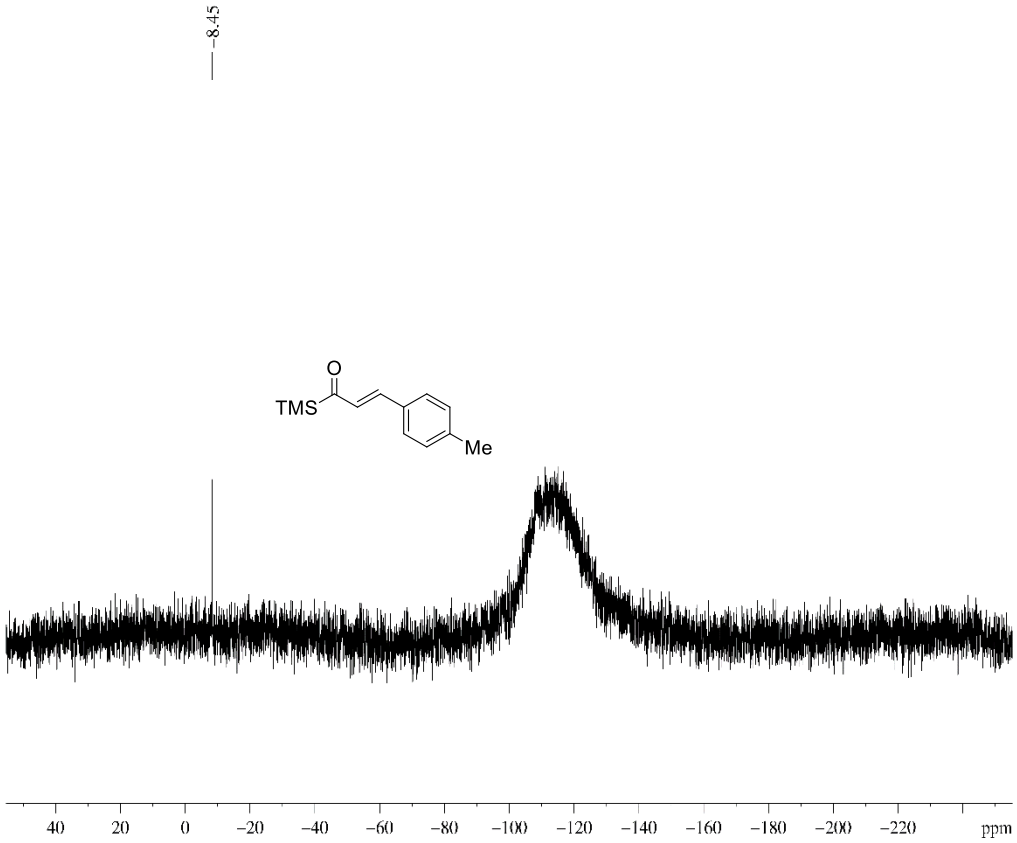

^{1}H (400 MHz, $CDCl_3$) and ^{13}C (100 MHz, $CDCl_3$)-NMR spectra of acylsilane **65b**

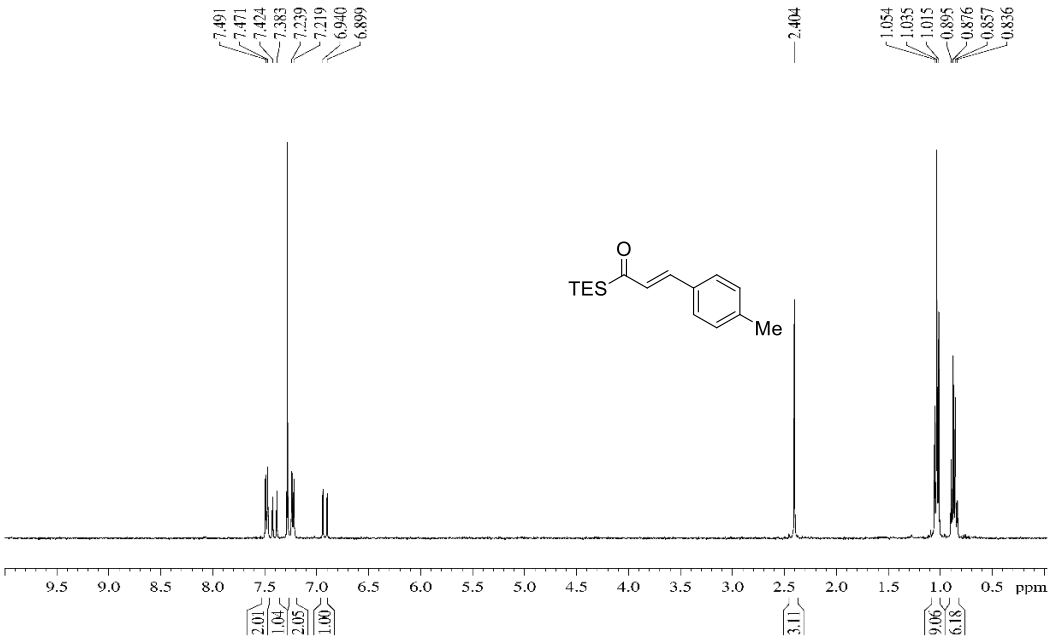

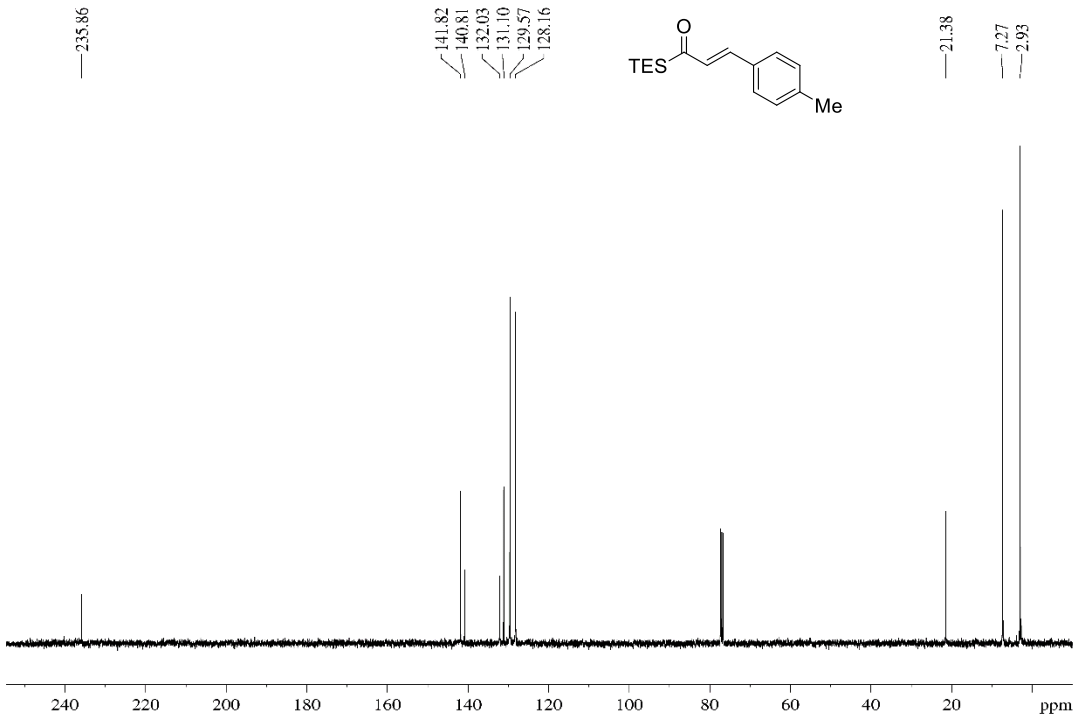

^{29}Si (80 MHz, $CDCl_3$)-NMR spectra of acylsilane **65b**

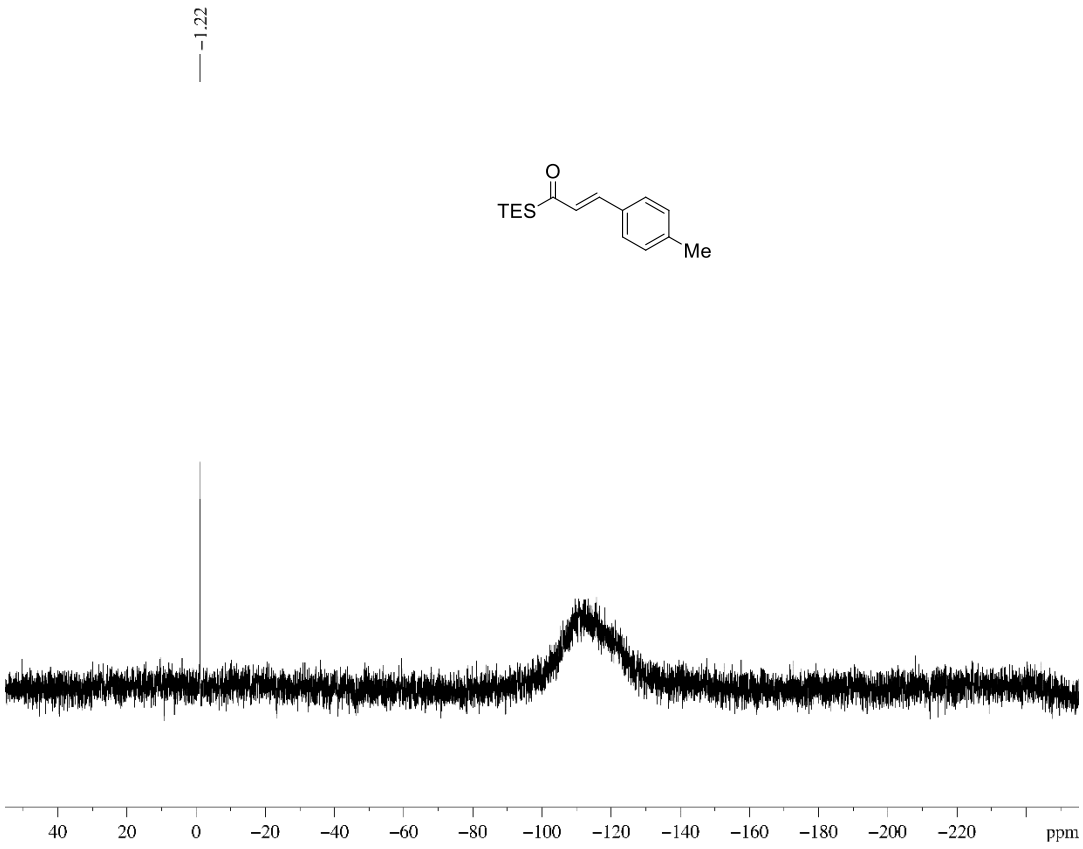

^{1}H (400 MHz, $CDCl_3$) and ^{13}C (100 MHz, $CDCl_3$)-NMR spectra of acylsilane **65c**

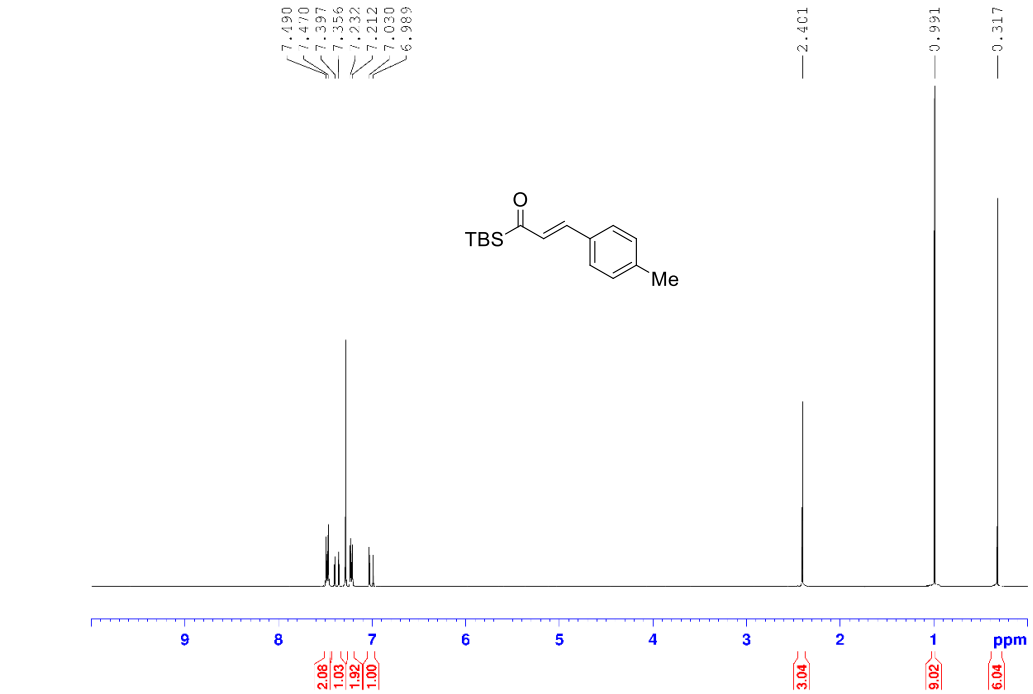

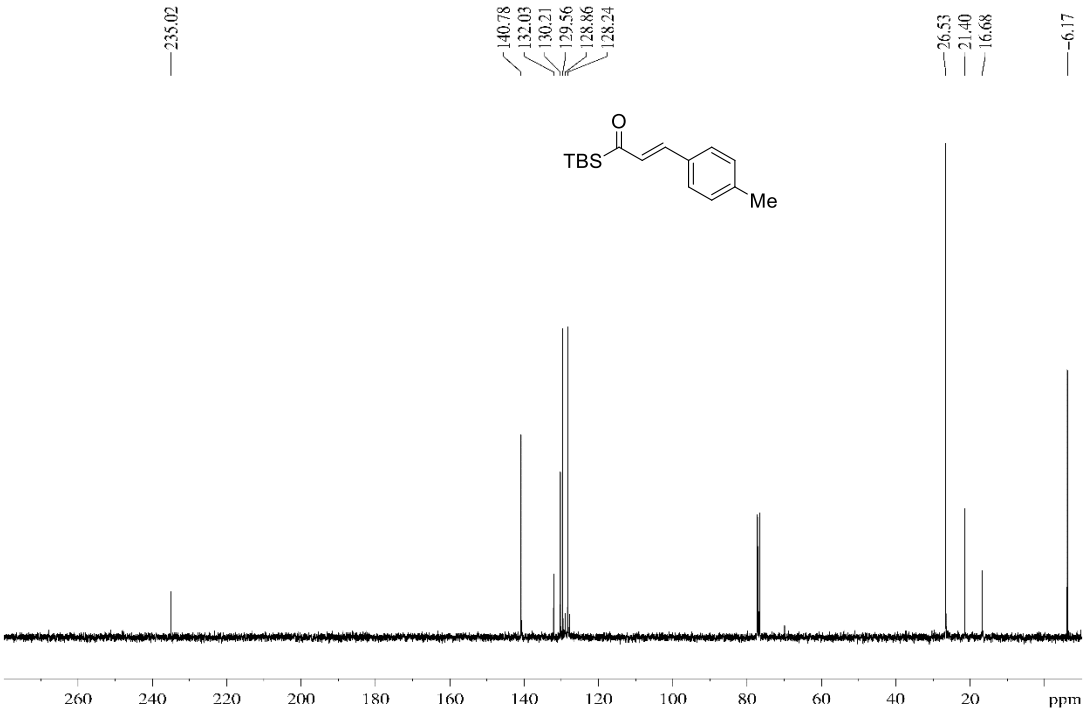

^{29}Si (80 MHz, $CDCl_3$)-NMR spectra of acylsilane **65c**

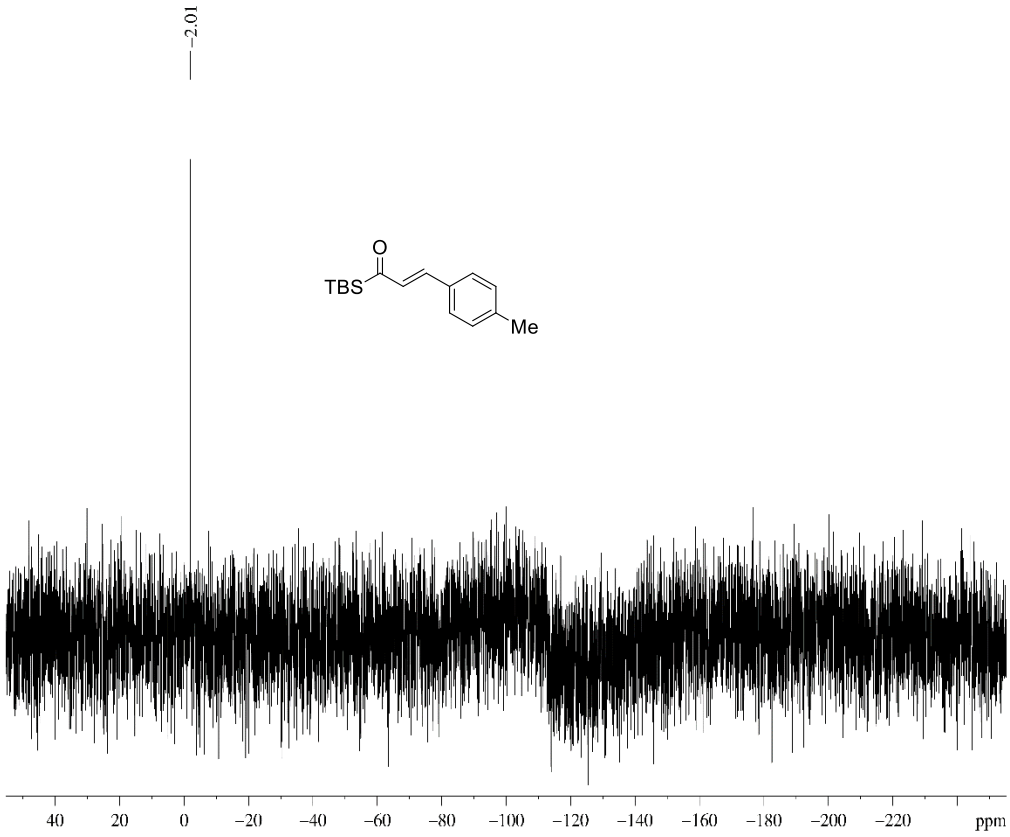

^{1}H (400 MHz, $CDCl_3$) and ^{13}C (100 MHz, $CDCl_3$)-NMR spectra of ethers **66d** and **67d**

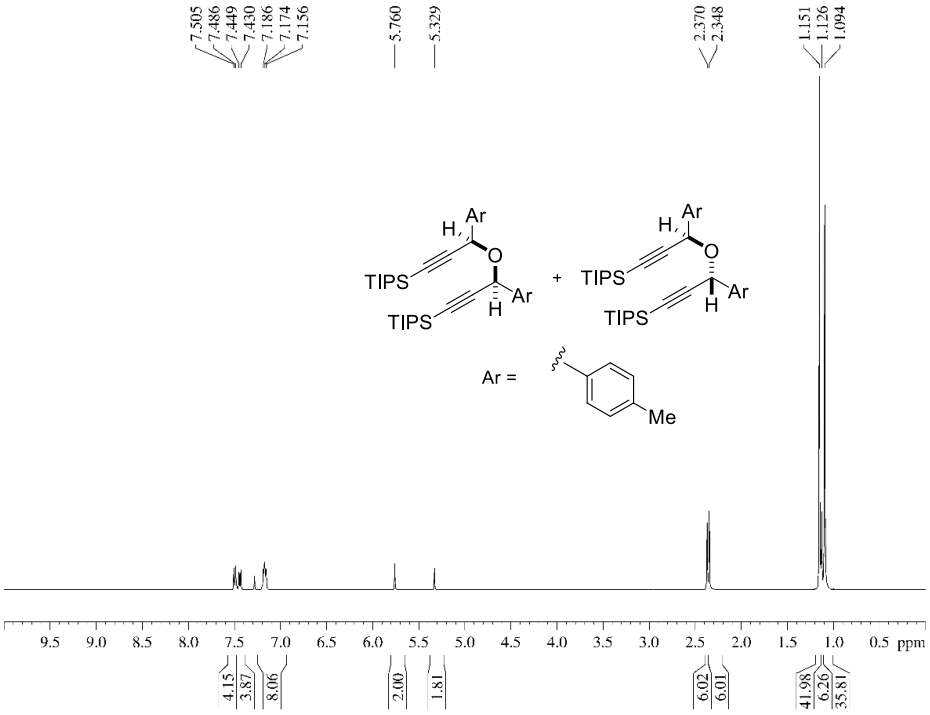

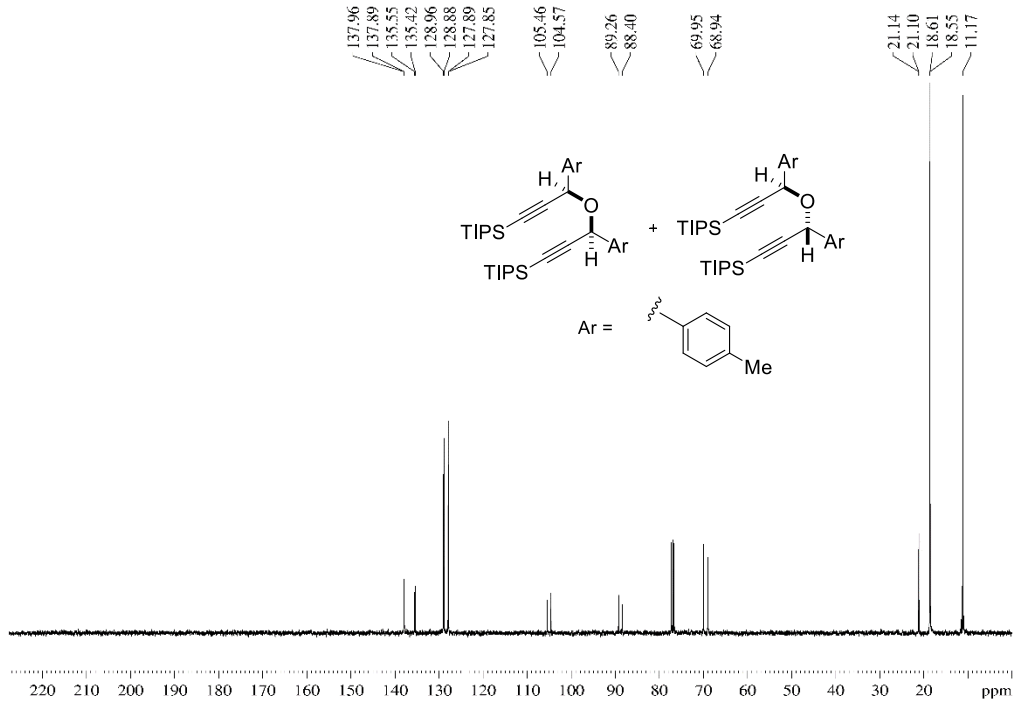

^{29}Si (80 MHz, $CDCl_3$)-NMR spectra of ethers **66d** and **67d**

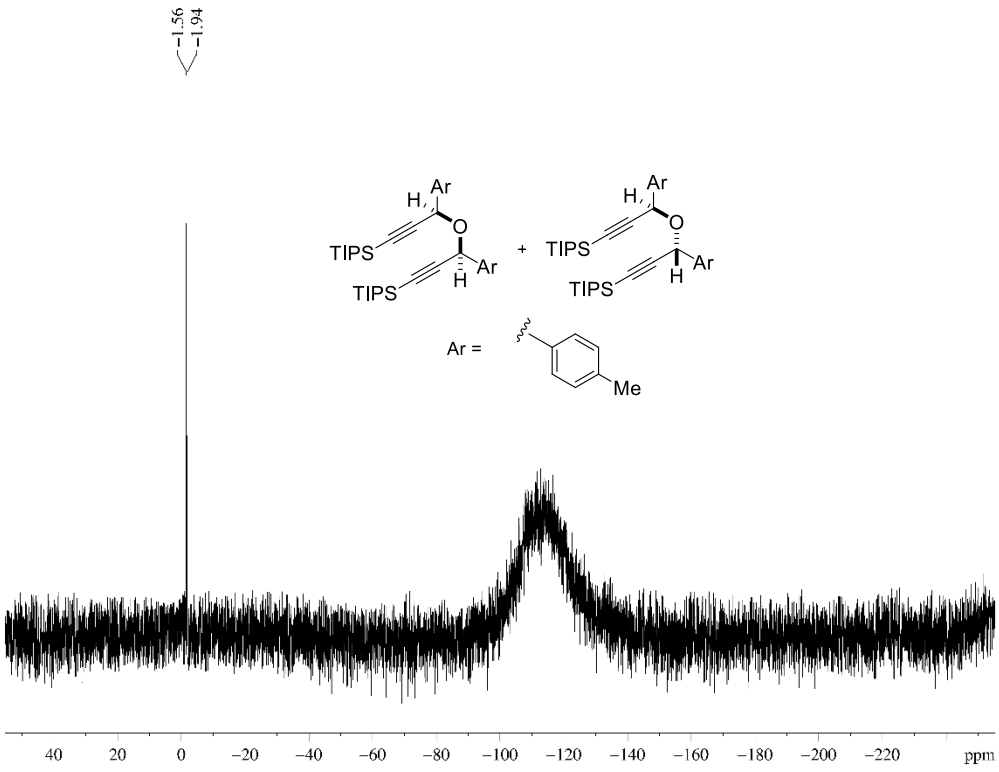

^{1}H (400 MHz, $CDCl_3$) and ^{13}C (100 MHz, $CDCl_3$)-NMR spectra of acylsilane **65e**

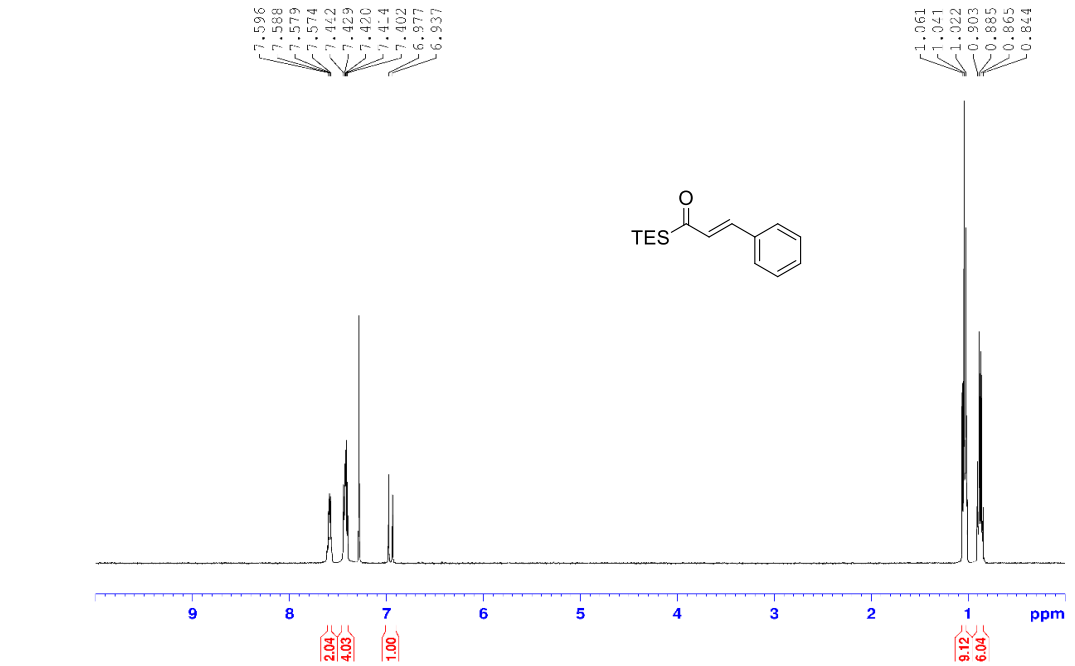

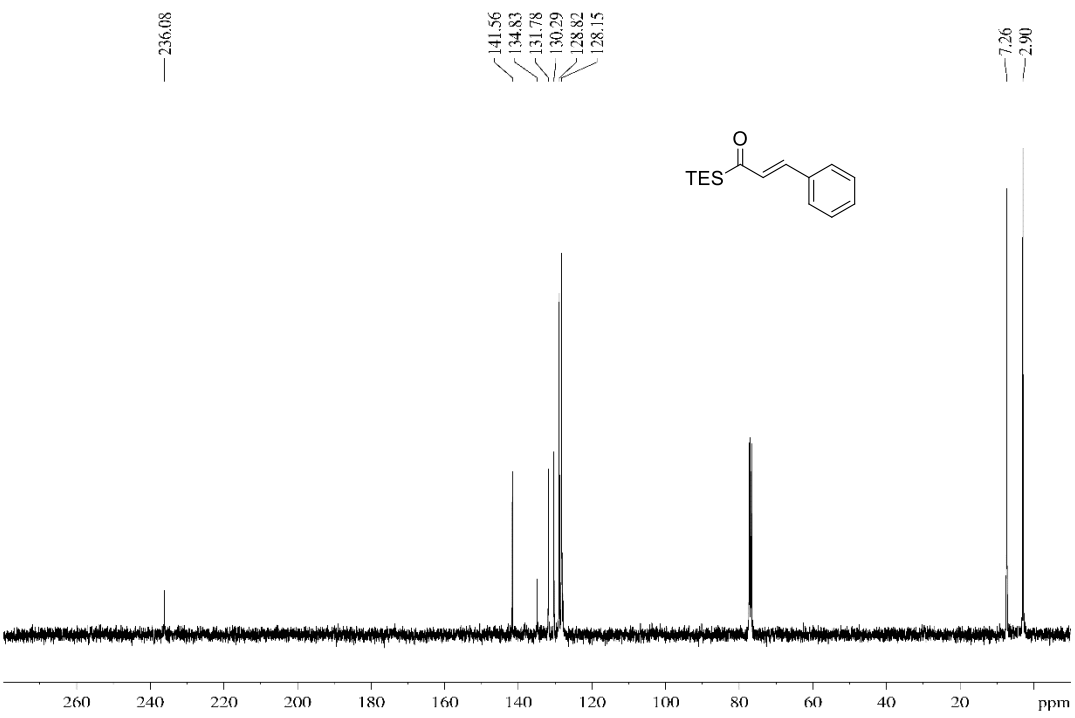

^{29}Si (80 MHz, $CDCl_3$)-NMR spectra of acylsilane **65e**

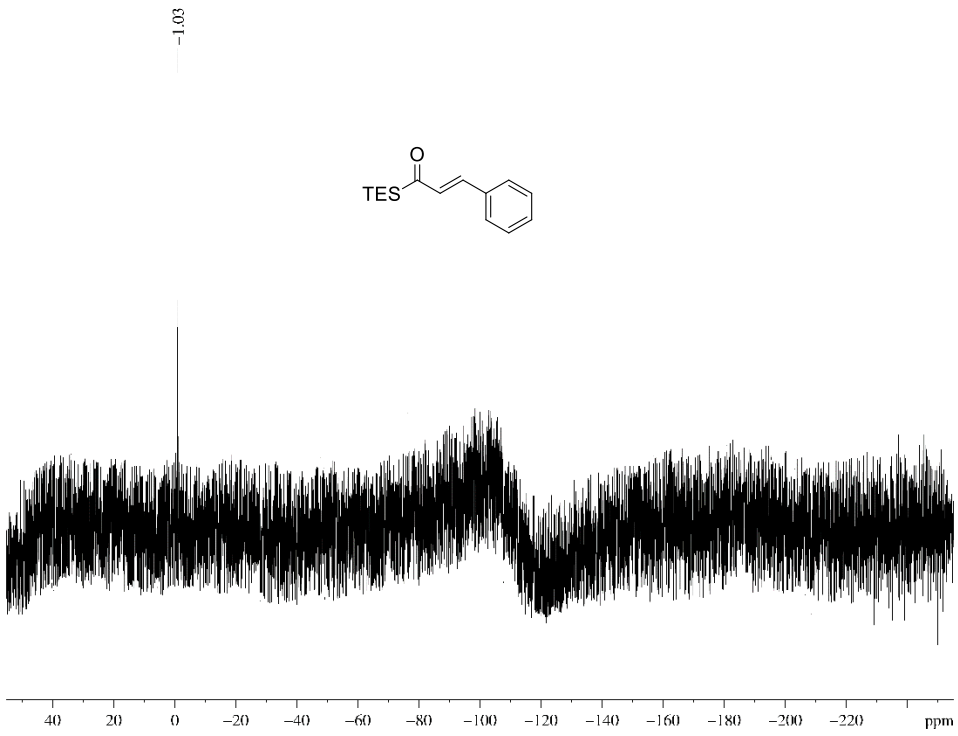

^{1}H (400 MHz, $CDCl_3$) and ^{13}C (100 MHz, $CDCl_3$)-NMR spectra of acylsilane **65f**

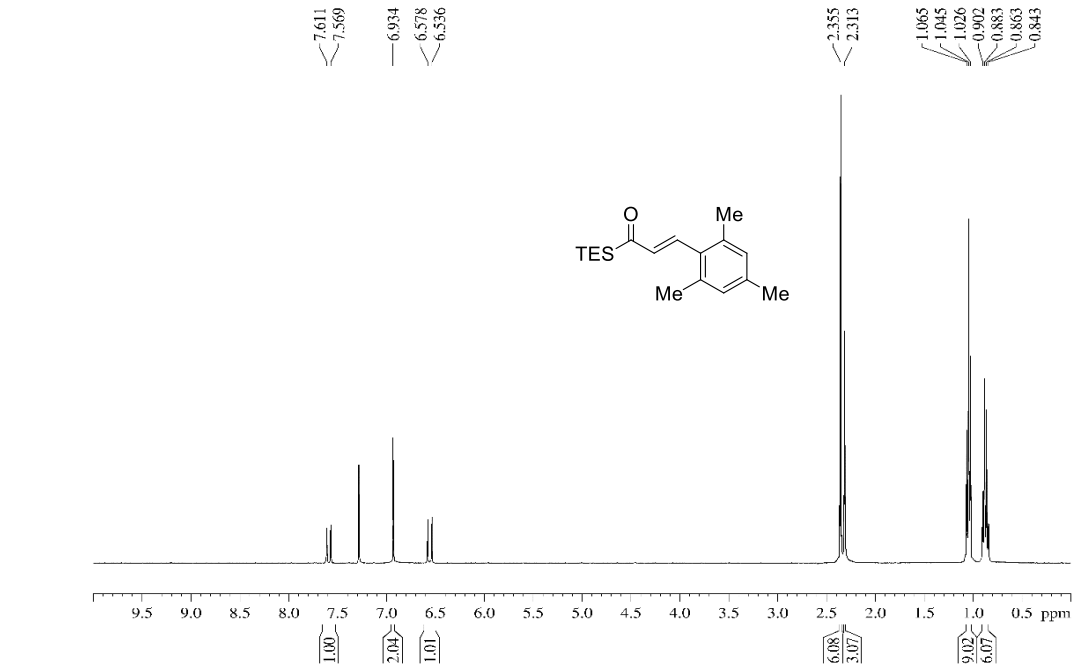

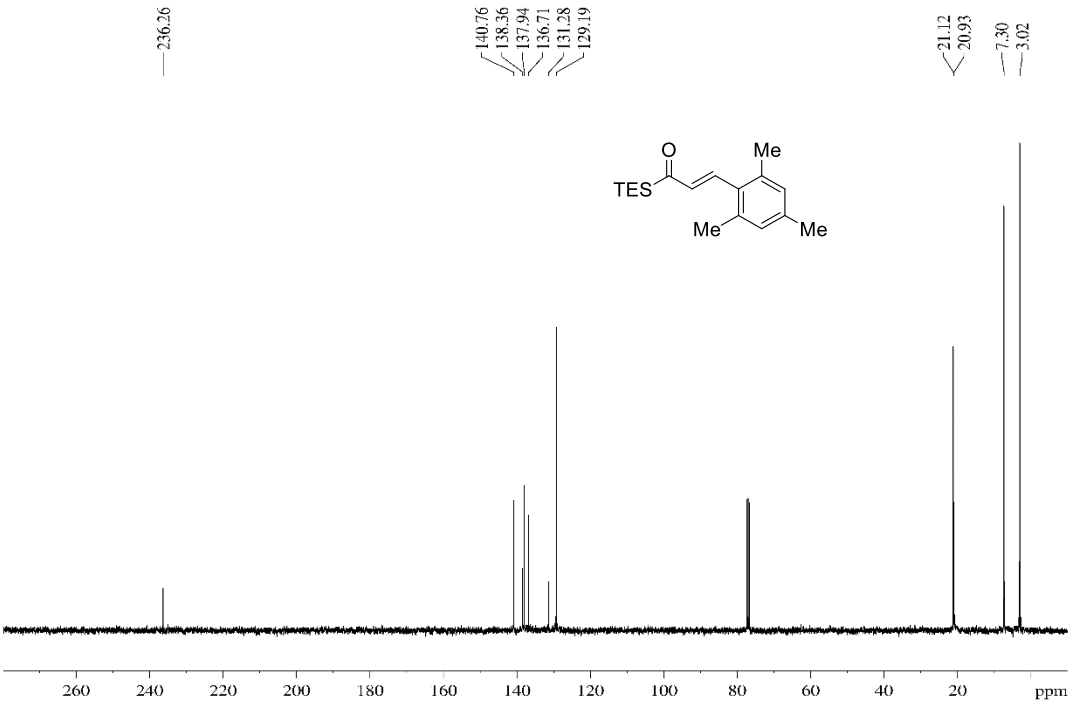

^{29}Si (80 MHz, $CDCl_3$)-NMR spectra of acylsilane **65f**

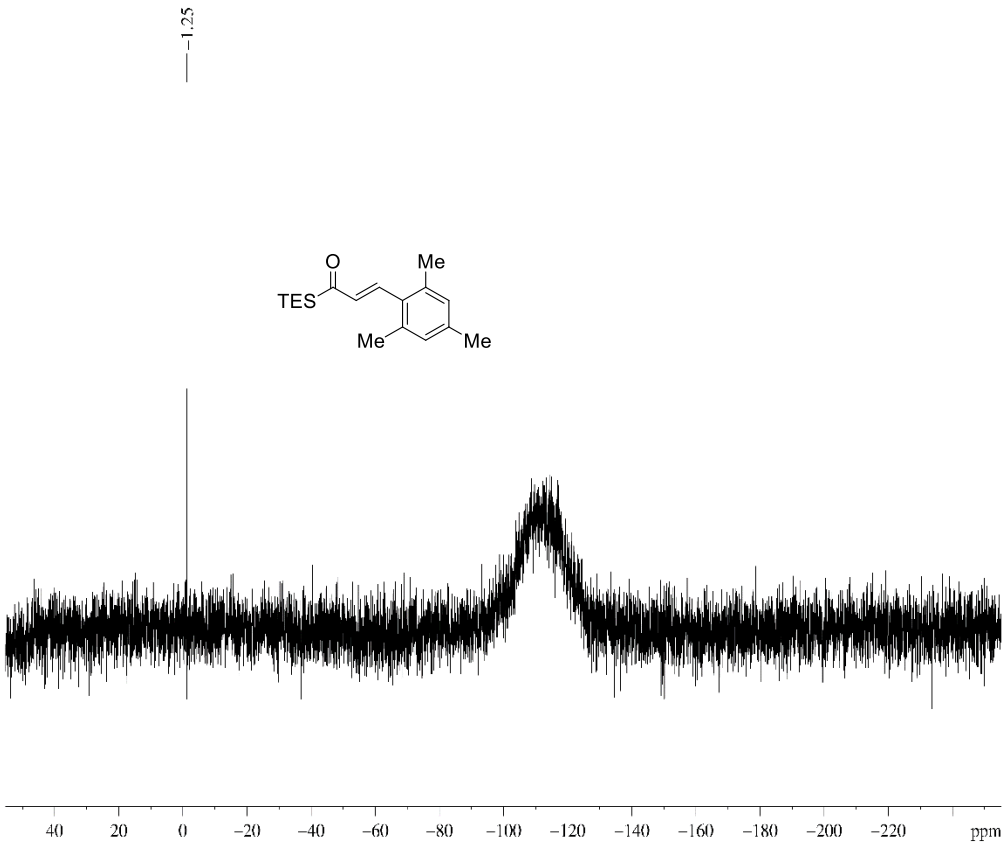

^{1}H (400 MHz, $CDCl_3$) and ^{13}C (100 MHz, $CDCl_3$)-NMR spectra of acylsilane **65g**

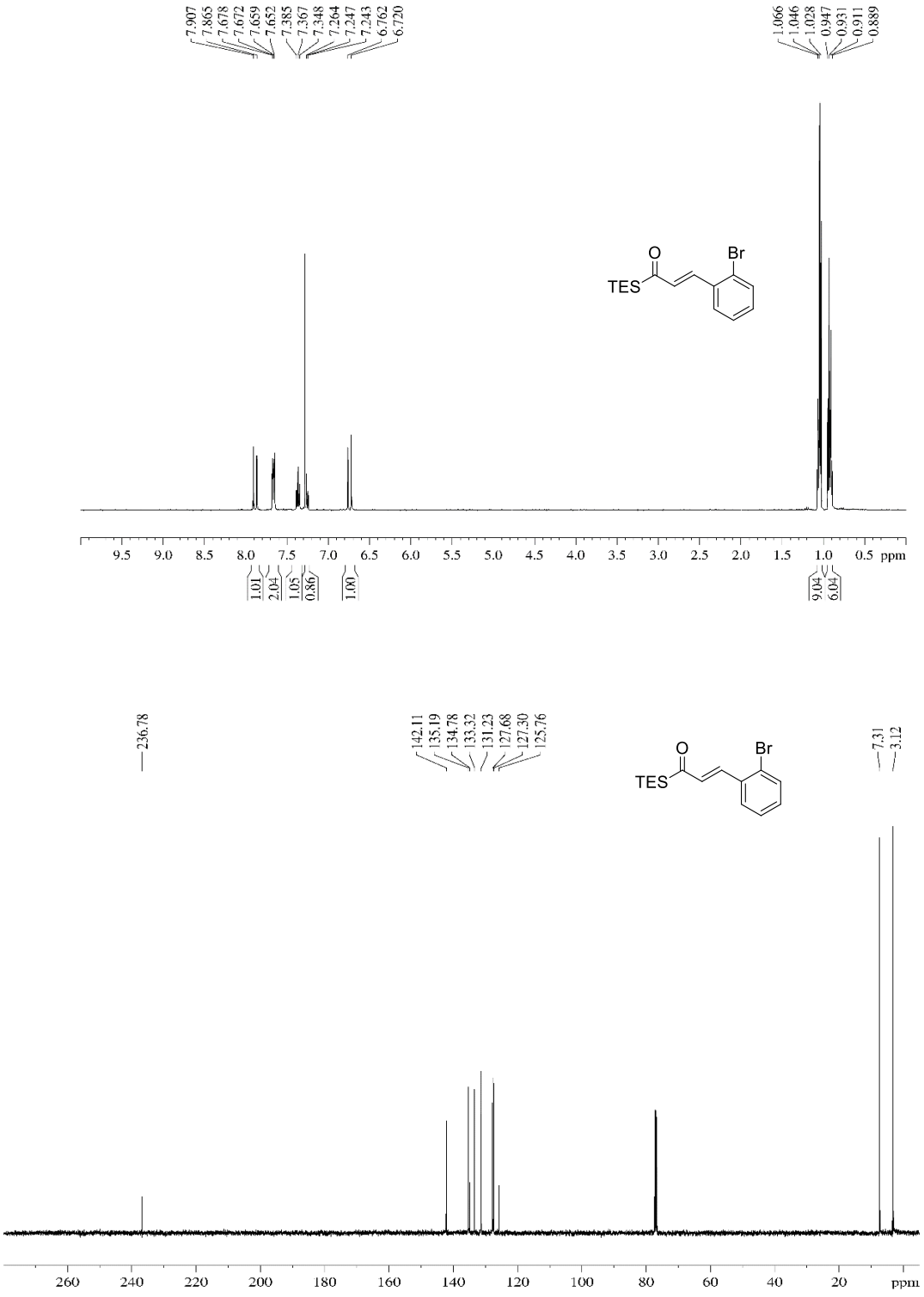

^{29}Si (80 MHz, $CDCl_3$)-NMR spectra of acylsilane **65g**

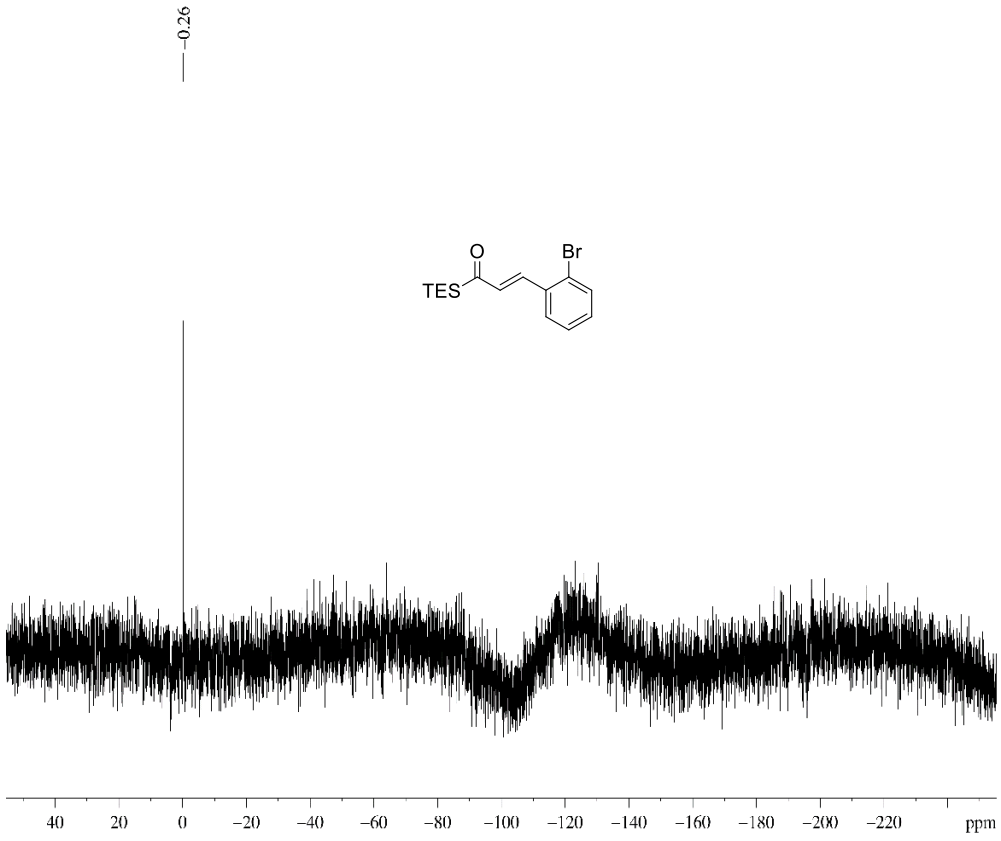

^{1}H (400 MHz, $CDCl_3$) and ^{13}C (100 MHz, $CDCl_3$)-NMR spectra of acylsilane **65h**

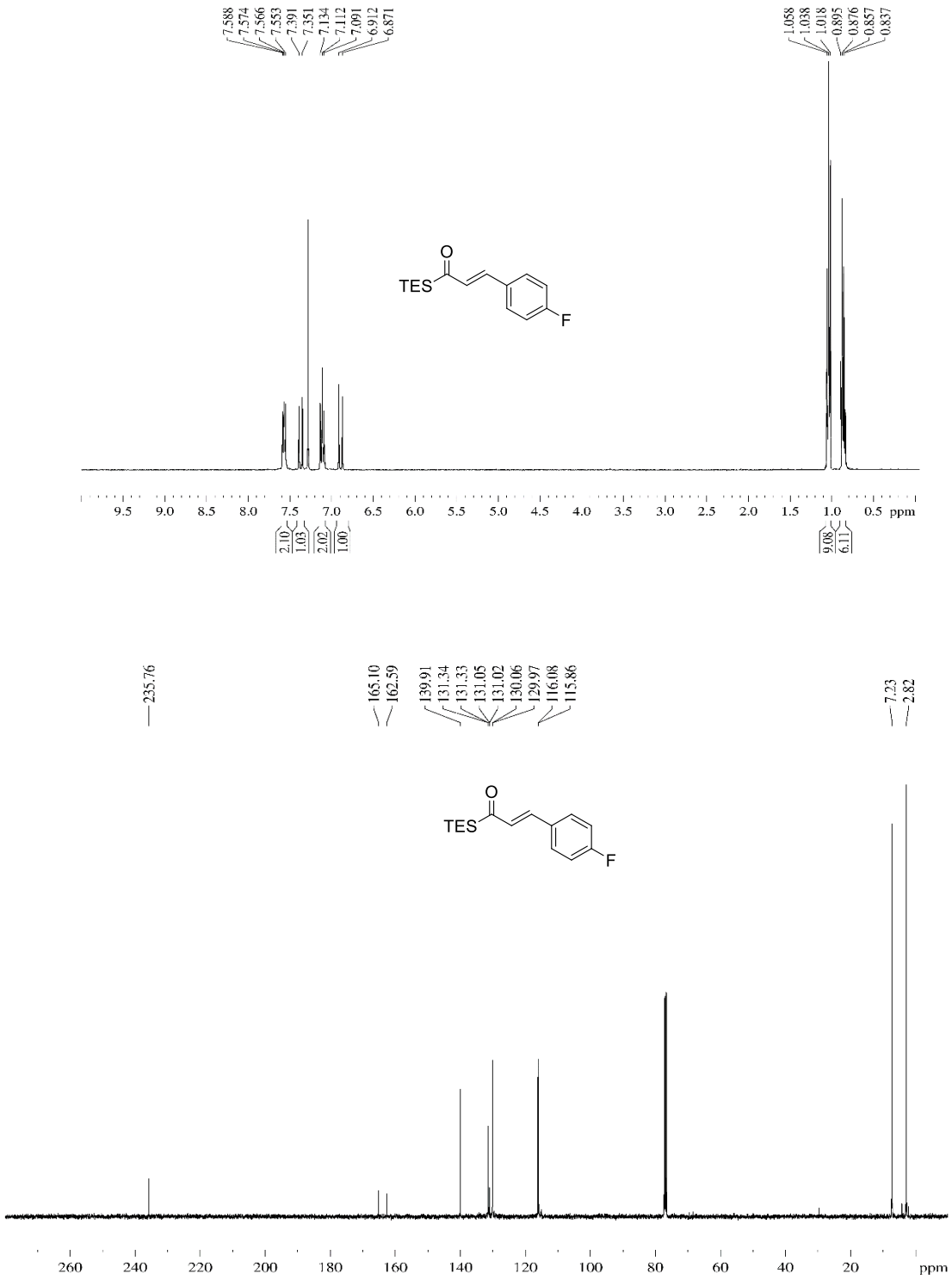

^{29}Si (80 MHz, $CDCl_3$)-NMR spectra of acylsilane **65h**

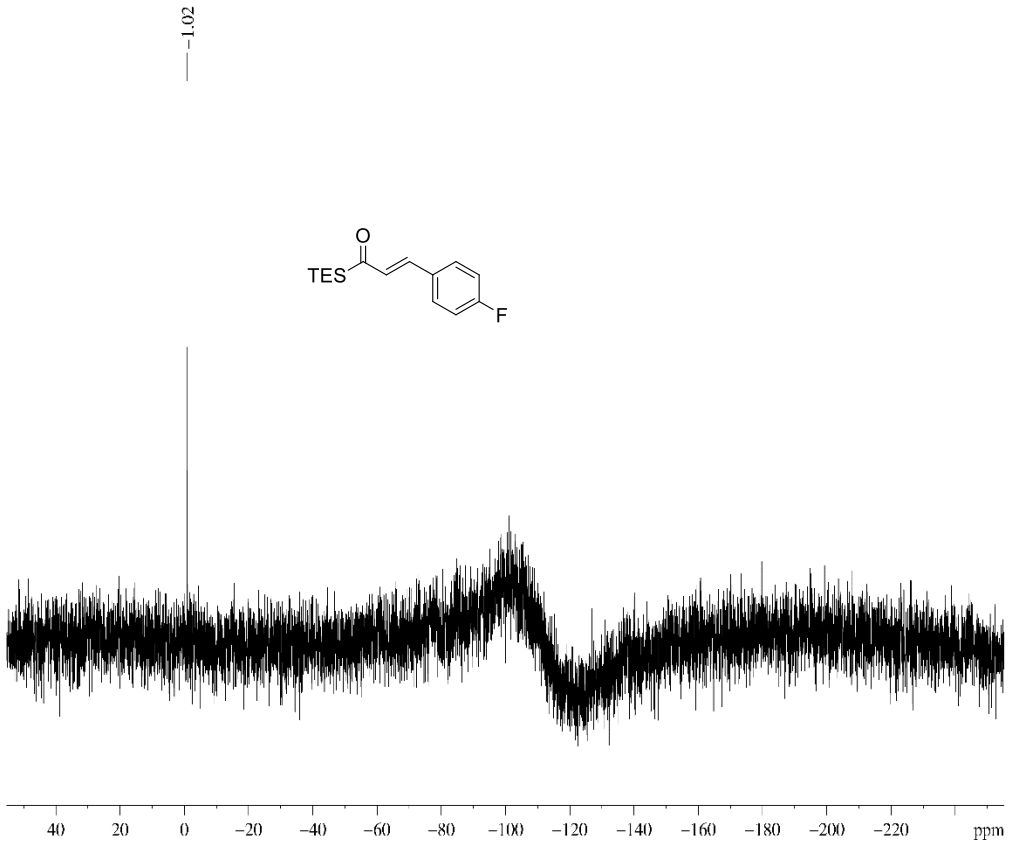

^{19}F (376 MHz, $CDCl_3$)-NMR spectra of acylsilane **65h**

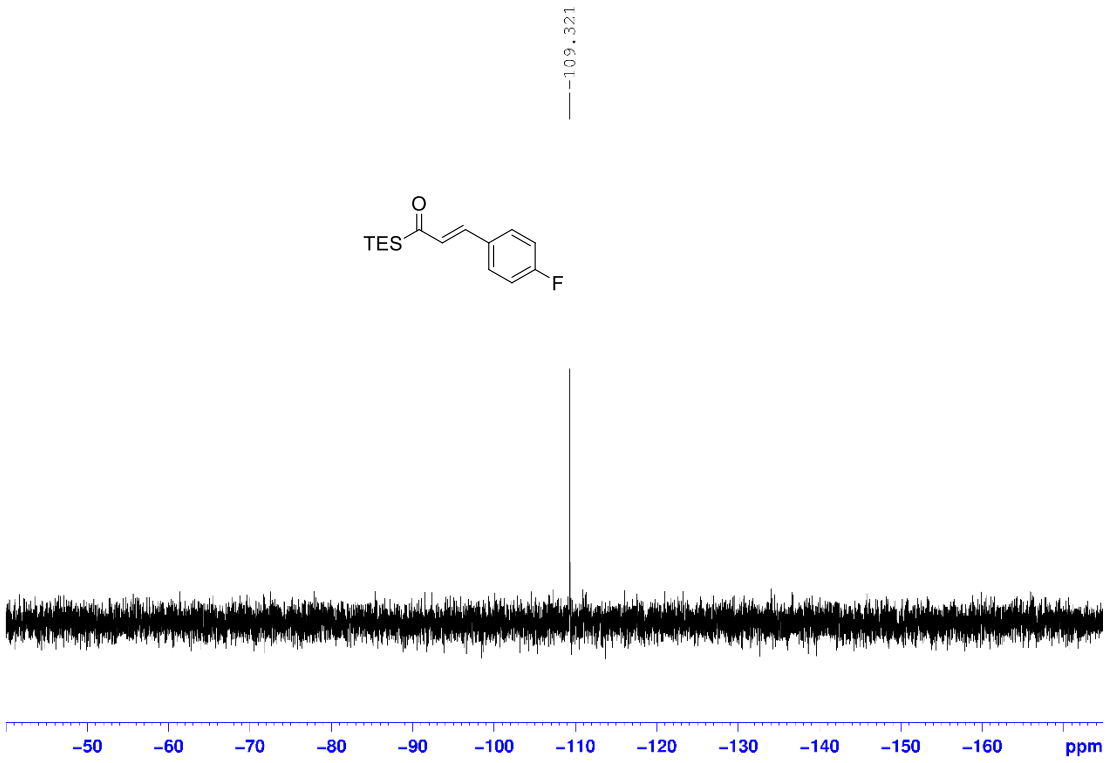

^{1}H (400 MHz, $CDCl_3$) and ^{13}C (100 MHz, $CDCl_3$)-NMR spectra of acylsilane **65i**

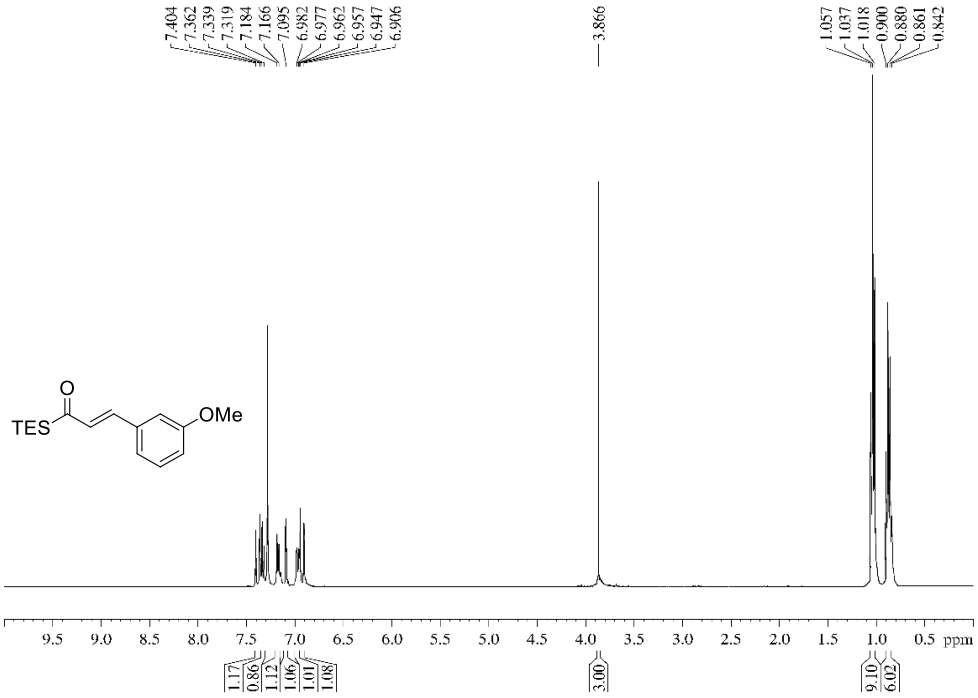

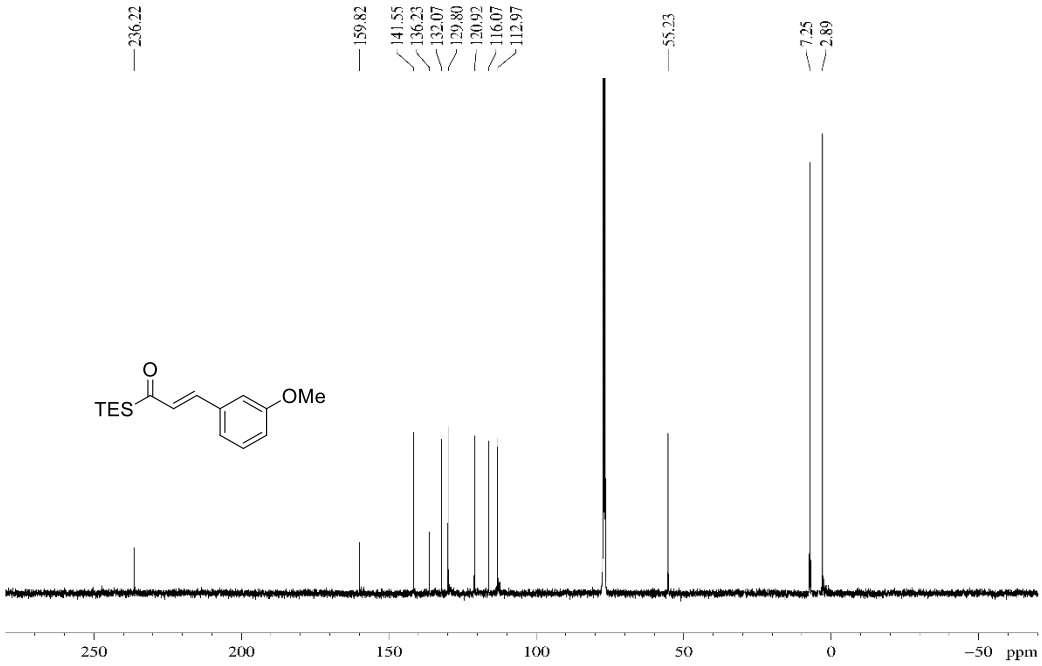

^{29}Si (80 MHz, $CDCl_3$)-NMR spectra of acylsilane **65i**

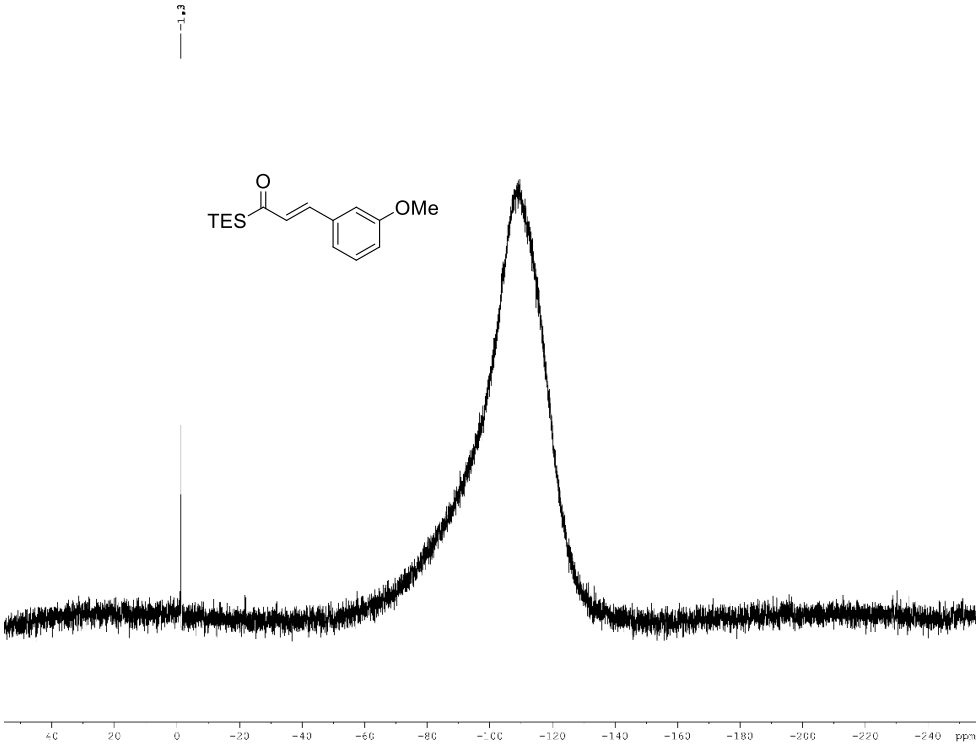

^{1}H (400 MHz, $CDCl_3$) and ^{13}C (100 MHz, $CDCl_3$)-NMR spectra of acylsilane **65j**

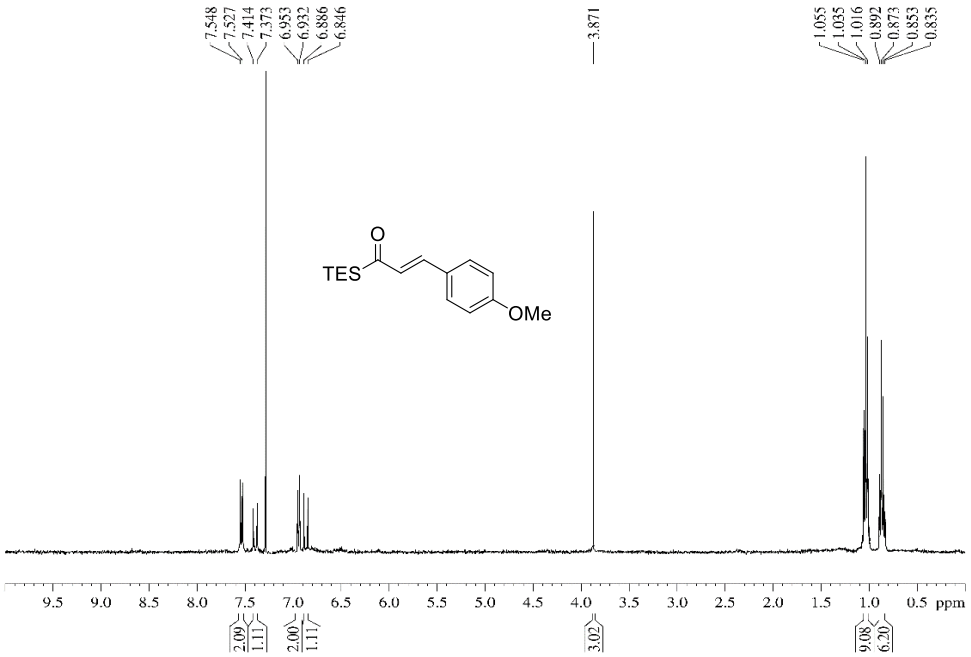

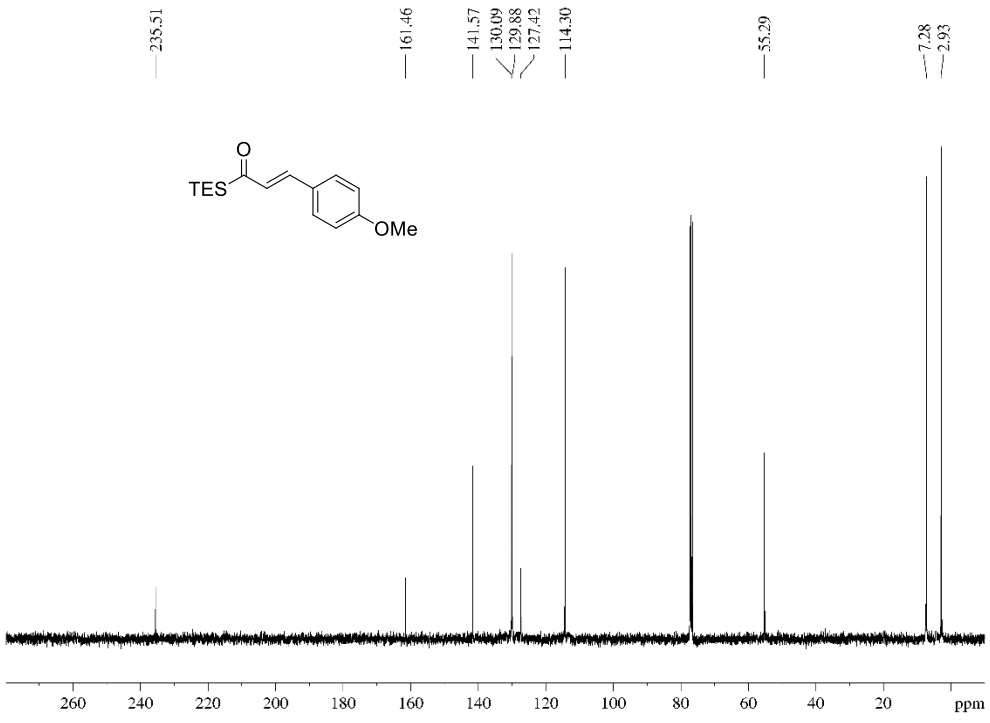

^{29}Si (80 MHz, $CDCl_3$)-NMR spectra of acylsilane **65j**

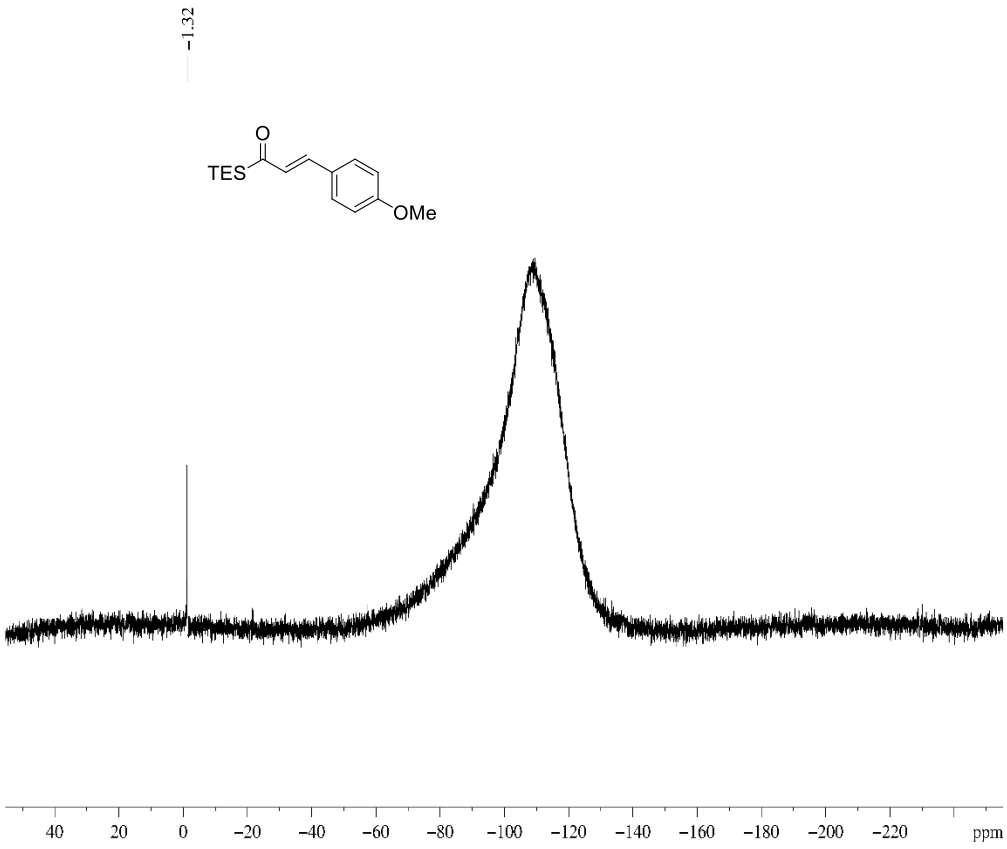

^{1}H (400 MHz, $CDCl_3$) and ^{13}C (100 MHz, $CDCl_3$)-NMR spectra of acylsilane **65k**

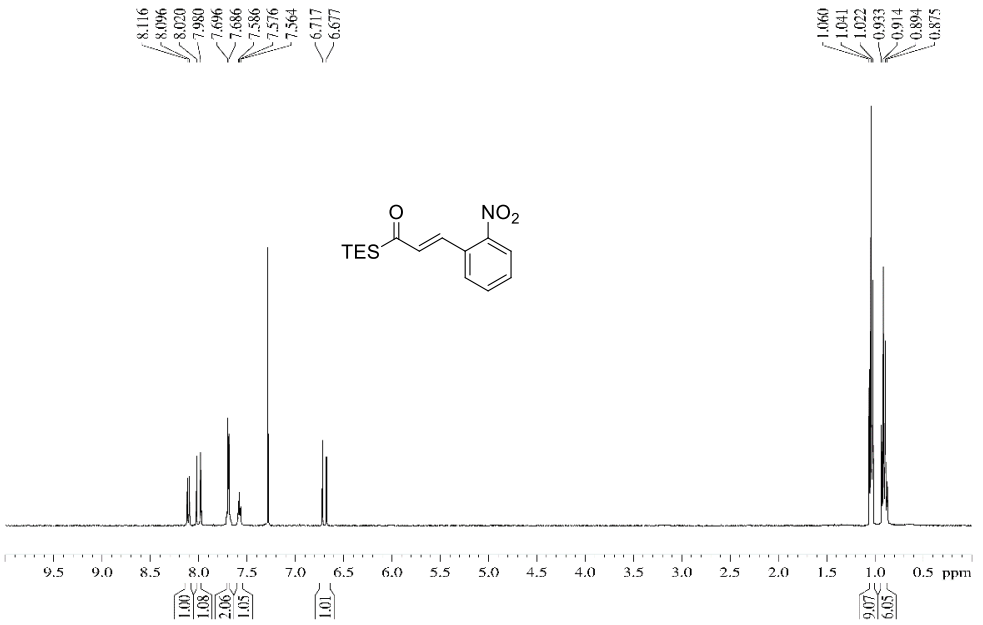

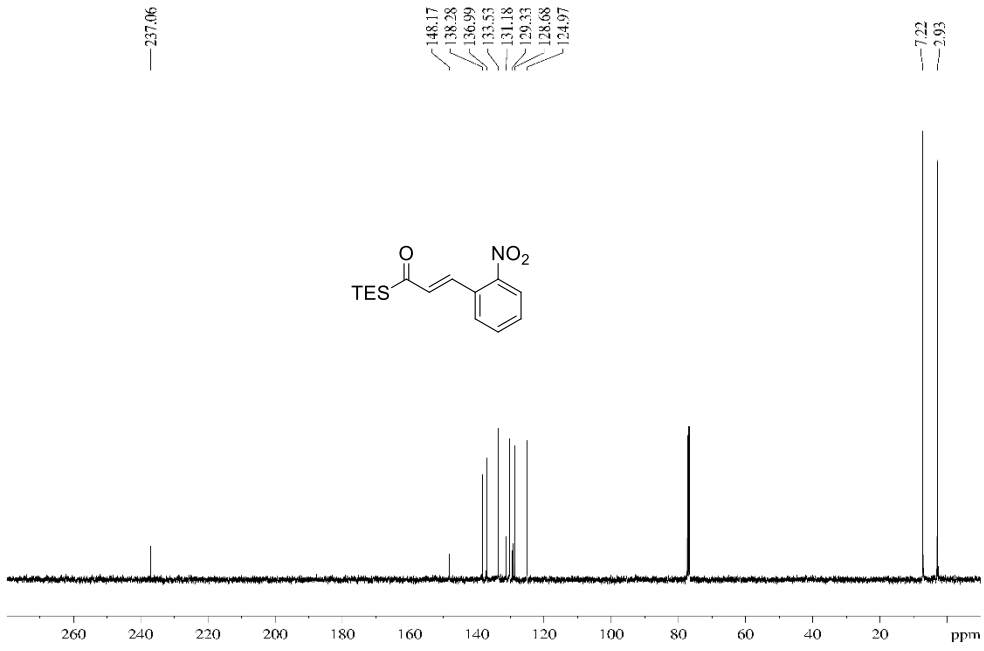

^{29}Si (80 MHz, $CDCl_3$)-NMR spectra of acylsilane **65k**

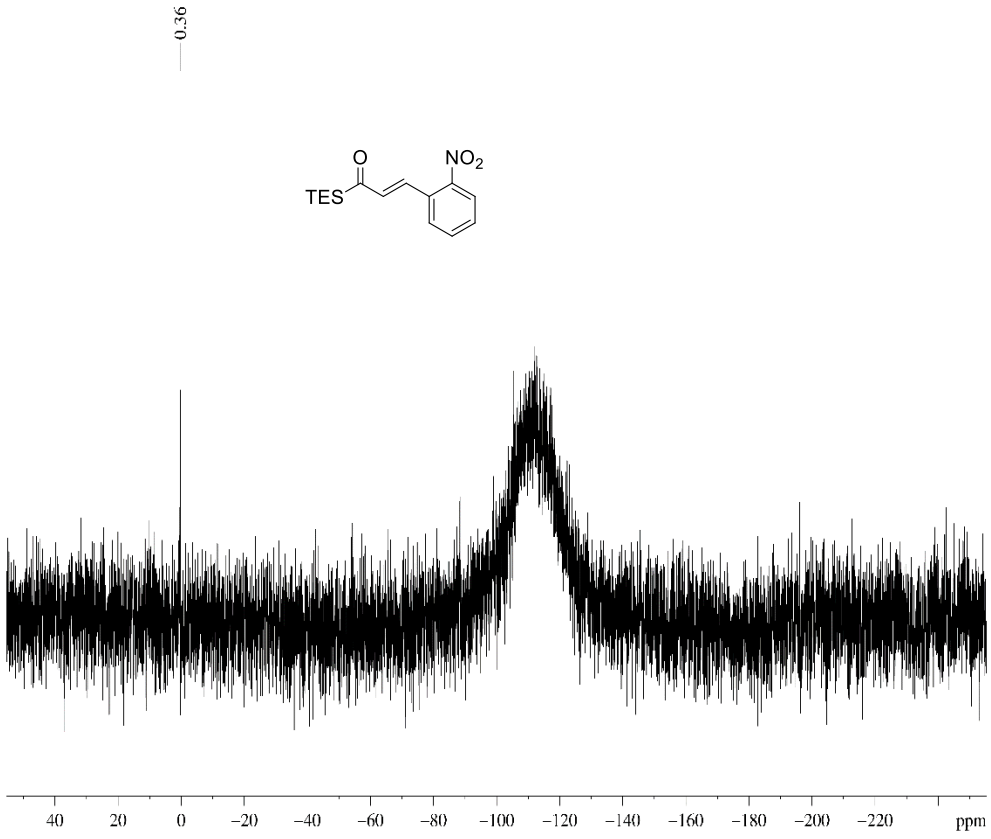

^{1}H (400 MHz, $CDCl_3$) and ^{13}C (100 MHz, $CDCl_3$)-NMR spectra of acylsilane **65l**

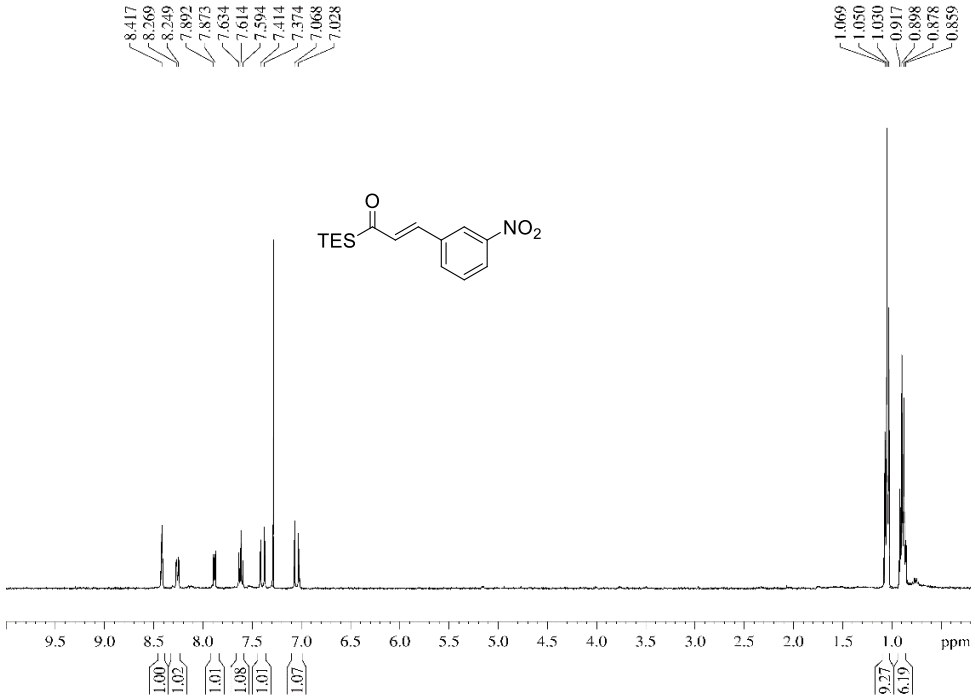

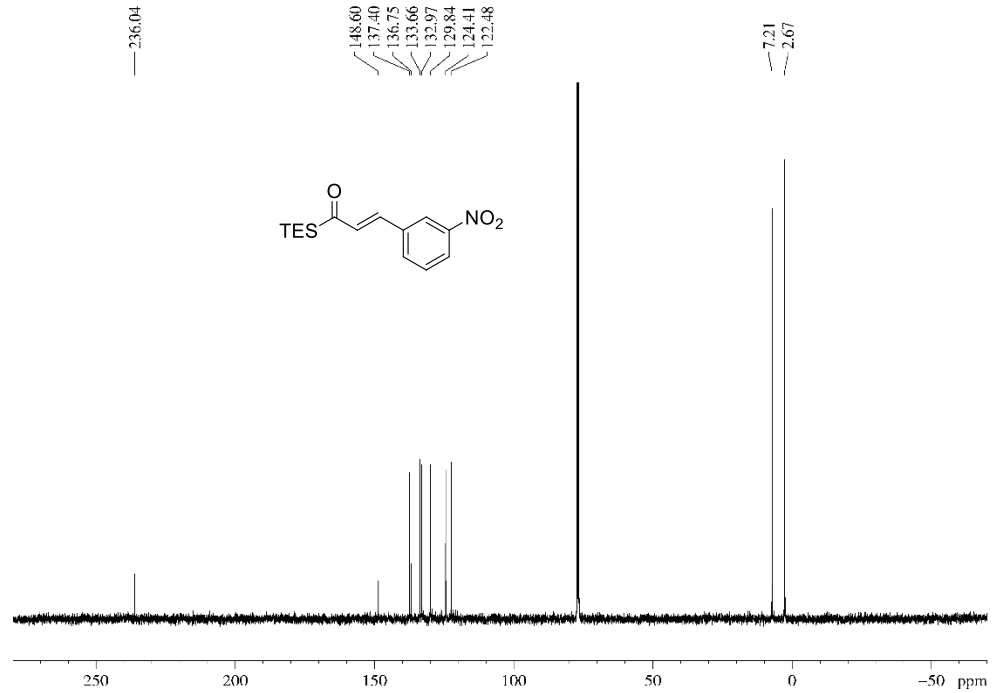

^{29}Si (80 MHz, $CDCl_3$)-NMR spectra of acylsilane **65l**

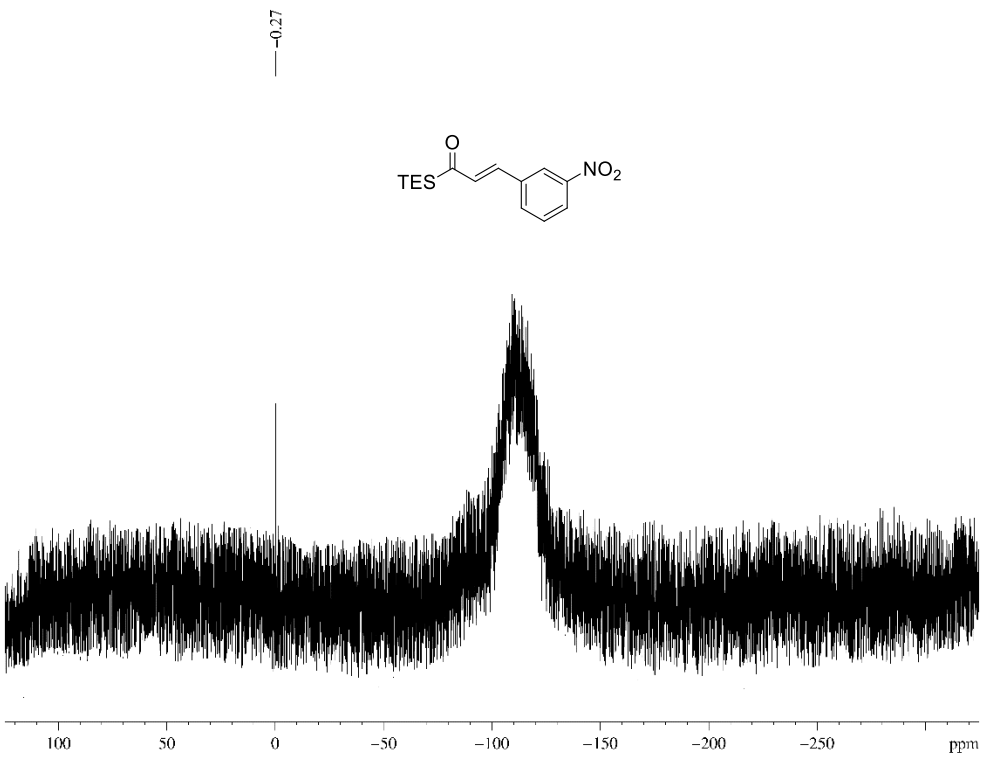

^{1}H (400 MHz, $CDCl_3$) and ^{13}C (100 MHz, $CDCl_3$)-NMR spectra of acylsilane **65m**

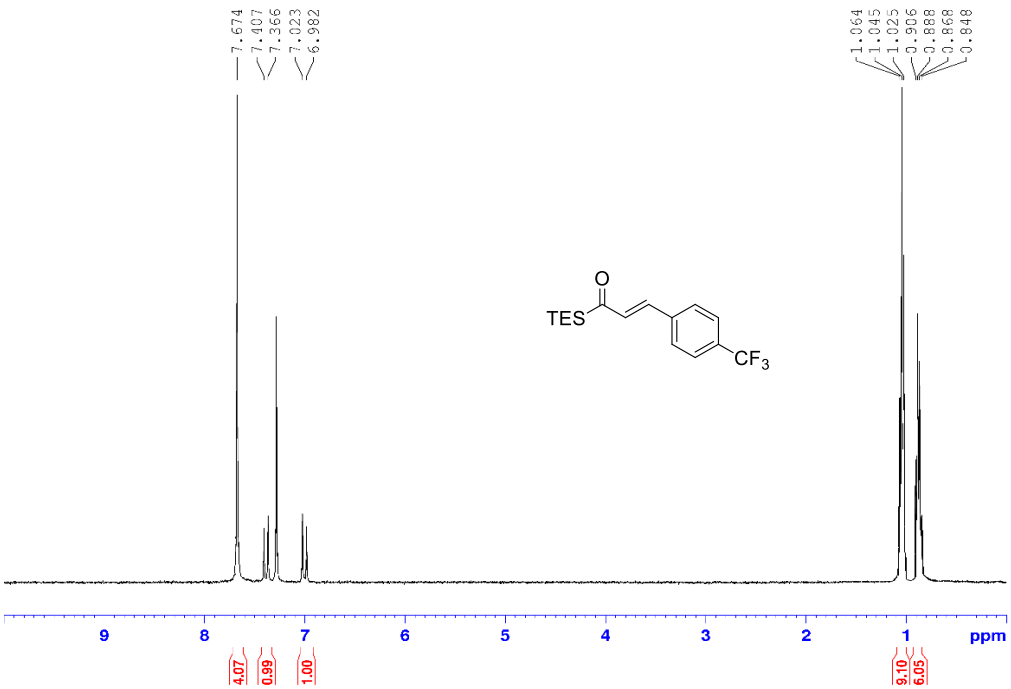

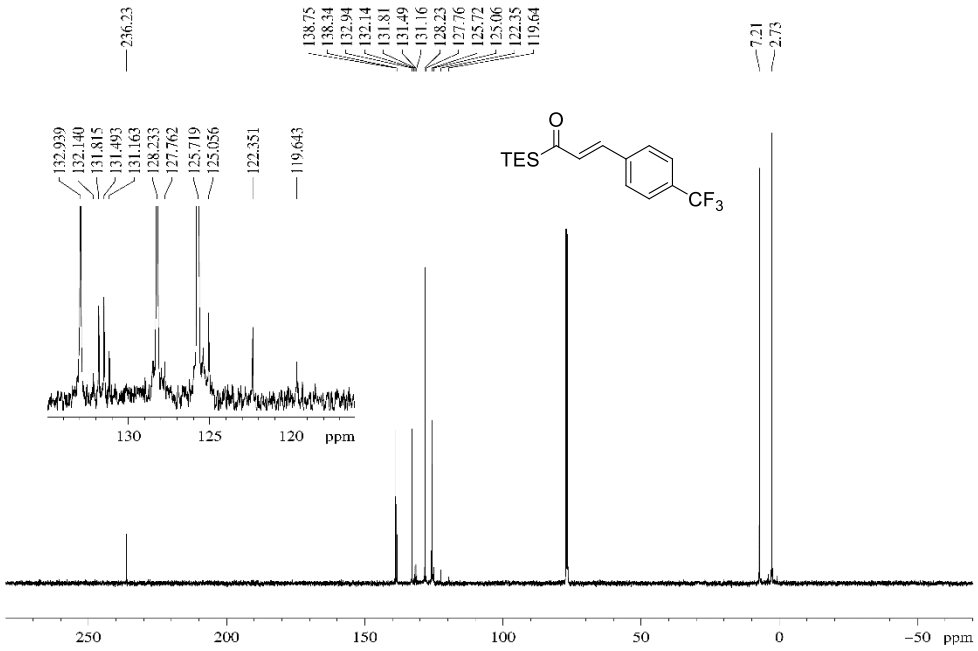

^{29}Si (80 MHz, $CDCl_3$)-NMR spectra of acylsilane **65m**

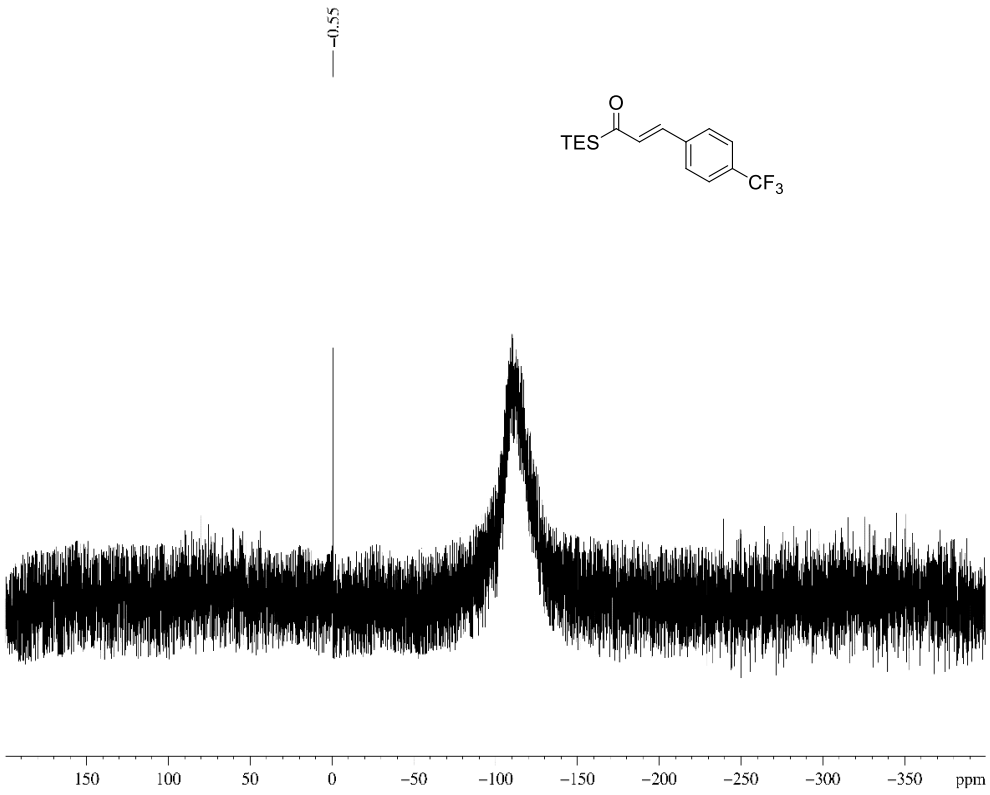

^{19}F (376 MHz, $CDCl_3$)-NMR spectra of acylsilane **65m**

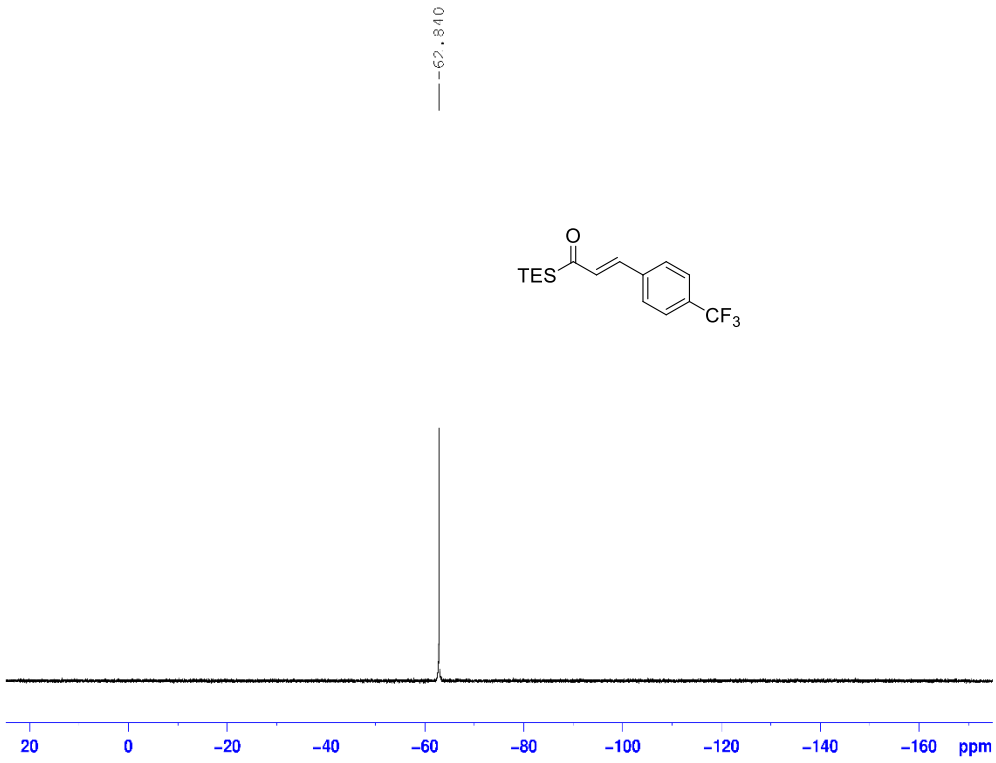

^{1}H (400 MHz, $CDCl_3$) and ^{13}C (100 MHz, $CDCl_3$)-NMR spectra of 1-Indanone **66n**

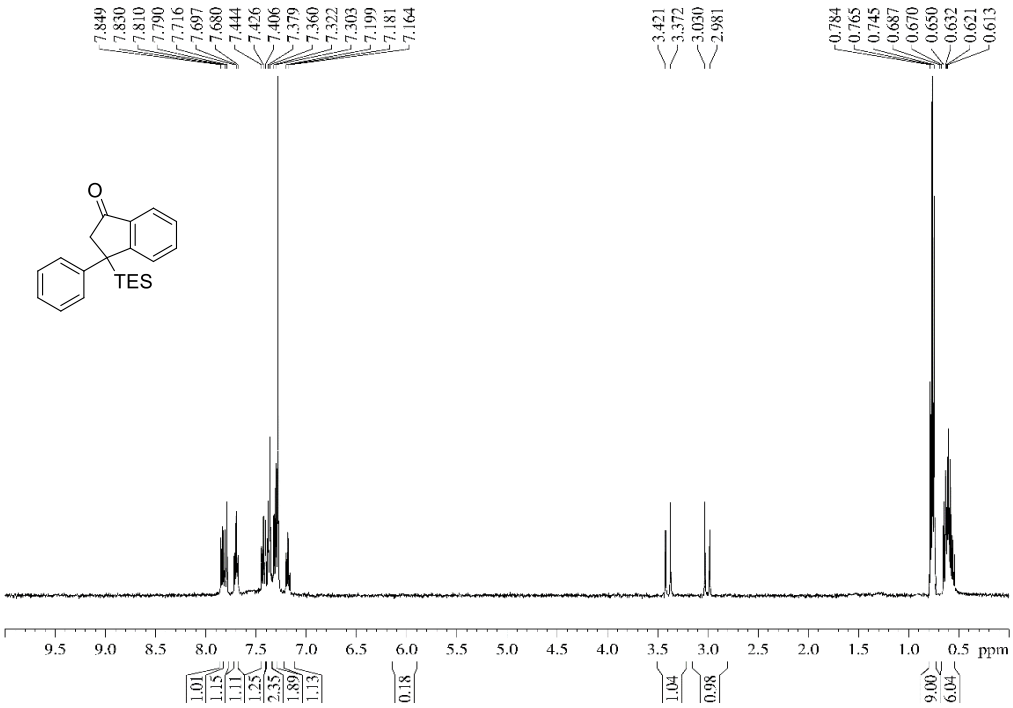

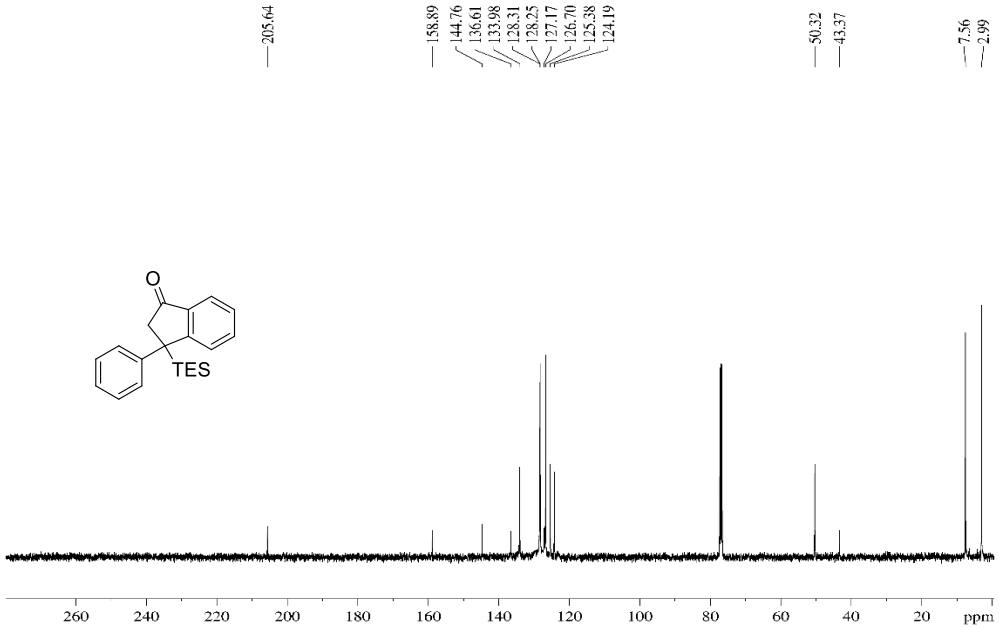

^{29}Si (80 MHz, $CDCl_3$)-NMR spectra of 1-Indanone **66n**

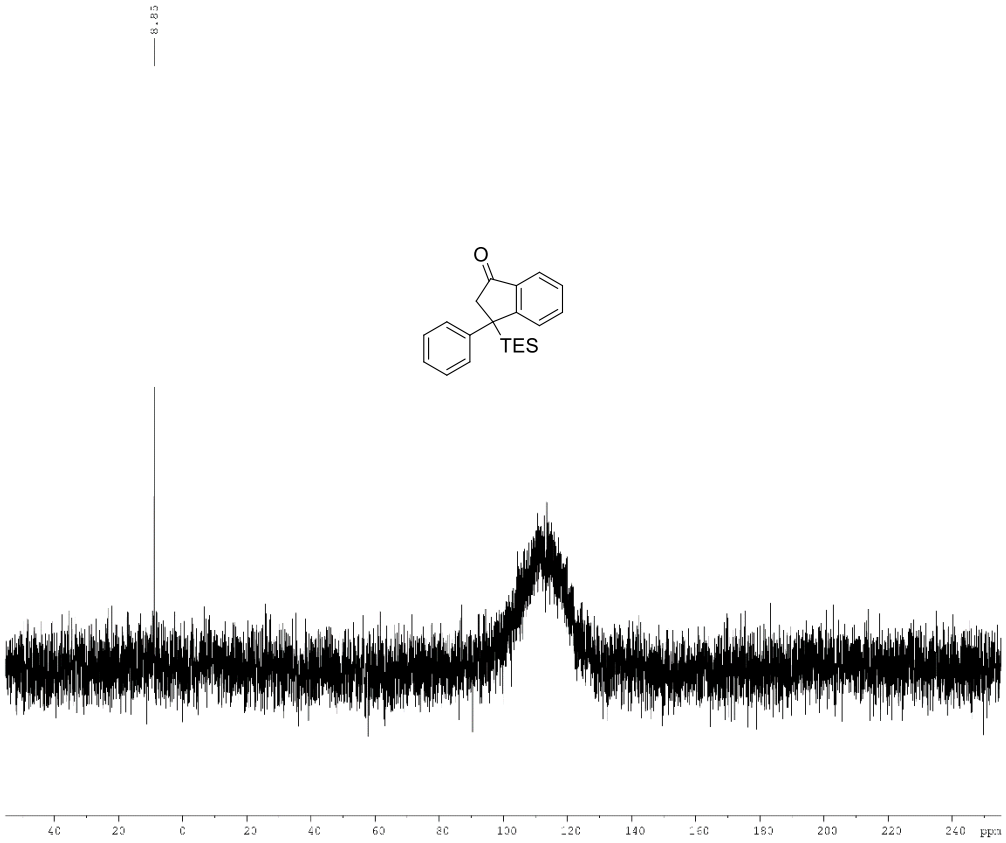

^{1}H (400 MHz, $CDCl_3$) and ^{13}C (100 MHz, $CDCl_3$)-NMR spectra of acylsilane **65o**

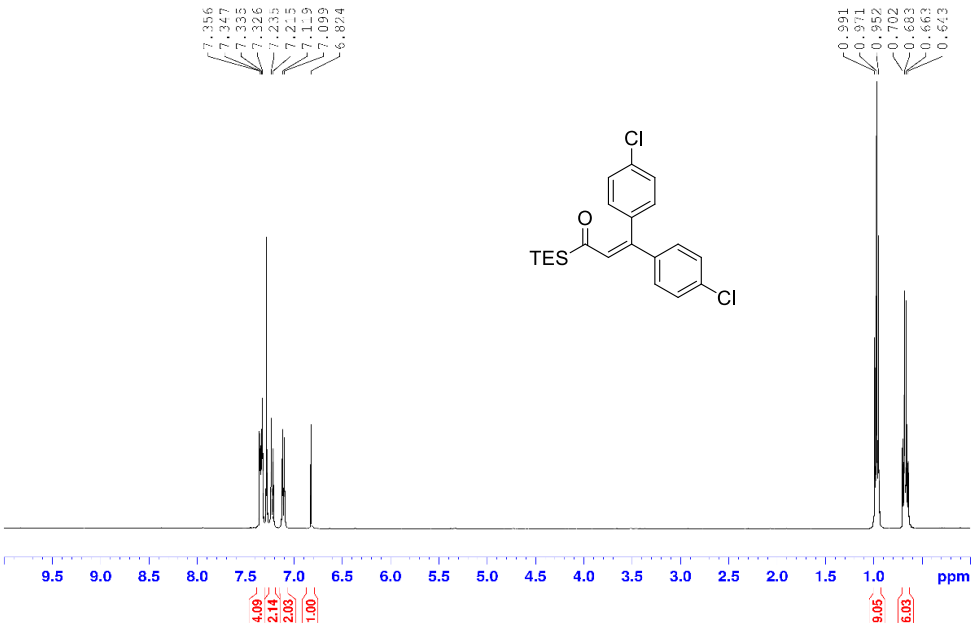

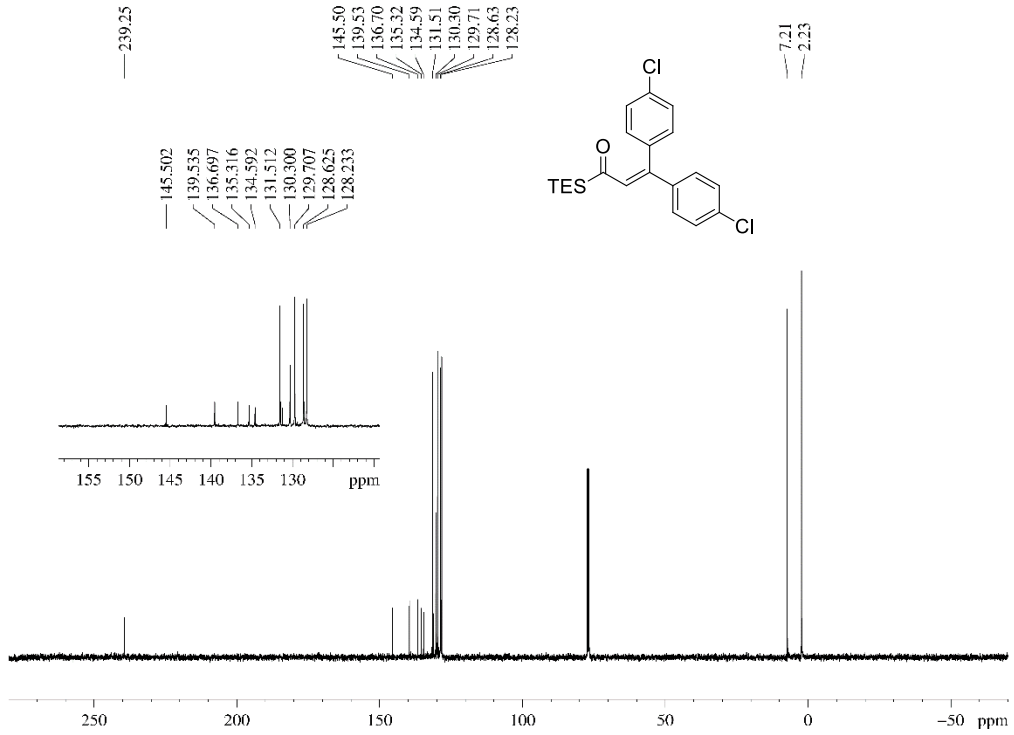

^{29}Si (80 MHz, $CDCl_3$)-NMR spectra of acylsilane **65o**

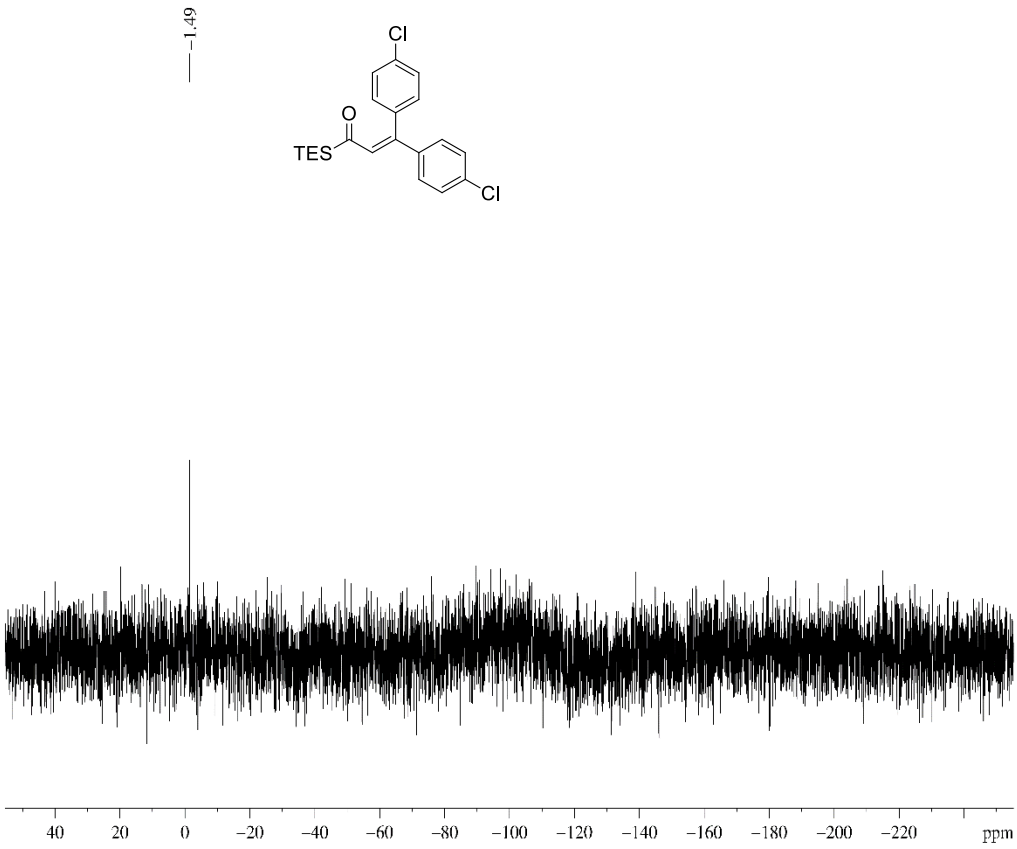

^{1}H (400 MHz, $CDCl_3$) and ^{13}C (100 MHz, $CDCl_3$)-NMR spectra of Enyne **66p**

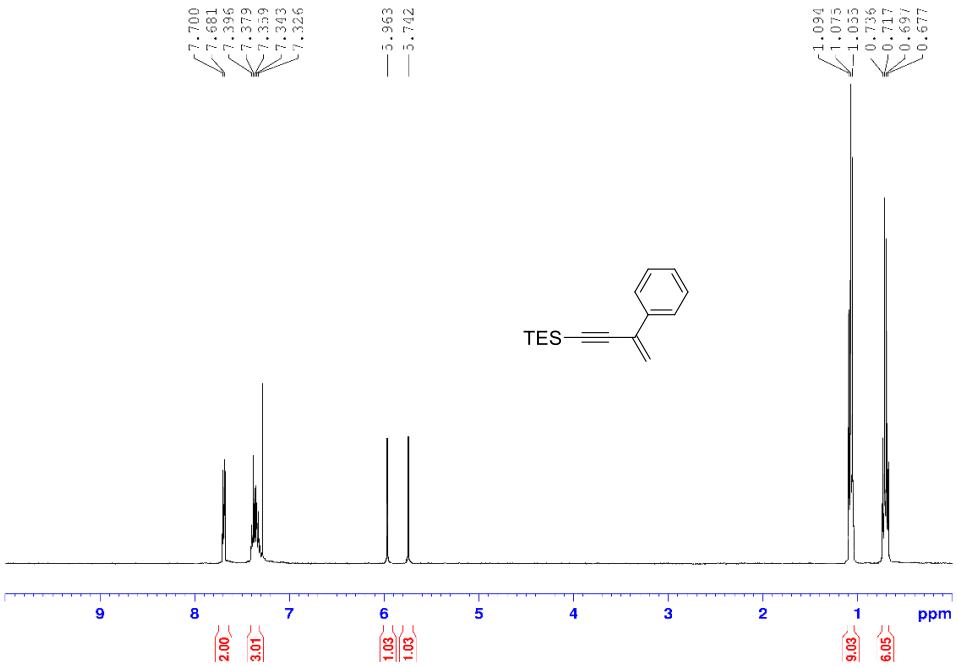

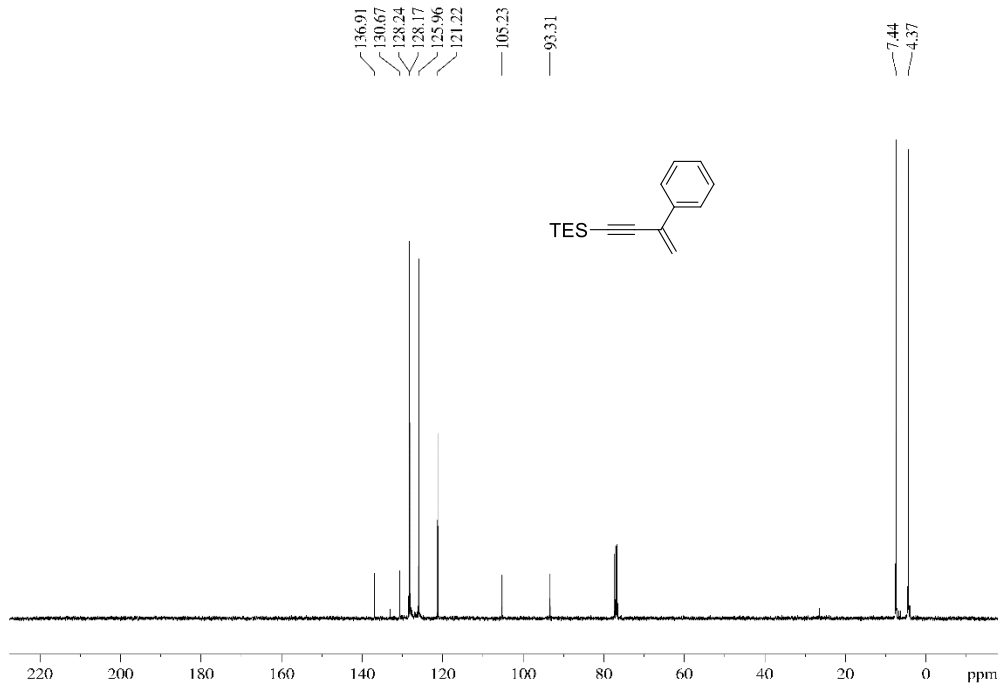

^{29}Si (80 MHz, $CDCl_3$)-NMR spectra of Enyne **66p**

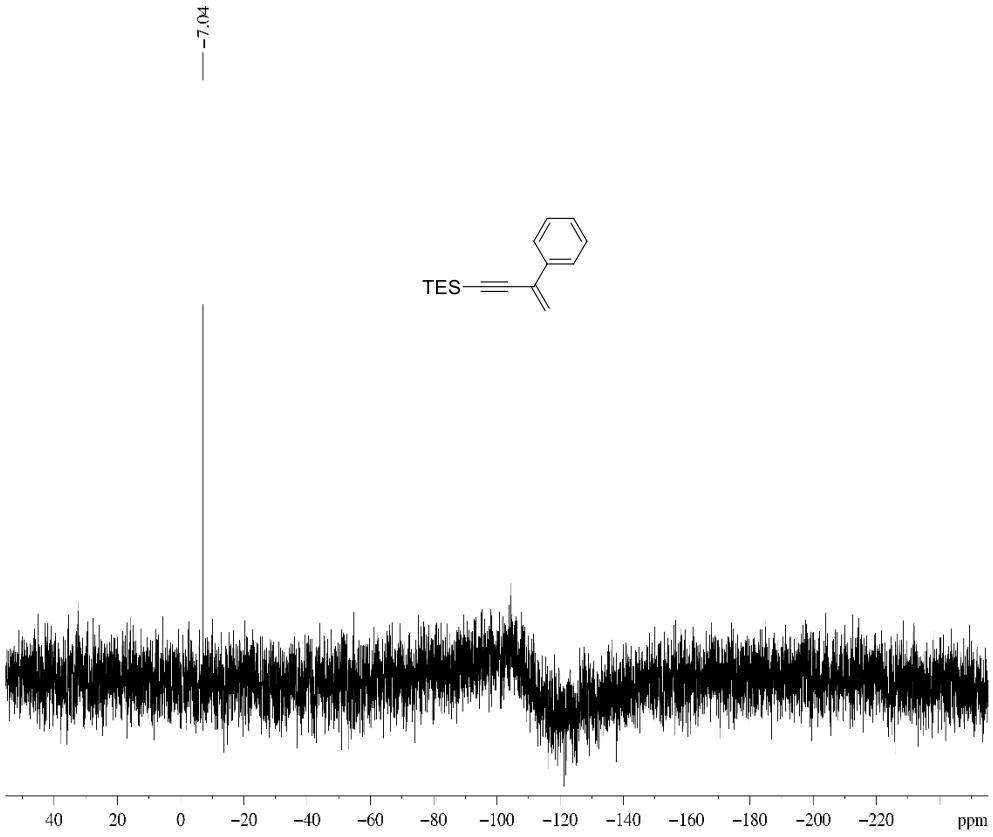

^{1}H (400 MHz, $CDCl_3$) and ^{13}C (100 MHz, $CDCl_3$)-NMR spectra of acylsilane **65p**

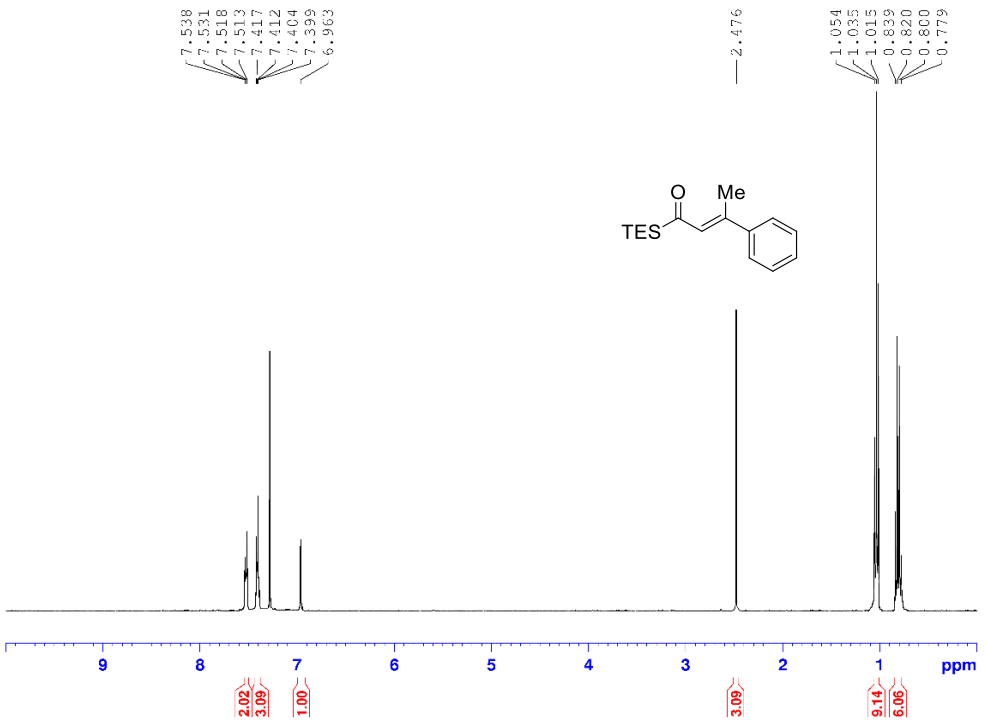

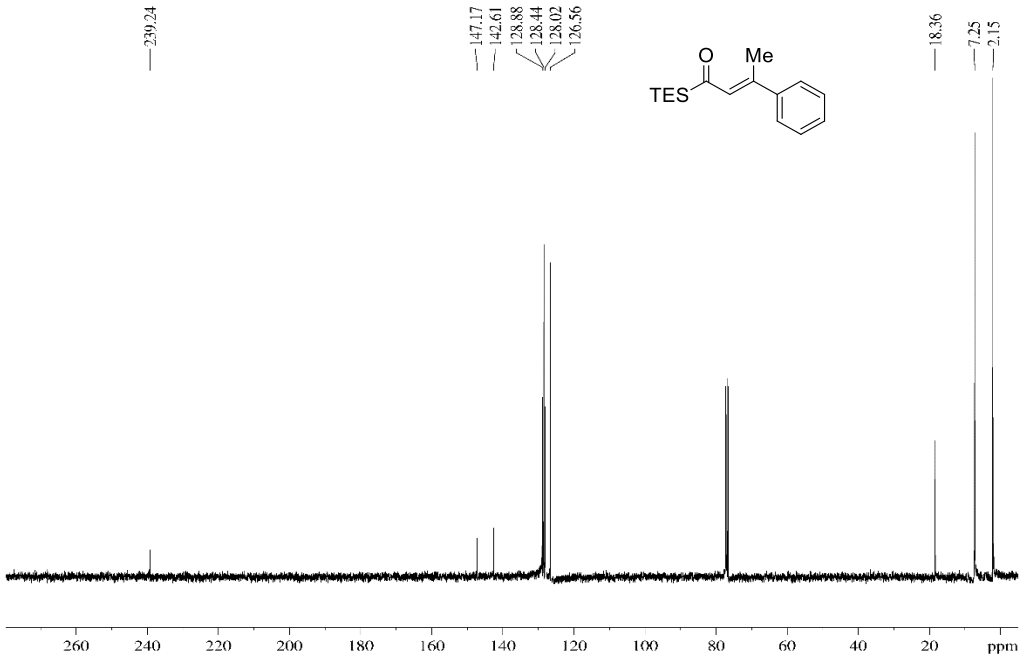

^{29}Si (80 MHz, $CDCl_3$)-NMR spectra of acylsilane **65p**

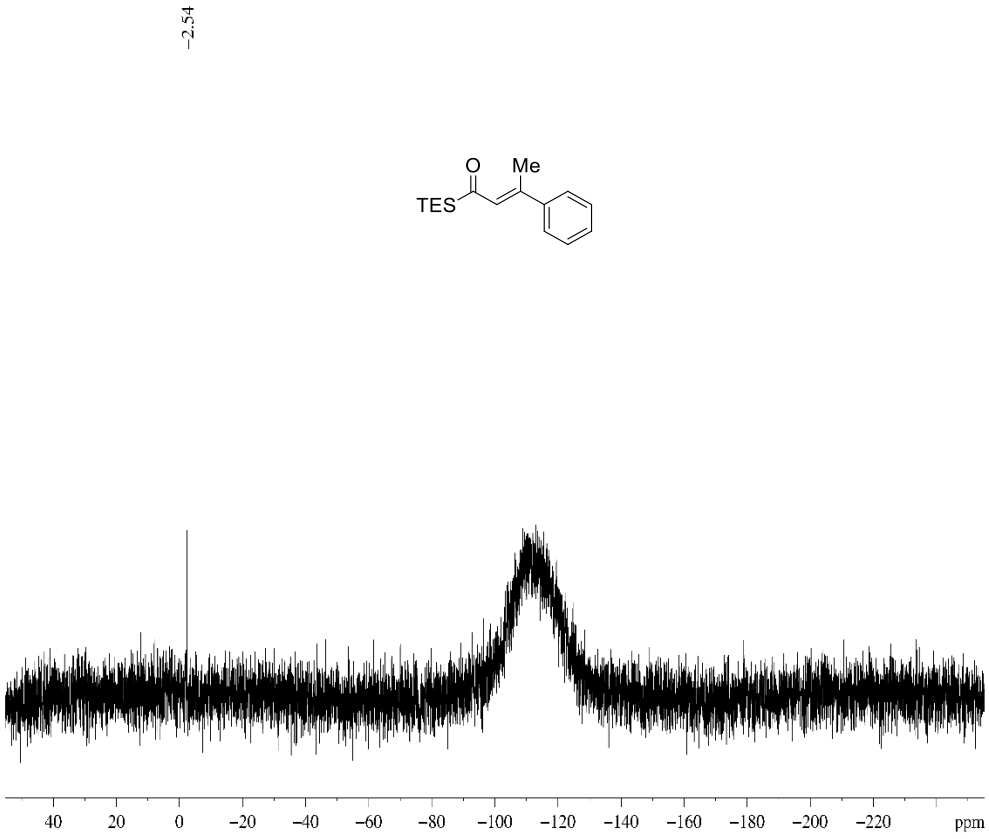

^{1}H (400 MHz, $CDCl_3$) and ^{13}C (100 MHz, $CDCl_3$)-NMR spectra of ketone **66q**

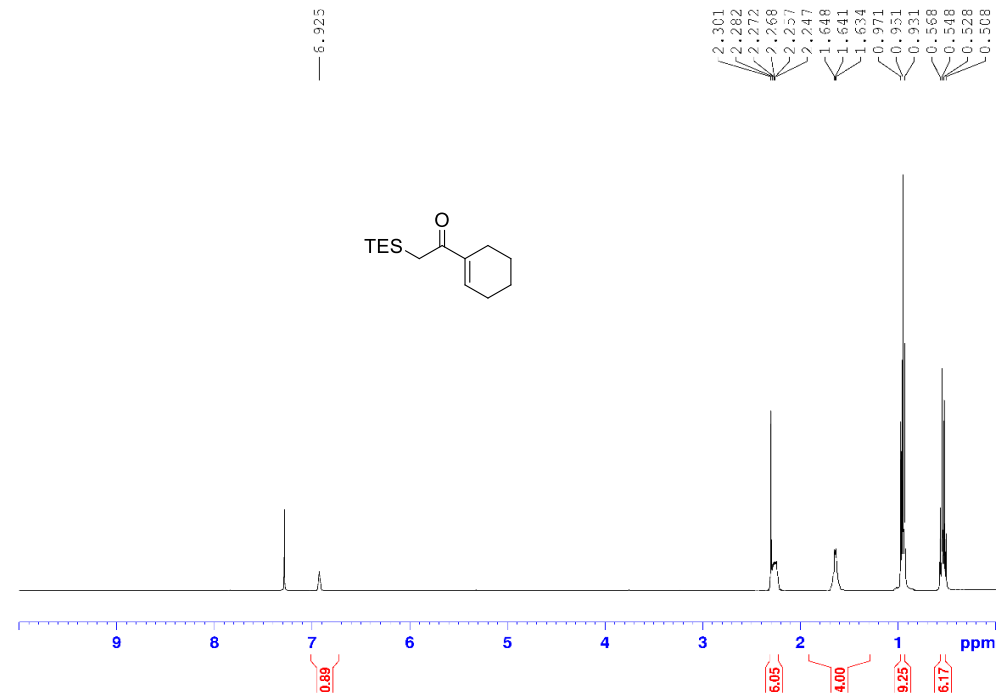

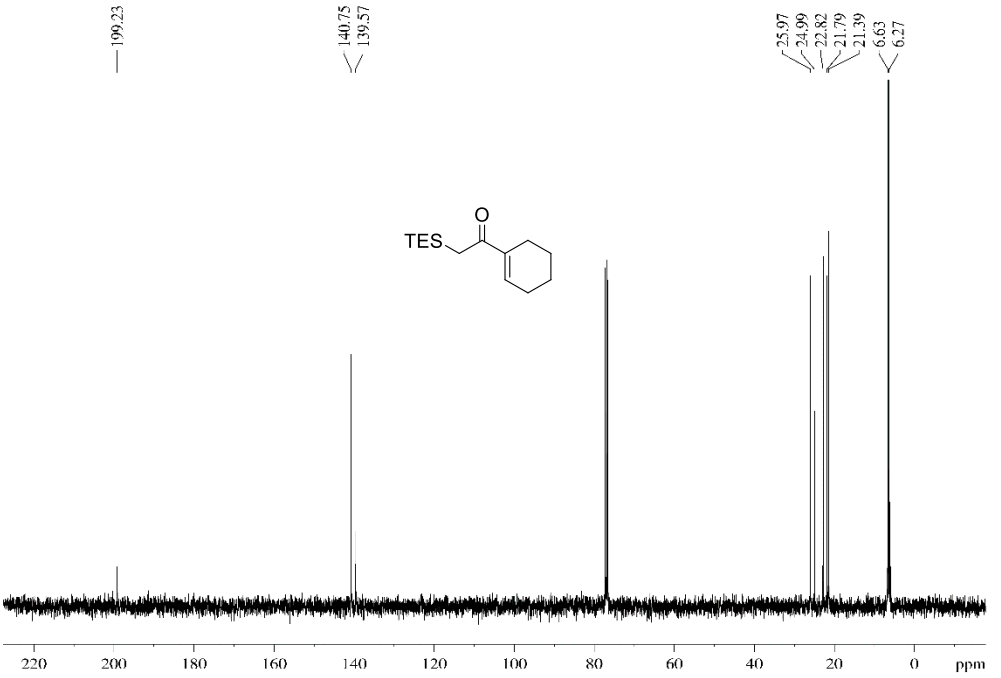

^{29}Si (80 MHz, $CDCl_3$)-NMR spectra of ketone **66q**

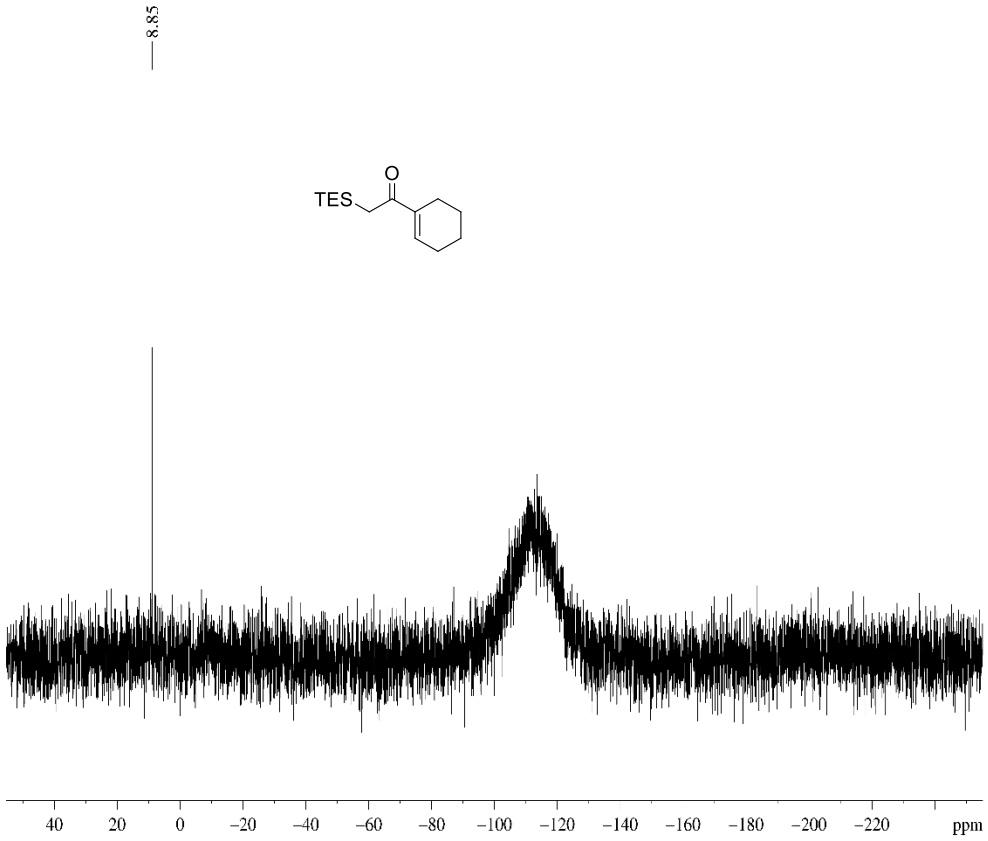

^{1}H (400 MHz, $CDCl_3$) and ^{13}C (100 MHz, $CDCl_3$)-NMR spectra of acylsilane **65t**

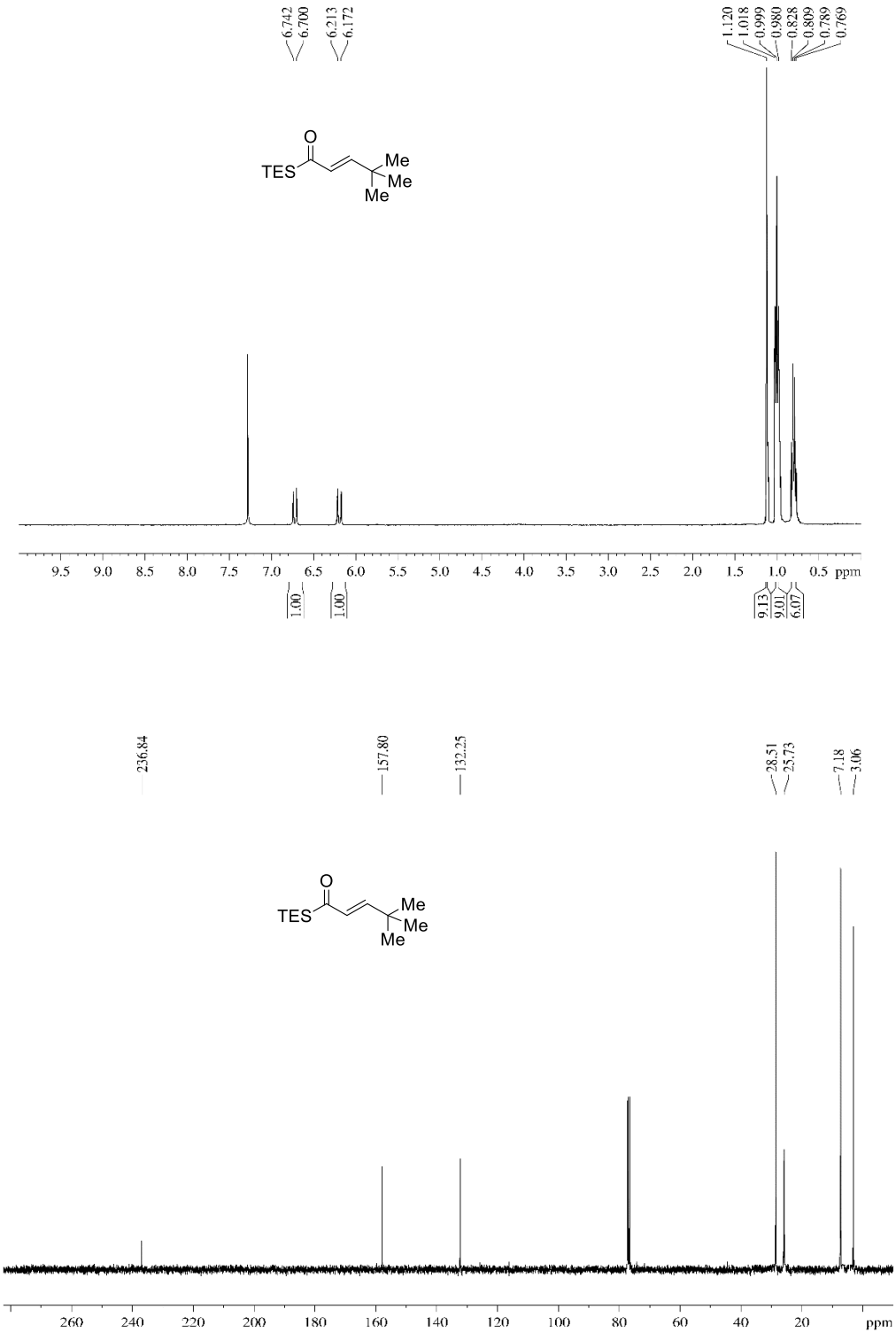

^{29}Si (80 MHz, $CDCl_3$)-NMR spectra of acylsilane **66t**

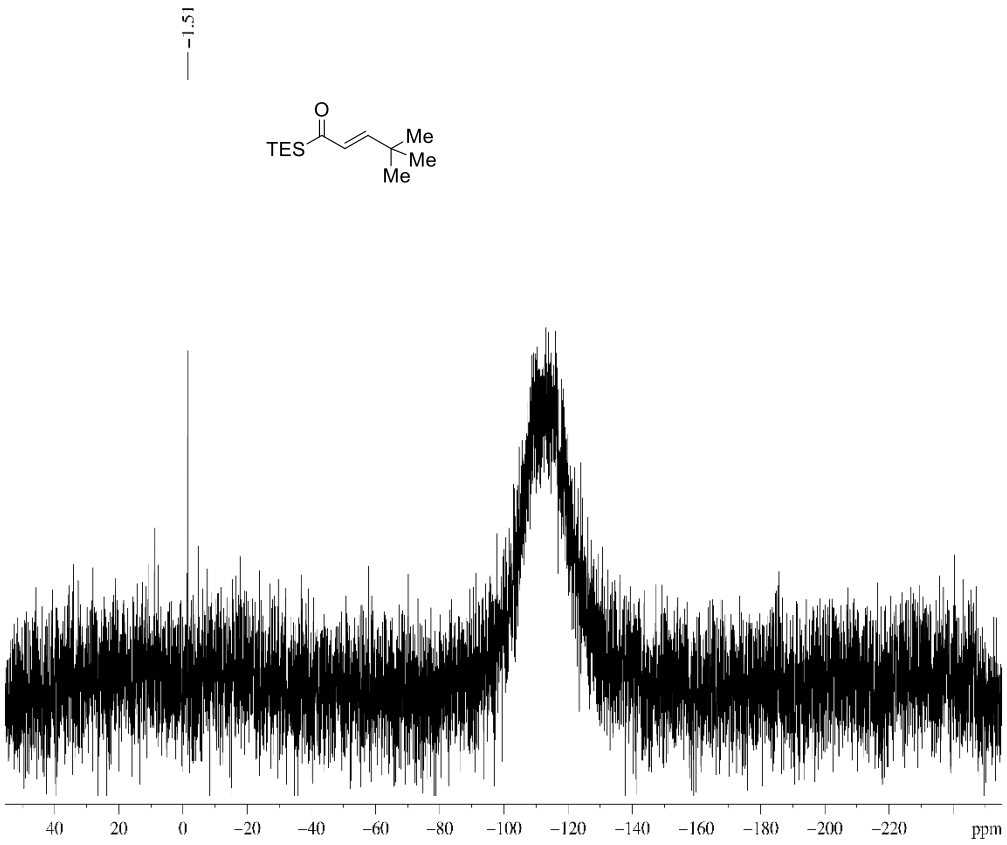

^{1}H (400 MHz, $CDCl_3$) and ^{13}C (100 MHz, $CDCl_3$)-NMR spectra of alcohols **64u** and **66u**

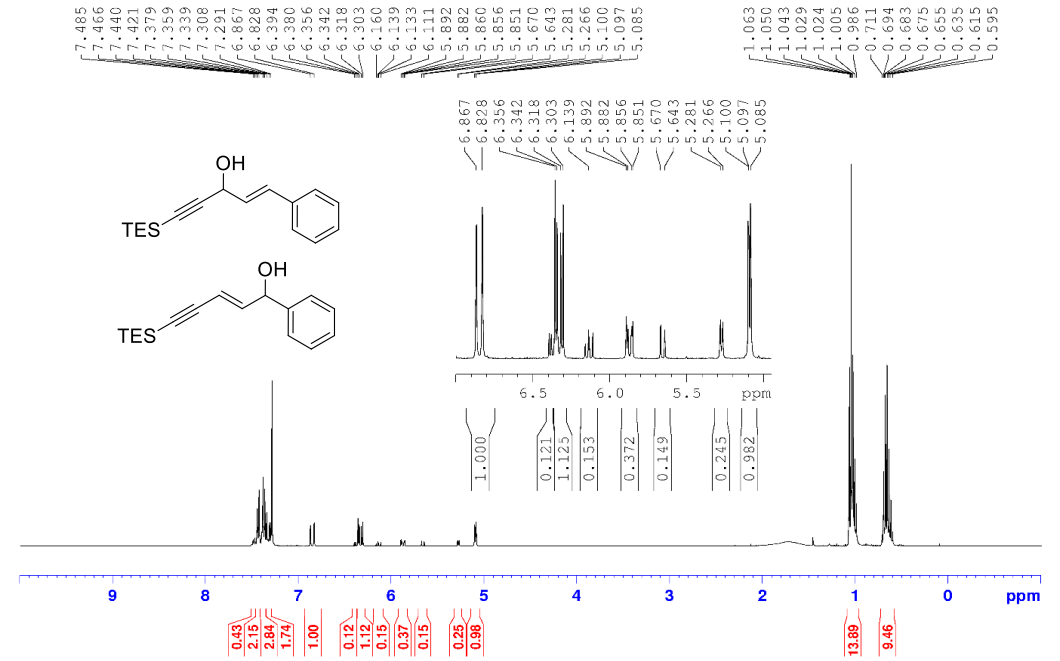

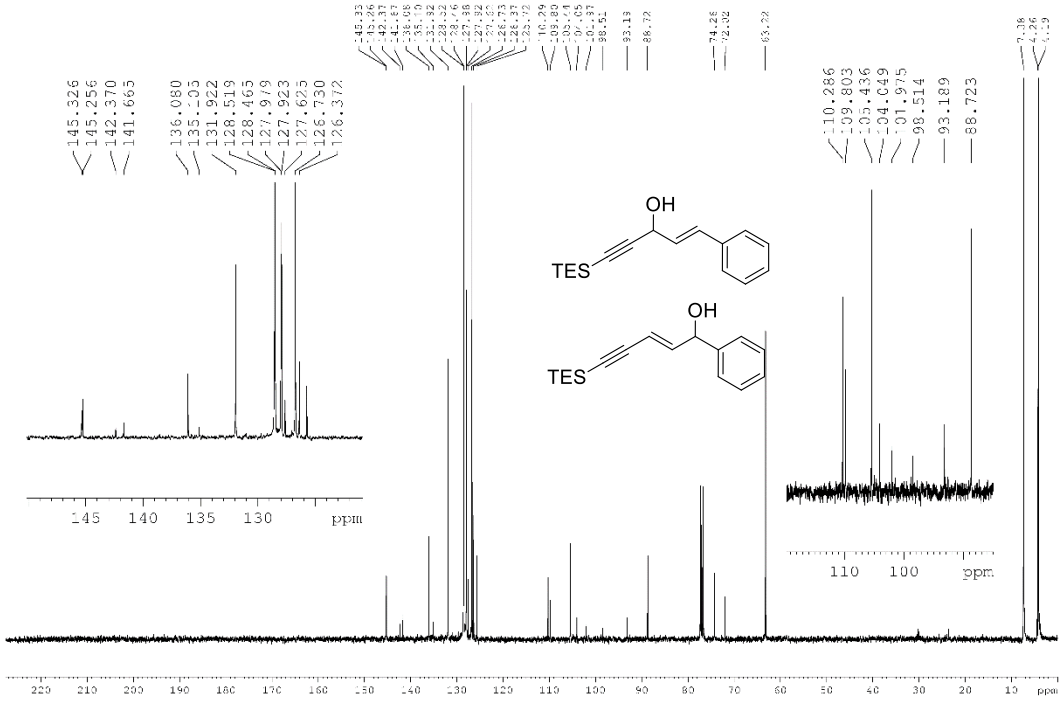

^{29}Si (80 MHz, $CDCl_3$)-NMR spectra of alcohols **64u** and **66u**

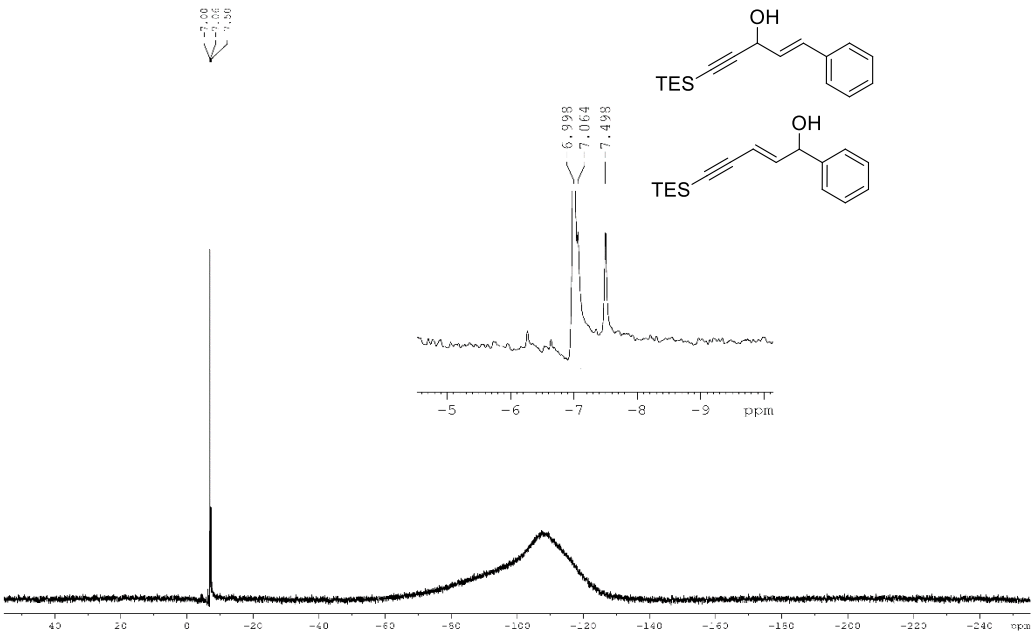

^{1}H (400 MHz, $CDCl_3$) and ^{13}C (100 MHz, $CDCl_3$)-NMR spectra of acylsilane **65u**

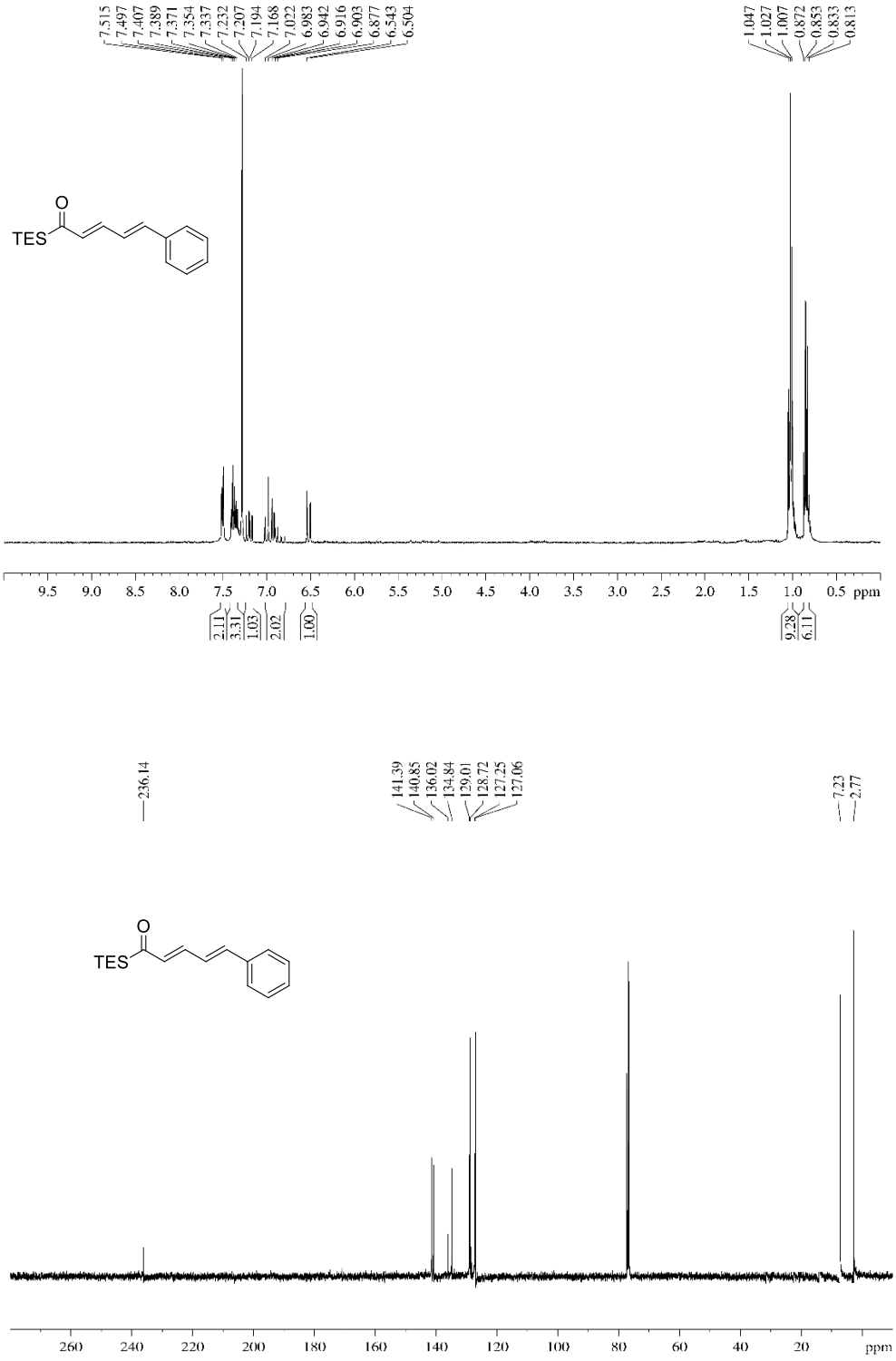

^{29}Si (80 MHz, $CDCl_3$)-NMR spectra of acylsilane **66u**

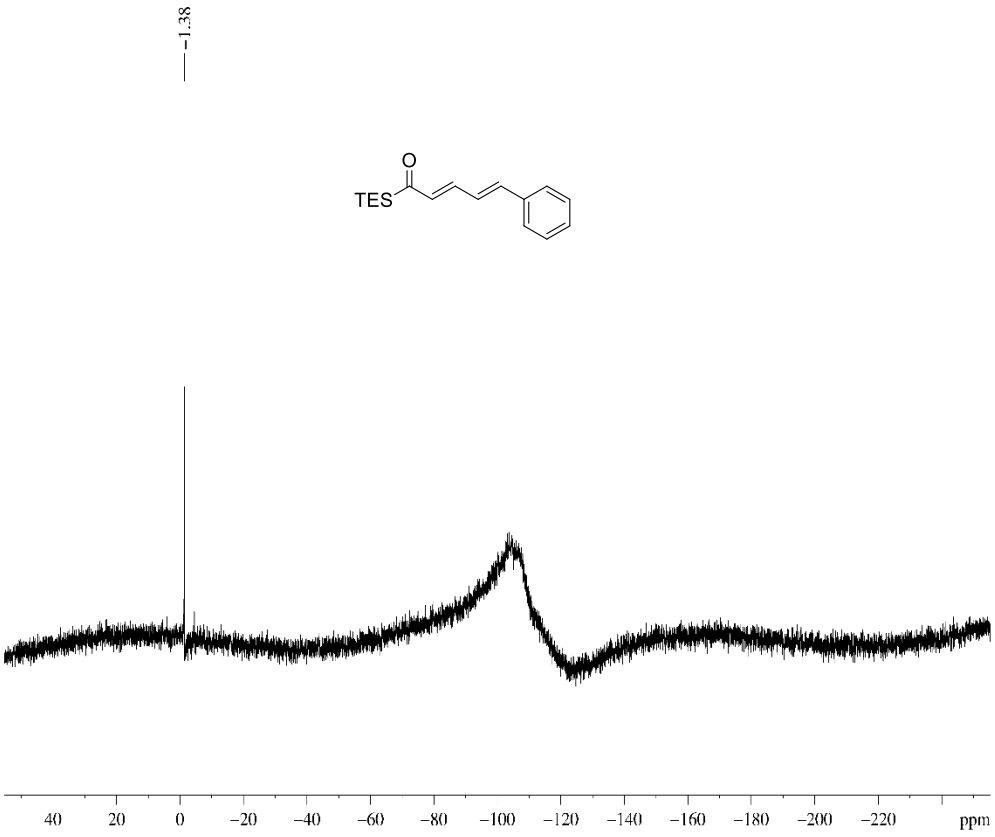

^{1}H (400 MHz, $CDCl_3$) and ^{13}C (100 MHz, $CDCl_3$)-NMR spectra of alcohols **66v** and **66v'**

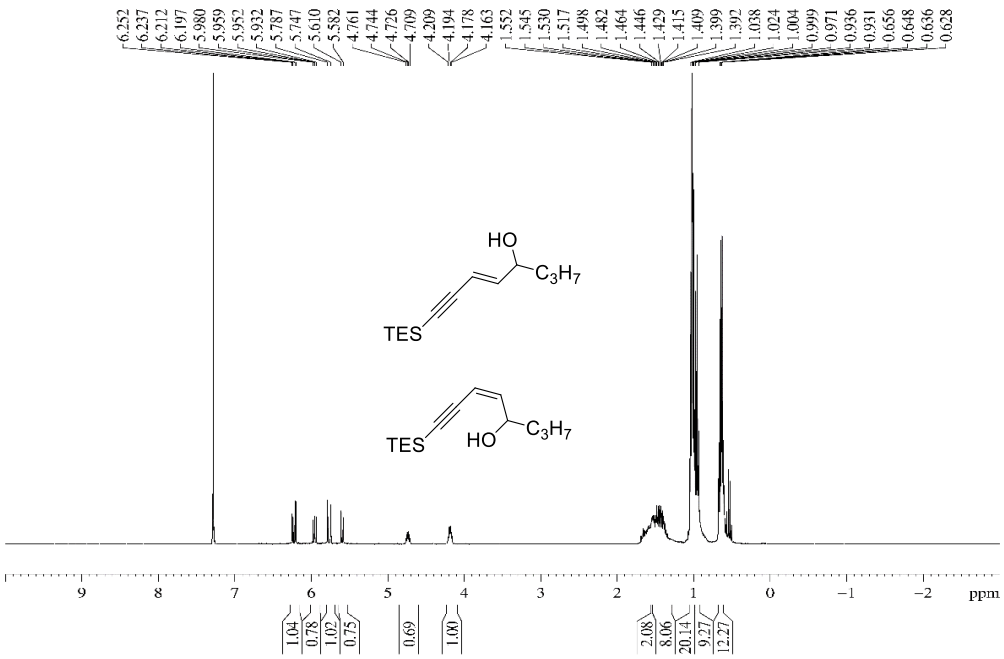

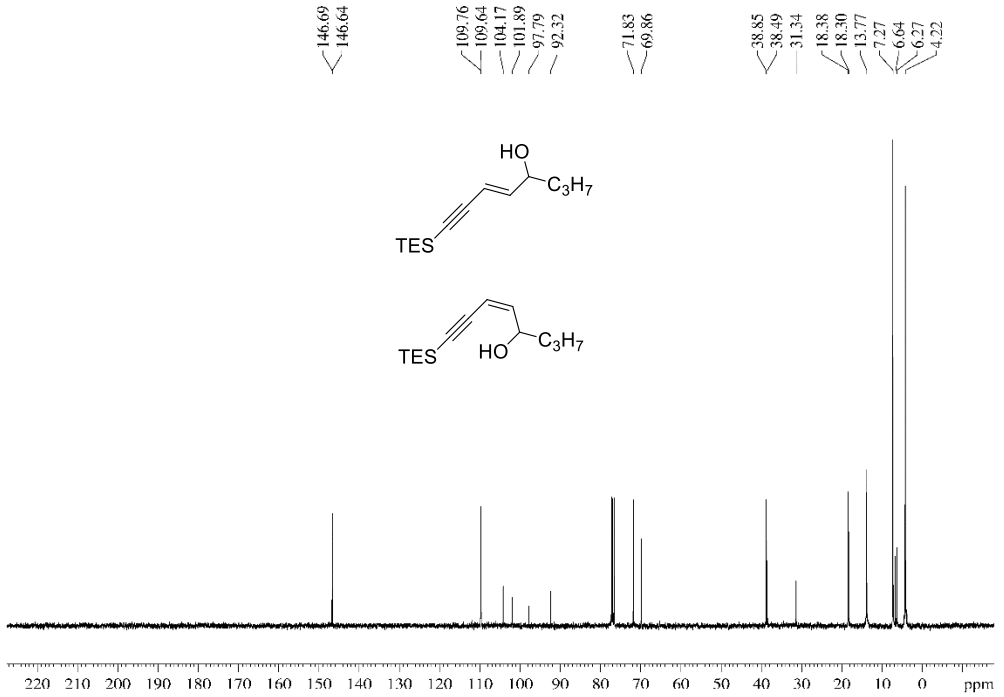

^{29}Si (80 MHz, $CDCl_3$)-NMR spectra of alcohols **64v** and **66v'**

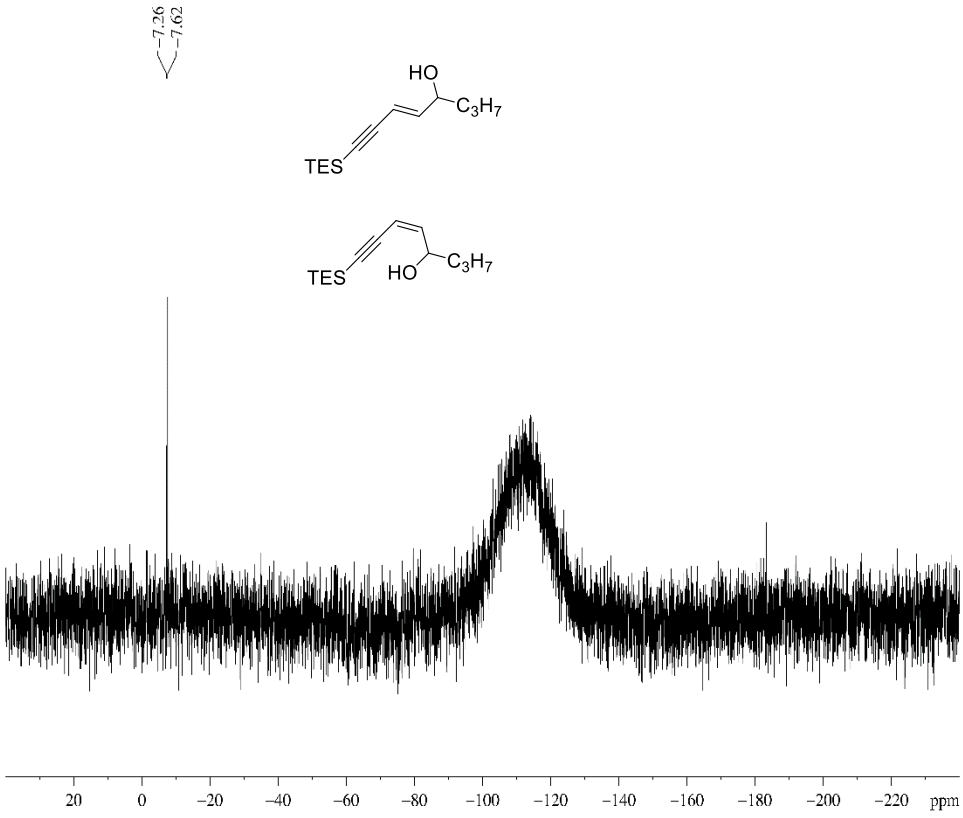

^{1}H (400 MHz, $CDCl_3$) and ^{13}C (100 MHz, $CDCl_3$)-NMR spectra of ketone **67v**

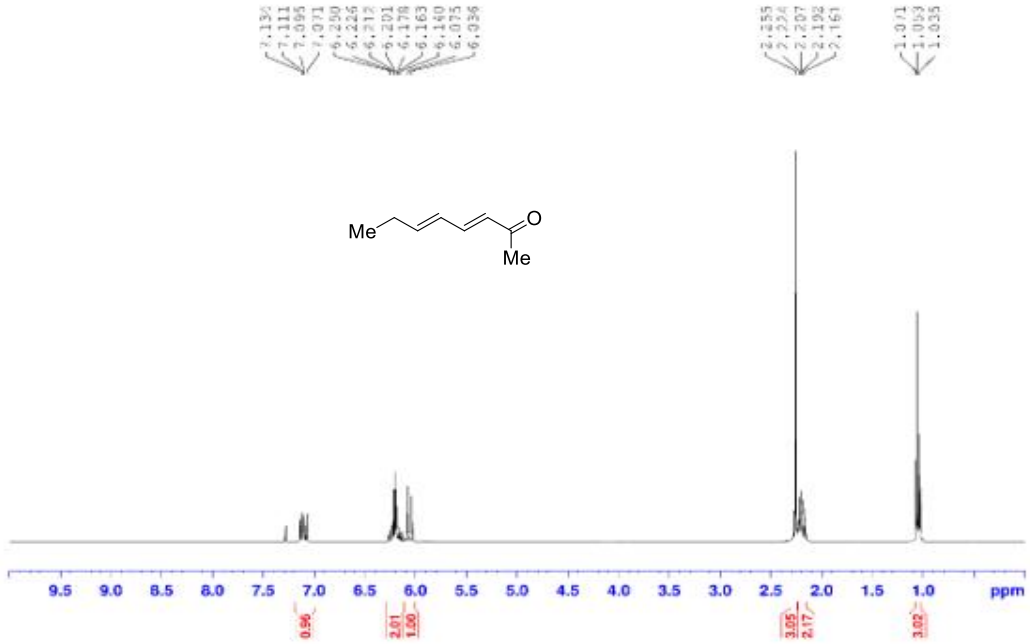

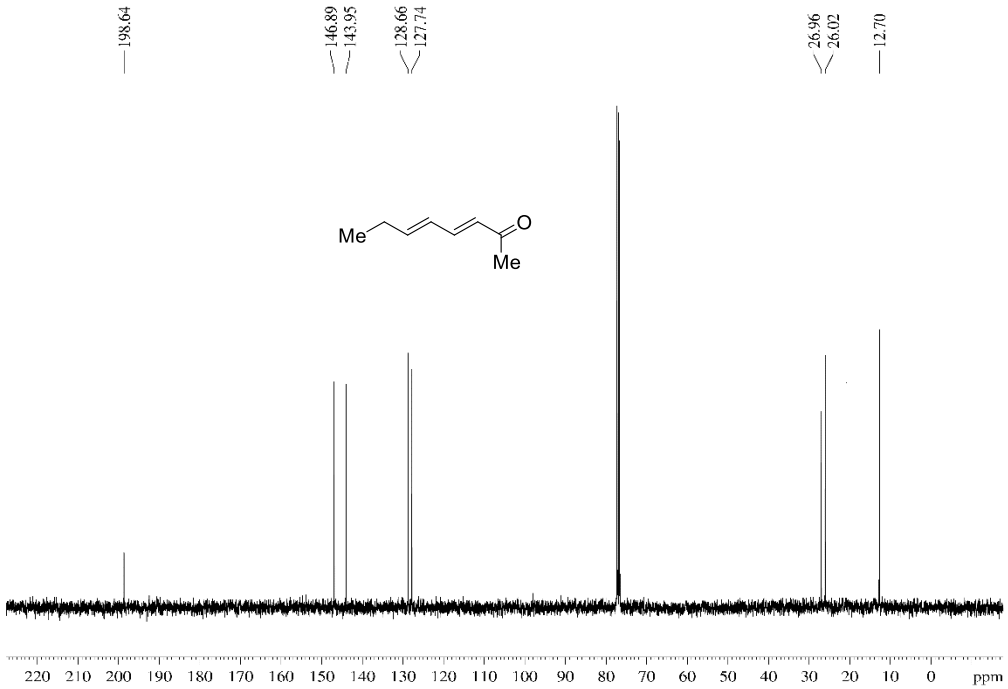

References

(1) Ley, S. V.; Baxendale, I. R. New Tools and Concepts for Modern Organic Synthesis. *Nat. Rev. Drug Discov.* **2002**, *1* (8), 573–586.

(2) Roy, D.; Uozumi, Y. Recent Advances in Palladium-Catalyzed Cross-Coupling Reactions at Ppm to Ppb Molar Catalyst Loadings. *Adv. Synth. Catal.* **2018**, *360* (4), 602–625.

(3) Studer, A.; Curran, D. P. Catalysis of Radical Reactions: A Radical Chemistry Perspective. *Angew. Chemie Int. Ed.* **2016**, *55* (1), 58–102.

(4) Ianni, A.; Waldvogel, S. Reliable and Versatile Synthesis of 2-Aryl-Substituted Cinnamic Acid Esters. *Synthesis (Stuttg).* **2006**, *2006* (13), 2103–2112.

(5) Dong Wook Kim, †; Choong Eui Song, ‡ and; Dae Yoon Chi*, †. Significantly Enhanced Reactivities of the Nucleophilic Substitution Reactions in Ionic Liquid. *J. Org. Chem.* **2003**, *68* (11), 4281–4285.

(6) Iranpoor, N.; Firouzabadi, H.; Khalili, D.; Motevalli, S. Easily Prepared Azopyridines As Potent and Recyclable Reagents for Facile Esterification Reactions. An Efficient Modified Mitsunobu Reaction. *J. Org. Chem.* **2008**, *73* (13), 4882–4887.

(7) Baughman, T. W.; Sworen, J. C.; Wagener, K. B. The Facile Preparation of Alkenyl Metathesis Synthons. *Tetrahedron* **2004**, *60* (48), 10943–10948.

(8) Seebach, D. Methods of Reactivity Umpolung. *Angew. Chemie Int. Ed. English* **1979**, *18* (4), 239–258.

(9) Seebach, D.; Corey, E. J. Generation and Synthetic Applications of 2-Lithio-1,3-Dithianes. *J. Org. Chem.* **1975**, *40* (2), 231–237.

(10) Read de Alaniz, J.; Rovis, T. A Highly Enantio- and Diastereoselective Catalytic Intramolecular Stetter Reaction. *J. Am. Chem. Soc.* **2005**, *127* (17), 6284–6289.

(11) Enders, D.; Niemeier, O.; Balensiefer, T. Asymmetric Intramolecular Crossed-Benzoin Reactions by N-Heterocyclic Carbene Catalysis. *Angew. Chemie Int. Ed.* **2006**, *45* (9), 1463–1467.

(12) SEEBACH, D.; WILKA, E.-M. Alkylation of 2-Lithio-1,3-Dithianes with Arenesulfonates of Primary Alcohols. *Synthesis (Stuttg).* **1976**, *1976* (07), 476–477.

(13) Nicolaou, K. C.; Mathison, C. J. N.; Montagnon, T. New Reactions of IBX: Oxidation of Nitrogen- and Sulfur-Containing Substrates To Afford Useful Synthetic Intermediates. *Angew. Chemie Int. Ed.* **2003**, *42* (34), 4077–4082.

(14) Fleming, F. F.; Funk, L.; Altundas, R.; Tu, Y. Deprotecting Dithiane-Containing Alkaloids. *J. Org. Chem.* **2001**, *66* (19), 6502–6504.

(15) Liu, J.; Wong, C.-H. An Efficient Method for the Cleavage of P-Methoxybenzylidene (PMP), Tetrahydropyranyl (THP) and 1,3-Dithiane Protecting Groups by Selectfluor™. *Tetrahedron Lett.* **2002**, *43* (22), 4037–4039.

(16) Brook, A. G. Molecular Rearrangements of Organosilicon Compounds. *Acc. Chem. Res.* **1974**, *7* (3), 77–84.

(17) Luo, Y.-R.; Luo, Y.-R. *Comprehensive Handbook of Chemical Bond Energies*; CRC Press, 2007.

(18) Akira Tsubouchi, *; Kotaro Onishi, A.; Takeda*, T. Stereoselective Preparation of 1-Siloxy-1-Alkenylcopper Species by 1,2-Csp2-to-O Silyl Migration of Acylsilanes. *J. Am. Chem. Soc.* **2006**, *128* (44), 14268–14269.

(19) Page, P. C. B.; Klair, S. S.; Rosenthal, S. Synthesis and Chemistry of Acyl Silanes. *Chem. Soc. Rev.* **1990**, *19* (2), 147–195.

(20) Kei Takeda, *,†, ‡; Hidekazu Haraguchi, † and; Okamoto‡, Y. A New Strategy for Construction of Eight-Membered Carbocycles by Brook Rearrangement Mediated [6 + 2] Annulation. *Org. Lett.* **2003**, *5* (20), 3705–3707.

(21) Bensari, A.; Zaveri, N. T. Titanium(IV) Chloride-Mediated Ortho-Acylation of Phenols and Naphthols. *Synthesis (Stuttg).* **2003**, No. 2, 267–271.

(22) Seyferth, D.; American Chemical Society. *New Applications of Organometallic Reagents in Organic Synthesis : Proceedings of a Symposium at the American Chemical Society National Meeting Held in New York City, April 6-9th, 1976*; Elsevier Scientific Pub. Co., 1976.

(23) Nickon, A.; Lambert, J. L. S. J. **Homoenolate Anions**. *J. Am. Chem. Soc.* **1962**, *84* (23), 4604–4605.

(24) Nickon, A.; Lambert, J. L.; Lambert, S. J. Homoenolization and Related Phenomena. IV. Evidence for Homoenolate Anions [1,2]. *J. Am. Chem. Soc.* **1966**, *88* (9), 1905–1910.

(25) Buechi, G.; Wuest, H. Synthesis of (+-)-Nuciferal. *J. Org. Chem.* **1969**, *34* (4), 1122–1123.

(26) Goswami, R. A New Method for Generating Trichlorotitanium(IV) Ester Homoenolates. Direct Tin-Titanium Exchange. *J. Org. Chem.* **1985**, *50* (26), 5907–5909.

(27) Nakamura, E.; Kuwajima, I. Homoenolate Anion Precursor. Reaction of Ester Homoenol Silyl Ether with Carbonyl Compounds. *J. Am. Chem. Soc.* **1977**, *99* (22), 7360–7362.

(28) Nakamura, E.; Shimada, J.; Kuwajima, I. A Ring-Opening Reaction of 1-Siloxy-1-Alkoxycyclopropanes. Preparation of Main-Group Metal Homoenolates of Alkyl Propionate. *Organometallics* **1985**, *4* (4), 641–646.

(29) Nakamura, E.; Kuwajima, I. Palladium Catalyzed Reactions of Propionate Homoemolate. Arylation, Vinylation, and Acylation. *Tetrahedron Lett.* **1986**, *27* (1), 83–86.

(30) Nakamura, E.; Aoki, S.; Sekiya, K.; Oshino, H.; Kuwajima, I. Carbon-Carbon Bond-Forming Reactions of Zinc Homoenolate of Esters. A Novel Three-Carbon Nucleophile with General Synthetic Utility. *J. Am. Chem. Soc.* **1987**, *109* (26), 8056–8066.

(31) Johnson, C. R.; Marren, T. J. Trimethylsilyl Chloride/Tetramethylethylenediamine Facilitated Additions of Organocopper Reagents (RCu) to Enones. *Tetrahedron Lett.* **1987**, *28* (1), 27–30.

(32) Ryu, I.; Matsumoto, K.; Ando, M.; Murai, S.; Sonoda, N. Synthesis of β-Mercuri Ketones by the Reaction of Siloxycyclopropanes with Mercuric Acetate and Their Conversion to α-Methylene Ketones and γ-Ketoesters. *Tetrahedron Lett.* **1980**, *21* (44), 4283–4286.

(33) Ryu, I.; Murai, S.; Sonoda, N. A Novel Synthesis of .Beta.-Trichlorostannyl Ketones from Siloxycyclopropanes and Their Facile Dehydrostannation Affording 2-Methylene Ketones. *J. Org. Chem.* **1986**, *51* (12), 2389–2391.

(34) Bennett, M. A.; Watt, R. Acyl Group Migration to a Co-Ordinated Double Bond: A Stable π-

Oxapropenyl Complex of Manganese. *J. Chem. Soc. D* **1971**, *0* (2), 95–96.

(35) Kuwajima, I.; Kato, M. 1-Trimethylsilylallylic Alcohols as Homoenolate Precursors. Stereo- and Regio-Specific Synthesis of Silyl Enol Ethers. *J. Chem. Soc. Chem. Commun.* **1979**, *0* (16), 708–709.

(36) Aoki, S.; Fujimura, T.; Nakamura, E.; Kuwajima, I. Palladium-Catalyzed Arylation of Siloxycyclopropanes with Aryl Triflates. Carbon Chain Elongation via Catalytic Carbon-Carbon Bond Cleavage. *J. Am. Chem. Soc.* **1988**, *110* (10), 3296–3298.

(37) Aoki, S.; Nakamura, E.; Kuwajima, I. Synthesis of 4-Keto Pimelates by Palladium-Catalyzed Carbonylativesymmetrical Coupling of Siloxycyclopropanes. *Tetrahedron Lett.* **1988**, *29* (13), 1541–1542.

(38) Aoki, S.; Fujimura, T.; Nakamura, E.; Kuwajima, I. Palladium- and Platinum-Catalyzed Reaction of Siloxycyclopropanes with Acid Chlorides. A Homoenolate Route to 1,4-Dicarbonyl Compounds. *Tetrahedron Lett.* **1989**, *30* (47), 6541–6544.

(39) Aoki, S.; Nakamura, E. Synthesis of 1,4-Dicarbonyl Compounds by Palladium-Catalyzed Carbonylative Arylation of Siloxycyclopropanes. *Synlett* **1990**, *1990* (12), 741–742.

(40) Fujimura, T.; Aoki, S.; Nakamura, E. Synthesis of 1,4-Keto Esters and 1,4-Diketones via Palladium-Catalyzed Acylation of Siloxycyclopropanes. Synthetic and Mechanistic Studies. *J. Org. Chem.* **1991**, *56* (8), 2809–2821.

(41) Kang, S.-K.; Yamaguchi, T.; Ho, P.-S.; Kim, W.-Y.; Yoon, S.-K. Palladium-Catalyzed Coupling and Carbonylative Coupling of Silyloxy Compounds with Hypervalent Iodonium Salts. *Tetrahedron Lett.* **1997**, *38* (11), 1947–1950.

(42) Rosa, D.; Orellana, A. Palladium-Catalyzed Cross-Coupling of Cyclopropanols with Aryl Halides Under Mild Conditions. *Org. Lett.* **2011**, *13* (1), 110–113.

(43) Rosa, D.; Orellana, A. Palladium-Catalyzed Cross-Coupling of Cyclopropanol-Derived Ketone Homoenolates with Aryl Bromides. *Chem. Commun.* **2013**, *49* (47), 5420–5422.

(44) Nithiy, N.; Orellana, A. Palladium-Catalyzed Cross-Coupling of Benzyl Chlorides with Cyclopropanol-Derived Ketone Homoenolates. *Org. Lett.* **2014**, *16* (22), 5854–5857.

(45) Ydhyam, S.; Cha, J. K. Construction of Seven-Membered Carbocycles via Cyclopropanols. *Org. Lett.* **2015**, *17* (23), 5820–5823.

(46) Park; Cha. Palladium-Mediated Ring Opening of Hydroxycyclopropanes. *Org. Lett.* **2000**, *2* (2), 147–149.

(47) Cheng, K.; Walsh, P. J. Arylation of Aldehyde Homoenolates with Aryl Bromides. *Org. Lett.* **2013**, *15* (9), 2298–2301.

(48) Martinez, A. M.; Cushmac, G. E.; Rocek, J. Chromic Acid Oxidation of Cyclopropanols. *J. Am. Chem. Soc.* **1975**, *97* (22), 6502–6510.

(49) Iwasawa, N.; Hayakawa, S.; Isobe, K.; Narasaka, K. Generation of β-Keto Radicals from Cyclopropanol Derivatives by the Use of Manganese(III) 2-Pyridinecarboxylate as an Oxidant and Their Reactions with Olefins. *Chem. Lett.* **1991**, *20* (7), 1193–1196.

(50) Iwasawa, N.; Hayakawa, S.; Funahashi, M.; Isobe, K.; Narasaka, K. Generation of *β* -Carbonyl

Radicals from Cyclopropanol Derivatives by the Oxidation with Manganese(III) 2-Pyridinecarboxylate and Their Reactions with Electron-Rich and -Deficient Olefins. *Bull. Chem. Soc. Jpn.* **1993**, *66* (3), 819–827.

(51) Iwasawa, N.; Funahashi, M.; Hayakawa, S.; Narasaka, K. Synthesis of Medium-Sized Bicyclic Compounds by Intramolecular Cyclization of Cyclic β-Keto Radicals Generated from Cyclopropanols Using Manganese(III) Tris(2-Pyridinecarboxylate). *Chem. Lett.* **1993**, *22* (3), 545–548.

(52) Narasaka, K. Generation of Radical Species by One Electron Oxidation with Metallic Compounds for the Construction of Carbon Skeletons. *Pure Appl. Chem.* **1997**, *69* (3), 601–604.

(53) Iwasawa, N.; Funahashi, M.; Hayakawa, S.; Ikeno, T.; Narasaka, K. Synthesis of Medium-Sized Bicyclic Compounds by Intramolecular Cyclization of Cyclic *β* -Keto Radicals Generated from Cyclopropanols Using Manganese(III) Tris(Pyridine-2-Carboxylate) and Its Application to Total Synthesis of 10-Isothiocyanatoguaia-6-Ene. *Bull. Chem. Soc. Jpn.* **1999**, *72* (1), 85–97.

(54) Chiba, S.; Cao, Z.; El Bialy, S. A. A.; Narasaka, K. Generation of β-Keto Radicals from Cyclopropanols Catalyzed by $AgNO_3$. *Chem. Lett.* **2006**, *35* (1), 18–19.

(55) Ishida, N.; Okumura, S.; Nakanishi, Y.; Murakami, M. Ring-Opening Fluorination of Cyclobutanols and Cyclopropanols Catalyzed by Silver. *Chem. Lett.* **2015**, *44* (6), 821–823.

(56) Zhao, H.; Fan, X.; Yu, J.; Zhu, C. Silver-Catalyzed Ring-Opening Strategy for the Synthesis of β- and γ-Fluorinated Ketones. *J. Am. Chem. Soc.* **2015**, *137* (10), 3490–3493.

(57) Huang, F.-Q.; Xie, J.; Sun, J.-G.; Wang, Y.-W.; Dong, X.; Qi, L.-W.; Zhang, B. Regioselective Synthesis of Carbonyl-Containing Alkyl Chlorides via Silver-Catalyzed Ring-Opening Chlorination of Cycloalkanols. *Org. Lett.* **2016**, *18* (4), 684–687.

(58) Kevin I. Booker-Milburn, *, †; J. Leighton Jones, †; Graham E. M. Sibley, †; Richard Cox, ‡ and; Meadows‡, J. New Fe(III)-Mediated Radical Cascade Reactions of Cyclopropyl Silyl Ethers. *Org. Lett.* **2003**, *5* (7), 1107–1109.

(59) Li, Y.; Ye, Z.; Bellman, T. M.; Chi, T.; Dai, M. Efficient Synthesis of β-CF_3 /SCF_3 -Substituted Carbonyls via Copper-Catalyzed Electrophilic Ring-Opening Cross-Coupling of Cyclopropanols. *Org. Lett.* **2015**, *17* (9), 2186–2189.

(60) Kirihara, M.; Kakuda, H.; Ichinose, M.; Ochiai, Y.; Takizawa, S.; Mokuya, A.; Okubo, K.; Hatano, A.; Shiro, M. Fragmentation of Tertiary Cyclopropanol Compounds Catalyzed by Vanadyl Acetylacetonate. *Tetrahedron* **2005**, *61* (20), 4831–4839.

(61) Li, A.-H.; Beard, D.; Coate, H.; Honda, A.; Kadalbajoo, M.; Kleinberg, A.; Laufer, R.; Mulvihill, K.; Nigro, A.; Rastogi, P.; et al. One-Pot Friedländer Quinoline Synthesis: Scope and Limitations. *Synthesis (Stuttg).* **2010**, *2010* (10), 1678–1686.

(62) Minetto, G.; Raveglia, L. F.; Sega, A.; Taddei, M. Microwave-Assisted Paal-Knorr Reaction - Three-Step Regiocontrolled Synthesis of Polysubstituted Furans, Pyrroles and Thiophenes. *European J. Org. Chem.* **2005**, *2005* (24), 5277–5288.

(63) and, M. J. S.; DeShong*, P. Reductive Cyclization of O-Nitrophenyl Propargyl Alcohols: Facile Synthesis of Substituted Quinolines†. *Org. Lett.* **2007**, *9* (17), 3209–3212.

(64) Yang, X.; Li, L.; Li, Y.; Zhang, Y. Visible-Light-Induced Photocatalytic Aerobic Oxidative C_{sp3} –H Functionalization of Glycine Derivatives: Synthesis of Substituted Quinolines. *J. Org. Chem.* **2016**, *81* (24), 12433–12442.

(65) Abbiati, G.; Arcadi, A.; Marinelli, F.; Rossi, E.; Verdecchia, M. Rh-Catalyzed Sequential Hydroarylation/Hydrovinylation-Heterocyclization of β-(2-Aminophenyl)-α,β-Ynones with Organoboron Derivatives: A New Approach to Functionalized Quinolines. *Synlett* **2006**, No. 19, 3218–3224.

(66) Bin Yan; Yebing Zhou; Hao Zhang; Jingjin Chen, A.; Liu*, Y. Highly Efficient Synthesis of Functionalized Indolizines and Indolizinones by Copper-Catalyzed Cycloisomerizations of Propargylic Pyridines. *J. Org. Chem.* **2007**, *72* (20), 7783–7786.

(67) Larock, R. C.; Kuo, M.-Y. Palladium-Catalyzed Synthesis of Quinolines from Allylic Alcohols and o-Iodoaniline. *Tetrahedron Lett.* **1991**, *32* (5), 569–572.

(68) Mahajan, J. P.; Suryawanshi, Y. R.; Mhaske, S. B. Pd-Catalyzed Imine Cyclization: Synthesis of Antimalarial Natural Products Aplidiopsamine A, Marinoquinoline A, and Their Potential Hybrid NCLite-M1. *Org. Lett.* **2012**, *14* (22), 5804–5807.

(69) Waibel, M.; Cramer, N. Palladium-Catalyzed Arylative Ring-Opening Reactions of Norbornenols: Entry to Highly Substituted Cyclohexenes, Quinolines, and Tetrahydroquinolines. *Angew. Chemie Int. Ed.* **2010**, *49* (26), 4455–4458.

(70) Gowrisankar, S.; Lee, H. S.; Kim, J. M.; Kim, J. N. Pd-Mediated Synthesis of 2-Arylquinolines and Tetrahydropyridines from Modified Baylis–Hillman Adducts. *Tetrahedron Lett.* **2008**, *49* (10), 1670–1673.

(71) Cho, C. S.; Kim, J. U. An Approach for Quinolines via Palladium-Catalyzed Heck Coupling Followed by Cyclization. *Tetrahedron Lett.* **2007**, *48* (22), 3775–3778.

(72) Cho, C. S. Palladium-Catalyzed Sonogashira Coupling Reaction Followed by Isomerization and Cyclization. *J. Organomet. Chem.* **2005**, *690* (17), 4094–4097.

(73) Mahanty, J. S.; De, M.; Das, P.; Kundu, N. G. Palladium-Catalyzed Heteroannulation with Acetylenic Carbinols as Synthons-Synthesis of Quinolines and 2,3-Dihydro-4(1H)-Quinolones. *Tetrahedron* **1997**, *53* (39), 13397–13418.

(74) Stone, M. T. An Improved Larock Synthesis of Quinolines via a Heck Reaction of 2-Bromoanilines and Allylic Alcohols. *Org. Lett.* **2011**, *13* (9), 2326–2329.

(75) Kulinkovich, O. G. The Chemistry of Cyclopropanols. *Chem. Rev.* **2003**, *103* (7), 2597–2632.

(76) Wang, D.-W.; Wang, X.-B.; Wang, D.-S.; Lu, S.-M.; Zhou, Y.-G.; Li, Y.-X. Highly Enantioselective Iridium-Catalyzed Hydrogenation of 2-Benzylquinolines and 2-Functionalized and 2,3-Disubstituted Quinolines. *J. Org. Chem.* **2009**, *74* (7), 2780–2787.

(77) Cheng, K.; Carroll, P. J.; Walsh, P. J. Diasteroselective Preparation of Cyclopropanols Using Methylene Bis(Iodozinc). *Org. Lett.* **2011**, *13* (9), 2346–2349.

(78) Murai, S.; Aya, T.; Sonoda, N. Synthesis via Silyl Alkenyl Ethers. IV. Synthesis of 1-Hydroxybicyclo[n.1.0]Alkanes from Silyl Alkenyl Ethers. Novel Class of Cyclopropanols. *J. Org. Chem.* **1973**, *38* (25), 4354–4356.

(79) Taylor, A. P.; Robinson, R. P.; Fobian, Y. M.; Blakemore, D. C.; Jones, L. H.; Fadeyi, O. Modern Advances in Heterocyclic Chemistry in Drug Discovery. *Org. Biomol. Chem.* **2016**, *14* (28), 6611–6637.

(80) Eicher, T.; Hauptmann, S.; Speicher, A. *The Chemistry of Heterocycles : Structure, Reactions, Synthesis and Applications*; Wiley-VCH, 2012.

(81) Minisci, F.; Bernardi, R.; Bertini, F.; Galli, R.; Perchinummo, M. Nucleophilic Character of Alkyl Radicals—VI : A New Convenient Selective Alkylation of Heteroaromatic Bases. *Tetrahedron* **1971**, *27* (15), 3575–3579.

(82) Minisci, F.; Fontana, F.; Vismara, E. Substitutions by Nucleophilic Free Radicals: A New General Reaction of Heteroaromatic Bases. *J. Heterocycl. Chem.* **1990**, *27* (1), 79–96.

(83) Seiple, I. B.; Su, S.; Rodriguez, R. A.; Gianatassio, R.; Fujiwara, Y.; Sobel, A. L.; Baran, P. S. Direct C−H Arylation of Electron-Deficient Heterocycles with Arylboronic Acids. *J. Am. Chem. Soc.* **2010**, *132* (38), 13194–13196.

(84) Ji, Y.; Brueckl, T.; Baxter, R. D.; Fujiwara, Y.; Seiple, I. B.; Su, S.; Blackmond, D. G.; Baran, P. S. Innate C-H Trifluoromethylation of Heterocycles. *Proc. Natl. Acad. Sci.* **2011**, *108* (35), 14411–14415.

(85) Gianatassio, R.; Kawamura, S.; Eprile, C. L.; Foo, K.; Ge, J.; Burns, A. C.; Collins, M. R.; Baran, P. S. Simple Sulfinate Synthesis Enables C□H Trifluoromethylcyclopropanation. *Angew. Chemie Int. Ed.* **2014**, *53* (37), 9851–9855.

(86) Fujiwara, Y.; Dixon, J. A.; O'Hara, F.; Funder, E. D.; Dixon, D. D.; Rodriguez, R. A.; Baxter, R. D.; Herlé, B.; Sach, N.; Collins, M. R.; et al. Practical and Innate Carbon-Hydrogen Functionalization of Heterocycles. *Nature* **2012**, *492* (7427), 95–99.

(87) Ma, X.; Herzon, S. B. Intermolecular Hydropyridylation of Unactivated Alkenes. *J. Am. Chem. Soc.* **2016**, *138* (28), 8718–8721.

(88) Mai, D. N.; Baxter, R. D. Unprotected Amino Acids as Stable Radical Precursors for Heterocycle C–H Functionalization. *Org. Lett.* **2016**, *18* (15), 3738–3741.

(89) Jin, J.; MacMillan, D. W. C. Alcohols as Alkylating Agents in Heteroarene C-H Functionalization. *Nature* **2015**, *525* (7567), 87–90.

(90) Matsui, J. K.; Primer, D. N.; Molander, G. A. Metal-Free C–H Alkylation of Heteroarenes with Alkyltrifluoroborates: A General Protocol for 1°, 2° and 3° Alkylation. *Chem. Sci.* **2017**, *8* (5), 3512–3522.

(91) McCallum, T.; Barriault, L. Direct Alkylation of Heteroarenes with Unactivated Bromoalkanes Using Photoredox Gold Catalysis. *Chem. Sci.* **2016**, *7* (7), 4754–4758.

(92) Li, G.-X.; Morales-Rivera, C. A.; Wang, Y.; Gao, F.; He, G.; Liu, P.; Chen, G. Photoredox-Mediated Minisci C-H Alkylation of N-Heteroarenes Using Boronic Acids and Hypervalent Iodine. *Chem. Sci.* **2016**, *7* (10), 6407–6412.

(93) Kan, J.; Huang, S.; Lin, J.; Zhang, M.; Su, W. Silver-Catalyzed Arylation of (Hetero)Arenes by Oxidative Decarboxylation of Aromatic Carboxylic Acids. *Angew. Chemie Int. Ed.* **2015**, *54* (7), 2199–2203.

(94) Garza-Sanchez, R. A.; Tlahuext-Aca, A.; Tavakoli, G.; Glorius, F. Visible Light-Mediated Direct Decarboxylative C–H Functionalization of Heteroarenes. *ACS Catal.* **2017**, *7* (6), 4057–4061.

(95) DiRocco, D. A.; Dykstra, K.; Krska, S.; Vachal, P.; Conway, D. V.; Tudge, M. Late-Stage Functionalization of Biologically Active Heterocycles Through Photoredox Catalysis. *Angew. Chemie Int. Ed.* **2014**, *53* (19), 4802–4806.

(96) Huff, C. A.; Cohen, R. D.; Dykstra, K. D.; Streckfuss, E.; DiRocco, D. A.; Krska, S. W. Photoredox-Catalyzed Hydroxymethylation of Heteroaromatic Bases. *J. Org. Chem.* **2016**, *81* (16), 6980–6987.

(97) O'Brien, A. G.; Maruyama, A.; Inokuma, Y.; Fujita, M.; Baran, P. S.; Blackmond, D. G. Radical C□H Functionalization of Heteroarenes under Electrochemical Control. *Angew. Chemie Int. Ed.* **2014**, *53* (44), 11868–11871.

(98) O'Hara, F.; Blackmond, D. G.; Baran, P. S. Radical-Based Regioselective C–H Functionalization of Electron-Deficient Heteroarenes: Scope, Tunability, and Predictability. *J. Am. Chem. Soc.* **2013**, *135* (32), 12122–12134.

(99) Bume, D. D.; Pitts, C. R.; Lectka, T. Tandem C-C Bond Cleavage of -Cyclopropanols and Oxidative Aromatization by Manganese(IV) Oxide in a Direct C-H to C-C Functionalization of Heteroaromatics. *European J. Org. Chem.* **2016**, *2016* (1), 26–30.

(100) Lu, S.-C.; Li, H.-S.; Xu, S.; Duan, G.-Y. Silver-Catalyzed C2-Selective Direct Alkylation of Heteroarenes with Tertiary Cycloalkanols. *Org. Biomol. Chem.* **2017**, *15* (2), 324–327.

(101) Alexiev, A.; Bontchev, P. R. A New Catalytic Reaction for Determination of Silver. *Mikrochim. Acta* **1970**, *58* (1), 13–19.

(102) Bonchev, P. R.; Aleksiev, A. A. Use of Marcus's Theory for Selecting Activators of Homogeneous Catalytic Reactions. *Theor. Exp. Chem.* **1975**, *9* (2), 144–147.

(103) Anderson, J. M.; Kochi, J. K. Silver(I)-Catalyzed Oxidative Decarboxylation of Acids by Peroxydisulfate. Role of Silver(II). *J. Am. Chem. Soc.* **1970**, *92* (6), 1651–1659.

(104) Elek, G. Z.; Borovkov, V.; Lopp, M.; Kananovich, D. G. Enantioselective One-Pot Synthesis of α,β-Epoxy Ketones via Aerobic Oxidation of Cyclopropanols. *Org. Lett.* **2017**, *19* (13), 3544–3547.

(105) Duncton, M. A. J. Minisci Reactions: Versatile CH-Functionalizations for Medicinal Chemists. *Medchemcomm* **2011**, *2* (12), 1135.

(106) Kuhnert, L.; Pehl, K.-W. Oscillations in the Belousov-Zhabotinskii System (BZR) Catalysed by Bis-Bipyridine-Silver Complexes. *Chem. Phys. Lett.* **1981**, *84* (1), 155–158.

(107) Joshaghani, M.; Bahadori, M.; Rafiee, E.; Bagherzadeh, M. Oxidative Transformation of Organic Compounds Using Bis(Bipyridine)Silver(II) Peroxydisulfate. *Arkivoc* **2008**, *2007* (16), 260–265.

(108) Bowmaker, G. A.; Effendy; Marfuah, S.; Skelton, B. W.; White, A. H. Syntheses, Structures and Vibrational Spectroscopy of Some 1:1 and 1:2 Adducts of Silver(I) Oxyanion Salts with 2,2'-Bis(Pyridine) Chelates. *Inorganica Chim. Acta* **2005**, *358* (14), 4371–4388.

(109) Blondel, C. Recent Experimental Achievements with Negative Ions. *Phys. Scr.* **1995**, *58*, 31–42.

(110) Nikolaev, A.; Legault, C. Y.; Zhang, M.; Orellana, A. The Acid-Free Cyclopropanol-Minisci Reaction Reveals the Catalytic Role of Silver–Pyridine Complexes. *Org. Lett.* **2018**, *20* (3), 796–799.

(111) Baxter, R. D.; Liang, Y.; Hong, X.; Brown, T. A.; Zare, R. N.; Houk, K. N.; Baran, P. S.; Blackmond, D. G. Mechanistic Insights into Two-Phase Radical C–H Arylations. *ACS Cent. Sci.* **2015**, *1* (8), 456–462.

(112) Patel, N. R.; Flowers, R. A. Uncovering the Mechanism of the Ag(I)/Persulfate-Catalyzed Cross-Coupling Reaction of Arylboronic Acids and Heteroarenes. *J. Am. Chem. Soc.* **2013**, *135* (12), 4672–4675.

(113) Tauber, J.; Imbri, D.; Opatz, T.; Tauber, J.; Imbri, D.; Opatz, T. Radical Addition to Iminium Ions and Cationic Heterocycles. *Molecules* **2014**, *19* (10), 16190–16222.

(114) Brook, A. G. Triphenylsilyl Phenyl Ketone. *J. Am. Chem. Soc.* **1957**, *79* (16), 4373–4375.

(115) Zhang, H.-J.; Priebbenow, D. L.; Bolm, C. Acylsilanes: Valuable Organosilicon Reagents in Organic Synthesis. *Chem. Soc. Rev.* **2013**, *42* (21), 8540–8571.

(116) Boyce, G. R.; Greszler, S. N.; Johnson, J. S.; Linghu, X.; Malinowski, J. T.; Nicewicz, D. A.; Satterfield, A. D.; Schmitt, D. C.; Steward, K. M. Silyl Glyoxylates. Conception and Realization of Flexible Conjunctive Reagents for Multicomponent Coupling. *J. Org. Chem.* **2012**, *77* (10), 4503–4515.

(117) Discussion Addendum for: [3 + 4] Annulation Using a [Β-(Trimethylsilyl) Acryloyl]Silane and the Lithium Enolate of an Α,Β-Unsaturated Methyl Ketone: (1R,6S,7S)-4-(Tert-Butyldimethylsiloxy)-6-(Trimethylsilyl)Bicyclo [5.4.0]Undec. *Org. Synth.* **2012**, *89*, 267–273.

(118) Smith, III, A. B.; Wuest, W. M. Evolution of Multi-Component Anion Relay Chemistry (ARC): Construction of Architecturally Complex Natural and Unnatural Products. *Chem. Commun.* **2008**, *0* (45), 5883–5895.

(119) Moser, W. H. The Brook Rearrangement in Tandem Bond Formation Strategies. *Tetrahedron* **2001**, *57* (11), 2065–2084.

(120) Jankowski, P.; Raubo, P.; Wicha, J. Tandem Transformations Initiated by the Migration of a Silyl Group. Some New Synthetic Applications of Silyloxiranes. *Synlett* **1994**, *1994* (12), 985–992.

(121) Kuwajima, I. Synthetic Organic Reactions by Means of Reactive Nucleophiles Generated through Rearrangement of a Silyl Group. *J. Organomet. Chem.* **1985**, *285*, 137–148.

(122) Soderquist, J. A.; Hassner, A. Synthetic Methods. 15. Unsaturated Acyl Derivatives of Silicon, Germanium, and Tin from Metalated Enol Ethers. *J. Am. Chem. Soc.* **1980**, *102* (5), 1577–1583.

(123) Reich, H. J.; Kelly, M. J.; Olson, R. E.; Holtan, R. C. Silyl Ketone Chemistry : Preparation and Reactions of Unsaturated Silyl Ketones. *Tetrahedron* **1983**, *39* (6), 949–960.

(124) Reich, H. J.; Kelly, M. J. Silyl Ketone Chemistry. Synthesis and Reactions of Olefinic and Acetylenic Silyl Ketones. *J. Am. Chem. Soc.* **1982**, *104* (4), 1119–1120.

(125) Danheiser, R. L.; Fink, D. M.; Okano, K.; Tsai, Y. M.; Szczepanski, S. W. A Practical and Efficient Synthesis of .Alpha.,.Beta.-Unsaturated Acylsilanes. *J. Org. Chem.* **1985**, *50* (25), 5393–5396.

(126) Meyer, K. H.; Schuster, K. Umlagerung Tertiärer Äthinyl-Carbinole in Ungesättigte Ketone. *Berichte der Dtsch. Chem. Gesellschaft (A B Ser.* **1922**, *55* (4), 819–823.

(127) Cadierno, V.; Crochet, P.; García-Garrido, S. E.; Gimeno, J. Metal-Catalyzed Transformations of Propargylic Alcohols into α,β-Unsaturated Carbonyl Compounds: From the Meyer–Schuster and Rupe Rearrangements to Redox Isomerizations. *Dalt. Trans.* **2010**, *39* (17), 4015–4031.

(128) Engel, D. A.; Dudley, G. B. The Meyer–Schuster Rearrangement for the Synthesis of α,β-Unsaturated Carbonyl Compounds. *Org. Biomol. Chem.* **2009**, *7* (20), 4149–4158.

(129) Swaminathan, S.; Narayanan, K. V. Rupe and Meyer-Schuster Rearrangements. *Chem. Rev.* **1971**, *71* (5), 429–438.

(130) Narasaka, K.; Kusama, H.; Hayashi, Y. Rearrangement of Allylic and Propargylic Alcohols Catalyzed by the Combined Use of Tetrabutylammonium Perrhenate(VII) and *p* -Toluenesulfonic Acid. *Chem. Lett.* **1991**, *20* (8), 1413–1416.

(131) Narasaka, K.; Kusama, H.; Hayashi, Y. Rearrangement of Allylic and Propargylic Alcohols Catalyzed by the Combined Use of Tetrabutylammonium Perrhenate (VII) and p-Toluenesulfonic Acid. *Tetrahedron* **1992**, *48* (11), 2059–2068.

(132) Li, Z.-Y.; Wang, M.; Bian, Q.-H.; Zheng, B.; Mao, J.-Y.; Li, S.-N.; Liu, S.-Z.; Wang, M.-A.; Zhong, J.-C.; Guo, H.-C. Highly Enantioselective Addition of Trimethylsilylacetylene to Aldehydes Catalyzed by a Zinc-Amino-Alcohol Complex. *Chem. - A Eur. J.* **2011**, *17* (21), 5782–5786.

(133) Guthrie, J. P. Hydrolysis of Esters of Oxy Acids: P K_a Values for Strong Acids; Brønsted Relationship for Attack of Water at Methyl; Free Energies of Hydrolysis of Esters of Oxy Acids; and a Linear Relationship between Free Energy of Hydrolysis and P . *Can. J. Chem.* **1978**, *56* (17), 2342–2354.

(134) Hilmar Weinmann, *; Michael Harre; Harribert Neh; Klaus Nickisch; Carlo Skötsch, A.; Tilstam, U. The Rupe Rearrangement: A New Efficient Method for Large-Scale Synthesis of Unsaturated Ketones in the Pilot Plant. *Org. Process Res. Dev.* **2002**, *6* (3), 216–219.

(135) Wang, D.-W.; Wang, X.-B.; Wang, D.-S.; Lu, S.-M.; Zhou, Y.-G.; Li, Y.-X. Highly Enantioselective Iridium-Catalyzed Hydrogenation of 2-Benzylquinolines and 2-Functionalized and 2,3-Disubstituted Quinolines. *J. Org. Chem.* **2009**, *74* (7), 2780–2787.

(136) Ruthenium-Catalyzed Synthesis of 3-Substituted Quinolines from 2-Aminobenzyl Alcohol and Aldehydes. *Bull. Korean Chem. Soc.* **2005**, *26* (12), 2038–2040.

(137) Das, S.; Maiti, D.; De Sarkar, S. Synthesis of Polysubstituted Quinolines from α-2-Aminoaryl Alcohols Via Nickel-Catalyzed Dehydrogenative Coupling. *J. Org. Chem.* **2018**, *83* (4), 2309–2316.

(138) Qu, F.; He, P.; Hu, R.-F.; Cheng, X.-H.; Wang, S.; Wu, J. Efficient Synthesis of Quinolines via a Knoevenagel/Staudinger/Aza-Wittig Sequence. *Synth. Commun.* **2015**, *45* (24), 2802–2809.

(139) Shintani, R.; Okamoto, K.; Hayashi, T. Rhodium-Catalyzed Isomerization of α-Arylpropargyl Alcohols to Indanones: Involvement of an Unexpected Reaction Cascade. *J. Am. Chem. Soc.* **2005**, *127* (9), 2872–2873.

(140) Matsuya, Y.; Koiwai, A.; Minato, D.; Sugimoto, K.; Toyooka, N. Novel Sequential 1,4-Brook Rearrangement–Wittig Reaction: New One-Pot Approach for Silyl Dienol Ethers. *Tetrahedron Lett.* **2012**, *53* (44), 5955–5957.

(141) Downey, C. W.; Mahoney, B. D.; Lipari, V. R. Trimethylsilyl Trifluoromethanesulfonate-

Accelerated Addition of Catalytically Generated Zinc Acetylides to Aldehydes. *J. Org. Chem.* **2009**, *74* (7), 2904–2906.

(142) Ma, S.; Wu, B.; Zhao, S. Mild and Efficient Synthesis of (*Z*)-α-Chloroalkylidene-β-Lactones via the $PdCl_2$ -Catalyzed Cyclocarbonylation of 2-Alkynols. *Org. Lett.* **2003**, *5* (23), 4429–4432.

(143) Ma, D.; Yu, Y.; Lu, X. *Highly Stereoselective Isomerization of Ynones to Conjugated Dienones Catalyzed by Transition-Metal Complexes*; 1989; Vol. 54.